

*CHANGE AND PROCESSES
OF CHANGE ON
SHORE PLATFORMS.*

A thesis
submitted in partial fulfilment
of the requirements for the Degree of
Doctor of Philosophy in Geography
in the
University of Canterbury

ANNA JANE TAYLOR

*UNIVERSITY OF CANTERBURY
2003*

GB
458.55
T238
2003

ABSTRACT.

This thesis examines morphological change and processes causing change on shore platforms formed in five different lithologies around New Zealand. Study platforms located at Kaikoura, Akaroa Harbour and Lake Waikaremoana are variously eroded into limestone, greywacke, basalt and two types of mudstone.

Rates and patterns of surface change are presented from three years of monitoring using a micro-erosion meter. Shore platform rock characteristics are described from observations of lithological features and with expressions of rock strength calculated by point load testing, Schmidt hammer testing, and a rock mass strength index. Marine processes were investigated by using deepwater wave data and direct measurement of wave induced flows on a shore platform. Weathering processes were assessed from observation of morphology and laboratory tests.

Annual rates of surface change ranged from 0.01mm.yr^{-1} to 12.82mm.yr^{-1} . All marine rock surfaces measured showed dynamic changes with both surface swelling and lowering measured. Mean rates of surface lowering on the basalt were 0.29mm.yr^{-1} , greywacke 0.78mm.yr^{-1} , limestone 1.19mm.yr^{-1} , Kaikoura mudstone 1.41mm.yr^{-1} and Lake Waikaremoana mudstone 9.13mm.yr^{-1} . These rates are similar to published rates from previous shore platform studies and are of sufficiently great magnitudes that they can have formed the current shore platforms over the period that water levels have been at present relative levels.

Rock characteristics differed between platforms yet profiles displayed similar form and dimensions. Platform orientation is across lines of weakness, both bedrock dip and strike, on all rock types examined. Platforms are therefore wholly eroded and not related to lithology. The three tests conducted to assess rock strength reflected strength of bedrock, surface rock and the body of rock as a whole. Rocks were classified as moderately strong (greywacke) through to very weak (Lake Waikaremoana mudstone). Comparison of elements of platform morphology and rate of surface change with rock characteristics showed no correlations with bedrock strength. Surface strength showed positive correlations to platform width and surface strength and rock mass strength showed negative correlations to gradient and

elevation. There were no strong trends between rock characteristics and surface level change. These observations contradict concepts of rock strength control of morphology given in the literature.

Investigation of marine processes showed that all but the smallest waves break before reaching the seaward edge of the shore platforms studied. Simultaneous measures of wave parameters in deepwater and onshore showed reductions of up to 67% in wave height and over 90% in wave energy and wave energy flux. It is an important finding of this study that the highest energy deepwater waves do not necessarily deliver the highest energy to the shore platform. Therefore, it is not applicable to use deepwater wave parameters or calculated breaking wave height as indicators of onshore wave assailing force to characterise the wave environment at shore platforms.

Direct measurements of velocity fields across a shore platform are reported for the first time in the geomorphic literature. Flows of up to $2.54\text{m}\cdot\text{s}^{-1}$ were recorded. Flow velocity was highest in the centre of the platform showing that wave force did not dissipate in a consistent way as waves flowed onto and across the platform. There were strong lateral components to flow and high levels of turbulence. Direct measurement of flow has enabled quantitative estimation of Clapotis, shock pressures, water hammer, hydrostatic pressure, shear stress, air compression, cavitation and abrasion for the first time on shore platforms. Air compression in rock cavities and abrasion are capable of erosion as independent mechanisms. Other mechanisms in combination may cause erosion at the micro scale.

Quantification of the competence and capacity of wave induced flow in sediment transport on shore platforms was undertaken. Removal of sediment from platform surfaces is an integral component of processes forming shore platforms and has not previously been quantified. It was shown that flow was competent to transport coarse sand at all locations across the platform while the flow measured had potential to move boulder-sized sediment. Net potential sediment transport was offshore and large blocks could be removed from the platform over the period of 2 to 3 tidal cycles. This differs from other coastal environments where net potential sediment movement can be in both on and offshore directions.

Morphological evidence of weathering processes included: honeycombs, salt crystallisation, rock disintegration, solution patterns and water layer weathering. Tests for susceptibility of each rock type to weathering mechanisms of wetting and drying and saturation showed that Lake Waikaremoana mudstone, Kaikoura mudstone and parts of the basalt were most susceptible to weathering by these mechanisms. Greywacke was least susceptible. Given the importance of wetting and drying suggested in the literature as a mode of shore platform development, it is an important finding that not all rocks in which shore platforms are formed are susceptible to this form of weathering. It was shown that susceptibility of rocks to weathering was not a strong control on shore platform morphology or erosion rates.

Through investigation of processes it has been shown that there are complex controls on the morphological development of shore platforms. These controls could not be explained using models of shore platform development currently available therefore a model of shore platform development has been presented in this thesis. It is based on a process – response model and provides a more universal framework within which to view shore platform development.

CONTENTS

| | |
|--|-----------|
| ABSTRACT | ii |
| LIST OF FIGURES | ix |
| LIST OF TABLES | xiii |
| LIST OF SYMBOLS | xiv |
| ACKNOWLEDGEMENTS | xvi |
| CHAPTER ONE PROCESSES OF CHANGE ON SHORE PLATFORMS..... | 1 |
| 1.1 Introduction..... | 1 |
| 1.2 Shore platform research..... | 3 |
| 1.2.1 <i>Factors important to shore platform development.</i> | 9 |
| 1.2.1.1 Rocks..... | 9 |
| 1.2.1.2 Waves..... | 10 |
| 1.2.1.3 Weathering..... | 11 |
| 1.2.1.4 Water Level..... | 12 |
| 1.2.1.5 Biology..... | 13 |
| 1.2.2 <i>Measurement of processes.</i> | 13 |
| 1.2.3 <i>Models of shore platform development.</i> | 14 |
| 1.2.4 <i>Questions in shore platform development.</i> | 19 |
| 1.3 Summary..... | 22 |
| 1.4 Thesis outline..... | 22 |
| CHAPTER TWO FIELD AREAS AND SHORE PLATFORM MORPHOLOGIES | 24 |
| 2.1 Introduction..... | 24 |
| 2.2 Rationale for choice of field sites..... | 24 |
| 2.3 Field site locations..... | 25 |
| 2.4 Field site environments..... | 26 |
| 2.4.1 <i>Kaikoura Peninsula.</i> | 27 |
| 2.4.2 <i>Raramai Arch.</i> | 29 |
| 2.4.3 <i>Robinson's Bay, Akaroa Harbour.</i> | 31 |
| 2.4.4 <i>Long term sea level.</i> | 33 |
| 2.4.5 <i>Lake Waikaremoana.</i> | 33 |
| 2.4.6 <i>Summary</i> | 35 |
| 2.5 Classification of shore platforms..... | 35 |
| 2.5.1 <i>Morphometric characterization.</i> | 39 |
| 2.5.1.1 Orientation..... | 39 |
| 2.5.1.2 Width..... | 40 |
| 2.5.1.3 Gradient..... | 41 |
| 2.5.1.4 Elevation..... | 42 |
| 2.5.2 <i>Definition of morphometric elements of shore platforms.</i> | 43 |
| 2.5.2.1 Orientation: | 44 |
| 2.5.2.2 Width: | 44 |
| 2.5.2.3 Gradient: | 44 |
| 2.5.2.4 Elevation: | 44 |
| 2.5.2.5 Roughness: | 45 |
| 2.6 Profile descriptions..... | 46 |
| 2.6.1 <i>Method.</i> | 46 |
| 2.6.2 <i>AK1</i> | 47 |
| 2.6.3 <i>AK2.</i> | 48 |
| 2.6.4 <i>KM2.</i> | 49 |
| 2.6.5 <i>KM3.</i> | 50 |

| | |
|---|------------|
| 2.6.6 KM7..... | 51 |
| 2.6.7 RM1..... | 52 |
| 2.6.8 WK1..... | 53 |
| 2.6.9 WK2..... | 54 |
| 2.6.10 Comparison of morphologies..... | 55 |
| 2.7 Summary..... | 60 |
| CHAPTER THREE SURFACE LEVEL CHANGES..... | 61 |
| 3.1 Methodology..... | 62 |
| 3.2 Measurements of surface changes..... | 70 |
| 3.3 Patterns of surface level change..... | 81 |
| 3.3.1 Temporal patterns of surface change..... | 81 |
| 3.3.2 Magnitude of surface changes..... | 84 |
| 3.3.3 Location of surface changes..... | 86 |
| 3.3.4 Nature of surface level changes..... | 88 |
| 3.4 Average rates of surface change..... | 89 |
| 3.4.1 Calculation of rates of surface change (multiple duration method)..... | 92 |
| 3.4.1.1 Comparison of methods..... | 95 |
| 3.4.2 Rates of surface change from longer term data..... | 96 |
| 3.4.3 Rate of change compared to the residual..... | 97 |
| 3.4.4 Average rates of surface change for each rock type..... | 98 |
| 3.5 Summary..... | 100 |
| CHAPTER FOUR ROCK CHARACTER AND RESISTANCE TO EROSION..... | 103 |
| 4.1 Introduction..... | 103 |
| 4.2 Description of Lithologies..... | 104 |
| 4.2.1 Rock types..... | 104 |
| 4.2.2 Structure..... | 104 |
| 4.2.3 Profile lithology..... | 105 |
| 4.3 Are shore platforms wholly eroded features?..... | 109 |
| 4.4 Lithological control on shore platform morphology..... | 110 |
| 4.5 Rock strength..... | 114 |
| 4.5.1 Indices of rock strength..... | 117 |
| 4.5.2 Methods used to measure rock strength..... | 118 |
| 4.5.2.1 Point load testing..... | 119 |
| 4.5.2.2 Schmidt hammer testing..... | 120 |
| 4.5.2.3 Mass strength assessment..... | 120 |
| 4.5.3 Rock strength of shore platforms studied..... | 121 |
| 4.5.4 Comparison of rock strength indices..... | 125 |
| 4.5.5 Variations in rock strength..... | 127 |
| 4.5.5.1 Spatial variation across a surface..... | 128 |
| 4.5.6 Reduction of rock strength..... | 130 |
| 4.6 Rock control of shore platform morphology..... | 132 |
| 4.6.1 Rock strength control at the platform wide scale..... | 138 |
| 4.6.2 Choice of index of rock strength for use in shore platform studies..... | 141 |
| 4.6.3 Rock control at the profile scale and micro scale..... | 142 |
| 4.7 Rock susceptibility to weathering..... | 145 |
| 4.8 Summary..... | 145 |
| CHAPTER FIVE WAVES ON SHORE PLATFORMS..... | 148 |
| 5.1 Introduction..... | 148 |
| 5.1.1 Why waves are important..... | 149 |
| 5.1.2 Previous measures of wave assailing force on shore platforms..... | 151 |
| 5.2 Wave Environments of Study Sites..... | 154 |
| 5.2.1 Methods of description of wave environments..... | 154 |
| 5.2.1.1 Statistical methods..... | 154 |
| 5.2.1.2 Spectral methods..... | 155 |

| | |
|---|------------|
| 5.2.1.3 Comparison of methods | 155 |
| 5.2.2 <i>Records of wave environments for New Zealand</i> | 156 |
| 5.2.2.1 Published records of wave environments for east coast, South Island | 157 |
| 5.2.3 <i>Wave environments directly offshore from study sites</i> | 160 |
| 5.2.3.1 KM2, KM3, KM7 and RM1 wave environment. | 160 |
| 5.2.3.2 AK1 and AK2 wave environment. | 163 |
| 5.2.3.2.1 Swell propagation. | 164 |
| 5.2.3.2.2 Wind wave generation. | 171 |
| 5.2.3.2.3 Combination of swell and wind waves. | 172 |
| 5.2.3.3 WK1 and WK2 wave environment | 174 |
| 5.2.4 <i>Comparison of offshore wave environments with rate of surface change</i> | 175 |
| 5.3 Changes as waves move from deepwater onto the shore platform. ... | 178 |
| 5.3.1 <i>Wave theories</i> | 180 |
| 5.3.2 <i>Location of wave breaking in relation to study profiles</i> | 181 |
| 5.3.3 <i>Frequency of wave breaking with respect to platforms</i> | 183 |
| 5.4 Comparison of deepwater, onshore and across shore flows. | 189 |
| 5.4.1 <i>Measurement methods</i> | 190 |
| 5.4.1.2 Instrumentation | 191 |
| 5.4.1.2.1 Wave buoy | 191 |
| 5.4.1.2.2 Vector (acoustic Doppler velocity meter)..... | 192 |
| 5.4.1.2.3 Marsh McBirneys (electro magnetic current meters) | 194 |
| 5.4.1.3 Calibration..... | 195 |
| 5.4.1.4 Sampling | 195 |
| 5.4.1.5 Post processing of data..... | 197 |
| 5.4.2 <i>Differences between deepwater and onshore (platform) wave parameters</i> . 198 | |
| 5.4.2.1 Wave period (T) | 200 |
| 5.4.2.2 Wave height (H) | 202 |
| 5.4.2.3 Wave velocity (u) | 203 |
| 5.4.2.4 Wave energy (E) and wave energy flux (Q)..... | 204 |
| 5.4.2.5 Where does the energy go? | 207 |
| 5.4.3 <i>Wave induced water flow across KM3</i> | 216 |
| 5.4.3.1 Flow velocity..... | 217 |
| 5.4.3.2 Flow direction | 222 |
| 5.4.3.3 Turbulence | 226 |
| 5.5 Summary | 231 |
| CHAPTER SIX WAVE INDUCED PROCESSES ON SHORE PLATFORMS..... | 235 |
| 6.1 Introduction..... | 235 |
| 6.2 Proposed modes of wave erosion. | 236 |
| 6.2.1 <i>Standing waves</i> | 236 |
| 6.2.1.1 Clapotis. | 236 |
| 6.2.2 <i>Breaking waves</i> | 238 |
| 6.2.2.1 Shock or impact pressures..... | 238 |
| 6.2.2.2 Water Hammer. | 239 |
| 6.2.3 <i>Broken waves</i> | 240 |
| 6.2.3.1 Hydrostatic pressure. | 240 |
| 6.2.3.2 Water mass friction / shear stress. | 243 |
| 6.2.3.3 Cavitation. | 250 |
| 6.2.3.4 Air compression. | 252 |
| 6.2.3.5 Quarrying / Plucking. | 258 |
| 6.2.3.6 Abrasion. | 260 |
| 6.2.4 <i>Combinations of modes</i> | 262 |
| 6.3 Sediment entrainment. | 265 |
| 6.3.1 <i>Sediment entrainment theories</i> | 266 |
| 6.3.2 <i>Sediment movement in the coastal environment</i> | 274 |
| 6.3.3 <i>Sediment movement on KM3</i> | 276 |
| 6.3.3.1 Potential sediment entrainment on KM3..... | 277 |
| 6.3.3.2 Sediment entrained on KM3. | 278 |

| | |
|---|------------|
| 6.3.3.3 Vector sediment entrainment summations. | 278 |
| 6.3.3.4 Potential sediment transport distances. | 285 |
| 6.3.3.5 Longinov's method. | 287 |
| 6.3.4 <i>Wave effectiveness</i> | 295 |
| 6.4 Summary..... | 302 |
| CHAPTER SEVEN WEATHERING..... | 305 |
| 7.1 Introduction..... | 305 |
| 7.2 Weathering mechanisms..... | 306 |
| 7.2.1 <i>Mechanical weathering</i> | 306 |
| 7.2.1.1 <i>Frost action</i> | 306 |
| 7.2.1.2 Salt weathering..... | 307 |
| 7.2.1.3 Mineral expansion..... | 308 |
| 7.2.1.4 Wetting and drying..... | 309 |
| 7.2.2 <i>Chemical weathering</i> | 310 |
| 7.2.2.1 Solution..... | 310 |
| 7.2.3 <i>Biological weathering</i> | 310 |
| 7.3 Measurement of weathering on shore platforms..... | 313 |
| 7.3.1 <i>Assessment of weathering made for this study</i> | 314 |
| 7.3.2 <i>Reduction of rock strength</i> | 315 |
| 7.3.3 <i>Morphological evidence</i> | 315 |
| 7.3.4 <i>Susceptibility tests</i> | 318 |
| 7.3.4.1 Slake-durability..... | 318 |
| 7.3.4.1.1 Method..... | 319 |
| 7.3.4.1.2 Results..... | 320 |
| 7.3.4.2 Wetting and drying..... | 321 |
| 7.3.4.2.1 Method..... | 321 |
| 7.3.4.2 Results..... | 322 |
| 7.3.4.3 Saturation..... | 326 |
| 7.3.4.3.1 Method..... | 326 |
| 7.3.4.3.2 Results..... | 327 |
| 7.4 Weathering as a control in shore platform morphological change..... | 329 |
| 7.5 Summary..... | 332 |
| CHAPTER EIGHT SPATIAL VARIATION AND SHORE PLATFORM DEVELOPMENT | 334 |
| 8.1 Introduction..... | 334 |
| 8.2 Shore platform development in the New Zealand temperate climate..... | 336 |
| 8.3 Profile scale..... | 341 |
| 8.4 Micro scale..... | 350 |
| 8.5 Shore platform development..... | 351 |
| 8.5.1 <i>The formation (erosion) zone</i> | 352 |
| 8.5.1.1 Spatial restrictions on erosive processes..... | 353 |
| 8.5.1.2 Morphological limits..... | 356 |
| 8.5.2 <i>Process – response model (within the zone of formation)</i> | 358 |
| 8.6 Summary..... | 361 |
| CHAPTER NINE CONCLUSIONS..... | 364 |
| 9.1 Control of rock type..... | 368 |
| 9.2 Weathering processes..... | 370 |
| 9.3 Wave processes..... | 371 |
| 9.4 The nature of the equilibrium of shore platforms..... | 375 |
| 9.5 Further research..... | 376 |
| REFERENCES | 378 |

LIST OF FIGURES

| | |
|---|----|
| Figure 1.1: Global distribution of rocky coasts & shore platform studies. | 4 |
| Figure 1.2: Stages in the development of the shore profile (Johnson 1919). | 15 |
| Figure 1.3: Challinor's diagram to explain consistency in the form of the coast profile as the sea advanced landward (Challinor 1949). | 16 |
| Figure 1.4: The parallel retreat model (Trenhaile 1974a) | 16 |
| Figure 1.5: Factors affecting erosion of rocky coasts (Sunamura 1994)..... | 18 |
| Figure 1.6: Vertical distribution of assailing force of waves and resisting force of rocks. (Sunamura 1992)..... | 18 |
| Figure 2.1: Map showing location of shore platform study profiles. | 26 |
| Figure 2.2: Kaikoura Peninsula showing shore platform lithology (Kirk 1977). ... | 27 |
| Figure 2.3: Marine terraces of the Kaikoura Peninsula (Ota <i>et al.</i> 1996)..... | 28 |
| Figure 2.4: Map of Raramai Arch shore platform. | 30 |
| Figure 2.5: Coastal features of the Akaroa Harbour..... | 31 |
| Figure 2.6: Map of Robinsons Bay Point shore platform. | 32 |
| Figure 2.7: Lake Waikaremoana with the shore platform profiles indicated. | 34 |
| Figure 2.8: Classification of rocky coasts. (Sunamura 1992)..... | 37 |
| Figure 2.9: Photo of fragmented seaward edge of KM3. | 38 |
| Figure 2.10: Gradient of shore platform at AK2. | 41 |
| Figure 2.11: Schematic of definitions and terminology adopted for this study. | 43 |
| Figure 2.12: Surveyed profile of AK1. | 47 |
| Figure 2.13: Surveyed profile of AK2. | 48 |
| Figure 2.14: Surveyed profile of KM2. | 49 |
| Figure 2.15: Surveyed profile of KM3. | 50 |
| Figure 2.16: Surveyed profile of KM7. | 51 |
| Figure 2.17: Surveyed profile of RM1. | 52 |
| Figure 2.18: Surveyed profile of WK1. | 53 |
| Figure 2.19: Surveyed profile of WK2. | 54 |
| Figure 2.20: Relative position of MEM bolt sites on profiles vs. elevation..... | 57 |
| Figure 2.21: Hypsographic curves for each study profile. | 58 |
| Figure 2.22: Surface elevations of rock surface. | 59 |
| Figure 3.1: Micro-erosion metres used for this study. | 63 |
| Figure 3.2: The bedstead frame. | 64 |
| Figure 3.3: Different surface level surrounding a water filled hole near KM2B. .. | 65 |
| Figure 3.4: Surface change measured for sites across AK1. | 71 |
| Figure 3.5: Surface change measured for sites across AK2. | 72 |
| Figure 3.6: Surface change measured for sites across KM2. | 73 |
| Figure 3.7: Surface change measured for sites across KM3. | 74 |
| Figure 3.8: Surface change measured for sites across KM7. | 75 |
| Figure 3.9: Surface change measured for sites across RM1. | 76 |
| Figure 3.10: Surface change measured for sites on the Raramai Arch platform. ... | 77 |
| Figure 3.11: Surface change measured for sites at Lake Waikaremoana. | 78 |
| Figure 3.12: Change of average surface level at selected MEM sites between 6/11/00 – 10/11/00 and 06/11/01 – 18/11/01. | 83 |
| Figure 3.13: Frequency bar graphs of change of average surface level between successive surveys | 84 |
| Figure 3.14: Plots showing contours of absolute average surface level..... | 87 |
| Figure 3.15: Duration between MEM surveys plotted against rate of surface level change calculated for every combination of surveys conducted at KM2B. | 91 |

| | |
|--|-----|
| Figure 3.16: Surface level changes for all durations measured on KM3C. | 93 |
| Figure 3.17: Comparison of average surface level rates of change obtained using the multiple duration method and the first and last survey method..... | 95 |
| Figure 3.18: Average rate of change vs. residual. | 97 |
| Figure 3.19: Average rate of change vs. Residual as a proportion of average rate. | 98 |
| Figure 4.1: Rock surface near AK1D. | 106 |
| Figure 4.2: Rock surface near KM2D. | 107 |
| Figure 4.3: Rock surface near KM7B. | 108 |
| Figure 4.4: Rock surface near RM1B. | 108 |
| Figure 4.5: Rock surface near WK1mem. | 109 |
| Figure 4.6: Strike of bedrock compared to the orientation of the landward cliff... .. | 110 |
| Figure 4.7: Correlations of bedrock strike or dip with platform width & gradient. | 111 |
| Figure 4.8: Structural classes according to rock dip and strike relative to the landward cliff face. (Trenhaile 1999). | 112 |
| Figure 4.9: Comparison of profiles a). Width and b). Gradient. | 113 |
| Figure 4.10: Specimen shape requirements for point load block tests | 119 |
| Figure 4.11: Rock strength as tested using point load & schmidt hammer methods..... | 127 |
| Figure 4.12: Contour pattern of spatial variation in surface strength near KM3B. | 129 |
| Figure 4.13: Average rate of surface change vs. Degree of weathering. | 132 |
| Figure 4.14: Shore platform width compared to a) bedrock strength, b) surface strength and c) mass strength of rock | 133 |
| Figure 4.15: Shore platform gradient compared to a) bedrock strength, b) surface strength and c) mass strength of rock | 134 |
| Figure 4.16: Shore platform elevation with respect to mean sea level compared to a) bedrock strength, b) surface strength and c) mass strength of rock | 135 |
| Figure 4.17: Shore platform roughness compared to a) bedrock strength, b) surface strength and c) mass strength of rock..... | 136 |
| Figure 4.18: Shore platform average rate of surface change compared to a) bedrock strength, b) surface strength and c) mass strength of..... | 137 |
| Figure 4.19: Shore platform surface rock strength of each profile compared to elements of morphology. | 143 |
| Figure 4.20: Shore platform surface rock strength compared to rate of surface change at individual MEM bolt sites..... | 144 |
| Figure 5.1: Factors affecting erosion of rocky coasts. (Sunamura 1994). | 150 |
| Figure 5.2: The 'black box' approach to shore platform development | 152 |
| Figure 5.3: Frequency of occurrence, as a percentage of each total record of a). H_s and b). T_z for wave buoy data from Kaikoura & Banks Peninsula. | 162 |
| Figure 5.4: Wave refraction diagram for banks peninsula for swell from 45° (Dingwall 1966). | 166 |
| Figure 5.5: Wave refraction diagram for Banks Peninsula for swell from 135° (Dingwall 1966). | 167 |
| Figure 5.6: Wave refraction diagram for Akaroa Harbour for swell from 135°. 168 | |
| Figure 5.7: Wave refraction diagram for Akaroa harbour for swell from 170° | 169 |
| Figure 5.8: Wind rose for Akaroa region. | 172 |
| Figure 5.9: Offshore wave height compared to a) platform width b) platform gradient and c) average rate of surface change. | 176 |
| Figure 5.10: Flow diagram showing transformations and action of sea waves..... | 178 |
| Figure 5.11: Areas of application of various wave theories (Komar 1998). | 180 |
| Figure 5.12: Controls on H_b for the Kaikoura coastal wave environment. | 182 |
| Figure 5.13: Locations of wave breaking shown in relation to KM3. | 184 |

| | |
|--|-----|
| Figure 5.14: Location where waves will break with respect to their deepwater height at mean sea level at KM3. | 184 |
| Figure 5.15: Frequency of occurrence of given H_s offshore from KM3. | 185 |
| Figure 5.16: Frequency of occurrence of H_b at a given distance from the landward boundary of the platform at KM3. | 185 |
| Figure 5.17: Frequency of occurrence of wave breaking at a given distance from the landward boundary of the platform at AK1. | 186 |
| Figure 5.18: Frequency of occurrence of wave breaking at a given distance from the landward boundary of the platform at AK2. | 186 |
| Figure 5.19: Frequency of occurrence of wave breaking at a given distance from the landward boundary of the platform at KM2. | 187 |
| Figure 5.20: Frequency of occurrence of wave breaking at a given distance from the landward boundary of the platform at KM7. | 187 |
| Figure 5.21: Frequency of occurrence of wave breaking at a given distance from the landward boundary of the platform at RM1. | 188 |
| Figure 5.22: Frequency of occurrence of wave breaking at a given distance from the landward boundary of the platform at WK1. | 188 |
| Figure 5.23: Frequency of occurrence of wave breaking at a given distance from the landward boundary of the platform at WK2. | 189 |
| Figure 5.24: Schematic showing location of velocity metres on KM3. | 191 |
| Figure 5.25: Vector probe showing orientation of beams. | 192 |
| Figure 5.26: Installation of Vector flow velocity instrument. | 193 |
| Figure 5.27: Installation of a Marsh McBirney ECM on the shore platform. | 194 |
| Figure 5.28: Schematic showing the problem of wave aliasing. | 196 |
| Figure 5.29: Schematic diagram of axis orientations of flow measurements. | 197 |
| Figure 5.30: Scatter plot showing deepwater wave period against onshore wave period for simultaneous 18 minute averages. | 202 |
| Figure 5.31: Scatter plot of deepwater wave height against onshore wave height, for simultaneous 18 minute periods. | 203 |
| Figure 5.32: Scatter plot of deepwater particle velocity against onshore water velocity, for simultaneous 18 minute periods. | 204 |
| Figure 5.33: Scatter plot of deepwater wave energy against onshore wave energy, for simultaneous 18 minute periods. | 205 |
| Figure 5.34: Scatter plot of deepwater wave energy flux against onshore wave energy flux, for simultaneous 18 minute periods. | 206 |
| Figure 5.35: Scatter plot of deepwater wave energy flux against onshore wave energy flux incorporating measurements from this project & from Stephenson (1997). | 207 |
| Figure 5.36: Significant swash excursions vs. Significant wave height. (Komar 1998, <i>after</i> Guza and Thornton 1982). | 208 |
| Figure 5.37: Schematic of shortwave / longwave energy transfers on a sand beach. (Guza and Thornton 1982). | 209 |
| Figure 5.38: Two onshore wave spectra recorded on 18/08/01. | 212 |
| Figure 5.39: Two onshore wave spectra recorded on 19/08/01. | 212 |
| Figure 5.40: Two onshore wave spectra recorded on 24/08/01. | 213 |
| Figure 5.41: Spectral peaks for onshore measured 18 minute wave spectra. | 214 |
| Figure 5.42: H_{s0} vs. Spectral peak power either side of $t=20s$ | 215 |
| Figure 5.43: A turbulent bore (Denny 1988). | 216 |
| Figure 5.44: Time series of flows. | 218 |
| Figure 5.45: Average and maximum velocities measured by each sensor over three tidal cycles on a). 18/08/01, b). 19/08/01 and c). 24/08/01. | 219 |

| | |
|--|-----|
| Figure 5.46: Average water depth vs. average velocity | 221 |
| Figure 5.47: Bar graphs of average flow showing direction. | 223 |
| Figure 5.48: Vector flow summations of average velocities on 18/08/01..... | 224 |
| Figure 5.49: Vector flow summations of average velocities on 19/08/01. | 225 |
| Figure 5.50: Vector flow summations of average velocities on 24/08/01..... | 225 |
| Figure 6.1: Clapotis or standing waves (Bagnold 1939). | 237 |
| Figure 6.2: Formation of shock pressures by a breaking wave (Bagnold 1939).... | 238 |
| Figure 6.3: Shear stress caused by a body of water moving over a stationary rock surface..... | 244 |
| Figure 6.4: Demarcation for shore platform initiation (Tsuji moto 1987). | 246 |
| Figure 6.5: Comparison of average flow velocities and flow velocities calculated using wave height and water depth..... | 248 |
| Figure 6.6: Critical velocities required for cavitation (Whipple et al 2000). | 251 |
| Figure 6.7: Deformation of rock surface at a joint due to application and release of water pressure. | 254 |
| Figure 6.9: Evidence of wave quarrying on shore platforms. | 259 |
| Figure 6.10: Sediment available for abrasion on shore platforms. | 261 |
| Figure 6.11: Modes of wave erosion & their distribution (Sanders 1968a). | 263 |
| Figure 6.12: Schematic illustration of forces and processes contributing to erosion by plucking (<i>after Whipple et al 2000</i>). | 263 |
| Figure 6.13: Sediment transport modes. (Richards 1982)..... | 267 |
| Figure 6.14: Critical entrainment velocities for given sediment sizes. | 269 |
| Figure 6.15: The Hjulstrom curve showing entrainment and transport velocities for given sediment sizes (Hjulstrom 1939)..... | 270 |
| Figure 6.16: Hjulstrom's curve with corrections (<i>after Novak 1973</i>). | 273 |
| Figure 6.17: Vector summations of the impulse of water flow on sediment for critical threshold velocities of: a). 0.1 m.s-1 b). 1.0 m.s-1 on 18/08/01..... | 281 |
| Figure 6.18: Vector summations of the impulse of water flow on sediment for critical threshold velocities of: a). 0.1 m.s-1 b). 1.0 m.s-1 on 19/08/01. | 282 |
| Figure 6.19: Vector summations of the impulse of water flow on sediment for critical threshold velocities of: a). 0.1 m.s-1 b). 1.0 m.s-1 on 24/08/01. | 283 |
| Figure 6.20: Oblique photo of KM3 showing channels along jointing. | 285 |
| Figure 6.21: Definition sketch of flow direction for applying Longinov's method | 288 |
| Figure 6.22: Proportional net velocity diagrams on 18/08/01. | 290 |
| Figure 6.23: Proportional net velocity diagrams on 19/08/01. | 291 |
| Figure 6.24: Proportional net velocity diagrams on 24/08/01. | 292 |
| Figure 6.25: Wave effectiveness plots for 18/08/01. | 297 |
| Figure 6.26: Wave effectiveness plots for 19/08/01. | 298 |
| Figure 6.27: Wave effectiveness plots for 24/08/01. | 299 |
| Figure 7.1: Weathered features observed on shore platforms | 316 |
| Figure 7.2: Evidence of biological weathering observed on shore platforms. | 317 |
| Figure 7.3: Slake-durability testing apparatus..... | 319 |
| Figure 7.4: Reduction in mass of samples from wetting and drying cycles. | 323 |
| Figure 7.5: Samples subjected to wetting and drying susceptibility testing. | 324 |
| Figure 7.6: Susceptibility of each rock type to 10 cycles of wetting and drying. .. | 324 |
| Figure 7.7: Water intake of rock samples over 70 hours of immersion | 328 |
| Figure 7.8: Correlation of susceptibility of shore platform rocks to weathering and rate of surface change. | 330 |
| Figure 8.1: Elevation of MEM sites vs. average rate of surface change. | 344 |
| Figure 8.2: Elevation of MEM sites vs. average rate of surface change. | 345 |
| Figure 8.3: Position of MEM site on the profile vs. average rate of erosion | 348 |

| | |
|--|-----|
| Figure 8.4: Normalised rates of erosion for each profile..... | 349 |
| Figure 8.5: A proposed model of shore platform development. | 352 |
| Figure 8.6: Hypsographic curves with respect to mean tidal levels. | 357 |
| Figure 8.7: Hypsographic curves with respect to max. and min. tidal levels. | 358 |
| Figure 8.8: Conceptual process – response model for shore platforms..... | 359 |

LIST OF TABLES

| | |
|--|-----|
| Table 1.1: Summaries of some published shore platform studies. | 5 |
| Table 2.1: Classification of roughness residual..... | 45 |
| Table 2.2: Morphometric parameters of study profiles. | 56 |
| Table 3.1: MEM site monitoring history. | 67 |
| Table 3.2: Rates of surface change for each MEM site. | 94 |
| Table 3.3: Rates of surface change measured between 1974 and 2000..... | 96 |
| Table 3.4: Students t-Test statistics comparing long and short term erosion rates. . | 97 |
| Table 3.5: Ave. representative rate of erosion and ave. residuals for rock types. | 99 |
| Table 4.1: General lithology of each study profile. | 105 |
| Table 4.2: Descriptive categories of rock strength (Selby 1980). | 121 |
| Table 4.3: Point load test results for all five rock types | 122 |
| Table 4.4: Schmidt hammer test results for all five rock types | 123 |
| Table 4.5: Rock mass strength classification for each rock type..... | 124 |
| Table 4.6: Rock strength: point load, Schmidt hammer and mass strength index. | 125 |
| Table 4.7: Rock strength rankings | 125 |
| Table 4.8: Compressive strength equivalent: point load & Schmidt hammer tests. | 130 |
| Table 5.1: Sea state code used for wave observations, (Kirk 1975a)..... | 157 |
| Table 5.2: Summary sea state data 1967 & 1971 to 1974 a). Kaikoura & b). Akaroa Head. | 158 |
| Table 5.3: Summary of a) wave height & b) wave period from deepwater data.... | 161 |
| Table 5.4: Frequency of occurrence of H_s offshore from KM2, KM3, KM7 and RM1. | 163 |
| Table 5.5: Frequency of occurrence of H_s offshore from AK1 and AK2. | 171 |
| Table 5.6: Frequency of occurrence of H_s heights offshore from WK1 and WK2. | 175 |
| Table 5.7: Summary of wave environments offshore from each profile..... | 175 |
| Table 5.8: Measured averages of wave parameters in deepwater and onshore. | 201 |
| Table 5.9: Turbulence measured at each sensor | 229 |
| Table 5.10: Measures of turbulence related to uniformity of flow | 230 |
| Table 6.1: Hydrostatic pressures calculated at KM3. | 241 |
| Table 6.2: Shear stresses at KM3 | 247 |
| Table 6.3: Modelled air compression pressures in joints at KM3. | 256 |
| Table 6.4: Sediment entrainment. The competence of flow on KM3 | 277 |
| Table 6.5: Potential net distance, in metres, of sediment movement on KM3 | 286 |
| Table 6.6: Calculation table used for Longinov's method | 289 |
| Table 7.1: Slake durability index (I_{d2}) for each rock type. | 320 |
| Table 7.2: Water content in sample as a % of dry mass before & after immersion | 327 |

LIST OF SYMBOLS

| | |
|-----------|--|
| A | initial dry mass of sample |
| B | final dry mass of sample |
| C | phase velocity |
| C_f | friction coefficient |
| d | water depth |
| D | width of air pocket |
| dD | increment of cliff retreat |
| dW | increment of platform down cutting |
| E | wave energy |
| F_R | rock resisting force |
| F_W | wave assailing force |
| g | acceleration due to gravity |
| h_b | depth of water at wave breaking |
| H | wave height |
| H_b | wave height at breaking |
| H_o | deepwater wave height |
| I_{d2} | slake-durability index |
| k | length of water column |
| k | wave number ($=2\pi/L$) |
| k_i | turbulent kinetic energy |
| K_b | refraction factor |
| K_s | shoaling factor |
| L | wave length |
| L_o | deepwater wave length |
| n | shoaling coefficient |
| p | hydrostatic pressure |
| p_o | hydrostatic pressure |
| p_v | vapour pressure |
| P | percent of time a given velocity is exceeded |
| P_c | point load under which a specimen fails |
| P_{max} | pressure of compressed air |
| P_o | initial (atmospheric) pressure |
| Q | wave energy flux |
| Q_o | deepwater wave energy flux |
| r | radius of a particle |
| s | distance from seabed |
| S_b | distance between orthogonals at point of wave breaking |
| S_c | load under which a block fails by shear |
| S_d | distance between orthogonals in deepwater |
| t | time taken for compression |
| t | time |
| T | wave period |
| u | flow velocity |
| u | water particle velocity |
| u_o | deepwater particle velocity |
| u_p | near bed velocity |

| | |
|-----------|--|
| u_t | rate of flow |
| u' | fluctuation from mean flow velocity (in the x direction) |
| \bar{u} | mean flow velocity |
| v' | fluctuation from mean velocity in the y direction |
| w | power (of flow) |
| w' | fluctuation from mean velocity in the z direction |
| x | distance in x direction |
| z | particle displacement from still water level |
| α | platform slope |
| σ | wave radian frequency ($=2\pi/T$) |
| σ | cavitation index |
| φ | angle of rest of particle |
| ρ | density, usually of seawater |
| τ | shear stress |
| γ | adiabatic compression of air |

ACKNOWLEDGEMENTS

This thesis would not have been possible without the support and encouragement of my supervisor Bob Kirk. During the course of this thesis he has been both a mentor and a friend who has given advice on more than just the thesis. Throughout my university education I have found Bob's style of teaching inspirational and I have gained much from this contact with him. Thanks Bob, for the enthusiasm and insight you have offered me.

Martin Single's co-supervision of this thesis has also been greatly appreciated. He has made many useful suggestions and has been a willing sounding board for ideas. I have also appreciated his recent, seemingly endless, round of reading of chapters on my behalf. Thanks Martin, I've learnt a lot from your input and hopefully you have learnt a little from all the hours of reading and discussions I've subjected you to.

I would like to thank my parents for their support both moral and financial throughout my education. They instilled in me a love of landscape and a desire to understand what I see. For that I am profoundly grateful. My wonderful Mother, Jane Taylor, has willingly spent hours sitting on platforms pushing buttons and keeping me company. Mum has also performed above and beyond the call of duty in her tireless proof reading and re-proof reading of drafts of this thesis. This has been the third family thesis she has proof read! A little bit of each ought to be yours Mum! Although Mum has proof read this thesis any mistakes still existing are entirely the responsibility of the author.

The Geography Department, University of Canterbury, provided funding for this thesis in the form of a grant to cover research costs and provided technical support. I would like to thank all the Geography Department technical staff who have helped me out at some stage. I would especially like to thank Justin Harrison who organised equipment and helped with the geological survey of profiles, Graham Furniss for macro advice and production John Thyne for general computer problem solving and Nick Key for his boat skipping skills.

Fieldwork for this thesis would not have been possible without the support of a great number of people not all of whom can be mentioned here. Thank-you especially to Jack van Berkel who always provided accommodation at the Edward Percival Marine Laboratory when I required it for myself and any field assistants I had with me. Thanks also to Dave Taylor and Emma Gibson for good company and an occasional bed at Kaikoua. I would also like to thank Dave Taylor for advice on things to do with marine zoology. I have had a great many field assistants who have been coerced, bribed or tricked into helping me out. Their help has been invaluable. I would most especially like to thank Sam Gough-Jones and Gail Cargill who both participated in multiple trips and tirelessly pressed buttons and my flatmate Kate (and her physio) who uncomplainingly lugged rocks up hills for me.

Thanks to the Geology department for the use of their geomechanical lab and to Cathy Knight for lessons in stone cutting and smashing (I had a great time!). Thanks to NIWA and the Zoology Department, University of Canterbury for use of wave buoy data. Thanks to Justin Cope at Environment Canterbury for providing data from the Banks Peninsula wave buoy.

To my fellow PhD's thank-you for the mutual support and company along the way, it has been a great experience. Thanks especially to Maree Hemmingsen for the exchange of coastal ideas and fun on field trips. Thanks to Peyman Zawar-Reza for mathematic advice and general light relief and to Gillian Blackler for the exchange of computing hints and hard learned short cuts. We should write a manual one day when we have some spare time!

Finally I would like to thank by partner Chris Johnston who has made the last three years of this thesis easier than they might otherwise have been. He has willingly acted as a field assistant, a sounding board and an adviser. Chris, your support, encouragement and love mean a lot to me. You'll be pleased to know that the year is now up!

CHAPTER ONE

PROCESSES OF CHANGE ON SHORE PLATFORMS

1.1 INTRODUCTION.

This thesis investigates and measures morphological change and processes causing change on shore platforms formed in five different lithologies around New Zealand. Shore platforms are wholly eroded, near horizontal, rock surfaces that occur between high and low tide levels on rocky coastlines around the world. It has been proposed that there are two distinct shore platform morphologies (Sunamura 1992). One type has a near horizontal rock surface bounded by an active marine cliff at the landward margin and an abrupt seaward drop at the seaward margin. The other type has a similar landward boundary but the near horizontal rock surfaces slope gently into the sea without a major break in slope. This categorisation of shore platforms is generally accepted and utilised in the current literature on shore platforms. However some publications outline several more 'types' of shore platforms between these two (Mii 1962, Trenhaile 1974b).

A significant body of literature on shore platforms has accumulated over the last 150 years with the question of formation guiding the main line of enquiry. However, despite this extended amount of focus, there still exists a range of theories within the literature regarding the fundamental mode of formation of shore platforms. Two poles of the debate that can be identified are:

- 1). that shore platforms are primarily marine in origin.
- 2). that shore platforms require subaerial weathering as a precursor to formation.

There are also a number of theories that assert some combination of both marine action and subaerial weathering is required in shore platform formation. This debate, here called waves vs. weathering is an enduring feature in shore platform literature, as solidly established as the shore platforms themselves.

Resolving the debate depends on understanding the forces resisting formation, the processes causing change and the balance between the two. Subsequent to this quantification of processes causing change on shore platforms, an indication of which of these processes, if any, are dominant is required. Therefore, further investigation of processes operating on shore platforms is necessary.

Another question that remains unanswered in the literature is that of shore platform equilibrium. This question is interlinked with that of formation and a number of different equilibrium forms and states have been suggested. Johnson (1919) and Sunamura (1992) outline shore platform development which reaches a static state of equilibrium and Edwards (1941) and Trenhaile (1974a) talk of shore platforms being dynamic in nature. Which, if any, of these proposed forms is correct remains to be answered.

The characteristics of the rock in which platforms are formed has often been cited as an important control on the rate of development and morphology of shore platforms (Bartrum 1935, Wentworth 1938, Jutson 1939, Edwards 1941, Hills 1949, Mii 1962, Sanders 1968a, Suzuki *et al.* 1970, Trenhaile 1972, 1974b, 1987, 2000, Bradley and Griggs 1976, Kirk 1977, Sunamura 1978, 1992, 1994, Gill and Lang 1983, Tsujimoto 1987, Trenhaile *et al.* 1998). Yet, the relationships presented are often contradictory therefore further clarification of the role of rock type in control of shore platform development is necessary.

The solid, rocky nature of shore platforms and the fact that they are wholly erosional in character makes them durable features within the landscape, especially when compared to other coastal landforms. For this reason abandoned or relict shore platforms are often used in the identification of past sea levels (Lawrie 1993, Bal 1997, Johnson and Libbey 1997), for reconstruction of paleo sea level records (Flemming 1965, Schulmeister *et al.* 1999) or identification of tectonic activity (Kelsey and Bochleim 1994, Ota *et al.* 1996). Work of this nature involving relict shore platforms has been conducted under the assumption that shore platforms form at or near sea level. Yet the literature of active platforms near present sea level shows that they occur at a range of elevations. The

relationship between contemporary shore platforms and current sea level should first be established before relict shore platforms are used for identification of previous relative sea levels (Cotton 1963).

Another reason for understanding contemporary changes on shore platforms and the role of processes in their formation is to enable sensible management of these coastal zones as they are being subjected to increasing pressure from human use and occupation.

This study, therefore, has the following major objectives.

- 1). Investigation of the control of rock type on shore platform morphology and shore platform development.
- 2). Investigation of the nature and activity of some processes of wave action and weathering as causes of change on shore platforms.
- 3). Quantification of change and of patterns of change for elucidation of both control and processes occurring on shore platforms.
- 4). To develop measures of processes that are more appropriate for use in shore platform studies.
- 5). Investigation of the concept of equilibrium as it applies to shore platform development.

1.2 SHORE PLATFORM RESEARCH.

In order to gain an understanding of the questions that remain unanswered in shore platform research a review of shore platform research to date is required.

Shore platforms were first discussed in scientific literature in the mid 19th century, notably by Dana (1849) and have been studied sporadically since, by a relatively small number of coastal scientists (Table 1.1). Shore platforms have been estimated to make up 20 – 30% of New Zealand's 10,000kms of coast (Kirk 1977). It is likely that a similar percentage or greater of the global coastline is also comprised of shore platforms, given Emery and Kuhn's (1982) estimate that 80% of the world's coastline can be

classified as backed by cliffs. Despite this, relatively little research has been undertaken on shore platforms when compared to the vast body of research that exists for sand beaches. The global distribution of work that has been done has been concentrated in a few locations, largely reflecting the activities of a small number of workers in Australasia, Canada, Britain and Japan (figure 1.1).

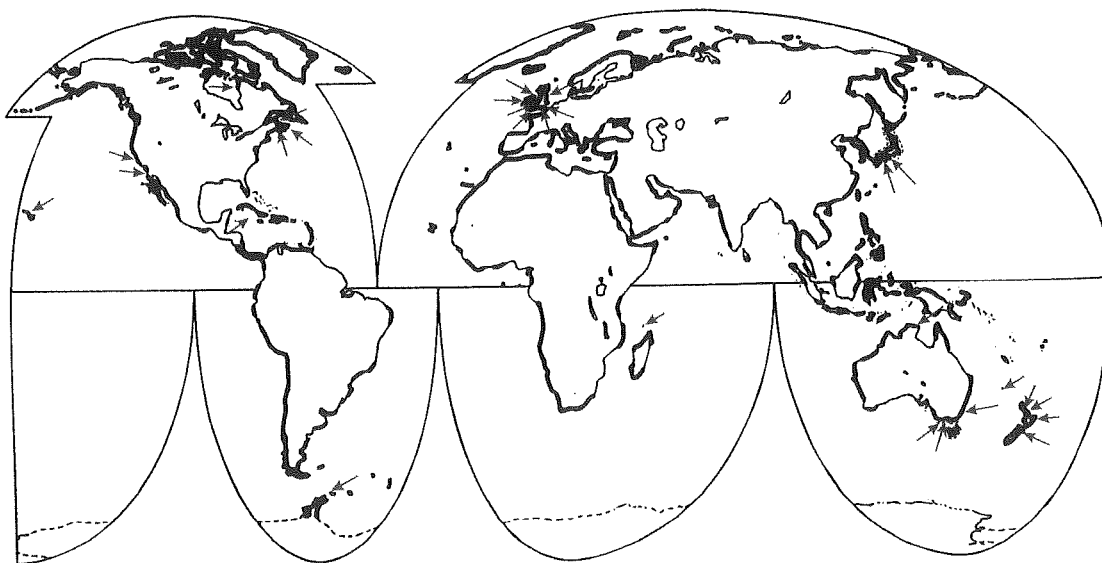


Figure 1.1: Global distribution of rocky coasts (Emery and Kuhn 1982) and shore platform studies (see table 1.1). Rocky coasts are shown with heavy black lines and locations where shore platforms have been studied are shown with red arrows.

Recent published literature includes two textbooks on rocky coasts, both with extensive sections on shore platforms (Trenhaile 1987, Sunamura 1992) and two review papers specifically outlining current shore platform research (Trenhaile 1980, Stephenson 2000). This chapter therefore, includes a synopsis of shore platform research rather than a full review. Greater elaboration of the literature will be given where it is directly relevant to topics covered in each separate chapter.

Table 1.1 presents a synopsis of most published investigations on shore platforms. It can be seen from this and figure 1.1 that research has been focused in a limited number of environments, despite the extensive occurrence of rocky coasts globally. This sparsity of measurement has meant that there is a lack of variety of morphogenic

Table 1.1: Summaries of some published shore platform studies.

| Author | Year | Location | Mode of platform formation / Conclusions | Measurements |
|------------------------|-------|--|---|--|
| Dana | 1849 | New Zealand and New Holland | wave cut | general observation |
| Bartrum | 1916 | Bay of Islands, New Zealand | weathered down to saturated level | general observation |
| Johnson | 1919 | (general theory) | wave cut - until static state attained | general observation |
| Bartrum | 1935 | North Island, New Zealand | two modes of formation - weathering and wave cut | general observation |
| Wentworth | 1938 | Oahu, Hawaii | wave cut then modified by weathering (water-layer) | observation of morphology |
| Jutson | 1939 | Sydney, Australia | wave cut (normal and ultimate profiles) | observation of morphology |
| Wentworth | 1939 | Oahu, Hawaii | wave cut then modified by weathering (solution benching) | observation of morphology |
| Edwards | 1941 | Victoria and Tasmania, Australia | storm wave cut | observation of morphology and quantified compressive strength of rock |
| Challinor | 1949 | (general theory) | wave cut - parallel retreat model | general observation |
| Hills | 1949 | Victoria, Australia | wave cut (recognised effects of other processes) | observation of morphology |
| Jutson | 1949 | Lorne, Australia | wave cut | observation of morphology |
| Jutson | 1954 | Lorne, Australia | wave cut | observation of morphology |
| Mii | 1962 | Tanabe Bay, Japan | combination of processes - marine erosion, subaerial weathering, sea level change | field surveys, observation of morphology, deepwater wave data and refraction diagrams, published tide timetables |
| Hodgkin | 1964 | Norfolk Island | biological erosion and solution of limestone | erosion pins and plastercasts, observation of morphology |
| So | 1965 | Isle of Thanet, England | storm wave cut | levelled profiles |
| Bird and Dent | 1966 | New South Wales, Australia | weathered | observation of morphology, levelled profiles |
| McLean J.F. | 1967 | Northeast Coast, South Island, New Zealand | genetic model of development, wave energy important | levelled profiles, air photos |
| Healy | 1968 | Whangaparaoa Peninsula, New Zealand | contribution of bioerosion | observation of morphology |
| McLean R.F. & Davidson | 1968 | Gisborne, New Zealand | wave energy was not a control on morphologic dimensions | airphoto analysis, field survey, wave refraction diagrams |
| Sanders | 1968a | Tasmania, Australia | combination of processes - hydraulic action and subaerial weathering the most important | levelled profiles, geomechanical testing, observation of morphology |
| Sanders | 1968b | Laboratory | wave cut | physical modelling |
| Trenhaile | 1972 | Vale of Glamorgan, Wales | wave cut - lithological controls important | levelled profiles identification of rock type |

Table 1.1 continued: Summaries of some published shore platform studies.

| | | | | |
|---------------------|-------|---|--|--|
| Trenhaile | 1974a | England and Wales | wave cut | levelled profiles, identification of rock type, fetch length |
| Trenhaile | 1974b | England and Wales | wave cut - classification of shore platforms | levelled profiles, identification of rock type, fetch length |
| Bradley & Griggs | 1976 | Ben Lomond Mountain coast, California | marine origin, with influence of rock type on morphology | surveyed profiles, offshore wave data, observation of morphology |
| Trudgill | 1976a | Aldabra Atoll, Indian Ocean | quantified biological erosion | MEM measurement, chemical analysis |
| Trudgill | 1976b | Aldabra Atoll, Indian Ocean | quantified biological erosion | MEM measurement, chemical analysis |
| Kirk | 1977 | Kaikoura, New Zealand | combination of processes - subaerial and marine | surveyed profiles, MEM measurement, observation of morphology |
| Robinson | 1977a | Northeast Yorkshire, England | marine erosion at the cliff foot and weathering on the plane | surveyed profiles, MEM measurement, observation of morphology |
| Robinson | 1977b | Northeast Yorkshire, England | marine erosion at the cliff foot and weathering on the plane | surveyed profiles, MEM measurement, observation of morphology |
| Robinson | 1977c | Northeast Yorkshire, England | marine erosion at the cliff foot and weathering on the plane | surveyed profiles, MEM measurement, observation of morphology |
| Sunamura | 1978 | Izu Peninsula, Japan | combination of processes, headland platforms - marine origin, bay platforms - marine and weathering origin | surveyed profiles, description of deepwater waves |
| Trenhaile | 1978 | Gaspe, Canada | wave cut, gradient of platform controlled by tidal range | surveyed profiles, description of deepwater waves |
| Emery & Kuhn | 1980 | LaJolla, California | cliffs eroded via weathering and abrasion (marine action) | observation of morphology |
| Spencer | 1981 | Grand Cayman Island, West Indies | solution of limestone | MEM measurement |
| Trenhaile & Layzell | 1981 | East Canada, Australia, New Zealand and Britain | wave cut | mathematical modelling |
| Trenhaile & Rudakas | 1981 | Gaspe, Canada | contribution of freeze thaw | - |
| Gill & Lang | 1983 | Otway Coast, Australia | wave cut | surveyed profiles, MEM measurements |
| Hansom | 1983 | South Shetland Islands, Antarctica | role of ice in cold environments | surveyed profiles, observation of morphology |
| Trenhaile & Mercan | 1984 | Gaspe and Nova Scotia, Canada | contribution of ice action | laboratory experiments, field measurement of rock samples |
| Viles & Trudgill | 1984 | Aldabra Atoll, Indian Ocean | comparison of long and short term MEM measurements | MEM measurements |
| Robinson & Jerwood | 1987 | Brighton, England | the effect of frost and salt weathering | observation of morphology |

Table 1.1 continued: Summaries of some published shore platform studies.

| | | | | |
|-------------------|-------|---------------------------------|---|--|
| Trudgill | 1987 | Co. Clare, Eire | investigation of bioerosion processes | various analysis |
| Tsujimoto | 1987 | Various, Japan | demarcation for platform initiation based on rock strength and wave assailing force | surveyed profiles, geomechanical rock testing, description of deepwater waves |
| Dionne & Brodeur | 1988 | Hudson Bay, Canada | the importance of frost weathering and ice action | - |
| Mottershead | 1989 | Start-Prawle Peninsula, England | salt spray weathering | MEM measurements |
| Sunamura | 1991 | Laboratory | wave cut and dependent on rock strength | physical modelling |
| McKenna et al | 1992 | Northeast coast, Ireland | wave cut | analysis of photographs, field surveys, tracer experiments |
| Nott | 1994 | Darwin Coast, Australia | sub aerial weathering dominant in tropical environments | surveyed profiles, observation of morphology |
| Sunamura | 1994 | (general theory) | wave cut with rock control of morphology | - |
| Stephenson & Kirk | 1996 | Kaikoura, New Zealand | comparison of long and short term MEM measurements | MEM measurements |
| Stephenson & Kirk | 1998 | Kaikoura, New Zealand | weathering dominates | surveyed profiles, geomechanical rock testing, direct measurement of waves on platform |
| Trenhaile et al | 1998 | New Brunswick, Canada | wave cut , rock hardness related to platform gradient | surveyed profiles, Schmidt hammer rock testing |
| Trenhaile | 1999 | Wales, Canada and Japan | wave cut, width increased with wave intensity | surveyed profiles, deepwater wave data, published tide timetables |
| Stephenson & Kirk | 2000a | Kaikoura, New Zealand | weathering dominates | surveyed profiles, geomechanical rock testing, direct measurement of waves on platform |
| Stephenson & Kirk | 2000b | Kaikoura, New Zealand | weathering dominates | surveyed profiles, geomechanical rock testing, direct measurement of waves on platform |
| Trenhaile | 2000 | (general theory) | wave cut | mathematical modelling |
| Stephenson | 2001 | Kaikoura, New Zealand | weathering dominates | surveyed profiles, geomechanical rock testing, direct measurement of waves on platform |
| Stephenson & Kirk | 2001 | Kaikoura, New Zealand | weathering dominates | surveyed profiles, geomechanical rock testing, direct measurement of waves on platform |
| Trenhaile | 2001 | (general theory) | wave cut | mathematical modelling |

conditions necessary for the establishment of meaningful causative relationships (Trenhaile 1974a). This problem has been further compounded by the fact that studies have often been based within one single shore platform environment (table 1.1). Also, historically much shore platform work has been descriptive rather than quantitative. This has meant that possible comparison between studies has been limited.

Much of the early work on shore platforms was descriptive with speculation on processes of formation being based on observation of morphologies at a limited number of locations (Sanders 1968a). Shore platforms were viewed as static, or very slowly developing landforms rather than dynamic features on which current change could be measured. By the mid 1960's the need for quantitative data relating to morphology and morphologic change had begun to be addressed (Hodgkin 1964, So 1965, McLean 1967, Sanders 1968a, Trenhaile 1972). This recognition of the fact that, without hard data, formation processes would never be agreed upon either coincided with, or was encouraged by, the development of instrumentation capable of measuring changes in this slowly evolving environment. Surveyed measures of shore platform morphology have been reported since the late 1960s (So 1965, McLean 1967, Sanders 1968a, Trenhaile 1974a). However, rates of morphological change on shore platforms were more difficult to quantify due to the lack of accurate instrumentation adequate for the measurement of the slow process of rock erosion over a short time period. The development of the micro erosion meter (MEM) in the late 1960's (High and Hanna 1970) enabled accurate quantification of horizontal surface erosion rates on shore platforms at the sub millimetre scale. This method has been used a number of times since (Trudgill 1976, Kirk 1977, Robinson 1977a, 1977b, Spencer 1981, Mottershead 1989, Stephenson and Kirk 1996, 1998). Unfortunately, despite the use of MEMs, reported rates of change on shore platforms are still restricted both spatially and temporally. However, assessment of rates of the back-cutting of landward cliffs of shore platforms have been undertaken by a significant number of researchers using both terrestrial and aerial photography (see Sunamura 1992: appendix 2).

1.2.1 FACTORS IMPORTANT TO SHORE PLATFORM DEVELOPMENT.

A general theme propagating through the shore platform literature is that there are a number of aspects which may be significant in controlling development on shore platforms. These include: the rock in which the platform is formed, the waves incident on the platform, weathering of the rock, variations in water level and both floral and faunal biota on the platform. While most authors acknowledge that processes related to all of these five aspects occur on shore platforms the degree of significance of each in the development of shore platforms is debated. This is a reflection of the fact that the mechanisms by which processes effect change are not clearly understood. Trenhaile (1987:206) stated that “few investigations have been concerned with determining the mode or efficiency of the wave erosional processes” and the same is true for processes of weathering. Sanders (1968a) recognised that a number of interrelated factors contributed to the formation of shore platforms but that the relative contribution of each was in question. The relative roles of these factors is still in question.

1.2.1.1 ROCKS

The rock in which a shore platform is formed is considered important in terms of lithology, structure, strength, and susceptibility to weathering.

Gill (1972) suggested that the strength of the rock in which the platform was formed dictated the platform morphology. Tsujimoto (1987), in presenting a demarcation between shore platforms and cliffs stated that rock strength, represented by compressive strength, was a critical condition for initiation of shore platform development. He based this demarcation on measurements of 25 shore platforms around Japan. He further developed this demarcation providing, in terms of a ratio of rock strength and wave energy, a critical condition which defined a boundary between two distinct types of shore platform morphology (Type-A and Type-B) (see figure 2.8).

Rock strength has been related to platform elevation with respect to sea level with platforms formed in harder rocks being related to higher elevations (Trenhaile 1987). Sunamura (1991) conducted laboratory experiments where modelled cliffs of differing hardness were exposed to simulated wave conditions. He found that in softer rocks, platforms formed at lower elevations in relation to still water level.

Edwards (1941) found a relationship between rock hardness as measured by compressive strength, and platform width. On shore platforms of the Victorian and Tasmanian coasts, Australia he found that the widest shore platforms occurred in rocks of compressive strength between 3000-16000p.s.i. In rocks of hardness either greater or less than this shore platforms were narrow, absent or incipient.

Tsujimoto (1987) and Sunamura (1994) found decreasing platform gradients with increasing rock hardness for sites around Japan. However, conversely, Trenhaile (1974a, 1978) found increases in platform gradient with increasing resistance of the rock to erosion on shore platforms in England and Gaspé, Canada.

It has been suggested that the strata of the bedrock, dip, strike and width of bedding, controls the morphology of the platform. Trenhaile (1987) presented a hierarchy of shore platform structures based upon variations in rock strike and dip with platforms being more developed in rocks with horizontal bedding plains. Platform width was significantly correlated to this hierarchy in southern Kii Peninsula, Japan and Gaspé, Canada (Trenhaile 1987).

1.2.1.2 WAVES.

Many publications place great importance on waves as fundamental erosive agents on shore platforms (see table 1.1) and wave action is a major element in a number of models of shore platform development (section 1.2.3). Takahishi (1977) found a positive relationship between platform width and wave exposure which was used as an indicator of wave energy for platforms in Japan. On the open Pacific coast, where wave energy was greatest, he found platforms with an average width of 60m whereas on the less

exposed Japan Sea coast average platform width was 50m. On the Inland Sea coast, where wave energy was lowest, average platform width was 40m. In contradiction to this finding a number of researchers have shown widest platforms in sheltered embayments and narrowest platforms on exposed headlands (Edwards 1941, Duckmanton 1974, Kirk 1977).

Stephenson and Kirk (2000a) have questioned the importance of waves in erosion of shore platforms. They measured wave height directly on shore platforms at Kaikoura, New Zealand, and showed that wave induced shear stresses were inadequate to cause erosion of the rock surface. Whether waves are the primary mode of erosion on shore platforms, or not, is therefore a contentious issue.

However, without the removal of debris created by erosive processes, rock surfaces would become armoured and erosion of the underlying bedrock would cease. This is often acknowledged, even by proponents of weathered shore platforms, but not often emphasised (Bartrum 1935, Wentworth 1938, Hills 1949, Mii 1962, Bradley and Griggs 1976, Robinson 1977a, Emery and Kuhn 1980, McKenna *et al.* 1992). Despite the fundamental function of waves as transporters of sediment off shore platforms no investigation of the competence (size of sediment carried) or the capacity (quantity of sediment carried) of waves in this environment has previously been conducted, to the author's knowledge. It is possible that quantification of this nature could help elucidate the extent to which the processes of erosion, be they waves or weathering, are required to break up the rock prior to removal.

1.2.1.3 WEATHERING.

The function of weathering in shore platform development has been recognised by researchers in three different ways:

- 1). as fundamental to the formation of shore platforms.
- 2). as a method of weakening the rock to the point where it becomes susceptible to wave erosion.

3). as a modifier of the surface after initial formation has been accomplished.

Stephenson and Kirk (2000b) used wetting and drying cycles as an indication of weathering and showed a correlation between these cycles and surface down wasting. From this and direct measurement of waves on the platform they concluded that weathering was fundamental to shore platform development at Kaikoura.

Trenhaile (2001) included a reduction factor which accounted for weathering when assessing the integral strength of the rock in a model of shore platform development.

Wentworth (1938, 1939) asserted that after initial erosion of the shore platform was accomplished by wave action the surface was subsequently levelled and flattened by processes of weathering.

It still remains to be shown whether weathering is a requirement of shore platform formation or only a factor in the rate of shore platform change in the form of reducing the strength of the rock or modifying the surface.

1.2.1.4 WATER LEVEL.

That water level plays a role in shore platform development has been recognised since the first treatise on shore platforms appeared. Dana (1849) hypothesised that the exact level of the platform was determined by the point at which the line of wave action was greatest and this was controlled by tidal level. The very fact that shore platforms develop at, or near water level makes the importance of this factor evident.

Tidal changes in sea level control the elevation at which erosive processes operate (Trenhaile 1987). In the case of waves it is the level at which they work, and in the case of weathering, the number of wetting and drying cycles. Trenhaile (1987) has related tidal range to platform gradient showing steeper shore platform gradients in locations of greater tidal range. Also, using examples from Canada, England, Wales, Japan and

Australasia he showed that platform width increased with tidal range. However the correlation was not strong and this was accounted for as the influence of other factors.

1.2.1.5 BIOLOGY.

Biology has usually been accorded a secondary role in the development of shore platforms modifying the surface, rather than forming it as such. The role of Biota can be both erosive and/or protective. A small amount of research has been undertaken quantifying individual aspects of shore platform modification by biota. Organisms have been shown to erode the rock through feeding mechanisms (McLean 1967) or boring (Trudgill 1976a) and to protect it via armouring (Hodgkin 1964). On the shore platforms of Aldabra Atoll in the Indian Ocean, Trudgill (1976a) estimated that solution of limestone from biological activity accounted for 10% of all contemporary erosion and that boring molluscs accounted for 36 – 64% of all contemporary erosion.

Hills (1949) suggested that growth of algae and vegetation over shore platform surfaces prevented wave quarrying and Stephenson (1997a) reported that algal growth periodically prevented drying of the surface on shore platforms at Kaikoura, New Zealand thus restricting weathering of the rock surface. Kirk (1977) attributed large seaweed present on the seaward edge of platforms with the ability to dissipate significant amounts of wave energy. Everard *et al.* (1964) noted that seaweed attaches to the rock with a holdfast and when ripped off in times of high energy wave attack can cause the removal of portions of the rock itself. At Macquarie Island, Southern Ocean, Smith and Bayliss-Smith (1998) documented losses, for one year, of at least 1.56 tonnes of rock per km of coast from a shore platform using measurements of freshly quarried bedrock attached to bull-kelp (*Durvillaea antarctica*) uprooted during storms.

1.2.2 MEASUREMENT OF PROCESSES.

Despite the recognition of aspects important to shore platform development, very little direct measurement of processes causing morphological change has been undertaken. This may reflect the difficulty of direct measurement of some factors, for example waves, in this environment. Direct measures of rock strength and lithological features

have been made both in *situ* and through laboratory testing (Tsujiimoto 1987, Stephenson 1997a). Only one geomorphic study has directly measured wave action on shore platforms (Stephenson and Kirk 2000a) and there has been no extensive investigation of the nature of wave flows onto and across shore platforms. Weathering patterns and amounts have been inferred from morphological evidence (Robinson 1977a, 1977b, 1977c) and wetting and drying cycles (Sanders 1968a, Stephenson and Kirk 2000b). Water level changes have been measured directly using either temporary or permanent tide gauges (Sanders 1968a, Trenhaile and Layzell 1981, Stephenson 1997a). A limited number of processes of change caused by biological components have been measured in very specifically focused studies (Trudgill 1976a, 1976b) and others have been mentioned in passing but not quantified (McLean 1967, Kirk 1977, Stephenson and Kirk 2000b).

This lack of direct quantification of process, for whatever reason, has meant that process has often been inferred from morphological evidence (e.g. Robinson 1977a, 1977b) and as Mii (1962) noted, morphology can be a notoriously ambiguous indicator of process. It has also meant that answering the question of shore platform formation has been approached via the use of modelling.

A discussion of models of shore platform development is therefore relevant to processes of change on shore platforms and presented in the following section. The purpose of this thesis is not to debate or verify models of shore platform development, but as most imply process occurring on shore platforms an understanding of them is important.

1.2.3 MODELS OF SHORE PLATFORM DEVELOPMENT.

Early models of shore platform development were based on qualitative observation.

Johnson (1919) proposed a model of shore platform evolution based on the Davisian concept of cyclic landform formation. He suggested that development occurred through a sequence of stages (figure 1.2). The initial stage was a submerged rock coast into

which the erosive power of waves caused back-cutting. Subsequent stages saw the cliff face progressively eroded landward by wave action until eventually the platform became wide enough to cause sufficient dissipation of wave energy so that erosion was no longer possible. When this final stage was attained the platform was in a state of static equilibrium and remained thus until the system was 'rejuvenated' by a change in base level.

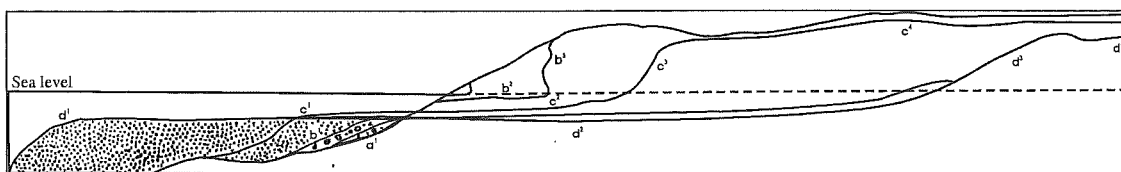


Figure 1.2: Stages in the development of the shore profile (Johnson 1919:fig. 32).

Bartrum (1935) proposed that shore platforms could be formed in two different ways. Either by the action of storm waves cutting a near horizontal surface into the cliff (Bartrum 1924) or by the weathering of rock down to a level of saturation related to the water table (Bartrum 1916). Wave transport removed the debris created by the weathered rock offshore, allowing further weathering to occur. He termed platforms formed in this manner 'Old Hat' type, after the colloquial name of the island on which this hypothesis was based.

Wentworth (1938, 1939) suggested that wave quarrying of rock was initially responsible for the formation of shore platforms on Oahu, Hawaii, but that water-layer weathering and solution planing had subsequently become the dominant processes of formation.

Edwards (1941) proposed that shore platforms existed because of a differential rate of back cutting of the low and high tide cliffs. Shore platforms were in a dynamic state of equilibrium related to the rate at which both cliffs were being eroded. He suggested that this related to factors of wave strength and rock strength.

Challinor (1949) agreed with the notion that shore platforms were wave-cut in origin but challenged the well established view of Johnson (1919) by suggesting that the near horizontal surface would be eroded to a level low enough that it would "not be allowed to impede the action of waves." (Challinor 1949:213) He proposed that there was

constancy in the form of the shore platform, as the sea advanced landwards with both width and gradient being maintained (figure 1.3). This has since been termed a parallel retreat model.

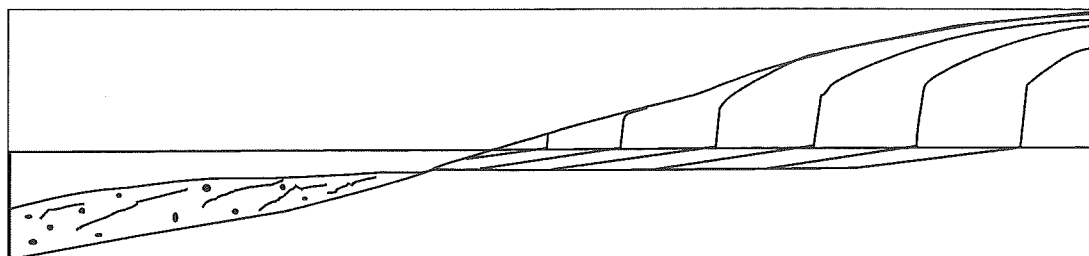


Figure 1.3: Challinor's diagram to explain consistency in the form of the coast profile as the sea advanced landward (Challinor 1949, fig.1).

This idea was further developed by Trenhaile (1974a) who modelled the geometric changes of shore platforms assuming parallel retreat. If platform gradient maintained dynamic equilibrium (figure 1.4) then rates of erosion should conform to a geometric equation (equation 1.1)

$$dD = dW \tan \alpha \quad \text{Equation 1.1}$$

where: dD = increment of platform down cutting with time
 dW = increment of cliff retreat with time
 α = platform slope

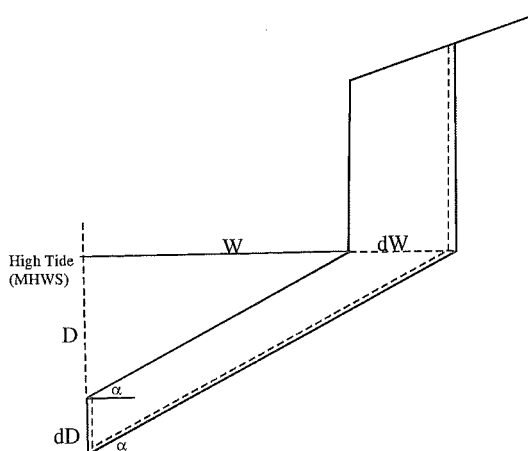


Figure 1.4: The parallel retreat model (Trenhaile 1974a: fig. 6)

The degree of adjustment of platform gradient to contemporary processes could then be assessed. Field evidence from shore platforms in England and Wales was used to calibrate this model. For this type of retreat to occur uniform erosion rates across the platform are required.

Kirk (1977), using measurements of surface change on shore platforms at Kaikoura, New Zealand, proposed a dual system of development. He suggested that consistent differences in rates of surface erosion across shore platform profiles meant it was unlikely that a single dominant mode controlled shore platform development but, rather, a gradient of processes occurred. With sub-aerial processes dominating on the upper (landward) zone and marine processes dominating on the lower (seaward) zone.

A number of Japanese researchers have approached the modelling of shore platform development through the use of geomechanical principles by defining the relationship between forces that cause erosion and the factors that resist it on a rocky coastline. They hypothesised that the forces causing erosion were those of the assailing forces of waves, F_W , and factors resisting erosion were those of rock strength, F_R (Sunamura 1992, Tsujimoto 1987). The model suggested that shore platform development was dependent on the relationship between F_W and F_R . When or where $F_W > F_R$ shore platforms would occur (Sunamura 1992). It also illustrated factors that either increased or reduced the strength of these two variables (Sunamura 1994) (figure 1.5). Figure 1.6 shows the vertical distribution of the two forces, F_W and F_R , and as such implies the way in which the platform physically develops.

Tsujimoto (1987) provided a demarcation, using field observations, between cliffs and the development of shore platforms based on the balance between F_W and F_R . Sunamura (1991) refined this model with laboratory work giving various stages of development for shore platforms formed in lithologies with different F_R .

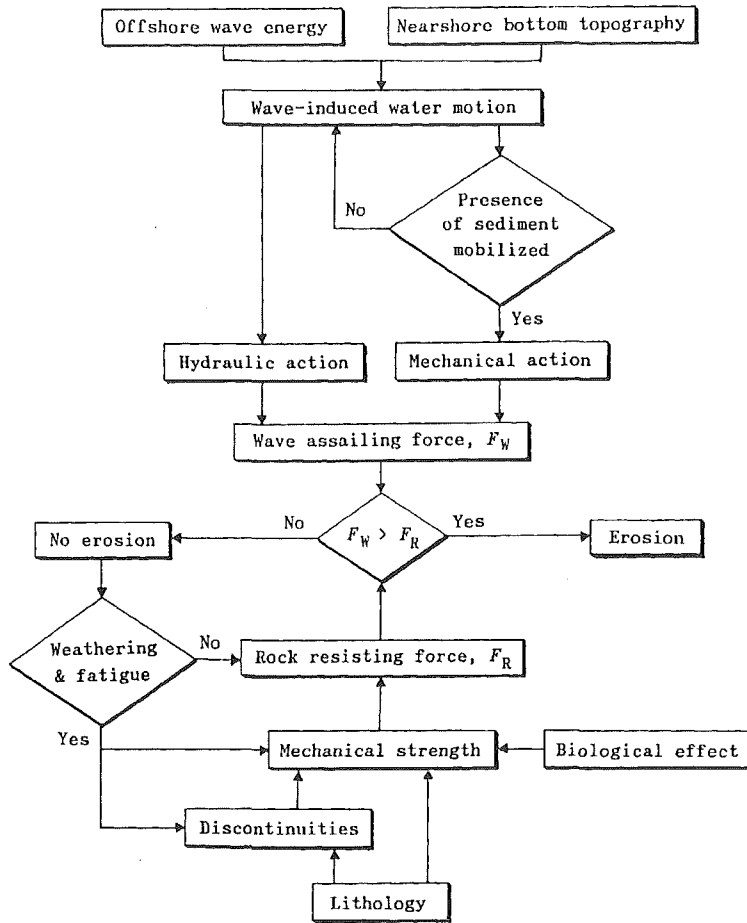


Figure 1.5: Factors affecting erosion of rocky coasts (Sunamura 1994: fig. 1)

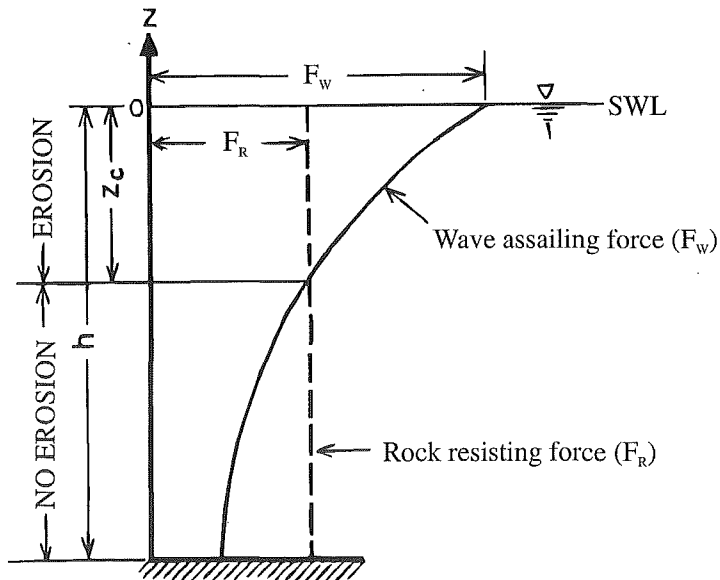


Figure 1.6: Vertical distribution of assailing force of waves and resisting force of rocks. (Sunamura 1992: figure 7.18)

The evident differences in these models and the continued debate on exact modes of development of shore platforms emphasises the fact that questions on shore platform genesis still remain unanswered.

1.2.4 QUESTIONS IN SHORE PLATFORM DEVELOPMENT.

The concept that wave driven processes dominate shore platform development has been fundamental to much shore platform research in the last 20 years. It is usually accepted, if only implicitly, that the notion of a balance between the forces of erosion and the forces resisting erosion are important in the formation of shore platforms. However the exact nature of these forces and the role each plays still remains an important question in shore platform research. The number of varying, and sometimes conflicting, models of shore platform development within the literature emphasises the fact that the question of how shore platforms develop has yet to be satisfactorily answered and even current processes of shore platform development are not well defined. A number of important questions therefore remain unanswered.

Interlinked with the question of how shore platforms develop is that of shore platform equilibrium. This is best illustrated by the fact that the models of shore platform development presented in the previous section all rely on the underlying assumption that shore platforms attain an equilibrium form. However, not all models assume the same state of equilibrium. It has been suggested that platforms may reach a static equilibrium form, as in Johnson's (1919) model, or a dynamic equilibrium, as in a parallel retreat model or variations of the state of equilibrium depending on the model presented. The suggestion that two distinct shore platform morphologies occur, as described in section 1.1, makes determination of an 'ultimate' form difficult. As does the need to infer initial shape, i.e. prior to platform development, and the assumption that current processes are the same as those that were fundamental in the initial formation of platforms. The early models of Johnson (1919), Bartrum (1916, 1924, 1935), Wentworth (1938, 1939) and Challinor (1949) were based on observation of morphology with no quantification of parameters offered. This made validation of theories proposed difficult and, at best,

limited. Without measurements of changes that have occurred it is not possible to say if an equilibrium form had been reached by particular platforms under study. Even with the advent of quantitative measures of change, validation of models continues to be difficult. For example Trenhaile (1974a) presented rates of surface change in the Vale of Glamorgan as validation of a parallel retreat model. However, surface change measured at Kaikoura did not fit this model (Kirk 1977).

In an effort to overcome these problems some researchers have turned to the use of laboratory modelling (Sanders 1968a 1968b, Sunamura 1991). The danger with this method is that an assumption of the dominant process is usually made prior to set up of simulations and this defines the elements represented. However it does provide a good basis for further investigation.

Often proposed relationships are based on the patterns observed within one environment. This poses a number of questions. Are patterns of change universal or platform specific? Are there consistent patterns of change? Kirk (1977) showed surface erosion rates at Kaikoura, New Zealand were lowest in the centre of the platforms and became greater both seaward and landward of this. Using the same measuring technique Stephenson and Kirk (1998) showed a slightly different pattern on the same platforms with highest rates occurring on the landward margins of the platforms and a reduction of rate seaward of this.

Very little measurement of processes on shore platforms has been undertaken. Therefore, understanding of the contribution of each process to shore platform development is limited. Tsujimoto (1987:49) states 'In discussing the influence of lithology in a dynamic study of shore platform formation it is necessary to properly assess the kind and degree of processes operating on a coast'. The same would also be true for the influence of waves and other factors. Sunamura (1994) noted that quantification of F_W and F_R used in his model of shore platform development was difficult. To represent F_W Tsujimoto (1987) used deepwater breaking wave height as an indication of wave energy arriving at the shore platform. However this did not fully account for the effects of wave propagation onto the shore platform. Stephenson and

Kirk (2000a) showed that deepwater wave energy was drastically reduced by the time waves reached shore platforms at Kaikoura, New Zealand.

Therefore, which aspects of wave assailing force are important? Representative measures used have included fetch length (Trenhaile 1974a, 1974b, Takahashi 1977), deepwater wave energy (Tsujimoto 1987) and shear stress calculated from wave height (Tsujimoto 1987, Stephenson and Kirk 2000a). Is it correct to assume theories and patterns of shoaling developed for sand beach environments apply to the shore platform environment? Some direct processes of wave erosion have been proposed, such as water hammer and cavitation, but none have been quantified in the shore platform environment (Sanders 1968a, Trenhaile 1987, Sunamura 1992).

A variety of different measures have also been used to represent F_R , including compressive strength (Edwards 1941, Tsujimoto 1987, Stephenson and Kirk 2000b) and *in situ* methods such as Schmidt hammer (Tsujimoto 1987, Trenhaile *et al.* 1998, Stephenson and Kirk 2000b) and sonic testing (Tsujimoto 1987). All of which may give very different values of strength for the same piece of rock. Which of these reveals the most about the processes of shore platform development?

No direct measurements of weathering have been made but possible amounts have been assessed by the correlation of wetting and drying cycles to erosion rates (Stephenson and Kirk 2000b) or from visual evidence (Wentworth 1938, 1939, Hodgkin 1964, Nott 1994).

There is a need for greater understanding of processes that cause changes on shore platforms and direct measurement and quantification of their capabilities as shore platform forming agents. Numerous authors have noted the need for greater understanding of mechanisms of process on shore platforms and that this can only be accomplished through direct measurement (Trenhaile 1987, Tsujimoto 1987, Sunamura 1992, Stephenson 2000).

1.3 SUMMARY.

In shore platform research a clear understanding of which process or processes are most dominant in shore platform development and the effect these processes have on morphology is lacking. Until accurate quantification of the effects of different processes operating on shore platforms is undertaken in a wide variety of environments and from this a dominant process becomes evident, the wave vs. weathering debate will continue *ad infinitum*. This quantification is hindered by lack of knowledge of exactly what these processes may be and the mechanisms by which they operate.

This thesis will add further to the limited body of literature documenting shore platform change by direct measurement of surface change on shore platforms developed in five different lithologies. It looks to address the problem of clarification of processes operating on shore platforms and assessment of their capacity in shore platform development by direct measurement of aspects of rock characteristics and wave action. To recap the thesis objectives, through quantification of processes on shore platforms the following objectives will be addressed:

- 1). Investigation of the control of rock type on shore platform morphology and shore platform development.
- 2). Investigation of the nature and activity of some processes of wave action and weathering as cause changes of on shore platforms.
- 3). Quantification of change and of patterns of change for elucidation of both control and processes occurring on shore platforms.
- 4). To develop measures of processes that are more appropriate for use in shore platform studies.
- 5). Investigation of the concept of equilibrium as it applies to shore platform development.

1.4 THESIS OUTLINE.

This thesis has been broadly divided into four sections, an introduction, elements resisting erosion, processes causing erosion and a summary. The two middle sections

are organised based on the concept of Sunamura (1992) of a balance between forces resisting erosion and those causing erosion on shore platforms. This concept has been utilised as a convenient method for dividing processes into manageable units.

The introduction section includes Chapters 1, 2 and 3. Chapter 1 has briefly reviewed past research on shore platform development and identified questions that still need to be addressed. It has also outlined the objectives for this thesis. Chapter 2 introduces the study areas used for this thesis. Profiles across shore platforms developed in five different rock types at various locations around New Zealand have been used for this investigation. The environments in which the shore platforms are formed and the shore platforms themselves are described. Chapter 3 presents measurements of rates and patterns of surface change along each study profile.

The section on elements resisting erosion is presented in Chapter 4. Chapter 4 discusses the character of the rock type in which each shore platform is formed. This includes aspects of lithology and rock strength.

The section on processes causing erosion is covered in Chapters 5 – 7. Chapters 5 and 6 look at wave induced processes and Chapter 7 at processes of weathering. Chapter 5 describes the wave environment at each study site and presents direct measurement of wave flows onto and across a shore platform. Chapter 6 uses measured aspects of wave induced flows to assess processes of wave erosion on shore platform surfaces. The second half of the chapter discusses the capacity and competence of the flow in moving sediment. Chapter 7 investigates the processes of weathering that occur on shore platforms and gives relative susceptibilities of each rock type to weathering.

The last section draws together measurements and relationships discussed in the first three sections by looking at the spatial differences in shore platform development. Chapter 8 discusses the processes presented in Chapters 4 – 7 with respect to spatial variation and the relative contribution of each to shore platform development. It presents a model of shore platform development. Chapter 9 presents the conclusions of this thesis and proposes some avenues for further research.

CHAPTER TWO

FIELD AREAS AND SHORE PLATFORM MORPHOLOGIES

2.1 INTRODUCTION

Shore platforms are found within a wide variety of environments and formed on many different lithologies. Strong notions in literature on shore platform development are that rock strength is a fundamental factor in controlling the type of development on rocky coasts and the rate at which that development occurs. However, aspects of lithology and shore platform morphology are intricately related and these relationships have not yet been satisfactorily defined (Trenhaile 1987, Sunamura 1992, Stephenson 2000).

This chapter describes the field areas and environments in which study sites are located. The morphology of the shore platform at each site is described and compared. Comparison of morphology may also yield detail on how each shore platform was formed and on water flows across the surface adding to process description.

2.2 RATIONALE FOR CHOICE OF FIELD SITES.

The rationale behind the choice of field sites was to locate shore platforms in a range of different rock types, of varying hardness, on which change could be monitored using the micro erosion meter (MEM) technique. This technique measures sub millimetre surface change with a portable gauge. Bolts are secured into the rock and used to relocate the gauge in exactly the same position for each successive surface measurement (section 3.1) (High and Hanna 1970, Stephenson 1997b).

Another criterion for selection of sites was to find locations that also allowed for measurement of other aspects of processes, for example, wave flow across the platform, rock strength and weathering.

2.3 FIELD SITE LOCATIONS.

Shore platforms formed in five different lithologies on coastlines around New Zealand were selected for study in this thesis (figure 2.1). At Lake Waikaremoana shore platforms have formed in mudstone. On the Kaikoura Peninsula shore platforms are formed in mudstone and limestone. Shore platforms at Raramai Arch Point are formed in greywacke and at Robinson's Bay Point they are formed in basalt. Characteristics of each of these rock types are described in sections 2.6 and 4.2 of this thesis.

Profiles orientated across the shore platforms were established at each of the study sites. Field measurement of morphology and monitoring of surface change across the profiles was an important part of the experimental design for this thesis. In all, eight re-locatable, shore-normal profiles were either established or reactivated across the selected platforms. The names given to each profile are listed in figure 2.1. Each profile was surveyed and MEM monitoring sites were located at roughly regular intervals across the horizontal portion of each profile. A number of individual MEM monitoring sites were also established on the shore platforms at Raramai Arch and Robinson's Bay within close proximity to study profiles.

Three of the study profiles were located on the Kaikoura Peninsula continuing the use of previously established profiles (Kirk 1977, Stephenson 1997a). Two of these were on mudstone, KM2 and KM3 and the third on limestone, KM7. For the sake of continuity, names used in previous studies at these locations have been used in this thesis. A new profile and eight individual MEM sites were established by the present writer on a greywacke platform south of Kaikoura at Raramai Arch, RM1. Two new profiles and three individual MEM sites were established by the present writer on a basalt platform at Robinson's Bay in Akaroa Harbour, AK1 and AK2. Around the shores of Lake Waikaremoana two new profiles, WK1 and WK2 and 3 other individual MEM sites were established on mudstone benches. The work at Lake Waikaremoana was undertaken as part of a wider project for Genesis Power Ltd. as part of their water use consent conditions, which investigates shoreline change around the lake (Allan *et al.* 1999).

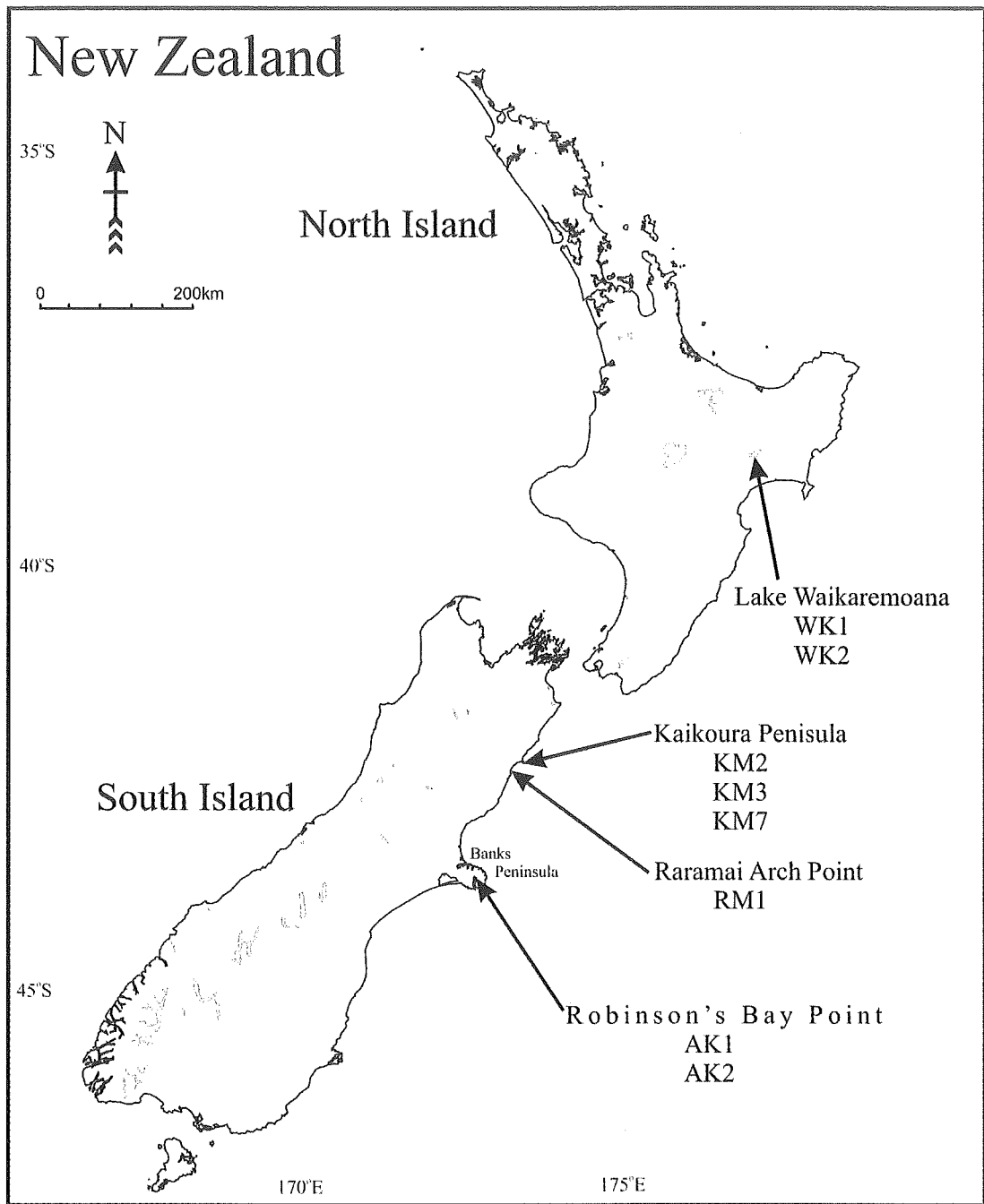


Figure 2.1: Map showing location of shore platform study profiles.

2.4 FIELD SITE ENVIRONMENTS.

This section broadly describes the field areas in which profiles are located. Aspects that are considered important in relation to the study of shore platforms and the understanding of processes on them are outlined. These include morphology, rock type characteristics, atmospheric climate, wave climate, tides and sea (water) level. Detailed morphological description of the study profiles themselves is made in

section 2.6. Detailed examination of rock characteristics is presented in Chapter 4 and of wave climates in Chapters 5 and 6.

2.4.1 KAIKOURA PENINSULA.

The Kaikoura Peninsula is located on the northeast coast of the South Island of New Zealand ($42^{\circ}25'S$: $173^{\circ}42'E$). It projects 4.5 km seaward from the general northeast-southwest strike of the coast in the form of a plateau with several terraces, the highest being 108 m above sea level. It covers a total area of 5.2 km^2 (figure 2.2). The seaward margins of the peninsula are flanked by intertidal shore platforms of various sizes covering some 0.77 km^2 (Kirk 1977).

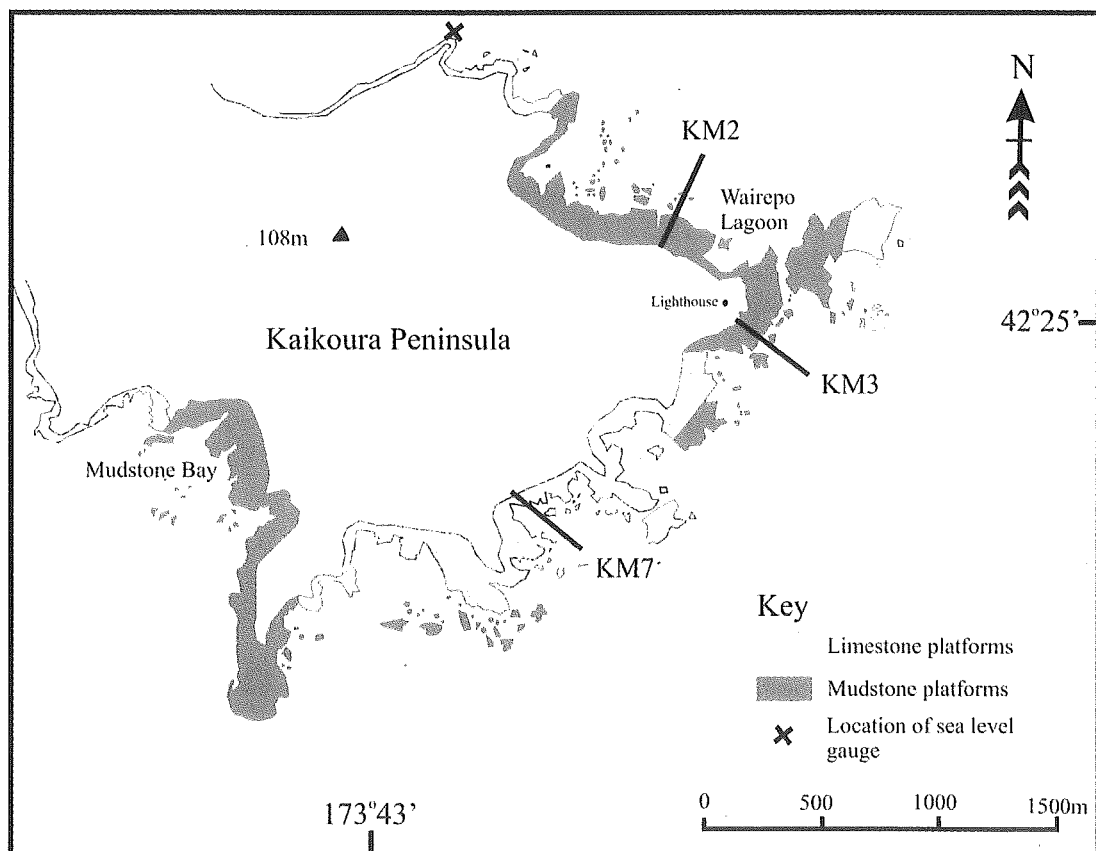


Figure 2.2: Kaikoura peninsula showing shore platform lithology (Kirk 1977). (Note that the seaward cliff-line irregularity is reduced due to the scale of the map.)

The rocks that make up the Kaikoura Peninsula are sedimentary and are Upper Cretaceous and Tertiary in age. The two units of rock in which the shore platforms are formed are Paleocene Amuri limestones and Oligocene grey-marls (mudstone). The geological structure of the peninsula comprises a slightly asymmetrical anticline

flanked on either side by two synclines, the axial planes of which strike northeast-southwest parallel to the general trend of the adjacent coast (Duckmanton 1974). Shore platforms are eroded across all three of these structures and their alignment is intersected by the platforms in a variety of ways, giving a range of relationships between shore platform orientation and local dip and strike around the peninsula. There is extensive secondary folding and faulting, particularly of the limestone, which is in general a harder more brittle rock. This has resulted in the surfaces of the platforms formed in the limestone displaying a wider variety of morphology than those developed in the mudstone (Kirk 1977).

Terraces on the peninsula (figure 2.3), apparently interglacial surfaces (Kirk 1977), occur at a variety of heights and are testimony to the interplay of eustatic sea level change and tectonic activity through the Quaternary. A net Quaternary uplift in excess of 100m was estimated by Suggate (1965) with average rates of 1.1 m.ka^{-1} reported by Ota *et al.* (1996). Duckmanton (1974) identified the most recent uplift from relict raised beaches as having been in the order of 2m. He suggested that this tectonic activity initiated deposition of sediment on the raised platforms on the eastern flank of the peninsula and led to the development of barrier beaches behind which lagoons formed at Wairepo and Mudstone Bay. The margin of the peninsula thus presents relict platforms as well as presently active ones.

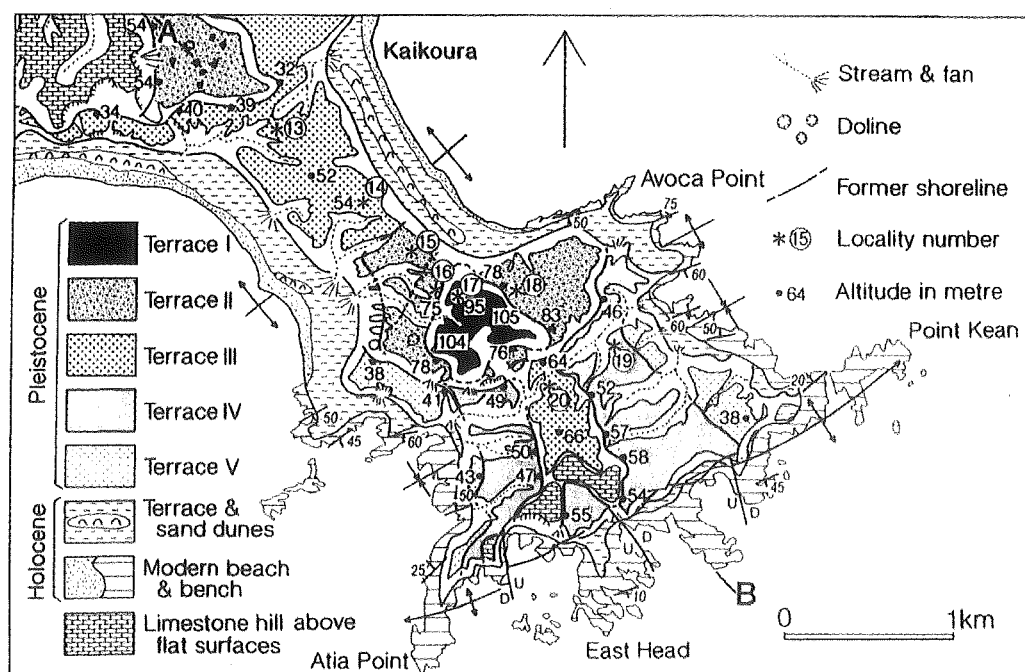


Figure 2.3: Marine terraces of the Kaikoura Peninsula (Ota *et al.* 1996 fig.9)

The climate of the Kaikoura region is temperate. Long term data from a weather station (New Zealand Meteorological Service) located on the peninsula at a height of 108m asl was examined to describe the main climatic variations. Monthly average temperatures range from 7.7°C in July to 16.2°C in January and frost occurs on average on 40 days per year although this will be less at sea level. Average annual rainfall recorded between 1945 and 1980 was 888 mm.yr⁻¹ (Stephenson 1997a). The placement of New Zealand within the westerly wind belt results in a progression of high and low pressure systems and associated fronts across the country (Sturman and Tapper 1996). At Kaikoura this results in a dominance of winds from the South, however, there is also a strong northeasterly component resulting from sea breeze conditions.

Dominant wind directions are important in the generation of wind and swell waves arriving at the Kaikoura coast. Generally the wave climate of the East Coast of the South Island can be characterized as a high-energy oceanic swell environment where long periods of relatively calm seas are interspersed with high-energy storms (Kirk 1977). Both near field wind waves and southerly swell conditions occur. Wind waves are generally smaller, steeper and closely coupled to the wind conditions and swells are of a longer period, more regular, and totally uncoupled from their generating wind. New Zealand's 7 to 10 day weather cycle synchronizes very closely to the southerly swell environment (Kirk *in* Sturman and Spronken-Smith 2001). Storms can occur at any time of the year and there is no distinct seasonal pattern to either the wind conditions or the associated waves and swell.

Kaikoura has a micro tidal range with mean annual tidal variations of 1.3m. This has been calculated from 6 years of sea level data recorded by a sea level gauge installed jointly by Geography Department, University of Canterbury and NIWA on the Wharf (figure 2.2). The maximum tidal range was 2.23m and the minimum range was 0.96m.

2.4.2 RARAMAI ARCH.

Raramai Arch is located 13kms southwest of Kaikoura. The coast to the south of the Kaikoura Peninsula continues the general northeast-southwest strike with steep relief

to sea level. Mountains with over 2000m of elevation occur within 20 km of the shore and corresponding ocean depths occur within similar distances offshore (Kirk 1977). The coast is comprised of small shore platforms with a maximum of approximately 200m alongshore and 70m in width, interspersed with narrow mixed sand and gravel beaches. These platforms are not as extensive as those formed on the Kaikoura Peninsula. The bedrock is dominated by massive, well indurated and complex greywacke of the Kawhia series in the Torlesse group. At Raramai Arch (42°28'S: 173°33'E) a shore platform has formed in greywacke seaward of an unnamed point and covers 3075 m² (figure 2.4). From this point there is steep relief directly landward with elevations of 450m being reached within 1000m.

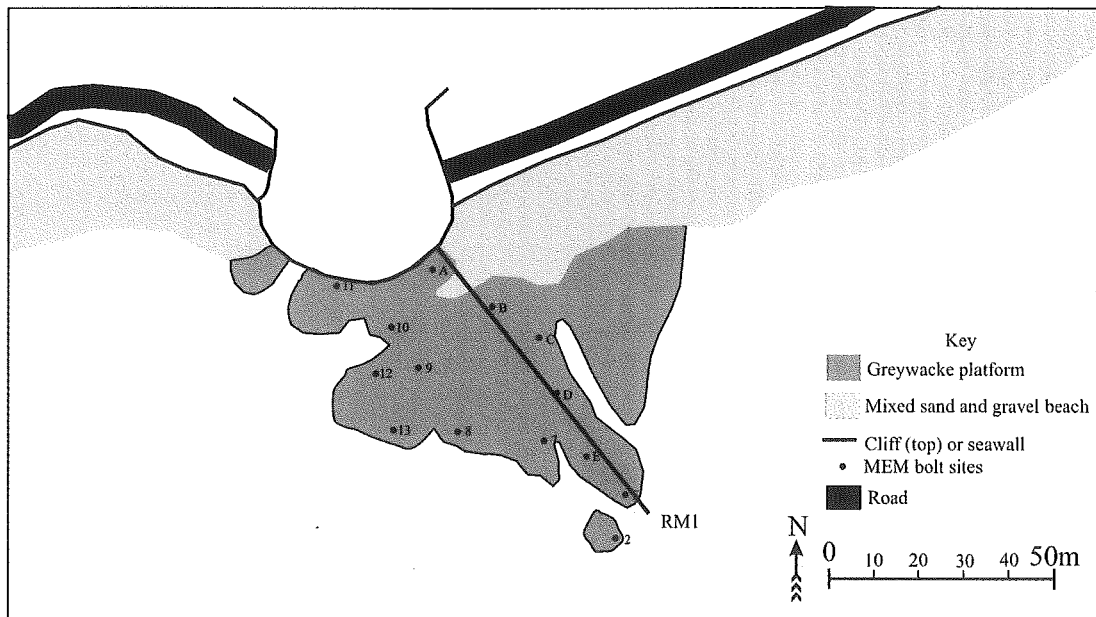


Figure 2.4: Map of Raramai Arch shore platform. Constructed using an aerial-photograph and direct topographic survey.

No information was available on the tectonic state of the stretch of coast on which Raramai Arch is located. However uplift rates of 1.7m.ka⁻¹ are documented for the Haumuri Bluffs 12 km to the south of Raramai Arch (Ota *et al.* 1996). This suggests that the Raramai area is also tectonically active

The proximity of Raramai Arch to the Kaikoura Peninsula means that it experiences very similar climatic, wave and tidal conditions as outlined for the Kaikoura Peninsula environment.

2.4.3 ROBINSON'S BAY, AKAROA HARBOUR.

Akaroa Harbour is formed in the caldera of the southern most of two Cenozoic intraplate volcanoes, which make up Banks Peninsula (Sewell *et al* 1992). It is encircled by a radial pattern of spurs and valleys reaching a maximum height of 841m asl. The axis of the Harbour extends directly south. About a quarter of the land slopes inward to the harbour basin and the remainder radiates outwards from the crater rim to the open sea. It is composed of a suite of lava flows of mildly alkaline to trachyte basalt of the Miocene French Hill formation with a number of dykes present (Sewell *et al* 1992).

The majority of the coastline exposed to the open ocean consists of cliffs of the plunging variety described by Cotton (1951). The coastline making up the inner shores of the Harbour consists of alternating sandy/muddy bays interspersed between rocky headlands, many of which have shore platforms (figure 2.5).

The study profiles were located on a point between Robinson's Bay and Duvauchelle's Bay. (43°46'S: 172°57'E) (figure 2.5). The platform covers an area of 4925m² (figure 2.6).

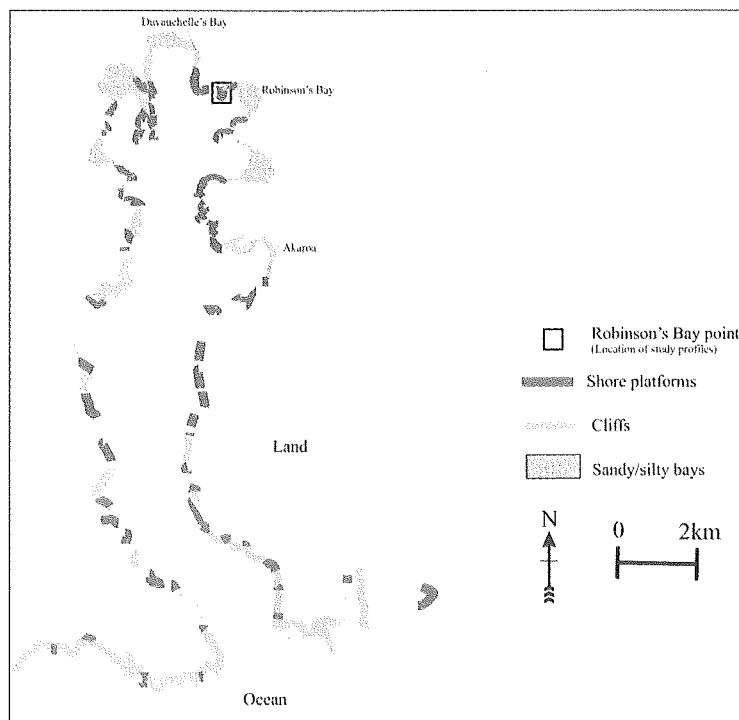


Figure 2.5: Coastal features of the Akaroa Harbour. Constructed using NZ Navy Chart 6324 (1:30 000) and an aerial-photograph.

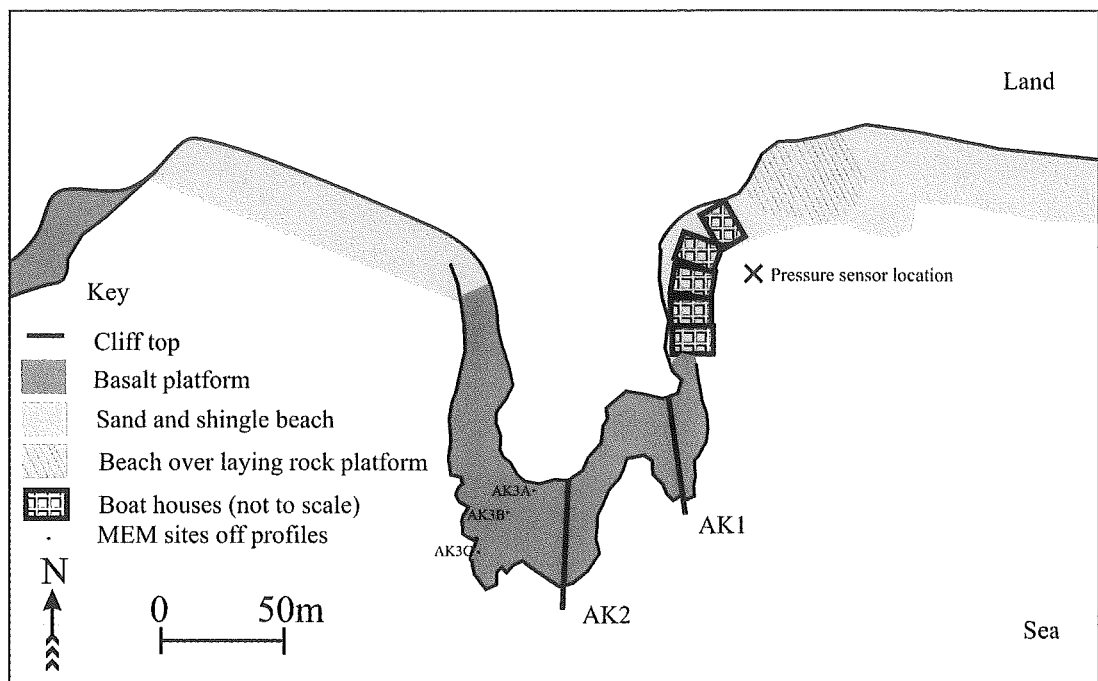


Figure 2.6: Map of Robinsons Bay Point shore platform. Constructed using an aerial-photograph and direct topographic survey.

Banks Peninsula is considered to have been tectonically stable for at least the last 125 000 years as interpreted from, among other features, relict shore platforms at 1m and 5-8m above sea level on both the southwest and northwest flanks of the Peninsula (Lawrie 1993, Bal 1997, Shulmeister *et al* 1999).

Relict platforms that occur on the southwestern edge of the Peninsula at 1 m asl are similar in morphology to the ones currently at intertidal level within the harbour. The relict shore platforms were also formed in rock of the French Hill formation. A comparison of the two platforms formed at different times could provide the basis of future study on the present and past development of shore platforms.

The climate of Akaroa Harbour is also temperate. The closest available long-term weather station is a New Zealand Meteorological Service station 45 km to the east at Christchurch. The Christchurch statistics provide a generally accurate picture although, because of its enclosed nature, the weather at Akaroa varies slightly to that at Christchurch. Mean maximum temperatures range from 11.3°C in July to 22.5°C in January and ground frost occurs on average 69 days per year. Mean annual rainfall between 1969 and 1998 was 635 mm.

Like Kaikoura, dominant winds at Christchurch were from the south together with a strong northeasterly component. The topography of the Akaroa area would protect the Harbour from some of the northeasterly winds.

The general wave climate acting upon the exposed flanks of Banks Peninsula is the same as that described for the Kaikoura region (see section 5.2.3.1). However within the Harbour the effects of wave shoaling and topographic protection from northerly directions results in the sea being calm for a much greater proportion of the time.

No permanent sea level gauges have been installed in Akaroa Harbour. Therefore a temporary gauge (a Greenspan pressure transducer) was installed 20 m directly seaward of a boat ramp (figure 2.6) for 8 months for this study. The sensor logged 15 minute averages of water depth and was surveyed into benchmarks on the shore platform. The mean tidal range was 1.5m making this region micro tidal. There was a maximum tidal range of 2.9m and a minimum tidal range of 1.3m.

2.4.4 LONG TERM SEA LEVEL.

The New Zealand coast has been subject to global sea level change. Relative sea level curves for the Canterbury Coast, New Zealand, presented in Shulmeister and Kirk (1993) give a general impression of long term sea level changes that will have been experienced at all marine sites in this study. Essentially the sea reached its present level between 6000-7000 years before the present. Assuming there has been no significant relative change in this level due to tectonic activity then the processes that form shore platforms have been working at this level for about (or at least) 6000-7000 years. However, tectonic uplift is a factor for the profiles on the Kaikoura peninsula.

2.4.5 LAKE WAIKAREMOANA.

Lake Waikaremoana is located in the Wairoa basin on the East Coast of the North Island (38°47' S : 177°05'E). It is a fresh water lake formed behind two natural landslides which blocked the Waikaretaheke River valley approximately 2500 years

before the present (Marshall 1927). The Lake covers an area of 55.74 km² with 92.5 km of coast (figure 2.7). 42% of the coastline is composed of shore platforms formed in soft mudstone. Long tracts of cliffed sandstone make up 50% of the coastline and the remaining 8% is composed of small sand or gravel pocket beaches or turf shores (Allan *et al* 2002). The two main geological components of the Lake Waikaremoana basins are sandstone and mudstone of Miocene age.

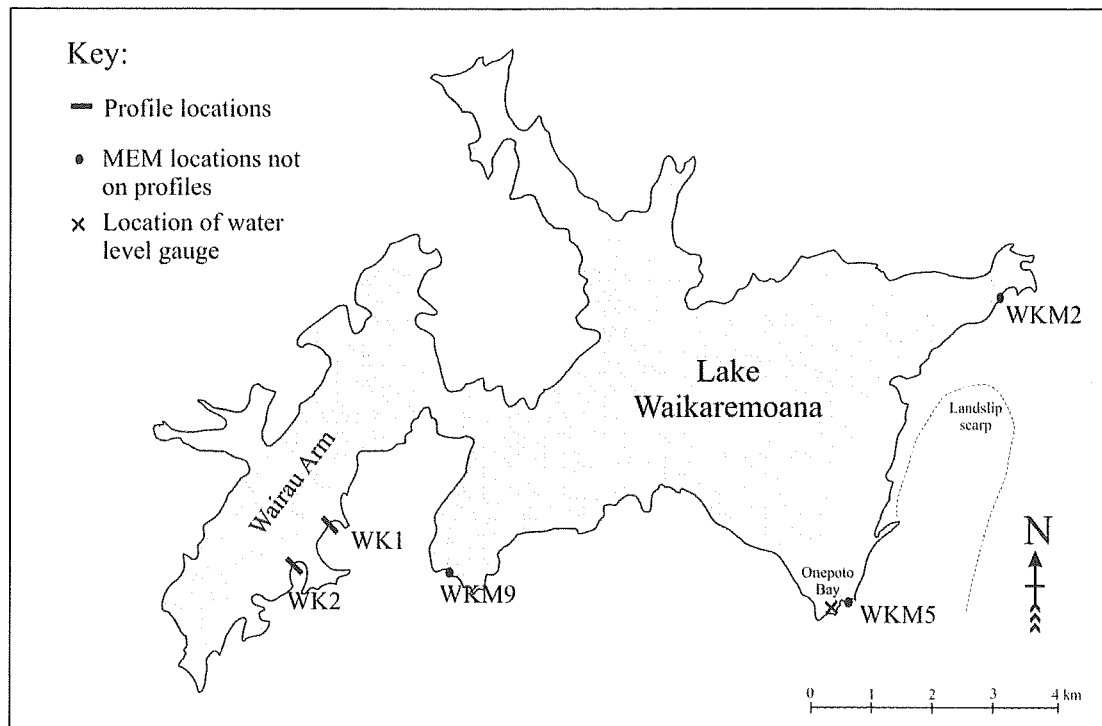


Figure 2.7: Lake Waikaremoana with the shore platform profiles indicated.

The Lake Waikaremoana area experiences a ‘mild and wet’ climate. Temperatures vary from a mean maximum of 8.9°C in July to 20.5°C in February with ground frosts occurring on average 38 days per year. Rainfall occurs frequently throughout the year with the highest levels in winter and lowest levels in spring. Total annual rainfall is 2148mm per year. Predominant winds are from the northwest, southwest and north, the strongest of these being those from the northwest and north directions (Allan *et al* 2002).

The enclosed nature of this water body means that all waves formed are closely coupled to the wind. Maximum wave heights of between 0.5m and 1m occur, on average 26 days per year. The predominant wind conditions suggest that the largest waves are concentrated on the Eastern and Southern shores of the lake. Different

arms of the lake can experience different wave conditions at the same time due to topographic channeling of winds.

Water levels at Lake Waikaremoana have been well documented (Marshall 1927, Matthews 1992, Allan *et al.* 1999). In 1946 the lake level was artificially lowered 5 metres to 582m asl to aid in stabilization of the natural dam for the installation of a hydroelectricity scheme. This has remained the mean level of the lake today with the exception of a brief lowering of the level during the 1960's to allow for tree stump clearance. So, the present shoreline has essentially had 56 years in which to establish. Lake levels are presently controlled by a management regime operated for hydropower generation that restricts levels to a 3m range between 580.29 to 583.29 m asl. This may be exceeded during flood events. Effectively this compares to a meso tidal regime in the vertical dimension.

2.4.6 SUMMARY

Shore platforms studies in this thesis have developed in a range of rock types and across a variety of geological structures. Rock types in which the shore platforms studied are formed include sedimentary, mildly metamorphic and igneous rocks and shore platforms are eroded across lithologies with a range of dip and strike. The shore platforms studied are formed at the margins of both fresh and salt water bodies with effectively micro and meso tidal ranges. All study sites are within temperate climates so mechanical weathering and moderate chemical weathering processes could be expected. There is moderate biological activity on the marine platforms.

2.5 CLASSIFICATION OF SHORE PLATFORMS.

Shore platforms are wholly eroded, relatively planar surfaces formed in solid rock and usually backed by a cliff. The majority of a shore platform's surface occurs between the high and low levels of the tide. They have been recognized in the literature as distinctive coastal features since the mid nineteenth century. Much of the literature on them, especially the early work, was primarily descriptive with deduction of process based on observations of morphology. Often this description

lacked rigorous definition making comparison between different studies and sites difficult. There is still a lack of uniformity with basic definition of aspects of shore platform morphology and possibly, even more fundamentally, of recognition of these features in the field. Many contradictions and discrepancies in definition of shore platforms occur. The need for consolidated definition of what a shore platform is has been recognised by a number of researchers (McLean 1967, Sanders 1968a, Trenhaile 1974b, 1987, 1999, Robinson 1977a, Sunamura 1983, 1992).

A number of differing definitions of shore platforms by different authors follow.

McLean (1967:2) defined a shore platform as “a solid rock feature with a well defined, sub-horizontal surface most of which lies between extreme high spring tide level and extreme low spring tide level. Shore platforms may be backed by an active cliff or beach”. Sanders (1968a) outlined a similar criteria. Robinson (1977a:237) stated that shore platforms were “gently sloping surfaces exposed at low tides on eroded coasts”. Mii (1962) referred to shore platforms as erosion planes in front of sea cliffs and distinguished these according to their elevation compared to mean sea level. In all Mii (1962) distinguished seven types of shore platform profiles each with distinctive characteristics. Trenhaile (1974b) classified four categories of intertidal platform-ledges in England and Wales.

- a). Contemporary shore platforms
- b). Lithologically controlled storm ledges
- c). ‘Raised’ shore platforms
- d). ‘Raised’ storm ledges

These were defined according to lithological control on processes and antecedent conditions.

Sunamura (1983, 1992), in an attempt to add uniformity to definition, divided hard (solid) rock coasts into just three major categories based on morphology. Two of these were types of shore platforms and the third was plunging cliffs (figure 2.8). Both platform types were considered to be wholly eroded in nature and formed in solid rock with backing cliffs. He designated Type A platforms as those with gently seaward-sloping ramps and Type B platforms as those with nearly horizontal surfaces and seaward scarps at the low tide level.

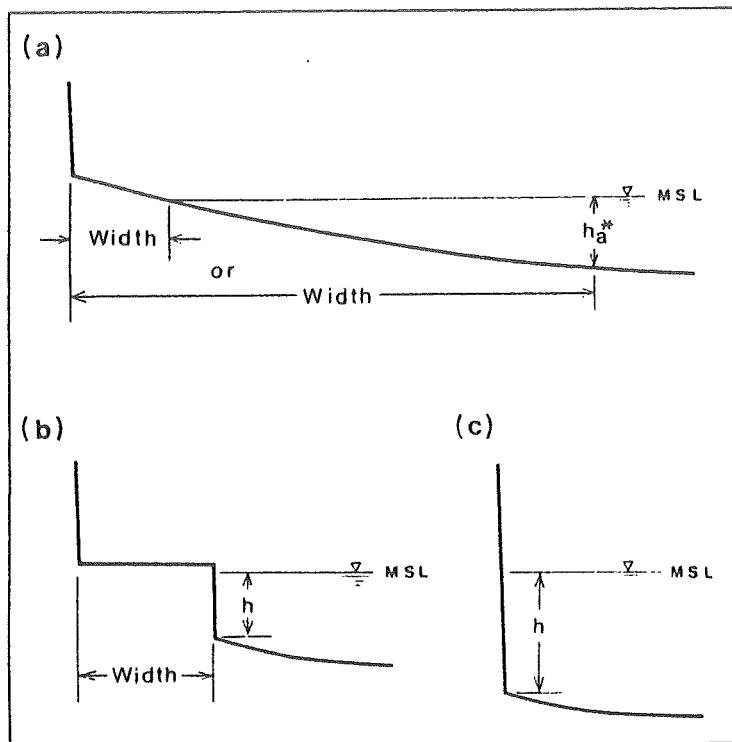


Figure 2.8: Classification of rocky coasts. Schematic cross-section of the three major morphologies. a) Type A shore platform, b) Type B shore platform, c) Plunging cliffs (Sunamura 1992:fig. 7.2).

This classification is, by necessity, a simplistic one and based on the notion that the morphology of platforms is controlled by a balance between the attacking force of the waves (F_w) and the resisting force of the rock (F_R). The Type A and Type B designations for shore platforms are widely used in contemporary shore platform literature and provide a good basis for general comparison, under the proviso they are used in a rigorous manner. However the universal applicability of Sunamura's categorization has still to be fully tested (Sunamura 1992, Stephenson 2000). In reality there is not necessarily a strict demarcation but many variations, reflecting lithological factors, weathering properties of rocks, tides, degree of exposure to wave assault and inheritance (Sunamura 1992). Therefore, the distinction between shore platforms is often not as sharp as figure 2.8 suggests.

When faced with distinguishing and classifying shore platforms in the field for the present study a number of problems arose. When categorizing the platforms of the Kaikoura Peninsula there were difficulties in identifying the platform boundaries. The seaward cliff of KM3 is fragmented and difficult to define precisely. It has deeply incised channels and reefs, made up of stack-like rock outcrops, along its

edge (figure 2.9 and 2.2). At KM2 the level of low tide occurred on the gently sloping near horizontal surface. For this reason the platform has previously been classified Type A (Stephenson 1997a). However the occurrence of a scarp or seaward drop approximately 10m seaward from this point, (figure 2.15), calls into question the validity of this classification. It is hypothesized that tectonic movement may have caused a variation in contemporary platform surface level orientation. Although, this may not be the only possible process causing changes in the shape and orientation of the surface of the shore platform profile.



Figure 2.9: Photo of fragmented seaward edge of KM3. Showing difficulty of boundary definition in shore platform description.

Another difficulty in the classification of shore platforms occurs when the horizontal surface of the platform has some relief. In the case of the Kaikoura Peninsula there are channels which are up to 2 m in depth and protrusions of up to 1m in height on some of the 'horizontal' surfaces.

Problems in classification and definition of shore platforms arise for two main reasons.

- 1). Classifications are not based purely on morphological grounds. The use of tidal level to define one or more of the boundaries includes a changeable process factor within the classification.
- 2). Morphology may be influenced by factors not included in the assessment of the assailing forces of waves (F_W) or the resisting forces of rocks (F_R).

In some cases the influence is profound. Such factors could include a change in base level through tectonic activity. The question of inheritance as a factor in formation of shore platform morphology has long been a topic of discussion (e.g. Trenhaile 1987). With 2m of tectonic uplift at Kaikoura this is an important but poorly understood factor, as is sea level change.

Shore platforms studied in this thesis will be assigned to Sunamura's (1992) Type-A and Type-B categorization, where possible, for ease of comparison with other examples in the international literature. However mention will be made where difficulties arose.

2.5.1 MORPHOMETRIC CHARACTERIZATION.

When describing shore platforms it is useful to consider a number of morphometric aspects. These include orientation, width, gradient and elevation. Characterization of shore platforms, comparisons between different platforms, models of shore platform development and the question of shore platform equilibrium all rely heavily on these aspects being rigorously defined in a consistent manner. It would therefore, be useful to have agreed criteria for defining dimensions of these different elements of shore platform morphology. Unfortunately this does not exist. A number of authors have defined aspects of measurements made (McLean 1967, Sanders 1968a, Robinson 1977a, Sunamura 1992, Trenhaile 2000, Stephenson 1997a) but more often there is very little clarity of exactly what has been measured.

This section outlines definitions used in the literature to measure the parameters of orientation, width, gradient and elevation. Section 2.5.2 gives definitions used in this study.

2.5.1.1 ORIENTATION.

Orientation of the shore platform profiles drawn in Sunamura's schematic classification (figure 2.8) is assumed to be as described by Tsujimoto (1987) which was in a representative location on the shore platform and along a line extended "perpendicular to the general trend of the landward cliff" (Tsujimoto 1987:55).

2.5.1.2 WIDTH.

The width of a platform is generally considered to be the horizontal distance between high tide level and low tide level (Mii 1962, Sanders 1968a, Robinson 1977a, Trenhaile 2000). However this definition sometimes includes slight variations. The landward boundary as defined by Robinson (1977a) extends either to the foot of the cliff or to mean high water level. Sunamura (1992) suggests platforms extend to the landward cliff base. Trenhaile (2000) defines the width of the platform as the horizontal distance extending from mean low water to mean high water of spring tides and then, in the same paper, uses the foot of the cliff as a boundary for the measurement of the platform gradient. Thus, difficulty in quantifying the width of shore platforms stems from the problem of boundary definition as exemplified above.

Use of water levels as boundaries for morphological features introduces a number of problems. The main one being that water levels are inherently not morphological criteria. This leads to problems with practical identification of a mean water level and also definition of particular water levels. Should use be made of mean high water or mean high spring tide level? For example, what should be done when using mean high spring tide level in locations where no spring tides occur, such as the Canterbury Bight. Tidal levels do not account for the effects of wave run-up and storm setup and therefore do not necessarily reflect the highest water level attained on a shore platform. This is an important consideration as this is the maximum level to which processes of wave action and marine wetting and drying are able to operate. Figure 2.8 suggests that the landward cliff foot and high water level coincide. If this is not the case or if there is a beach present on the backshore which boundary should be used?

Problems of boundary definition may also occur at the seaward margin of platforms. In some cases the seaward cliff edge of the shore platform lacks or loses definition. At KM3 deeply incised channels and reefs fragment the rock surface (figure 2.9). In the field, an assessment of all factors needs to be made resulting in a boundary definition based on the observer's judgement.

2.5.1.3 GRADIENT.

The gradient of a platform is one of the primary components in parallel retreat models of shore platform development, which have been used by Challinor (1949), Kirk (1977) and Trenhaile (1974a). Use of gradient means that vertical erosion rates directly determine horizontal retreat rates of the platform. Therefore an accurate quantification of this parameter is essential.

As with defining the width of platforms one of the main problems with assessing their gradient is definition of the boundaries. Stephenson (1997a) used the gradient between his most seaward and most landward MEM bolt sites as representative of platform gradient. However this does not measure aspects of morphology directly and although it could be applied in this study it was not considered universally applicable and therefore was not used. The gradient defined by Mii (1962:29) was “the degree of inclination measured with regard to the erosion plane” where the erosion plane was the near horizontal surface of the shore platforms. However, he did not directly define the boundaries of this plane. Sunamura (1992) and Trenhaile (2000) both defined the gradient as being the slope of the plane between the cliff foot and the seaward limit of the shore platform. This results in a generalised, uniform gradient for the entire platform. Assessment of the gradient at KM2 was made using this definition. Figure 2.10 shows that the gradient of a line drawn between the boundary points of the platform did not represent the gradient of the majority of the horizontal surface of the platform.

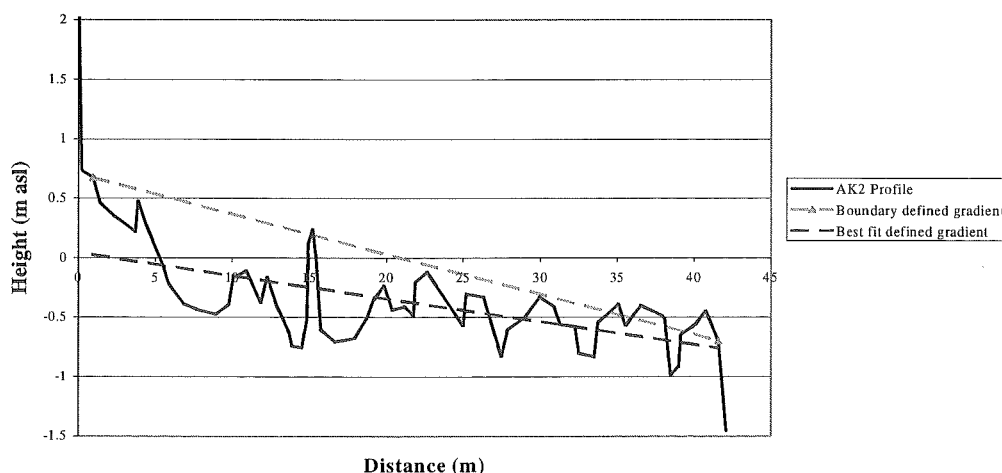


Figure 2.10: Gradient of shore platform at AK2. As represented by a line drawn between the landward cliff foot and the seaward limit of the platform (grey dashed line). The black dashed line shows the gradient of the majority of the horizontal surface.

Added to the boundary problem is the occurrence of local scale topography or non-uniformity of gradient across a platform. Robinson (1977a) is the only author to have addressed this problem directly. He measured gradients across the platform profile in 1 metre segments and applied best segment analysis.

Sanders (1968a) distinguishes horizontal shore platforms from sloping ones using a cut off of a 3° gradient. Similarly Sunamura's (1992) Type A platforms are gently sloping and his Type B platforms are nearly horizontal. However no definite boundary gradient is given. The demarcation depends, rather, on the shape of the profile and a comparison of this to the level of low tide.

2.5.1.4 ELEVATION.

Elevation has often been used as part of the classification of the shore platforms. For example, "high tide platforms", "low tide platforms" (Mii 1962) and "intertidal platforms" (Denny 1988). Shore platforms are usually defined as near horizontal rock surfaces extending between high and low tidal levels. Therefore, strictly speaking, the platform would extend across all elevations between these levels. For this reason it is important to define which part of the platform is being measured to obtain a given elevation. Establishing the elevation of platforms with respect to sea level is important if relict shore platforms are to be used as indicators of past sea levels. Also, there is much debate on the relationship between exposure of shore platforms and their elevation.

It is usual for the elevation of the platform to be related to some sea level datum such as mean sea level. However detail of exactly how this has been accomplished is often unstated. Bradley and Griggs (1976) present one of the few rigorous descriptions of how shore platform elevation was measured. They surveyed profiles across platforms, measuring elevation at a sufficient number of points to adequately define a local average elevation.

When working with morphometric elements of shore platforms in any rigorous scientific way, problems include simple agreement on definitions and practicalities of measurement. There needs to be a standardization of definitions used in shore

platform studies, including clear outlines as to how measurements were obtained. This is unlike beach environments where a more generally accepted, though by no means uniform, set of morphological criteria are in place (Zenkovich 1967, Komar 1998). For this reason definitions of morphometric aspects used in this study are outlined in the following section.

2.5.2 DEFINITION OF MORPHOMETRIC ELEMENTS OF SHORE PLATFORMS.

This section defines measurements of shore platform morphology used in this study. Figure 2.11 is a schematic showing terminology adopted and definition of some morphological aspects of profile measurement.

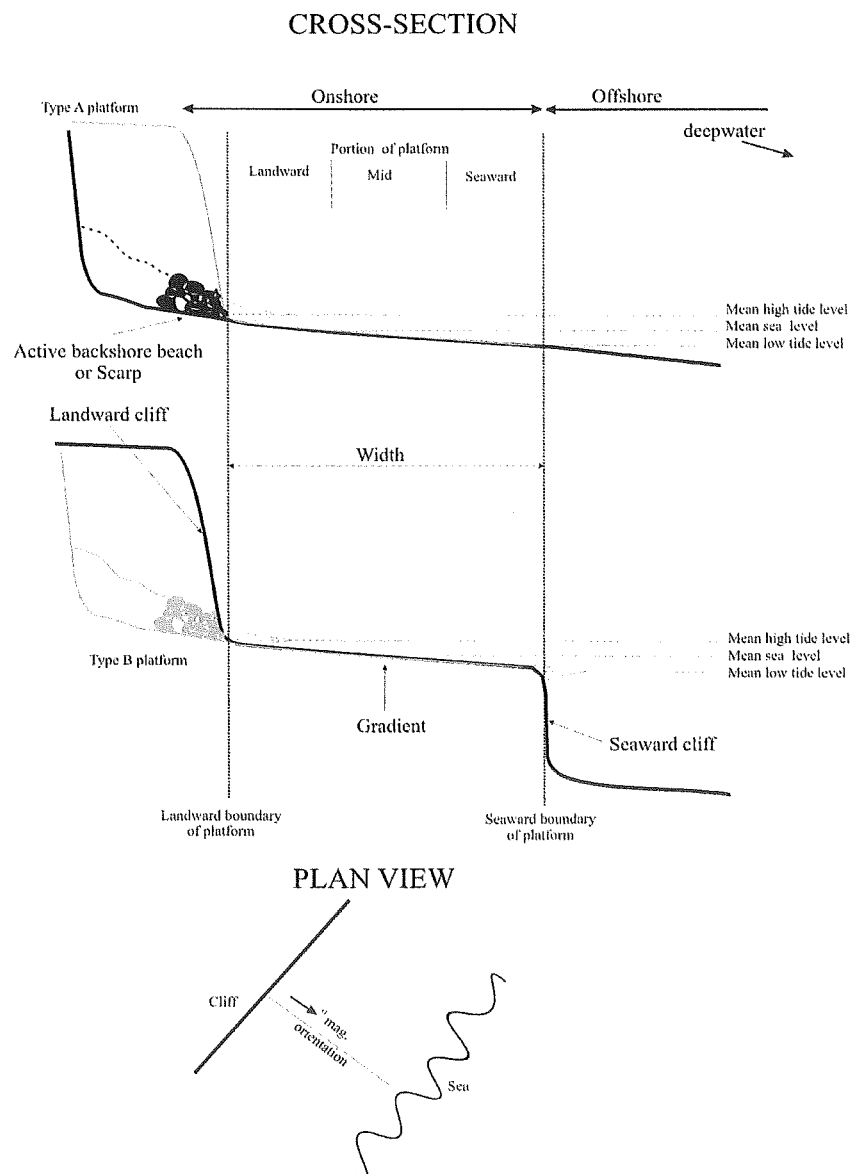


Figure 2.11: Schematic of definitions and terminology adopted for this study. (See text for greater detail)

2.5.2.1 ORIENTATION:

Profiles were extended perpendicular to the general trend of the landward cliff and the orientation of this line was measured as the angle from north (magnetic) in the seaward direction.

2.5.2.2 WIDTH:

Width is the horizontal distance, in metres, from the landward cliff foot, landward scarp or the base of the active backshore beach to the seaward cliff (for platforms defined as Type B in Sunamura's classification scheme) or the mean low tidal level (for platforms defined as Type A in Sunamura's classification scheme). These are respectively defined as the landward and seaward boundaries of the shore platform. Where the seaward cliff was fragmented the location of the most consolidated seaward edge was used. Figure 2.11 shows the high water level coinciding with the cliff foot. This generally occurred on the study platforms investigated but may not be the case on shore platforms universally. Extension of the landward boundary of shore platforms to the cliff foot or active backshore beach takes account of the highest point of marine action rather than using the standard high tide levels.

2.5.2.3 GRADIENT:

Gradient is the slope of a line of best fit through the points defining the profile between the seaward and landward boundaries, as defined for width. It is expressed in either degrees of inclination from horizontal or as a dimensionless ratio of vertical change in height / width.

2.5.2.4 ELEVATION:

Elevation is the mean elevation, in metres, of the platform surface between the seaward and landward boundaries in relation to mean sea level. Mean sea level at Kaikoura was defined using a sea level gauge installed on the Kaikoura wharf by the Geography Department, University of Canterbury and NIWA (figure 2.2). Mean sea level at Akaroa was related to water level data collected by a pressure sensor installed temporarily in Robinson's Bay from 30/07/2001 to 01/04/2002 (figure 2.6). At Lake Waikaremoana water level was obtained from a water level gauge located in Onepoto Bay and operated by Genesis Power (figure 2.7).

2.5.2.5 ROUGHNESS:

Although this aspect of shore platform morphology is not often mentioned in the shore platform literature it is considered important here both on its descriptive merit alone and as an indicator of the degree to which the shape of the surface varies from the gradient which has been expressed in terms of a straight line. Roughness has been defined with measures of variance, in meters, from the gradient line in both vertical and horizontal directions. Plots of each profile were used with measurements interpolated for every 0.25m interval between the landward and seaward boundaries. From these the standard deviation of the residual sum of squares was calculated for both the horizontal and vertical directions. This gives the mean variation of points along the profile from the best fit (gradient) line. The greater the residual roughness number the greater the roughness of the profile. As the profile was measured to the nearest 0.25m this dictates the scale to which roughness has been defined using this method.

Roughness residuals have been assigned an arbitrary classification based on observation to make description of this parameter more tangible for the reader (table 2.1). As residuals in the horizontal direction are also dependent on platform width broad classifications have been made.

Table 2.1: Classification of roughness residuals.

| Roughness residual (m) | | Descriptive classification |
|------------------------|--------------|----------------------------|
| vertical | horizontal | |
| 0.00 - 0.14 | 0.0 - 9.9 | very smooth |
| 0.15 - 0.19 | 10.0 - 19.9 | smooth |
| 0.20 - 0.24 | 20.0 - 29.10 | moderately rough |
| 0.25 - 0.29 | 30.0 - 39.9 | rough |
| >0.30 | >40 | very rough |

The roughness parameter helps to describe the morphology of shore platforms and reflects the lithology and the way in which the rock breaks apart. It is also an

important aspect in the constraining and directing of water flow across a shore platform. This will be discussed further in Chapter 6.

2.6 PROFILE DESCRIPTIONS.

This section describes and defines the shore platform profiles used in this study.

2.6.1 METHOD.

Profiles were surveyed along a shore-normal line extending from the backshore cliff to the deepest point possible. Onshore surveying was conducted using a Sokkia 'Set 3E' Total Station theodolite and single prism which has an instrumental error of $\pm 1\text{mm}$. Measurement of the profile morphology was based on identifying and surveying breaks in slope. The locations of all MEM sites were surveyed relative to the profiles. Data was reduced to a common datum (section 2.4) relative to sea level for each site.

Offshore survey of profiles was conducted using a Raytheon Surveying Fathometer, Model DE-719C, echosounder mounted on an aluminum boat. The echosounder operates at 208 HZ and has a sampling rate of 534 soundings per minute providing very good resolution in shallow water. It is accurate to within $\pm 2.5\text{cm}$ (0.5% of the indicated depth) (Allan *et al.* 1999). The onshore profile was continued offshore through the use of fixed markers onshore. Sounding began at the last point of the onshore survey and was extended as the boat maneuvered in an offshore direction in a straight line at as consistent a speed as possible. Horizontal distance was measured either by fixing the location of the sounder relative to the shore using GPS or by paying out a line marked at 5m intervals and secured on the shore. The sounder was calibrated for local water conditions by 'chain-barring'. This involved a 300x300mm metal plate being suspended a specific distance below the sounding transducer and the speed of the sounder adjusted accordingly to give a true depth reading. The trace was digitized using ArcInfo and imported into EXCEL where it was combined with the onshore survey data.

Profiles drawn for each site include locations of MEM sites and arrows indicating boundaries used for defining shore platform morphologies. Letters naming each

MEM site are shown on the figures. Morphometric parameters were measured as defined in section 2.5.2.

2.6.2 AK1

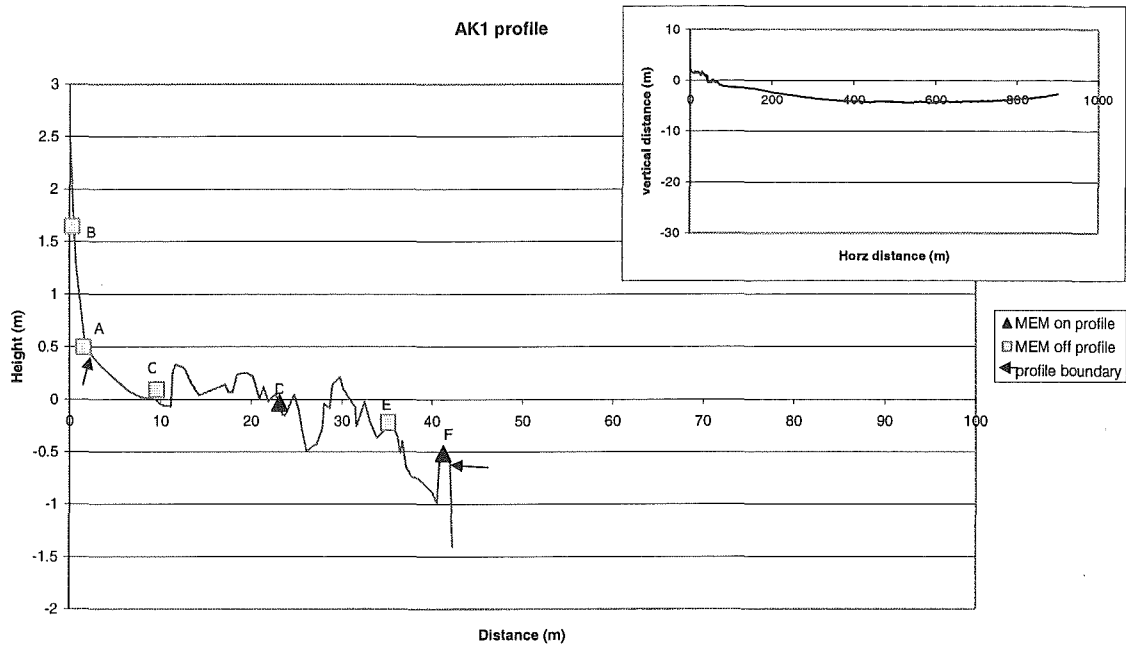


Figure 2.12: Surveyed profile of AK1. Inset shows full profile including offshore survey.

The platform at AK1 (figure 2.12) is formed in basalt off a point to the north of Robinson's Bay (figure 2.6). The platform is backed by an active cliff approximately 30m high and is a Type-B in Sunamura's classification system. It is orientated almost directly south (176°). The platform has a width of 40.4m at the profile and a gradient of $1^{\circ}25'$ tilting towards the ocean. There is a seaward drop of 1.34m and the seafloor extending seaward from here is gently sloping and composed of sand and mud. The offshore portion of the profile crosses a bay and can be seen in the upward curve of the surface towards the end of the profile.

The surface of the platform is moderately rough in the vertical and very smooth horizontally. Some scattered cobbles and pebbles occasionally covered the platform surface between 5 - 10m from the landward cliff.

Five MEM sites were distributed reasonably evenly along the profile with a sixth (AK1B) being located above high tide level on a small ledge in the cliff. AK1C was within close proximity to loose sediment.

2.6.3 AK2.

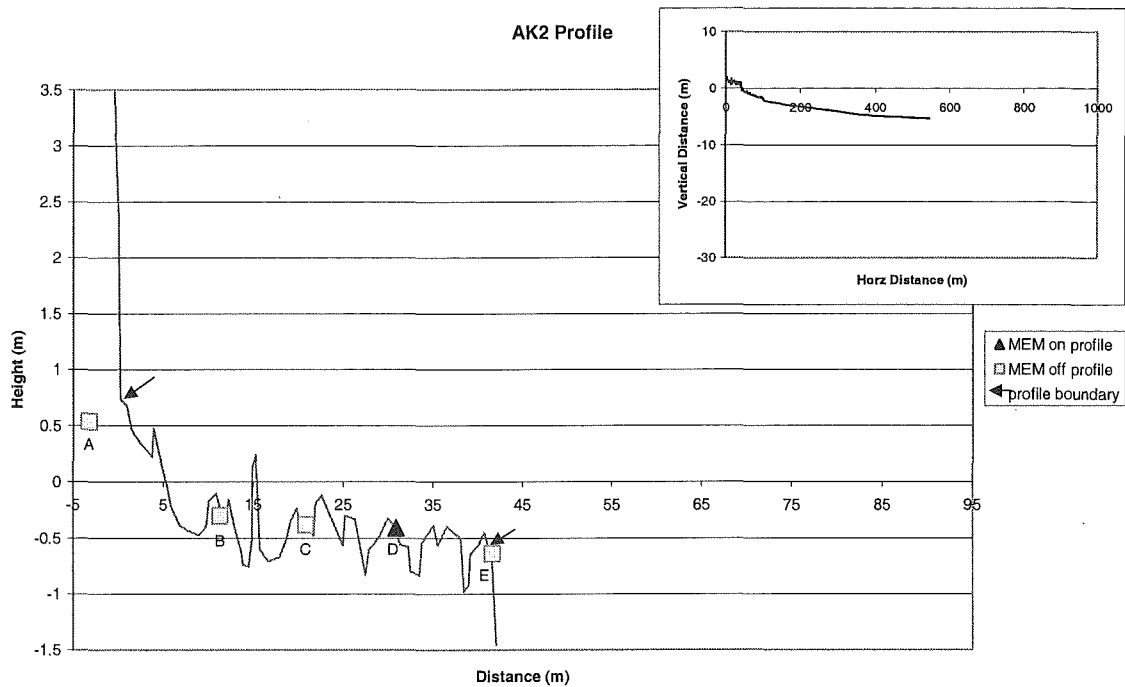


Figure 2.13: Surveyed profile of AK2. Inset shows full profile including offshore survey.

Profile AK2 (figure 2.13) is located approximately 200m north around the point from AK1. It is also formed in basalt and has a similar offshore profile with a gently sloping seafloor composed of sand and mud. A 30m high active cliff backs the platform at this point and the width is 40.7m. The orientation of the profile is 184° and the surface has a gradient of $1^\circ 07'$. There was a seaward drop of 0.87m and in Sunamura's classification system it is a Type-B platform. The surface is moderately rough vertically and very smooth horizontally. A dyke formed at right angles across the profile has resulted in a raised protuberance 15m from the landward cliff.

Five MEM sites were established along or near to the profile at roughly regular intervals. The most landward site is located 1.2 m to the east of the profile due to the difficulty of installation directly at the cliff foot on the profile itself.

Three further MEM sites were established on this platform as shown in figure 2.6.

2.6.4 KM2.

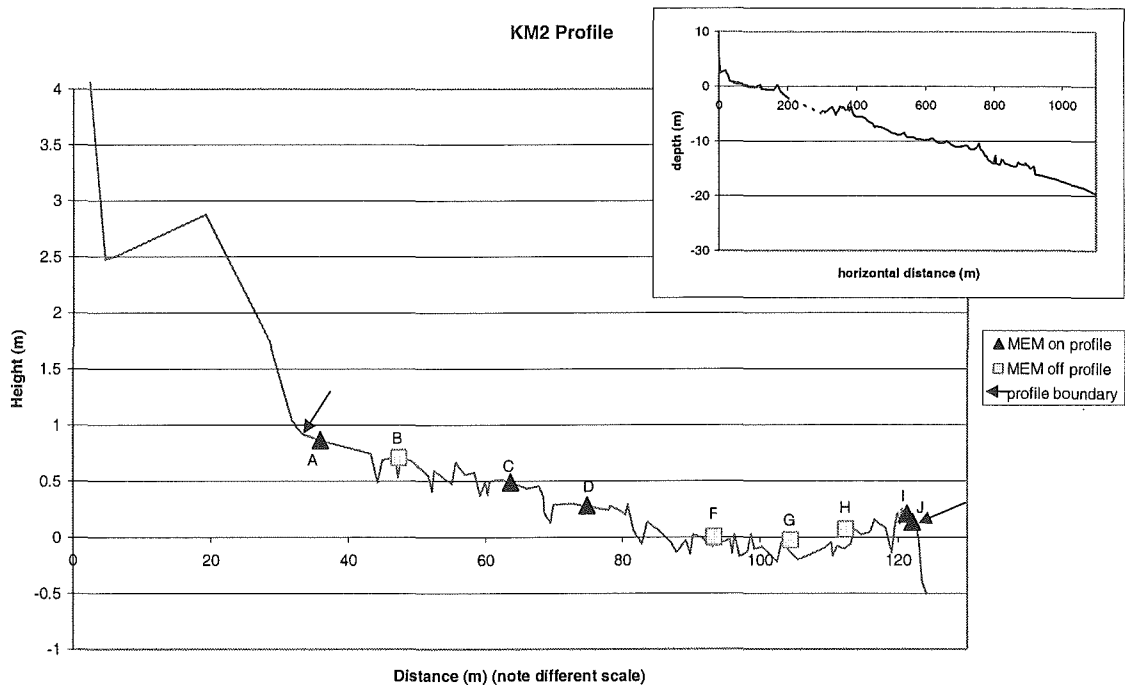


Figure 2.14: Surveyed profile of KM2. Inset shows full profile including offshore survey.

The shore platform at KM2 (figure 2.14) is formed in mudstone and backed by an active cobble beach that encloses the remnants of a lagoon between it and an abandoned marine cliff. The surface slopes gently towards the ocean with a gradient of $0^{\circ}32'$ and there is no distinct drop off at the low tide level. The profile extends in a northerly (10°) direction and is 89.1m wide. The profile displays some concavity between 80 and 120m from the landward edge and a small rampart exists immediately seaward of this. The surface of KM2 is vertically and horizontally smooth. Seaward of the rock surface the profile becomes very gently sloping with a sandy bottom (Stephenson 1997a). A number of small submerged offshore reefs are evident on the offshore portion of the profile.

Nine MEM sites were utilized along this profile. Three of these (KM2C, KM2G and KM2I) were established in 1974 (Kirk 1977) the remainder were installed in 1993 (Stephenson 1997a). The bolts of a tenth MEM site (KM2E) on this profile eroded out of the rock surface at some stage between 12/02/1999 and 15/4/1999. KM2A is located within 5 m of the limestone cobbles that make up the backing beach.

2.6.5 KM3.

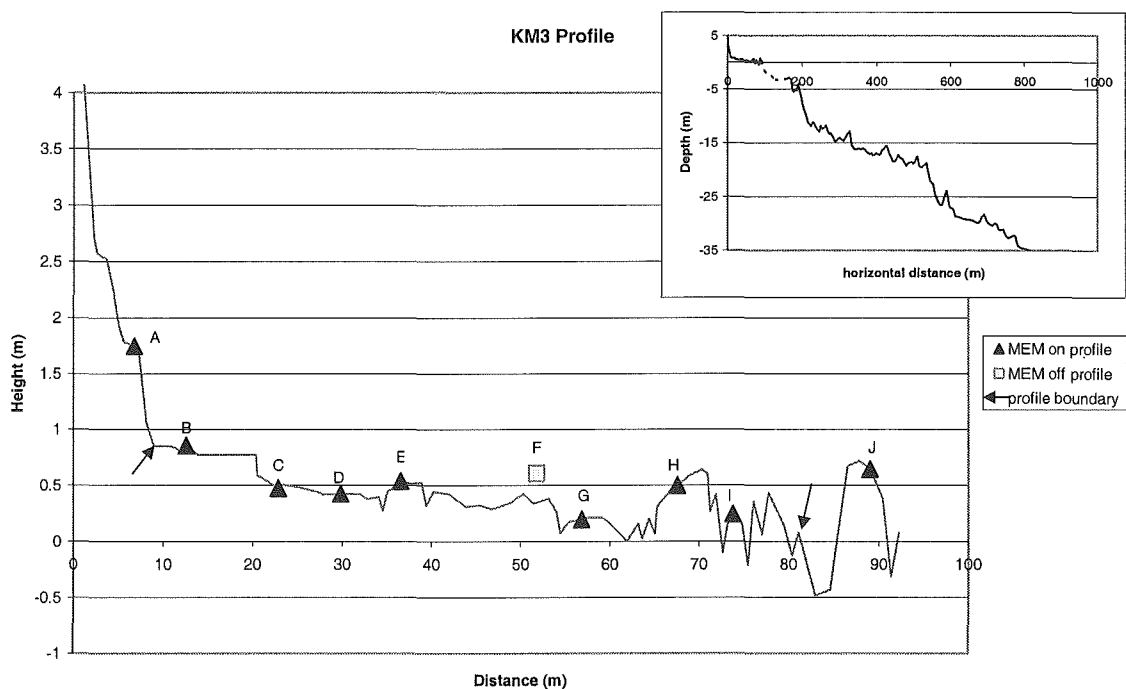


Figure 2.15: Surveyed profile of KM3. Inset shows full profile including offshore survey.

The platform at KM3 (figure 2.15) is formed in mudstone and the profile has an orientation of 133° . It is backed by an active cliff of approximately 60m in height. The seaward edge of the platform is not well defined with large channels dividing up large blocks of rock forming offshore reefs. The depth of water in front of the profile is 0.73 m and a rampart of 0.5 – 1m above the general surface of the platform is evident. The width at this point on the platform is 72.1m and the gradient is $0^{\circ}26'$ towards the ocean. In Sunamura's classification scheme this platform is Type-B. The surface is smooth both vertically and horizontally. A number of channels cross the profile following the joints within the rock and there is an 0.9 m downward step

7m from the landward cliff. A smaller downward step (0.25m) occurs another 12m seaward of this. Offshore the profile shows some submerged reefs interspersed by smoother surfaces.

10 MEM sites were utilized along this profile. The most landward site is 1.75m above msl and is very rarely inundated by the tides. The most seaward site is located on the block separated from the platform, proper, by a large channel. Three of the sites (KM3E, KM3G and KM3I) date back to installation in 1974 (Kirk 1977), the remainder were installed in 1993 (Stephenson 1997a).

2.6.6 KM7.

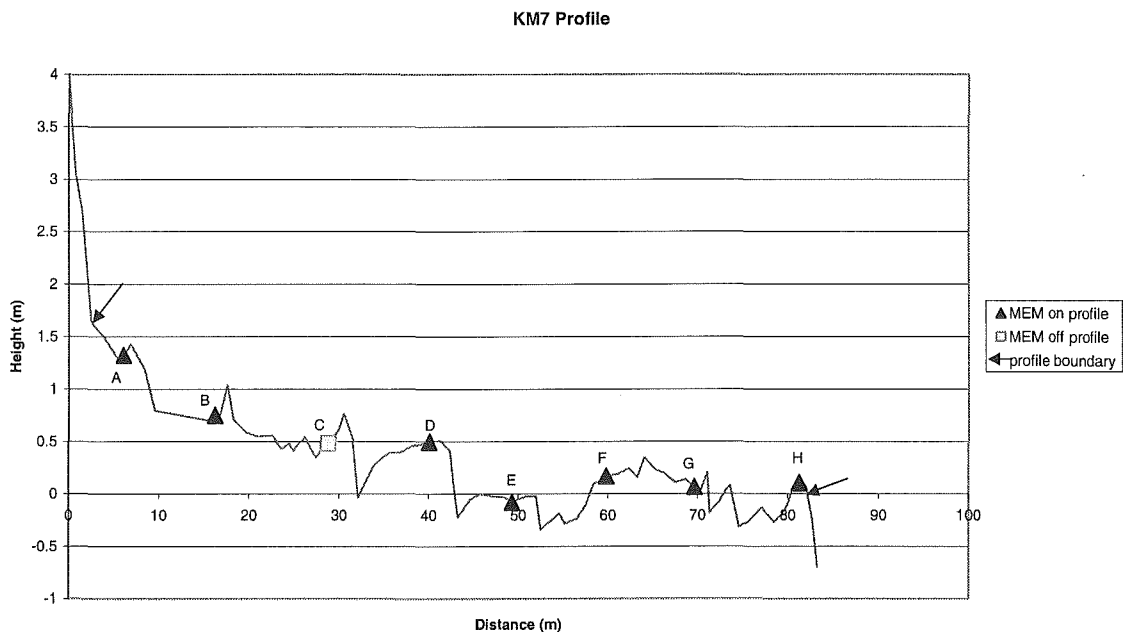


Figure 2.16: Surveyed profile of KM7.

The platform at KM7 (figure 2.16) is formed in limestone, which has been subjected to intense folding and faulting. It is backed by a cliff of approximately 80m in height and the rock surface at the seaward edge slopes gently away under the water. The platform is therefore designated as a Type A platform in Sunamura's (1992) classification scheme. Between approximately 300 - 500 m seaward of the edge of the platform is a reef of out cropping remnant limestone and mudstone surfaces. This reef meant that offshore echo sounding from this profile was not possible.

The gradient of KM7 is $0^{\circ}53'$ and it has a mean elevation of 0.27 m above sea level. Its surface is extensively fractured and a number of small channels corresponding to some of these fractures cross the profile. The surface is moderately rough in the vertical direction and smooth in the horizontal direction. The movement of sediment from a limestone cobble beach directly to the north of the profile intermittently causes the formation of a small ephemeral beach at the foot of the cliff base.

Eight MEM bolt sites installed in 1993 (Stephenson 1997a) at regular intervals along this profile were utilized for this study.

2.6.7 RM1.

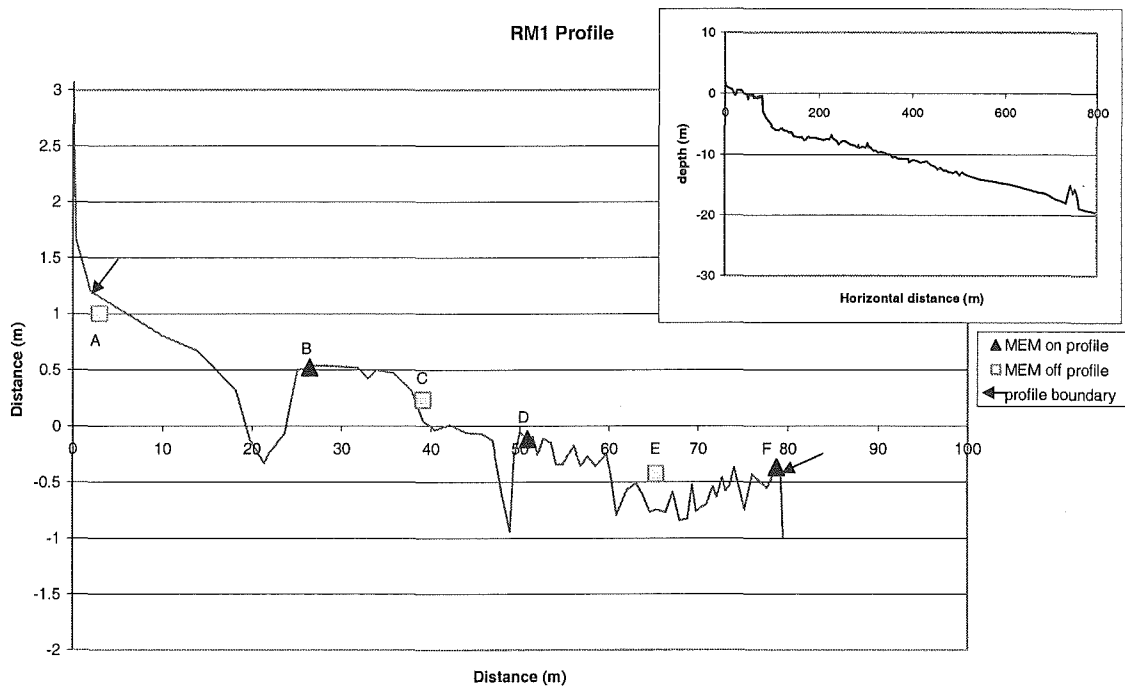


Figure 2.17: Surveyed profile of RM1. Inset shows full profile including offshore survey.

The profile at Raramai Arch (figure 2.17) traverses an extensively fractured greywacke platform backed by 50 – 60m high cliffs. A mixed sand and gravel beach extends to the north of the platform and sometimes has excursions onto the platform at the foot of the landward cliff filling the channel seen on the profile at 20m. RM1 is 74.2 m in width and has a slope of $1^{\circ}05'$ tilting towards the ocean. The seaward part of the profile from 45m beyond the landward cliff to the seaward cliff is slightly concave and is traversed by 2 channels the deepest of which is 0.75m in depth. The

depth of the seaward drop is 1.9m. In Sunamura's classification scheme this is a Type-B platform. The surface of RM1 is vertically rough and horizontally smooth. The offshore profile slopes smoothly seaward and a submerged reef was evident 750m from the shore. The offshore sea floor directly seawards of the platform has cobbles on it for approximately 30m and beyond this is sandy (Taylor, pers. comm. 2003).

Six MEM bolt sites were installed along this profile for this study, although the fractured nature of the greywacke made installation directly on the profile impossible in places. RM1A and RM1B were both located within 5m of a supply of unconsolidated sand and gravel. However at the latter location a 0.65m step prevented sediment reaching the platform surface. Eight other MEM bolt sites were also installed on the platform at Raramai Arch the locations of which can be seen in figure 2.4. RM11 was located above the level of the highest tides at 2.11m above msl. RM7 was rendered inoperative due to human interference in April 1999.

2.6.8 WK1.

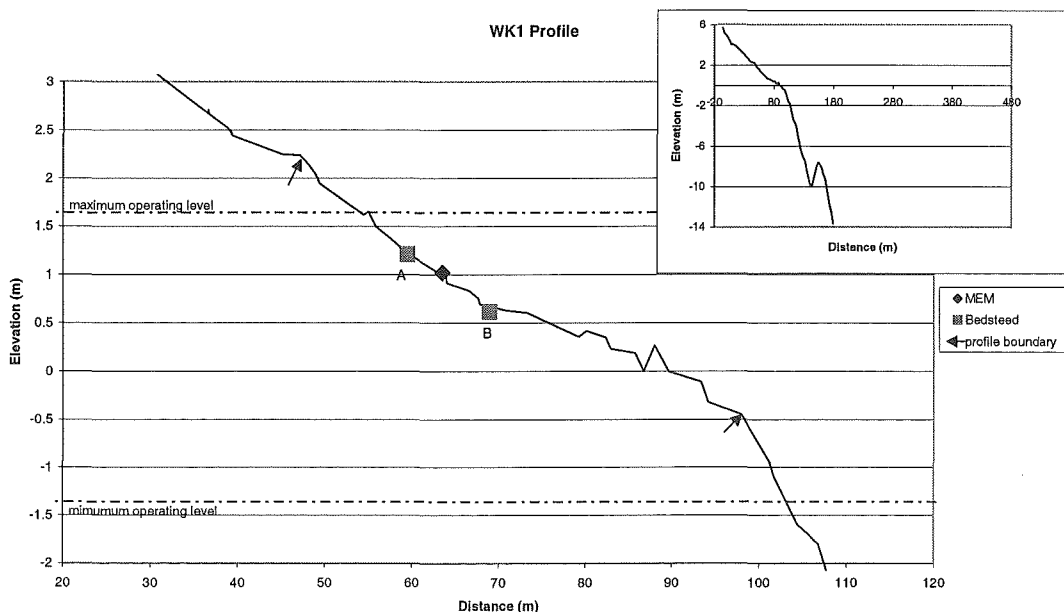


Figure 2.18: Surveyed profile of WK1. Inset shows full profile including offshore survey.

The shore platform at WK1 (figure 2.18) is formed in soft friable mudstone off a point in the Wairoa arm of Lake Waikaremoana. In Sunamura's classification scheme it is designated as a Type-A platform as it has no distinct lakeward drop. The profile has a width of 49.8m and a gradient of $2^{\circ}13'$. The mean elevation relative to mean lake level is 0.81m. The platform itself is backed by a small beach of weathered mudstone and landward of this the surface is scrub covered but continued to slope gently ($\sim 3^{\circ}$) until backed by a steep forested slope as shown in figure 2.19. Overall the profile is slightly concave in shape and very smooth.

A MEM bolt site and two Bedstead bolt sites were installed in January 1999.

2.6.9 WK2.

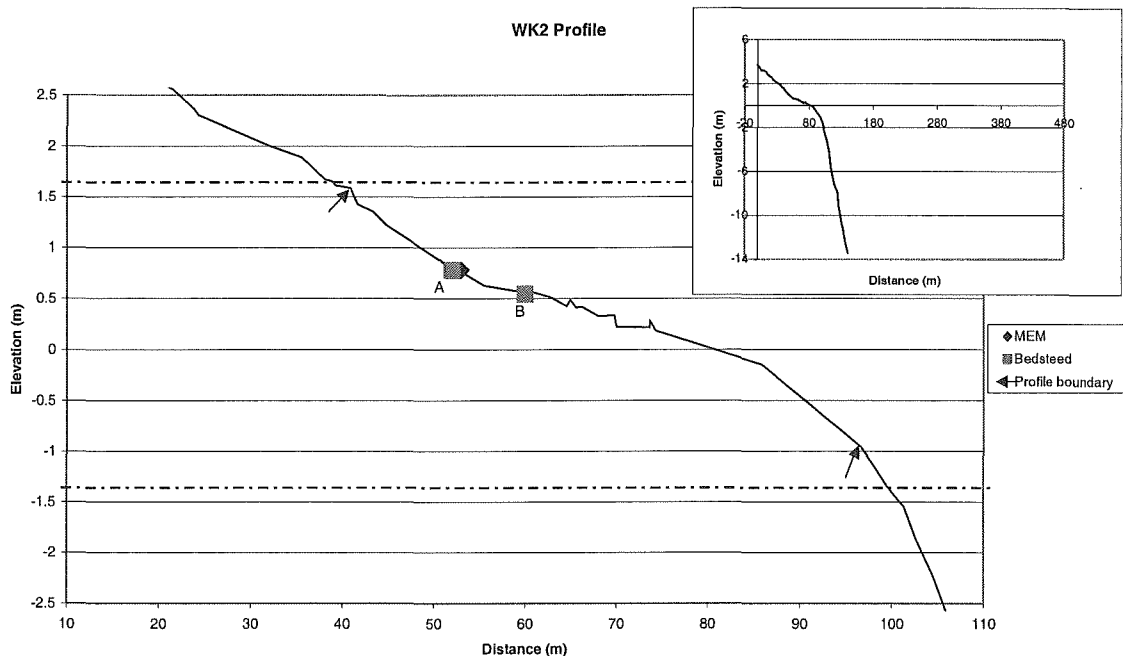


Figure 2.19: Surveyed profile of WK2. Inset shows full profile including offshore survey.

The platform at WK2 (figure 2.19) is also formed off a point in mudstone and located to the west of WK1 (figure 2.7). It is a Type-A platform in Sunamura's classification scheme. It has a width of 57.3m and a gradient of $2^{\circ}13'$. The upper half of the profile, above 582m asl, is slightly concave and the lower half is slightly convex. The mean elevation of the profile is 0.65m above mean lake level. The surface of the profile is very smooth in both the vertical and horizontal aspects.

A MEM bolt site and two Bedstead bolt sites were also installed at WK2 in January 1999.

Both the profiles used at Lake Waikaremoana are slightly different to the majority of the mudstone platforms formed on the shores of the lake in that they are wider and flatter because of their location on headlands. These profiles were utilized for this study rather than shorter steeper ones for two reasons. Platforms studied at Raramai and Akaroa are also formed off headlands and installation of the MEM system for measurement of surface change was possible on the surfaces of these platforms whereas it was not possible on the steeper surfaces.

2.6.10 COMPARISON OF MORPHOLOGIES.

The previous sections described each study profile individually. In this section a comparison is made of the morphometric aspects of the profiles formed in each different lithology. Table 2.2 presents morphometric characteristics for each of the 8 study profiles.

The platforms formed in Basalt are the narrowest of those studied with the two profiles, AK1 and AK2, both being just over 40 m wide. The two Type A platforms studied at Lake Waikaremoana are between 49 and 60 m wide and the remainder of the study profiles are over 70m wide. It is not necessarily those platforms formed in the 'hardest' rocks that are narrowest (section 4.6).

Platform gradients of profiles range from $0^{\circ}26'$ to $2^{\circ}41'$. There is a weak negative correlation ($R^2 = 0.4$) between width as an independent variable and gradient with the shorter platforms having steeper gradients. However, more data would be required to verify this relationship with any confidence.

The mean elevation of platforms varied between 0.81m above mean water level to 0.37m below mean water level. This difference in elevations is significant when considering the level shore platforms develop in relation to sea level and will be further investigated in section 4.6 with respect to parameters of rock strength.

Table 2.2: Morphometric parameters of study profiles.

| profile name | location | lithology | strike (mag°) | dip (mag°) | surface roughness | | orientation (mag°) | width (m) | gradient (°) | mean elevation (m asl) | backshore |
|--------------|---|-----------|---------------|------------|-------------------|----------------|--------------------|-----------|--------------|------------------------|-------------------------|
| | | | | | vertical (y) | horizontal (x) | | | | | |
| Ak1 | Akaroa Harbour Robinson's Bay point | Basalt | 280 | +70 | 0.20 | 7.00 | 176 | 40.4 | 1°25' | -0.11 | cliff (~30m) |
| Ak2 | Akaroa Harbour Robinson's Bay point | Basalt | 317 | +69 | 0.24 | 9.09 | 184 | 40.7 | 1°07' | -0.37 | cliff (~30m) |
| Km2 | Kaikoura Peninsula Wairepo Lagoon | Mudstone | 260 | +45 | 0.14 | 10.87 | 10 | 89.1 | 0°32' | 0.22 | active cobble beach |
| Km3 | Kaikoura Peninsula Point Kean | Mudstone | 130 | -55 | 0.15 | 13.35 | 133 | 72.1 | 0°26' | 0.36 | cliff (~60m) |
| Km7 | Kaikoura Peninsula Third Bay | Limestone | 65 | +35 | 0.23 | 12.46 | 126 | 78.7 | 0°53' | 0.27 | cliff (~80m) |
| Rm1 | Raramai Arch point | Greywacke | 250 | -80 | 0.25 | 10.26 | 138 | 74.2 | 1°05' | -0.22 | cliff (~50m) |
| Wk1 | Lake Waikaremoana Wairau arm | Mudstone | 315 | -20 | 0.11 | 2.48 | 255 | 49.8 | 2°41' | 0.81 | forested steep slope |
| Wk2 | Lake Waikaremoana Wairau arm | Mudstone | 338 | -32 | 0.11 | 2.94 | 295 | 57.3 | 2°13' | 0.65 | forested steep slope |

It is also important to note that the gradients of platforms between the landward cliff and the seaward edge are not always smooth seaward facing slopes. Therefore, distribution of elevations along a shore platform profile are not necessarily progressive. This can be seen in figure 2.20 which plots relative position of MEM bolt sites on profiles against the elevation of each site.

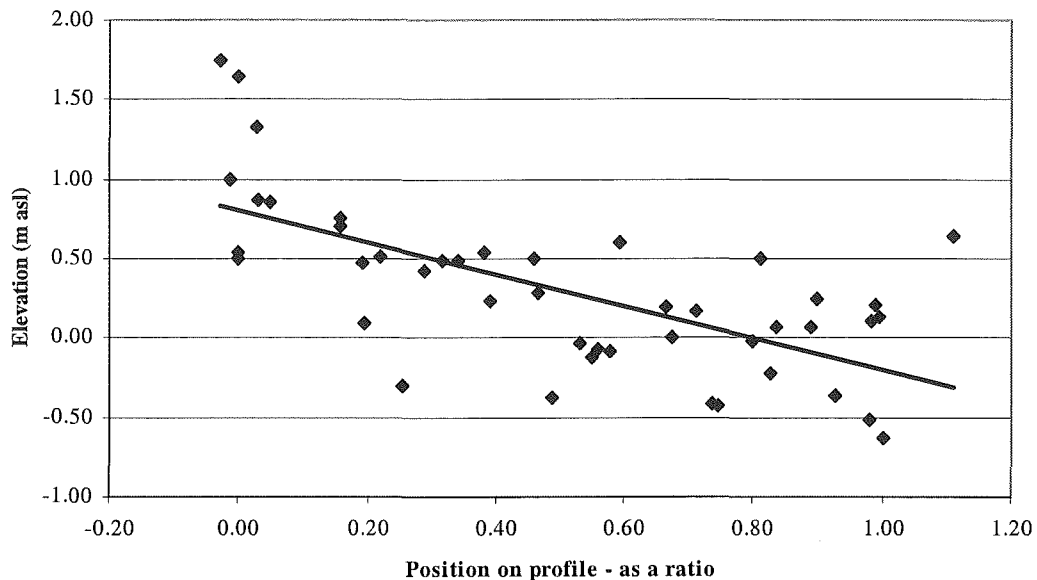


Figure 2.20: Relative position of MEM bolt sites on profiles vs. elevation of MEM bolt sites in relation to mean sea level. The position of each MEM site on the profile is given as a ratio of the total width of the platform where 0 represents locations at the landward cliff and 1 those at the seaward cliff. Some MEM sites were located outside these boundaries.

This means that processes related to progression of factors across the platform, i.e. the tide rising and falling, will not always correlate directly to the elevation of a specific location in relation to sea level.

It is also possible to analyze the distribution of elevation around mean sea level for each platform using hypsographic curves. These plot the cumulative frequency of elevations measured at regular intervals along a profile. Elevation was interpolated at 0.25m intervals across each shore platform study profile and hypsographic curves for each profile are shown in figure 2.21.

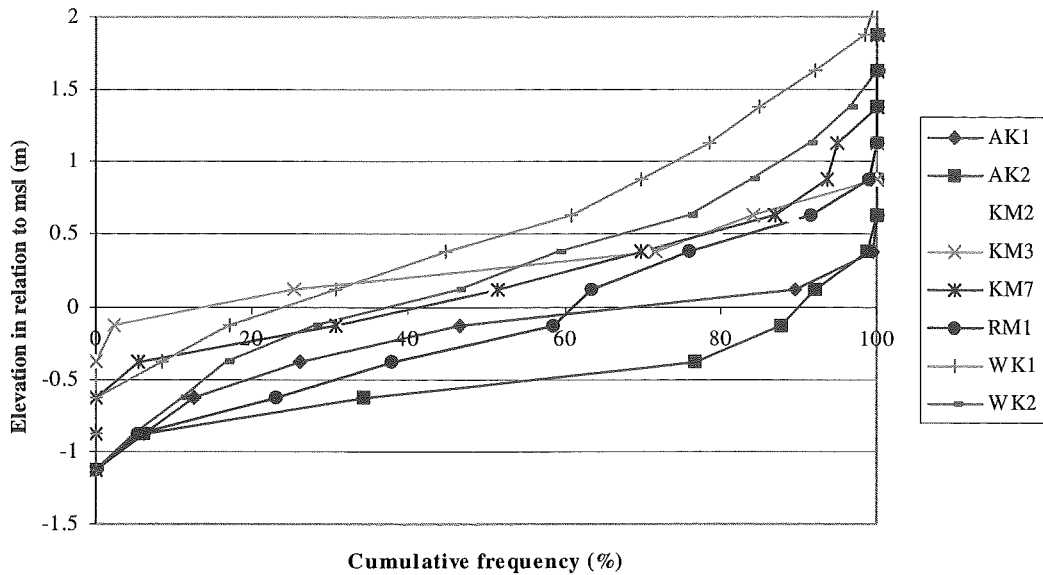


Figure 2.21: Hypsographic curves showing frequency of elevation at 0.25m intervals for each study profile.

All platforms show broadly similar distribution patterns with between 20 and 80 % of elevations distributed evenly over a narrow range of elevations. This is shown in the gentle slope of the centre portions of each curve. The profile at RM1 is the only exception to this showing a steeper step in the distribution of elevations around mean sea level. Although the curves for each profile follow similar patterns the actual distributions show that in general the greater portion of the platforms formed in the basalt and greywacke are below mean sea level. The profiles at KM2, KM3, KM7, WK1 and WK2 all had at least 60% or more of their elevations above mean sea or water level. No attempt has been made to assess reasons for these differences in level between different shore platforms here or in the literature. However this type of analysis may be a useful tool for investigating the relationship of shore platform elevation to mean sea level and the question of elevation of equilibrium profiles. It warrants further investigation using a wider range of shore platforms.

The roughness of each profile has been described at the coarse scale of greater than 0.5m of horizontal length (section 2.5.2.5 and table 2.1). This is useful when assessing the shore platform as a whole but full description of the nature of the surface should include assessment of the roughness of different rock types at a smaller scale. This may reflect something of the nature of the different rock types in which each platform is formed. Figure 2.22 shows digital elevation models of one

2450mm² area of shore platform surface for each profile. These were constructed from measurement of the elevation of 120 points relative to an arbitrary datum, sampled in a grid pattern using the Traversing MEM. The MEM method is described more fully in section 3.1. Wireframe plots were drawn using Surfer Golden Software mapping system. One representative MEM site per profile was selected for presentation in figure 2.22. An analysis of surface roughness at the micro scale has been made on a subjective basis.

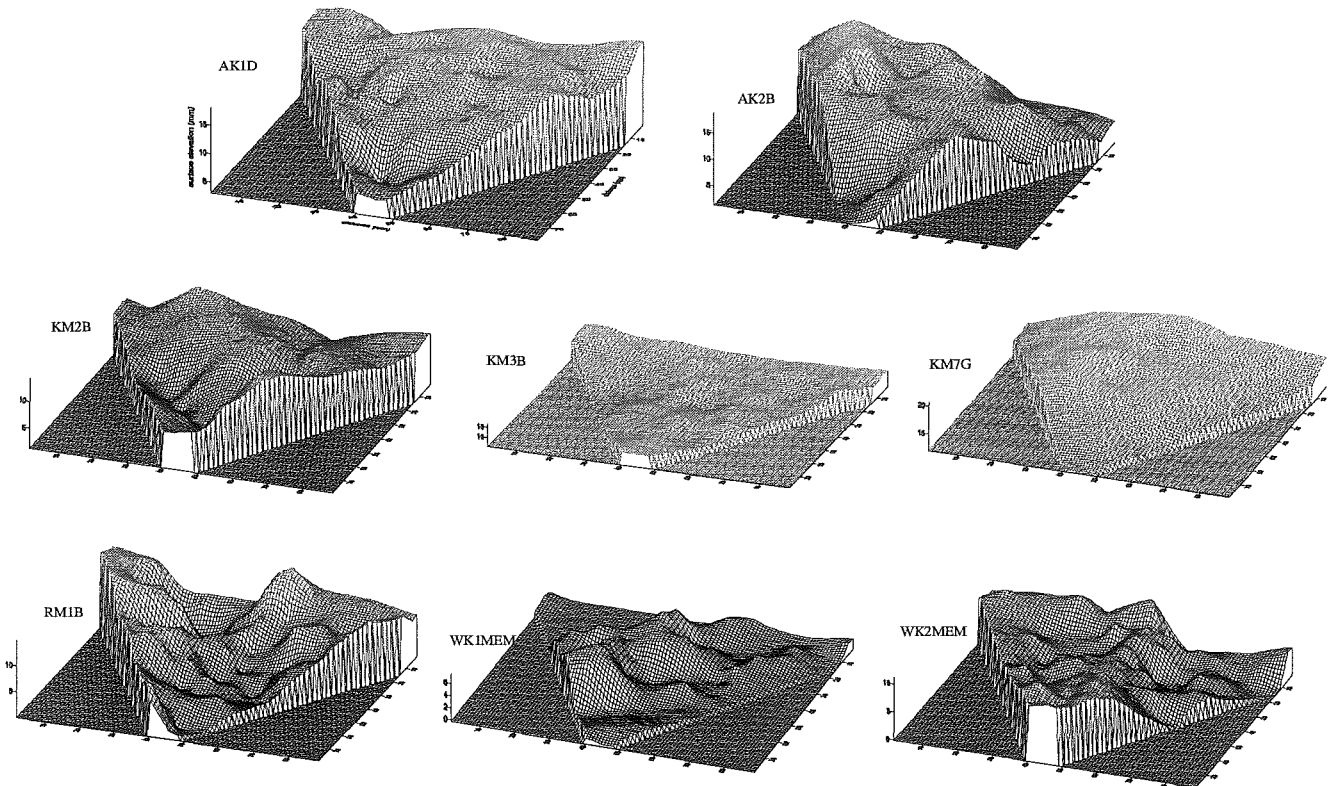


Figure 2.22: Surface elevations of rock surface. Representative wireframe contour plots for each study profile.

At this smaller (micro) scale there are also differences in roughness of the rock surfaces in which each platform has formed. At the micro scale both the basalt and greywacke are rougher than the Kaikoura mudstone and limestone with a greater range of elevations covered more frequently over the 2450mm² area. The Lake Waikaremoana mudstone also shows a jagged surface pattern over this smaller area. This differs from the large scale roughness of profiles WK1 and WK2 and reflects the weathered nature of the surface.

2.7 SUMMARY.

Platforms studied in this thesis have been formed in five different lithologies: limestone and mudstone at Kaikoura, greywacke at Raramai Arch, basalt at Robinsons Bay Point and mudstone at Lake Waikaremoana. This chapter has described the environmental conditions of the study sites and the morphology of each of the eight study profiles.

All the platforms studied experience a temperate climate. Those at Kaikoura and Raramai Arch are exposed to a high energy storm wave environment and the platforms at Robinson's Bay Point and on the shores of Lake Waikaremoana are exposed to lower energy wave environments due to the confined nature of both water bodies.

Important morphometric parameters of shore platforms defined include orientation, width, gradient, elevation and roughness. Roughness was measured at two scales of greater than half a metre and less than 0.1m. Each profile was described according to these parameters. Platforms studied in this thesis are eroded across a range of rock dips and strikes and have widths ranging from 40.4m to 89.1m. Gradients are between $2^{\circ}41'$ and $0^{\circ}26'$ and mean elevations vary between 0.81m above mean water level to 0.37m below mean water level.

CHAPTER THREE

SURFACE LEVEL CHANGES.

This chapter presents measurements of surface change on the shore platforms studied for this thesis. Measurements were made using the same method (micro erosion metre) on all rock types and are therefore comparable. Quantification and characterisation of surface change on shore platforms is an important step towards gaining an understanding of the way in which these landforms develop. It also gives an indication of the response of shore platform rocks to processes.

Many of the models presented in Chapter 1 use some measure or concept of surface lowering as a determinant of shore platform development. However, few robust quantitative assessments of the process of surface change on shore platforms have been undertaken. It is important therefore to characterize and quantify this process on a variety of shore platforms in order to provide a clearer understanding of what is actually happening.

As the process of surface lowering of rock on shore platforms is relatively slow, quantification is difficult. Any technique developed for measuring rock surface erosion faces a number of problems. These include the need for sub millimetre accuracy, on a short-term scale, the need for one or more unchanging datum points within close proximity to the measurement location and as little disturbance of the rock surface as possible during measurement. Different measurement techniques have been reported in the literature including: weathering of inscriptions (Emery 1941), erosion pins (Hodgkin 1964), plaster-casts of rock surfaces around embedded pins (Hodgkin 1964), micro erosion meters (Trudgill 1976, Robinson 1977a, 1977b, 1977c, Kirk 1977, Spencer 1981, Gill and Lang 1983, Viles and Trudgill 1984, Mottershead 1989, Stephenson and Kirk 1996, 1998, 2000a, 2000b) and laser scanners (Williams *et. al.* 2000). To date the most effective of these and the most widely utilised has been the micro erosion meter (MEM) technique. The MEM technique was utilised in this study.

To allow comparison between varying rock types it was considered important that a consistent method of surface lowering measurement was used at all monitored sites on each different rock type in this study. This was undertaken in order to eliminate any error at such a fine scale inherent between different measurement techniques. To this end the same instruments were also used at all sites.

3.1 METHODOLOGY.

The micro erosion metre was first described by High and Hanna (1970) and has been used by a number of researchers since for the quantification of surface lowering on shore platforms (Trudgill 1976, Robinson 1977a, 1977b, 1977c, Kirk 1977, Spencer 1981, Gill and Lang 1983, Viles and Trudgill 1984, Mottershead 1989, Stephenson and Kirk 1996, 1998, 2000a, 2000b). It utilises a measuring gauge of sub-millimetre accuracy relocated in exactly the same location on the rock surface for each successive survey. A description of the MEM method as it pertains to this study follows.

At each survey site three expanding masonry bolts were installed. They were recessed below the rock surface at the apex points of an equilateral triangle measuring 150 mm on each side. Each bolt was secured using a machined screw pin with a hemispherical surface on the top. An engineering gauge mounted on a triangular plate with legs at each apex is then placed on these bolts with the base of the legs resting on the hemispherical surface. Exact relocation is accomplished via Kelvin's clamp principle where the base of each leg is shaped differently in order to facilitate exact placement in three dimensions. One foot is cone shaped, one wedge shaped and the third is flat. The gauge then measures the distance from the plate to the surface of the rock. The bolts provide an arbitrary datum from which measurements are made to a high degree of accuracy, under the proviso that the bolts remain undisturbed (Kirk 1977). As the surface of the rock erodes the bolts are progressively exposed. At some sites, bolts were eroded out of the rock surface completely after a period of time (see end piece). At Kaikoura this occurred over a time period of greater than 3 years and in some cases bolts have been in place for in excess of 28 years. At Lake Waikaremoana one set of bolts were eroded out of the surface within one year.

Two different micro erosion meter (MEM) gauges were used for this project.

- 1). A mechanical MEM (figure 3.1 a) with a mechanical engineering gauge set off centre in a plate which, by rotation of the tripod, gives three separate measures at each site (described by Kirk 1977). The instrumental error of this gauge is $\pm 0.01\text{mm}$.
- 2). A traversing MEM (figure 3.1 b) with an electronic gauge mounted on arms set at 120° intervals. This gauge is placed on a triangular stand with legs and ball bearings glued along each side enabling exact relocation of 120 separate points within a triangle of 2450 mm^2 (described by Stephenson 1997b). The traversing MEM logs directly into a lap top computer using a DOS based spreadsheet programme. The instrumental error of this gauge is $\pm 0.001\text{mm}$

In some locations the distance to the rock surface from the plate required the addition of probe extensions. This was only possible with the mechanical MEM. Both instruments were calibrated at regular intervals during the study period using a specially machined steel block.

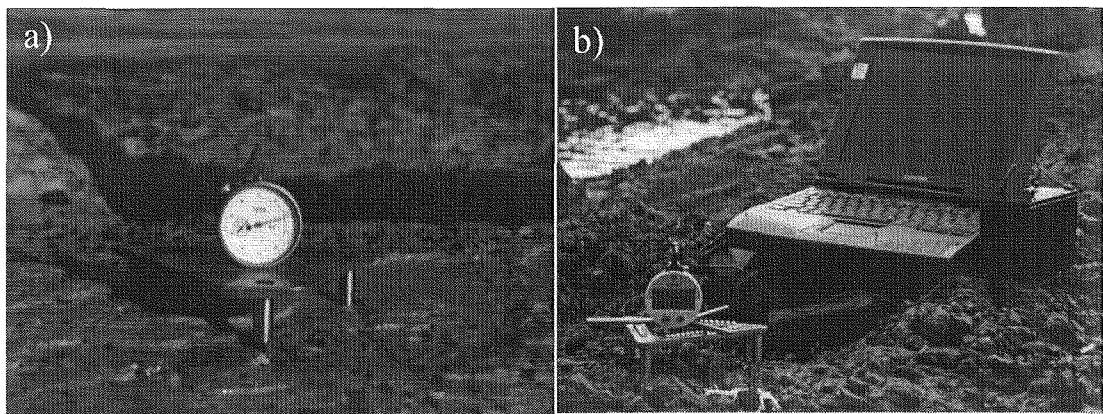


Figure 3.1: Micro erosion metres used for this study. a). mechanical MEM, b). traversing MEM.

Installation of the bolts for use in this measuring technique was difficult in some locations. Restriction in the ranges of the gauges meant that sites needed to be located on relatively horizontal surfaces. Also, both the greywacke and basalt fractured easily, especially when assaulted with an industrial hammer action drill. This meant that placement of sites in highly fractured zones was not possible. Both these factors may bias the results to some extent. However, quantification of this

bias will not be possible until less obtrusive micro erosion measuring methods are available for comparison.

At Lake Waikaremoana the mudstone in which the shore platforms are formed is highly friable. This made drilling bolt holes within close proximity to each other difficult. For this reason another instrument which utilises more widely spaced bolts was used in conjunction with MEM measurements. This instrument, called a Bedstead frame (figure 3.2), consists of a frame with guide holes drilled into it at regular intervals and mounted on three legs spaced 580mm apart. It relocates exactly using Kelvin's clamp principle and measurements are made between the frame and the rock using a stainless steel probe.

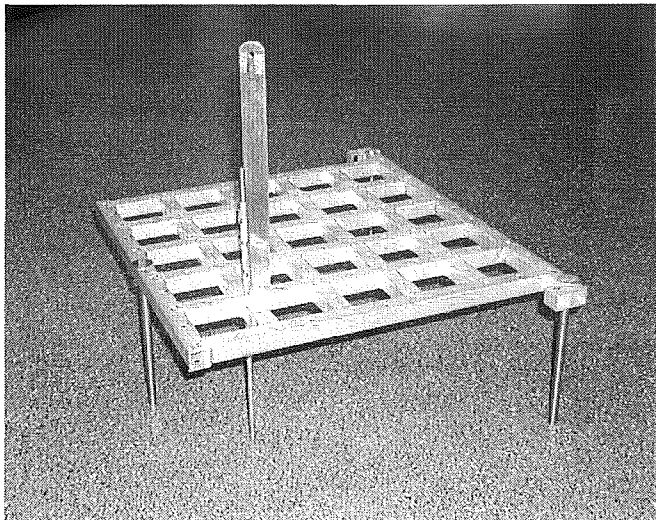


Figure 3.2: The bedstead frame.

Both MEM and bedstead frame sites were installed at Lake Waikaremoana in order to give a comparison across measurement methods. Both methods yielded similar results of surface change within this environment and were therefore considered comparable.

At all sites some disturbance of the rock surface during bolt installation was inevitable. However this was kept to a minimum and once bolts were installed the surfaces were left to rest and settle for up to one month prior to initial measurement.

The possible effects of the bolt holes, or the bolts themselves, on surface change was minimised by measurements being made of only the centre portion of the rock

between the bolt holes. No measurements were made within 40 mm of bolt holes. The possible effect of the bolt holes on rock surface changes was not investigated here. Visually, in most cases, there appeared to be very little effect. However in a few instances on the Kaikoura mudstone the effect of water sitting in the holes could be seen but was not quantified. At these sites the region in immediate proximity to the holes remained noticeably higher than the surrounding surface. Figure 3.3 is an example of the effect of water remaining pooled between tides in a hole on a mudstone surface near KM2B. Note that this hole is larger than the bolt holes and is shown here as an example because the effect was clearly discernible.

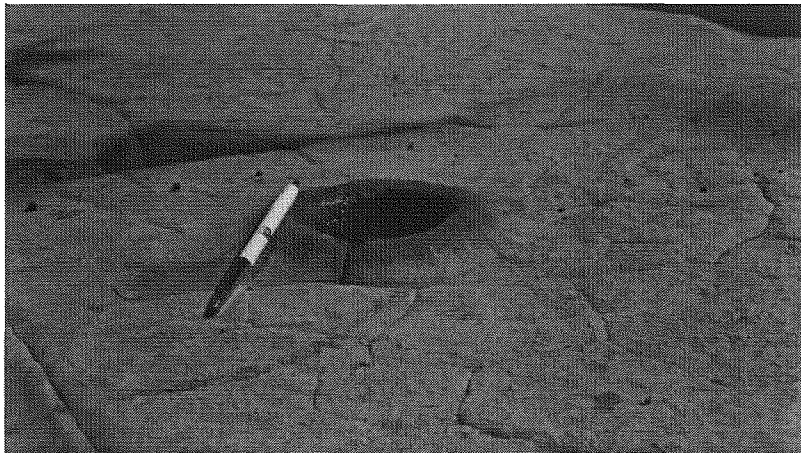


Figure 3.3: Different surface level surrounding a water filled hole near KM2B. Note that the hole is larger than bolt holes where similar raised edges occasionally occurred but at a smaller scale. The pen is 135mm in length.

The validity of using micro scale measurements to characterise average rates of erosion on shore platforms has been questioned by Kirk (1977) and Trenhaile (1987). Trenhaile (1987) suggested that erosion at a larger scale, in the form of chips and removal of blocks associated with the more easily fractured parts of the surface would not be measured by using the MEM technique. The necessity of installing MEM bolt sites away from fracture zones etc. could exclude measurement of erosion at what some assume to be the most vulnerable part of the rock.

An attempt was made in this study, by use of photogrammetry to develop a larger scale method of measurement which would give an indication of erosion, in the form of chips and removal of blocks. Photogrammetry uses stereo photography of the rock to produce a digital elevation model (DEM) of the surface. It has been successfully used to monitor a number of geomorphological features (Lane *et. al.*

1998). Two of these are soil surface development (Merel and Farries 1998) and sub-aerial riverbed gravels (Lane *et. al.* 1996).

Photogrammetry was trialed at 3 – 6 sites on each rock type with a total of 15 sites in all being monitored using this method. At each site a 900cm² area of surface was photographed in stereo. A requirement of this method of surface monitoring is that at least three constant datum points must be present within successive photographs. To fulfil this requirement the bolts of MEM sites were utilised. It was intended that successive DEMs taken at 2 –3 month intervals over a two year period would provide further information on surface change at a scale greater than that of the MEM monitoring.

At the 15 sites monitored using this method over the two year period no discernible erosion occurred at a scale larger than that measured by the MEM technique. The greater accuracy acquired using the MEM methods was therefore considered to be a more useful measure of surface change. Photogrammetry may be a useful method of measuring erosion of shore platform surfaces, if developed at a larger scale and over a longer period than trialed here. This longer period observation was not within the time scope of this thesis.

While an accurate method with which to measure this larger scale erosion has yet to be developed, the MEM gives the best possible quantification of rock surface change available at this time. The scale of change measured also means that this is a base rate of erosion for the shore platform. Any larger chunks of rock removed from the platform surface will therefore add to overall erosion. Rates measured using the MEM method have been shown to be more than capable of forming present day platforms at Kaikoura (Kirk 1977).

Another concern expressed about the use of the MEM technique has been the reliability of measurements made over a geomorphically short time span, of what is, temporally, a relatively slow process (Trenhaile 1987, Viles and Trudgill 1984). Stephenson and Kirk (1996) compared long and short term data measured at 15 individual MEM sites on the Kaikoura Peninsula. They compared measurements at each site made over a 20 year period with those made over a 2 year period and found

that the average lowering rate for both the shorter and longer term data were in statistical agreement. This concern will be further addressed in section 3.4.2.

A third concern about the use of MEM techniques in assessment of shore platform surface change is the extrapolation of measurement of a small area to an entire platform. As Stephenson and Kirk (1996:210) state ‘Clearly this is dependent on how much area is to be considered and the degree of variability in the morphogenetic environment.’ The question of how many sites were required to give an accurate representation of overall erosion rate for a shore platform was addressed by Mottershead (1989) who suggested that 30 measurements were sufficient to calculate a representative mean annual lowering rate on the Start-Prawle Peninsula, UK. Stephenson and Kirk (1996) showed statistically, that 30 measurements characterised surface lowering rates adequately on the Kaikoura Peninsula. For this reason greater than 30 individual measurements were used on each shore platform monitored in this study.

Locations of MEM bolt sites were given in section 2.6 with between 5 and 10 sites positioned along each study profile. A number of sites on the Kaikoura peninsula were installed prior to commencement of this study (section 2.6) and have records extending up to 27 years in length. Table 3.1 presents a record of monitoring of each MEM site undertaken for this thesis. It includes previous monitoring of each site installed prior to this thesis.

Table 3.1: MEM site monitoring history.

| site | date of installation | total length of record (days) | monitoring | | | |
|------|----------------------|-------------------------------|------------|---------------------------|-------------------|--------------------------|
| | | | author | dates of monitoring | number of surveys | interval between surveys |
| AK1A | Apr 1998 | 950 | This study | 11 Apr 1998 - 16 Nov 2000 | 12 | 2-3 months |
| AK1B | Apr 1998 | 950 | This study | 11 Apr 1998 - 16 Nov 2000 | 12 | 2-3 months |
| AK1C | Apr 1998 | 950 | This study | 11 Apr 1998 - 16 Nov 2000 | 12 | 2-3 months |
| AK1D | Apr 1998 | 950 | This study | 11 Apr 1998 - 16 Nov 2000 | 12 | 2-3 months |
| AK1E | Apr 1998 | 950 | This study | 11 Apr 1998 - 16 Nov 2000 | 12 | 2-3 months |
| AK1F | Apr 1998 | 950 | This study | 11 Apr 1998 - 16 Nov 2000 | 12 | 2-3 months |
| AK2A | Apr 1998 | 950 | This study | 11 Apr 1998 - 16 Nov 2000 | 12 | 2-3 months |
| AK2B | Apr 1998 | 950 | This study | 11 Apr 1998 - 16 Nov 2000 | 12 | 2-3 months |
| AK2C | Apr 1998 | 950 | This study | 11 Apr 1998 - 16 Nov 2000 | 12 | 2-3 months |
| AK2D | Apr 1998 | 950 | This study | 11 Apr 1998 - 16 Nov 2000 | 12 | 2-3 months |
| AK2E | Apr 1998 | 950 | This study | 11 Apr 1998 - 16 Nov 2000 | 12 | 2-3 months |

Table 3.1 continued: MEM site monitoring history.

| | | | | | | |
|------|----------|------|----------------|---------------------------|----|-------------|
| AK3A | Apr 1998 | 950 | This study | 11 Apr 1998 - 16 Nov 2000 | 12 | 2-3 months |
| AK3B | Apr 1998 | 950 | This study | 11 Apr 1998 - 16 Nov 2000 | 12 | 2-3 months |
| AK3C | Apr 1998 | 950 | This study | 11 Apr 1998 - 16 Nov 2000 | 12 | 2-3 months |
| KM2A | Dec 1993 | 2470 | Stephenson '97 | 22 Dec 1993 - 28 Feb 1996 | 5 | 2-9 months |
| | | | This study | 13 May 1998 - 26 Sep 2000 | 12 | 2-3 months |
| KM2B | Dec 1993 | 2470 | Stephenson '97 | 22 Dec 1993 - 28 Feb 1996 | 6 | 2-9 months |
| | | | This study | 13 May 1998 - 26 Sep 2000 | 12 | 2-3 months |
| KM2C | Mar 1974 | 9681 | Kirk '77 | 29 Mar 1974 - Mar 1975 | 6 | 2 months |
| | | | Stephenson '97 | 22 Dec 1993 - 28 Feb 1996 | 5 | 2-9 months |
| | | | This study | 13 May 1998 - 26 Sep 2000 | 12 | 2-3 months |
| KM2D | Dec 1993 | 2470 | Stephenson '97 | 22 Dec 1993 - 28 Feb 1996 | 6 | 2-9 months |
| | | | This study | 13 May 1998 - 26 Sep 2000 | 12 | 2-3 months |
| KM2E | Mar 1974 | 9084 | Kirk '77 | 29 Mar 1974 - Mar 1975 | 6 | 2 months |
| | | | Stephenson '97 | 22 Dec 1993 - 28 Feb 1996 | 4 | 2-9 months |
| | | | This study | 13 May 1998 - 12 Feb 1999 | 4 | 2-3 months |
| KM2F | Dec 1993 | 2470 | Stephenson '97 | 22 Dec 1993 - 28 Feb 1996 | 5 | 2-9 months |
| | | | This study | 13 May 1998 - 26 Sep 2000 | 12 | 2-3 months |
| KM2G | Feb 1974 | 9343 | Kirk '77 | 26 Feb 1974 - Mar 1975 | 6 | 2 months |
| | | | Stephenson '97 | 22 Dec 1993 - 28 Feb 1996 | 5 | 2-9 months |
| | | | This study | 13 May 1998 - 26 Sep 2000 | 12 | 2-3 months |
| KM2H | Dec 1993 | 2470 | Stephenson '97 | 22 Dec 1993 - 28 Feb 1996 | 4 | 2-9 months |
| | | | This study | 13 May 1998 - 26 Sep 2000 | 12 | 2-3 months |
| KM2I | Feb 1974 | 9343 | Kirk '77 | 26 Feb 1974 - Mar 1975 | 6 | 2 months |
| | | | Stephenson '97 | 22 Dec 1993 - 28 Feb 1996 | 4 | 2-9 months |
| | | | This study | 13 May 1998 - 26 Sep 2000 | 12 | 2-3 months |
| KM2J | Dec 1993 | 2470 | Stephenson '97 | 22 Dec 1993 - 28 Feb 1996 | 6 | 2-9 months |
| | | | This study | 13 May 1998 - 26 Sep 2000 | 12 | 2-3 months |
| KM3A | Dec 1993 | 2516 | Stephenson '97 | 21 Dec 1993 - 27 Feb 1996 | 6 | 2-9 months |
| | | | This study | 13 May 1998 - 10 Nov 2000 | 13 | 2-3 months |
| KM3B | Dec 1993 | 2516 | Stephenson '97 | 21 Dec 1993 - 27 Feb 1996 | 6 | 2-9 months |
| | | | This study | 13 May 1998 - 10 Nov 2000 | 13 | 2-3 months |
| KM3C | Dec 1993 | 2516 | Stephenson '97 | 21 Dec 1993 - 27 Feb 1996 | 5 | 2-9 months |
| | | | This study | 13 May 1998 - 10 Nov 2000 | 13 | 2-3 months |
| KM3D | Dec 1993 | 2471 | Stephenson '97 | 21 Dec 1993 - 27 Feb 1996 | 5 | 2-9 months |
| | | | This study | 13 May 1998 - 26 Sep 2000 | 12 | 2-3 months |
| KM3E | Feb 1974 | 9343 | Kirk '77 | 26 Feb 1974 - Mar 1975 | 6 | 2 months |
| | | | Stephenson '97 | 21 Dec 1993 - 27 Feb 1996 | 4 | 2-9 months |
| | | | This study | 13 May 1998 - 26 Sep 2000 | 12 | 2-3 months |
| KM3F | Dec 1993 | 2516 | Stephenson '97 | 21 Dec 1993 - 27 Feb 1996 | 5 | 2-9 months |
| | | | This study | 13 May 1998 - 10 Nov 2000 | 13 | 2-3 months |
| KM3G | Feb 1974 | 9388 | Kirk '77 | 26 Feb 1974 - Mar 1975 | 6 | 2 months |
| | | | Stephenson '97 | 21 Dec 1993 - 27 Feb 1996 | 5 | 2-9 months |
| | | | This study | 13 May 1998 - 10 Nov 2000 | 13 | 2-3 months |
| KM3H | Dec 1993 | 2516 | Stephenson '97 | 21 Dec 1993 - 27 Feb 1996 | 5 | 2-9 months |
| | | | This study | 13 May 1998 - 10 Nov 2000 | 12 | 2-3 months |
| KM3I | Feb 1974 | 9270 | Kirk '77 | 24 Jun 1974 - Mar 1975 | 6 | 2 months |
| | | | Stephenson '97 | 21 Dec 1993 - 27 Feb 1996 | 4 | 2-9 months |
| | | | This study | 13 May 1998 - 10 Nov 2000 | 12 | 2-3 months |
| KM3J | Dec 1993 | 2471 | Stephenson '97 | 21 Dec 1993 - 27 Feb 1996 | 6 | 2-9 months |
| | | | This study | 13 May 1998 - 26 Sep 2000 | 10 | 2-3 months |
| KM7A | Dec 1993 | 2471 | Stephenson '97 | 22 Dec 1993 - 2 Mar 1996 | 3 | 2-12 months |
| | | | This study | 25 May 1998 - 27 Sep 2000 | 11 | 2-3 months |
| KM7B | Dec 1993 | 2471 | Stephenson '97 | 22 Dec 1993 - 2 Mar 1996 | 5 | 2-12 months |
| | | | This study | 14 Mar 1998 - 27 Sep 2000 | 12 | 2-3 months |
| KM7C | Dec 1993 | 2471 | Stephenson '97 | 22 Dec 1993 - 2 Mar 1996 | 4 | 2-12 months |
| | | | This study | 14 Mar 1998 - 27 Sep 2000 | 12 | 2-3 months |
| KM7D | Dec 1993 | 2471 | Stephenson '97 | 22 Dec 1993 - 2 Mar 1996 | 3 | 2-12 months |
| | | | This study | 14 Mar 1998 - 27 Sep 2000 | 12 | 2-3 months |

Table 3.1 continued: MEM site monitoring history.

| | | | | | | |
|--------|----------|------|----------------|---------------------------|----|-------------|
| KM7E | Dec 1993 | 2471 | Stephenson '97 | 22 Dec 1993 - 2 Mar 1996 | 1 | 2-12 months |
| | | | This study | 14 Mar 1998 - 27 Sep 2000 | 8 | 2-3 months |
| KM7F | Dec 1993 | 2471 | Stephenson '97 | 22 Dec 1993 - 2 Mar 1996 | 4 | 2-12 months |
| | | | This study | 14 Mar 1998 - 27 Sep 2000 | 12 | 2-3 months |
| KM7G | Dec 1993 | 2471 | Stephenson '97 | 22 Dec 1993 - 2 Mar 1996 | 4 | 2-12 months |
| | | | This study | 14 Mar 1998 - 27 Sep 2000 | 12 | 2-3 months |
| KM7H | Dec 1993 | 2471 | Stephenson '97 | 22 Dec 1993 - 2 Mar 1996 | 4 | 2-12 months |
| | | | This study | 14 Mar 1998 - 27 Sep 2000 | 12 | 2-3 months |
| RM1A | Feb 1998 | 898 | This study | 23 May 1998 - 6 Nov 2000 | 12 | 2-3 months |
| RM1B | Feb 1998 | 898 | This study | 23 May 1998 - 6 Nov 2000 | 12 | 2-3 months |
| RM1C | Feb 1998 | 898 | This study | 23 May 1998 - 6 Nov 2000 | 12 | 2-3 months |
| RM1D | Feb 1998 | 898 | This study | 23 May 1998 - 6 Nov 2000 | 12 | 2-3 months |
| RM1E | Feb 1998 | 898 | This study | 23 May 1998 - 6 Nov 2000 | 9 | 2-3 months |
| RM1F | Feb 1998 | 898 | This study | 23 May 1998 - 6 Nov 2000 | 10 | 2-3 months |
| RM2 | Feb 1998 | 191 | This study | 23 May 1998 - 30 Nov 1998 | 3 | 2-3 months |
| RM7 | Feb 1998 | 521 | This study | 23 May 1998 - 26 Oct 1999 | 2 | 2-3 months |
| RM8 | Feb 1998 | 898 | This study | 23 May 1998 - 6 Nov 2000 | 7 | 2-3 months |
| RM9 | Feb 1998 | 898 | This study | 23 May 1998 - 6 Nov 2000 | 12 | 2-3 months |
| RM10 | Feb 1998 | 898 | This study | 23 May 1998 - 6 Nov 2000 | 12 | 2-3 months |
| RM11 | Feb 1998 | 898 | This study | 23 May 1998 - 6 Nov 2000 | 12 | 2-3 months |
| RM12 | Feb 1998 | 898 | This study | 23 May 1998 - 6 Nov 2000 | 12 | 2-3 months |
| RM13 | Feb 1998 | 898 | This study | 23 May 1998 - 6 Nov 2000 | 9 | 2-3 months |
| WK1mem | Jan 1999 | 1147 | This study | 20 Jan 1999 - 12 Mar 2002 | 3 | yearly |
| WK1bsA | Jan 1999 | 1147 | This study | 20 Jan 1999 - 12 Mar 2002 | 2 | yearly |
| WK1bsB | Jan 1999 | 0 | This study | 20 Jan 1999 - 12 Mar 2000 | 0 | yearly |
| WK2mem | Jan 1999 | 780 | This study | 20 Jan 1999 - 10 Mar 2001 | 1 | yearly |
| WK2bsA | Jan 1999 | 1147 | This study | 20 Jan 1999 - 12 Mar 2002 | 3 | yearly |
| WK2bsB | Jan 1999 | 1147 | This study | 20 Jan 1999 - 12 Mar 2002 | 3 | yearly |
| WKM2 | Jan 1999 | 1147 | This study | 20 Jan 1999 - 12 Mar 2002 | 2 | yearly |
| WKM5 | Jan 1999 | 1147 | This study | 20 Jan 1999 - 12 Mar 2002 | 3 | yearly |
| WKM9b | Jan 1999 | 1147 | This study | 20 Jan 1999 - 12 Mar 2002 | 3 | yearly |

A total of 65 MEM measurement sites were monitored for this study. Surveys of sites on marine platforms for this thesis were made at reasonably regular intervals of 2 to 3 months between 13 February 1998 and 16 November 2000. At Lake Waikaremoana surveys were made at yearly intervals between 20 January 1999 and 12 March 2002. Each site was surveyed between 4 and 13 times during the study period. The maximum record length was 1147 days at WK1MEM and WK2MEM.

Surveys were made during daylight hours and in dry weather only. Not all sites were measured on every possible occasion due to a number of factors. Some of the seaward sites were located on exposed surfaces, usually at the top of the seaward cliff, where waves made measurement impossible, even at low tide, during a number of field excursions. In some locations bolt sites were covered by sediment at the designated time of measurement. This occurred occasionally at KM7A and most

notably at sites on Lake Waikaremoana shore platforms where removal of debris would have disturbed the surface itself, leading to inaccurate results. Some sites were covered with vegetation and algal growth at various times of the year preventing accurate measurement of the surface. This was often the case at KM7D and RM1F. Species of algae included *Scytosiphon lomentaria*, *Porphyra columbina*, *Enteromorpha ramulosa* (Stephenson 1997) *Corallina officinalis* and *Lithothamnion species*.

Where barnacles (*Chaemosipho species*) or limpets (*Cellana species*) had established themselves on the rock surface between measurements they were carefully removed prior to measurement. Barnacles tended to grow on the more seaward sites at Raramai Arch and Robinson's Bay Point.

3.2 MEASUREMENTS OF SURFACE CHANGES.

Surface changes measured at each MEM bolt site are presented in figures 3.4 – 3.11. The surface level at each re-survey was calculated from the average level of all measurements taken at that site on that survey. Plots of change for each MEM bolt site along a profile have been drawn on the same figure and labelled accordingly, from A at the most landward site with others lettered in order from this to the most seaward (see figures 2.12 – 2.19). Surface level is shown, starting from a level of zero for the first survey. The surface level of successive surveys relative to this first survey are plotted. Negative numbers represent levels lower than the original and show erosion of the rock surface. Positive numbers represent surface levels higher than those of the original survey and show surface swelling. There was no unconsolidated sediment present on any of the surfaces when they were measured.

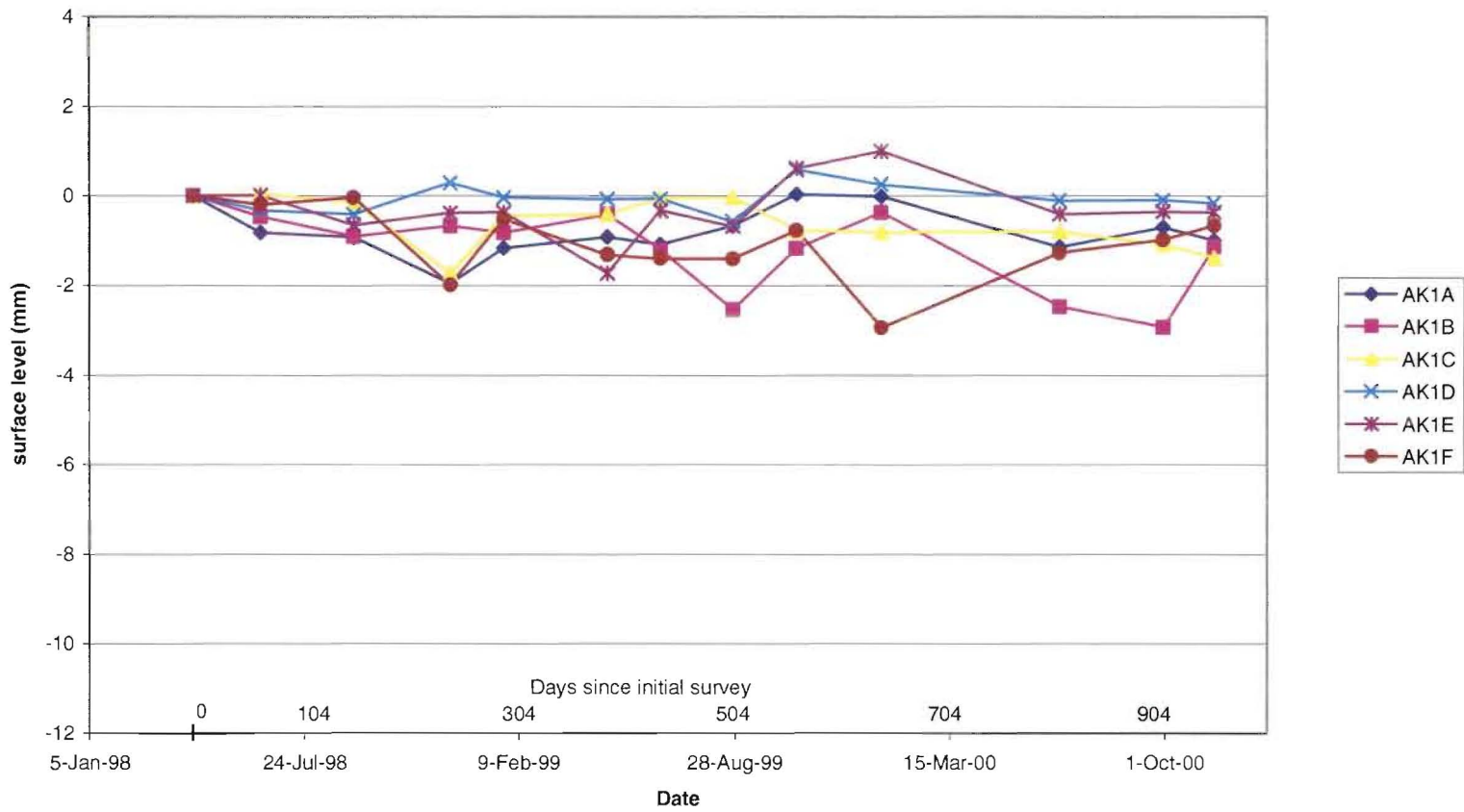


Figure 3.4: Surface change measured for sites across AK1. Surface level is shown as change from the first survey in mm. Duration between surveys is shown as dates and as number of days from initial survey.

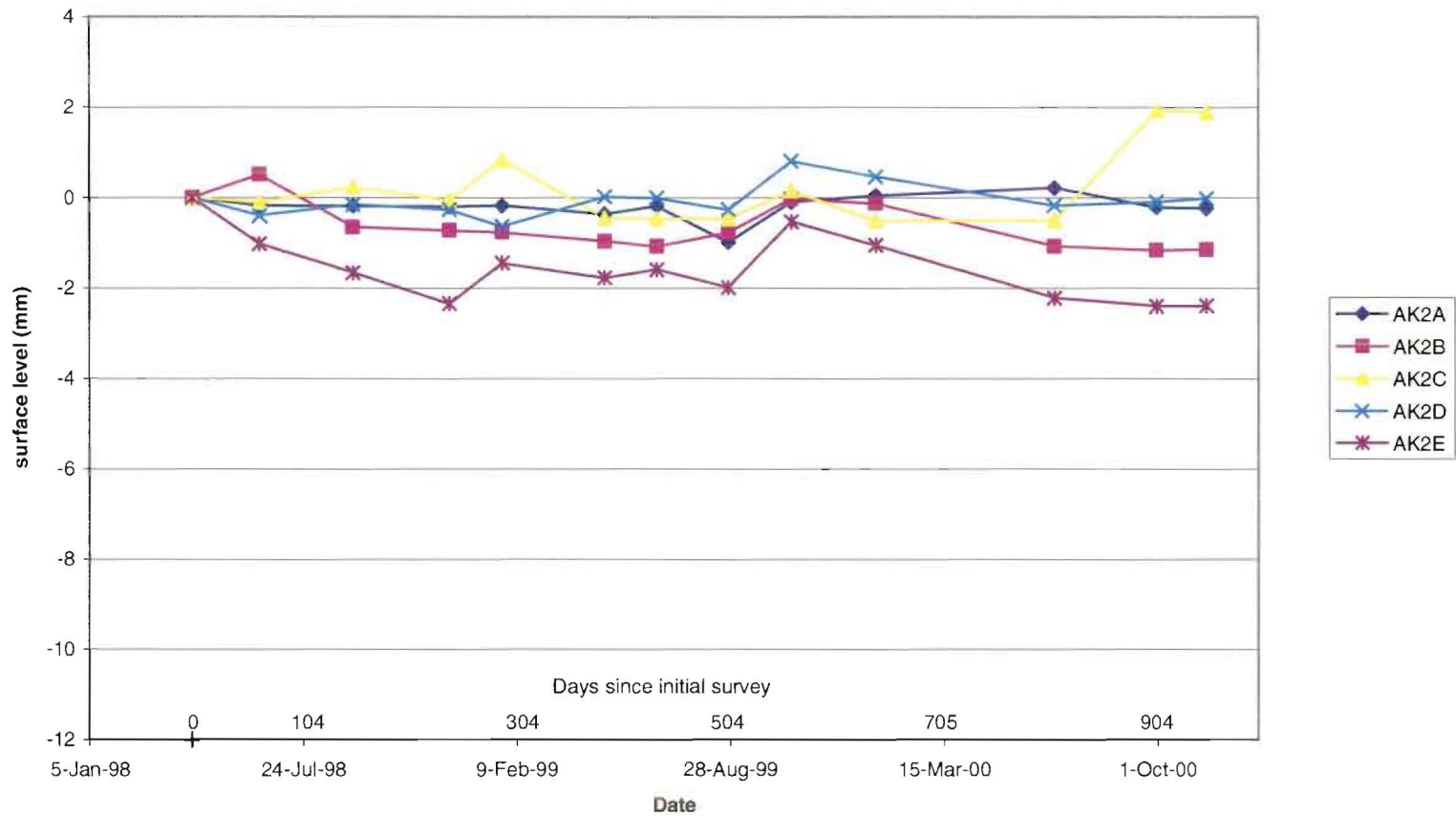


Figure 3.5: Surface change measured for sites across AK2. Surface level is shown as change from the first survey in mm. Duration between surveys is shown as dates and as number of days from initial survey.

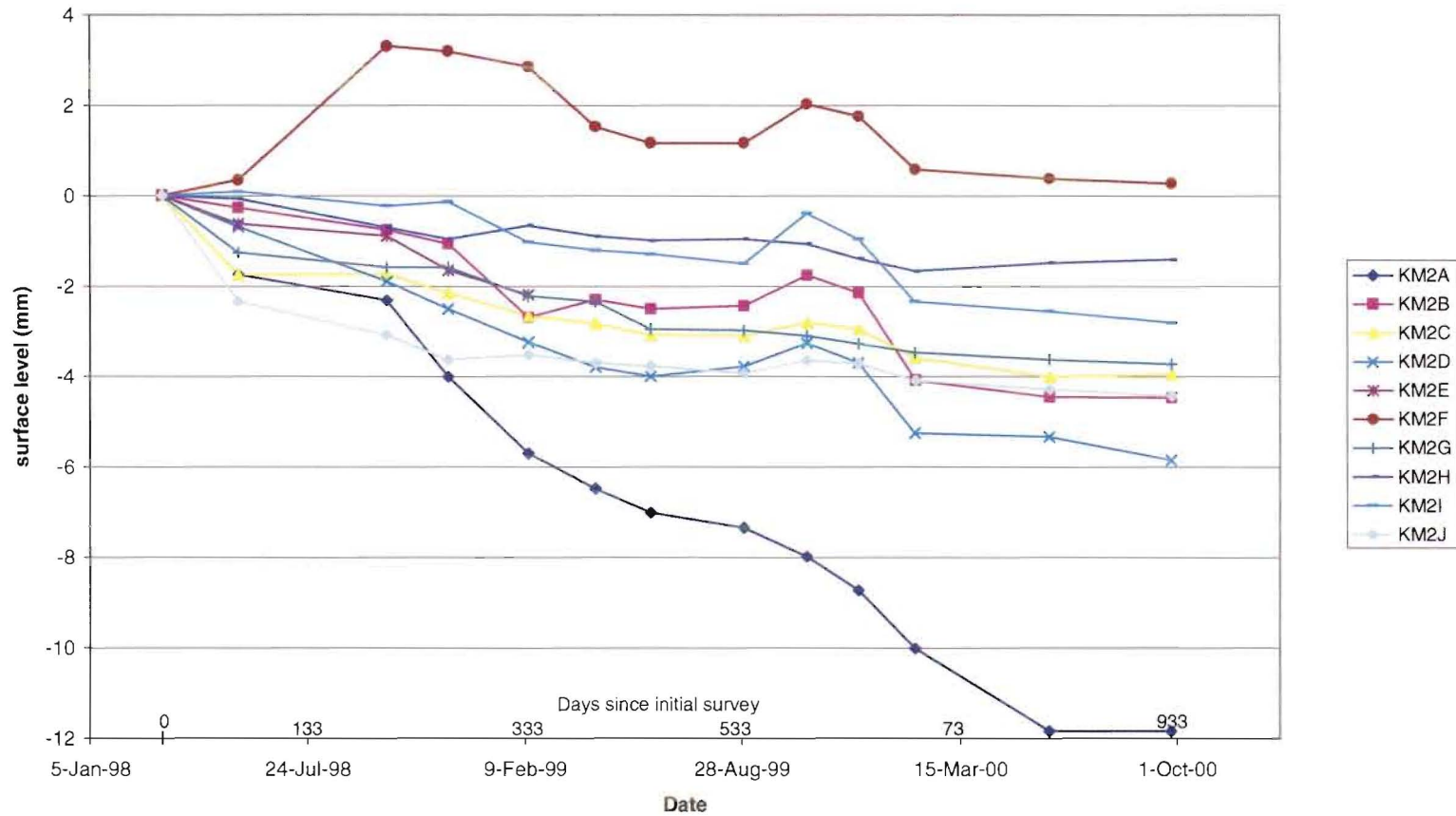


Figure 3.6: Surface change measured for sites across KM2. Surface level is shown as change from the first survey in mm. Duration between surveys is shown as dates and as number of days from initial survey.

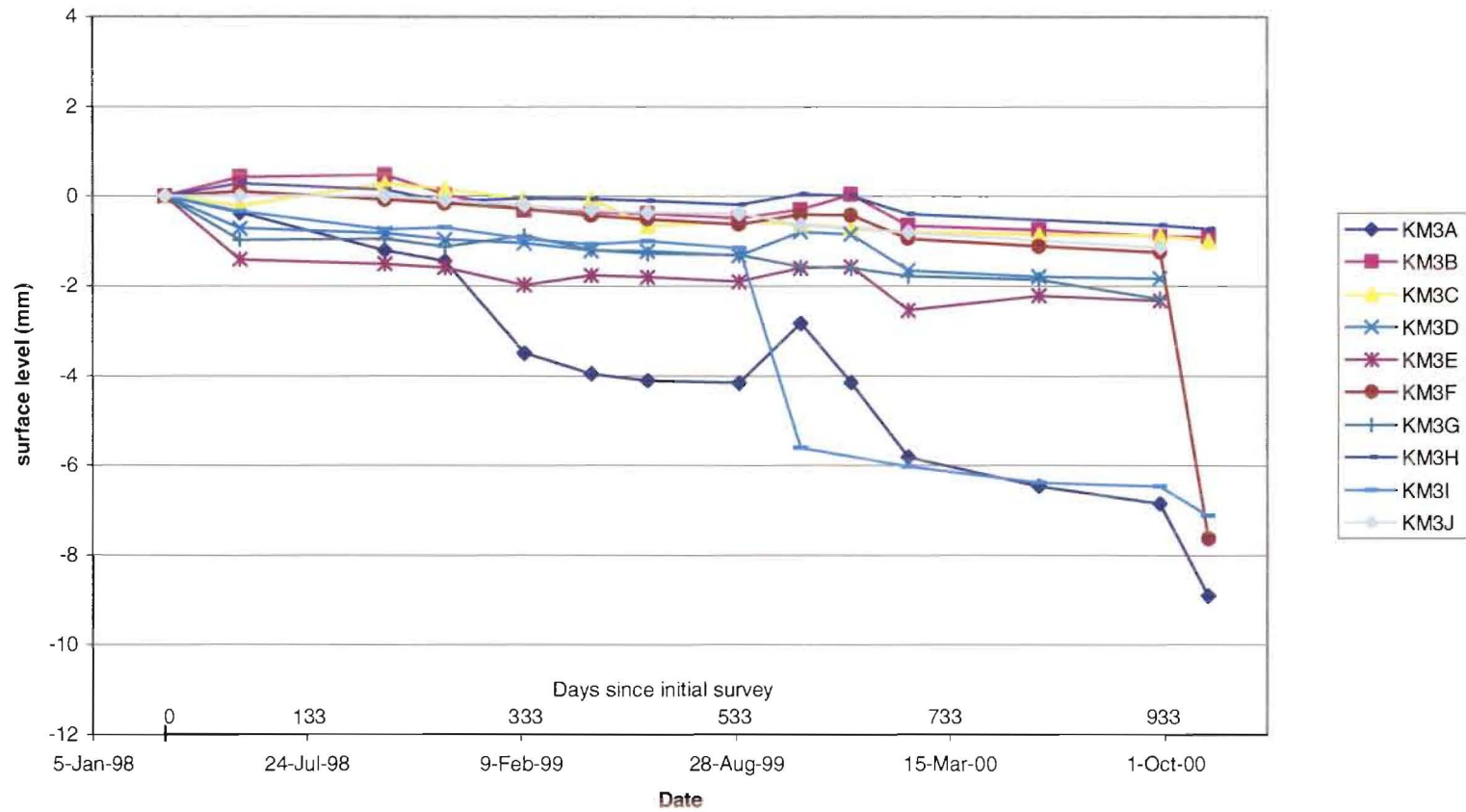


Figure 3.7: Surface change measured for sites across KM3. Surface level is shown as change from the first survey in mm. Duration between surveys is shown as dates and as number of days from initial survey.

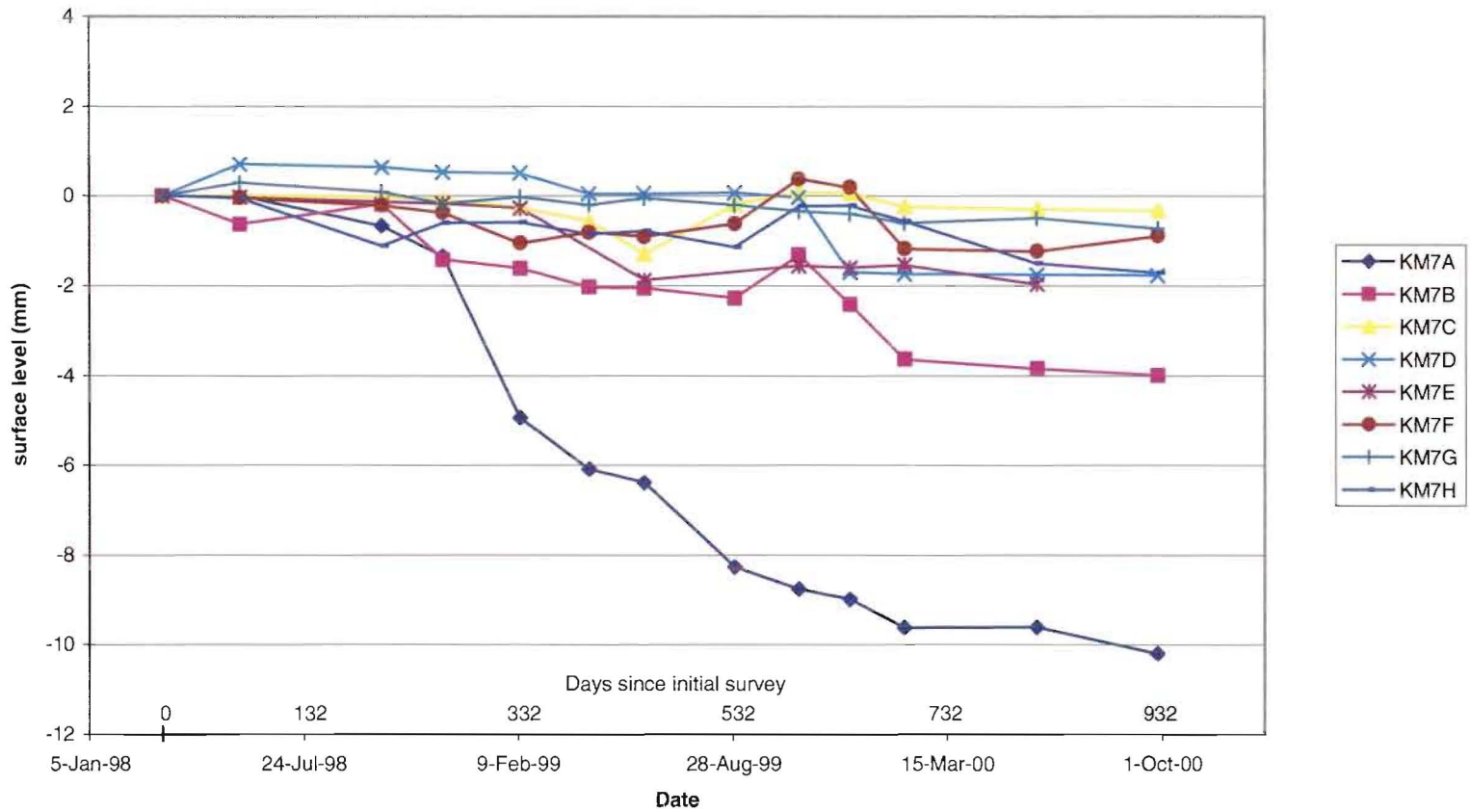


Figure 3.8: Surface change measured for sites across KM7. Surface level is shown as change from the first survey in mm. Duration between surveys is shown as dates and as number of days from initial survey.

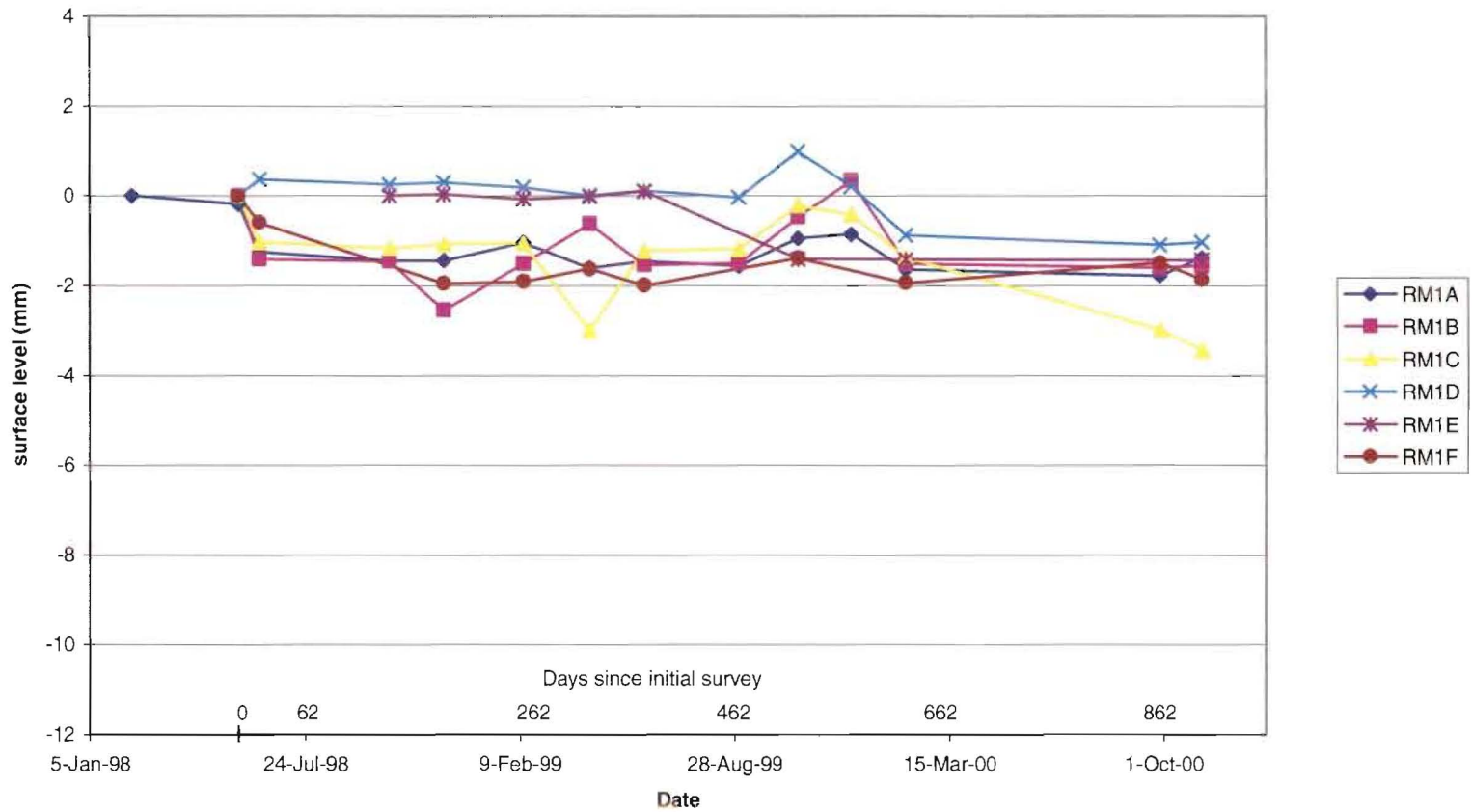


Figure 3.9: Surface change measured for sites across RM1. Surface level is shown as change from the first survey in mm. Duration between surveys is shown as dates and as number of days from initial survey.

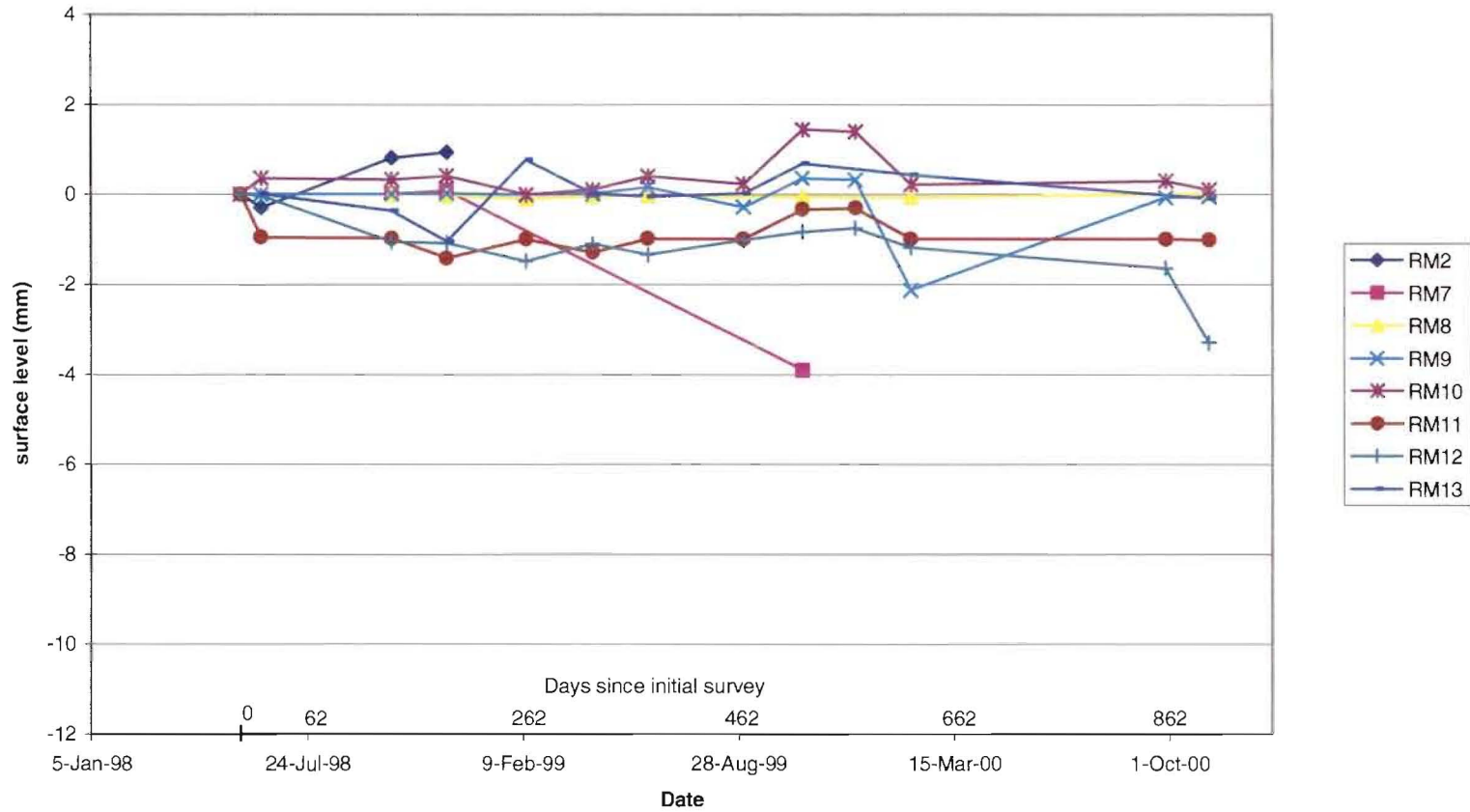


Figure 3.10: Surface change measured for sites on the Raramai Arch platform. Surface level is shown as change from the first survey in mm. Duration between surveys is shown as dates and as number of days from initial survey.

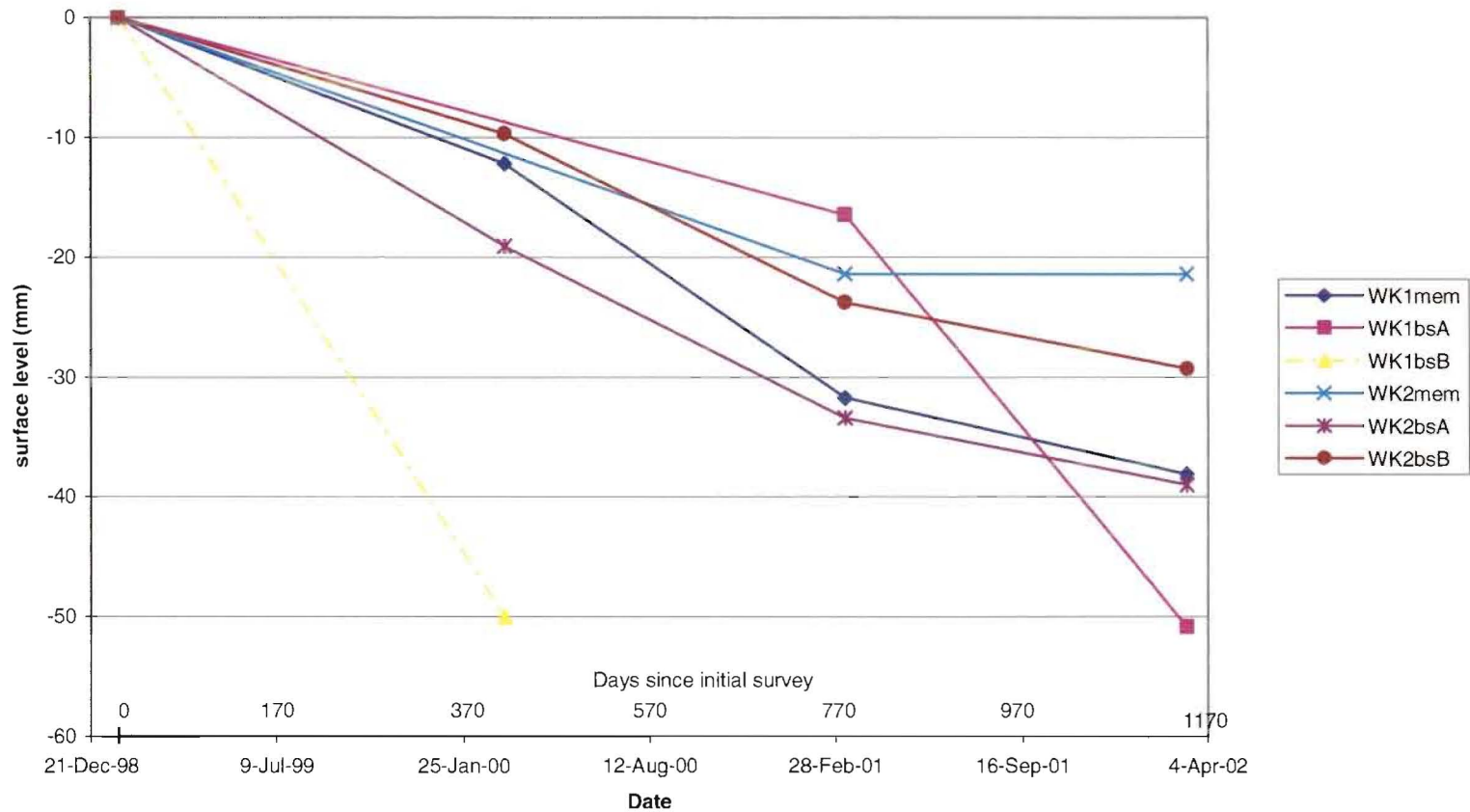


Figure 3.11: Surface change measured for sites on the shore platforms of Lake Waikaremoana. Surface level is shown as change from the first survey in mm. Surface change of WK1bsB was estimated as bolts were completely eroded out of the surface by the second survey. Duration between surveys is shown as dates and as number of days from initial survey.

As can be seen from figure 3.11 maximum changes in surface level occurred on the platforms at Lake Waikaremoana, where an excess of 50 mm of lowering was recorded over an 1147 day period at WK1bsA. Surface level changes occurring on shore platforms formed in other rock types were one to two orders of magnitude less than this. The greatest total surface change measured on the marine shore platforms studied was a lowering of 11.84 mm at KM2A over a 928 day period.

It was notable that both lowering and elevation of surfaces was measured on all rock types with the exception of the Lake Waikaremoana mudstone. A maximum rise in elevation of average surface level of 2.96 mm was measured at KM2F over a 206 day period and the majority of MEM sites showed some tendency for surface change in both vertical directions. Those sites that showed no evidence of elevated surface levels were KM2A, KM7A and all sites at Lake Waikaremoana.

This 'swelling' phenomenon (elevation of the surface) has been reported in previous shore platform studies by Kirk (1977), Stephenson and Kirk (1998 and 2001) and Stephenson *et al.* (in prep) at Kaikoura on mudstone and limestone and at other locations by Mottershead (1989) on greenschists and Stephenson *et al.* (in prep) on greywacke. The term 'swelling' was defined by Stephenson and Kirk (2001:6) as "the rise in elevation of a measurement point on a bedrock surface relative to the previous measurement." This study is the first time the swelling phenomenon has been reported over a wider range of rock types: mudstone, limestone, greywacke and basalt, all of which have been measured using the same method. It will be investigated more fully in section 3.3.4.

The surface level of MEM sites on AK1 and AK2 (figure 3.4 and 3.5) varied within envelopes of change of 4mm in the vertical extent. However, figure 3.4 and 3.5 show only very slight overall surface lowering.

Plots of surface levels on KM2 (figure 3.6) define a wide envelope of vertical variation from a rise in elevation to 3.30mm to erosion of 11.84mm. Overall surfaces showed a generally erosive trend with only KM2F displaying a rise in

average surface level of greater than 1.5mm. The plot of KM2A surface levels shows erosion at a greater rate than other sites on KM2.

Surface level changes on KM3 (figure 3.7) did not show as wide an envelope of change as those on KM2 (figure 3.6). Changes on KM3 were generally consistent with most surfaces lowering at a constant rate. Two of the sites, KM3I and KM3F, however experienced dramatic drops in surface level of 4.46mm and 6.39mm respectively. This was probably indicative of a larger portion of rock being removed from the measured surface between the successive surveys. KM3A showed higher rates of erosion than other sites on this profile.

Surface level change at KM7 (figure 3.8) defined an envelope of vertical change between 0.71mm and -10.20mm although the majority of sites were within 0.71mm to -4.00mm in extent. KM7A showed the greatest amount of total erosion on this profile over the study period with total average lowering of surface level of 10.20mm.

Landward MEM bolt sites of profiles on the Kaikoura Peninsula eroded significantly more than other sites on these profiles (figures 3.6, 3.7 and 3.8). This is likely to be the result of sediment supplies in close proximity to these locations causing abrasion of the surface. Distribution of rates of erosion across platforms will be discussed further in section 8.3.

Generally surface level changes on the greywacke at RM1 (figure 3.9) showed surface lowering. However, the vertical changes of most sites were variable and defined an envelope of change of between 0.99mm and -3.45mm. Average surface level of other sites on greywacke (figure 3.10) ranged between 1.44mm and -3.91mm.

Plots of surface level changes on profiles WK1 and WK2 (figure 3.11) all indicated rapid erosion.

3.3 PATTERNS OF SURFACE LEVEL CHANGE.

The data record surface change as the net effect of all the processes acting on the surface. In order to elucidate what is causing the measured surface change identification of patterns of change are required. It may then be possible to relate these patterns to processes thus identifying causative relationships. Comparison of patterns on each different rock type is also important in order to ascertain similarities and differences of change. Three methods of identifying patterns will be investigated in the following sections. Section 3.3.1 looks at temporal patterns of change. Sections 3.3.2 and 3.3.3 look at spatial patterns of change in the form of magnitude of change and location of change at a micro scale.

3.3.1 TEMPORAL PATTERNS OF SURFACE CHANGE.

The range of changes in surface levels evident at individual MEM sites, with both lowering and elevation measured on most surfaces, suggests that expansion and contraction of the rock is occurring. It is likely that this process is a precursor to erosion. Expansion and contraction is necessarily sequential and greater understanding of the process will be obtained with definition of the temporal aspect of the patterns of change.

As surface level surveys of each MEM bolt site were made on a 2-3 monthly basis it is only possible to identify patterns of change at a seasonal scale. These patterns have been identified visually from figures 3.4 to 3.11. Unfortunately it was not possible to stringently define cycles of change using a method such as frequency analysis due to the low numbers of data points defining the plots and a lack of observed regularity of both amplitude and frequency of change. However sequential patterns, rather than cyclic patterns, have been identified visually from figures 3.4 to 3.11 through the alternating periods of lowering and elevating of the surfaces.

The plots of surface change given in figures 3.4 – 3.11 appear to follow sequential patterns of change that are similar at most sites along a profile, although sometimes at differing vertical (spatial) scales. These sequential patterns occurred on all shore platforms studied but did not correspond closely to any seasonal cycle. Kirk (1977),

Robinson (1977b, 1977c), Mottershead (1989) and Stephenson and Kirk (1998, 2001) have all suggested that surface change on shore platforms was related to seasonal factors. This was not evident here.

It is possible that surface change responded to events or factors such as zoological influences or non-seasonal climatic conditions rather than seasonal controls.

The most clearly evident event was an episode of swelling which occurred on the surfaces of the marine shore platforms studied during early summer 1999/2000. On those sites that did not show swelling (KM2A and KM7A) a lessening in the rate of erosion was evident. Regular calibration of both MEM instruments throughout the entire survey period precluded the phenomena from being a result of instrumental error

As stated previously the spacing between surveys defines the scale to which any cycle or pattern can be identified. Using 2-3 monthly surveys it was only possible to identify patterns of surface change at a seasonal scale or greater.

Very little is known about the temporal scale of rock surface expansion and contraction on shore platforms. Stephenson and Kirk (2001) proposed that swelling episodes lasted for 3 to 4 months in some instances and that different episodes may be superimposed onto others of different time scales. However they made this speculation based on data also collected at 2-3 monthly intervals. Analysis of patterns over time scales of less than three months has not previously been published.

To investigate the possibility of smaller scale patterns of change the surface levels of three MEM sites (KM2B, KM7C and RM1B) were surveyed intensively over a two week period between 11/6/01 and 24/6/01 (figure 3.12). Surveys of surface level were made at approximately the same time of day every three days, conditions allowing. During one day at each of the three MEM sites, hourly surveys of surface level were conducted. KM2B was also surveyed on a daily basis between 6/11/00 and 10/11/00 (figure 3.12).

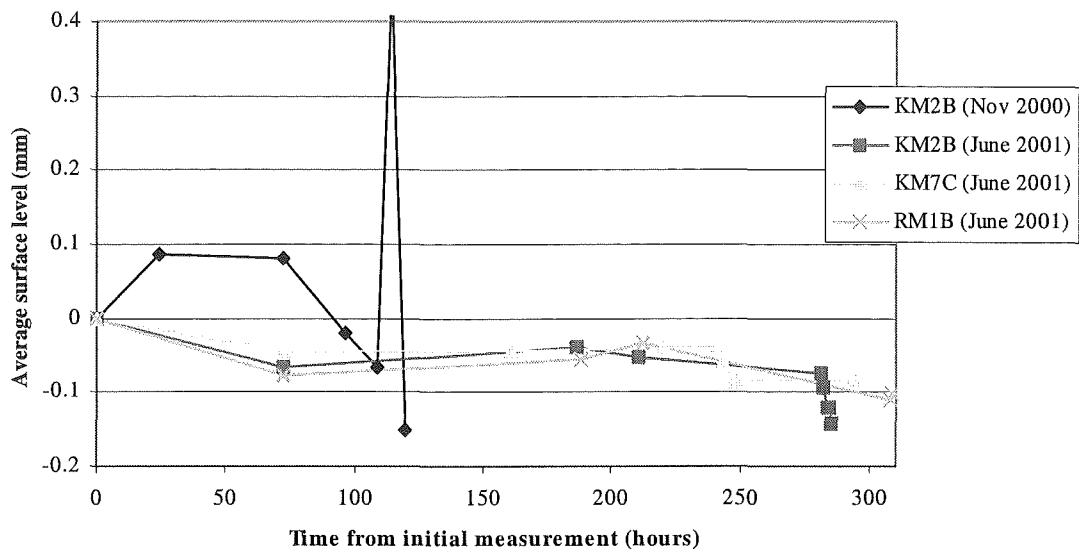


Figure 3.12: Change of average surface level at selected MEM sites between 6/11/00 – 10/11/00 and 06/11/01 – 18/11/01. The first measurement of each represents time and surface level zero. Time between measurements is given in hours.

No cyclic pattern was discernible in figure 3.12. The limited number of measurements and the short time period would make detection of any cycle difficult. However, figure 3.12 does show that significant changes of average surface level, both swelling and lowering, did occur over daily and even hourly intervals on the three rock types measured. These changes included both swelling and lowering of the surface. Figure 3.12 shows that rock surface level change on shore platforms occur at much shorter time scales than previously reported in other studies.

This is in agreement with findings of Stephenson *et al.* (in prep) who report surface changes of up to 3.378 mm over daily periods on mudstone at Kaikoura and on greywacke at Apollo Bay, Victoria, Australia.

Although this investigation has further demonstrated sequences of change of rock surface level on shore platforms, including the swelling phenomenon, more detailed study is required to fully characterise it. This would require regular surveys of surface level at intervals of short duration.

3.3.2 MAGNITUDE OF SURFACE CHANGES.

This section characterises the range of vertical changes measured on each rock type. This has been done in order to determine if the patterns of change in the vertical dimension are similar for each rock type.

The average surface change between each survey was calculated for all MEM sites. Frequency graphs of magnitude of change between surveys were constructed for each of the five rock types (figure 3.13). Average surface levels of sites have been used rather than surface change of individual measurement points. Individual point measurement showed changes of up to 10 mm between survey periods. These individual point changes will be further investigated in section 3.3.4.

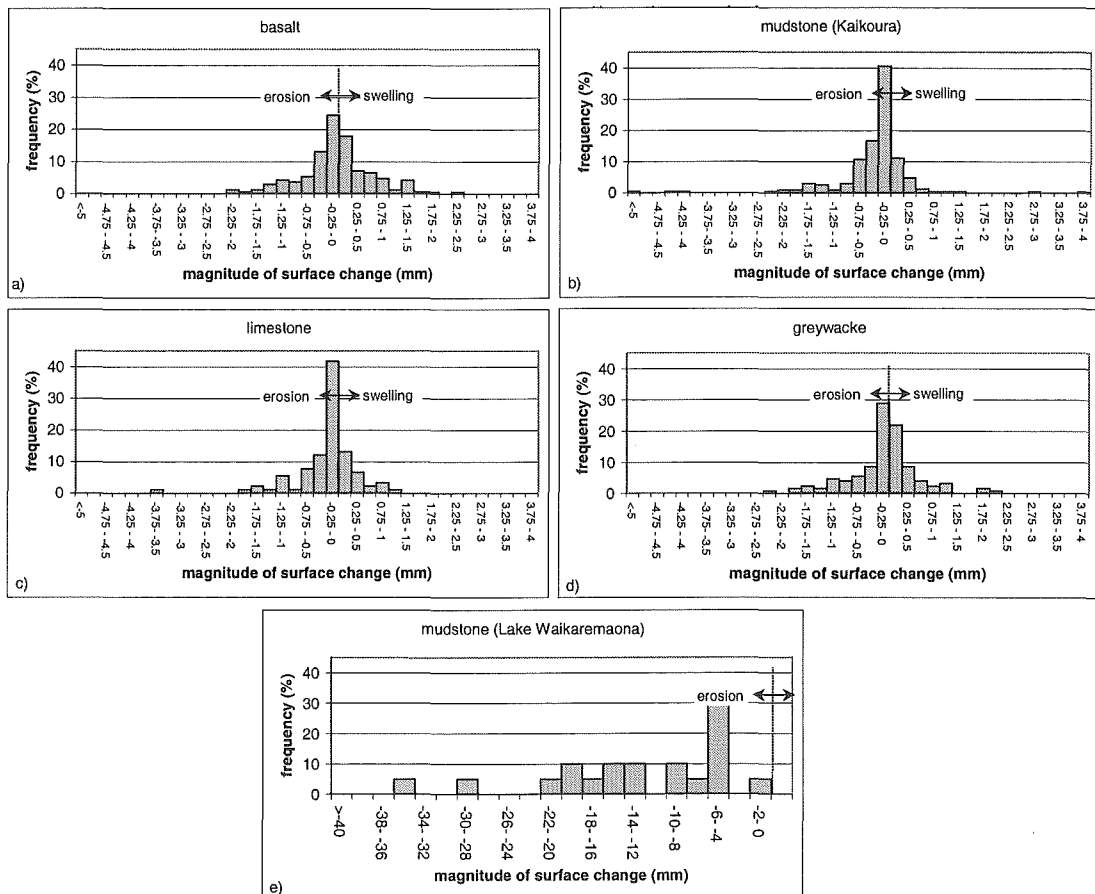


Figure 3.13: Frequency bar graphs of change of average surface level between successive surveys for a). basalt, b). mudstone (Kaikoura) c). limestone d). greywacke and e). mudstone (Lake Waikaremaona). Frequencies are given in percentages. Swelling is shown as positive surface change.

Maximum changes in average surface level between surveys were recorded at sites on mudstone at Lake Waikaremoana. All surface level changes at Lake Waikaremoana were erosive with the most frequent change between surveys being 4-6mm of erosion. The magnitude of surface changes between surveys at Lake Waikaremoana was significantly greater than any measured on the four other rock types studied. This can be partly accounted for by the greater duration between surveys at the Lake Waikaremoana sites but the rate of downwear of these platforms was still significantly higher than on the marine platforms studied.

On the marine shore platform surfaces both the largest single average lowering (6.39 mm) and the largest single average swelling (3.95 mm) between survey periods was recorded on the mudstone at Kaikoura. However, these measurements are isolated extremes. The histograms for both basalt and greywacke are more platykurtic, showing that changes in surface level between successive measurements were distributed across a larger range of magnitudes than those on the Kaikoura mudstone and the limestone surfaces. Changes in basalt and greywacke ranged from elevation of surface levels of 2.25 mm to lowering of 2.25 mm. This is a 4.5 mm range of average surface level changes between surveys. Surface changes on Kaikoura mudstone, excluding the extreme values, and on the limestone ranged between average elevation of 1.5 mm to average lowering of 2.25 mm. This is a 3.75mm range of changes.

The average magnitude of erosive events between surveys on the basalt was 0.48mm, on the mudstone at Kaikoura was 0.49mm, on the greywacke was 0.50mm, on the limestone was 0.44mm and on the mudstone at Lake Waikaremoana was 12.52mm. The greatest average magnitude of swelling between surveys was on the basalt platform (0.52mm). Average magnitude of swelling on the Kaikoura mudstone was 0.41 mm, on the greywacke was 0.40 mm and on the limestone was 0.33 mm. No swelling was measured on the mudstone at Lake Waikaremoana.

Those sites that showed no evidence of swelling all underwent greater levels of total erosion than most sites, with total surface erosion of at least 30 times greater than the average magnitude of swelling events. It is possible that these greater rates of

surface downwearing obliterated any evidence of swelling that may have occurred, making it difficult to detect, as suggested by Mottershead (1989).

Figure 3.13 shows that the magnitude of surface level change each rock type undergoes is significant. Measurements of all surfaces showed episodes of swelling as well as erosion, with the exception of the Lake Waikaremoana mudstone which showed only erosion. The range of changes measured on the basalt and the greywacke was larger than that of the Kaikoura mudstone and limestone. Shore platform surfaces are therefore dynamic in nature.

3.3.3 LOCATION OF SURFACE CHANGES.

The previous section gave average magnitude of surface level changes for each rock type. Using the data collected with the traversing MEM it is possible to investigate the spatial dynamics of these changes at the micro scale.

Figure 3.14 presents surface plots of the location and magnitude of absolute average surface level change between surveys for one MEM site on each rock type. Sites typical of each rock type have been chosen for presentation. The average surface level change between surveys was calculated for each of the 120 points measured by the traversing MEM and the absolute of this was taken to give total average amount of change for each point. Absolute average surface level changes were then plotted in wireframe contour form using Surfer Golden software mapping package.

Figure 3.14 gives both the magnitude of change measured and the distribution of locations of these changes within the measurement area.

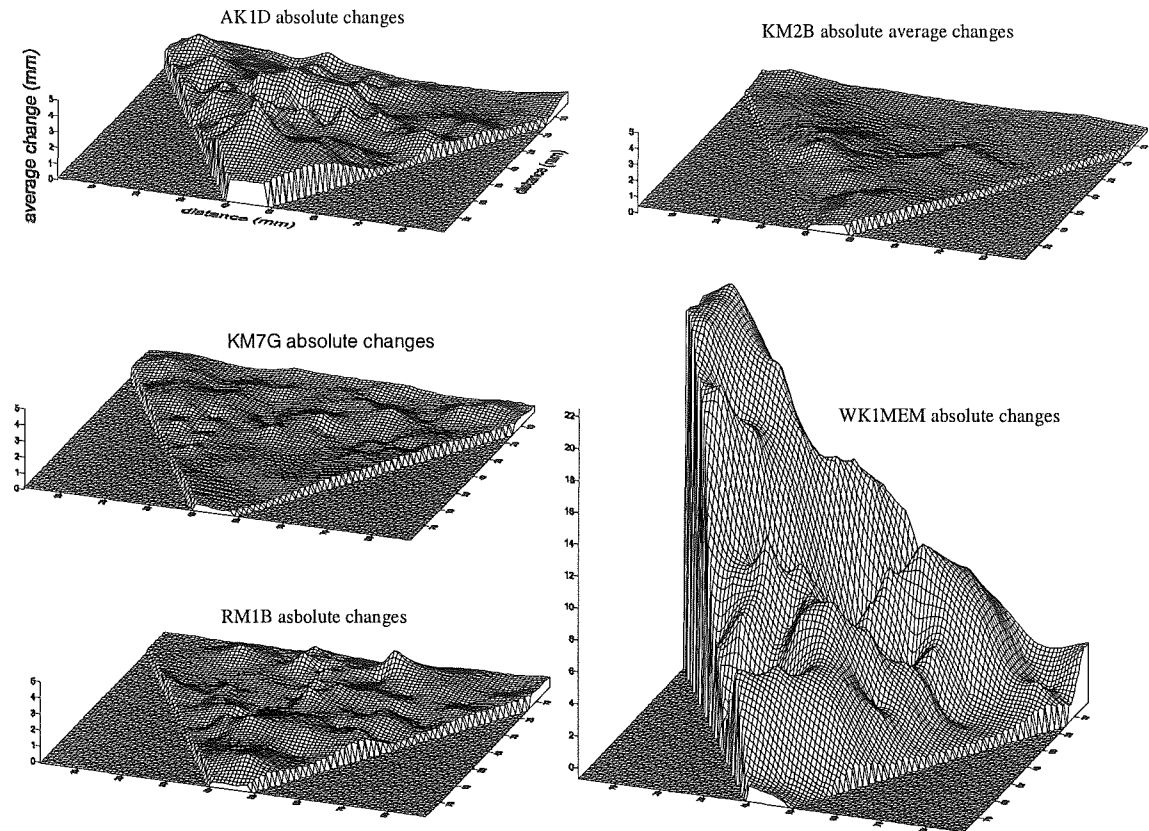


Figure 3.14: Plots showing contours of absolute average surface level change between surveys.

At this micro scale the surface of both the basalt and the greywacke (AK1D and RM1B) displayed complex patterns of change. The lumpy nature of these plots shows that while the entire area measured was dynamic there were also a large number of distinct locations where change of a greater magnitude than neighbouring points occurred. On the Kaikoura mudstone (KM2B) overall surface change was lower, as was the spatial variation of change with only a relatively few points of localised change. The surface at KM7G also displayed little total magnitude in change and only a few spots of local variation.

The large amount of erosion that occurred on the mudstone at Lake Waikaremoana has resulted in much greater vertical extent of this plot than on the other four rock types. However it is still possible to see that surface level changes were not spread evenly across the surface but concentrated at a number of apparently disconnected points. One side of this surface area is eroding at a noticeably faster rate than the other. This side is roughly orientated on the lakeward side of the plot.

Basalt displayed a greater spatial diversity in activity at this micro scale as well as going through a greater magnitude of variation. It is surprising that those rock types that displayed the greatest diversity in patterns of change both in magnitude and locality have the slowest long term rates of erosion.

3.3.4 NATURE OF SURFACE LEVEL CHANGES.

Both swelling and lowering of the surface occurred on all marine shore platforms studied regardless of rock type. The sequential pattern of change indicates that the rock surfaces were undergoing expansion and contraction in conjunction with erosion. Stresses caused by expansion and contraction of a rock surface are likely to be a precursor for erosion.

The shore platform surfaces formed in basalt and, to a lesser extent, the greywacke showed large magnitude changes in surface level during the measurement period without a corresponding net erosion of the surface (figures 3.4, 3.5, 3.9, 3.10 and 3.14). This leads to an important conclusion. There is a remarkable robustness evident in these rock types. They are capable of absorbing large scale surface changes without eroding.

At Kaikoura on the mudstone and limestone the uniform nature and the lower magnitude of surface changes suggests that these rock types are less able to withstand dynamic change without corresponding erosion of the surface. On the mudstone at Lake Waikaremoana both the dynamic nature of the surface level change and the high rates of erosion suggest that this is a rock type that is unable to withstand net erosion when subjected to changes of this nature.

In order to more fully understand the role of surface level changes as an erosive agent on shore platforms further study would be required. This would need to include greater definition of both temporal and spatial scales of the process and investigation of physical or chemical processes causing expansion and contraction of the rock surface.

3.4 AVERAGE RATES OF SURFACE CHANGE.

To allow general comparison of shore platform surface level changes on each different rock type studied and of each separate MEM site an average rate of change needs to be considered.

Previously documented assessments of average erosion rates on shore platforms have been calculated using the difference between two surface level surveys divided by the duration between these surveys. This has been assumed to give representative annual erosion rates in mm.yr^{-1} (Kirk 1977, Robinson 1977b, 1977c, Gill and Lang 1983, Viles and Trudgill 1984, Mottershead 1989, Stephenson 1997a, Stephenson and Kirk 1996, 1998, 2000a, 2000b). When quantifying average erosion rates where swelling was evident in the measurements Stephenson (1997a) excluded measurements that showed swelling since the previous measurement. Kirk (1977) used the algebraic sum of measured changes divided by the measurement period.

The dynamic nature of surface level change, as shown in the previous sections, presents a difficulty in the determination of an average erosion rate for each site. Spencer (1981:92) cautioned against the use of average erosion rates for a site stating that "a few high rates of erosion distort the magnitude of surface lowering". Distortion of this nature may also result from intermittent surface level elevation between surveys at individual locations as reported in section 3.3.3.

While the temporal scale of surface change as a result of expansion and contraction of the rock remains undefined, calculation of erosion rates using average surface level changes between only two surveys may misrepresent actual rates of change. It is not possible to predict the stage of the expansion/contraction sequence in which the rock surface will be when it is surveyed. This further complicates the calculation of a representative average erosion rate.

Distinguishing between expansion and contraction of the rock surface, and the process of erosion, becomes complicated when the magnitudes of the expansion events are of the same order as the erosion of the surface. It was shown in section 3.3.2 that the average magnitude of swelling events on the marine rock surfaces was

between 0.52 and 0.33 mm and occurred over varied intervals. At sites where only surface lowering was measured calculation of an average rate of erosion seemed to be a relatively simple matter. At sites where the amplitude of the swelling events were similar to the erosion rate itself (e.g. *KM3C*) calculation of an average rate was not so simple. The time at which the survey was made dictated the stage of the expansion / contraction, sequence when the rock surface was measured, and rates varied as a result. For example at *KM3C* very different rates of erosion were obtained using surveys taken at approximate yearly intervals. The rate of surface change calculated using surveys taken on 5/10/98 and 27/10/99 was $-0.862 \text{ mm.yr}^{-1}$. Whereas a rate of $-0.285 \text{ mm.yr}^{-1}$ was calculated using surveys of the same surface taken on 30/8/99 and 26/9/00.

Therefore the stage of the rock surface in the expansion /contraction sequence is an important factor to consider when calculating a representative erosion rate.

Also another important consideration is the duration between measurements. As stated in section 3.1 the validity of short term measurements of a temporally slow process such as rock surface erosion have been questioned (Trenhaile 1987, Viles and Trudgill 1984). Stephenson and Kirk (1996) showed that measurements collected using the MEM technique over a two year period were representative of longer term erosion rates on shore platforms at Kaikoura. It is implied that rates calculated using surveys separated by intervals shorter than this may not be representative.

As regular surveys were conducted at each MEM site during the study period it is possible to illustrate the importance of both the duration between measurements and stage of the rock surface in the expansion/contraction sequence at time of survey when calculating an average rate of surface change (Figure 3.15). Average rates of surface level change were calculated for every possible combination of any two surveys at *KM2B*. For example, the total surface change between survey 1 and survey 2 was divided by the duration between these two surveys. The same was done for measurements taken on survey 1 and survey 3, survey 2 and survey 3 etc.

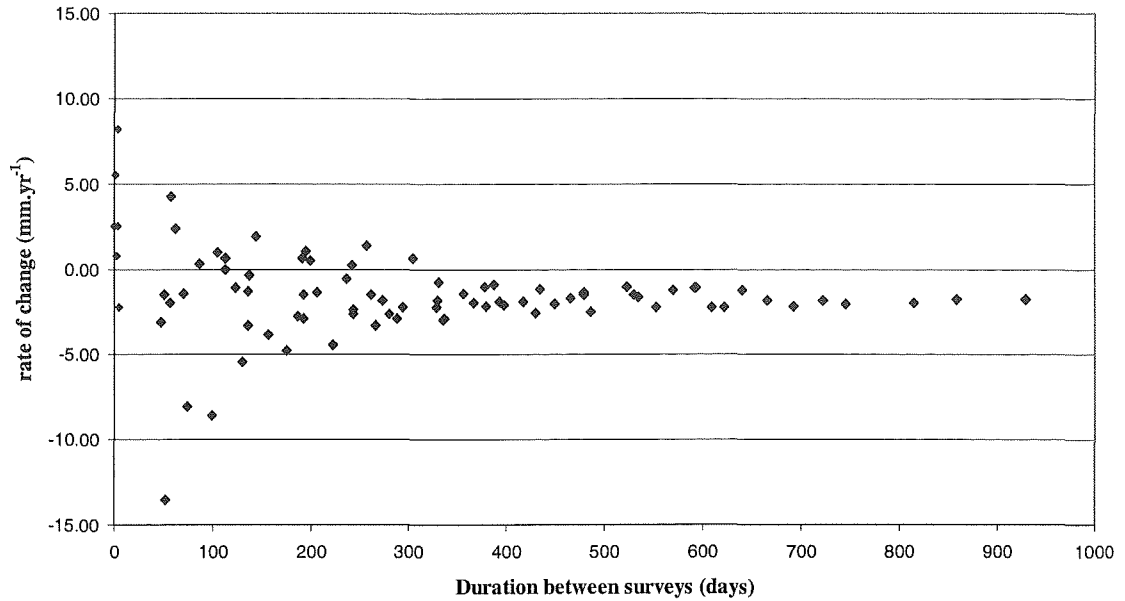


Figure 3.15: Duration between MEM surveys plotted against rate of surface level change calculated for every combination of surveys conducted at KM2B.

Figure 3.15 shows that average surface change calculated over shorter intervals had a wider degree of variability and as the interval between surveys increased this variability decreased. It is a remarkable and unexpected finding that measured surface change rates are a function of duration of the record.

Part of this effect is mathematical in that the time period increased in relation to the amount of surface change occurring. However, this does not account for all of the pattern shown in figure 3.15. Also figure 3.15 shows that for survey intervals of greater than 600 days, rates of change tended to show little variation. This pattern was similar on all rock types measured and supports Stephenson and Kirk's (1996) assertion that measurements over a 2 year period are representative of longer term rates. It also suggests that expansion and contraction of the rock surface has a temporal frequency of less than 600 days.

Until greater understanding of the processes causing rock surface level change are gained, correction for them at the time of field measurement can not be made. The numbers of factors that, undoubtedly, are involved would make it next to impossible to co-ordinate re-survey of sites at the same stage of the cycle each time. Therefore a

method for combating this problem was developed in the data analysis procedure. This method follows.

3.4.1 CALCULATION OF RATES OF SURFACE CHANGE (MULTIPLE DURATION METHOD).

The surface change measured between every possible combination of surveys (section 3.4) was plotted against the duration between these surveys for each MEM site. Actual surface changes were used as conversion of surface level measurements to rates of change between surveys tended to further complicate already complicated patterns. A line of best fit was plotted through these points and forced through the origin. From the slope of this line an average erosion rate was obtained. Best fit lines did not always show strong correlation of data points but a trend was always discernible. This was deemed acceptable as the trend or pattern was required rather than a causative relationship between the two components which is gained from regression analysis.

Figure 3.16 shows the graph constructed for calculation of average rate of surface change using the multiple duration method at KM3C. The spread of points around the best-fit line defined a band of variation of surface levels around a representative rate of change, as indicated in figure 3.16 by the shaded zone. The mean residual error of the points around the line of best fit was calculated using least squares and is presented for each site as an indication of the degree of variability of the surface over time as well as the amplitude of the swelling phenomena.

Calculation of rates of surface change using this multiple duration method give a clearer picture of the character of the surface change and filter out the problem of using single long duration measurements. It also circumvents problems associated with simple exclusion of swelling measurements.

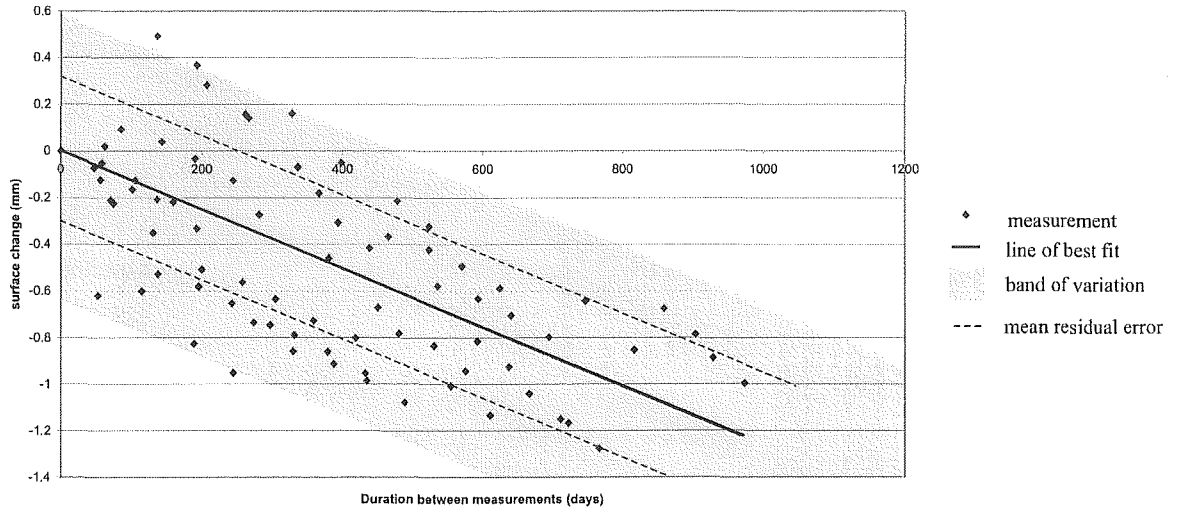


Figure 3.16: Surface level changes for all durations measured on KM3C. The gradient of the best fit line gives representative average rate of surface change and the shaded region shows the degree of variation in measurements as a result of swelling and contraction of the rock surface. Note that the shaded band does not show the value of the mean residual. The dashed line represents mean residual values.

Table 3.2 presents average rates of surface change for each MEM site calculated using this multiple duration method. Also presented are average rates of change calculated using the first and last survey measurements made at each site. Results from the multiple duration method showed that the maximum erosion rates of 12.82 mm.yr^{-1} were measured at WK1mem. Maximum erosion rate on marine platforms studied were 4.75 mm.yr^{-1} at KM2A. Table 3.2 includes mean residuals for each site, giving an indication of amplitude of the variation of surface changes from the representative average rate of change. Average residuals ranged from a maximum of 12.93 mm on the mudstone at Lake Waikaremoana and a minimum of 0.23 mm at KM3H.

Table 3.2: Rates of surface change for each MEM site. Negative numbers represent erosion of the surface.

| site | rate of change (mm.yr ⁻¹) multiple duration method | average residual | rate of change (mm.yr ⁻¹) first and last measurement method |
|--------|---|------------------|--|
| AK1A | -0.05 | 0.78 | -0.38 |
| AK1B | -0.77 | 0.97 | -0.36 |
| AK1C | -0.41 | 0.66 | -0.53 |
| AK1D | 0.01 | 0.42 | -0.06 |
| AK1E | -0.03 | 0.91 | -0.14 |
| AK1F | -0.28 | 1.07 | -0.25 |
| AK2A | 0.03 | 0.39 | -0.09 |
| AK2B | -0.42 | 0.61 | -0.44 |
| AK2C | 0.55 | 1.08 | -0.05 |
| AK2D | 0.07 | 0.49 | -0.01 |
| AK2E | -0.59 | 0.87 | -0.92 |
| AK3A | -0.10 | 0.84 | -0.29 |
| AK3B | -0.15 | 0.45 | -0.12 |
| AK3C | -0.14 | 0.68 | -0.19 |
| KM2A | -4.75 | 0.82 | -4.66 |
| KM2B | -1.77 | 0.85 | -1.76 |
| KM2C | -1.30 | 0.61 | -1.55 |
| KM2D | -2.17 | 0.79 | -2.30 |
| KM2E | -2.01 | 0.29 | -2.39 |
| KM2F | -0.18 | 1.55 | 0.11 |
| KM2G | -1.36 | 0.47 | -1.46 |
| KM2H | -0.59 | 0.29 | -0.56 |
| KM2I | -1.13 | 0.67 | -1.10 |
| KM2J | -1.27 | 0.98 | -1.74 |
| KM3A | -3.11 | 1.04 | -3.34 |
| KM3B | -0.48 | 0.33 | -0.34 |
| KM3C | -0.39 | 0.31 | -0.37 |
| KM3D | -0.61 | 0.37 | -0.72 |
| KM3E | -0.71 | 0.18 | -0.92 |
| KM3F | -1.83 | 1.75 | -0.49 |
| KM3G | -0.69 | 0.28 | -0.90 |
| KM3H | -0.32 | 0.23 | -0.27 |
| KM3I | -3.02 | 1.67 | -2.67 |
| KM3J | -0.57 | 0.09 | -0.53 |
| KM7A | -4.72 | 1.73 | -4.35 |
| KM7B | -1.54 | 0.70 | -1.57 |
| KM7C | -0.09 | 0.51 | -0.13 |
| KM7D | -0.98 | 0.79 | -0.70 |
| KM7E | -0.99 | 0.18 | -0.88 |
| KM7F | -0.33 | 0.69 | -0.35 |
| KM7G | -0.34 | 0.17 | -0.28 |
| KM7H | -0.53 | 0.60 | -0.67 |
| RM1A | -0.37 | 0.64 | -0.51 |
| RM1B | -0.13 | 1.09 | -0.64 |
| RM1C | -1.00 | 1.23 | -1.40 |
| RM1D | -0.57 | 0.64 | -0.42 |
| RM1E | -0.92 | 0.19 | -0.69 |
| RM1F | -0.31 | 0.78 | -0.19 |
| RM2 | 2.66 | 0.23 | 1.78 |
| RM7 | -4.30 | 0.34 | -3.75 |
| RM8 | 0.03 | 0.05 | 0.01 |
| RM9 | -0.07 | 0.85 | -0.03 |
| RM10 | 0.00 | 0.27 | 0.04 |
| RM11 | -0.06 | 0.57 | -0.41 |
| RM12 | -0.86 | 0.76 | -1.34 |
| RM13 | 0.05 | 0.69 | -0.04 |
| WK1mem | -12.82 | 4.08 | -12.13 |
| WK1bsA | -12.51 | 12.06 | -16.19 |
| WK1bsB | 0.00 | | ~50.00 |
| WK2mem | -10.01 | 0.00 | -10.01 |
| WK2bsA | -12.81 | 6.08 | -12.41 |
| WK2bsB | -9.78 | 3.50 | -9.33 |
| WKM2 | -10.75 | 12.93 | -9.20 |
| WKM5 | -6.21 | 2.08 | -6.27 |
| WKM9b | -7.28 | 3.58 | -7.34 |

3.4.1.1 COMPARISON OF METHODS.

For each MEM site the average rates obtained using the multiple duration method were compared to average rates calculated from the difference between the first and last measurements divided by the duration between those measurements. This was done to investigate the comparability of both methods of calculating rate of surface change and to assess the accuracy of using rates defined by just two surface measurements alone. Figure 3.17 shows the correlation between the results of the two methods. Both yielded very similar representative rates of surface change and were strongly correlated with an r of 0.98. This suggests that only two measurements, spaced with sufficient duration apart, are adequate to characterize the rate of erosion on a shore platform. However, the multiple duration method used to obtain average erosion rates given in table 3.2 is considered more useful when characterising rock surface changes on shore platforms through the inclusion of amplitude of change factor in the form of the residual. Measures of average rate of surface change used in this thesis are those obtained using the multiple duration method unless otherwise stated.

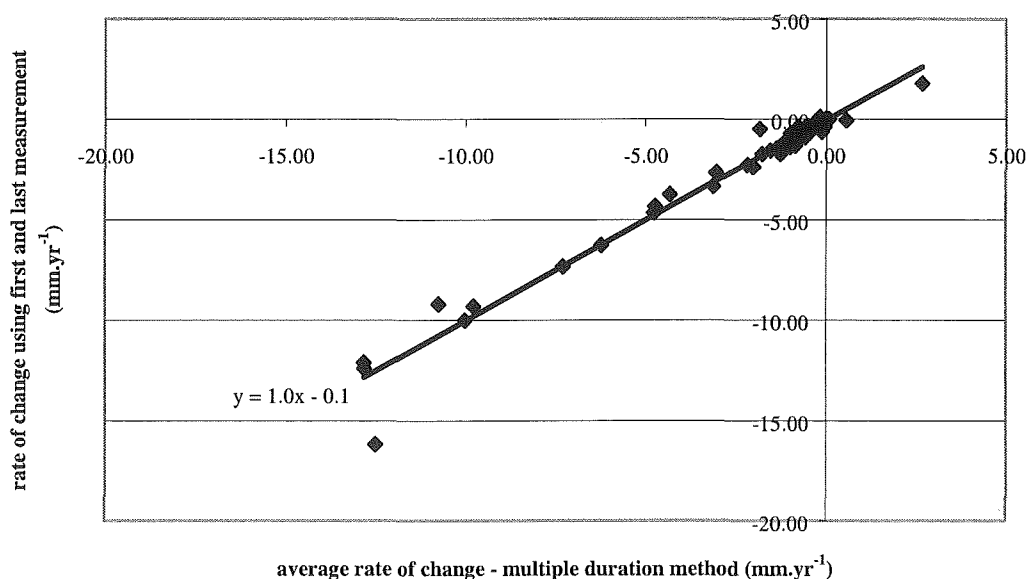


Figure 3.17: Comparison of average surface level rates of change obtained using the multiple duration method and the first and last survey method.

3.4.2 RATES OF SURFACE CHANGE FROM LONGER TERM DATA.

In section 3.1 it was noted that Stephenson and Kirk (1996) stated that MEM measurements of surface erosion on shore platforms spanning intervals of greater than two years were representative of longer term erosion. They showed this by comparison of short term (2 year) data with 20 years of data at Kaikoura. It is also possible to undertake similar analysis here.

Seven of the MEM sites monitored on the Kaikoura Peninsula were installed in 1974 (Kirk 1977). It is therefore possible to present amounts of surface change measured over periods of greater than 24 years (Table 3.3). No other shore platform surface monitoring network has been monitored for such an extensive time span. This enables comparison of downwear rates measured over quarter of a century to those measured over a three year period.

When assessing grand mean erosion rates using these data it is important to note that only the bolts remaining in the rock surface could be measured. Of the original 13 sites installed across profiles KM2 and KM3, 7 still remain measurable.

Table 3.3: Rates of surface change measured between 1974 and 2000. Included are rates of surface change measured between 1998-2000.

| site | duration between measurements (years) | surface change (mm) | rate of change (mm.yr ⁻¹) | rate of change 1998 - 2000 (mm.yr ⁻¹) |
|------------------|---------------------------------------|---------------------|---------------------------------------|---|
| KM2C | 26.5 | -36.38 | -1.37 | -1.3 |
| KM2E | 24.1 | -55.97 | -2.32 | -2.01 |
| KM2G | 26.6 | -32.15 | -1.21 | -1.36 |
| KM2I | 26.6 | -30.05 | -1.13 | -1.13 |
| KM3E | 26.6 | -11.28 | -0.42 | -0.71 |
| KM3G | 26.6 | -30.24 | -1.14 | -0.69 |
| KM3I | 26.4 | -46.64 | -1.77 | -3.02 |
| grand mean total | | | -1.34 | -1.46 |

Table 3.4: Students t-Test statistics comparing long and short term erosion rates.

| | Variable 1 | Variable 2 |
|---------------------|------------|------------|
| Mean | -1.34 | -1.46 |
| Variance | 0.35 | 0.67 |
| Observations | 7 | 7 |
| df | 6 | |
| t Stat | 0.58 | |
| P(T<=t) two-tail | 0.58 | |
| t Critical two-tail | 2.45 | |

The grand total mean rate of erosion measured since 1974 was 1.34mm.yr^{-1} . This compared to an erosion rate of 1.46mm.yr^{-1} for the same MEM sites measured between 1998 and 2000. The representativeness of the shorter, three year data set when compared with lowering rates calculated over a 24+ year period was tested using Student's t-Test for paired data (table 3.4). The t-statistic was 0.58 with 7 degrees of freedom and t-critical for a two-tail distribution was 2.45 at 5% probability. Therefore the hypothesis that shorter term surface change data are representative of surface change data measured over a longer time period can be accepted.

3.4.3 RATE OF CHANGE COMPARED TO THE RESIDUAL.

The absolute size of residuals varied in relation to the total average rates of surface change at each site (figure 3.18). As rate of change increased so did the amplitude of variation in the surface levels of the rock.

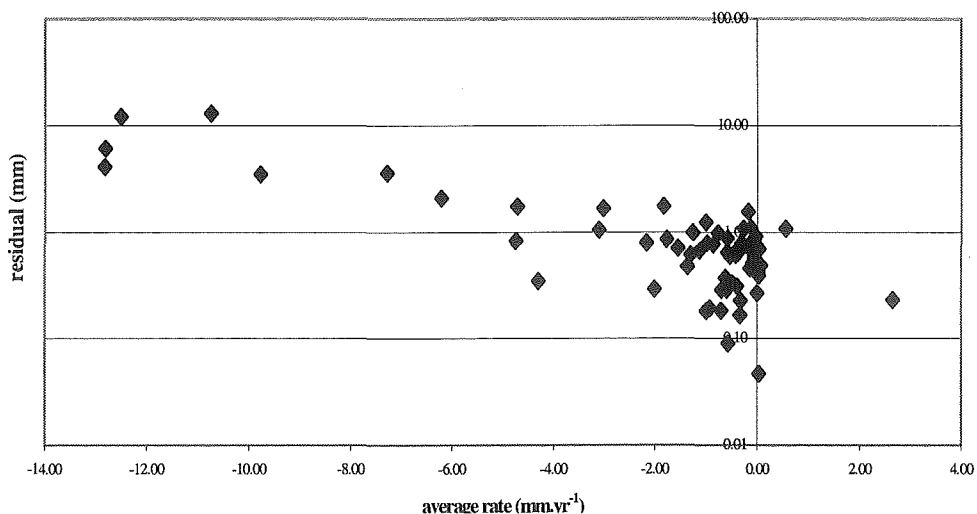


Figure 3.18: Average rate of change vs. residual. Where the residual is an indication of the measured variability of surface level. Note the log scale on the vertical axis.

Residuals, when calculated as a proportion of average rate of change for each site showed a negative power relationship with respect to average rates of erosion (figure 3.19). The closer to zero the average rate of surface change the greater the proportional amplitude of variation of changes. Although total amplitude of variation was greater for surfaces undergoing higher rates of change the magnitude of the variation was proportionally greater for surfaces with lower rates of change.

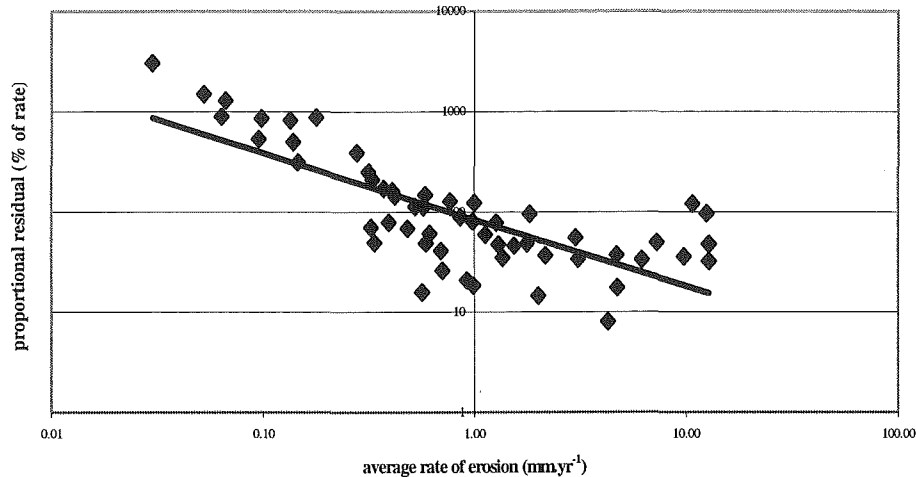


Figure 3.19: Average rate of change vs. residual as a proportion of Average rate. Where the residual is a measure of the variability of surface level measured. Note that scales are logarithmic and average rates of change are shown with erosion as positive.

3.4.4 AVERAGE RATES OF SURFACE CHANGE FOR EACH ROCK TYPE.

Average rates of surface change were calculated for shore platforms in each rock type (table 3.5) using an average of rates for each MEM site on that rock type. Rates varied for each rock type. The shore platforms formed in basalt had the lowest average rate of erosion at 0.29 mm.yr^{-1} . The shore platforms formed in greywacke were the next slowest downwearers (0.78 mm.yr^{-1}) and platforms in the mudstone at Lake Waikaremoana eroded at the greatest rate (9.13 mm.yr^{-1}).

Table 3.5: Average representative rate of erosion and average residuals for each rock type.

| rock type | average rate of change (mm.yr ⁻¹) | ave residual |
|---------------------------------|--|--------------|
| Basalt | -0.29 | 0.75 |
| Mudstone (Kaikoura) | -1.41 | 0.68 |
| Limestone | -1.19 | 0.67 |
| Greywacke | -0.78 | 0.60 |
| Mudstone (Lake Waikaremoana) | -9.13 | 6.33 |

The tectonic stability of Banks Peninsula (section 2.4.3) suggests that the relative water level of Akaroa Harbour has been at its present level since the sea reached its current height 6000 – 7000 years ago. At the current erosion rate of 0.29 mm.yr⁻¹ that would equate to 1.89 m of downwearing on the contemporary shore platforms. This is a sufficient amount of erosion to have formed the present platforms during 6000 – 7000 years of approximately present sea levels.

The relative water level at Kaikoura Peninsula has been influenced by tectonic activity since the sea reached its present height. The best available information tentatively suggested a 2 m episode of uplift between 300 – 1000 years ago (Duckmanton 1974). If the present relative sea level for the shore platforms on the Kaikoura Peninsula were taken to have been stable for the last 450 years this would equate to 0.63 m of erosion on the mudstone platforms and 0.54 m on the limestone platforms. Both these amounts are sufficient to have formed the current platforms. If this rate is representative of the erosion that has occurred during the last 6000 – 7000 years a total of 9.17 m of erosion has occurred on the mudstone platforms and 7.74 m total on the limestone platforms.

The shoreline at Raramai Arch was assumed to be tectonically active but the rate of uplift is unknown (section 2.4.2). Therefore, assuming relative water level at the Raramai Arch platform reached its present elevation 6000 – 7000 years before present this equates to 5.07 m of down wear on this platform.

At Lake Waikaremoana the water level was lowered to its present elevation 56 years before present. At the current average rate of surface change 0.58 m of erosion would have occurred since then. These shore platforms are very actively eroding.

Allan *et al.* 2002 analysed a number of sandstone boulders perched on mudstone pedestals at two locations on shore platforms around the shores of the Lake. They found the mean height of the pedestals was 0.31m above the platform surfaces and estimated from this an average downwearing rate of 5.86mm.yr⁻¹. The subsequent MEM data reported in this study has confirmed this estimate within its margin of error.

Rates of surface level change measured on marine shore platforms for this study are comparable to those reported in other published studies. Using MEM techniques of measurement erosion rates of between 1.53mm.yr⁻¹ (Kirk 1977) and 0.0 – 0.9 mm.yr⁻¹ (Robinson 1977b, 1977c) have been measured on shore platforms formed in a number of different lithologies. The rate of erosion measured on the mudstone at Lake Waikaremoana was an order of magnitude greater than any previously reported erosion rates on shore platforms.

3.5 SUMMARY

This chapter has quantified and characterised surface level changes measured on shore platforms studied for this thesis. Surface level change was measured with a micro erosion meter (MEM) which is a precision engineering gauge relocated in exactly the same position for each survey on bolts secured below the rock surface. It has been shown that rates measured by the MEM are base rates of erosion and were sufficient to have formed the contemporary platforms. Therefore this technique gives a useful indication of changes occurring on shore platforms in the study environments.

Up to ten MEM sites were monitored on each study profile. Those sites on the Kaikoura mudstone, limestone, greywacke and basalt were surveyed every 2 –3 months between March 1998 and November 2000. The sites on the Lake Waikaremoana mudstone were surveyed yearly between January 1999 and March

2002. Surface change has been presented in this chapter. The largest over all surface level change during the study period of 50+mm occurred on WK1bsA. The largest surface change measured during the study period on the marine shore platforms was 11.84mm at KM2A. As well as erosion of surfaces, “swelling” events were measured on all rock types with the exception of the Lake Waikaremoana mudstone. No cyclic patterns of surface level change were evident. However, there were distinct sequential patterns at both the 2-3 monthly and daily scales showing expansion and contraction of the rock surface. On the marine platforms the magnitude of changes between surveys varied. The basalt and greywacke showed a broad range of changes between surveys of 2.25mm swelling to 2.25mm lowering. The Kaikoura mudstone and limestone showed less of a range of changes between surveys of 1.5mm swelling to 2.25mm lowering. At Lake Waikaremoana average change between surveys was 4 – 6mm of erosion.

Using the traversing MEM data the spatial diversity of surface level change was investigated at the micro scale. Basalt and greywacke displayed a greater spatial diversity of variation and range of magnitudes of change in surface level than the limestone and Kaikoura mudstone. The range and diversity of surface level variations on the basalt and greywacke without corresponding erosion showed these two rock types are capable of absorbing large surface changes. The Kaikoura mudstone and the limestone were less able to withstand dynamic change without corresponding erosion. The dynamic nature of surface level change and high rates of erosion measured on the Lake Waikaremoana mudstone showed that it is unable to withstand surface level change without net erosion occurring.

Average rates of surface change were calculated for each MEM site. The dynamic nature of surface change measured on all rock types during the study period drew into question calculation of average rates from the generally accepted method of using the first and last survey measurements divided by the duration between them. Regular surveys allowed for analysis of the importance of duration between measurements and it was shown that rates of surface change are a function of duration of the record. A method of calculating average surface level change was developed and called a multiple duration method. This method uses surface level changes measured for all possible durations between all surveys taken at a site during

the study period. These changes are plotted against duration and the line of best fit through these points gives the average rate of change. The residual gives the magnitude of variation in surface level.

Average rates calculated in this manner were similar to those calculated using the first and last measurement of the three year sample period. However, they told more about the character of change over this time.

The average rate of erosion measured in the basalt was 0.29mm.yr^{-1} , on the greywacke was 0.78mm.yr^{-1} , on the limestone was 1.19mm.yr^{-1} , on the Kaikoura mudstone was 1.41mm.yr^{-1} and on the Lake Waikaremoana mudstone was 9.13mm.yr^{-1} .

Data from MEM sites spanning 24+ years showed that erosion rates were statistically similar to the three year period of measurement conducted for this study.

CHAPTER FOUR

ROCK CHARACTER AND RESISTANCE TO EROSION.

4.1 INTRODUCTION

World wide, shore platforms are formed in a wide variety of rock types under varied morphogenetic conditions (figure 1.1). This thesis investigates shore platforms formed in five different lithologies. An understanding of the similarities and differences exhibited between these rock types is important when looking at the effect of processes pertaining to their alteration and ultimately shore platform development. Many of the concepts and models of shore platform development are based on the notion that the bedrock presents a resistance to the processes causing erosion whether those processes are wave or weathering induced (see Trenhaile 1987, Sunamura 1992, Stephenson 2000 for summaries). It is important to identify the type of resistance that the rock offers and to quantify it in order to understand how the rock has been and is eroded.

The fact that shore platforms form in many different lithologies suggests that rock type is not a primary causative factor in their formation. However, it has been suggested that aspects of lithology may affect morphology of shore platforms and the rate at which they develop (Bartrum 1935, Wentworth 1938, Jutson 1939, Edwards 1941, Hills 1949, Mii 1962, Sanders 1968a, Suzuki *et al.* 1970, Trenhaile 1972, 1974b, 1987, 2000, Bradley and Griggs 1976, Kirk 1977, Sunamura 1978, 1992, 1994, Gill and Lang 1983, Tsujimoto 1987, Trenhaile *et al.* 1998).

The shore platforms studied in this thesis have formed in basalt, limestone, greywacke and two different types of mudstone. This is a selection that encompasses a variety of rocks of quite different natures and characteristics including sedimentary (limestone and mudstones), mildly metamorphic (greywacke) and igneous rocks (basalt). This chapter compares and contrasts the rock characteristics that each study profile traverses. Lithology of each profile is described and three different measures of rock strength of each rock type are presented. The controls exerted by aspects of lithology and rock strength on shore platform morphology and morphological change

are investigated and an indication of the most appropriate indices of rock strength for use in shore platform research is given.

4.2 DESCRIPTION OF LITHOLOGIES

A good basis for understanding landform development is in description of the feature. This section provides descriptions of the lithology and characteristics of the rock into which each shore platform studied for this thesis is formed.

4.2.1 ROCK TYPES.

Profiles AK1 and AK2 are formed in basalts of the Miocene French Hill formation. This formation is made up of a suite of lava flows ranging from mildly alkaline basalt to trachyte basalt (Sewell *et al.* 1992). The mudstone at Kaikoura which KM2 and KM3 cross is an Oligocene greymarl. This is a bedded calcareous mudstone of the Waima formation and is Tertiary in age (Lensen 1975). The limestone at KM7 is Paleocene Amuri limestone which is a white to light grey sandy limestone (Lensen 1975). RM1 traverses a complex, massive and well indurated rock, locally known as greywacke. This greywacke is bedded and Mesozoic in age, being of the Kawhai series in the Torlesse group (Lensen 1975). The mudstone at Lake Waikaremoana over which profiles WK1 and WK2 cross is Miocene in age and has been classified variously as 'silty mudstone', 'sandy mudstone' or 'sandy siltstone' (Allan *et al.* 2002).

4.2.2 STRUCTURE.

The orientation of bedding and fracture planes of shore platform rocks studied was identified by geological surveys at each profile site. Observations were made along the line of each profile. These were conducted using a tape measure and Brunton compass. The compass can be used to measure both direction and angle of inclination from horizontal. Assessment included measurement of the strike and dip of dominant bedding or fracture planes and the strike and dip of any secondary sets that were evident. Also noted were the spacing, roughness, separation, infilling, and

persistence of discontinuities and the presence of ground water where it was evident. Discontinuities included fractures, joints, faults, fissures and cracks.

Bedding planes and major fracture zones were readily identifiable in the mudstones, greywacke and limestone. The basalt is volcanic in origin and therefore lacks bedding planes, though it is layered. Therefore, at AK1 and AK2 it was possible to identify major and minor fracture planes that were generally consistent over the width of the platforms. Strike was measured in degrees from magnetic North and also in comparison to the general orientation of the landward cliff. Dip was measured in degrees from horizontal. The direction of the dip is given as both a magnetic compass direction and in relation to the ocean (or lake) where + indicates dip facing towards the water body and – indicates dip facing away from the water body.

4.2.3 PROFILE LITHOLOGY

Table 4.1 gives a summary of general aspects of lithology including the dip and strike of dominant bedding planes of each profile, and the angle between rock strike and cliff orientation.

Table 4.1: General lithology of each study profile.

| profile | rock type | strike (mag °) | dip (°) | strike of landward cliff (mag °) | angle between strike and cliff (°) |
|---------|-----------|----------------|-----------|----------------------------------|------------------------------------|
| AK1 | basalt | 280 | 70S (+) | 219 | 61 |
| AK2 | basalt | 317 | 69S (+) | 156 | 19 |
| KM2 | mudstone | 260 | 45N (+) | 100 | 20 |
| KM3 | mudstone | 132 | 57 NE (-) | 43 | 89 |
| KM7 | limestone | 65 | 35E (+) | 36 | 29 |
| RM1 | greywacke | 251 | 81E (-) | 228 | 23 |
| WK1 | mudstone | 315 | 20NE (-) | 165 | 30 |
| WK2 | mudstone | 338 | 32NE (-) | 205 | 47 |

At AK1 the general strike of the basalt is 280° dipping at 70° towards the ocean. At this point on the platform the strike of this steeply dipping rock runs at an angle of 61° to the general trend of the landward cliff. There are two distinct sets of secondary fracture planes. These are also both steeply dipping, and strike so that they form roughly triangular patterns of fractures on the rock surface (figure 4.1). The spacing of these secondary fracture zones is between 50 – 300mm and defines the boundaries of blocks that were occasionally observed to have been displaced from the platform surface (figure 4.1).



Figure 4.1: Rock surface near AK1D. Showing patterns formed by dominant and secondary fracture planes. Arrow indicates space where block has been removed. Object is 280mm long.

The lithology at AK2 is similar to that of AK1. The dip is also (69°) however, the strike of the rock forms a lesser angle to the orientation of the cliff (19°) at this point on the platform. The sizing and relative positioning of secondary fault planes is comparable to those at AK1. A dyke crosses the profile approximately 15m from the landward cliff (figure 2.14). This dyke is 0.4m in width and stands 0.75m above the general height of the platform surface at this point.

KM2 is formed in mudstone that strikes at an angle of 20° to the landward edge of the shore platform which is a beach comprised of limestone cobbles. The rock dips at 45° towards the ocean. Two secondary fracture planes were evident. One strikes at right angles to the major bedding plane and dips at 80° . The other strikes almost parallel to the major bedding plane and has a dip of 12° . These bedding planes

outline trapezoid zones of fracturing that are evident at a variety of scales. Structures of approximately 1m in scale have smaller structures (100-300mm) nested within them (figure 4.2). These zones also occasionally outline locations where blocks have been removed from the shore platform surface (figure 4.2). However, removal of only a very few such blocks was observed during the study period. Some of the fractures were filled with muddy sand.

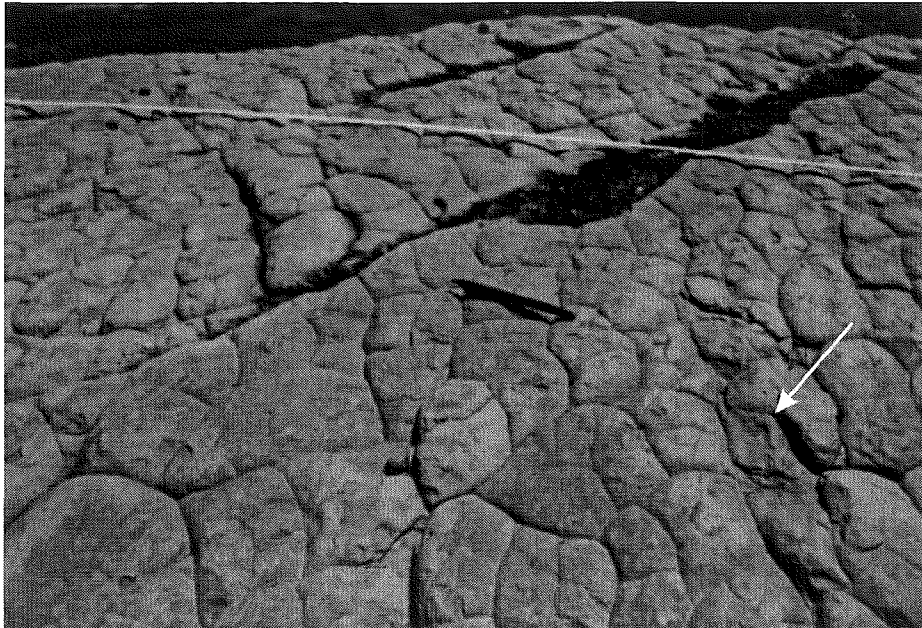


Figure 4.2: Rock surface near KM2D. Showing surface pattern defined by bedding planes. Arrow indicates position where a block has been removed. The pen in the centre of the picture is 135mm in length.

KM3, also formed in mudstone, traverses bedding planes that are of a similar size and relative position as those at KM2. KM3 has a slightly steeper dip of 57° in the landward direction. The angle between the major bedding planes and the cliff at this point on the shore platform is almost a right angle (89°).

KM7 is formed in limestone with a general strike of 65° and dip of 35° towards the ocean. The limestone has been subjected to intense folding and faulting and dip and strike varies along the profile as a result of this. The general dip and strike given above reflect the dominant direction of the bedding. Some areas of variation from this were evident along the profile. The general strike of the bedrock is at an angle of 29° to the landward cliff. Secondary fracture sets cross the main bedding with dips of 62° and 80° striking 35° and 95° respectively. The limestone is thinly bedded (figure 4.3).

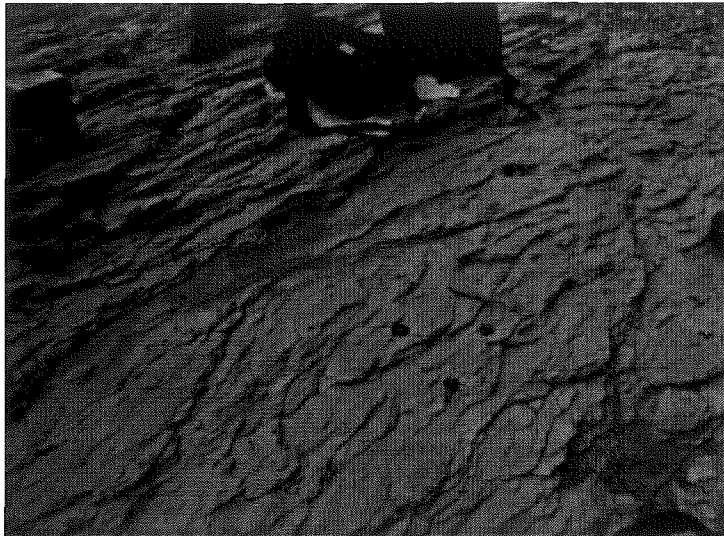


Figure 4.3: Rock surface near KM7B. MEM bolts, located centre right in the picture, form a triangle of 150mm along each side.

RM1 is formed in greywacke that is highly fractured. The dominant bedding plane runs at an angle of 23° to the strike of the landward cliff and is steeply dipping away from the ocean at an angle of 81° . Secondary fracture zones with dips of 60° and 35° and strikes of 106° and 344° respectively were evident and defined trapezoid structures at the rock surface (figure 4.4). Fractures were fine and no unconsolidated material was evident within fractures. Two channels that crossed the profile (section 2.6.7) both coincided with the main bedding planes of the rock.

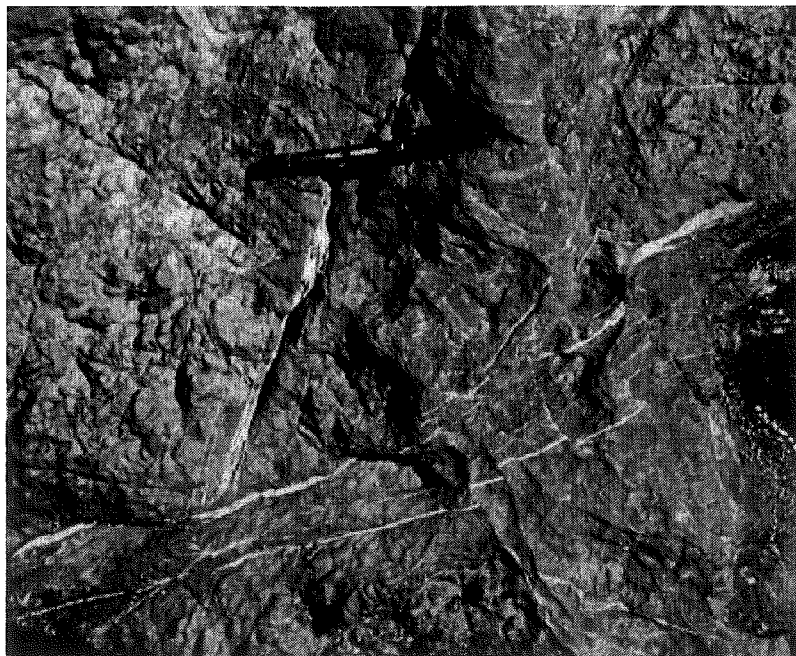


Figure 4.4: Rock surface near RM1B. Pen is 145mm in length.

The mudstone at Lake Waikaremoana in which the two profiles WK1 and WK2 are formed is highly friable (figure 4.5). Exposed surfaces, especially those further from the lake edge are deeply weathered. The bedding planes on both WK1 and WK2 are gently dipping (20° and 32° respectively) away from the lake and strike at angles of 30° and 47° to the orientation of the backing beach on each platform.



Figure 4.5: Rock surface near WK1MEM. Lens cap is 50mm in diameter.

4.3 ARE SHORE PLATFORMS WHOLLY ERODED FEATURES?

It was stated in Chapter 1 that shore platforms are wholly erosional in origin. This was based on the fact that they appear to be ‘cut’ into solid rock.

Figure 4.6 shows the direction of strike of the bedrock in relation to the orientation of the landward cliff for each of the eight profiles studied. It can be seen that all shore platforms studied in this thesis are orientated across dip and strike of lithology. There was no pattern evident in platform orientation with relation to dip or strike of the rock. This truncation of lithology can only be caused by erosion of the bedrock. Hence the shore platforms studied in this thesis are clearly wholly erosional in origin and are orientated in relation to the sea or lake rather than to lithological controls.

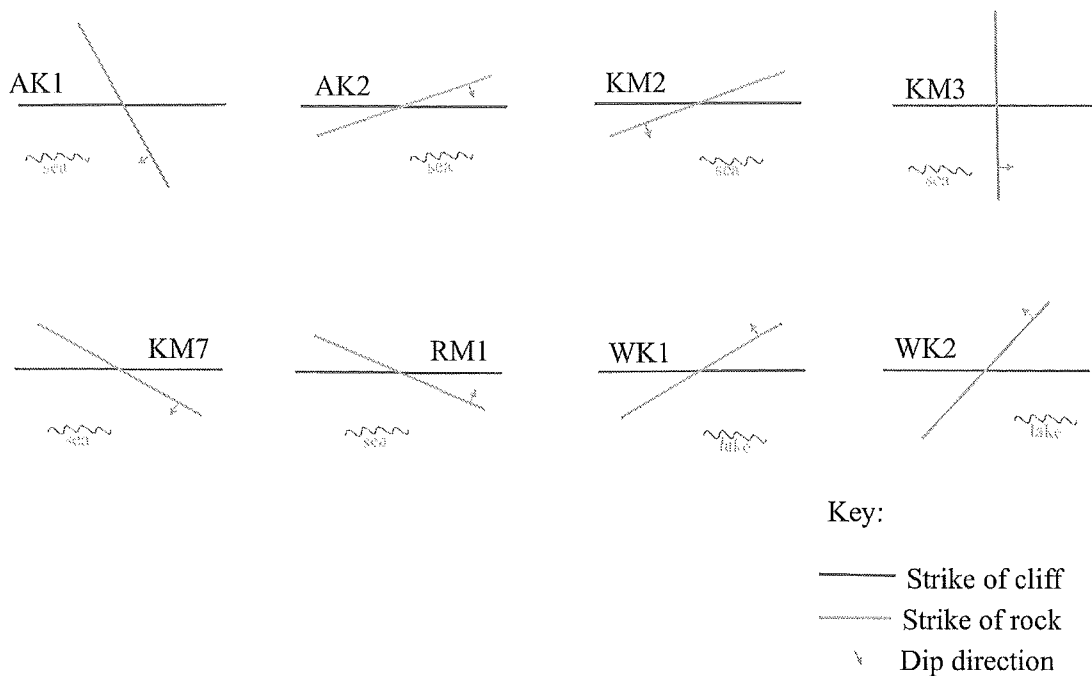


Figure 4.6: Strike of bedrock in comparison to the orientation of the landward cliff at each profile.

It seems that erosion of shore platforms studied for this thesis does not follow lines of weakness within the bedrock. Erosion caused by processes related purely to the rock structure would tend to preferentially erode the weaker zones i.e. along the bedding planes. It was shown in figure 4.6 that the shore platforms have formed, for the most part, regardless of the lines of weakness within the rock.

4.4 LITHOLOGICAL CONTROL ON SHORE PLATFORM MORPHOLOGY.

Although shore platforms appear to form regardless of lithology, on the larger scale, the notion that aspects of lithology control the present morphology of shore platforms and rates of change of morphology has been suggested by a number of authors (Edwards 1941, Mii 1962 Sanders 1968a, Sunamura 1973, Gill and Lang 1983, Tsujimoto 1987, Trenhaile 1987, 1999).

Investigations of the control of the lithological factors of bedrock strike and dip on aspects of shore platform morphology are discussed in this section. Figure 4.7 presents plots comparing bedrock strike to platform width and platform gradient and

bedrock dip to the same two aspects of morphology. No direct correlations were found between any of these factors. The lithological components of rock strike and dip show no direct control over the morphological components of width and gradient on the shore platforms studied for this thesis.

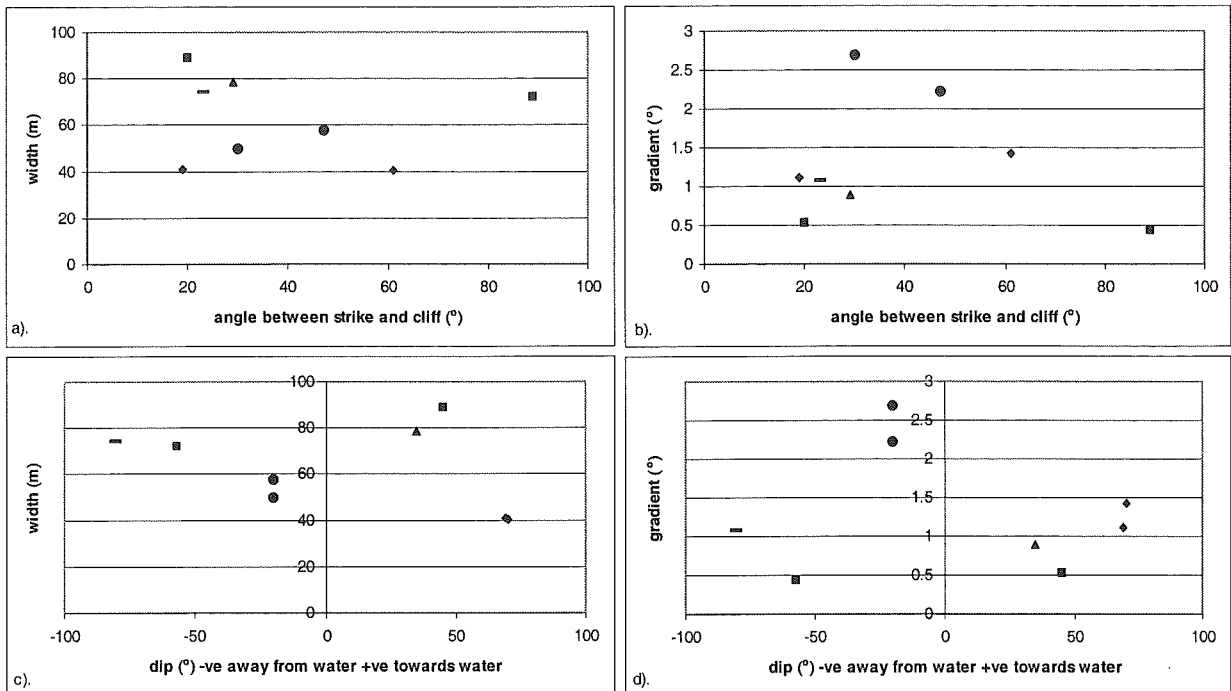


Figure 4.7: Correlations of bedrock strike or dip with platform width and gradient. Each rock type is plotted using a different symbol; greywacke (—), limestone (▲), basalt (◆), Kaikoura mudstone (■) and Lake Waikaremoana mudstone (●). a). angle between strike and cliff vs. width, b). angle between strike and cliff vs. gradient, c). dip vs. width and d). dip vs. gradient.

The lack of direct relationships shown in figure 4.7a-d add further strength to the statement that shore platforms form regardless of the underlying bedrock lithology.

The dip and strike of the rock were analysed as separate components of lithology in figure 4.7. However, the two aspects may exert control in combination. Trenhaile (1987) stated that the combination of bedrock dip and strike in relation to the incoming waves was a determining factor in the morphology of shore platforms. He presented eight structural classes of shore platforms categorised according to the rock dip and strike in relation to the cliff face (figure 4.8).

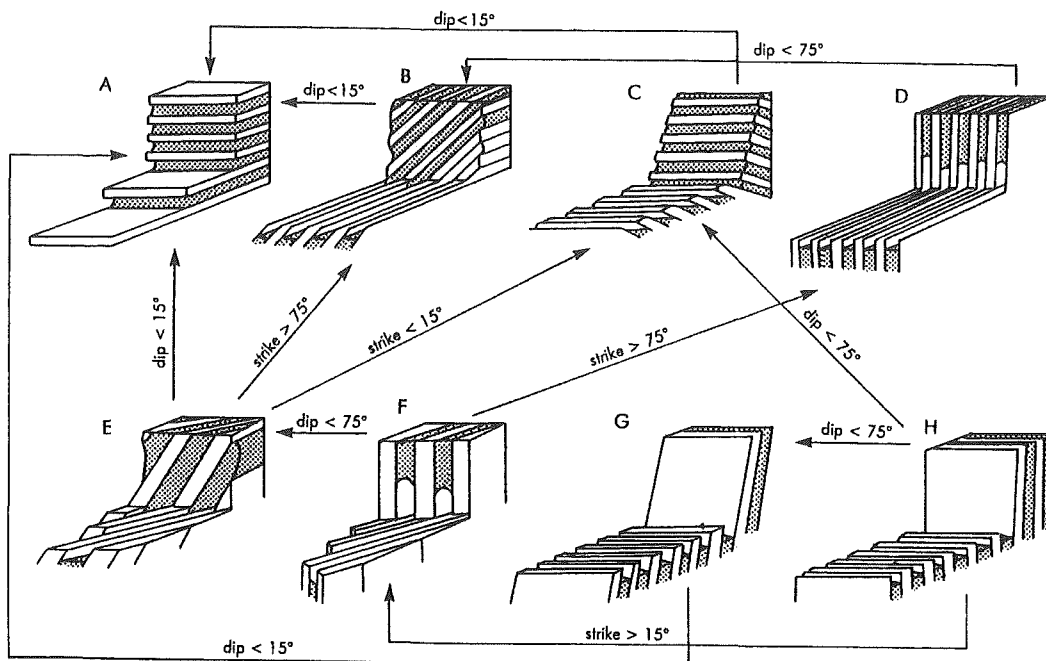


Figure 4.8: Structural classes according to rock dip and strike relative to the landward cliff face. Arrows represent promotions within class hierarchy according to changes in strike and dip (Trenhaile 1999:fig3).

“The structural classes are ranked in descending order according to their predicted susceptibility to mechanical wave erosion” (Trenhaile 1999:360). Those in category A are considered by Trenhaile to be weakest or most susceptible and those in category H strongest or least susceptible. This ranking is made on the assumption that the combination of dip and strike of the shore platform bedrock encountered by incoming waves is of relevance as it ‘determines the degree of protection afforded by resistant strata to weaker beds’ (Trenhaile 1999:360) and that waves are the primary erosive force.

This model suggests that platforms with dip and strike orientated similar to those of category A will be most extensive with greatest width and platforms classed in each successive category will be progressively narrower.

Profiles studied in this thesis were classified into categories according to figure 4.8. Platform category was plotted against platform width to test Trenhaile’s model as applied to the shore platforms studied for this thesis (figure 4.9a). Although this model did not address gradient in relation to the combination of rock dip and strike it seems logical to assume that some relationship between the two would exist. A plot of platform category against platform gradient was also constructed (figure 4.9b).

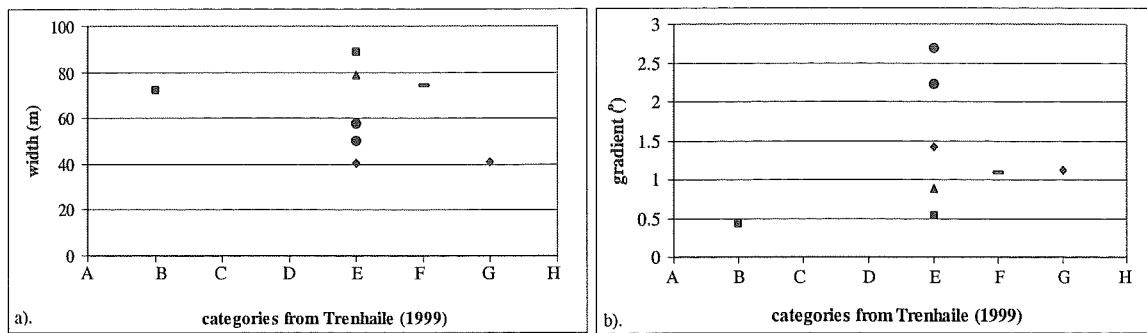


Figure 4.9: Comparison of profiles (classified according to figure 4.8) to a). width and b). gradient. Each rock type is plotted using a different symbol; greywacke (—), limestone (▲), basalt (◆), Kaikoura mudstone (■) and Lake Waikaremoana mudstone (●).

Figures 4.9 a and b both show a grouping of profiles in category E that cover a range of both width and gradient. No clear relationship is discernable in either figure.

According to Trenhaile’s model a negative trend would be expected with a hierarchical relationship and platforms in category A being the widest. Figure 4.9 shows that no hierarchical relationship is evident either in relation to platform width or gradient for this study.

The limited number of profiles used in this analysis may mean that the hierarchy is not well defined. However the profiles studied here do not adhere to the relationship suggested by Trenhaile (1999). This may be because of other aspects of rock structure or differences in morphogenetic environments. Also Trenhaile (1999) states that factors other than dip and strike may cause some changes in the positions of intermediate classes in the hierarchy e.g. bed thickness, joint density and variations in the direction of wave attack. He does not, however, outline how this may occur.

This section has shown that the orientation of shore platforms studied for this thesis bears no relationship with underlying rock lithology. It has also been shown that rock dip and strike do not control aspects of shore platform width and gradient.

4.5 ROCK STRENGTH

The inherent strength of a rock body resists forces of erosion and holds bedrock intact. Quantification of this strength will therefore give an indication of the susceptibility of a rock to erosion. Some models of shore platform development rely heavily on an understanding and quantification of rock strength as a factor controlling shore platform formation and the rate of development (Trenhaile and Layzell 1981, Sunamura 1992, Trenhaile 1999).

Therefore in order to understand processes causing changes on shore platforms an understanding of those factors resisting change must also be obtained. Traditionally the resistance forces of a body of rock have been defined in terms of rock strength and this can be tested and quantified in a variety of ways. Geomechanical quantification of rock strength involves assessment of the structure of the rock mass and the nature of its discontinuities (Brown 1981, Charnicheel 1989), and a large number of tests have been developed to assess various aspects of rock strength.

Choosing an appropriate means of characterising rock strength should reflect the nature of the forces that are causing erosion. The resistance that a body of rock is able to offer depends on the way in which processes are trying to break that rock apart. For example, waves cause external frictional stresses as water flows across the rock surface. Therefore the resistance the rock can offer to these forces needs to be assessed in terms of mechanical properties such as compressive and shear strengths. Weathering processes work both mechanically by applying external stresses, especially in fractures, and chemically by causing internal crystalline stresses. The resistance a rock presents to mechanical weathering is in terms of mechanical properties such as compressive and shear strengths but the resistance offered against chemical weathering, such as solution, is in terms of chemical properties such as the bonding and crystalline structure of the rock.

An example of the importance of characterising rock strength in terms of the nature of the forces causing erosion is found in Suzuki *et al.* (1970). In southern Japan they described a wash board relief formed on shore platform surfaces with alternating layers of mudstone and tuff. Compressive and impact strength tests conducted on the

different rock types showed the mudstone to be the stronger rock. Despite this, the mudstone was eroding more rapidly than the tuff. As compressive and impact strength tests indicate the resistance of rock to erosion by shear forces it was concluded that the mudstone was more susceptible to weathering in the form of wetting and drying than the tuff. The platform was eroded by weathering rather than by wave action (Suzuki *et al.* 1970).

There is a large body of literature investigating rock strength, for engineering purposes, and many standard tests have been developed to provide comparable, quantitative data and predictive information. Unfortunately this geomechanical literature is not often referred to in geomorphic studies.

Engineering assessments of rock strength usually include analysis of the rock structure or direct strength testing combined with analysis of the nature of discontinuities. Analysis of the structure of rock mass can be done through investigation of the chemical composition and bonding of the minerals within the rock and gives an indication of rock strength. This includes measurement of porosity, density and absorption. These properties all give an indication of how well the chemical and mineral bonding of the rock holds together under specific conditions. Tests of these factors are not always easy, or are expensive to carry out as specific equipment is required.

It is also possible to test, directly, the strength of the intact rock by loading a sample of the rock with pressure and recording the amount of pressure that it is able to withstand before failure. This is referred to as the bulk strength and there are various standard methods for testing it such as uniaxial core compressive testing and point load testing (Brown 1981). These methods require removal and preparation of samples from the actual body of rock and are usually performed in laboratory conditions.

Tests have also been developed to assess the *in situ* surface strength of rock. The most commonly used is the Schmidt hammer test which measures the elasticity of the rock surface (Day and Goudie 1977).

Analysis of the nature of discontinuities within the rock body tends to be less rigorously tested and based on careful description of aspects such as joint spacing, orientation, continuity and persistence (Brown 1981). Discontinuities within the rock generally act to reduce its intact strength.

When classifying rock strength geomorphologists have tended to use less rigorous testing methods than engineers. There may be a number of reasons for this including a lack of access to testing equipment, the large areas of rock that require assessment and an interest in the surface layer of the rock rather than the unchanged internal structure of the rock. This general description of rock strength has hindered causative comparisons by not providing a rigorous basis on which to compare between rock types or even within a single rock body (Day and Goudie 1977, Selby 1980).

To address this issue Selby (1980) developed an index of rock mass strength. This method is based on simple surface testing of rock strength and observation of aspects of lithology. Each aspect is ranked and weighted to give the final index. It can be used to compare the strength of large areas of rock and has been employed in this study (section 4.5.2.3).

Comparable measures of rock strength in shore platform studies are not common. Most studies, at least, name the rock type in which the shore platforms have been formed. In some studies it has been assumed that certain rock types are 'harder' than others, but no quantification of hardness has been given (e.g. Bartrum 1935, Trenhaile 1974a, Bradley and Griggs 1976). Only a few studies go on to further quantify rock strength.

Edwards (1941) was the first to put a quantitative value on the strength of shore platform rocks. He gave compressive strength values for shore platforms in Victoria and Tasmania, Australia. Unfortunately there was no description of the testing method included with the results. Since then compressive strength has been used as an indication of the strength of shore platform rocks by Suzuki *et al.* (1970), Takahashi (1977), Tsujimoto (1987), Sunamura (1978) and Stephenson and Kirk (2000b). In these studies compressive strength values were obtained through

compression testing in the laboratory. An indication of compressive strength of shore platform rocks has also been obtained through *in situ* testing of the elasticity of the rock surface using Schmidt hammers (Suzuki *et al.* 1970, Tsujimoto 1987, Sunamura 1978, Trenhaile *et al.* 1998 and Stephenson and Kirk 2000b).

A comprehensive geomechanical analysis of rock strength on shore platforms was conducted by Tsujimoto (1987). Recognising that both intact rock strength and discontinuities were important in the assessment of overall strength of shore platform bedrock, he developed a ratio relating the compressive strength (uniaxial core compression test) to a measure of bedrock joint structure. This measure was obtained through *in situ* sonic testing of the bedrock. Unfortunately this comprehensive approach to rock strength analysis has not been replicated in other shore platform research to the author's knowledge. Part of the difficulty is the expense of sonic testing equipment. It was beyond the scope of the budget for this project to assess rock strength using sonic techniques. Therefore, this study assesses fractures within the bedrock using a less costly and, unfortunately, less objective observational method (section 4.5.2.3).

4.5.1 INDICES OF ROCK STRENGTH

From the previous section it is apparent that only a few studies of shore platforms have used quantifiable indices of rock strength and that these indices have been varied. There is a need for more geomechanically based definitions of shore platform rock strength before robust analysis of the control of various characteristics of the rock on platform morphology can be undertaken.

Assessment of rock strength should be made in a way that reflects the processes of nature, so that an index is obtained, that gives an indication of how resistant shore platform rocks are to the erosive forces that are acting on them. A wide variety of processes have been hypothesised as active in erosion of rocks of shore platforms but no clearly dominant processes have yet been defined. Therefore, careful consideration is required before choice of index of rock strength is made. To this end three different tests of rock strength have been conducted for this thesis, defining three different indices of rock strength. This section describes methods used to

define the indices. Sections 4.5.3 and 4.5.4 compare rock strength of each platform obtained using the three different indices.

4.5.2 METHODS USED TO MEASURE ROCK STRENGTH

This section outlines methods used to measure the strength of the rock each shore platform was formed in.

For comparative purposes among shore platform studies an indication of the compressive strength of the shore platform rocks was required.

Compressive strength (S_c) is the load per unit area under which a block fails by shearing or splitting and can be given by equation 4.1

$$S_c = \frac{P_c}{A} \quad \text{Equation 4.1}$$

Where P_c is the load under which a specimen fails and A is the cross-sectional area (Tsujiimoto 1987).

A standard uniaxial core compressive strength test used by Tsujimoto (1987) and Stephenson (1997a) was attempted for this study. In this test a machine is used to apply a constant rate of axial load to a uniform sized rock specimen until failure occurs. The specimen is required to be in the form of a circular cylinder of 50mm in diameter and a height of 2.5 – 3 times the diameter. It must have flat ends and be free from abrupt irregularities (Brown 1981). The fractured nature of many of the rocks that formed the shore platforms studied in this thesis prevented preparation of rock samples as specified above in all but one instance (Kaikoura mudstone). Therefore uniaxial core compressive strength testing was not possible.

It was possible to conduct tests of point load compression and Schmidt hammer rebound and to make mass strength assessments for each rock type. The method is presented for each test in the remainder of this section and the results are presented and discussed in sections 4.5.3 – 4.5.6.

4.5.2.1 POINT LOAD TESTING.

An indication of compressive strength of each rock type in which the shore platforms in this study are formed was obtained using the point load testing method. This is a slightly less rigorous test than the uniaxial core compression test. Point load testing requires rock specimens in the form of cut blocks or irregular lumps. These are then broken by application of concentrated load through a pair of spherically truncated platens (ISRM 1985). The method used for this thesis followed the instructions laid out in ISRM (1985). Large blocks ($\sim 0.4\text{m}^3$) of bedrock were collected from locations close to study profiles on each rock type. These were cut into blocks of standard size (figure 4.10) in a laboratory, where the diameter (D) was $50\pm 20\text{mm}$.

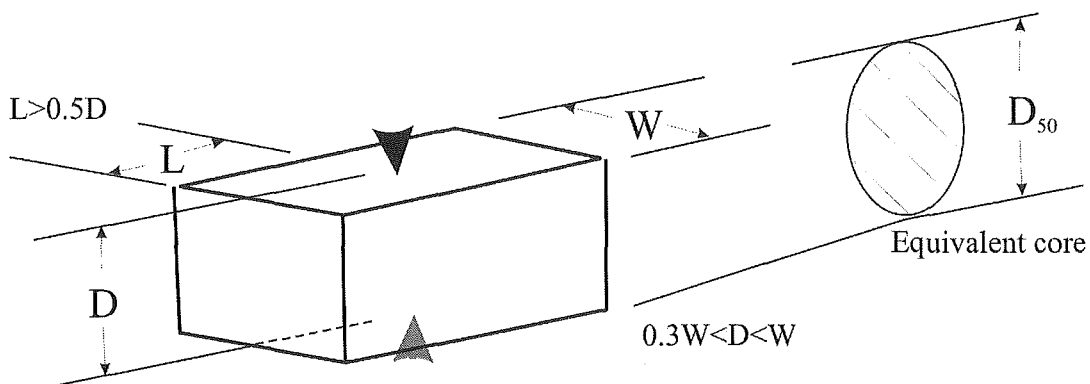


Figure 4.10: Specimen shape requirements for point load block tests (ISRM 1985:fig.3c).

Block dimensions were measured to an accuracy of $\pm 2\%$. All specimens were tested after being air dried for at least 40 hours. Samples were tested dry in order to match natural conditions as closely as possible. It was noted during *in situ* drilling of shore platform surfaces that rock below the surface layer was dry even when the top layer was wet. Samples were tested with load acting at right angles to the planes of weakness of the rock sample and tests were only considered valid when surface fracturing passed through both loading points. Between 10 and 27 valid tests were obtained for each of the five rock types. Failure loads were corrected to give 50mm core equivalent compressive strength values according to instructions given by ISRM (1985).

4.5.2.2 SCHMIDT HAMMER TESTING.

Rock strength was tested *in situ* using an N-type Schmidt hammer. The Schmidt hammer was designed for *in situ* testing of concrete and has been successfully used by geomorphologists to make rapid field measurements of the surface strength of rocks (Day and Goudie 1977, Selby 1980, Williams and Robinson 1983). The hammer measures the distance of rebound of a mass from a controlled impact of the mass on a rock surface. The distance of rebound gives a relative measure of surface hardness or strength (Day and Goudie 1977). Rock surfaces were tested when dry and the hammer was oriented vertically. Surfaces tested were flat, free from flakes and dirt and as far from fractures as possible. The effect of fractures is to lower the surface strength of the rock body (Hucka 1965, Day and Goudie 1977). The variability of readings meant that at least 30 impacts were made at each site and the average of these was reported as per the Schmidt hammer guidelines. Each impact was made at a fresh location as repeated testing of the same spot increases the rebound values due to local partial crushing of the rock (Day and Goudie 1977). Schmidt hammer testing was undertaken at 3 locations on each profile, close to MEM bolt sites, but not on them.

4.5.2.3 MASS STRENGTH ASSESSMENT.

Both point load and Schmidt hammer testing give locationally specific strengths of the bedrock and rock surface respectively. Selby (1980) suggested that the type of rock strength defined by testing of specific locations is not necessarily the type of strength that keeps a landform together. He developed a method of assessment to give a relative value for mass strength of the rock, as a whole. This accounts not only for intact rock strength, but also fractures and weathering, all of which combine to facilitate erosion of the bedrock. Selby (1980) identified seven rock mass parameters used in engineering classifications that are also relevant in geomorphic analysis. The seven parameters used are: intact rock strength, weathering, spacing of joints, joint orientations, width of joints, continuity of joints and outflow of groundwater. Each parameter is divided into five hierarchical categories and weighted according to relative importance. Weighted parameters are summed to give a relative index of rock mass strength. Field classification of parameters is

based on straightforward measurement and observation. Rock masses with total ratings of 100-91 are classified as very strong, 90-71 strong, 70-51 moderate, 50-26 weak and <26 very weak (refer to table 4.2). Field assessment of each of the seven parameters was made for this study at each profile in conjunction with the geological survey outlined in section 4.2.2.

4.5.3 ROCK STRENGTH OF SHORE PLATFORMS STUDIED

Selby (1980) divides rock strength into five categories of very strong, strong, moderately strong, weak and very weak, based on values obtained from different strength tests (table 4.2). He categorises values for point load compression strength testing, Schmidt hammer rebound testing and mass strength index as shown in table 4.2. This gives a qualitative comparison of rock strength given by different types of tests. This descriptive definition of strength will be used throughout this chapter in conjunction with actual indices of strength in order to give an impression of the strength of the rocks in which the shore platforms studied are formed compared to rock strengths in general.

Table 4.2: Descriptive categories of rock strength (Selby 1980).

| rock strength category | point load compressive strength (MPa) | Schmidt hammer rebound number | mass strength index number |
|------------------------|---------------------------------------|-------------------------------|----------------------------|
| very weak | 0.04-1.0 | 10-35 | <26 |
| weak | 1.0-2.0 | 35-40 | 26-50 |
| moderately strong | 2.0-4.0 | 40-50 | 51-70 |
| strong | 4.0-8.0 | 50-60 | 71-90 |
| very strong | >8.0 | >60 | 91-100 |

Table 4.3 presents the results of rock strength of each different rock type from point load testing. The first column gives the average value. Also presented are the standard deviations of test results and the maximum and minimum test values measured.

Table 4.3: Point load test results for all five rock types. Qualitative strength is based on values given in table 4.2.

| Rock type | point load testing (MPa) | | | | qualitative rock strength |
|------------------------------|--------------------------|--------------------|---------|---------|---------------------------|
| | average | standard deviation | maximum | minimum | |
| basalt | 1.79 | 1.97 | 7.44 | 0.19 | weak |
| mudstone (Kaikoura) | 1.03 | 0.27 | 1.32 | 0.49 | weak |
| limestone | 1.92 | 1.00 | 3.18 | 0.12 | weak |
| greywacke | 2.14 | 1.46 | 4.62 | 0.47 | moderately strong |
| mudstone (Lake Waikaremoana) | 1.70 | 1.44 | 3.79 | 0.50 | weak |

Point load testing resulted in a range of average $I_{s(50)}$ compression strengths between 2.14 and 1.03 MPa. This encompasses rocks of weak and moderately strong character (Selby 1980). The strongest rock tested this way was the greywacke and the weakest the Kaikoura mudstone.

Surprisingly the Lake Waikaremoana mudstone was relatively strong in terms of point load compressive strength given its friable nature. However, testing of this rock was restricted to the small number of ten accepted tests due to the difficulty of preparation of samples. Much of the rock fragmented during cutting.

The variation in point load tests of all rock types was large as shown by the standard deviation of testing. Tests on the basalt gave a standard deviation of 1.97MPa which was greater in magnitude than the average point load strength measured. Standard deviations of other rock types were not as high ranging from 0.27MPa of test mean on the Kaikoura mudstone to 1.46MPa on the greywacke. Although greywacke had the highest mean point load strength, the strongest individual specimen sampled was from the basalt. Basalt showed the greatest variation in point load strength with a standard deviation of $\pm 110\%$ of the mean value.

Table 4.4 presents the results of Schmidt hammer testing on each of the five different rock types. The first column gives the average rebound value. Also presented are the standard deviations of test results and the maximum and minimum test values measured on each rock type.

Table 4.4: Schmidt hammer test results for all five rock types. Qualitative strength is based on values given in table 4.2.

| rock type | Schmidt hammer testing (rebound number) | | | | qualitative rock strength |
|------------------------------|---|--------------------|---------|---------|---------------------------|
| | average | standard deviation | maximum | minimum | |
| basalt | 22 | 5.4 | 41 | 16 | very weak |
| mudstone (Kaikoura) | 32 | 5.7 | 45 | 10 | very weak |
| limestone | 31 | 7.3 | 44 | 10 | very weak |
| greywacke | 44 | 10.8 | 79 | 12 | moderately strong |
| mudstone (Lake Waikaremoana) | 19 | 1.7 | 22 | 17 | very weak |

Schmidt hammer mean rebound values ranged from 19 on the mudstone at Lake Waikaremoana to 44 on the greywacke. In terms of general rock strength (table 4.2) rocks were either very weak (Lake Waikaremoana mudstone, basalt, limestone and Kaikoura mudstone) or moderately strong rock (greywacke).

The mean rebound number for the basalt was low in comparison to the Kaikoura mudstone, limestone and greywacke. This result may not only reflect the inherent surface strength of the rock but could also be influenced by the rough nature of the surface. Williams and Robinson (1983) reported field trials that indicated Schmidt hammer readings were a function of not only the hardness of the surface but also the texture. Smooth planar surfaces gave readings of up to 30% higher than rough or irregular surfaces of the same rock type. They stated that Schmidt hammer readings were ‘representative only of a given rock and a given surface texture of that rock’ (Williams and Robinson 1983:292). The surface of the basalt, at a micro scale, was noticeably rougher than the Kaikoura mudstone or limestone (figure 2.23). However, as it is these properties that are exposed to erosion, comparison between rock types of different surface textures should be adequate for the purposes of this study.

Variations in testing ranged from a maximum test result of 79 on the greywacke to a minimum of 10 on both the Kaikoura mudstone and limestone. As 10 is the lowest accurate rebound value measurable by the N-Type Schmidt hammer being used this minimum value does not necessarily represent the weakest possible part of the

surface. Standard deviations of rebound numbers in testing were between 10.8 on the greywacke and 1.7 on the Lake Waikaremoana mudstone.

Mudstone at Lake Waikaremoana had a comparatively low standard deviation of 9% of the mean value (19). Standard deviations of other rock types ranged between 18 – 25% of mean values. This low standard deviation at Lake Waikaremoana is more a reflection of difficulty in testing the mudstone at Lake Waikaremoana using the Schmidt hammer method rather than a lack of uniformity of the strength of the rock surface. The weathered nature of the surface made locating suitable test sites difficult and many of the tests registered below 10 on the rebound scale. As this is below the accurate measurement scale of the hammer these results were discarded.

Assessment of the shore platform rocks using Selby's (1980) rock mass strength index is given in table 4.5. Presented are descriptions and ratings for each parameter in the rock mass classification scheme for each of the five rock types studied in this thesis. As joint orientation was measured relative to the slope of the landform it was not applicable in the shore platform situation as surfaces are essentially horizontal. Therefore each rock type was given a neutral value of 14 for this parameter.

Table 4.5: Rock mass strength classification according to Selby (1980) for each rock type.

| rock type | intact strength | weathering | joint spacing | joint orientation | width of joints | continuity of joints | ground water | index total | qualitative rock strength |
|------------------------------|-----------------|-----------------------|--------------------------|-------------------|-----------------|--|--------------------|-------------|---------------------------|
| basalt | very weak (5) | slight (9) | seamy / fractured (18) | n/a (14) | 0.1 - 1mm (6) | continuous - no infill (5) | none (6) | 63 | moderately strong |
| mudstone (Kaikoura) | very weak (5) | slight - moderate (8) | seamy / fractured (18) | n/a (14) | 0.1 - 1mm (6) | continuous - no infill / thin infill (5) | none / trace (5.5) | 61 | moderately strong |
| limestone | very weak (5) | slight (9) | fractured (15) | n/a (14) | 0.1 - 1mm (6) | continuous - no infill (5) | none (6) | 60 | moderately strong |
| greywacke | moderate (14) | slight (9) | seamy / fractured (18) | n/a (14) | 0.1 - 1mm (6) | continuous - no infill (5) | none (6) | 72 | strong |
| mudstone (Lake Waikaremoana) | very weak (5) | high (5) | fractured / crushed (12) | n/a (14) | 1 - 5mm (5) | continuous - thin infill (4) | trace (5) | 50 | weak |

Assessment of mass strength using this method showed that strengths ranged from weak (Lake Waikaremoana mudstone) through to strong (greywacke).

4.5.4 COMPARISON OF ROCK STRENGTH INDICES.

Table 4.6 presents results of the three different assessments of rock strength for each rock type in one table. The three different methods used for testing the strength of each of the five rock types gave varied results.

Table 4.6: Rock strength, assessed using point load and Schmidt hammer tests and the rock mass strength index.

| rock type | point load (MPa) | Schmidt (rebound number) | mass strength (Selby's index) |
|------------------------------|------------------|--------------------------|-------------------------------|
| basalt | 1.79 | 22 | 63 |
| mudstone (Kaikoura) | 1.03 | 32 | 61 |
| limestone | 1.92 | 31 | 60 |
| greywacke | 2.14 | 44 | 72 |
| mudstone (Lake Waikaremoana) | 1.70 | 19 | 50 |

From the three different tests of rock strength, relative rankings of the five rock types from strongest to weakest can be derived (table 4.7). Rankings of the five rock types studied in this thesis were different for each index of rock strength.

Table 4.7: Rock strength rankings. Where 1 = the strongest rock type and 5 = the weakest.

| Rank \ Test | Point load | Schmidt hammer | Mass strength |
|-------------|------------------------------|------------------------------|------------------------------|
| 1 | greywacke | greywacke | greywacke |
| 2 | limestone | mudstone (Kaikoura) | basalt |
| 3 | basalt | limestone | mudstone (Kaikoura) |
| 4 | mudstone (Lake Waikaremoana) | basalt | limestone |
| 5 | mudstone (Kaikoura) | mudstone (Lake Waikaremoana) | mudstone (Lake Waikaremoana) |

This difference in rankings is a reflection of the fact that each test measures a different aspect of rock strength. The point load test measures the compressive strength of bedrock with test samples obtained from subsurface, unweathered bedrock. Schmidt hammer tests the rock surface strength and reflects the state of the surface, including degree of weathering, fractures and texture. Both these tests sample at a specific point and results are extrapolated to the entire rock body. The mass strength assessment evaluates the rock body as a whole and therefore considers the strength at the landform scale.

From table 4.7 it can be seen that the greywacke was highest ranked in all three tests. It is the strongest of the shore platform bedrocks studied in this thesis, in all aspects.

The limestone, comparatively, was internally strong but its surface strength was weaker and when assessed as a whole rock mass it was relatively weak. This weakness of the rock mass was due mainly to the extensive folding and faulting of the rock which has caused extensive fracturing.

The basalt was relatively strong internally and as a whole rock body but its surface strength was significantly weaker than all other rock types except the Lake Waikaremoana mudstone. As noted in the previous section this may be a true reflection of a weaker surface or a reflection of the rougher surface texture. Figure 2.22 showed that at the micro scale the basalt is more angular than either the Kaikoura mudstone or limestone.

The bedrock of the Kaikoura mudstone was relatively weak, internally, but had a comparatively high surface strength. This is interesting. The reason for this is unknown but may reflect less surface weathering or the smoother nature of the surface. It is also possible that the top weathered layer of rock is more frequently removed thereby leaving unweathered surfaces exposed more often relative to the other rock types. This is an avenue of investigation that warrants further study.

The Lake Waikaremoana mudstone was generally weakest in all three strength aspects.

Quantification of three different aspects of strength for each rock has been given in this section. Point load testing measured bedrock strength, Schmidt hammer testing measured surface rock strength and the mass strength index assessed the overall strength of the rock body. Each test gave a different ranking of the five different rock types in terms of relative strength. From this it could be concluded that shore platforms formed in each different rock type will be susceptible to different processes of erosion. This is an important consideration when investigating the control of rock strength on shore platform morphology and when defining an index of rock resistance force suitable for use in studies of shore platform development.

4.5.5 VARIATIONS IN ROCK STRENGTH.

When characterising rock strength it is important to consider variation as well as mean values in order to obtain an overall impression of the character of the rock. Tables 4.3 and 4.4 gives standard deviations of test results and maximum and minimum values measured for point load and Schmidt hammer testing of each rock type. These were described in section 4.5.3. Graphical representation of variations in strength of each rock type in the form of standard deviation of test results of point load and Schmidt hammer testing is given in figure 4.11.

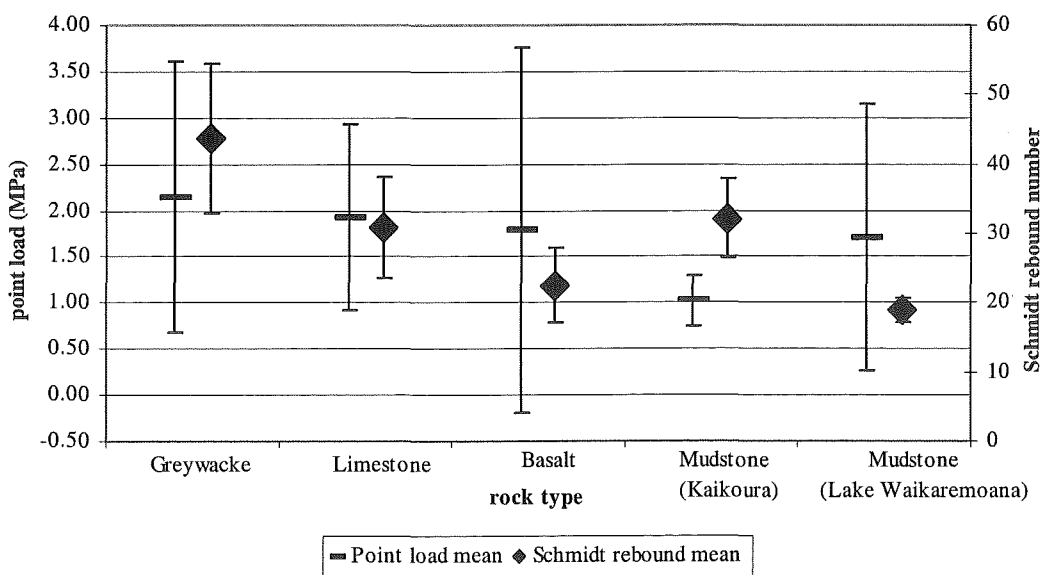


Figure 4.11: Rock strength as tested using point load and Schmidt hammer methods. The central point gives mean value and the bars show standard deviation of all test results for each rock type.

Figure 4.11 emphasises the fact that there was a large variation in point load testing results. Basalt showed the greatest variation with a standard deviation of $\pm 110\%$ of the mean value. The greywacke, limestone and Lake Waikaremoana mudstone all had large standard deviations for point load tests ranging between $\pm 85\%$ and $\pm 52\%$ of their respective mean values. Kaikoura mudstone showed a relatively small variation in test results of only $\pm 26\%$ of the mean value. The bedrock strength of basalt is therefore spatially varied and diverse in character, as are the strengths of the greywacke, limestone and Lake Waikaremoana mudstone. This diversity would be expected to result in differential weathering and erosion rates on the basalt shore platform.

Variations of measurements around the mean values for Schmidt hammer testing were less than those of point load testing and the magnitudes of standard deviations were more consistent between rock types with greywacke, basalt, limestone and Kaikoura mudstone recording standard deviations between 18-25% of mean values and Lake Waikaremoana mudstone had a standard deviation of 9% of the mean value.

Rock surface strength as tested by the Schmidt hammer had smaller standard deviations than bedrock strength tested by the point load method. This suggests that surface strength is more uniform in nature than bedrock strength. However, the different strength testing methods and the different units used for analysis means that comparisons of this nature between results can only be made very tentatively.

4.5.5.1 SPATIAL VARIATION ACROSS A SURFACE.

The standard deviations of measurements of surface rock strength (table 4.4) show that surfaces of all rock types studied displayed a range of different surface strengths. This emphasises the importance of a mean result representative from at least 30 rebound tests as outlined in the testing procedure.

The spatial diversity of rock strength over a small area of rock surface was investigated on an area of mudstone at Kaikoura. Schmidt hammer readings were

taken on consistent 0.05m spaced grid points over a surface area of mudstone of 1m x 0.5m. From this uniform testing pattern a contour map of surface strength was plotted (figure 4.12a) using Surfer Golden Software mapping package.

Figure 4.12a shows that surface strength ranged from Schmidt hammer rebound values of 37 (weak rock) to 10 (very weak rock) within a 0.5m² area. This is a remarkable amount of variation in surface strength across a small area which, visually, appears relatively uniform (figure 4.12b).

The smoother surface of the Kaikoura mudstone lent itself to systematic sampling of this nature. It was not possible to carry out similar studies on the other rock types due to their rougher surface characteristics. As magnitudes of standard deviations of surface testing were similar for each of the rock types it is reasonable to assume that these rock types would also display complex spatial variations in rock surface strength.

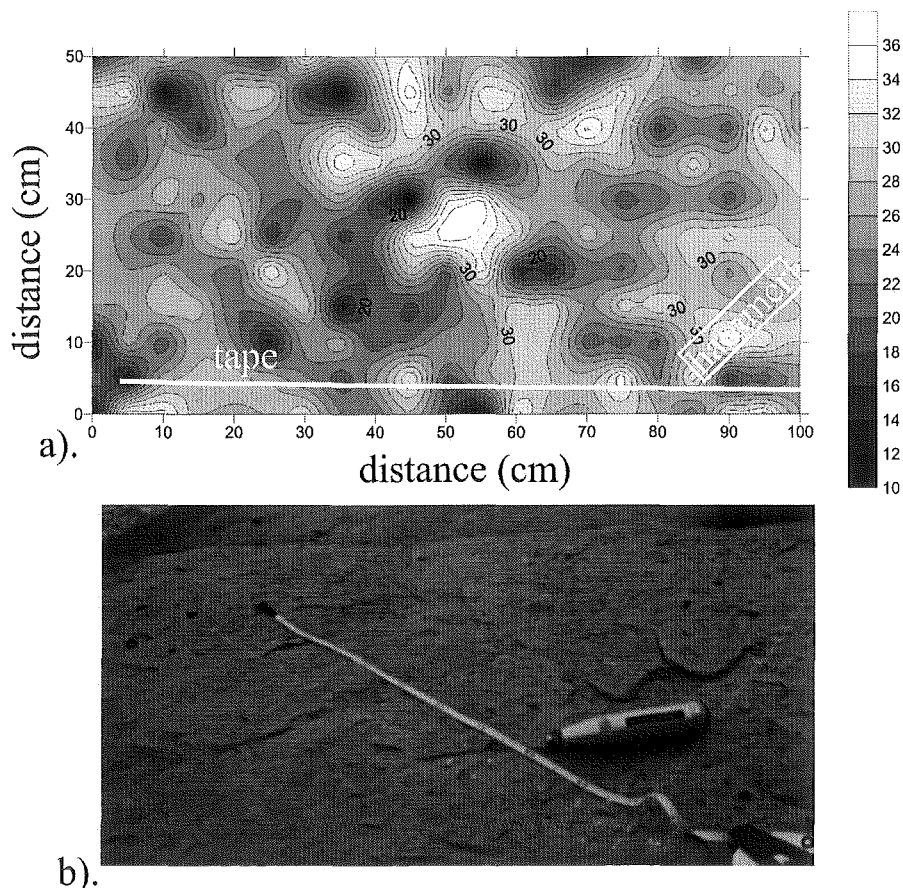


Figure 4.12: a) Contour pattern depicting the spatial variation in surface strength of 0.5m² of rock surface near KM3B. Tests were made at 0.05m spaced grid points. The contour map was plotted using Surfer Golden Software mapping package. b) Photo of the surface tested. Hammer is 280mm in length.

The surface strength of the mudstone at Kaikoura has been shown to be spatially diverse (figure 4.12a). This diversity of pattern shown in figure 4.12a is similar in character to the diverse pattern shown in shore platform surface change at the micro scale (figure 3.14). This leads to the conclusion of a causative link between surface strength of rock and surface level changes at similar spatial scales where the general relationship is uncertain. This link has yet to be fully investigated and is an avenue for future research.

4.5.6 REDUCTION OF ROCK STRENGTH.

By converting point load and Schmidt hammer rebound values into equivalent uniaxial core compressive strengths it is possible to compare measured bedrock strength with surface strength. From this an indication of the amount of weathering of the surface can be obtained, in terms of reduction of rock strength.

Conversion from both point load and Schmidt hammer rebound values to an equivalent uniaxial core compressive strength is possible using correlation graphs and equations developed for this purpose (ISRM1985, Day and Goudie 1977, Brown 1981, Charnicheal 1989). Graphs and equations were based on laboratory testing of a wide range of rock samples.

Table 4.8 presents compressive strength equivalent values for both point load and Schmidt hammer rebound mean results for each rock type. Conversions for point load data were made using a correlation graph provided in ISRM (1985) and conversion from Schmidt hammer values were made using a conversion equation provided by Day and Goudie (1977).

Table 4.8: Compressive strength equivalent values for point load and Schmidt hammer testing for each rock type.

| rock type | point load | Schmidt hammer |
|------------------------------|------------------------------|------------------------------|
| | compressive equivalent (MPa) | compressive equivalent (MPa) |
| basalt | 40 | 4.7 |
| mudstone (Kaikoura) | 22 | 11.4 |
| limestone | 45 | 10.4 |
| greywacke | 50 | 33.2 |
| mudstone (Lake Waikaremoana) | 38 | 3.6 |

For the basalt and the Lake Waikaremoana mudstone compressive strength equivalents from point load and Schmidt hammer tests are an order of magnitude different. Basalt point load core compressive strength equivalent was 40MPa compared to a Schmidt hammer core compressive strength equivalent of 4.7MPa. The rock type that showed the least difference between core compressive strength equivalents of the two tests was the greywacke with a point load equivalent of 50MPa and a Schmidt hammer equivalent of 33.2MPa.

Although conversion to a standard measure of uniaxial core compressive strength may enable useful comparison between tests, the reported accuracy of conversion equations and graphs is not great (ISRM 1985). Rather, it is recommended to use the actual test results directly where possible and in this way make a comparison between rock types (Day and Goudie 1977). However compressive strength equivalents do provide a good basis for comparison between the different indices of rock strength.

As point load test results represent the intact rock strength of the bedrock and Schmidt hammer rebound results represent the surface strength, the difference between the two gives the degree to which rock strength has been reduced at the surface. This can be used as an indication of the degree of weathering of the surface rock.

The least weathered shore platform surface was the one formed in the greywacke where surface strength was 34% that of the bedrock strength. The Kaikoura mudstone showed a 48% reduction in strength at the surface. The limestone and basalt both showed greater reductions of 77% and 88% respectively and the most highly weathered rock was the Lake Waikaremoana mudstone with reduction in strength of 91% at the surface.

Given broadly similar morphogenetic conditions it is expected that surfaces with a greater degree of weathering would erode at a greater rate. There was no such correlation between the reduction in rock strength at the surface and average rate of surface change (figure 4.13). Those rock types with greater average rates of surface change were not necessarily the most weathered at the surface, where the reduction

of rock strength between bedrock and the surface has been taken as an indication of degree of weathering.

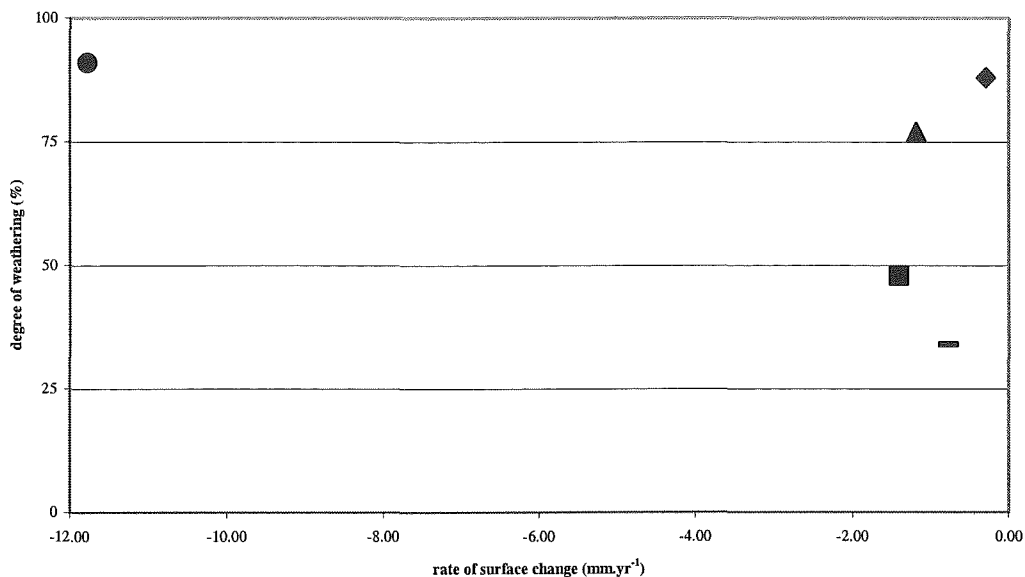


Figure 4.13: Average rate of surface change vs. degree of weathering. Degree of weathering is given as the percent reduction between bedrock and surface strength rock strength for each rock type.

There may be a number of reasons for this lack of correlation, related to variations in morphogenetic conditions, the rate at which weathered material can be removed from each rock type or as stated previously conversions to equivalent compressive core strengths may have some significant component of error. These are possible avenues for future investigation.

4.6 ROCK CONTROL OF SHORE PLATFORM MORPHOLOGY.

This section investigates the control of each of the three measured indices of rock strength on aspects of morphology and morphological change. Measured indices of rock strength were point load or bedrock strength, Schmidt hammer rebound or surface strength, and mass strength of the rock. Figures 4.14 – 4.18 show plots of each of the three measured indices of rock strength as related to shore platform width, gradient, elevation, surface roughness and rate of surface change.

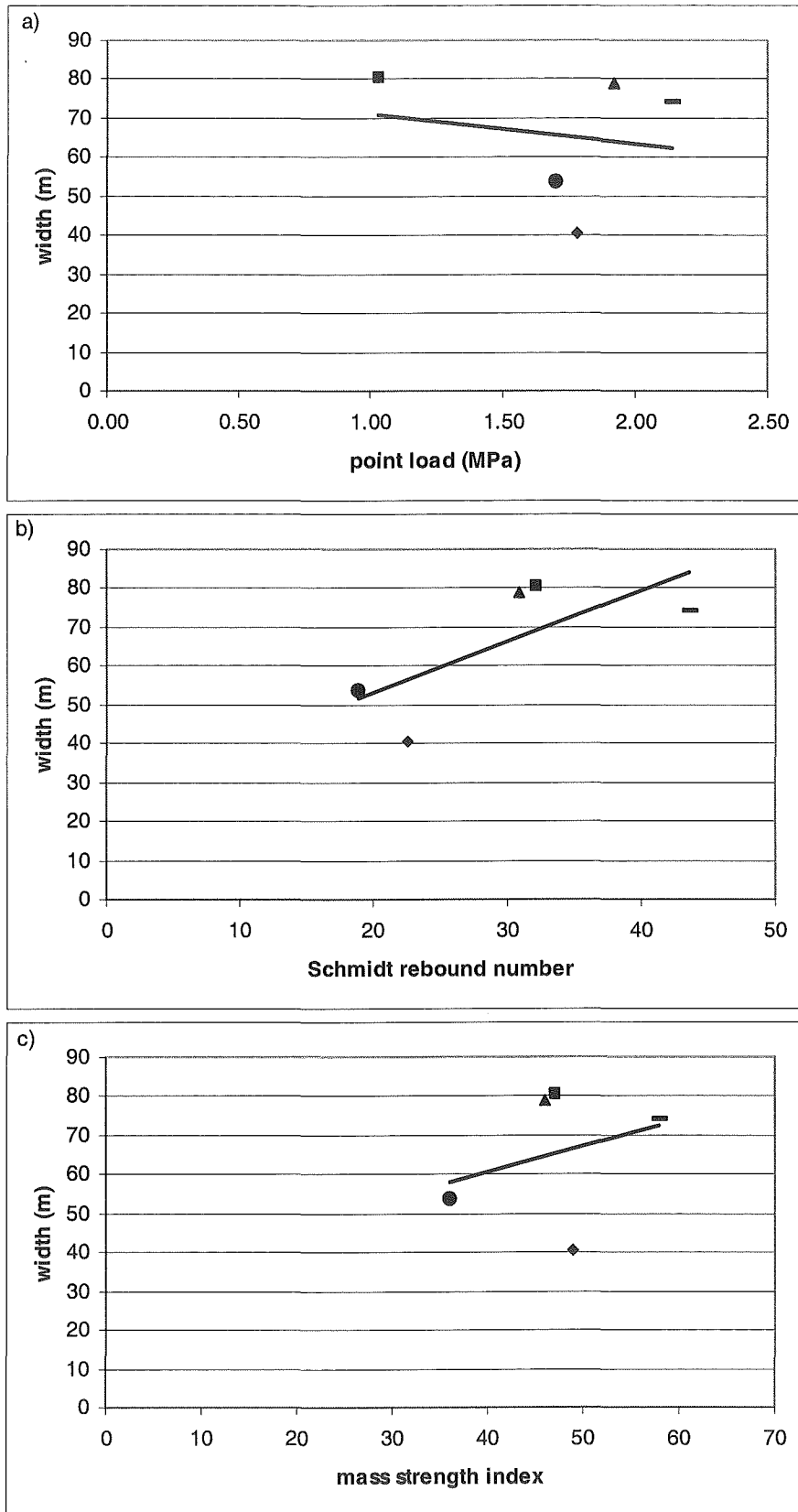


Figure 4.14: Shore platform width compared to a) bedrock strength, b) surface strength and c) mass strength of the rock in which each shore platform is formed. Each rock type is plotted using a different symbol; greywacke (—), limestone (▲), basalt (◆), Kaikoura mudstone (■) and Lake Waikaremoana mudstone (●).

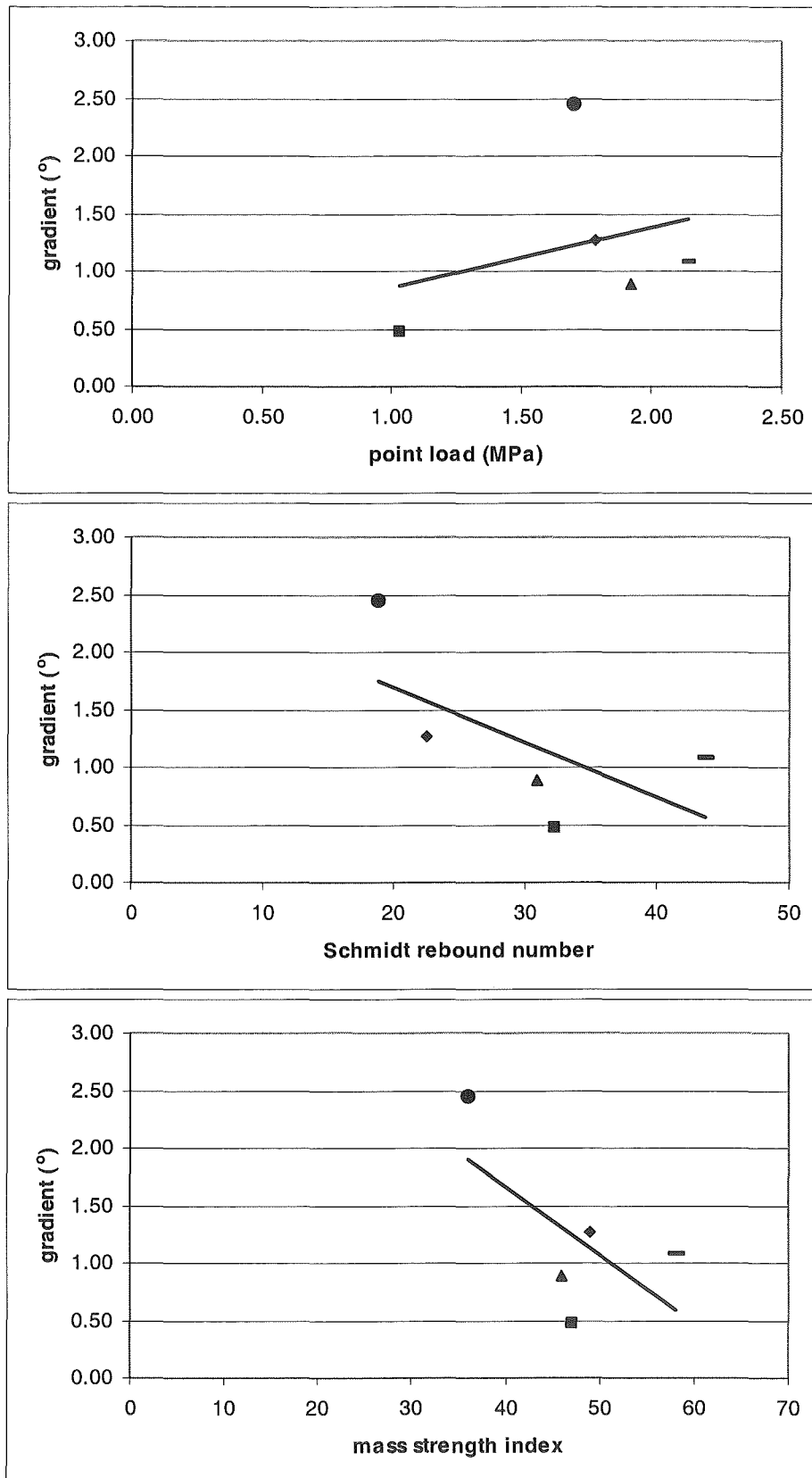


Figure 4.15: Shore platform gradient compared to a) bedrock strength, b) surface strength and c) mass strength of the rock in which each shore platform is formed. Each rock type is plotted using a different symbol; greywacke (—), limestone (▲), basalt (◆), Kaikoura mudstone (■) and Lake Waikaremoana mudstone (●).

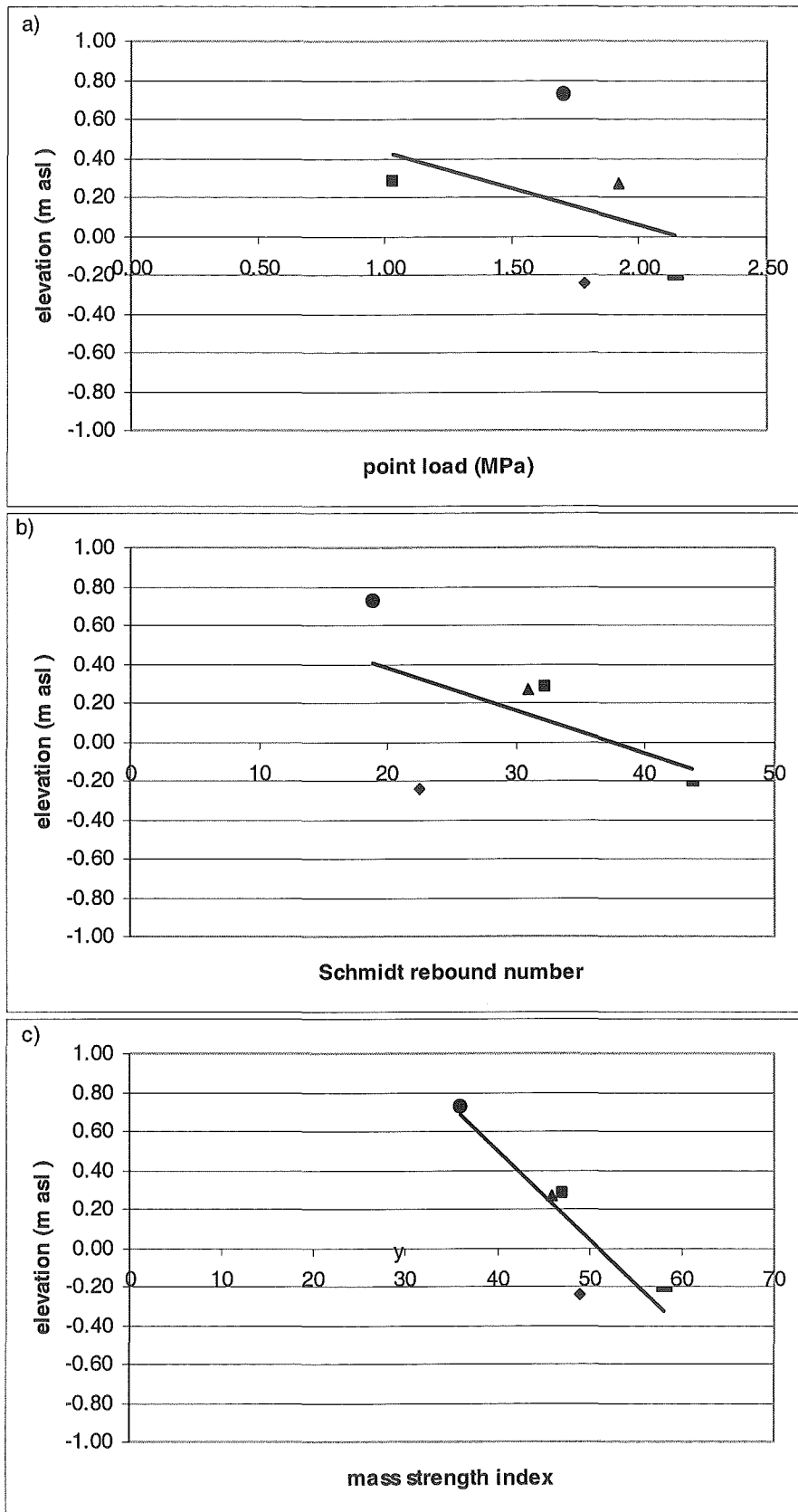


Figure 4.16: Shore platform elevation with respect to mean sea level compared to a) bedrock strength, b) surface strength and c) mass strength of the rock in which each shore platform is formed. Each rock type is plotted using a different symbol; greywacke (—), limestone (▲), basalt (◆), Kaikoura mudstone (■) and Lake Waikaremoana mudstone (●).

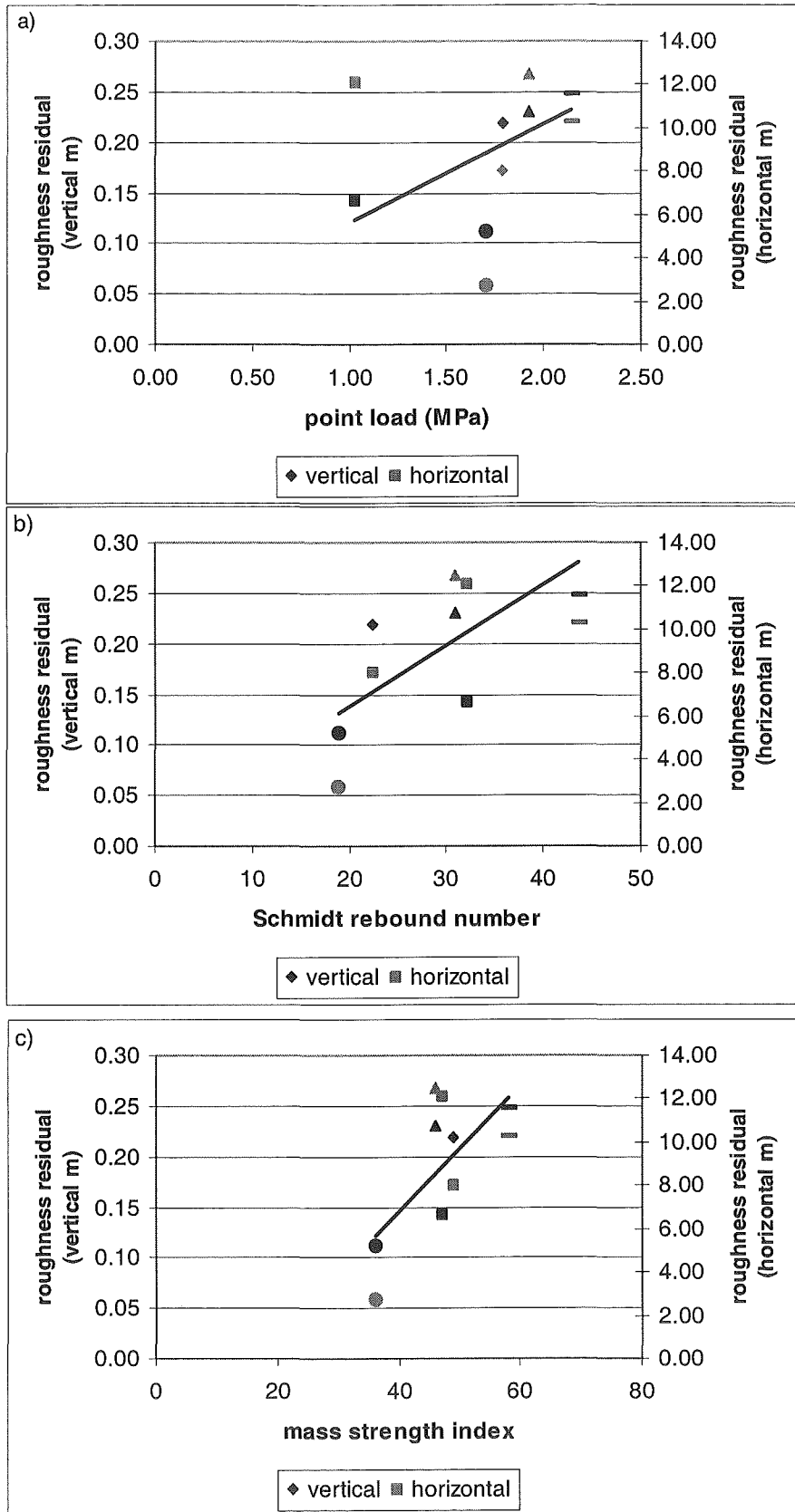


Figure 4.17: Shore platform roughness compared to a) bedrock strength, b) surface strength and c) mass strength of the rock in which each shore platform is formed. Both the vertical and horizontal components of roughness have been plotted. Each rock type is plotted using a different symbol; greywacke (—), limestone (\blacktriangle), basalt (\blacklozenge), Kaikoura mudstone (\blacksquare) and Lake Waikaremoana mudstone (\bullet).

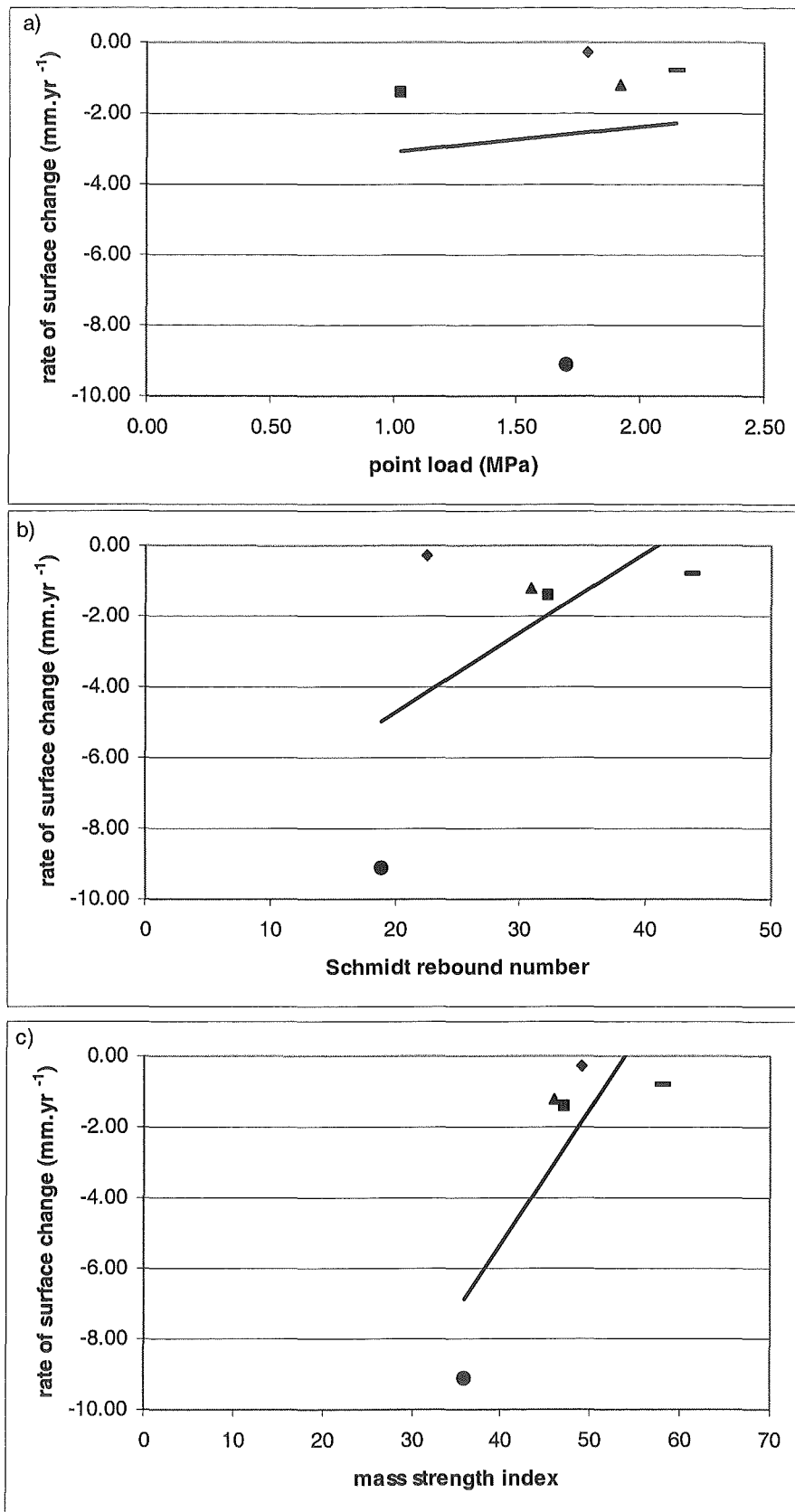


Figure 4.18: Shore platform average rate of surface change compared to a) bedrock strength, b) surface strength and c) mass strength of the rock in which each shore platform is formed. Each rock type is plotted using a different symbol; greywacke (—), limestone (▲), basalt (◆), Kaikoura mudstone (■) and Lake Waikaremoana mudstone (●).

4.6.1 ROCK STRENGTH CONTROL AT THE PLATFORM WIDE SCALE.

Figure 4.14 shows that there was a strong positive correlation between surface rock strength and width ($r=0.71$). Shore platforms studied were generally wider in rocks with greater surface strength. No relationships between bedrock strength of mass strength and width were shown.

Trenhaile (1987:219) stated that “it is logical to assume that the widest wave-cut shore platforms develop in the weaker rocks” and studies in Japan (Takahashi 1977) and California (Bradley and Griggs 1976) found narrower platforms formed in stronger rocks. The positive relationship shown in figure 4.14b contradicts this proposition as have a number of other studies. Patterns of narrower platforms formed in weaker rocks have been reported by So (1965) on the Isle of Thanet and by Robinson (1977c) in Northern Yorkshire. This variety of relationships between rock strength and platform width serves to emphasise that the causative relationship between rock strength and shore platform morphology is complex. This relationship is also complicated by the choice of rock strength indices and leads to questioning of there being a causative relationship between rock strength and platform width as an indicator of shore platform development.

Figure 4.15 shows that the relationships between shore platform gradient and both rock surface strength and rock mass strength were negative. No distinct relationship was shown between bedrock strength and gradient. In this study shore platforms with surfaces closer to horizontal were found in the stronger rock types. This finding agrees with observed patterns reported by Gill (1972) and Gill and Lang (1983) who observed that gradients were lower on more resistant rocks in Victoria, Australia.

However this finding contradicts a number of propositions presented in the literature. Trenhaile and Layzell's (1981) model of shore platform development postulates steeper gradients on shore platforms developed in stronger rock types and observations of some workers have found this pattern (Sanders 1968a, Bradley and Griggs 1976, Kirk 1977). No robust explanation for this relationship has been proposed. The general concept seems to be that platforms reach an equilibrium having a horizontal surface and that platforms developing in weaker rocks will attain equilibrium more quickly. Therefore under stable relative sea level conditions shore

platforms in weaker rocks will have developed further towards a flat gradient than stronger rocks.

One possible explanation for the general relationship shown in figure 4.15 of steeper gradients on rocks of weaker surface strength is that on rocks of varied strength different mechanisms of erosion may dominate. The dominant mechanism of erosion will determine the pattern of erosion across the shore platform surface thus controlling the gradient with the result of different gradients occurring on shore platforms formed in different rock strengths.

Figure 4.16 shows that for platforms studied in this thesis there was a strong negative correlation ($r=0.89$) between rock mass strength and platform elevation (figure 4.16c) and the same general trend is shown for both surface strength and bedrock strengths in relation to elevation (figure 4.16a and b). Platforms on stronger rocks were formed at lower mean elevations with respect to mean water level. This is an unexpected finding.

Both physical models (Sunamura 1991) and mathematical models (Trenhaile and Layzell 1981) have posited higher mean elevations with increased rock hardness when other variables such as waves were held constant. Observational studies have also reported mean elevation increasing with increasing hardness of rock (Sanders 1968a, Gill 1972, Kirk 1977, Gill and Lang 1983). Bartrum (1935) and So (1965) observed that shore platforms tended to be at higher elevations on headlands than in bays with the implication that shore platforms on headlands were formed in harder rocks. However, the accuracy of measures of shore platform elevation with respect to sea level in micro-tidal environments has been questioned (Trenhaile 1987). The elevations of all profiles studied in this thesis were surveyed in relation to accurate sea level gauges within the local environment of each profile.

It is possible that the negative relationship between rock strength and shore platform elevation shown in figure 4.16 has been influenced by tectonic activity. The Kaikoura peninsula is tectonically active (section 2.4.1) and therefore relative sea levels, with regard to platform elevation may have varied when compared to those of the shore platforms studied in other environments. As with the relationship of shore

platform rock strength in relation to gradient it is also possible that different mechanisms of erosion are required to form shore platforms in rock of different strengths. These mechanisms may work towards a different surface elevation with respect to water level.

The roughness of platform surfaces is strongly correlated to the mass strength of the rock ($r=0.81$), with rougher surfaces in both the horizontal and vertical aspects on stronger rocks (figure 4.17c). This strong positive relationship is also found with both bedrock and surface strength (figure 4.17a and b), although it is not as strong with $r=0.69$ and $r=0.68$ respectively. The strength of the rock is an important control on roughness of shore platform surfaces. This is logical, as factors such as fractures are important in defining the shape of the surface.

Another important aspect of rock strength in control of shore platform surface roughness is variation in strength of each rock type. There was a good positive correlation ($r=0.75$) between vertical roughness and standard deviation of bedrock strength. Shore platforms displaying a greater range of bedrock strengths had rougher surfaces. This would be the result of differential erosion of weaker parts of the rock.

Both surface strength and mass strength show a positive correlation with rate of surface change (figure 4.18b and c). Shore platform surfaces that experienced greater erosion rates (negative surface change) were generally on weaker rock. This correlation was strongest for mass strength ($r=0.82$). This concurs with the notion that the greater the resistance of the rock to erosion the slower the rate of shore platform development.

It is interesting that the index of rock strength that showed the strongest correlation with rate of surface change was the mass strength index. Mass strength assessed rock strength at a macro scale and rate of surface change was assessed at the micro scale using the MEM technique.

In figures 4.14 – 4.18 measures from all shore platforms studied have been included. However, the magnitude difference in the Lake Waikaremoana data in elevation and

rate of surface change may bias the causative relationships shown. The Lake Waikaremoana morphogenetic environment differs from the four other shore platform environments in its lack of a tidal regime and the less energetic wave environment.

Generally, for shore platforms studied in this thesis, the strength of the bedrock was not strongly correlated with any of the five assessed aspects of morphology (figures 4.14a – 4.18a). Surface strength and mass strength both displayed stronger correlations than bedrock strength with all aspects of morphology that were assessed (figures 4.14b and c – 4.18b and c). Both surface strength and mass strength show positive relationships to platform width (figures 4.14b and c) whereas the trend shown for bedrock strength vs. platform width is negative (figure 4.14a). A similar contradiction occurs in comparison of the rock strength to platform gradient. Surface strength and mass strength both show negative relationships (figures 4.15b and c) and bedrock strength shows a positive trend (figure 4.15a). This highlights the fact that the index used to measure rock strength in shore platform studies effects the causative relationships shown.

The relationships shown in figure 4.13 between rock strength and aspects of shore platform morphology highlight the complex nature of rock strength controls on shore platform morphology.

4.6.2 CHOICE OF INDEX OF ROCK STRENGTH FOR USE IN SHORE PLATFORM STUDIES.

The different relationships shown in figures 4.14 – 4.18 emphasise the fact that the index of rock strength chosen in shore platform studies will have a great influence on relationships portrayed. This was especially evident with respect to platform width and gradient.

There were no strong correlations between elements of morphology and bedrock strength measured in the form of the point load index. Therefore compressive strength of the intact bedrock rock does not appear to be a useful measure of rock strength on shore platforms with regard to explaining shore platform morphology.

Correlations between morphology and surface strength in the form of the Schmidt hammer rebound index were stronger with correlation values of between $r=0.52$ and $r=0.71$. Stronger still were the strength of correlations between morphology and mass strength with values of between $r=0.63$ and $r=0.93$.

As noted in section 4.5.1 the resistance a rock presents depends on the nature and location of the processes of erosion. Therefore, useful indices of rock strength in shore platform studies appear to be either Schmidt hammer surface strength or rock mass strength. As these indices evaluate the surface strength of the rock it is appropriate that they be used when assessing the effect of processes that primarily occur at the platform surface.

Further definition of which index of rock strength to use depends on the aspects of shore platform processes that are being investigated. As the rock mass strength index assesses the resistance of the rock at a macro, or landform scale, it would be the most appropriate index to use in analysis of the platform as a whole.

Schmidt hammer testing is spatially confined and therefore assesses rock strength at a micro scale and so would be appropriate for use when assessing the effect of processes at this scale. The main advantage of Schmidt hammer testing over mass strength assessment is that it requires less subjective input.

4.6.3 ROCK CONTROL AT THE PROFILE SCALE AND MICRO SCALE.

As the Schmidt hammer allowed non-destructive and relatively quick, extensive spatial coverage of measurement across the surfaces of the platforms it was possible to calculate an average surface strength for each profile as well as each rock type. This allowed for further analysis providing greater detail of the relationship between surface rock strength and morphological elements of the shore platforms. Figure 4.19 presents correlations between surface strength of each profile compared to platform width, gradient, elevation, surface roughness and rate of surface change.

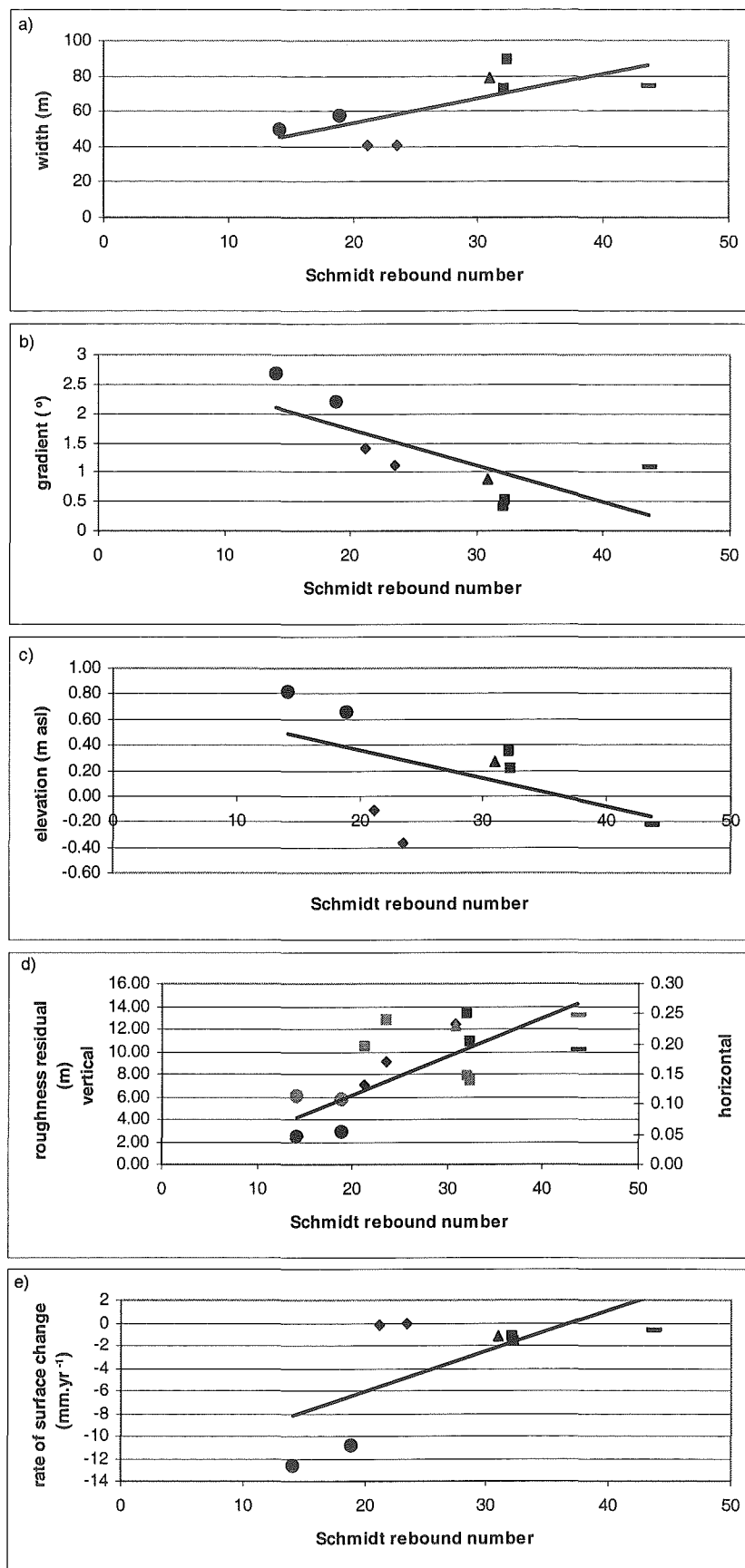


Figure 4.19: Shore platform surface rock strength of each profile compared to elements of morphology. Shore platform morphological elements are a) width, b) gradient, c) elevation, d) surface roughness and e) rate of surface change. Each rock type is plotted using a different symbol; greywacke (—), limestone (▲), basalt (◆), Kaikoura mudstone (■) and Lake Waikaremoana mudstone (●).

Surface strength compared to platform width (figure 4.19a) shows a strong ($r=0.71$) positive correlation. Figure 4.19b shows a strong ($r=0.75$) negative correlation between gradient and surface strength. A weaker negative relationship ($r=0.49$) is shown with elevation (figure 4.19c). Roughness shows a good positive correlation ($r=1.78$) to surface strength for all profiles studied. Figure 4.19e shows a negative relationship between rate of surface change and surface rock strength. However, this is somewhat distorted by the high rates of surface down-wear recorded at Lake Waikaremoana.

These relationships shown in figure 4.19 are similar to those shown in figures 4.14 – 4.18 thereby adding more weight to the relationships described in section 4.6.1.

The extensive spatial coverage of surface rock strength testing also made it possible to investigate the relationship between rock strength and rate of surface change at a more detailed scale. Figure 4.20 plots the average rate of surface change at individual MEM bolt sites against the mean rebound numbers of surface rock strength testing performed close to each specific bolt site. There was a generally positive relationship between these two variables but the correlation was not significant.

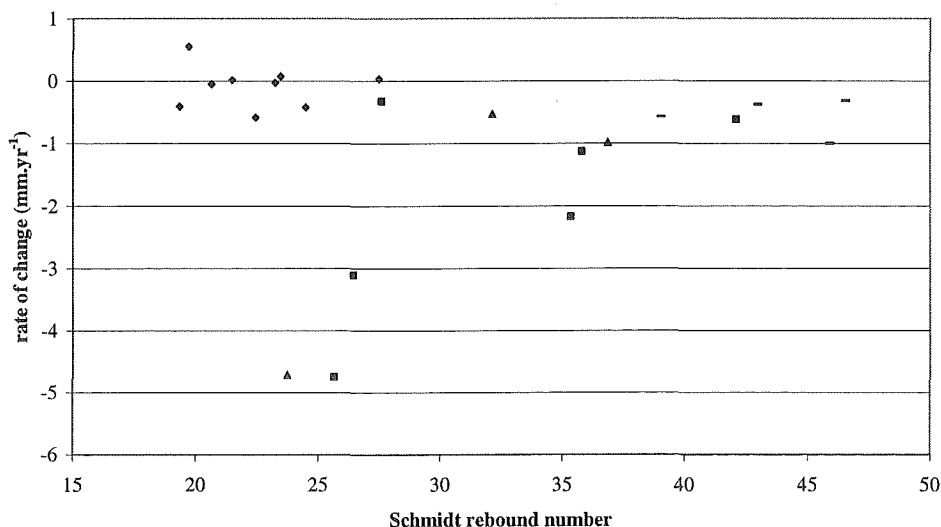


Figure 4.20: Shore platform surface rock strength compared to rate of surface change at individual MEM bolt sites. Note that Lake Waikaremoana results have been excluded, as Schmidt hammer testing near MEM bolt sites was not possible. Each rock type is plotted using a different symbol; greywacke (—), limestone (▲), basalt (◆) and Kaikoura mudstone (■).

Figure 4.20 shows two distinct populations with the results from the basalt forming one group and the remainder following the general trend of increased rate of erosion with lower rock surface strength. This must reflect something of the nature of the rock and the way in which it erodes. Further elucidation of this notion would require detailed study of the rock surface and erosive processes.

When discussing this plot (figure 4.20) it is important to note that the more location specific surface strength measures highlight the importance of spatial surface variations in strength. Testing close to MEM bolt sites may not accurately represent the surface strength of the portion of rock being measured for surface change. This can be seen in the large variation in surface strength within 10-20cm² of area in figure 4.12.

4.7 ROCK SUSCEPTIBILITY TO WEATHERING.

This chapter has presented measurements of rock strength obtained from direct testing of rock samples from each rock type or *in situ* testing of the surface at each study profile. It is important to note that processes of weathering may reduce this intact strength of the rock through disintegration or deterioration of the rock. This leads to a weakening of the integrity of the rock structure. Section 4.5.6 discussed the observed reduction in rock strength between the bedrock and the surface on each platform but this provided no insight into the mechanisms or effects of weathering in relation to shore platform development. The processes of weathering and their effects on rock strength will be further addressed in Chapter 7.

4.8 SUMMARY.

This chapter has described the character and nature of the rocks into which each of the shore platforms studied for this thesis are formed. Descriptions of lithology of the platform bedrock at each profile have been given and rock strength has been assessed using three different indices. Using these findings the role of rock character

in shore platform development and as a control on morphology has been investigated.

It has been shown that at the locations studied the shore platforms truncate lithology. Dip and strike of the bedrock was orientated at a range of different angles to the landward cliffs of profiles. This observation has led to the conclusion that shore platforms are wholly erosional features and that erosion of the shore platforms studied for this thesis does not follow lines of weakness within the bedrock.

The strength of each rock type was characterised by three different indices. These were derived from three tests of rock strength each of which assessed a different aspect of the strength of the rock. The tests were, point load compressive test which gives an indication of bedrock strength, Schmidt hammer rebound test which gives an indication of surface rock strength and a rock mass assessment which gives an index for the strength of the entire rock body.

The greywacke was the strongest rock according to all three indices. It had a bedrock strength of 2.14MPa, a Schmidt hammer rebound number of 44 and a rock mass index of 72. The weakest rock was the Lake Waikaremoana mudstone with a bed rock strength of 1.70, and surface strength of 19 (rebound number) and a mass strength index of 50. The Kaikoura mudstone, limestone and the basalt had strength values ranging between the greywacke and the Lake Waikaremoana mudstone.

The clear differences that were shown between measures of strength of individual rock types using the three different indices highlights the importance of choice of index and that this will have a great influence on relationships portrayed. The choice of index should provide an assessment of rock strength that relates to the nature of the erosive processes that will be occurring in the environment. It was found in this chapter that the most useful indices of rock strength in shore platform studies of the three presented here were those that assessed the strength at the surface. These were the Schmidt hammer test for smaller scale more detailed assessment and the rock mass index for platform wide scale of assessment. Point load compressive testing revealed little about the rock strength in relation to shore platform development.

Rock types have also been characterised in terms of variations in rock strength that were measured in each test. For point load testing the basalt showed the greatest variation with a standard deviation of $\pm 110\%$ of the mean value. The Kaikoura mudstone showed the least variation with a standard deviation of $\pm 26\%$ of the mean value. The other rock types had standard deviations of between $\pm 85\%$ and $\pm 52\%$ of mean values. Variations in Schmidt hammer tests were lower with standard deviations being between $\pm 25\%$ and $\pm 9\%$ of mean values. This variation in strength will reflect in the way the rock breaks down and the spatial response of the shore platform development to processes of erosion.

The role of rock strength in control of shore platform morphology and development has been shown to not be strong over all. It was shown that there were some correlations between some rock strength indices measured and some aspects of shore platform morphology but these relationships were only limited in extent.

Given the notion prevalent within the literature that shore platform development and morphology is controlled by rock type and strength and that platforms in stronger rocks would be narrower and higher there were some surprising, although not always strong, relationships shown. These were, that the widest platforms were generally on the strongest rock, that gradient decreased with increasing rock strength, that generally platforms on weaker rocks were at higher elevations with respect to sea level and that there was no strongly discernable relationship between rate of surface change and rock strength.

This chapter has shown that the nature of rock strength control on shore platform development and morphology is more complex than is apparent from the literature.

CHAPTER FIVE

WAVES ON SHORE PLATFORMS.

5.1 INTRODUCTION

The notion that wave action is a fundamental process in the formation of shore platforms is dominant in the international literature on shore platforms (Dana 1849, Johnson 1919, Bartrum 1935, Jutson 1939, 1949, 1954, Edwards 1941, Challinor 1949, Hills 1949, So 1965, Trenhaile 1974a, 1978, 1987, 1999, Bradley and Griggs 1976, Robinson 1977a, Sunamura 1978, 1991, 1992, Trenhaile and Lazell 1981, Gill and Lang 1983, Tsujimoto 1987). Some models have been based on a balance between the assailing forces of waves and the resisting forces of rocks (Tsujimoto 1987, Sunamura 1992, 1994, Trenhaile 1999). Therefore a study of processes on shore platforms should include description of the wave environment impacting on those shore platforms.

This chapter describes the wave environments of each study site. The differing location of study profiles means that each is exposed to a different wave environment. KM2, KM3, KM7 and RM1 all have similar unlimited marine fetches and are exposed to high energy wave action. Profiles AK1 and AK2 are exposed to a combination of waves from both marine and enclosed water body origins. Profiles WK1 and WK2 at Lake Waikaremoana are exposed only to the limited fetch wave environment of an enclosed water body.

Notwithstanding the emphasis that has been placed on wave action in the debate on shore platform development very little direct measurement of waves on shore platforms has been undertaken. Section 5.4 of this chapter describes direct measurement of waves onto and across the shore platform at KM3.

5.1.1 WHY WAVES ARE IMPORTANT.

Coastal literature, in general, places a great emphasis on the concept of waves as the primary agents of morphological change on the shore. Waves are among the primary components in the much referred to process-response model of Krumbein (1964). Zenkovich (1967:12) stated that "Waves are the main factor in the alteration of coasts". He goes on to say "All changes in coasts and in the coastal portion of the sea bed are brought about by the energy of waves from the open sea" (Zenkovich 1967:22) and that work is affected directly by wave impact and transportation of sediments and indirectly by the action of currents, which develop when a wave breaks. The concept that waves are of primary importance in coastal change is also prevalent in disciplines other than geomorphology. This is evident in the opening line from an engineering text which states "One of the facts of life in the ocean that affects engineering activities is the omnipresence of waves" (Herbich 1990:1).

This inherent belief that waves are fundamental to processes of morphological change in the coastal zone also holds in most shore platform studies. This is evident in the nature of many of the names given to these geomorphological features: "Storm wave platform" (Bartrum 1926), "sloping wave bench" (Edwards 1941), "wave-cut terrace" (Dietz 1963), "wave cut bench" (Thornbury 1954), "wave-cut platform" (Sunamura 1975, Bradley and Griggs 1976) and "wave-cut shore platform" (Trenhaile 1987). The more generally accepted non-generic term shore platform reflects the continued uncertainty within the literature as to the degree of importance of wave processes in their formation.

Models of shore platform development are structured such that if wave intensity increases while all other factors remain constant the platform width and rate of change will increase (Trenhaile and Lazell 1981, Tsujimoto 1987, Sunamura 1992). When presenting factors affecting erosion of rocky coasts Sunamura (1992, 1994) considered that the balance between the assailing forces of the waves and the resisting forces of the rocks is of primary importance. He regarded other factors as subsets of either rock strength or wave assailing force (figure 5.1).

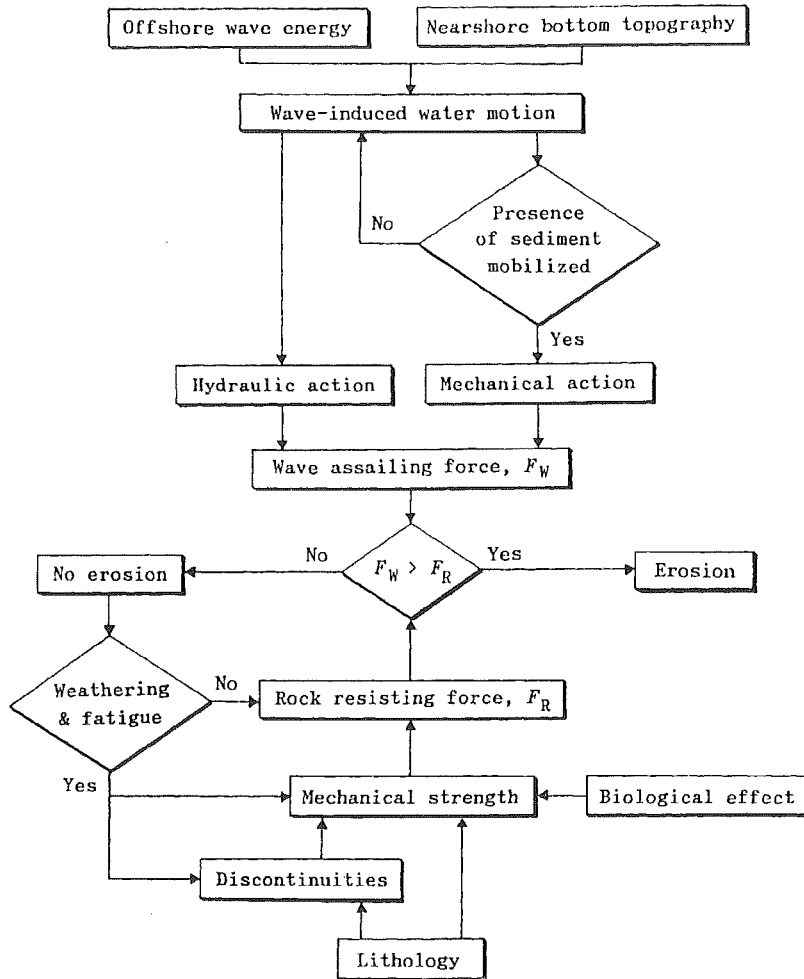


Figure 5.1: Factors affecting erosion of rocky coasts. “Ultimate factors are wave assailing force, F_W and rock resistance force, F_R .” (Sunamura 1994:fig 1).

Some field studies of shore platforms observed widest shore platforms where wave action was most vigorous (Everard *et al.* 1964, So 1965, Trenhaile 1972, 1999, Takahashi 1977, Tsujimoto 1987). However, wider shore platforms in sheltered wave environments have also been reported (Bartrum 1935, Edwards 1941, Hills 1949, 1972, Bird and Dent 1966). The relationships between shore platform width and wave intensity are therefore complicated in nature.

The relationship between wave intensity and shore platform gradient also appears to be complicated. Trenhaile (1987) suggested that wave cut platforms are horizontal in vigorous storm wave environments where tidal range is small. This supported the

assertions of Bartrum (1935), Jutson (1949, 1954), Edwards (1941) and Cotton (1963) that horizontal surfaces can be cut by waves. Although exactly how this is accomplished is unclear.

Trenhaile (1987) noted that clarification of relationships between platform morphology and wave intensity, as an indication of wave assailing force, is difficult due to a general lack of wave data from rock coastlines. Until comprehensive measurement of wave action in the shore platform environment is undertaken these relationships will remain unclear.

5.1.2 PREVIOUS MEASURES OF WAVE ASSAILING FORCE ON SHORE PLATFORMS.

Some shore platform studies have included surrogate measures of wave action but only a very few have measured wave action directly on shore platforms. In shore platform studies there has been a distinct lack of direct measurement of wave energy, wave disturbance or wave assailing force on shore platforms (Trenhaile 1987, Sunamura 1992, Gaylord 2000, Stephenson and Kirk 2000a).

The length of exposed fetch offshore from a shore platform has been used in some studies as an indicator of relative wave assailing forces reaching a shore platform (Trenhaile 1974b, Robinson 1977c, Takahashi 1977). The amount of exposed fetch is equated to maximum possible wave energy reaching the shore. Takahashi (1977), Trenhaile (1987) and Tsujimoto (1987) have shown correlations between shore platform width, as an indication of degree of shore platform development and exposure to longer fetches.

Zoologists working on intertidal rocky shore environments (shore platforms) use the term 'exposure' in relation to the amount of wave energy that is translated onto the shore at a given location (Gaylord 1999). Thomas (1986) described an exposure index derived from wind velocity, direction, duration and effective fetch and used it as a descriptor for

biological littoral zonation. He related the amount of deepwater wave energy directly to the onshore wave conditions.

Measures of deepwater wave energy offshore from platforms have been used as indicators of wave assailing force at the platform (Mii 1962, Suzuki *et al.* 1970, Bradley and Griggs 1976, Takahashi 1977, Sunamura 1978, Tsujimoto 1987, Trenhaile 1999). Parameters of wave height, either directly measured or hindcast, were used to calculate deepwater wave energy values. This use of deepwater wave energy does not elucidate actual processes of wave assailing force on shore platforms (figure 5.2).

This ‘black box’ approach, using deepwater wave parameters, has been taken because ultimately it is desirable to predict wave effects at the shore from meteorological information. This meteorological information is more easily obtained than direct deepwater wave measurements and can be used to forecast or hindcast deepwater sea state variables. However, use of deepwater wave parameters for this purpose has limitations. They reflect nothing, or very little, of the nature of the processes occurring at the shore (figure 5.2) and it has been shown that wave energy reduces dramatically as waves approach shore platforms (Stephenson and Kirk 2000a).

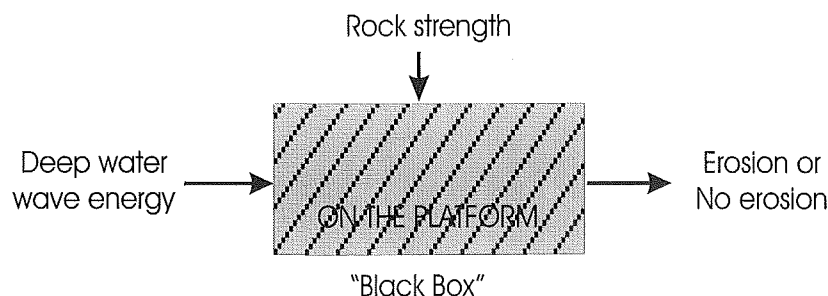


Figure 5.2: The ‘black box’ approach to shore platform development where verification or elucidation of the processes is lacking.

To try, in part to overcome this ‘black box’ problem and account for changes that may be occurring as waves move from deepwater to onshore Tsujimoto (1987) applied various shoaling and refraction equations to ascertain the impacting wave energy, pressure and shear forces at the shore platform.

Laboratory experiments have been conducted by Sanders (1968a, 1968b) and Sunamura (1991) where wave tanks were used to generate simulated deepwater wave conditions. These waves were shoaled across scale model seafloors towards model cliffs and assessment of the impact of the waves on the cliffs over time was recorded. However, as these experiments implicitly assumed that wave action was the primary formative process in morphological change they do not report direct measurement of the wave environment at the model/water interface. Process was inferred from measuring the morphological change after a given amount of time.

Williams and Roberts (1995) inferred wave forces on a shore platform in south Wales, from the measurement of pebble impact on a specially designed instrument located directly on the shore platform. Pebble impacts recorded by the sensor were related to the velocity and turbulence of the water.

Castilla *et al* (1998) and Taylor (2003) used maximum water velocity recorders (dynamometers) to directly measure maximum water force on shore platforms in central Chile and South Island, New Zealand respectively. This type of dynamometer was a ping pong ball like drogue attached by a line to a spring within a casing. This casing is attached to the rock surface. As the force of the waves on the drogue extends the spring a marker is moved to and held at the point of greatest extension. The spring loading means that only maximum water velocities at the specific location over the measurement period are obtained.

Stephenson and Kirk (2000a) measured water pressure at two sites along a profile across a shore platform at Kaikoura as waves moved over them at high tide. Pressure was converted to wave height and using this the shear force at the platform surface was calculated. They also compared these onshore measures of wave energy to a measure of deepwater wave energy. In terms of providing a description of how waves move across platforms this was a good starting point. However, there are also problems with this approach in that wave height on the shore platform might not relate directly to the velocity of the water over the surface at the point of measurement.

To date the most comprehensive description of flow patterns on shore platforms using direct measurement was given by Gaylord (1999). He used 2-axis cantilever-style drag-sphere flow probes to measure water velocities at single locations on four different platforms in California.

For this study measurements of water velocities induced by wave action were made directly on the shore platform at KM3. Results of these measurements are reported in section 5.4.

5.2 WAVE ENVIRONMENTS OF STUDY SITES.

This section describes the general deepwater wave environments at each of the study sites.

5.2.1 METHODS OF DESCRIPTION OF WAVE ENVIRONMENTS.

Generally deepwater wave data are used to describe sea state conditions prevailing at a particular location. These data are usually sourced from locations as close as possible to study areas. The raw data are either used directly, especially if the study area is in deepwater, or the data are processed to account for changes that may occur as waves move away from the area of generation and through different depths of water.

Wave environments or particular sea states contain a range of wave sizes and are not monochromatic. They can therefore be usefully described using either statistical parameters or spectral analysis.

5.2.1.1 STATISTICAL METHODS

Longuet-Higgins (1952) showed that the range of waves in a given deepwater swell state follow that of a Rayleigh distribution. Therefore statistical description of any swell state is possible using parameters such as wave height (H), wave period (T), significant wave height (H_s) and root mean square wave height (H_{rms}). Traditionally descriptions of sea

states and consequent wave environments have used the two recorded parameters of significant wave height (H_s) and average wave period (T). H_s is defined as the average height of the highest one third of waves measured over a given time period (Thompson and Vincent 1984). T is the time between successive wave crests averaged over the given time period. It can be obtained using the zero upcrossing method defined in IAHR (1989).

A combination of H_s and T statistics with indications of joint probability of occurrence give a good general description of the wave climate of a region. Munk (1944) proposed uniform procedures for observing waves using H_s and T . Sverdrup and Munk (1947) pioneered the use of this combination of parameters when they employed them as input parameters in a method for hindcasting of wave events or wave climates. Tucker (1963) presented standard parameters for use in analysis of sea wave records and IAHR (1989) gave a comprehensive list of wave parameters and wave related functions.

5.2.1.2 SPECTRAL METHODS

Spectral analysis describes the full spectrum of waves present and is used to provide a more comprehensive description of sea state. It describes the way energy is distributed with respect to the range of frequencies present in a given record.

5.2.1.3 COMPARISON OF METHODS

Thompson and Vincent (1985) noted that it is difficult to inter-relate statistical and spectral descriptions of sea state, especially in shallow water. Therefore a consistency of use and understanding is important.

Choice of which method to use depends on what is required from the data, how it is to be analysed and what form of data is available. Both methods have drawbacks. Describing a sea state using statistical parameters may give the impression that a wave train is monochromatic. This can cause problems when trying to relate waves to

process. In the same way, much laboratory work uses monochromatic waves, which may also create problems when performing real world comparison. Spectral analysis of a wave environment requires detailed data collection, which is not often possible and can be fraught with logistical problems.

For this thesis wave environments are described using statistical parameters. This gives an adequate general representation of the deepwater wave environment at each site. Specifically, deepwater measures of wave height and direction have been used and water velocity and wave energy was obtained from this statistical data. Spectral analysis of the wave environments has been conducted to a limited extent when greater elucidation of changes in wave patterns were required and where data allowed this type of analysis.

5.2.2 RECORDS OF WAVE ENVIRONMENTS FOR NEW ZEALAND

As the extensive measurement required to define wave environments offshore from each study profile was beyond the scope of this thesis, descriptions of wave environments reported in the literature and in regions relevant to study sites are outlined in this section.

There are very few published records outlining the characteristics of the New Zealand wave environment. A unified method of description is lacking in those that are available and very little long term wave data has been recorded. Wave buoys have been installed temporarily at various locations for limited periods but these data are sparse and often not readily available to the general researcher. Also descriptions of wave environments at specific sites are not often applicable at other locations around New Zealand. Macky *et al.* (1995) described the wave climate of the western Bay of Plenty but topographical differences mean that this is of little relevance to the sites studied in this thesis on the east coast of the South Island. Ewans and Kibblewhite (1992) compared the spectral signatures measured by two deepwater wave rider buoys. One was located on the east coast and one on the west coast of the North Island. They used 'spectral families' as a way of describing the wave climate and found that on average the east coast is less energetic than the west coast with a persistent long-period southerly swell on the west

coast side. However their location of the east coast wave rider buoy near Great Barrier Island would have resulted in the buoy being protected by the East Cape from the southerly swells incident on the majority of the New Zealand coast. Therefore their wave spectra should not be extrapolated as representative of the wave climate along the east coast of the South Island.

5.2.2.1 PUBLISHED RECORDS OF WAVE ENVIRONMENTS FOR THE EAST COAST, SOUTH ISLAND.

McLean (1968) and Kirk (1972, 1973, 1974, 1975a) compiled reports outlining summary sea state statistics around New Zealand for the years 1967, 1971-74. These were based on daily visual observations of the sea state from various locations, provided by the New Zealand Meteorological Service. Observations were made from both the Kaikoura Peninsula and Akaroa Head lighthouses (figures 2.2 and 2.5). An ordinal scale was used which gave a description of the sea surface with regard to wave action. Table 5.1 outlines the classifications used and gives an indication of the corresponding wave height.

Table 5.1: Sea state code used for wave observations, description and associated wave height (Kirk 1975a)

| Ordinal scale | wave height (m) |
|---------------|-----------------|
| calm | 0 and 0 - 0.1 |
| smooth | 0.1 - 0.5 |
| slight | 0.5 - 1.25 |
| moderate | 1.25 - 2.5 |
| rough | 2.5 - 4 |
| very rough | 4 - 6 |
| high | 6 - 9 |
| very high | 9 - 14 |
| phenomonal | 14 + |

The distributions of sea states over the time period, 1967 and 1971- 1974, were broadly similar with very little seasonal component. Table 5.2 shows the percentage of the observations in each sea state category at Kaikoura and Akaroa Head.

Table 5.2: Summary sea state data recorded for the years 1967 and 1971 to 1974 at a). Kaikoura and b). Akaroa Head.

a).

| sea state | frequency of observation (% of year) for given years | | | | | |
|------------|--|------|------|------|------|---------|
| | 1967 | 1971 | 1972 | 1973 | 1974 | average |
| calm | 20 | 33 | 34 | 38 | 31 | 31 |
| smooth | 52 | 46 | 48 | 45 | 48 | 48 |
| slight | 24 | 15 | 13 | 13 | 17 | 16 |
| moderate | 4 | 2 | 4 | 3 | 4 | 3 |
| rough | 0.1 | 4 | 0.1 | 0.2 | 0.5 | 1 |
| very rough | 0 | 0 | 0 | 0 | 0 | 0 |
| high | 0 | 0 | 0 | 0 | 0 | 0 |
| very high | 0 | 0 | 0 | 0 | 0 | 0 |
| phenomonal | 0 | 0 | 0 | 0 | 0 | 0 |

b).

| sea state | frequency of observation (% of year) for given years | | | | | |
|------------|--|------|------|------|------|---------|
| | 1967 | 1971 | 1972 | 1973 | 1974 | average |
| calm | 2 | 1 | 0 | 1 | 2 | 1 |
| smooth | 17 | 20 | 16 | 17 | 20 | 18 |
| slight | 54 | 53 | 52 | 65 | 46 | 54 |
| moderate | 19 | 17 | 22 | 18 | 23 | 20 |
| rough | 8 | 8 | 9 | 0 | 8 | 7 |
| very rough | 0 | 0.3 | 1 | 0 | 1 | 0 |
| high | 0 | 0 | 0 | 0 | 0 | 0 |
| very high | 0 | 0 | 0 | 0 | 0 | 0 |
| phenomonal | 0 | 0 | 0 | 0 | 0 | 0 |

At Kaikoura for the majority (79 %) of time the sea state was classified smooth or calm with wave heights of between 0 – 0.5 m. Maximum wave heights greater than 2.5 m were recorded 1% of the time. At Akaroa Head for the majority (54 %) of time waves were between 0.5 – 1.25 m in height. Maximum wave heights of between 4 – 6 m were recorded 0.5 % of the time.

These statistics were based on visual observations taken, once per day, from the land and therefore may not correspond directly to deepwater wave conditions.

To further describe the wave environments of east coast, South Island, McLean (1972) collated visual observations of wave characteristics from ship reports made within the Kaikoura coastal region, approximately 32 km offshore. The most predominant wave

period recorded was 12 seconds. However, Tomlinson (1971 *in* McLean 1972) reported average dominant wave periods of 6 – 8 seconds. The distribution of wave directions was bimodal with 42 % of waves from the north and northeast and 17 % from the south. Swells came predominantly (43 %) from the south with 31 % from the north and northeast.

Pickrill and Mitchell (1979) described ocean wave characteristics around New Zealand based on 17 collective years of wave records. They described the east coast of the South Island as a high energy lee shore with a mixed wave climate made up of southerly swells originating in the westerly wind belt south of New Zealand and locally generated southerly and northerly storm waves. The majority of wave heights were between 0.5 - 2 m and wave periods were between 7 – 11 s. They noted a short period rhythmic cycle superimposed onto a very weak seasonal cycle. However the short term nature of many of the records meant that seasonal cycles were difficult to detect. They showed that in wave shadow areas on the northern sides of Banks Peninsula and Kaikoura Peninsula the refracted southerly component of wave environments was still recorded as prevalent within the environment.

Gorman and Laing (2001) presented the derivation of a wave hindcasting model developed to cover the New Zealand region and “fill the gaps in our wave record”. It was based on 15 years of climate data and they reported good accuracy. However the results are not publicly available for use at this time.

Also, in an effort to fill a gap in the published wave climate records around New Zealand the National Institute of Water and Atmosphere (NIWA), in conjunction with Environment Canterbury (ECan), installed a deepwater directional wave buoy in February 1999, 17 Kilometres to the east of Banks Peninsula in 90 metres of water. This buoy has recorded wave height (significant and maximum), wave period and wave direction for a period of 3 years to date. Significant wave height (H_s) ranged from 0.6–6.76 m with a mean H_s of 1.84 m and mean period (T) of 6.74 s. T ranged between 3.9–11.6 s with the larger, longer waves originating from the south. In all 64 % of waves came from the south and southeast (Walsh 2002).

5.2.3 WAVE ENVIRONMENTS DIRECTLY OFFSHORE FROM STUDY SITES.

The previous section described published records of sea states for the east coast of the South Island and these give a general indication of wave environments in the region. However the different locations of study sites (figure 2.1) mean that factors such as topography and local climate may result in wave environments different from these general descriptions. The general descriptions have not necessarily come from direct deepwater measurement of parameters at the study sites but from remote observation or measurement.

This section gives descriptions of wave environments specific to each study site based on direct wave measurements made close to the site and where these were not available from hindcasting methods or a combination of both.

As the degree of exposure of a site dictates both, the nature of the offshore environment and the translation of deepwater waves to the shore platforms, a description of exposure at each site is also provided.

5.2.3.1 KM2, KM3, KM7 AND RM1 WAVE ENVIRONMENT.

Profiles KM2, KM3, KM7 and RM1 are all exposed directly to open sea of the Kaikoura region with extensive uninterrupted fetches. Profiles at KM3, KM7 and RM1 are orientated towards the southeast and the shore platforms at these locations are exposed to waves from approximately 45 degrees (northeast) to 225 degrees (southwest). The aspect of KM2 differs in that it is orientated towards the northeast and is exposed to waves from approximately 315 degrees (northwest) to 135 degrees (southeast). This would result in less direct wave attack from the largest southerly swells at KM2 but north and northeast waves can also be of significant size (section 5.2.2.1).

At Kaikoura no long term measurements of the wave environment have been made but two separate sets of short-term data collection have been undertaken using deepwater non-directional wave buoys. These will be used to define the deepwater wave environment of sites KM2, KM3, KM7 and RM1.

In 1996 a buoy was installed 8 km east of the peninsula and recorded wave heights for a period of 38 days between 1 June 1996 and 9 July 1996 (Stephenson 1997a). During the course of this thesis a deepwater non-directional wave buoy was installed by NIWA in 30 m of water 2 km east of the Kaikoura peninsula. It recorded half hourly averages of H_s and T for 9 days between 16 August 2001 and 24 August 2001. Table 5.3 gives the frequency of waves in each category recorded during both time periods. Included are frequencies from data collected by the Banks Peninsula wave buoy (section 5.2.2.1). The 1996 data are from averages of daily summaries and the 2001 data are shown as both average daily summaries and average ½ hourly summaries.

Table 5.3: Summary of a) wave height (H) and b) wave period (T) data from two deepwater wave buoys installed temporarily to the east of the Kaikoura peninsula in 1996 and 2001 and wave height data from a permanent deepwater wave buoy installed east of Banks Peninsula. Percentage frequency of occurrence is shown based on daily averages for 1996 and 2001a and ½ hourly averages for 2001b and Banks Peninsula.

| a). H_s (m) | frequency of occurrence (% of record) | | | |
|---------------|---------------------------------------|-------|-------|-----------------|
| | 1996 | 2001a | 2001b | Banks Peninsula |
| 0.0 - 0.5 | 0 | 0 | 0 | 0 |
| 0.5 - 1.0 | 2.6 | 0 | 0 | 4.8 |
| 1.0 - 1.5 | 23.7 | 22.2 | 28.9 | 29.3 |
| 1.5 - 2.0 | 47.4 | 44.4 | 46.8 | 27.0 |
| 2.0 - 2.5 | 13.2 | 33.3 | 24.0 | 16.2 |
| 2.5 - 3.0 | 10.5 | 0 | 0.4 | 7.9 |
| 3.0 - 3.5 | 0 | 0 | 0 | 4.1 |
| 3.5 - 4.0 | 2.6 | 0 | 0 | 2.4 |
| 4.0 - 4.5 | 0 | 0 | 0 | 3.2 |
| 4.5 - 5.0 | 0 | 0 | 0 | 3.2 |
| 5.0 - 5.5 | 0 | 0 | 0 | 1.3 |
| > 5.5 | 0 | 0 | 0 | 0.5 |

| b). T (s) | frequency of occurrence (% of record) | | | |
|-----------|---------------------------------------|-------|-------|-----------------|
| | 1996 | 2001a | 2001b | Banks Peninsula |
| <4 | 0 | 0 | 0.4 | 0 |
| 4 - 5 | 0 | 0 | 3.0 | 0.2 |
| 5 - 6 | 26.3 | 11.1 | 18.6 | 2.6 |
| 6 - 7 | 31.6 | 55.6 | 26.6 | 12.2 |
| 7 - 8 | 28.9 | 33.3 | 38.8 | 22.1 |
| 8 - 9 | 13.2 | 0 | 8.0 | 24.7 |
| 9 - 10 | 0 | 0 | 3.4 | 17.6 |
| 10 - 11 | 0 | 0 | 1.1 | 10.8 |
| 11 - 12 | 0 | 0 | 0 | 6.3 |
| >12 | 0 | 0 | 0 | 3.5 |

The non-seasonality of wave climates on the east coast of South Island noted by McLean (1968), Kirk (1972, 1973, 1974, 1975a) and Pickrill and Mitchell (1979) suggests that these short term Kaikoura wave buoy data may describe annual wave environments for

this region. However, extrapolation of such short term data is not necessarily accurate. For this reason a comparison of this and long term data recorded by the wave buoy east of Banks Peninsula was made. There is open sea between Banks Peninsula and Kaikoura Peninsula and the regions off each peninsula have the same exposure to synoptic wind conditions in terms of fetch and aspect. Therefore, it is reasonable to assume wave environments are similar. However, confirmation of this assumption is required.

Figure 5.3 shows a graphical comparison of frequency of wave height (figure 5.3a) and frequency of wave period (figure 5.3b) recorded at each buoy. Similar patterns for both H_s and T_z are evident and there were strong correlations ($r \geq 0.91$) between both H_s and T_z frequencies of the Banks Peninsula data set and each of the Kaikoura data sets. As the Banks Peninsula data set covers a much longer time span than either of the two Kaikoura data sets it shows slightly higher frequency of occurrence in the larger wave height categories and lower frequency of occurrence in the dominant (1 – 2 m) wave height categories. This is due to the greater likelihood of occurrence of the rarer, larger and longer period waves within the data set.

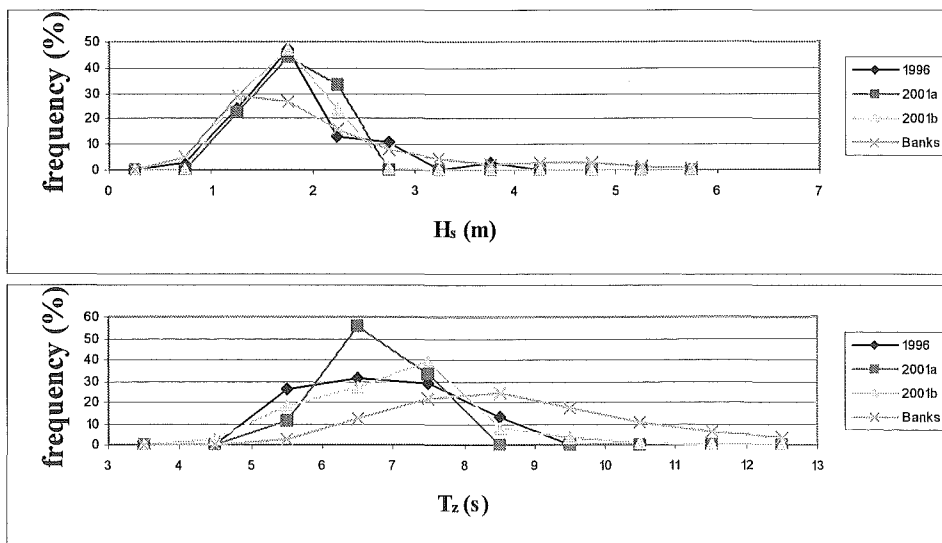


Figure 5.3: Frequency of occurrence, as a percentage of each total record of a). significant wave height (H_s) and b). wave period (T_z) for wave buoy data from Kaikoura (1996, 2001a, 2001b) and Banks Peninsula.

The deepwater wave environment directly offshore from KM2, KM3, KM7 and RM1 is therefore comparable to that recorded by the Banks Peninsula wave buoy.

The wave climate in the deepwater offshore from profiles KM2, KM3, KM7 and RM1 is dominated by southerly swell conditions. Average H_s is 1.8 m and average T is 6.7 s. Absolute calm conditions (H_s of 0 – 0.5 m) are rare and waves larger than 5 m occur less than 2 % of the time. The dominant H_s of 1.0 – 2.0 m occurs 56 % of the time. Table 5.4 shows the frequency of occurrence of significant wave heights offshore from KM2, KM3, KM7 and RM1.

Table 5.4: Frequency of occurrence of significant wave heights offshore from KM2, KM3, KM7 and RM1.

| H_s (m) | frequency of occurrence (%) |
|-----------|-----------------------------|
| 0.0 - 0.5 | 0 |
| 0.5 - 1.0 | 4.8 |
| 1.0 - 1.5 | 29.3 |
| 1.5 - 2.0 | 27.0 |
| 2.0 - 2.5 | 16.2 |
| 2.5 - 3.0 | 7.9 |
| 3.0 - 3.5 | 4.1 |
| 3.5 - 4.0 | 2.4 |
| 4.0 - 4.5 | 3.2 |
| 4.5 - 5.0 | 3.2 |
| 5.0 - 5.5 | 1.3 |
| 5.5 - 6.0 | 0.4 |
| 6.0 - 6.5 | 0.1 |
| 6.5 - 7.0 | 0.04 |
| 7.0+ | 0 |

5.2.3.2 AK1 AND AK2 WAVE ENVIRONMENT.

Profiles AK1 and AK2 are located in the topographically confined and sheltered head of the Akaroa harbour (figure 2.5). The maximum effective fetch onto these profiles is 4.05 km from the southwest. The enclosed nature of the Harbour means that these profiles are not exposed to the full power of the wave environment as measured at the Banks Peninsula deepwater wave buoy. Frequently, during this study 1.5 - 2m swell

was observed at the entrance to the harbour at the same time as no wave activity was evident directly offshore from AK1 and AK2.

The wave environment offshore from these profiles is composed of a combination of swell waves, generated in deepwater that have propagated into the Harbour and near field wind waves generated within the Harbour itself. There have been no direct measurements of the wave environments in the Akaroa Harbour. Therefore, frequencies of each of these two components of wave generation that combine to make up the wave environment will be described separately and combinations discussed subsequently.

5.2.3.2.1 SWELL PROPAGATION.

As swell waves propagate from deepwater into the shallow water of Akaroa Harbour the friction of the seabed causes both shoaling and refraction. Waves are considered to be in deepwater when they have no interaction with the seafloor. Shoaling is the result of the interaction of the wave with the sea floor, which causes changes in wave energy and shape. Refraction is the deformation (or bending) of the wave crest.

The change in height of the wave (H_b) as it propagates into the Harbour can be calculated using equation 5.1.

$$H_b = H_o K_s K_b \quad \text{Equation 5.1}$$

Where H_o is the deepwater wave height, K_s is a shoaling factor and K_b is a refraction factor.

The shoaling factor for the Akaroa Harbour was calculated using equation 5.2. Komar and Gaughan (1972) derived this equation by evaluating the energy flux of waves in deepwater and at the breaker zone according to linear wave theory and fitting the result to laboratory data. The equation is therefore semi-empirical and gives the best approximation for changes caused by shoaling (Komar 1998).

$$\frac{H_b}{H_o} = \frac{0.563}{(H_o/L_o)^{1/5}} \quad \text{Equation 5.2}$$

Where H_b gives the breaker height after shoaling has occurred, H_o is the deepwater wave height and L_o is the deepwater wavelength. L_o was calculated using the linear wave theory approximation for deepwater waves (equation 5.3).

$$L_o = \frac{gT^2}{2\pi} \quad \text{Equation 5.3}$$

The refraction factor was obtained through construction of refraction diagrams. These are graphical plots of incoming wave crests with corresponding orthogonals and give a general picture of the spread of wave energy over an area of coastline. Refraction diagrams are constructed using the offshore topography and a reduction factor that predicts the changing path of oncoming wave fronts due to their interaction with the sea floor (Johnson *et al.* 1948). Using the principle of conservation of energy flux a refraction factor can be calculated from the changes in distance between orthogonals. Orthogonals show the distribution of energy along the wave crest. As they either diverge or converge according to the refraction of the wave front corresponding dispersal or intensification of the energy occurs and from this a refraction factor can be calculated (equation 5.4).

$$K_b = \left(\frac{S_d}{S_b} \right)^{1/3} \quad \text{Equation 5.4}$$

Where S_d is the distance between Orthogonals along a wave crest in deepwater and S_b is the distance between the same Orthogonals at the point of wave breaking. This calculation applies to waves which are about to break, when, according to solitary wave theory energy is proportional to the cube of wave height.

Dingwall (1966) presented two refraction diagrams for the sea off Banks Peninsula (figures 5.4 and 5.5). He used wave approach angles of 45 degrees and 135 degrees and

wave periods of 10 seconds based on available wave observations, which suggested these were the prevailing conditions. Figures 5.4 and 5.5 show that very little wave energy is transmitted into the Akaroa Harbour under the most common wave conditions and that the most successful transmission of wave energy up the harbour occurs under southeast (135 degree) swell conditions.

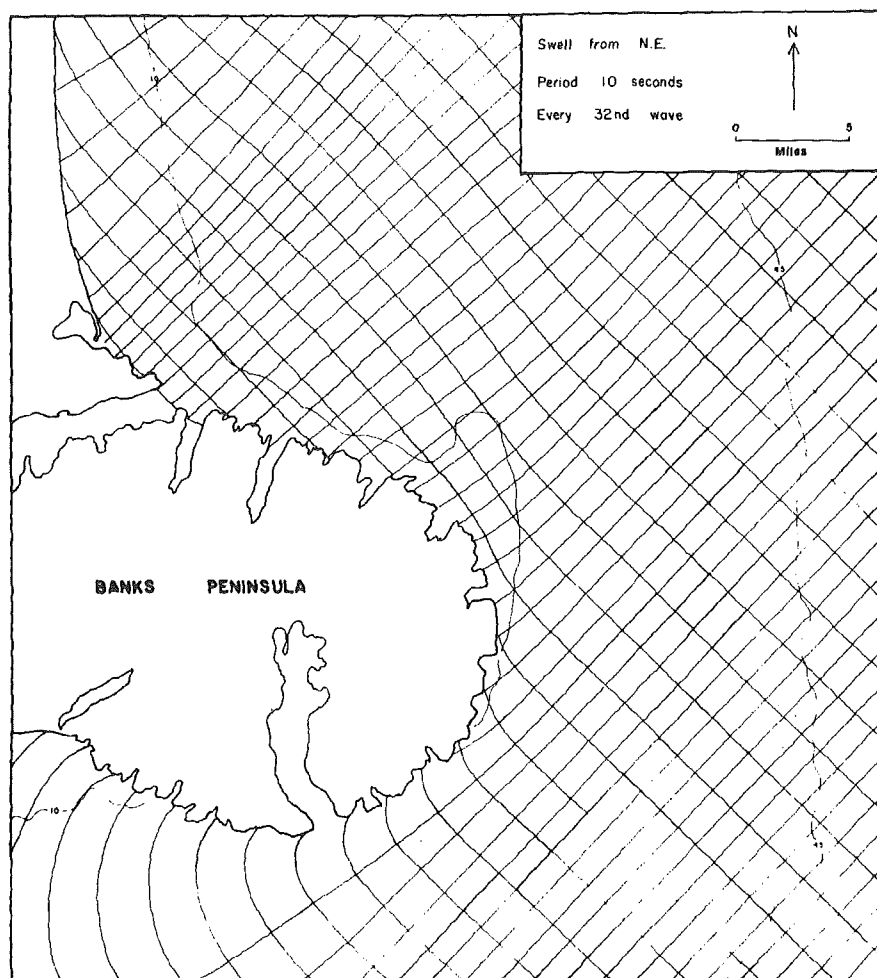


Figure 5.4: Wave refraction diagram for Banks Peninsula for swell from 45° (Dingwall 1966:fig 6).

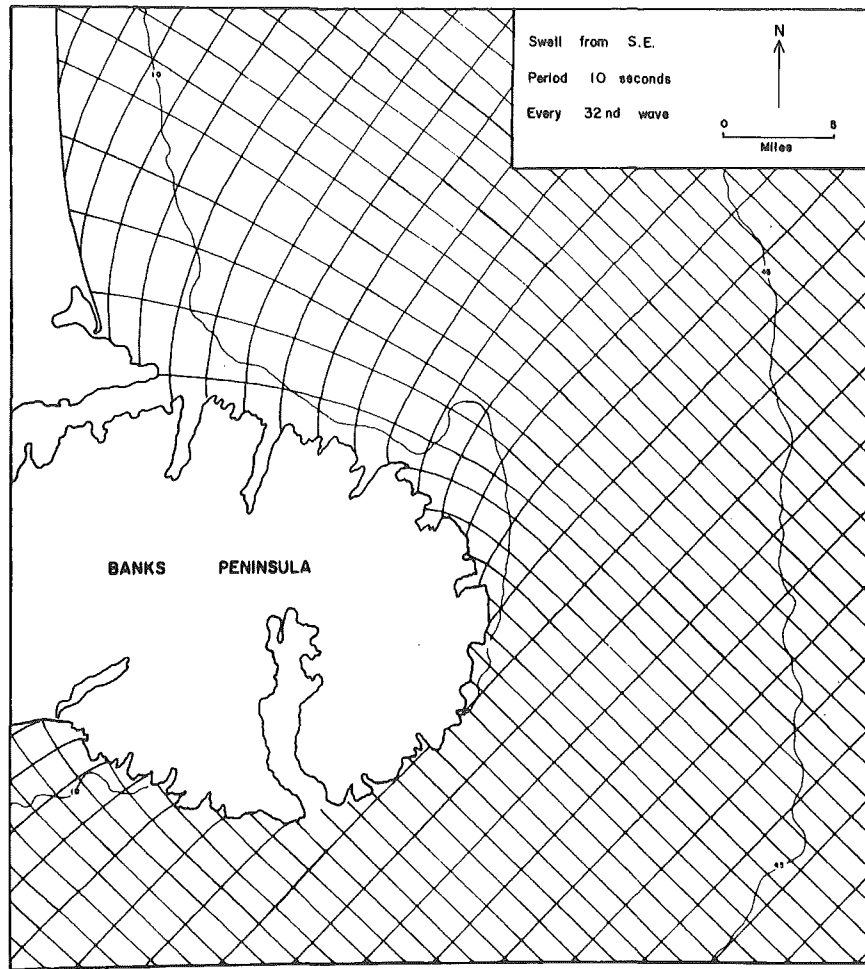


Figure 5.5: Wave refraction diagram for Banks Peninsula for swell from 135° (Dingwall 1966:fig 5).

Larger scale wave refraction diagrams (figures 5.6 and 5.7) were constructed for Akaroa Harbour using 135 degree wave approach, taking the work of Dingwall (1966) into account, and a 170 degree wave approach based on the prevailing deepwater wave conditions according to the Banks Peninsula wave buoy data. Diagrams were constructed using the method outlined by Johnson *et al* (1948) on 1:30 000 NZ navy chart 6324. Initial drawing was undertaken by hand and diagrams were subsequently digitised using CorelDraw.

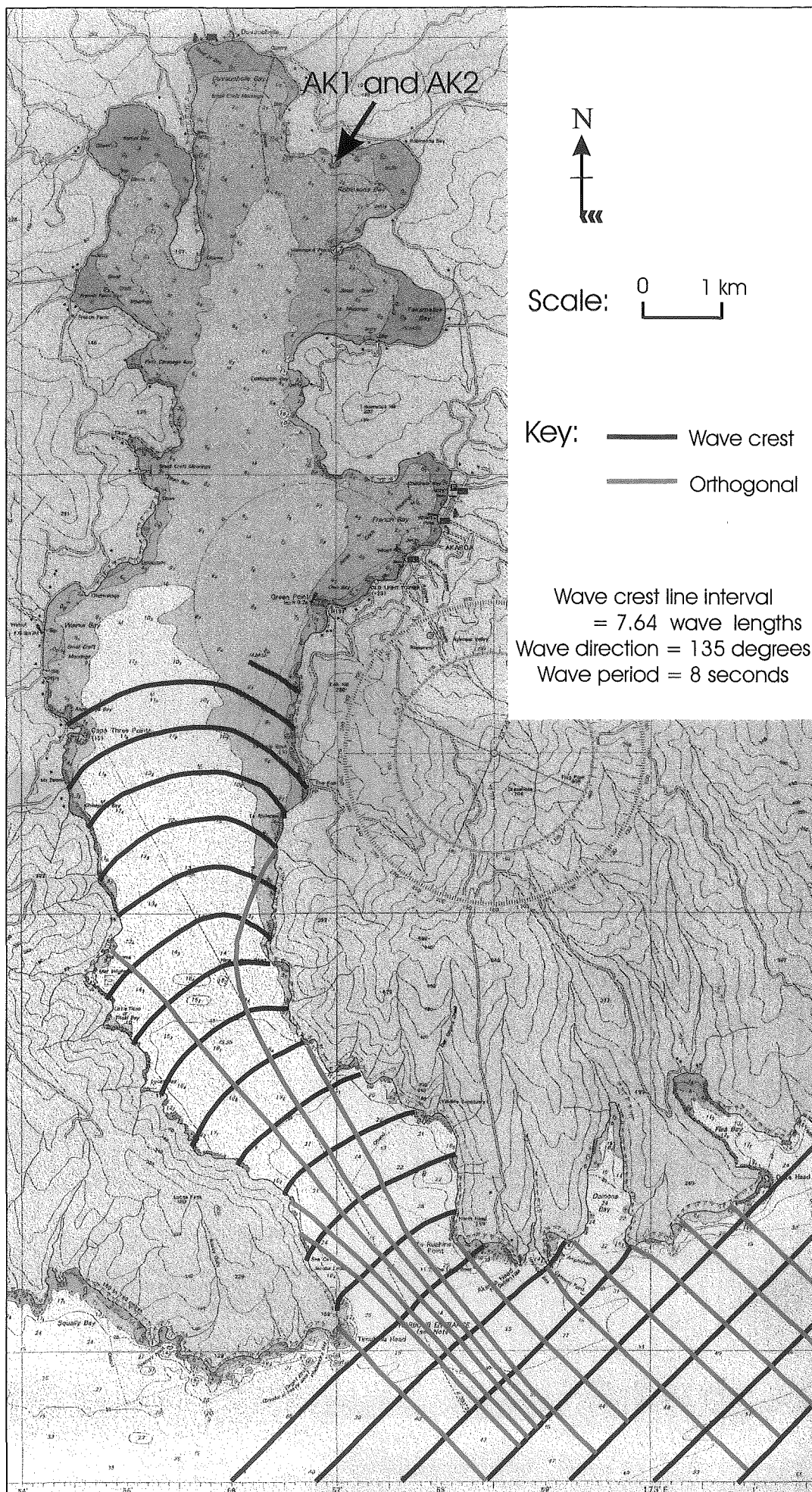


Figure 5.6: Wave refraction diagram for Akaroa Harbour for swell from 135°. (Scale is reduced from the original 1:30 000 diagram).

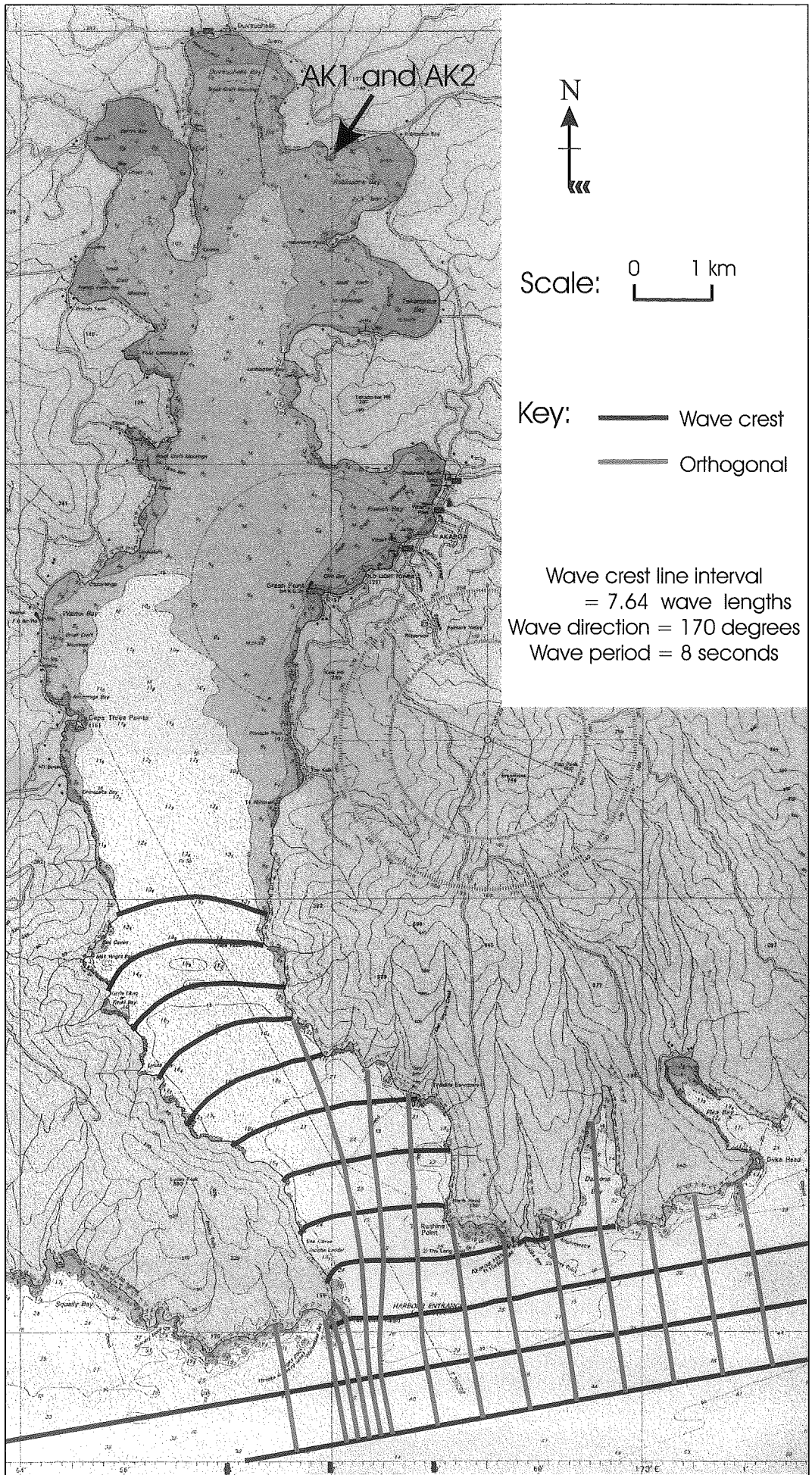


Figure 5.7: Wave refraction diagram for Akaroa Harbour for swell from 170°. (Scale is reduced from the original 1:30 000 diagram).

It is clear from figures 5.6 and 5.7 that refraction of swell from deepwater into Akaroa Harbour is significant, even under conditions when oncoming swell propagation is directly up the alignment of the harbour (135°).

The refraction divergence factor for swell propagating into Akaroa Harbour from 135 degrees with an 8 second period is $K_b = 0.171$. The divergence factor for swell from 170 degrees is $K_b = 0.159$.

Using equation 5.1 it is possible to calculate the breaker height at the head of the harbour after shoaling and refraction has occurred. For swell from 135° with a significant deepwater wave height of 6.76m ($H_{so(max)}$) the calculated maximum breaker height directly offshore from AK1 and AK2 is $H_b = 1.12m$. For swell from 135° under conditions of average significant deepwater wave height, $H_{so} = 1.8m$, the calculated breaker height directly offshore from AK1 and AK2 is $H_b = 0.23m$

Figures 5.4 – 5.7 show that not all waves generated in deepwater will propagate to the head of the Harbour and that the final height of swell, if it does propagate depends on the original deepwater direction. Therefore, calculation of frequencies of occurrence of propagated wave heights at the head of the Harbour was accomplished by dividing the Banks Peninsula wave buoy data into three sectors based on wave direction. Sectors were 225° to 85°, 85° to 155° and 155° to 225°. It was assumed that swell from northerly directions (225° to 85°) would not propagate into the Harbour. Figure 5.4 shows that by the time swell from the northeast direction reaches the entrance of the Akaroa Harbour there has been a significant divergence of the orthoginals. Therefore extreme dissipation of wave energy would have occurred by this point and no swell would propagate into the Harbour.

To ascertain final breaker heights offshore from AK1 and AK2 the refraction factor (K_b) calculated for wave angle approach of 135° was applied to swell from between 85° to 155° and K_b for swell from 170° was applied to swell from between 155° to 225°. The refraction factor calculated for wave approach of 135° was the largest possible for

Akaroa Harbour. Therefore using this K_b for swell from a range of directions will result in a slight overestimation of final breaker heights.

The second column of table 5.5 presents occurrence frequencies of significant wave heights for propagated swells reaching the water directly offshore from profiles AK1 and AK2 calculated in the manner described above.

Table 5.5: Frequency of occurrence of wave heights offshore from AK1 and AK2. The frequencies of propagated deepwater swell waves are shown in the second column. Frequencies of locally generated wind waves are in the third column. An estimate of the combination of the deepwater and wind waves is in the fourth column (see text for explanation).

| H_s (m) | frequency of occurrence (%) | | |
|------------|-----------------------------|------------|-------------|
| | propogated swell | wind waves | combination |
| 0 | 20 | 7 | 1 |
| 0.0 - 0.25 | 30 | 49 | 25 |
| 0.25 - 0.5 | 40 | 24 | 34 |
| 0.5 - 0.75 | 9 | 10 | 18 |
| 0.75 - 1.0 | 1 | 7 | 14 |
| 1.0 - 1.25 | 0 | 4 | 8 |
| 1.25 - 1.5 | 0 | 0 | 0 |
| 1.5+ | 0 | 0 | 0 |

5.2.3.2.2 WIND WAVE GENERATION.

Given the enclosed nature of the Akaroa Harbour and the fact that swell propagation is limited, sea state conditions created by near shore winds need to be considered when describing the typical wave environment offshore from AK1 and AK2. Hindcasting has been used to derive the wind wave regime in the Harbour for typical annual wind conditions.

Hindcasting uses wind and fetch data to model generation of wind waves in a given environment (see Allan 1998 for details on hindcasting techniques). A computer package called Lakewave (produced by M Hicks (NIWA) in conjunction with Geography Department, University of Canterbury) was used to hindcast significant wave heights directly offshore from AK1 and AK2. Lakewave uses the NARFET model

(Smith 1991) of wave prediction for enclosed water bodies reworked for New Zealand conditions.

The Akaroa Harbour was treated as a lake by drawing a straight line across the entrance, from the northern head to the southern head. The Lakewave programme then regarded the Harbour as a fully enclosed water body and appropriate fetch lengths were taken from this. Wind data used is given in figure 5.8. The wind rose in figure 5.8 was constructed using hourly wind data over a five year period (January 1995 – December 1999) from the closest weather station to the Akaroa Harbour (Le Bons Bay weather station, NIWA Climate data base). It was constructed in a DOS programme supplied by Prof. A Sturman, Geography Department, University of Canterbury.

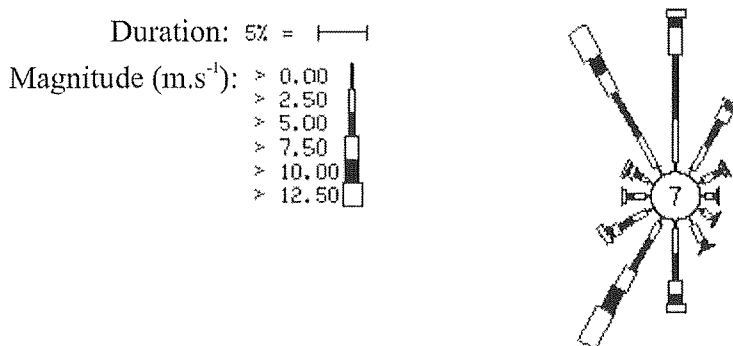


Figure 5.8: Wind rose for Akaroa region (based on 5 years of recorded wind data).

Table 5.5 gives frequencies of occurrence of H_s predicted by Lakewave. Simulated wind events blew for sufficient lengths of time for fully aroused sea states to occur. In every case a fully aroused sea was predicted to be reached in less than 1.5 hours.

5.2.3.2.3 COMBINATION OF SWELL AND WIND WAVES.

The second and third columns of table 5.5 present the frequencies of occurrence of wave heights for propagated deepwater swells and predicted wind waves offshore from AK1 and AK2. Although these two sea states can be regarded as independent each will not

necessarily occur in isolation. Remote generation of swell means that it may occur unrelated to prevailing wind conditions. Therefore, treating propagated swell and wind waves as discrete means that any two combinations of wave heights from each wave train may occur at the same time within the Harbour. Maximum heights will be produced when addition of waves from each wave train occurs. However interaction of waves is complex and simple addition of wave heights does not account for interference effects created by differing wave forms and directions of propagation.

Simple probability combinations of the two different wave climate frequencies are not realistic either as the two events will very rarely occur in isolation. Wind generated waves occur because irregularities in the surface of the water are enlarged by the wind. If a swell wave is present within the harbour the wind will blow across this and for energy to be added to the existing waves the wind blowing across the crests has to be faster than the crests themselves, creating a lower pressure hence increasing the wave height. Swell waves will only increase in size if the energy contributed by the wind is greater than that of the existing waves. Also, rather than adding energy a wind with the 'wrong' direction or speed, for example, may change other aspects of the waves such as their shapes.

This restriction on the addition of energy to the waves by wind must mean that there is a transition from a swell dominated wave environment to a wind wave dominated environment within the Harbour. It has been assumed that this will occur when predicted wind waves are of similar height to swell waves. In table 5.5 a frequency of wave height occurrence for the combination of swell and wind waves has been calculated by assuming each wind wave category will dominate only when swell waves are smaller. However, accurate modelling of the combination of sea states is complex so these frequencies of wave occurrence should be regarded as an estimate only.

Based on this estimate, at AK1 and AK2 the majority of waves (92%) are under 1m in height and there are significant periods (26%) of calm water or very small (0– 0.25 m) waves. Maximum predicted wave height was 1.25m. The wave environment offshore from AK1 and AK2 has very low energy wave activity.

Field verification of the estimated wave climate given in table 5.5 is difficult due to the lack of wave data available for the Akaroa Harbour. However, measurements of waves were made over a 20 minute period at high tide on 6/02/02 using the pressure sensor installed for tidal observations (section 2.4.3). Unfortunately this sensor was not located in an ideal site for wave observation as it was within a wave shadow area (figure 2.6). Pressure was sampled at 5 Hz and converted to water depth. A significant wave height, $H_s = 0.15$ m was recorded. An estimated H_s of 0.5m was observed 100m seaward of AK2 during the time of measurement.

During the time of measurement deepwater swell conditions at the Banks Peninsula wave buoy were $H_s = 5.79$ m from 146° and there was an 8 m.s^{-1} southwesterly (220°) wind which had been blowing for at least 3 hours (NIWA climate data base). Using Lakewave, wind waves of 0.57 m would result from these wind conditions. From equation 5.1 and recorded deepwater wave conditions predicted propagated swell height would be $H_b=0.98$ m.

H_s recorded at the pressure sensor was smaller than either predicted swell or wind wave heights. This suggests that frequencies given in table 5.5 over estimate actual wave heights within the Akaroa Harbour.

5.2.3.3 WK1 AND WK2 WAVE ENVIRONMENT

The Lakewave programme was used to predict the typical wave environment offshore from WK1 and WK2 as no direct measurements of waves have been undertaken at Lake Waikaremoana. Annual wind data, based on a ten year record (Matthews 1992) was used as input for Lakewave. Predicted frequencies of occurrence of significant wave heights offshore from WK1 and WK2 are given in table 5.6. This is a low energy wave environment with predicted maximum significant wave height of 0.75m and for 75% of the time waves are generally 0.25m or less in height. In the main body of the lake (figure 2.7) maximum significant wave heights of 1.3m are predicted.

Table 5.6: Frequency of occurrence of significant wave heights offshore from WK1 and WK2.

| H_s (m) | Frequency of occurrence (%) |
|------------|-----------------------------|
| 0.0 - 0.25 | 73 |
| 0.25 - 0.5 | 26 |
| 0.5 - 0.75 | 1 |
| 0.75 - 1.0 | 0 |
| 1.0 - 1.25 | 0 |
| 1.25 - 1.5 | 0 |
| 1.5+ | 0 |

5.2.4 COMPARISON OF OFFSHORE WAVE ENVIRONMENTS WITH RATE OF SURFACE CHANGE.

As noted in section 5.1.2 many studies have used measures of the deepwater wave environment as an indication of the wave assailing force at the shore platform. The assumed magnitude of this assailing force has then been used to define relationships of control on platform morphology. As in Tsujimoto's (1987) demarcation of shore platform initiation which was based on a balance of F_W and F_R . Section 5.2.3 provided descriptions of the wave environments offshore from each study profile. Table 5.7 is a summary of these giving either measured or predicted maximum significant wave heights and average significant wave heights for each profile. Maximum significant wave heights ranged between 6.7m off the Kaikoura coast to 0.8m offshore from WK1 and WK2. Average significant wave heights ranged between 1.8m and 0.2m.

Table 5.7: Summary of wave environments offshore from each profile.

| H_s (m) | AK1 | AK2 | KM2 | KM3 | KM7 | RM1 | WK1 | WK2 |
|-----------|-----|-----|-----|-----|-----|-----|-----|-----|
| maximum | 1.3 | 1.3 | 6.7 | 6.7 | 6.7 | 6.7 | 0.8 | 0.8 |
| average | 0.6 | 0.6 | 1.8 | 1.8 | 1.8 | 1.8 | 0.2 | 0.2 |

If significant wave height is used as an indicator of onshore wave assailing force it is possible to make a comparison between this and platform width, platform gradient and average rate of surface change at each profile in order to investigate the control

deepwater wave energy exerts over shore platform morphology and shore platform development in the form of rate of surface change.

Wave height has been used here as a surrogate for wave energy. This has been done because wave energy is directly proportional to the square of wave height (see equation 5.8).

Figure 5.9 plots H_s (both maximum and average) offshore from each profile against a) platform width, b) platform gradient and c) average rate of surface change measured on each profile.

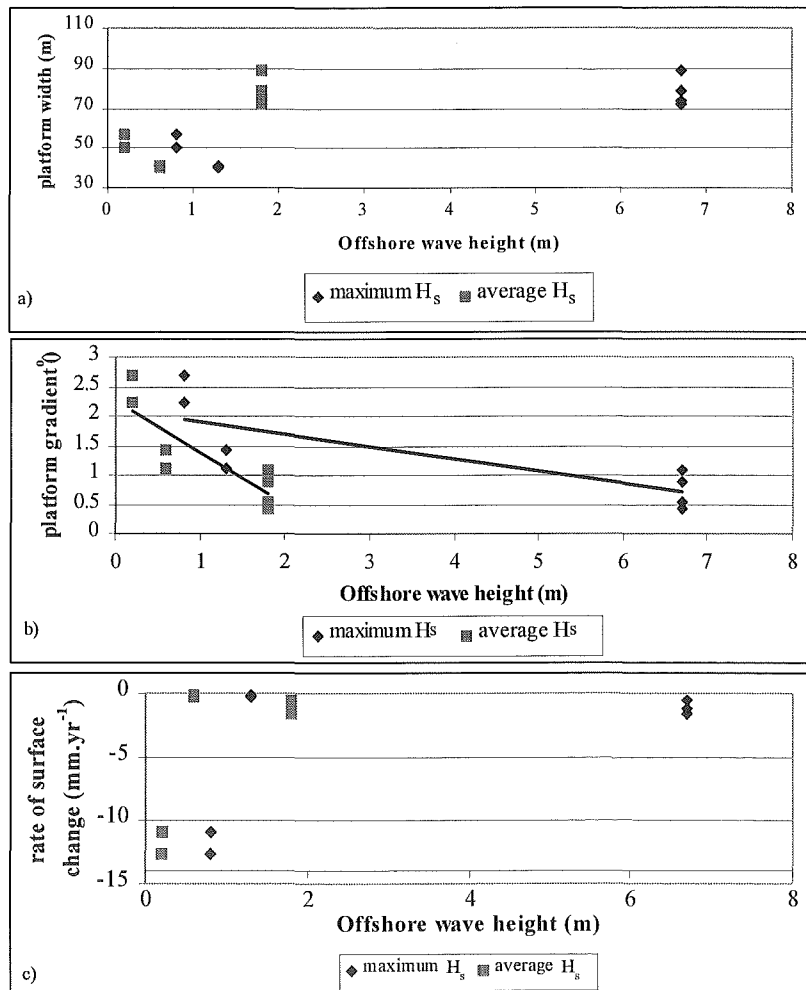


Figure 5.9: Offshore wave height compared to a) platform width b) platform gradient and c) average rate of surface change. Wave heights are given as both maximum significant height and average significant height in meters.

There are obvious clusters of points on each plot as groups of profiles were exposed to the same general wave environments. This makes it difficult to define relationships between the two factors shown in each plot with any certainty. There is a trend towards wider platforms with greater offshore wave height (figure 5.9a) although this is not well defined.

Figure 5.9b shows a negative trend with shallower gradients occurring on platforms with larger offshore wave heights. The correlations between maximum significant wave heights and gradient and average significant wave heights and gradient were $r=0.84$ and $r=0.77$ respectively. These suggest a strong relationship but the result may be somewhat biased by the grouping of the data. However the observation of steeper gradients on the less active wave environments does support the model of Trenhaile and Layzell (1981) that suggested gradient of 'wave-cut' platforms is least where wave action is strongest. No robust explanation for this relationship has been offered.

Figure 5.9c shows that there is no correlation between offshore wave height and rate of surface change at each platform. For the shore platforms studied in this thesis there is no distinct relationship between the offshore deepwater wave environment and the rate of surface change.

This does not necessarily mean that there is no relationship between the assailing force of the waves and shore platform development. Just that, for this study there was no relationship between deepwater wave height and shore platform surface change. This may mean one of two things. Wave assailing force is not a direct control on shore platform development or deepwater wave height, when used as an indicator of wave energy is not a true indication of wave assailing force on shore platforms.

This question of the use of deepwater wave parameters as indicators of wave assailing force and wave activity on shore platforms is an important one. Virtually nothing is known about the translation of wave energy from deepwater onto the shore platform. Some shore platform studies have used shoaling equations and theory developed for sand beaches to account for changes in wave energy (Mii 1962, Tsujimoto 1987).

However, how applicable these theories are to the shore platform environment has not been tested. The only direct comparison of deepwater and on shore platform wave energy has been published by Stephenson and Kirk (2000a) who showed a reduction in wave energy of greater than 91% as waves moved from deepwater onto the shore platform at Kaikoura.

The next section addresses changes that occur as waves move from deepwater onto the shore platform at KM3.

Section 5.4.3 looks at flow across shore platforms caused by wave action.

5.3 CHANGES AS WAVES MOVE FROM DEEPWATER ONTO THE SHORE PLATFORM.

As waves generated in deepwater move into shallow water they are subject to change. Figure 5.10 presents a flow diagram showing the transformation and actions of sea waves as they move shoreward.

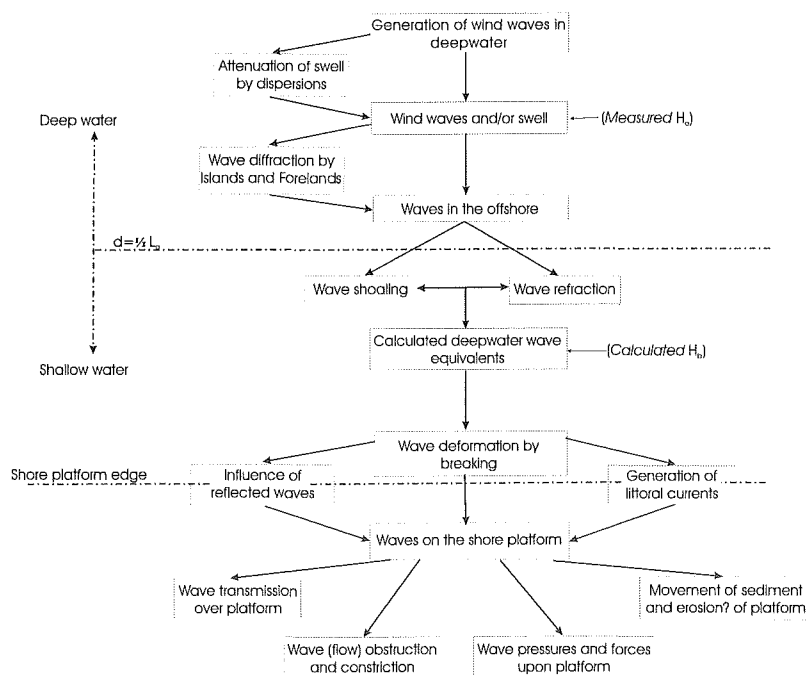


Figure 5.10: Flow diagram showing transformations and action of sea waves (after Goda 1990).

Initially waves are generated in deepwater and propagate outwards from the generation zone as swell. Deepwater waves propagate by oscillatory motion of the water through which they pass. (Detail on wave generation and propagation can be found in many texts including Bascom (1980), Denny (1988), Komar (1998)). Measurement of deepwater waves can be made directly by equipment such as wave buoys and pressure sensors. Water depth is defined in relation to the length of the wave. Shallow water occurs at a depth of equal to or less than $\frac{1}{2}$ the deepwater wave length (L_0).

Figure 5.10 shows that as waves move into shallow water they undergo processes of both shoaling and refraction. Shoaling is the interaction of the wave with the sea floor, which causes changes in wave energy and shape. Refraction is the deformation (or bending) of the wave crest. Both processes may occur simultaneously.

As waves propagate into shallow water the presence of the seabed changes the orbital motion of the water. Waves steepen and eventually reach a point where the wave is no longer able to maintain form and collapse (breaking) occurs. On breaking much of the energy of the wave is lost to turbulence, noise and heat and the whole body of water moves forward as a wave of translation rather than in the deepwater, oscillatory manner. This type of wave is referred to as a bore (Denny 1988).

The location of wave deformation by breaking with respect to the shore platform edge as shown in figure 5.10 will be discussed further in section 5.3.2. The effects of shoaling and refraction on wave parameters can either be measured directly or calculated in accordance with theories specifically developed for this purpose (section 5.3.1).

The action and effects of waves once they reach the shore platform can be grouped into four categories (figure 5.10). As transmission of waves across the platform occurs they will exert pressures and forces and may cause both movement of sediment and erosion of the platforms. These may be considered the assailing forces of waves. Flow caused by waves may also be constricted and obstructed by platform morphology. Section 5.4.3 and Chapter 6 present further discussion of these aspects of waves on shore platforms.

5.3.1 WAVE THEORIES

Wave theories have been developed to calculate components of waveform and dynamics under changing conditions. They describe and predict wave behaviour. Most theories are based on conservation of energy flux as the wave propagates shoreward and model aspects of the wave itself such as, celerity (velocity), wave length, water particle displacement and energy. The simplest and most commonly used theory is Linear (Airy) Theory based on equations of a sinusoidal waveform and conservation of energy flux. Other theories include Stokes theory (a 2nd order derivative theory), cnoidal and solitary wave theory. The latter two use more complex closely fitting equations to define the waveform. (For greater explanation of wave theory see Denny (1988) or Komar (1998)).

Each theory is suited to deriving different aspects of changing waves and each tends to work better in different circumstances. Figure 5.11 shows under which circumstances each theory is most efficient.

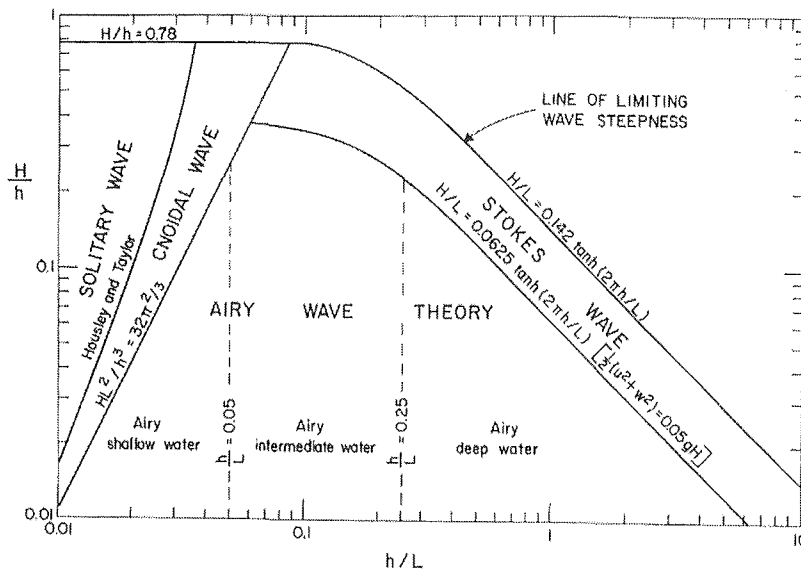


Figure 5.11: The areas of application of various wave theories as a function of the ratios H/h and h/L where H is wave height, h is water depth and L is wave length (Komar 1998).

From figure 5.11 it can be seen that modelling holds till the point of breaking. After this water flow becomes more complex and has not been successfully modelled mathematically. Empirical and descriptive methods have been adopted when investigating waves at and after breaking (Komar 1998).

Tsujimoto (1987) used H_b calculated from deepwater wave parameters and linear wave theory as an indication of wave assailing force on shore platforms around Japan. In this way he used linear wave theory to account for changes that may have occurred as waves shoaled through shallow water. However, before wave theories are used to give an indication of wave assailing force on a shore platform knowledge of the location of breaking with respect to the shore platform should be ascertained.

5.3.2 LOCATION OF WAVE BREAKING IN RELATION TO STUDY PROFILES.

The location of wave breaking relative to the shore can be attained from equation 5.5.

$$H_b = 0.78h_b \qquad \text{Equation 5.5 (CERC 1984)}$$

Where H_b is the height of the wave at breaking (after shoaling and refraction effects) and h_b is the depth of water at breaking. This equation is a working model, which has been developed based on empirical evidence, and is only accurate when the nearshore bottom slope is very gradual. The Shore Protection Manual (CERC 1984) presents empirically derived graphs of H_b/h_b for a range of other nearshore surface slopes. However, as nearshore seafloors of all study sites are of gradual slope equation 5.5 provides a useful rule of thumb for this study. It has also been used in shore platform studies by Tsujimoto (1987) and Stephenson (1997a).

Knowledge of the wave environment offshore from each profile (tables 5.4, 5.5, 5.6 and 5.7) makes it possible to calculate wave breaking locations in relation to the shore platforms studied for this thesis. Frequencies of significant wave heights given in table

5.5 and 5.6 for AK1, AK2, WK1 and WK2 are predicted breaking wave heights having accounted for shoaling and refraction effects and can therefore be utilised directly in equation 5.5. Further investigation of the effect of shoaling on wave height is required for sites KM2, KM3, KM7 and RM1 before breaker height can be calculated using equation 5.5.

The effect of shoaling on wave height frequencies at these sites can not be calculated using equation 5.2 directly as data used to compile table 5.4 did not include synchronised wave period and wave height measurements.

Progression of a wave through shallow water causes it to change height, generally steepening, but not always. It was necessary therefore to investigate the controls on H_b in the Kaikoura environment (figure 5.12). Figure 5.12 shows the change in wave height calculated using equation 5.2 for the range of different wave conditions recorded by the Banks Peninsula wave buoy data (Walsh 2002). Both wave height and wave period are plotted against the difference in wave height after shoaling. It can be seen that there was no direct systematic relationship between H_o and H_b , but rather that T is the controlling factor on H_b . Increases of up to 1m in wave height and decreases of less than 0.04m were predicted by equation 5.2 for this environment.

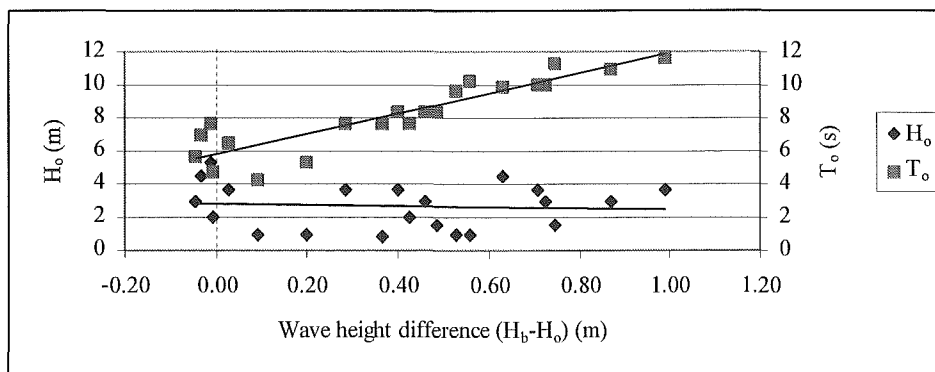


Figure 5.12: Controls on H_b for the Kaikoura coastal wave environment. The difference between wave breaking height and deepwater wave height is plotted against deepwater wave height (H_o) and deepwater wave period (T).

It is important to remember that equation 5.2 was developed for sand beaches where the nature of the unconsolidated sediment will cause energy dissipation of waves of shorter

period and taking into account the margin of error involved in this method of calculation it is reasonable to assume that wave height only increases during shoaling in these circumstances. Therefore, it was deemed adequate to use measured values of H_0 instead of calculated H_b values when calculating wave breaking depth using equation 5.5 for KM2, KM3, KM7 and RM1.

The influence of refraction has been neglected in the calculation of depth of wave breaking for profiles at KM2, KM3, KM7 and Raramai. As described earlier they are directly exposed to waves from a large range of directions. Refraction is considered to be relatively small and difficult to calculate accurately for these sites.

Predicted locations of frequency of wave breaking with respect to shore platforms were calculated for each profile (figures 5.16 – 5.23). The method of calculation is described for one profile (KM3) but frequencies only are shown for all others.

5.3.3 FREQUENCY OF WAVE BREAKING WITH RESPECT TO PLATFORMS.

Figure 5.13 shows the profile of KM3 and the location of wave breaking relative to the platform, for the maximum wave conditions $H_s = 6.76$ m and the average wave conditions $H_s=1.8$ m at the highest recorded tidal level, mean water level and the lowest recorded tidal level. From this it can be seen that even at the highest tides average size waves will break seaward of the platform.

As breaker height is restricted by depth (equation 5.5) a plot of maximum breaker height with respect to measured profile depth was constructed (figure 5.14). Plots were constructed for mean sea level and topography that deepened in the landward direction was filtered. Filtering was done as waves will break at the point where they first encounter their breaking depth as they progress towards the shore. In figure 5.14 the solid line shows H_b calculated with water depth directly and the dashed line shows filtered H_b for KM3.

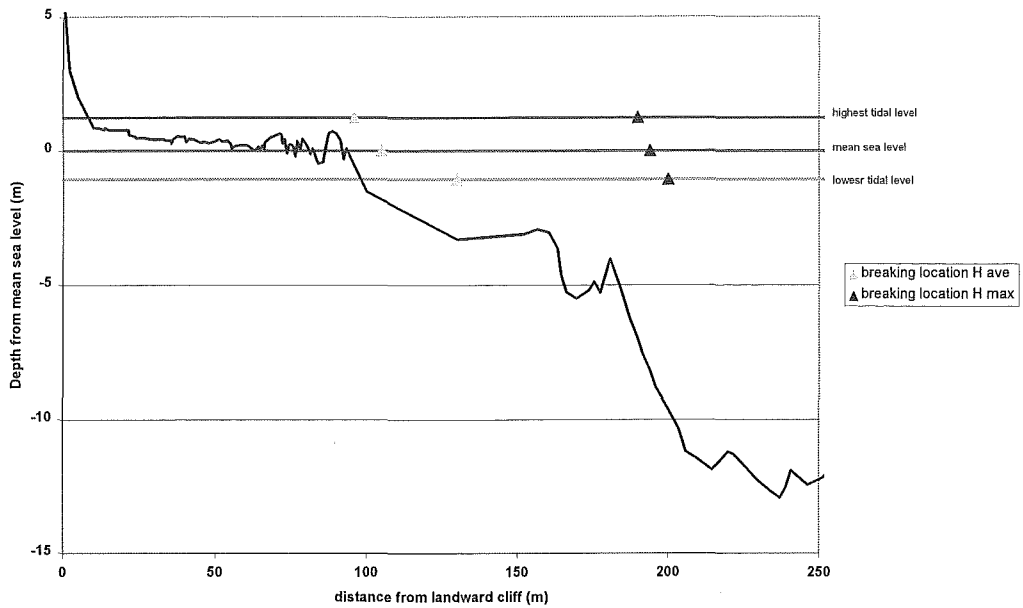


Figure 5.13: Locations of wave breaking for average H_s and maximum H_s shown in relation the profile at KM3.

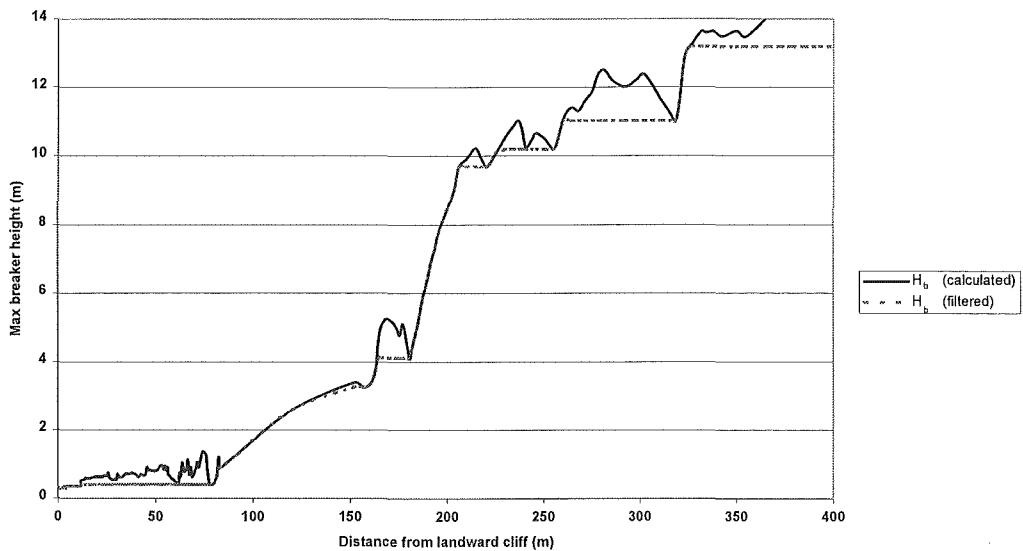


Figure 5.14: Location where waves will break with respect to their deepwater height at mean sea level at KM3. The location of breaking is shown as the distance in metres from the landward cliff.

From this and with a knowledge of significant deepwater wave height frequencies (figure 5.15) it was possible to establish the frequency of occurrence of waves breaking at given locations relative to the landward cliff of the shore platform (figure 5.16). Note that this is given for mean sea level so when considering any other tidal levels the graph would be displaced in either the seaward or landward direction. However as average tidal ranges are less than 1.5m (section 2.4.1) displacement would not be great.

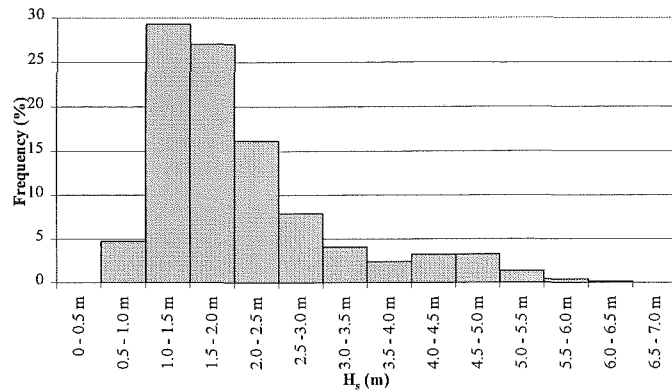


Figure 5.15: Frequency of occurrence of given significant wave heights (H_s) offshore from KM3.

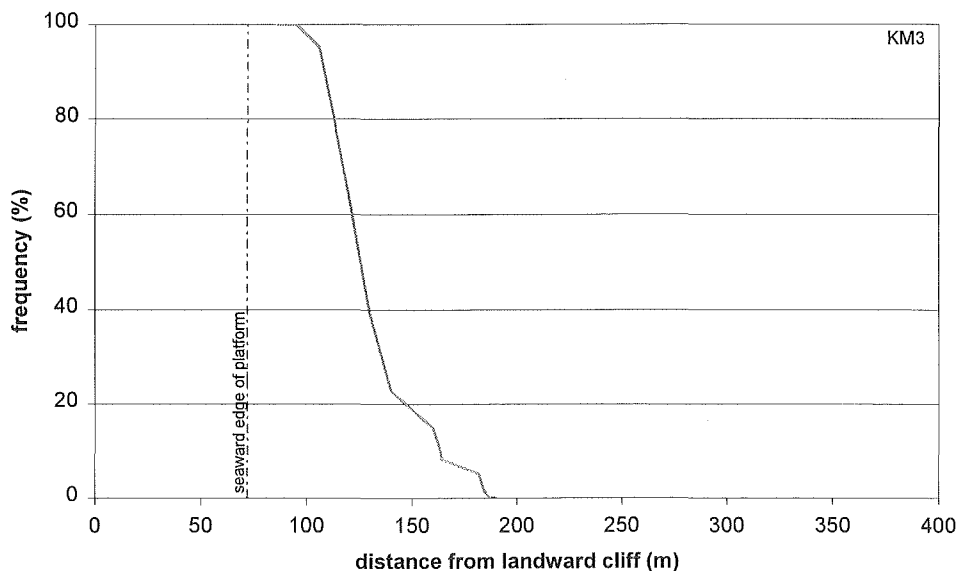


Figure 5.16: Frequency of occurrence of wave breaking at a given distance from the landward boundary of the platform at KM3.

Figure 5.16 shows that all but the smallest waves break before they reach the platform at KM3 and 50% of all waves have broken at least 25m seaward of the seaward cliff. The largest 10% of waves break 175m seaward of the platform.

Frequency of wave breaking graphs are presented for all other study profiles in figures 5.17 – 5.23.

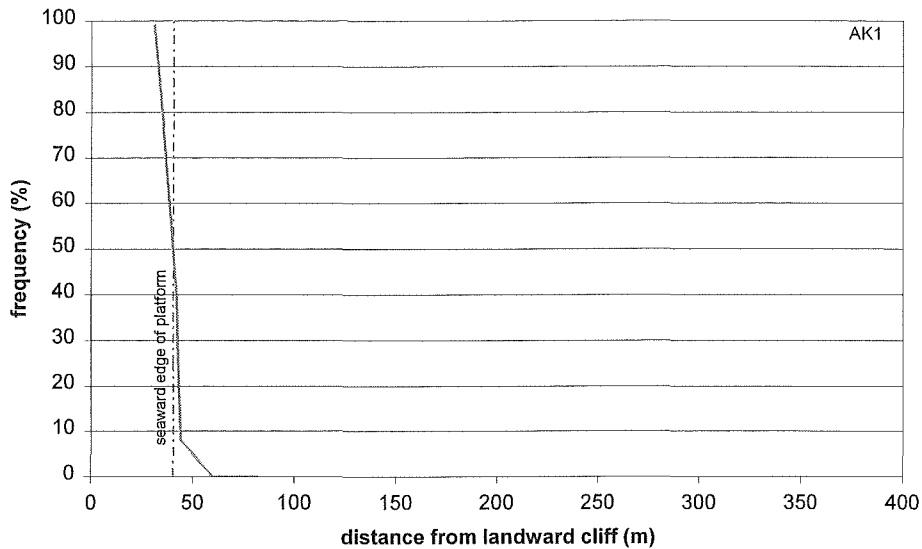


Figure 5.17: Frequency of occurrence of wave breaking at a given distance from the landward boundary of the platform at AK1.

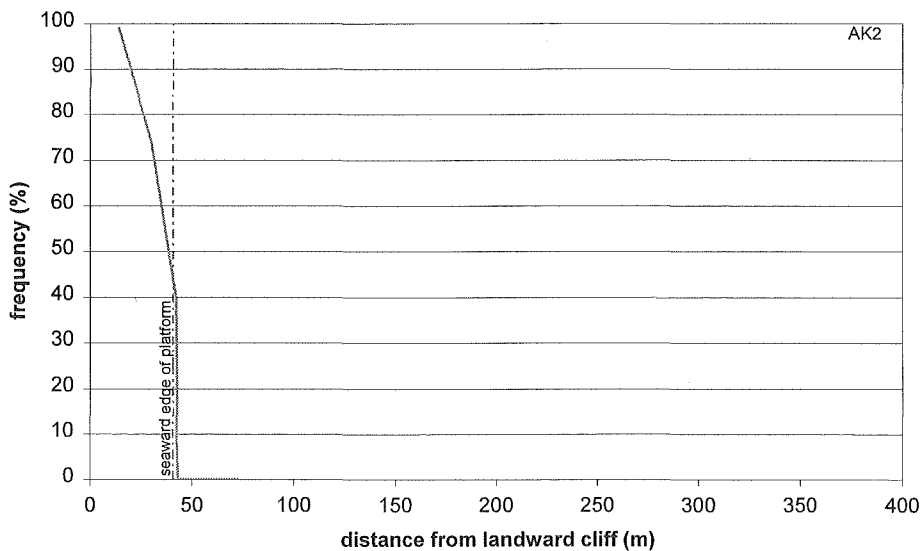


Figure 5.18: Frequency of occurrence of wave breaking at a given distance from the landward boundary of the platform at AK2.

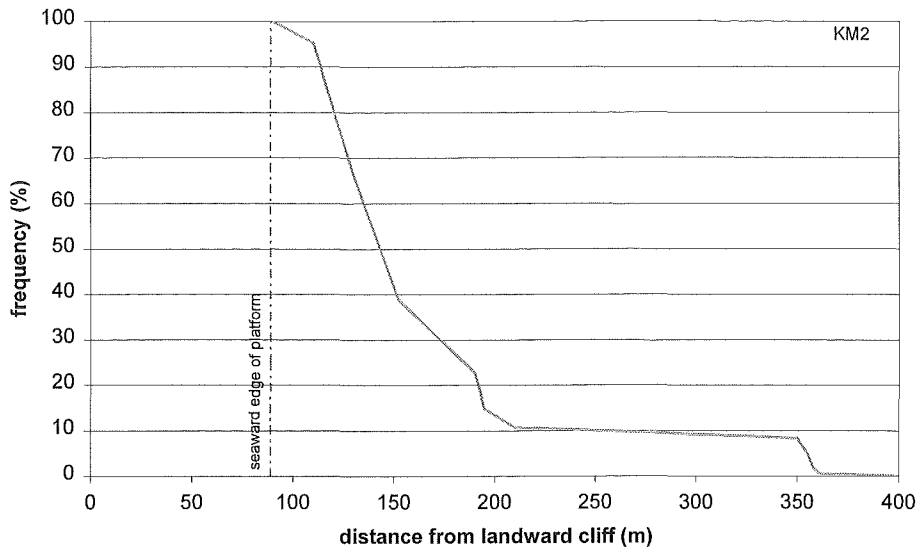


Figure 5.19: Frequency of occurrence of wave breaking at a given distance from the landward boundary of the platform at KM2.

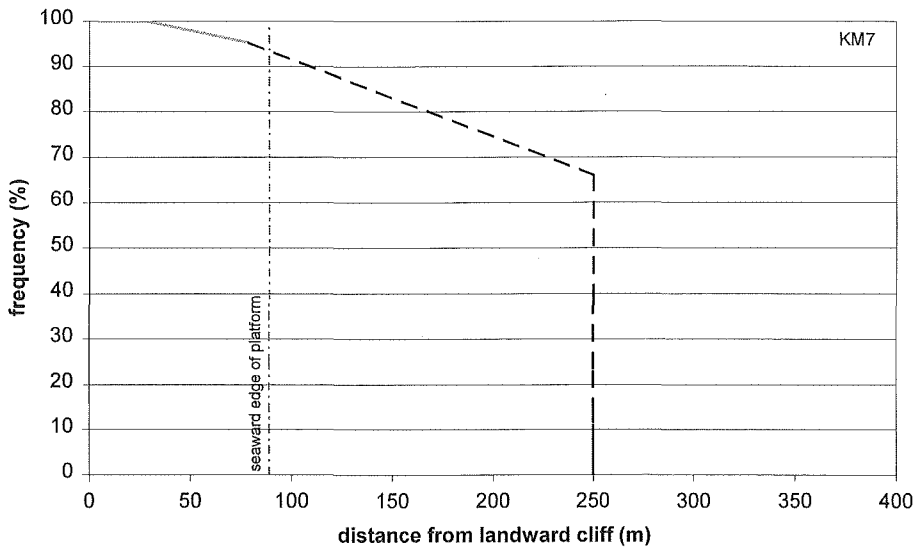


Figure 5.20: Frequency of occurrence of wave breaking at a given distance from the landward boundary of the platform at KM7.

At KM7 the existence of a reef 300-500m seaward of the platform (section 2.6.6) will mean that all but the smallest waves will break at this point before reaching the platform proper. Figure 5.20 has been drawn with a dashed line to show this is an estimate of frequency of wave breaking locations only.

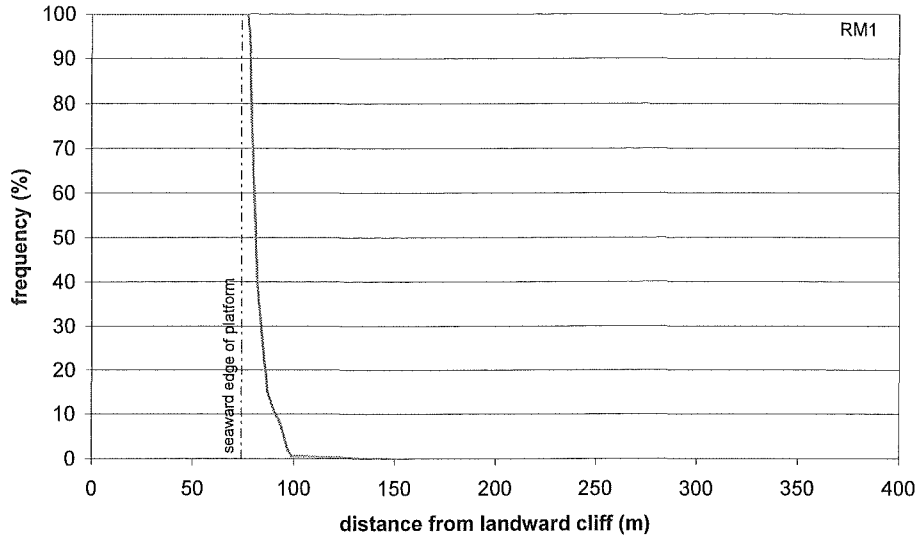


Figure 5.21: Frequency of occurrence of wave breaking at a given distance from the landward boundary of the platform at RM1.

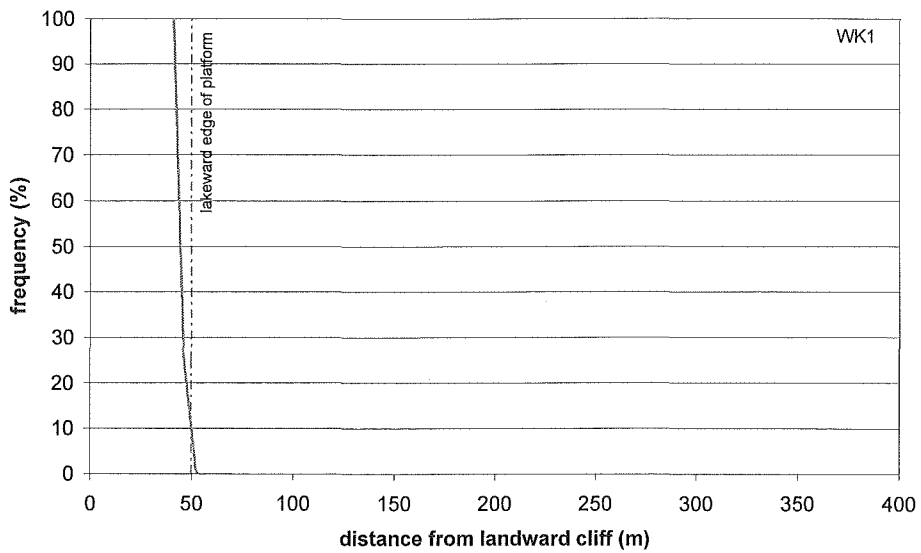


Figure 5.22: Frequency of occurrence of wave breaking at a given distance from the landward boundary of the platform at WK1.

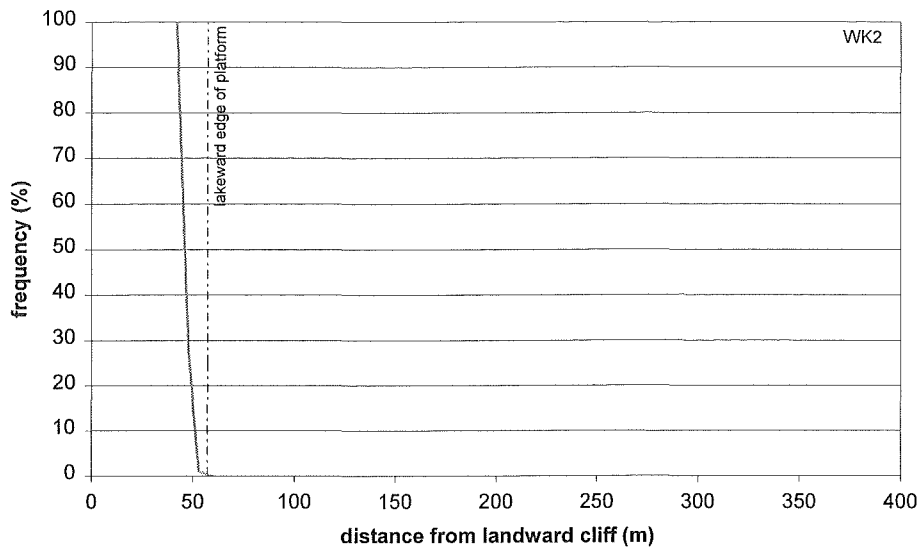


Figure 5.23: Frequency of occurrence of wave breaking at a given distance from the landward boundary of the platform at WK2.

With the exception of the very smallest waves all waves are broken before they get to the platforms (at all of the sites under study here). This finding concurs with that of Stephenson (1997a). It is therefore a solitary bore (or a smaller reformed wave) that flows onto and over any of the platforms. This has also been confirmed in general observation by the author.

5.4 COMPARISON OF DEEPWATER, ONSHORE AND ACROSS SHORE FLOWS.

The nature of broken waves is complex and current mathematical modelling of wave breaking or flow after breaking is of limited value and simplistic when compared to the empirical evidence of broken wave behaviour. Representation of flow is not good enough to be useful and the lack of accuracy of models makes them inadequate as a prediction tool. Much of the broken wave modelling discussed in the international literature has been for the purposes of engineering and protection of structures (see Goda 1990) or for flows on sand beaches (see Komar 1998).

Therefore, as there is currently no satisfactory theory to predict the flow of waves onto and across a shore platform, the description of empirical evidence is imperative. The remainder of this chapter is devoted to such description. Section 5.4.1 details methods of measurement of flow onto and across the shore platform at KM3. The differences measured between deepwater and on shore platform wave parameters are presented in section 5.4.2 and descriptions of flow patterns across the shore platform at KM3 are presented in section 5.4.3.

Direct measurements of flow induced by wave action were undertaken at KM3. Flow measurements were made at only one study profile due to logistical considerations. Securing of flow velocity instruments to the rock platform was an arduous undertaking because of fractures in the mudstone. Securing instruments to the more easily fractured surfaces of other study profiles such as greywacke and basalt proved too tenuous and was therefore not undertaken. Measurements of flows presented in this project should therefore be regarded in the nature of a pilot study to be extended onto different morphologies at a future date.

5.4.1 MEASUREMENT METHODS.

Measurements of flow on the shore platform at KM3 were undertaken during two separate sampling periods. KM3 is 72.1m in width and orientated towards the southeast with unlimited fetch and exposure to the high energy southerly swell environment (section 2.6.5). During each set of measurements three separate fluid velocity meters were attached to the shore platform along the profile at KM3. One was an acoustic Doppler velocity meter and the other two were electro magnetic current meters. Figure 5.24 is a schematic diagram showing the locations of the velocity meters. Locations for installation of instruments were chosen so that they were on surfaces that were as flat as possible without any obvious topographical obstructions within the close vicinity. This was to avoid the possibility of measuring flow controlled by local topography. Sampling of velocity was done at a height of between 100mm and 110mm from the platform surface to avoid measurement of flow directly disturbed by surface roughness.

Water flow was measured in 18 minute bursts on the hour every hour while water covered the platform, approximately 2.5 hours either side of high tide.

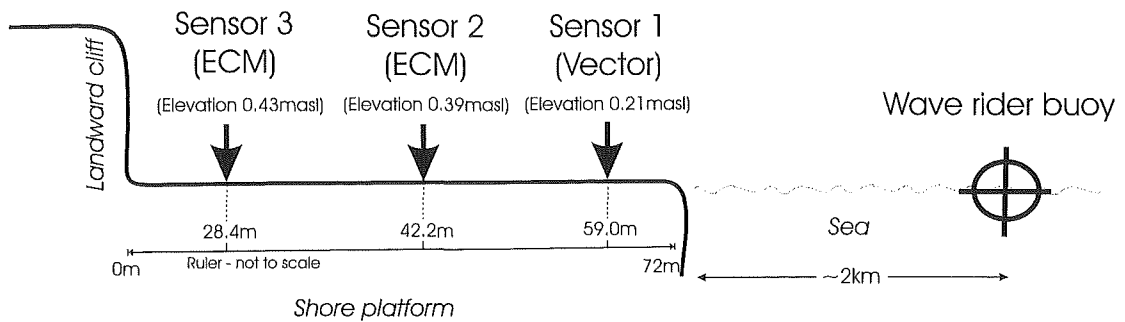


Figure 5.24: Schematic showing location of velocity metres on KM3

Initial flow measurements were conducted between 12 – 23 July 2001.

A second set of measurements were conducted between 18 – 24 August 2001. This second set was made in conjunction with an experiment undertaken by NIWA and the Zoology Department, University of Canterbury. During this experiment a non-directional deepwater wave rider buoy was installed approximately 2km east of the Kaikoura peninsula sampling continuously.

5.4.1.2 INSTRUMENTATION

5.4.1.2.1 WAVE BUOY

A non-directional deepwater wave buoy was installed, by NIWA, in 30m of water 2 km east of the North East Point of the Kaikoura Peninsula during the August 2001 field period. Deepwater wave data recorded at this buoy were provided by NIWA and the Zoology Department, University of Canterbury for use in this project. The buoy recorded half-hourly averages of wave height including, maximum, $H_{1/10}$ and H_s and wave period, T_z . Data from the wave buoy was not recorded as a continuous stream of water levels therefore was not in a form that could be spectrally analysed.

5.4.1.2.2 VECTOR (ACOUSTIC DOPPLER VELOCITY METER)

Sensor 1 was a Nortek Vector (acoustic Doppler velocity) Current Meter. This instrument samples instantaneous water velocity in three dimensions, at up to 64 Hz, using the acoustic Doppler principle. The Vector is a bistatic sonar that transmits short acoustic pulses through a central beam. These pulses are scattered back by reflectors in the water. Echoes are received and measured through three beams displaced off to the side of the transmission beam (figure 5.25). Reflectors are particles in the water, which include zooplankton, suspended sediment and air bubbles. It is assumed that these particles move within the water at the same velocity as the water itself.

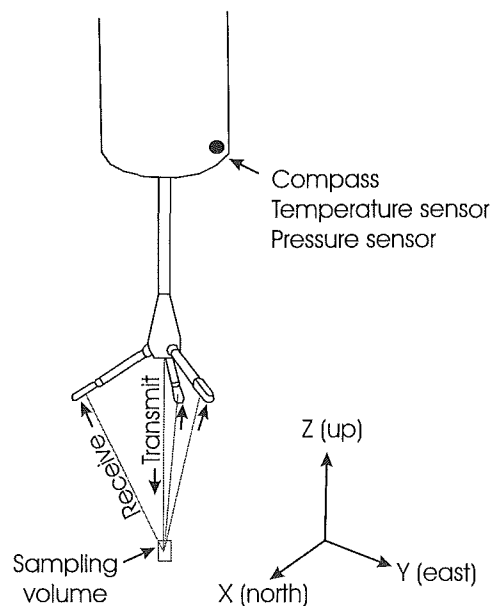


Figure 5.25: Vector probe showing orientation of beams and location of pressure sensor.

Water velocity is measured 157mm from the transmitter through a volume of 14x14mm. The configuration of the beams results in the Vector being more sensitive to the z velocity component (figure 5.25) than it is to the x or y velocity components. Consequently the z velocity component has a lower measurement uncertainty. Vector instrumental uncertainty is calculated by the vector software, provided by the manufacturer and has an accuracy of the larger of $\pm 0.25\%$ or $0.0025 \text{ m}\cdot\text{s}^{-1}$.

In addition to velocity the Vector samples water pressure, temperature, instrument tilt and direction through sensors located inside the casing (figure 5.25). These parameters are sampled every second during the sampling period, with the exception of pressure, which is sampled at the same rate as velocity. The Vector is capable of running in real time, connected to a laptop by cable, or stand-alone, sampling either continuously or in burst mode as determined by the configuration file. The configuration file is loaded and data down loaded using manufacturer provided software. Three text files are produced.

1. A summary of the configuration file.
2. Velocity and pressure data sampled at specified Hz rate.
3. Temperature sampled every second during the sampling period.

Down loaded data were processed using the ExploreV processing programme, developed by Nortek, and subsequently analysed in Excel spreadsheets.

The Vector was attached to a solid metal frame, which was bolted to the rock surface (figure 5.26). The frame was aligned so that it would cause the least interference at the location of measured flow and the flow was sampled 110 mm from the platform surface. It operated in the stand-alone mode during the recording period and was down loaded via cable to a laptop at completion of each sampling period. The vector was located on the most seaward location due to its stand-alone capabilities. Sensors 2 and 3 required cables connected to dry land for operation.

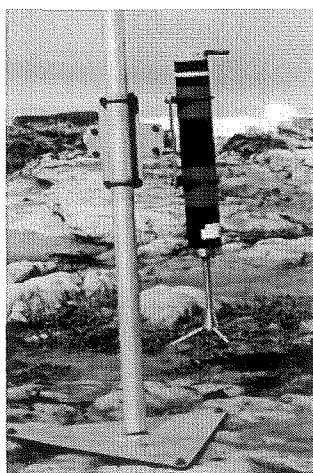


Figure 5.26: Installation of Vector flow velocity instrument near the seaward edge of the shore platform at KM3.

5.4.1.2.3 MARSH MCBIRNEYS (ELECTRO MAGNETIC CURRENT METERS)

Sensors 2 and 3 were Marsh McBirney Electromagnetic Current Meters (ECMs). These meters sample instantaneous water velocity in 2 dimensions (figure 5.27). Flow is measured by means of the Faraday principle of electromagnetic induction. The sensor generates a magnetic field through which the water (a conductor) moves producing a voltage that is proportional to its velocity.

The two ECMs were mounted on the platform using 1.5 m slotted poles (figure 5.27) and connected by cable to a Campbell 21X data logger situated at the base of the landward cliff at a level just higher than that of the highest tide. The ECM probes were located at a height of 100 mm above the platform surface and orientated so they measured flow on a horizontal plane parallel to the platform surface. The x and y axis (figure 5.27 and 5.29) of both instruments were orientated in the same compass direction. A programme was written for the 21X data logger to enable sampling of the x and y components of flow at 5 Hz for 18 minutes. Results were recorded as a text file, which was then analysed in an Excel workbook.

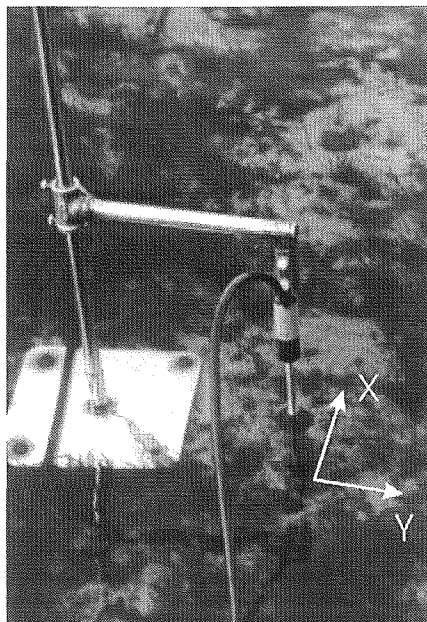


Figure 5.27: Installation of a Marsh McBirney ECM on the shore platform at KM3. The arrows show the axis of measurement of the instrument.

5.4.1.3 CALIBRATION

All three flow velocity instruments were calibrated separately, as per manufacturer instructions. They were all also calibrated against each other to check for comparability. This calibration was conducted in a field situation. Ideally a comparison of the two types of instrumentation should have been undertaken in a laboratory flume that provided a known steady flow. Unfortunately a suitable flume was not available. Comparison was therefore undertaken with gauges located close together, without causing interference to each other, in a stream where the flow appeared to be uniform. All three instruments recorded velocities that were within $\pm 0.05 \text{ m.s}^{-1}$. The different velocity metres were therefore assumed to be comparable for the purposes of this experiment.

Previous studies conducted in laboratory situations on the comparability of velocity measured by different current meters have shown that the velocities measured by acoustic Doppler meters are comparable to those of ECMs (Kraus *et al* 1994). Elgar *et al* (2001) compared measurements made using acoustic Doppler velocity meters and ECMs within the inner surf zone of a gently sloping sandy beach. They showed that the nearshore velocity field statistics measured by all instruments were similar. Variations in measurements between the Acoustic Doppler meters and the ECMs were less than 0.04 m.s^{-1} . The turbulent nature of a sandy beach surf zone would be similar in character to that of the shore platform environment.

5.4.1.4 SAMPLING

Instruments were set from a common clock and sampled simultaneously.

The flow environment was sampled on the hour every hour for 18 minutes while the tide covered the platform and the sensors were submerged. An 18 minute period was used as it is considered to be the length of time required to fully encompass the spectrum of the wave environment (CERC 1984, Komar 1998). Tucker (1963) used 10-minute periods in his analysis of records of sea waves. Guza and Thornton (1982) used 17 minute sections in their analysis of swash zone oscillations on a natural beach.

Sampling rates were selected to avoid wave aliasing. Wave aliasing occurs when sampling patterns misrepresent actual wave forms (figure 5.28). To avoid this enough samples need to be taken in order to define the wave and the flow accurately while also considering the memory capacity of the instruments. Accounting for the typical 6 to 10 second wave periods expected, it was considered that 5 Hz was regular enough to fully define the wave while avoiding wave aliasing.

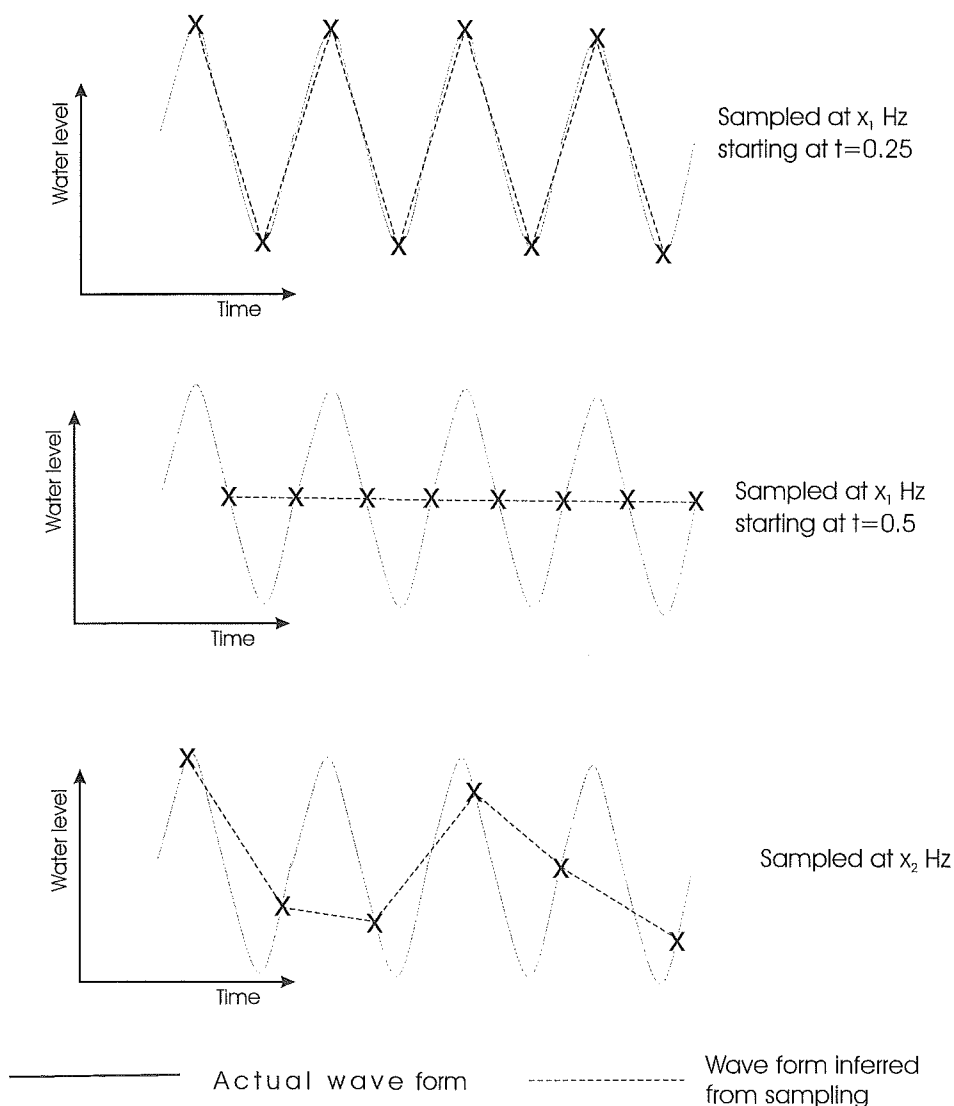


Figure 5.28: Schematic showing the problem of wave aliasing. A cross section of a waveform is shown through time with sampling points indicated. Inferred waveform from sampling is superimposed. When sampling fails to define the wave form accurately wave aliasing may occur.

The Vector sampled at 8 Hz and the ECMs at 5 Hz. 5 Hz was the maximum possible sampling rate for the ECMs in this configuration. Memory capacity restrictions meant that the ECMs data logger required down loading twice during the 18 minute recording period in order to acquire the complete data set and avoid over writing.

Sampling during the August 2001 field period was undertaken over 4 tidal cycles. Recording over all tidal cycles during the study period was not possible owing to a combination of equipment malfunction and rain causing inappropriate environmental conditions. The Vector sampled in burst mode recording 18 minutes of data at 8 Hz on the hour every hour synchronised with the ECMs.

5.4.1.5 POST PROCESSING OF DATA

Vector data were downloaded and processed in ExploreV, a programme provided as support software for the Vector instrument. The orientation of the Vector velocity data was rotated in order to correspond with the direction of ECMs data (figure 5.29).

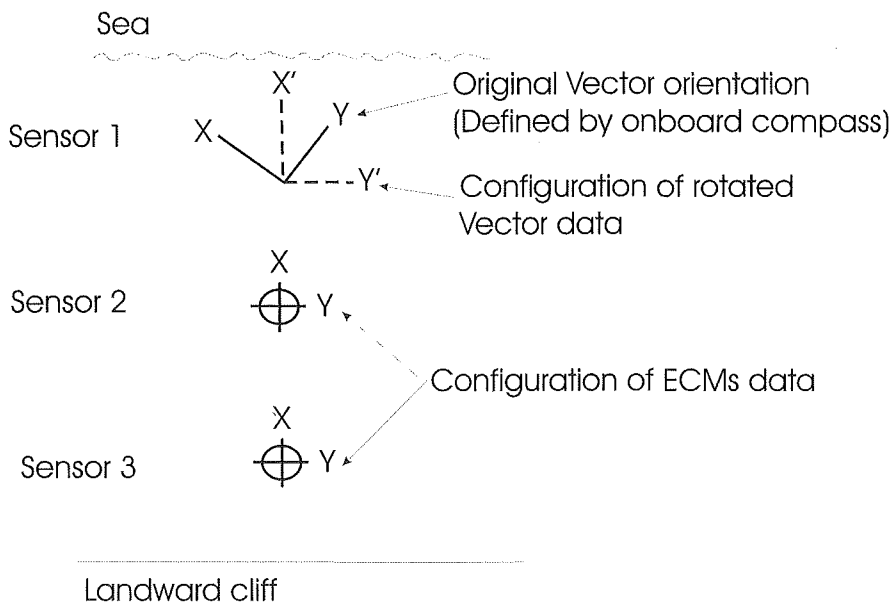


Figure 5.29: Schematic diagram of axis orientations of flow measurements shown in plan view. (Not to scale).

Velocity data from the Vector were also filtered to remove noise from the signal. Excessive amounts of air bubbles within the water will strongly reflect the acoustic signal and may cause large amounts of noise. The Vector reports the correlation along the three beams and from this it is possible to identify readings that are obvious spurious spikes in the data. The filter (a low pass filter) has the effect of eliminating incoherent sequences replacing them with values linearly interpolated between velocities before and after the incoherent sequence.

Vector files were sorted in a specifically developed Excel workbook to match velocity with pressure and time data. All files were then combined.

5.4.2 DIFFERENCES BETWEEN DEEPWATER AND ONSHORE (PLATFORM) WAVE PARAMETERS.

This section discusses measured changes in wave parameters as the waves propagated from deepwater onto the shore platform at KM3. The data used for these comparisons were averages of the 18 minute measurements made on the hour every hour at sensor 1 (figure 5.24) and synchronous half hourly averages measured at the deepwater wave buoy. Wave parameters discussed are wave period (T), maximum wave height (H_{\max}), significant wave height (H_s), water particle velocity (u) both maximum and average, maximum and average wave energy (E) and maximum and average wave energy flux (Q).

Wave height and period were measured directly at each instrument. The Vector converts pressure directly into water level above the sensor according to its internal calibration. Pressure was sampled at 8Hz. Water level measurements were processed using time series analysis in a specifically developed excel workbook. Analysis was based on the zero upcrossing method described by IAHR (1989). It yielded wave period, maximum wave height and significant wave height. Internal programming of the deepwater wave buoy produces half hourly averages of H_s and T automatically. Onshore water velocity (u) was measured directly by the Vector. No direct deepwater measure of water or wave velocity was made by the wave buoy. In order to compare the velocities at each location two measures of velocity at the wave buoy were calculated using Linear wave theory.

One was the phase velocity (C) of the wave form, which was calculated in m.s^{-1} using equation 5.6. This measures the velocity at which the waveform is travelling.

$$C = \frac{gT}{2\pi} \quad \text{Equation 5.6 (Komar 1998)}$$

Where T is the deepwater wave period and g is the gravitational constant (9.81m.s^{-2}).

The second measure of velocity in deepwater was water particle velocity (u_o). This was calculated using equation 5.7.

$$u_o = \frac{\pi H_o}{T} e^{kz} \cos(kx - \sigma t) \quad \text{Equation 5.7 (Komar 1998)}$$

Where k is the wave number and z is particle displacement from still water level. u_o was calculated at a fixed time $t = 0$ and location $x = 0$ and with particle displacement $z = H_o/2$ (maximum) and where $k = 2\pi/L_o$. Maximum water particle velocities were calculated in order to be directly comparable to the onshore velocity measures which are horizontal flow. Water particle velocity is an important factor to measure, as it is the water movement itself that will exert force on the platform rather than the somewhat intangible waveform.

In deepwater, phase velocity is usually an order of magnitude greater than water particle velocity. The waveform or wave energy travels faster than the water through which it moves. However, once waves have propagated into shallow water and break, water particles then travel at the same rate as the solitary waves. Therefore, here the actual velocity of the water, rather than that of the waveform is the most appropriate measure to be used for comparison.

Wave energy at each site was calculated using equation 5.8 from linear wave theory. This gives a measure of total energy per unit area of surface of wave crest.

$$E = \frac{1}{8} \rho g H^2 \quad \text{Equation 5.8}$$

Where H is the wave height at each location, ρ is the water density (1005 kg.m^{-3}) and g is the gravitational constant (9.81 m.s^{-2}).

Wave energy flux (Q) is the rate of energy flow past a point, or the power, of the waves. The Q of one meter of wave crest is gained from equation 5.9.

$$Q = ECn \quad \text{Equation 5.9}$$

Where n is a shoaling coefficient. In deepwater, C is the phase velocity and $n = \frac{1}{2}$ and in shallow water C is the solitary wave velocity and $n = 1$.

Table 5.8 presents a summary of these wave parameters measured simultaneously in deepwater and on the shore platform at KM3 during the August 2001 field period.

5.4.2.1 WAVE PERIOD (T)

Both deepwater and onshore wave periods were similar and between 5.2-7.6s. There was a maximum difference between the T_o and T of a 36% increase. Generally onshore T was slightly longer than that offshore at the same time. Figure 5.30 shows a scatter plot of the relationship between onshore and offshore T . There was a positive relationship with a strong correlation ($r=0.6$).

Linear wave theory asserts that there should be no change in T as waves move into shallow water. The variation from theory shown in figure 5.30 may be the result of wave breaking which usually occurs before the waves reach the shore platform or that simultaneous deepwater and onshore measurements encompass a slightly different set of waves (i.e. there was a time lag). Generally wave period was slightly longer onshore than in deepwater.

Table 5.8: Measured averages of wave parameters in deepwater and onshore during the August 2001 field period. Also shown are the differences between deepwater and onshore measure as a percentage change, where negative indicates an increase in the value. Parameters include: Wave period T (s), maximum wave height H_{\max} (m), average significant wave height H_s (m), phase velocity C ($\text{m}\cdot\text{s}^{-1}$), water particle velocity u ($\text{m}\cdot\text{s}^{-1}$), wave energy E ($\text{N}\cdot\text{s}^{-1}$), wave energy flux Q ($\text{N}\cdot\text{m}^{-1}\cdot\text{s}^{-1}$). The subscript o denotes deepwater wave parameters. (See text for full explanation of parameters).

| Date and start time of 18 minute recording | wave parameters | | | | | | | | | | | | | | | |
|--|-----------------|---------|------------|---------------|-------------|------------|--------------|-----------|------------|--|--|------------|--|--|--|------------|
| | T_o (s) | T (s) | Change (%) | H_o max (m) | H max (m) | Change (%) | H_{so} (m) | H_s (m) | Change (%) | u_o max ($\text{m}\cdot\text{s}^{-1}$) | u max ($\text{m}\cdot\text{s}^{-1}$) | Change (%) | C (phase) ($\text{m}\cdot\text{s}^{-1}$) | u_o ave ($\text{m}\cdot\text{s}^{-1}$) | u ave ($\text{m}\cdot\text{s}^{-1}$) | Change (%) |
| 18/8/01 14:00 | 5.3 | 6.1 | -14 | 3.3 | 0.5 | 86 | 2.2 | 0.3 | 85 | 2.5 | 1.4 | 44 | 8.3 | 1.5 | 0.4 | 72 |
| 18/8/01 15:00 | 5.4 | 5.9 | -9 | 5.9 | 0.5 | 92 | 2.5 | 0.4 | 85 | 5.1 | 1.4 | 72 | 8.5 | 1.7 | 0.5 | 70 |
| 18/8/01 16:00 | 5.2 | 5.9 | -13 | 5.2 | 0.6 | 89 | 2.5 | 0.4 | 83 | 4.6 | 1.9 | 59 | 8.2 | 1.8 | 0.5 | 71 |
| 19/8/01 15:00 | 6.8 | 6.9 | -2 | 2.2 | 0.7 | 68 | 1.5 | 0.4 | 70 | 1.1 | 1.6 | -46 | 10.6 | 0.7 | 0.5 | 37 |
| 19/8/01 16:00 | 6.2 | 7.1 | -13 | 2.6 | 0.6 | 76 | 1.5 | 0.5 | 67 | 1.5 | 1.5 | 0 | 9.7 | 0.8 | 0.5 | 41 |
| 19/8/01 17:00 | 6.1 | 6.8 | -12 | 2.2 | 0.6 | 72 | 1.6 | 0.4 | 74 | 1.3 | 1.7 | -28 | 9.5 | 0.9 | 0.5 | 45 |
| 19/8/01 18:00 | 5.3 | 7.2 | -36 | 3.1 | 0.6 | 79 | 2.0 | 0.4 | 79 | 2.3 | 1.5 | 35 | 8.3 | 1.3 | 0.5 | 65 |
| 24/8/01 07:00 | 7.5 | 6.6 | 13 | 2.3 | 0.3 | 85 | 1.5 | 0.2 | 85 | 1.1 | 1.5 | -42 | 11.8 | 0.7 | 0.4 | 34 |
| 24/8/01 08:00 | 7.5 | 7.4 | 2 | 2.5 | 0.5 | 81 | 1.5 | 0.3 | 78 | 1.2 | 1.6 | -39 | 11.7 | 0.7 | 0.5 | 27 |
| 24/8/01 09:00 | 7.1 | 7.4 | -4 | 2.7 | 0.5 | 80 | 1.4 | 0.4 | 76 | 1.3 | 1.8 | -32 | 11.0 | 0.7 | 0.5 | 30 |
| 24/8/01 10:00 | 7.6 | 7.0 | 7 | 2.7 | 0.4 | 85 | 1.5 | 0.3 | 81 | 1.2 | 1.3 | -10 | 11.8 | 0.7 | 0.5 | 31 |

| Date and start time of 18 minute recording | wave parameters | | | | | | | | | | | |
|--|--|--|------------|--|--|------------|--|--|------------|--|--|------------|
| | E_o max ($\text{N}\cdot\text{m}^{-2}$) | E max ($\text{N}\cdot\text{m}^{-2}$) | Change (%) | E_o ave ($\text{N}\cdot\text{m}^{-2}$) | E ave ($\text{N}\cdot\text{m}^{-2}$) | Change (%) | Q_o max ($\text{N}\cdot\text{m}^{-1}\cdot\text{s}^{-1}$) | Q max ($\text{N}\cdot\text{m}^{-1}\cdot\text{s}^{-1}$) | Change (%) | Q_o ave ($\text{N}\cdot\text{m}^{-1}\cdot\text{s}^{-1}$) | Q ave ($\text{N}\cdot\text{m}^{-1}\cdot\text{s}^{-1}$) | Change (%) |
| 18/8/01 14:00 | 13502 | 250 | 98 | 5697 | 126 | 98 | 55970 | 349 | 99.4 | 23614 | 53 | 99.8 |
| 18/8/01 15:00 | 43191 | 308 | 99 | 7580 | 160 | 98 | 182746 | 443 | 99.8 | 32071 | 82 | 99.7 |
| 18/8/01 16:00 | 33838 | 386 | 99 | 7458 | 207 | 97 | 138420 | 731 | 99.5 | 30507 | 105 | 99.7 |
| 19/8/01 15:00 | 5697 | 587 | 90 | 2627 | 239 | 91 | 30063 | 940 | 96.9 | 13863 | 109 | 99.2 |
| 19/8/01 16:00 | 8460 | 505 | 94 | 2663 | 272 | 90 | 41209 | 760 | 98.2 | 12972 | 129 | 99.0 |
| 19/8/01 17:00 | 6074 | 489 | 92 | 2961 | 197 | 93 | 28781 | 813 | 97.2 | 14030 | 94 | 99.3 |
| 19/8/01 18:00 | 11767 | 505 | 96 | 4831 | 217 | 96 | 48777 | 748 | 98.5 | 20028 | 103 | 99.5 |
| 24/8/01 07:00 | 6748 | 142 | 98 | 2847 | 65 | 98 | 39720 | 214 | 99.5 | 16760 | 29 | 99.8 |
| 24/8/01 08:00 | 7826 | 284 | 96 | 2885 | 142 | 95 | 45943 | 456 | 99.0 | 16936 | 70 | 99.6 |
| 24/8/01 09:00 | 8851 | 346 | 96 | 2555 | 151 | 94 | 48784 | 607 | 98.8 | 14084 | 72 | 99.5 |
| 24/8/01 10:00 | 8786 | 187 | 98 | 2773 | 104 | 96 | 51781 | 252 | 99.5 | 16343 | 47 | 99.7 |

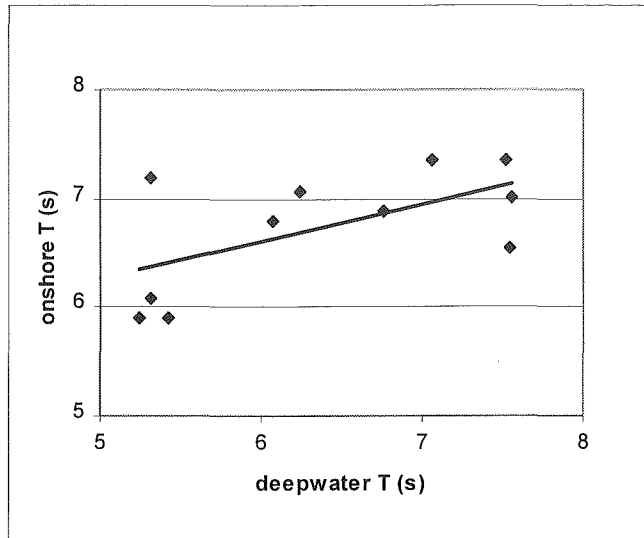


Figure 5.30: Scatter plot showing deepwater wave period against onshore wave period for simultaneous 18 minute averages.

5.4.2.2 WAVE HEIGHT (H)

Table 5.8 shows there were distinct decreases in both maximum H and H_s as waves moved onshore. The largest decrease measured was 92% with waves reducing in height from $H_{o(max)}=5.9\text{m}$ in deepwater to $H=0.5\text{m}$ on the shore platform. The smallest measured decrease in wave height was 67% with significant wave heights of $H_{s0}=1.5\text{m}$ in deepwater and $H_s=0.5\text{m}$ onshore. Waves undergo refraction and shoaling as they move shoreward and most have broken before they reach the shore platform (section 5.3) so a reduction in wave height was predicted. However the amount of reduction is considerable and worthy of note, especially when using deepwater H_s as a parameter to define wave assailing force on shore platforms.

Deepwater and onshore wave heights have been plotted in figure 5.31. This shows that wave height reduced as waves propagated from deepwater onto the shore platform. However, there was no evident direct relationship dictating the amount of this reduction.

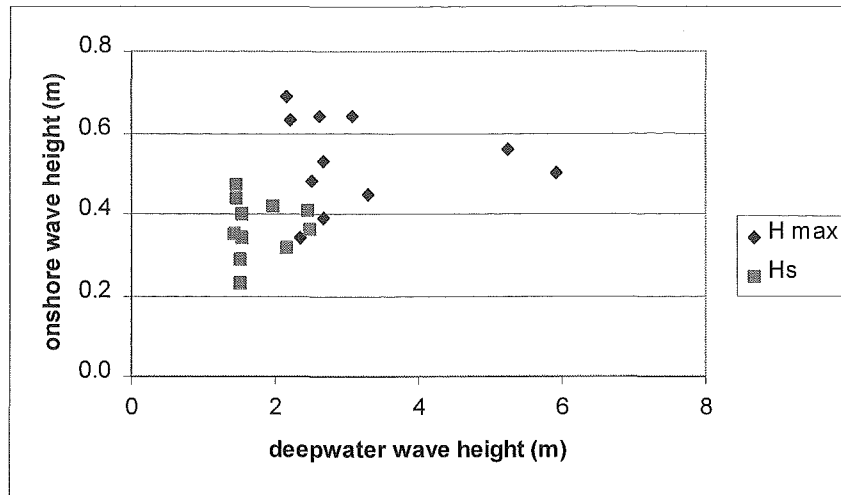


Figure 5.31: Scatter plot of deepwater wave height against onshore wave height, for simultaneous 18 minute periods. Maximum wave height and significant wave height are shown.

5.4.2.3 WAVE VELOCITY (U)

There were wide ranging differences between water particle velocities in deepwater and onshore with a maximum velocity of $5.1\text{m}\cdot\text{s}^{-1}$ occurring in deepwater while onshore velocity was $1.4\text{m}\cdot\text{s}^{-1}$. Conversely measurements of $1.1\text{m}\cdot\text{s}^{-1}$ were recorded in deepwater when onshore velocities were $1.6\text{m}\cdot\text{s}^{-1}$. Maximum velocities showed differences of between 72% decrease to 46% increase. Average velocities all decreased between 27% and 73%.

Figure 5.32 graphs deepwater particle velocity against onshore water particle velocity and shows no clear relationship between the two. This lack of relationship between deepwater velocities and on shore velocities is an important finding. Velocities of flow on the shore platform at KM3 were not directly dictated by offshore conditions.

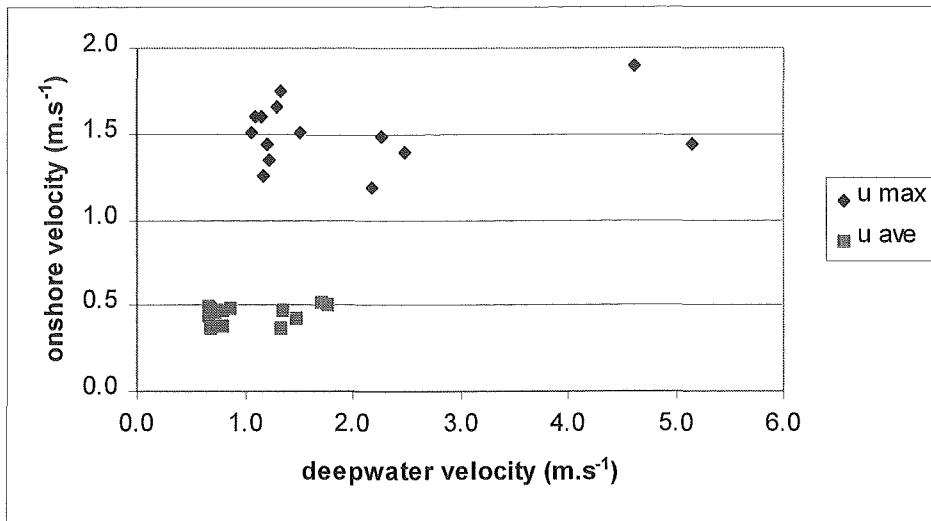


Figure 5.32: Scatter plot of deepwater particle velocity against onshore water velocity, for simultaneous 18 minute periods. Maximum water velocity and average water velocity are shown.

No direct comment upon water particle velocity in deepwater compared with the same measure onshore has been made in the coastal geomorphic literature. However, Kirk (1975b) measured onshore surf zone velocities directly using a specifically designed dynamometer and made visual observations of H_o and T_o at the same time. His measurements were conducted on steep sloping mixed sand and gravel beaches at Kaikoura, New Zealand. His data indicated increases in maximum velocities between deepwater and onshore of 55% to 900%. Smaller H_o conditions produced greater deepwater / onshore differences. Ingle (1966 *in* Kirk 1975b) measured maximum swash velocities on sand beaches in California which were up to 470% greater than the water particle velocities calculated for recorded incident deepwater wave conditions. From these two examples it can be seen that large differences in deepwater and onshore velocities have also been evident in other coastal environments.

5.4.2.4 WAVE ENERGY (E) AND WAVE ENERGY FLUX (Q)

Table 5.8 shows maximum deepwater wave energies of up to 43 191N.m⁻² and maximum average wave energies of 7 580N.m⁻² while onshore wave energy only reached a maximum of 587N.m⁻² and maximum average energy of 239N.m⁻². All

measurements showed reductions in energy between deepwater and onshore of greater than 90%. Reductions in maximum wave energy flux were all greater than 96.9% and reductions in average wave energy flux were all greater than 99%. These measures show significant reductions in energy as waves propagate from deepwater onto the shore platform.

Stephenson and Kirk (2000a) also measured reductions in wave energy flux of 91% or more. They made measurements at Kaikoura over 6 high tides using an onshore pressure sensor and an offshore non-directional wave buoy.

Figures 5.33 and 5.34 show plots of deepwater vs. onshore wave energy and energy flux respectively.

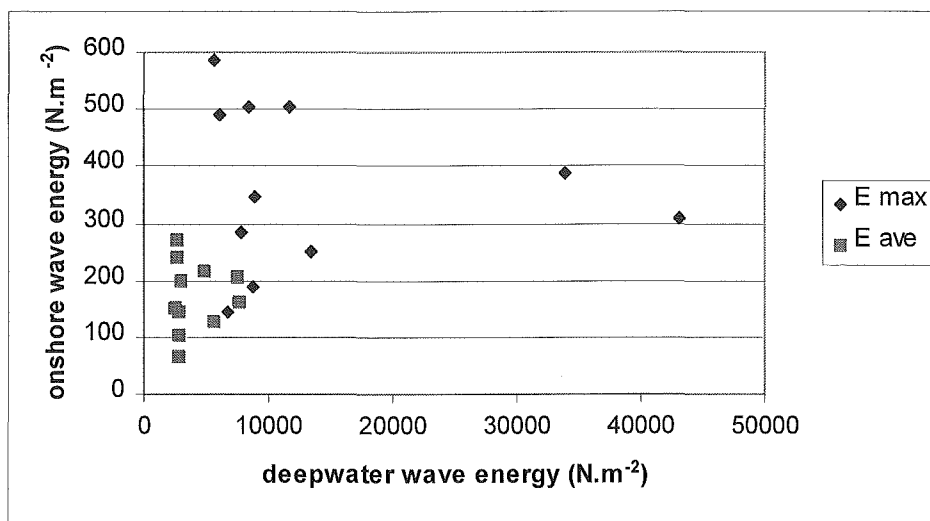


Figure 5.33: Scatter plot of deepwater wave energy against onshore wave energy, for simultaneous 18 minute periods. Maximum wave energy and significant wave energy are shown.

From figures 5.33 and 5.34 it can be seen that neither deepwater wave energy or wave energy flux correlate directly to onshore wave energy or wave energy flux. This finding questions the use of deepwater wave energy flux as an indicator of the wave assailing force on shore platforms. Section 5.1.2 outlined the frequent use of deepwater wave energy as an indication of wave assailing force on shore platforms.

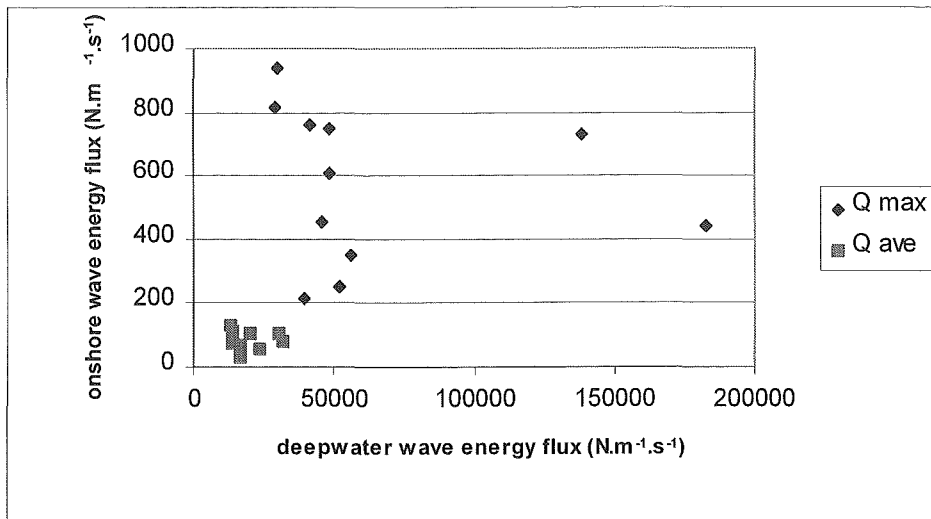


Figure 5.34: Scatter plot of deepwater wave energy flux against onshore wave energy flux, for simultaneous 18 minute periods. Maximum wave energy flux and significant wave energy flux are shown.

Accounting for the fact that there is clustering within the data, the graphs of both energy and energy flux changes (figures 5.33 and 5.34) show an interesting phenomenon. This is, that it is not necessarily the highest energy deepwater waves that deliver the highest energy to the shore platform.

To further investigate this proposal, data reporting wave energy flux changes between deepwater and on shore platform collected by Stephenson (1997a) at Kaikoura have been plotted with data from this study (figure 5.35). The inclusion of this data further emphasises the lack of a direct relationship between deepwater and on shore platform wave energy flux.

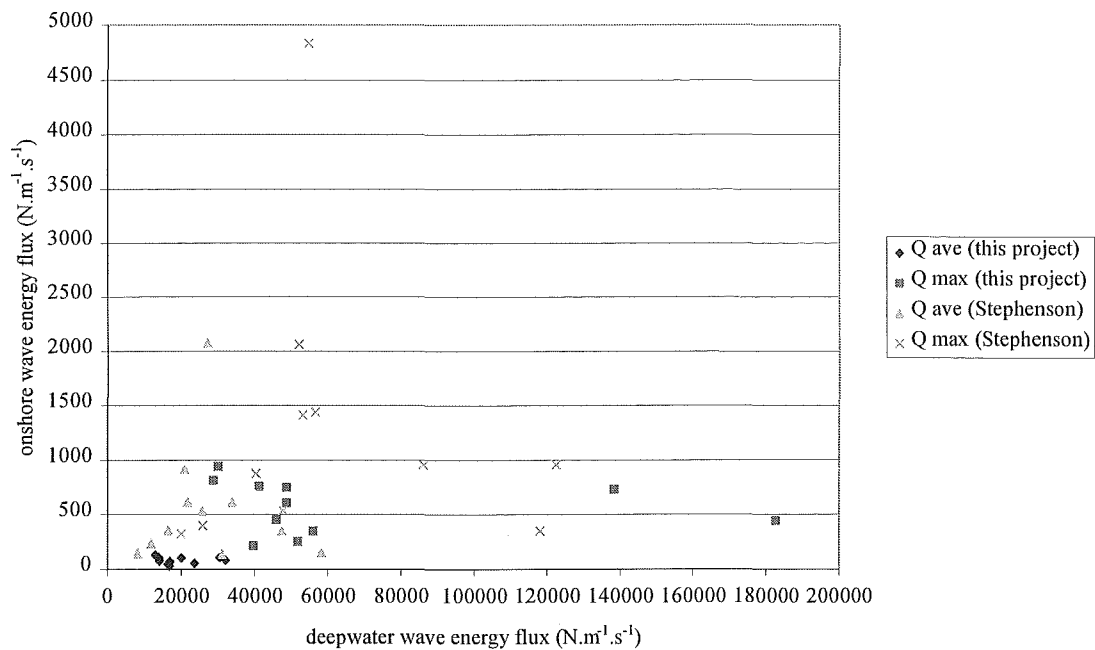


Figure 5.35: Scatter plot of deepwater wave energy flux against onshore wave energy flux which incorporates measurements from this project and from Stephenson (1997).

Table 5.8 and figures 5.31-5.35 have shown that use of deepwater wave energy for characterising onshore platform wave energy is problematic. No direct relationships were shown between measured parameters of wave height, water particle velocity, wave energy and wave energy flux in deepwater and the same parameters in shallow water.

5.4.2.5 WHERE DOES THE ENERGY GO?

It was shown in the previous section that significant energy loss occurred as waves propagated from deepwater onto the shore platform. Some dissipation of this energy is the result of wave breaking and all but the smallest waves were shown to have broken before they reached the platform (section 5.3). However, it is difficult to attribute losses of up to 99% entirely to breaking. As deepwater wave parameters are often used as surrogates for onshore wave energy it is important to investigate where energy is lost to the system.

Thompson and Vincent (1985) showed that although the range of wave sizes in a deepwater wave environment conforms to a Rayleigh distribution the same is not necessarily true for breaking waves. Treating breaking, and broken waves, as if they conform to a Rayleigh distribution may lead to erroneous results. However Thompson and Vincent (1985) show only small error in results as a consequence of this assumption so this would not explain energy loss of the magnitude reported in the previous section. There is still significant unexplained loss of energy to the system.

Assuming that energy within a system should be conserved Guza and Thornton (1982) suggested that it might be moved to different frequencies as waves approach the shore. When measuring the horizontal component of run up (swash excursion) on a sand beach in California, they found that both high and low frequency oscillations occurred. The infragravity (longer period) motions responded to offshore wave conditions where as the shorter period incident bores did not (figure 5.36).

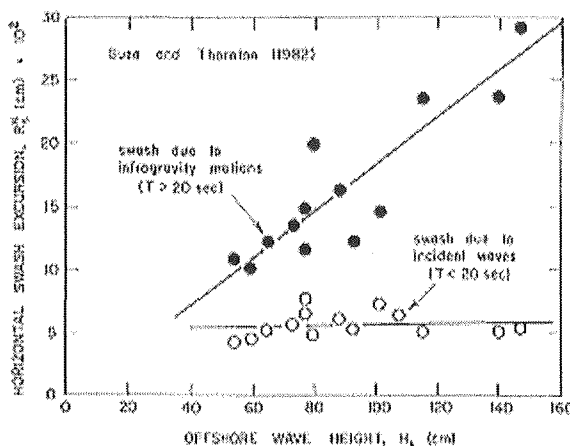


Figure 5.36: Significant swash excursions obtained from high and low frequency swash variance vs. significant wave height. (Komar 1998:fig 6-32, after Guza and Thornton 1982).

Guza and Thornton (1982) suggested that reflection and refraction of waves off the beach face created an interaction between the waves causing set up of longer period waves or infragravity motion (figure 5.37).

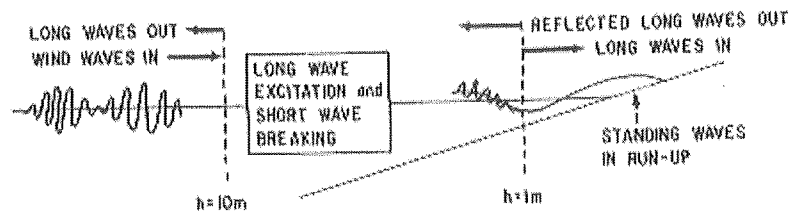


Figure 5.37: Schematic of shortwave / longwave energy transfers on a sand beach. (Guza and Thornton 1982: fig 8).

The morphology of shore platforms, especially those described by Sunamua (1992) as Type-B, presents an abrupt face to the incident waves. It is therefore feasible that the process of energy transfer to longer wave frequencies described by Guza and Thornton (1982) occurs on shore platforms. This may explain, at least in part, such high energy losses within the system.

In order to investigate this concept a comparison of deepwater and onshore spectral signatures at KM3 would have been ideal. Unfortunately collection of deepwater wave spectra was beyond the scope of this project. Lacking this, spectral analysis of onshore wave heights has been undertaken whilst three different deepwater wave conditions prevailed.

Spectral analysis breaks down a signal, in this case wave height vs. time for an 18 minute period, into constituent sinusoids of different frequencies. Spectral analysis was performed in Matlab using a fast Fourier transform algorithm. The transform was constrained using a Nyquist frequency of 4 Hz which is related to the sampling rate. Possible window effects, relating to the total length of time of sampling, were investigated by performing fast Fourier transforms on smaller subsets of data and comparing these to the spectral signatures of the full 18 minute data set. From these no change in the frequency / power distributions were evident therefore window effects can be discounted.

Figures 5.38, 5.39 and 5.40 each show two onshore wave spectra. Spectra shown in each figure were measured during a single high tide over which deepwater wave conditions were relatively consistent. Wave period in seconds is graphed against power.

Spectra for 18/08/01 (figure 5.38) both show a spread of energy across the range of wave periods with no significant peaks and relatively low overall energy. Deepwater wave conditions at 15:00 were $H_s=2.15\text{m}$ and $T=5.4\text{s}$ and at 16:00 $H_s=2.5\text{m}$ and $T=5.2\text{s}$.

Spectra for 19/08/01 (figure 5.39) show significant peaks at periods of between 13–15s as well as energy at the longer period end of the spectrum. There were relatively large overall amounts of energy. Deepwater wave conditions at 16:00 and 17:00 were $H_s=1.5\text{m}$, $T=6.2\text{s}$ and $H_s=1.6\text{m}$, $T=6.1\text{s}$ respectively.

Spectra for 24/08/01 (figure 5.40) show slightly lower peaks than those of 19/08/01. However, there was significantly more energy in the longer wave periods of both these spectra. Deepwater wave conditions at 08:00 and 09:00 were $H_s=1.5\text{m}$, $T=7.5\text{s}$ and $H_s=1.4\text{m}$, $T=7.1\text{s}$ respectively.

From figures 5.38, 5.39 and 5.40 it was evident that when there were longer period deepwater waves there were greater total onshore wave energies. When deepwater wave heights were larger the onshore wave energy was lower. This confirms the finding that use of deepwater wave parameters such as deepwater wave energy or wave height might be deceptive when attempting to quantify received onshore energy at Kaikoura. Again this emphasises the need for caution when using deepwater wave conditions to assess onshore assailing wave force.

To investigate possible changes in wave energy to longer frequency waves using figures 5.38, 5.39 and 5.40 spectral peaks of power greater than $4000\text{ N}\cdot\text{m}^3$ from each wave spectrum were measured. Figure 5.41 shows the power, in $\text{N}\cdot\text{m}^3$, plotted against peak spectra period, in seconds of each for these peaks.

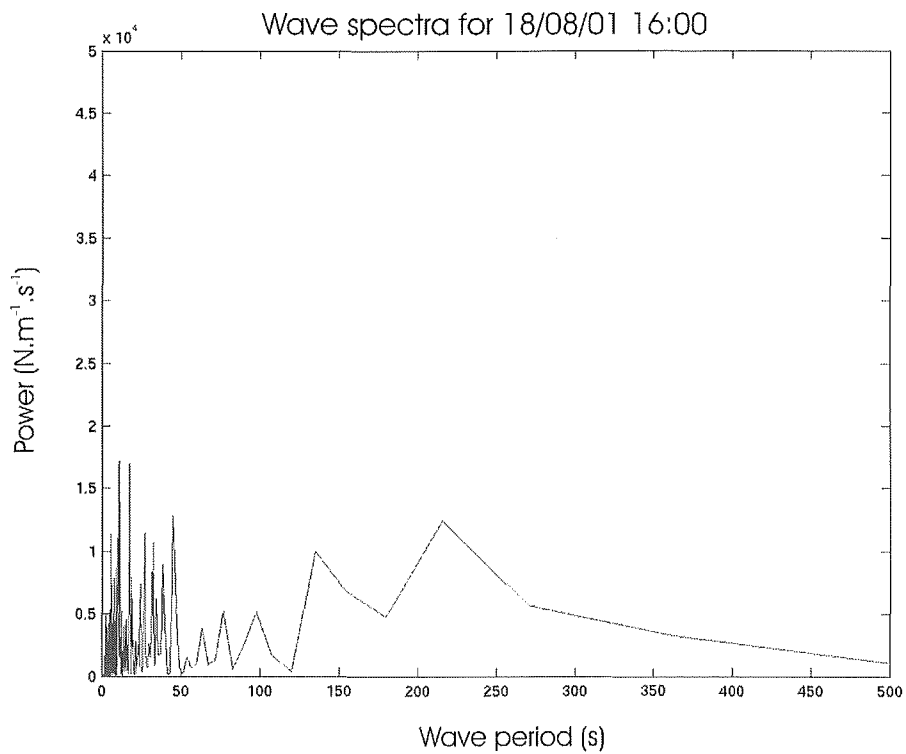
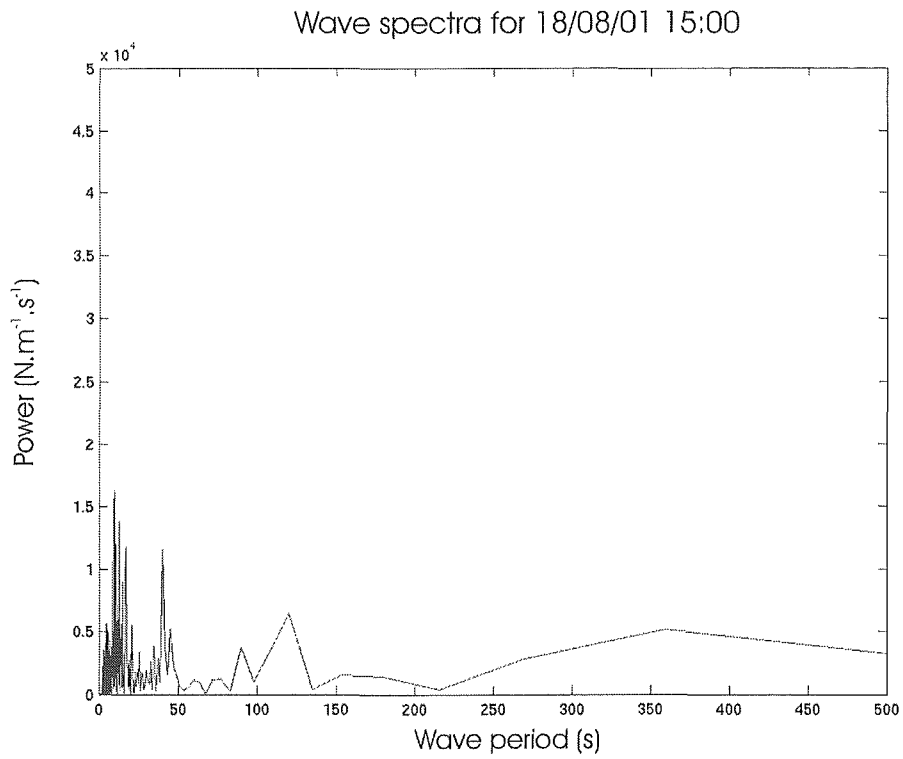


Figure 5.38: Two onshore wave spectra recorded on 18/08/01 at KM3 for 18 minutes from a. 15:00 and b. 16:00

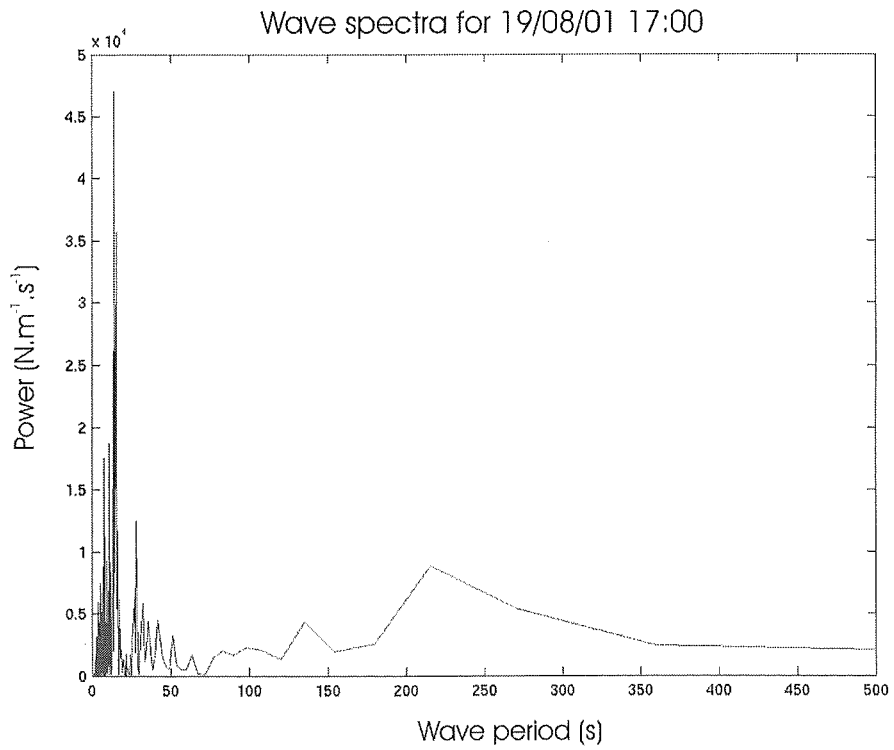
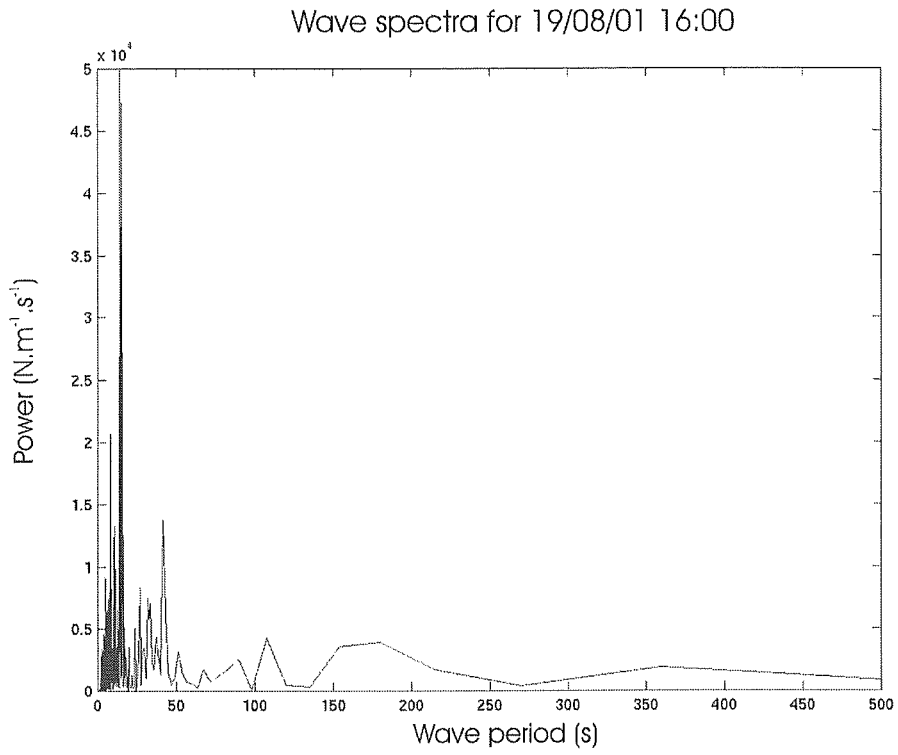


Figure 5.39: Two onshore wave spectra recorded on 19/08/01 at KM3 for 18 minutes from a. 16:00 and b. 17:00

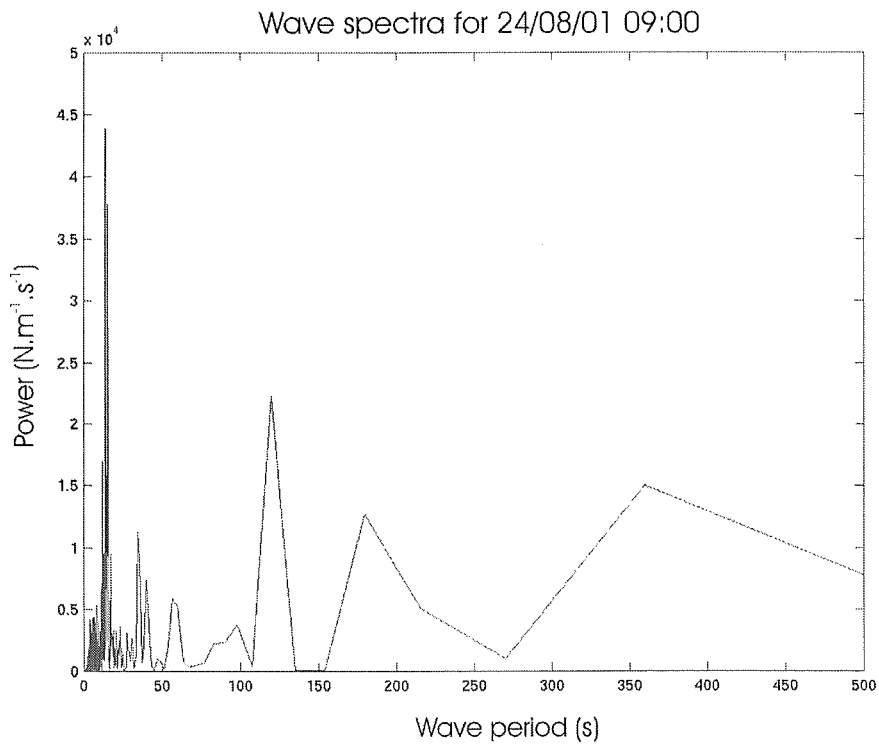
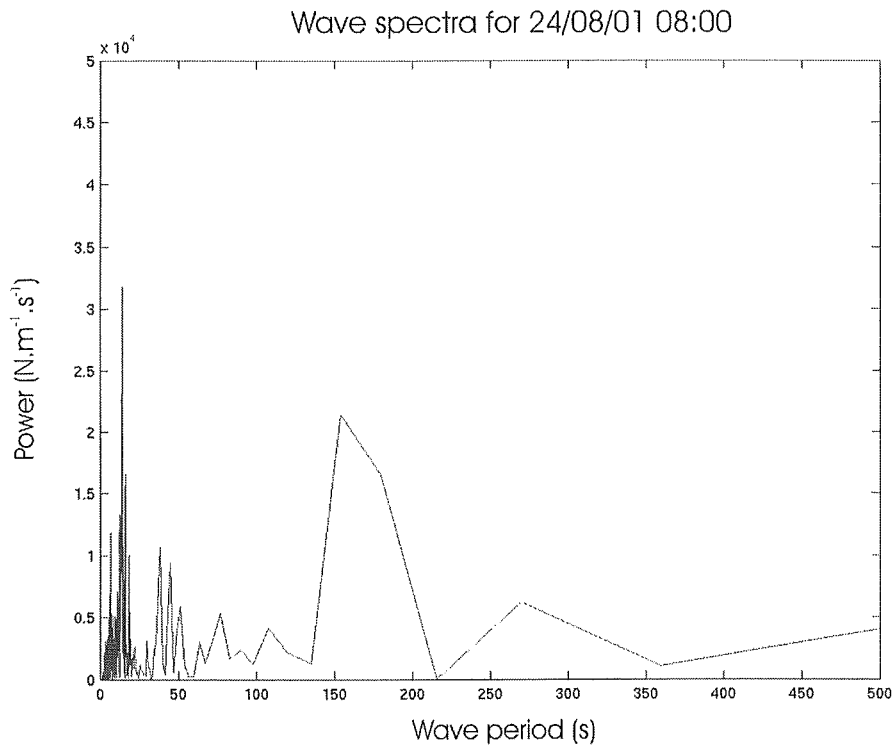


Figure 5.40: Two onshore wave spectra recorded on 24/08/01 at KM3 for 18 minutes from a. 08:00 and b. 09:00

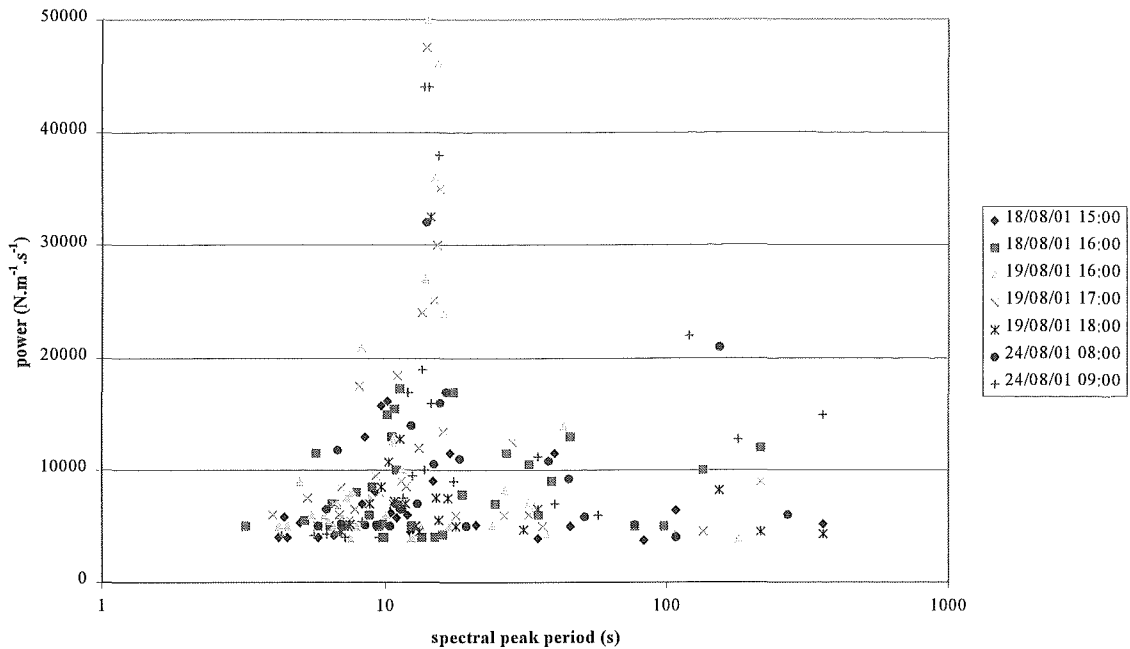


Figure 5.41: Spectral peaks for onshore measured 18 minute wave spectra. The period of each spectral peak is plotted against its power. Each 18 minute wave spectrum is shown using a different symbol. Note logarithmic scale on x axis.

Figure 5.41 shows that almost all spectral peaks occurred at higher periods than the corresponding deepwater T_0 of the same time. A significant number of the spectra had maximum peaks at or very close to $T=14s$. Other noticeable clusterings of peaks occurred at the longer period end of the spectra at $T=216s$ (3.6 minutes) and $T=360s$ (6 minutes). The dominant 14 s peak may be related to the groupiness of the wave trains. Deepwater wave spectra would be required to explore this hypothesis more fully.

The longer period oscillations noted in figure 5.41 may be an indication of harmonic wave forms established in relation to the incident wave conditions and the shape of the platform itself. The existence of longer period waves in the onshore platform record supports the possibility that wave energy may be transferred from short period incident waves to longer period infragravity waves.

Figure 5.42 was constructed to further investigate this possibility of an energy shift from short period sea state wave motions to longer infragravity period wave motions related to the incident wave conditions, as is characteristic of sand beaches. This shows

deepwater wave height plotted against the highest spectral peak either side of $T=20$ s for each spectra. It is modelled on the relationship shown in figure 5.36 established for sand beaches where infragravity waves increase in size as H_o increases.

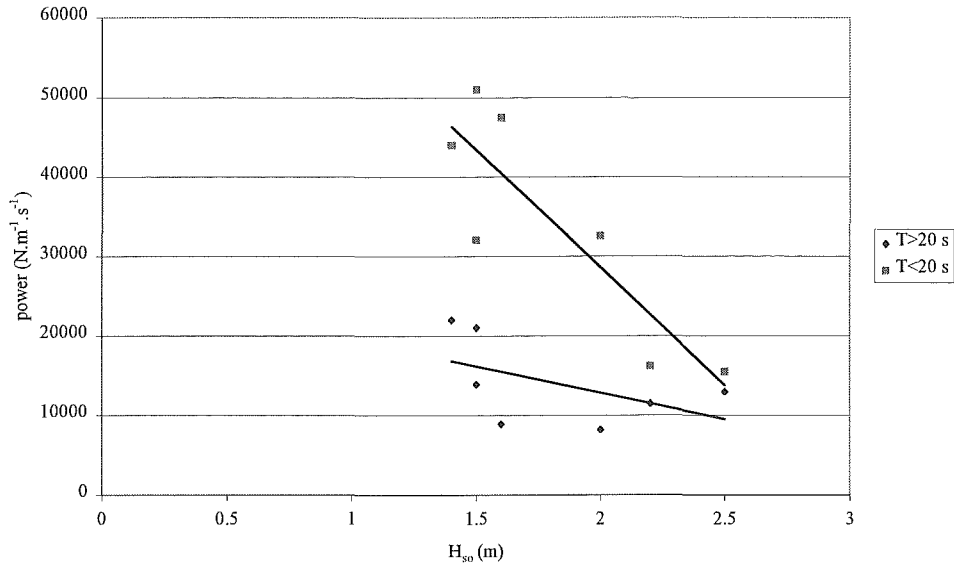


Figure 5.42: Deepwater significant wave height vs. spectral peak power for the highest peaks either side of $T=20$ s from wave spectra for 18 minute onshore wave data.

Infragravity motions (those longer than $T=20$) were evident in these data. However, there was very little direct relationship between these and deepwater wave height. For wave periods shorter than 20s a strong inverse relationship ($r = 0.87$) was evident between deepwater H_s and spectral peak power as an indication of dominant onshore platform wave frequency. Frequencies in patterns of flow on the shore platform (KM3) appear to be driven, in some way, at the time scale of incident waves. Interactions of water masses setting up infragravity waves appear to have a secondary effect on flow over the shore platform.

There was measurement of some movement of energy to higher frequency motions. However, the question of how much was not answered here due to the lack of deepwater spectral data.

5.4.3 WAVE INDUCED WATER FLOW ACROSS KM3

This section describes flow across the shore platform at KM3 measured during the August 2001 field period. An empirical statistical approach has been adopted rather than the theoretical one used in many shore platform studies. Flow velocities were recorded by sensors 1, 2 and 3 spaced across the profile of the shore platform at KM3 (figure 5.24). Data collection methods were described in section 5.4.1. The maximum water velocity recorded on the platform was 2.54 m.s^{-1} with average velocities for each 18 minute period ranging from 0.72 m.s^{-1} to 0.22 m.s^{-1} . A strong lateral component in direction of flow was evident and water movement across the platform was generally observed to be in the form of bores.

It was shown in section 5.3 that all but the smallest waves break before they reach the shore platform at KM3. Once waves have broken they propagate forward essentially as a bore. Denny (1988:91) states ‘regardless of the manner in which a wave breaks, the shape of the broken wave resembles that of a turbulent bore’. A bore is a turbulent body of water that occurs where there is an abrupt change in the level of water (figure 5.43).

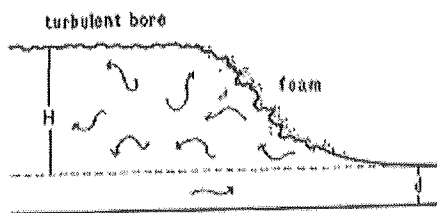


Figure 5.43: A turbulent bore (Denny 1988:fig 7.5a)

The bore itself is highly turbulent and its front face is steep and foaming with white water. The back slope of the bore is gradual and similar to that of a solitary wave. This is the typical type of wave that was visually observed crossing the study profiles.

“The present understanding of wave breaking process is such that there is simply no adequate substitution for empirical observations at each particular site” (Denny

1988:91). Thorough empirical observation of wave action on shore platforms has not been reported in the literature to date. For this reason the present section is a description of empirical observations made as waves crossed the shore platform at KM3.

Figure 5.44 gives a pictorial representation of the flow fields at each sensor over an 18 minute period on 18/08/01 beginning at 14:00. A time series for each sensor is shown where vectors represent the amplitude and direction of water flow of each consecutive measurement. Time series recorded simultaneously by each sensor are shown. Only one representative 18 minute period has been presented in order to give a visual impression of flows. Flow, in the horizontal plane at sensor 1 appeared highly turbulent but with a distinct rhythmic pattern. Flow at sensor 2 appeared less turbulent and more coherent, and was of slightly greater magnitude than at sensor 1. It was also rhythmic in nature. Flow at sensor 3 appeared reduced in magnitude but still reasonably coherent and distinctly rhythmic.

Measurements at sensor 1 showed comparatively dramatic variation in the direction of flow. Some of this may be accounted for by the fact that sensor 1 (the Vector) sampled at a higher rate allowing for greater resolution in the signal. It is also more sensitive to air bubbles in the flow which may cause noise in the signal. However, measurements of flow by the two different types of instrument have been shown to be comparable (section 5.4.1.3) and noise was accounted for by use of a processing filter (section 5.4.1.5). The dramatic variation recorded is therefore not considered to be spurious.

5.4.3.1 FLOW VELOCITY

Figure 5.45 shows bar graphs of average velocities measured at each sensor for each 18 minute period over three tidal cycles. Maximum recorded velocities are also included. Average flow velocity ranged from $0.72\text{m}\cdot\text{s}^{-1}$ to $0.22\text{m}\cdot\text{s}^{-1}$. Average flow velocities were always greatest at sensor 2 and least at sensor 3. This pattern persisted under varied deepwater wave conditions, which occurred on each different day (table 5.8). The same pattern occurred for maximum velocities with greatest velocities always recorded at sensor 2. The maximum velocity recorded during the study period was $2.54\text{m}\cdot\text{s}^{-1}$.

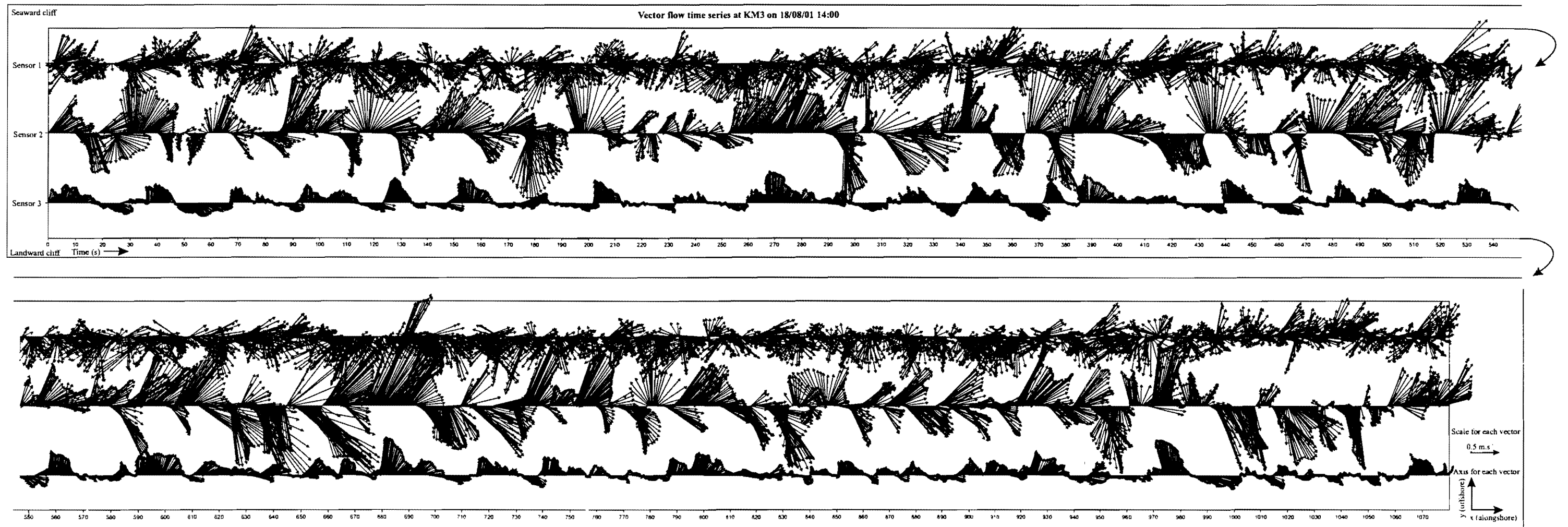


Figure 5.44: Time series of flows recorded simultaneously at sensors 1, 2 and 3 on KM3, on 18/08/01 between 14:00 and 14:18. Separate vectors are shown for each measurement. Sampling rate at sensor 1 was 8Hz and at sensors 2 and 3 was 5Hz. Magnitude of flow is proportional to vector length and direction of flow is represented by the direction of the vector where the diagram is in plan view and the x-y plane is shown.

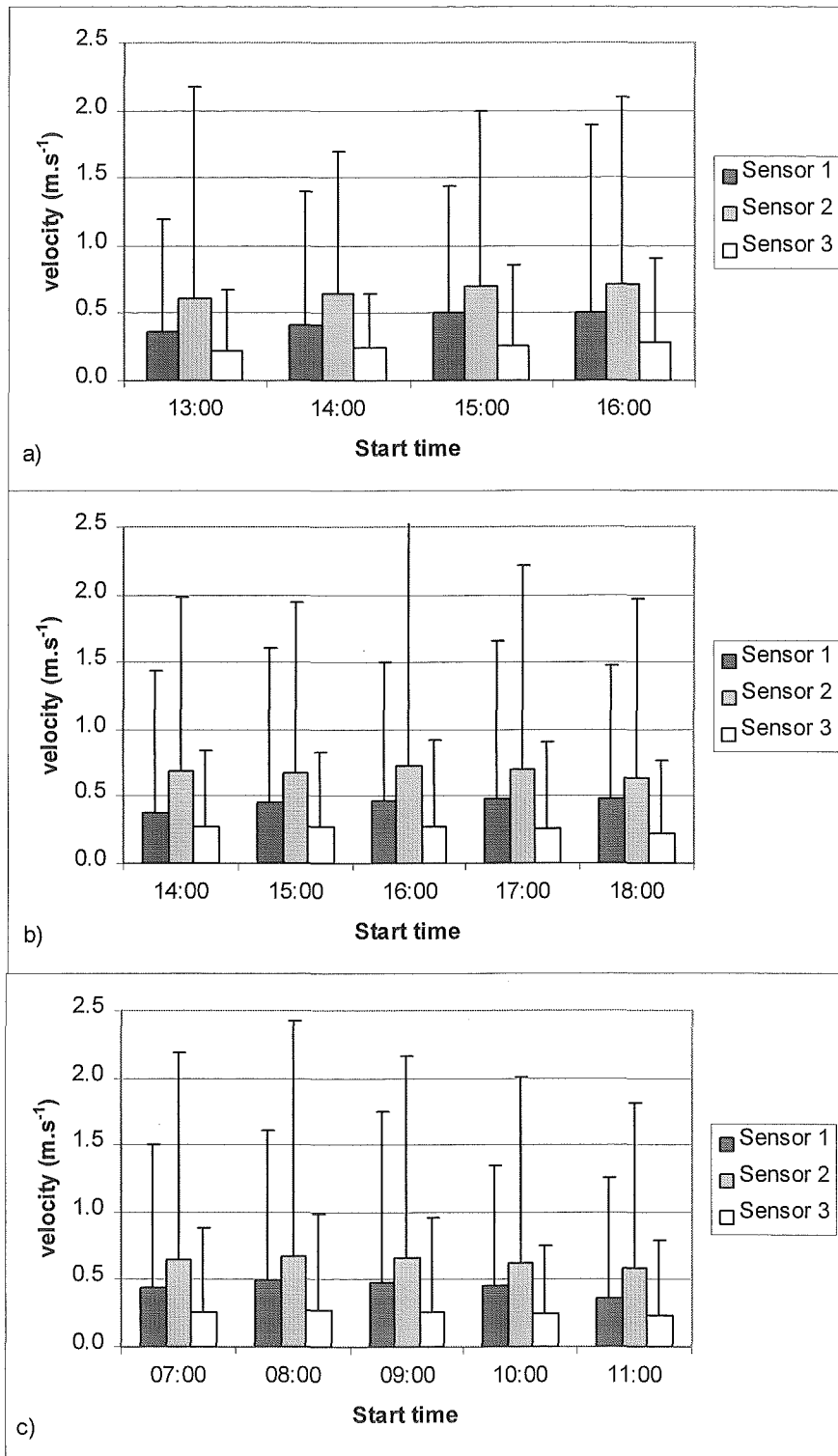


Figure 5.45: Average and maximum velocities measured by each sensor over 18 minute sampling periods at KM3 over three tidal cycles on a). 18/08/01, b). 19/08/01 and c). 24/08/01. The start time of each 18 minute sampling period is given.

Figure 5.45 shows that average flows were always significantly faster at sensor 2, in the centre of the platform, than at either sensor 1 on the seaward edge of the platform or at sensor 3 nearer the landward cliff.

Models of shore platform development assume that energy is dissipated at a constant rate as waves shoal across a platform (Johnson 1919, Sunamura 1992). Intuitively, it is expected that energy levels and hence the assailing force of the wave reduces the further the wave travels across the platform and wave energy is often used as an indication of the amount of ‘work’ (or erosion) a wave is capable of on a shore platform (Tsujiimoto 1987, Sunamura 1992).

From equation 5.8 the velocity of a wave in shallow water is directly related to the energy associated with that wave where

$$u^2 = gH \qquad \text{Equation 5.10}$$

Therefore the spatial variation in velocity measured at KM3 would suggest that the concept of a constant rate of energy dissipation across shore platforms does not necessarily hold. Velocities at sensor 2 in the centre of the platform were on average 0.21m.s^{-1} faster than those at sensor 1 on the seaward edge. By the time waves reached sensor 2 they had travelled 16.8 m further across the platform and yet higher velocities were recorded here. This variation in velocity has implications in terms of spatial variation of erosion by the waves and also in terms of patterns of sediment movement across the platform.

Average velocity at each sensor showed little variation either over the course of a tidal cycle or under differing deepwater wave conditions (figure 5.45). To show this more clearly figure 5.46 was constructed plotting average water depth at the time of flow measurement against average velocity. This shows that only very slight increases in velocity were recorded as water level changed through tidal oscillations. Flow velocities at sensor 1 are seen to be most closely linked to water level however this linkage is not

great. Once the platform was covered by the tide, flow velocities did not change greatly as a result of changes in water level.

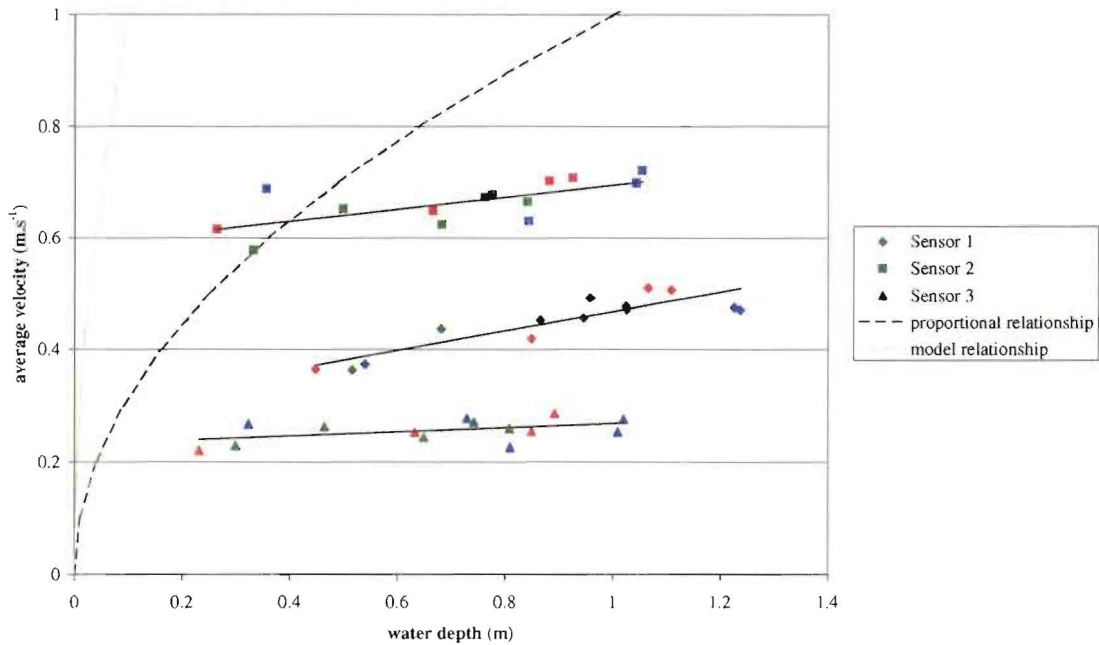


Figure 5.46: Average water depth vs. average velocity at each sensor during different stages of the tide while the water covered the shore platform. Recorded at KM3 on 18/08/01 (red symbols), 19/08/01 (blue symbols) and 24/08/01 (green symbols). The black dashed line shows the relationship $u^2 \propto d$. The grey dashed line shows the model relationship $u = \sqrt{gd}$.

It is also evident from figure 5.46 that at each sensor only a small range of velocities were recorded over the entire field period, despite varied deepwater wave conditions which ranged from $H_{s0} = 2.5\text{m}$ to 1.4m . Velocities at sensor 1 showed greatest variation with a standard deviation of 0.05 m.s^{-1} . At sensor 2 standard deviation was 0.04 m.s^{-1} and at sensor 3 standard deviation was 0.02m.s^{-1} .

Equation 5.10 gives a shallow water approximation for wave velocity derived from linear theory. The velocity under the wave is expected to be depth controlled. In very shallow water H can essentially be regarded as water depth. Therefore, the model relationship between water depth and velocity is $u = \sqrt{gd}$, from equation 5.10. This relationship is shown on figure 5.46 as a grey dashed line. Also included in figure 5.46 is the proportional relationship between velocity and water depth where $u^2 \propto d$ (black

dashed line). The velocities measured on the platform differ significantly from the anticipated model velocities.

These results suggest that flow velocities on the shore platform are not controlled by factors such as deepwater wave conditions or water depth on the platform but perhaps by the morphology of the platform itself. More extensive measurement over a greater range of deepwater wave conditions would be required to verify this hypothesis.

5.4.3.2 FLOW DIRECTION

As velocities shown in figure 5.45 are average magnitudes no indication of direction is given. The strength of flow in different directions is an important consideration when describing a flow regime. It helps to define where work will be directed. This section describes spatial patterns of flow measured at KM3.

Figure 5.47 shows average velocity of flows in the offshore, alongshore to the south, onshore and alongshore to the north directions. Each bar represents the average flow through a 90 degree wedge centred on that direction.

Average flows from each of the four directions were similar at sensors 1 and 3. Generally at sensor 2 onshore/offshore flow dominated. However, there was still a distinct lateral component to flow.

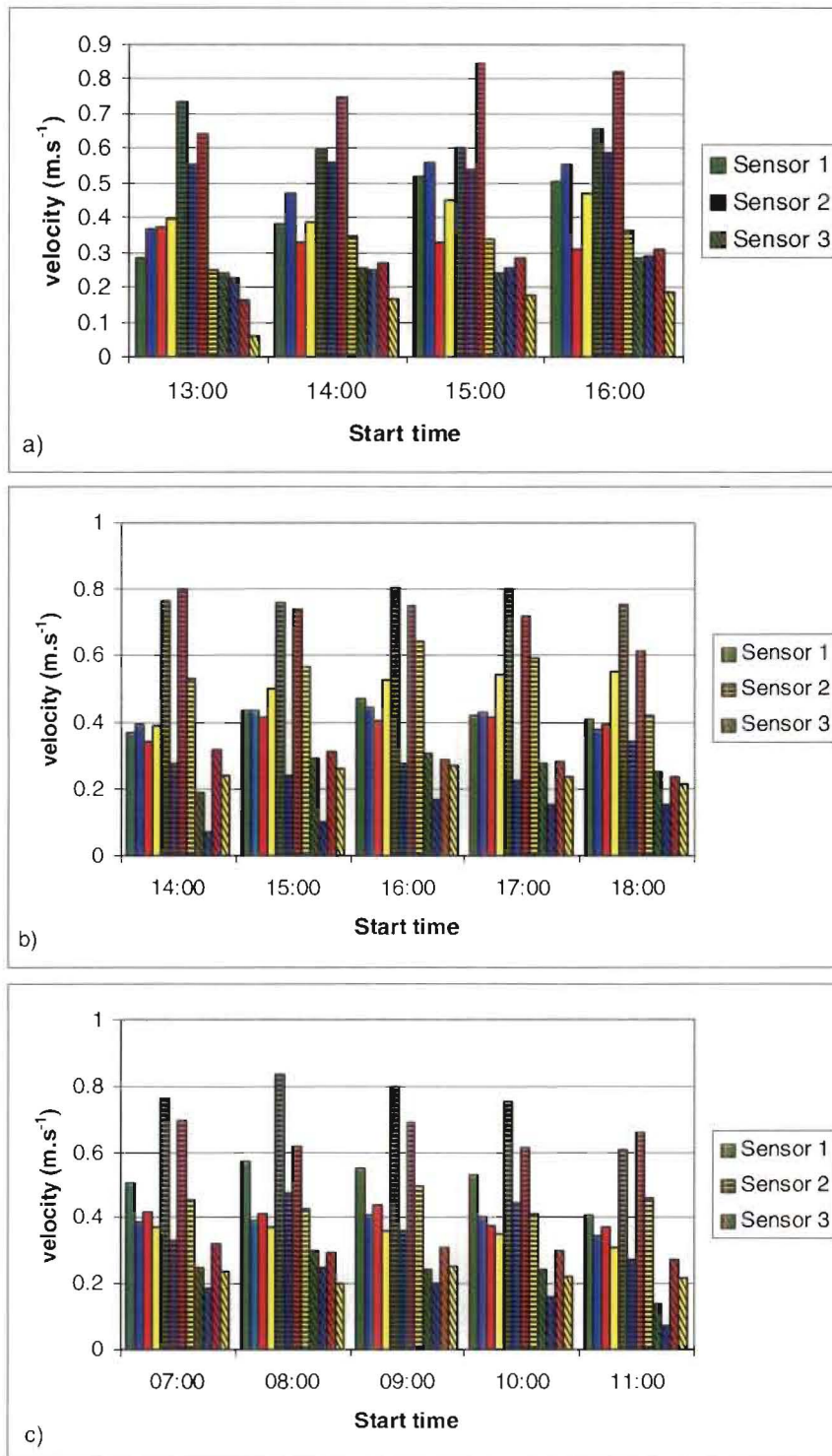


Figure 5.47: Bar graphs of average flow at KM3 in the offshore (green), alongshore to the south (blue), onshore (red), and alongshore to the north (yellow) directions. Flows through a 90° wedge centred on the given direction were averaged for each 18 minute period measured on a). 18/08/01, b). 19/08/01 and c). 24/08/01. The start time of each 18 minute period is given.

To further investigate directions of flow on the shore platform at KM3 vector summation diagrams of average velocity at each sensor over each 18 minute period were constructed (figure 5.48, 5.49 and 5.50). Flow measurements were categorised into eight different groups based on direction of flow. Average velocities of flow from each direction were calculated. Vectors representing these average velocities were summed and resultant vectors are shown. Resultant flow vectors show direction and magnitude of general flow at each location. Magnitudes of resultant general flow velocities ranged from 0.7 m.s^{-1} to 0.01 m.s^{-1} and almost all were directed alongshore showing considerable lateral component to flow on the shore platform at KM3. This lateral component of flow was especially evident at sensor 2 and appeared to be dependent on deepwater wave direction.

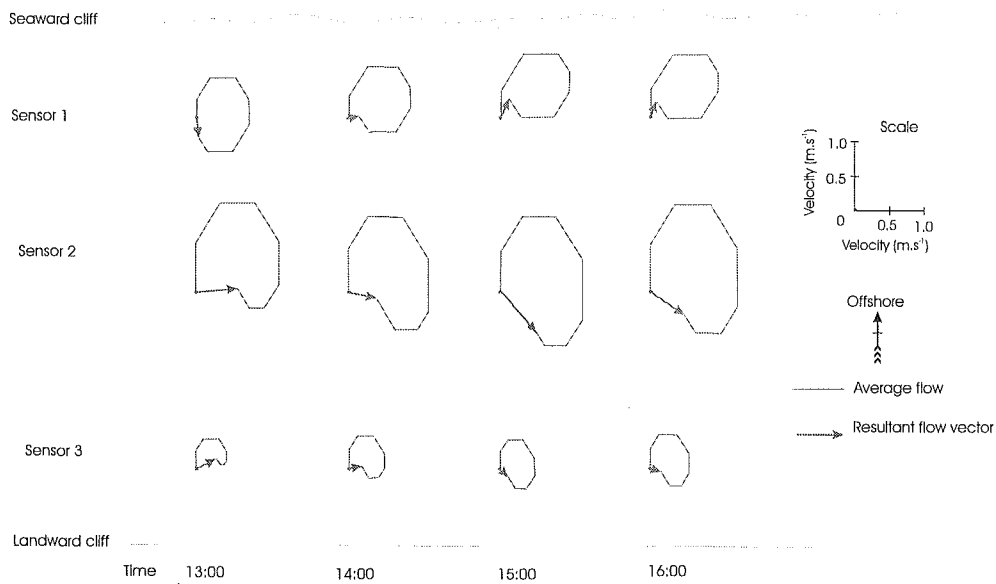


Figure 5.48: Vector flow summations of average velocities measured on 18/08/01. For each 18 minute run average flow velocity in 8 separate component directions is shown. Vectors representing flow in each component direction have been summed and the resultant flow vector is shown. A schematic plan view has been used to show vector summations for each sensor at given times. All measurements were taken when the tides allowed water to cover the platform.

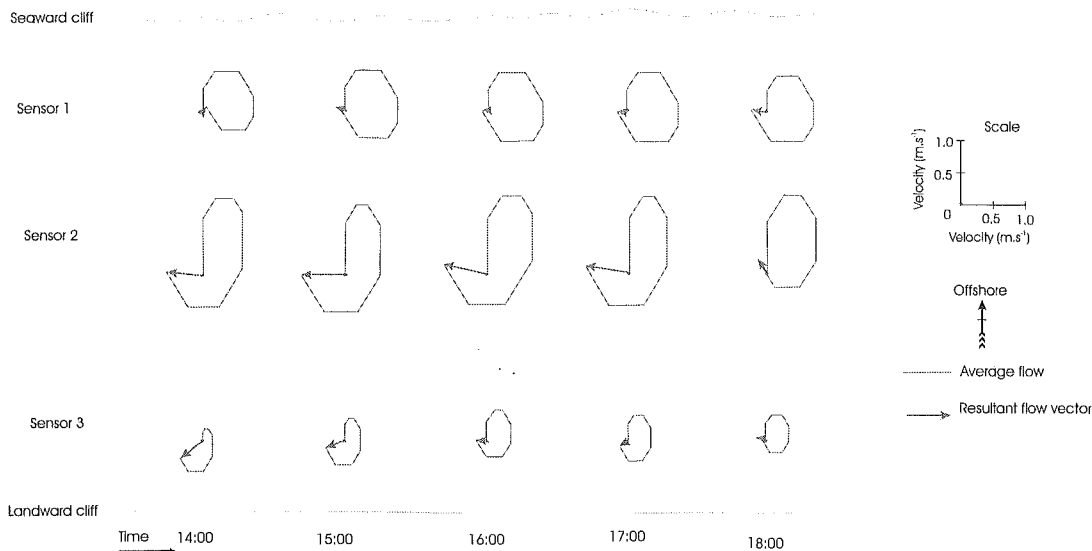


Figure 5.49: Vector flow summations of average velocities measured on 19/08/01. For each 18 minute run average flow velocity in 8 separate component directions is shown. Vectors representing flow in each component direction have been summed and the resultant flow vector is shown. A schematic plan view has been used to show vector summations for each sensor at given times. All measurements were taken when the tides allowed water the cover the platform.

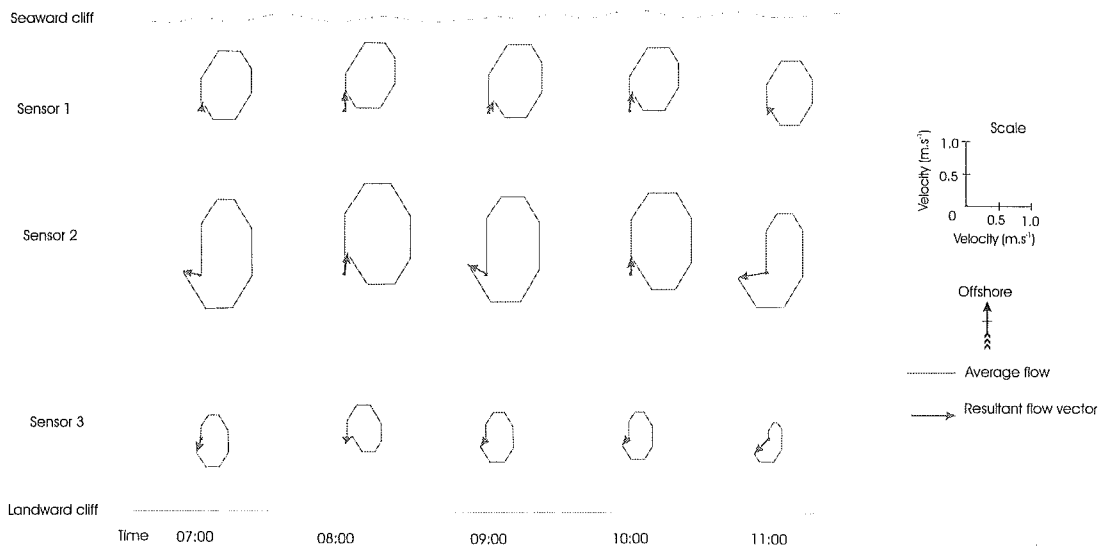


Figure 5.50: Vector flow summations of average velocities measured on 24/08/01. For each 18 minute run average flow velocity in 8 separate component directions is shown. Vectors representing flow in each component direction have been summed and the resultant flow vector is shown. A schematic plan view has been used to show vector summations for each sensor at given times. All measurements were taken when the tides allowed water the cover the platform.

Lateral flows along the shore platform at KM3 were of significant size when compared to total average flows and occurred, to a varying degree across the entire platform profile.

Gaylord (1999) also documented a strong lateral component to flow over shore platforms. He measured flows at single locations on four separate platforms in California.

Strong lateral components of flow evident at KM3 (figures 5.48, 5.49 and 5.50) show that flows do not only occur in a bimodal onshore / offshore pattern. This is an important finding as it means that weaknesses in the rocks are subjected to forces from a wide range of directions. This has implications for the way rocks may be broken apart and the influence of bedding planes and layers of weakness on development of shore platform morphology.

Trenhaile (1999) gave a hierarchy of shore platform susceptibility to erosion based on orientation of bedding planes and layers of weakness in relation to wave attack (figure 4.8). From this relative rate of development and morphological parameters of width were modelled (section 4.4). It was assumed that waves were perfectly refracted and implicitly implied that wave action was orientated in an onshore/offshore direction (Trenhaile 1999). Figures 5.47 –5.50 have shown that under varying angles of wave approach there are strong lateral components of wave induced flow across the platform at KM3. Therefore, wave assailing force is directed in more than just the onshore/offshore direction. Lateral flow therefore needs to be considered when assessing the assailing force of waves on shore platforms.

5.4.3.3 TURBULENCE

Turbulence is an important aspect of flow induced by the passage of bores. This section describes the type and magnitude of turbulence measured at KM3.

Turbulence is the random chaotic motion of water flow and is usually expressed in terms of the degree of randomness of flow around a mean velocity (Denny 1988). It includes rapid variability of flow in both direction and intensity (Thais and Magnaudet 1996). The structure of turbulent flow in shallow water is complex and can be detected at various different scales, often referred to as eddies. The amount and scale of turbulence depends on; the viscosity of the fluid, the nature and scale of the initial disturbance and the texture of the surface over which the flow is occurring. Turbulence at a scale less than the water depth, can be the result of bottom friction as water flows across a surface, wind shear at the water surface and wave breaking. Turbulence can also appear as large scale horizontal eddies influenced by bottom cover (Nadaoka and Yagi 1998). In an oceanic environment the nature, magnitude and scale of the turbulence also depends on the type of wave and the way it breaks (Denny 1989). Turbulence can create both lift and drag forces on a surface, enable aeration of the wave and cause dissipation of wave energy hence acting to slow wave propagation (Denny 1989). Effects of turbulence on the platform surface and on sediment movement will be discussed in Chapter 6.

A number of models have been developed to describe turbulence including eddy viscosity and mixing length layers (Nowell and Church 1979). However much of the work that has been undertaken on turbulence in water flow has been developed with the unidirectional flow of rivers in mind and wave-turbulence interactions have received little attention (Thais and Magnaudet 1996).

In fluid mechanics flow is described according to its uniformity and steadiness. Uniformity of flow relates to the flow direction and steadiness to the speed. A completely non-turbulent flow would be one that is of both uniform and steady state. Turbulence therefore is the deviation of flow from this state. As turbulence is essentially random, indications of turbulent intensity have been made using normal error statistics in order to define variation around a mean flow. Where \bar{u} is the mean stream wise flow velocity and u' is the fluctuation from the mean flow such that velocity at any given time $u(t) = \bar{u} + u'$. The root mean square (RMS) of u' (which is also the standard deviation of u) is then used to indicate the degree of intensity of fluctuations around a

stream-wise flow. Turbulence in each of the three dimensions can be calculated in the same manner.

There are obvious drawbacks to using a measure of turbulence related to stream-wise flow on a shore platform environment where underlying flow is, at the very least, bimodal, as the waves flow in and out and often includes a significant component of lateral flow as shown in section 5.4.3.2. Another measure used to describe turbulence is that of turbulent kinetic energy. This is calculated using equation 5.10 (Thais and Magnaudet 1996).

$$k_i = \frac{1}{2} \left(\overline{u'^2} + \overline{v'^2} + \overline{w'^2} \right) \quad \text{Equation 5.10}$$

However, field studies tend not to refer to turbulent kinetic energy due to the difficulty in differentiating the energy of the wave related motion from the energy of the turbulence. Often an estimate of the rate of energy dissipation caused by turbulence (ϵ) gained from velocity spectra is used in preference to turbulent kinetic energy (MacKenzie and Kiorboe 1995). However significant discrepancies appear amongst available ϵ_t estimates (Thais and Magnaudet 1996).

Although RMS measures of u' have drawbacks they do give a value with which to comparatively assess the magnitude of turbulence within the measured shore platform flows and are therefore used here. The remainder of this section presents measurements of turbulence made at KM3 during the August 2001 field period. Measures of the deviation from both steadiness and uniformity of flow are given.

Turbulence measured at KM3 with respect to the steadiness of the flow is presented in Table 5.9. Both the variation of flow in the onshore/offshore direction ($\sqrt{\overline{u'^2}}$) and in the horizontal plane (onshore/offshore and alongshore) ($\sqrt{\overline{u'^2 + v'^2}}$) are given.

Table 5.9: Turbulence measured at each sensor over 18 minute periods in relation to the changes in magnitude of the stream-wise flow ($\sqrt{u'^2}$) and changes in magnitude of the flow in the horizontal plane ($\sqrt{u'^2 + v'^2}$). Also shown, for comparison, are average flow velocities.

| Date and start time of 18 minute recording | Sensor 1 | | | Sensor 2 | | | Sensor 3 | | |
|--|---------------------------------------|---------------------------------------|---------------------------------------|---------------------------------------|---------------------------------------|---------------------------------------|---------------------------------------|---------------------------------------|---------------------------------------|
| | onshore/offshore (m.s ⁻¹) | horizontal plane (m.s ⁻¹) | Average velocity (m.s ⁻¹) | onshore/offshore (m.s ⁻¹) | horizontal plane (m.s ⁻¹) | Average velocity (m.s ⁻¹) | onshore/offshore (m.s ⁻¹) | horizontal plane (m.s ⁻¹) | Average velocity (m.s ⁻¹) |
| 18/08/01 13:00 | 0.24 | 0.39 | 0.36 | 0.53 | 0.60 | 0.61 | 0.16 | 0.20 | 0.22 |
| 18/08/01 14:00 | 0.25 | 0.43 | 0.42 | 0.54 | 0.61 | 0.65 | 0.20 | 0.24 | 0.25 |
| 18/08/01 15:00 | 0.30 | 0.49 | 0.51 | 0.59 | 0.66 | 0.70 | 0.21 | 0.27 | 0.25 |
| 18/08/01 16:00 | 0.30 | 0.49 | 0.51 | 0.62 | 0.69 | 0.71 | 0.24 | 0.29 | 0.29 |
| 19/08/01 14:00 | 0.27 | 0.42 | 0.38 | 0.66 | 0.70 | 0.69 | 0.21 | 0.25 | 0.27 |
| 19/08/01 15:00 | 0.32 | 0.48 | 0.46 | 0.63 | 0.69 | 0.67 | 0.23 | 0.26 | 0.28 |
| 19/08/01 16:00 | 0.31 | 0.49 | 0.47 | 0.67 | 0.75 | 0.72 | 0.24 | 0.29 | 0.28 |
| 19/08/01 17:00 | 0.31 | 0.49 | 0.48 | 0.66 | 0.73 | 0.70 | 0.23 | 0.27 | 0.25 |
| 19/08/01 18:00 | 0.29 | 0.46 | 0.47 | 0.63 | 0.68 | 0.63 | 0.22 | 0.25 | 0.23 |
| 24/08/01 07:00 | 0.37 | 0.47 | 0.44 | 0.69 | 0.75 | 0.65 | 0.23 | 0.28 | 0.26 |
| 24/08/01 08:00 | 0.40 | 0.49 | 0.49 | 0.69 | 0.76 | 0.68 | 0.24 | 0.30 | 0.27 |
| 24/08/01 09:00 | 0.41 | 0.50 | 0.48 | 0.68 | 0.74 | 0.67 | 0.23 | 0.28 | 0.26 |
| 24/08/01 10:00 | 0.37 | 0.46 | 0.45 | 0.64 | 0.70 | 0.62 | 0.23 | 0.27 | 0.24 |
| 24/08/01 11:00 | 0.32 | 0.40 | 0.36 | 0.58 | 0.63 | 0.58 | 0.18 | 0.22 | 0.23 |

Average magnitudes of turbulence in stream-wise flow were between 0.16 m.s^{-1} and 0.69 m.s^{-1} . Accounting for flow directions from the entire horizontal plane total turbulent variations of between 0.20 m.s^{-1} and 0.76 m.s^{-1} were measured. The scale of the turbulence measured is large when compared to average flow velocities (table 5.9). Magnitudes of erratic flow velocities caused by turbulence were between 92% and 112% of the average flow velocity.

Measures of turbulence made in relation to uniformity of flow at KM3 are presented in table 5.10. To give an impression of the rapidity with which flow changed direction, the average time it took for the flow to change direction by greater than 45 degrees in either a clockwise or anticlockwise direction was identified. Table 5.10 shows the average amount of time (in seconds) for flow to change more than $\pm 45^\circ$ for each 18 minute measurement period. The amount of variation from this mean time is also given in terms of a standard deviation.

Table 5.10: Measures of turbulence related to uniformity of flow measured at each sensor over 18 minute periods. Average times for flow to change direction $\pm 45^\circ$ and standard deviation of this measure are given. Times are given in seconds.

| Date and start time of 18 minute recording | Sensor 1 | | Sensor 2 | | Sensor 3 | |
|--|--|---------------------------|--|---------------------------|---|---------------------------|
| | average time for direction change (s) | standard deviation (s) | average time for direction change (s) | standard deviation (s) | average time for direction change (s) | standard deviation (s) |
| 18/08/01 13:00 | 1.1 | 1.0 | 4.6 | 4.1 | 6.4 | 6.2 |
| 18/08/01 14:00 | 1.4 | 1.6 | 4.1 | 4.0 | 3.9 | 3.5 |
| 18/08/01 15:00 | 1.7 | 1.8 | 3.3 | 2.9 | 3.0 | 2.7 |
| 18/08/01 16:00 | 1.9 | 2.2 | 3.4 | 3.2 | 3.3 | 2.7 |
| 19/08/01 14:00 | 1.1 | 1.1 | 8.7 | 7.1 | 10.9 | 8.8 |
| 19/08/01 15:00 | 1.6 | 1.7 | 3.6 | 3.0 | 4.1 | 3.3 |
| 19/08/01 16:00 | 1.6 | 1.7 | 3.2 | 2.9 | 3.6 | 3.2 |
| 19/08/01 17:00 | 1.7 | 1.7 | 3.1 | 2.3 | 3.2 | 2.6 |
| 19/08/01 18:00 | 1.7 | 1.8 | 3.3 | 2.7 | 3.1 | 2.6 |
| 24/08/01 07:00 | 1.5 | 1.6 | 4.2 | 3.7 | 4.4 | 3.5 |
| 24/08/01 08:00 | 1.8 | 2.0 | 4.1 | 4.0 | 3.4 | 2.9 |
| 24/08/01 09:00 | 1.7 | 1.9 | 3.2 | 2.5 | 3.4 | 2.7 |
| 24/08/01 10:00 | 1.6 | 1.8 | 3.5 | 2.9 | 3.7 | 3.1 |
| 24/08/01 11:00 | 1.1 | 1.2 | 4.3 | 4.3 | 5.6 | 4.5 |

At sensor 1 flows varied on average every 1.5 ± 1.6 seconds. At sensor 2 average variation in flow direction occurred every 4.0 ± 3.6 seconds and at sensor 3 flows varied on average every 4.4 ± 3.7 seconds.

The shore platform flow environment measured at KM3 was very turbulent. Both in terms of changes in magnitude of flow velocity and changes in direction of flow. The scale of turbulence measured at KM3 questions the value of average flows and associated shear stresses as indicators of process on shore platforms. A description of turbulent flow combined with mean flow may be more meaningful than mean flows or significant wave heights alone.

5.5 SUMMARY

The notion that wave action is a fundamental process in the formation of shore platforms is well established in the international literature. Some authors have presented relationships between shore platform morphology and development, and offshore wave parameters (Mii 1962, Suzuki *et al.* 1970, Bradley and Griggs 1976, Takahashi 1977, Sunamura 1978, Tsujimoto 1987, Trenhaile 1999). Some models of shore platform development assert that wave assailing force has significant control over shore platform development (Sunamura 1992, Trenhaile and Layzell 1981, Trenhaile 1999). Yet, there is still debate on the relative importance of wave action in erosion of shore platforms (Stephenson and Kirk 2000a, 2000b). Given the importance attributed to wave action in the shore platform development debate, this chapter has characterised the wave environment at each shore platform studied. It then described and discussed direct and comprehensive measurements made of the flow regime across the shore platform at KM3.

The wave environments offshore from each of the study profiles were described in section 5.2. In deepwater offshore from KM2, KM3, KM7 and RM1 maximum significant wave height is 6.7m and average significant wave height is 1.8m. The wave environment offshore from AK1 and AK2 is more sheltered and shoaling and refraction

of deepwater waves is significant, as is the contribution of locally generated wind waves. Maximum significant wave height is 1.3m and average significant wave height is 0.6m. Hindcasting was used to predict the offshore wave environment of the enclosed water body at WK1 and WK2. Maximum predicted significant wave height is 0.8m and average significant wave height is 0.2m. Study sites therefore encompassed a range of different intensity wave environments.

Deepwater wave parameters have been used as indicators of wave assailing force on shore platforms and hence regarded as a control of shore platform development by a number of authors (Mii 1962, Suzuki *et al.* 1970, Bradley and Griggs 1976, Takahashi 1977, Sunamura 1978, Tsujimoto 1987, Trenhaile 1999). A comparison of offshore wave environments at each profile and rate of profile surface change was conducted in this chapter. It was found that there was a trend towards wider platforms with greater offshore wave height. However, the grouped nature of the data meant that this could not be stated with any certainty. No direct relationship between deepwater wave height and rate of surface change was found. This questions the use of deepwater wave parameters as indicators of on-platform wave action.

In the literature the use of deepwater wave parameters as indicators of the onshore platform wave environment has been made as very few direct measurements of wave activity have been conducted on shore platforms. This lack of onshore wave data means that little is known about the relationship between deepwater and onshore platform wave parameters and a number of assumptions have been made. Tsujimoto (1987) used a calculated value of breaker height as an indication of wave assailing force at shore platforms assuming that waves will reach their greatest height and break directly on the platform. It has been shown in this chapter that all but the smallest waves have broken before reaching the seaward edge of platforms studied. Therefore, in these instances use of breaker height as an indication of wave assailing force would be inappropriate. Once waves have broken modelling of changes in wave parameters no longer holds.

Simultaneous measurement of wave parameters in deepwater and on the shore platform at KM3 have made a comparison of these two sets of parameters possible. This showed

significant changes in most parameters and no direct relationships to predict these changes. Significant wave period was slightly longer onshore than in deepwater, but the relationship between the two remained relatively constant. Wave height reductions of over 67% were recorded as waves propagated from deepwater onto the shore platform and changes in water particle velocity between deepwater and onshore varied between 72% reduction to a 46% increase. Reductions in wave energy and wave energy flux were dramatic with 90% or more of the wave energy being lost as waves moved from deepwater onto the shore platform at KM3. It has been shown that it was not necessarily the highest energy deepwater waves that delivered the highest energy to the shore platform. This is a significant finding as prediction of onshore wave assailing force is usually done by use of deepwater wave parameters.

These findings suggest that the use of offshore wave parameters as indicators of onshore platform wave assailing force should be made with caution until a clear relationship between the two is established.

If waves are the key agents of erosion on shore platforms then an understanding of the distribution of assailing forces across shore platforms is required. Section 5.4.3 described and discussed measured flow patterns across a shore platform. This has not been done before in the geomorphic shore platform literature.

Flow across the shore platform at KM3 was described from measurements made by three sensors spaced along the profile. Highest velocities were recorded in the centre of the platform with a maximum velocity of $2.54\text{m}\cdot\text{s}^{-1}$ recorded and a maximum average velocity of $0.72\text{m}\cdot\text{s}^{-1}$. Average velocities were lowest at $0.22\text{m}\cdot\text{s}^{-1}$ at sensor 3 on the landward portion of the platform. Flow velocities on the platform were not related to tidal level or offshore wave conditions. This is a surprising finding and it has been proposed in this chapter that flow velocity is controlled by another parameter such as platform morphology.

There were strong lateral components to flow at all three locations on the shore platform at KM3 under varied deepwater wave conditions. This is an important finding as it

shows that shore platform surface rocks are exposed to a more varied regime of flow than is often implicitly implied within the literature.

Flow was in general very turbulent in terms of both uniformity and steadiness of flow with measures of turbulence being of the same order of magnitude as average flow velocities. Turbulence was greatest at the sensor on the seaward edge of the platform. The levels of turbulence measured here mean that the contribution of turbulence to wave assailing force on shore platforms should not be overlooked. Turbulence will contribute lift and drag forces to flow induced shear. It will enable aeration of the flow and enhance dissipation of wave energy.

This chapter has described broad scale relationships and flow patterns across the shore platform at KM3. The next step from this research would be to extend measurements onto shore platforms formed in different lithologies, with different seaward profile shape and subjected to different wave environments to see if the same broad scale aspects are apparent. Another direction of research is to look at small-scale flow patterns to enable greater understanding of specific processes of wave assailing force.

The accurate characterisation of flow on the shore platform at KM3 made in this chapter will enable more informed investigation of wave induced erosive processes. This will be undertaken in the next chapter.

CHAPTER SIX

WAVE INDUCED PROCESSES ON SHORE PLATFORMS

6.1 INTRODUCTION.

The previous chapter presented a description of wave flows onto and across shore platforms. This chapter presents further characterisation and parameterisation of these flows. Assessment is undertaken as to whether erosion is actually accomplished by waves. Where erosion by waves is considered possible the way in which it operates and its extent on shore platforms has been investigated. The sediment carrying capacity and competence of flow on the shore platform at KM3 has been investigated.

The first section of this chapter outlines modes of wave erosion on rocky shore platforms as proposed by other researchers. The feasibility of each of these modes is investigated given the flow regime measured at KM3 and described in Chapter 5. Later in this chapter the competence and capacity of waves as a mode of sediment transportation off shore platform is described and defined. Quantifiable elements of wave or flow force are presented with a discussion of possible capabilities of these consequent forces.

Many researchers assert that waves provide the primary force to erode shore platforms (section 5.1). However specifics on how this erosion is accomplished are somewhat lacking (figure 5.2). A wide variety of modes of wave erosion have been proposed within the published shore platform literature but very few are substantiated by direct evidence. In most cases morphology has been used as an indicator of process, notwithstanding that form is an ambiguous indicator of process. In the absence of quantitative (or even qualitative) information on how waves flow across a shore platform it has been necessary in the past to assess modes of wave erosion via conjecture and speculation. Given the lack of reliable and robust modelling of breaking and broken wave dynamics theorising of this nature would seem to be somewhat futile. Despite this a large number of proposed modes of wave erosion have been outlined in the literature

based on the duration and distribution of the hydrostatic, hydrodynamic and mechanical aspects of water flow as related to waves. The bulk of wave erosion literature is engineering based and attempts to assess the forces that structures within the marine zone will be required to withstand.

6.2 PROPOSED MODES OF WAVE EROSION.

This section outlines proposed modes of wave erosion of hard rock shore platform surfaces and assesses the likelihood of the occurrence of each mode under the flow regime outlined in Chapter 5. Modes discussed are Clapotis, shock or impact pressures, water hammer, hydrostatic pressure, water mass friction, cavitation, air compression, plucking and abrasion.

The action of waves can be grouped into three different force mechanism categories: hydrostatic (the pressure of the water itself), hydrodynamic (the movement of the water) and mechanical (the loading of the water with sediment). It is also possible to break wave action into three groups, on a temporal basis, related to the point during the evolution of a wave, at which the mode of erosion occurs. These groups are waves prior to breaking or under standing wave conditions, waves at the point of breaking and broken waves. In this chapter modes of wave erosion have been separated into the latter three categories for ease of understanding and mention of the type of force mechanism each mode falls into has been made. Definitions of modes of wave erosion given in the literature are sometimes a little unclear and may also vary between authors. In these instances some of the different definitions have been presented here and the most useful definition adopted.

6.2.1 STANDING WAVES.

6.2.1.1 CLAPOTIS.

Clapotis is caused by the formation of a standing wave at a vertical face. It has been referred to as a mode of erosion for cliffs (Sunamura 1992). However some authors suggest that it may occur, to a limited extent, on shore platforms (Sanders 1968a,

Sunamura 1992). Clapotis form as the result of the interaction of waves and wave reflections from a vertical structure (figure 6.1). The differing oscillation patterns of the two opposing waves interact to form a vertical jet, which collapses on itself (Bagnold 1939).

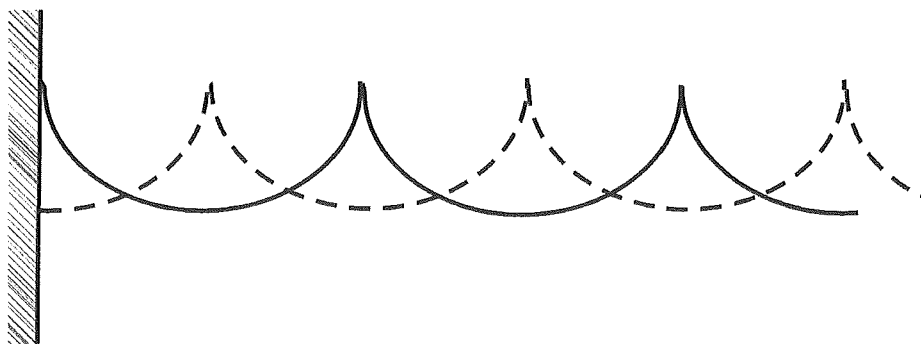


Figure 6.1: Clapotis or standing waves formed by the interaction of incident and reflected waves from a vertical face (Bagnold 1939:fig 7).

When this jet occurs at the rock face, a cliff or sea wall, it exerts a hydrodynamic pressure on the structure. For Clapotis to occur very specific conditions are required. The incident wave must be unbroken and the water at the rock face must be deep enough so that no wave interactions occur with the seafloor.

Formation of Clapotis against the landward cliffs of any of the shore platforms in this study was not possible due to the lack of adequate water depth in front of the cliffs even at the highest tides. Sanders (1968a) suggested that Clapotis may occur against the seaward cliffs of shore platforms at low tide. This is very unlikely to occur on the shore platforms studied for this thesis, as the seaward cliffs are fragmentary and jagged. The reflection of waves from these 'faces' will also be fragmentary thus hampering the set up of the required wave interactions to form Clapotis. Suitable Clapotis forming reflection of waves from seaward cliff faces will also be hampered by the protective cover of marine growth that exists e.g. *Durvillaea antarctica* (bull kelp). This acts to dissipate wave energy and may change wave shape at this point. Clapotis is therefore not a feasible mode of wave erosion on the shore platforms studied for this thesis.

6.2.2 BREAKING WAVES.

6.2.2.1 SHOCK OR IMPACT PRESSURES.

Shock or impact pressures are the result of a moving wave contacting a stationary rock face producing a hydrodynamic impact force. Wave shock is proposed as a mode of wave erosion on shore platforms by Bagnold (1939), Zenkovich (1967), Sanders (1968a), Trenhaile (1987), and Sunamura (1992).

Wave shock occurs when air is trapped by the jet which issues from the top of an unstable wave as it begins to break (Figure 6.2 a). This air is then compressed as the remaining portion of the wave continues to advance (figure 6.2 b and c). Finally the air bursts upwards with a low booming sound and the formation of much spray (figure 6.2 d). Wave shock pressures only occur when a wave breaks directly onto a vertical structure. Furthermore the wave must break in such a location that a pocket of air is trapped between it and a vertical wall positioned parallel to the wave front. (Bagnold 1939).

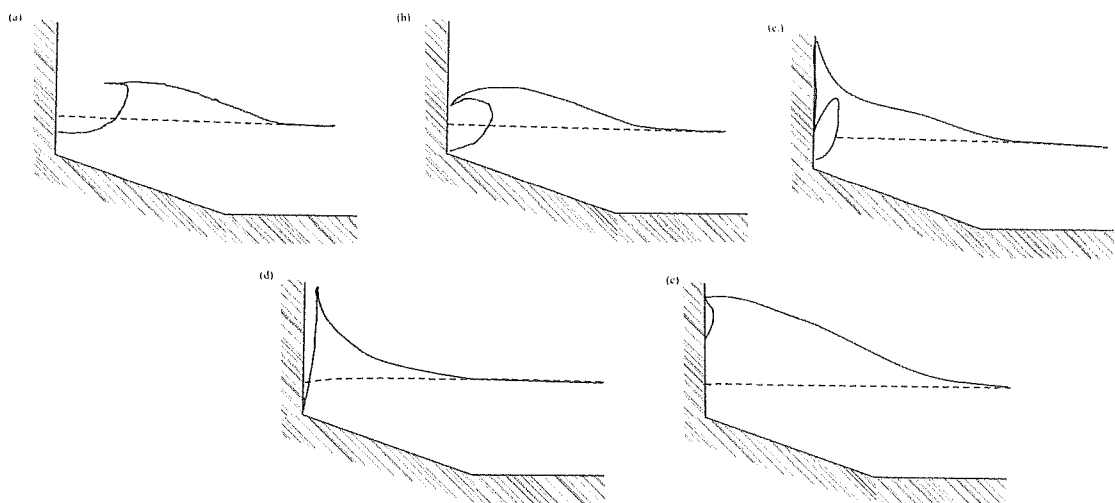


Figure 6.2: The formation of shock pressures by a breaking wave. (a) formation of a jet as the wave begins to break, (b) trapping of air by the jet, (c and d) subsequent history of the break, (e) a break occurring slightly later (Bagnold 1939:figs 11 and 12).

Bagnold (1939:209) further clarifies the conditions under which shock pressures will occur by stating that ‘the only case in which shock pressures appear ever to be produced’ is when the wave breaks slightly later than the one shown in figure 6.2a-d and the air

cushion is much thinner in the horizontal direction as shown in figure 6.2 e. Therefore, for wave shock to occur the following conditions must be met. The wave must arrive at the vertical wall when the base of the wall is permanently submerged. The vertical wave front must be very flat and the air cushion thin. 'The condition is therefore extremely critical' (Bagnold 1939:210). Bagnold's success at creating this phenomenon in the laboratory was patchy and depended on very specific combinations of wave parameters. However pressures produced under laboratory conditions were of short duration and high intensity (10 times greater than ordinary hydrostatic wave pressure). Artificially produced wave shock was rare in the laboratory and Bagnold failed to measure breaking wave shock of this origin in the field, as did Millar *et al.* (1974). Denny (1985) also failed to measure any wave shock pressures in more than 100 hours of observation at an exposed intertidal site. According to Trenhaile (1987) the rarity of occurrence is more than compensated for by the magnitude of the event when, or if, it happens on a shore platform.

It was shown in section 5.3.3 that at all study sites all but the very smallest incident waves break before they reach the shore platform. None would ever reach the vertical landward cliff at the required stage for the production of shock pressures described above to occur.

6.2.2.2 WATER HAMMER.

Water hammer is the impact between a body of water and a solid (Trenhaile 1987). It has been proposed as a mode of wave erosion on shore platforms by Sanders (1968a), Trenhaile (1987), and Sunamura (1992).

The incompressibility of water means that when a moving body of water impacts a stationary, solid, body of rock a shock pressure in the form of water hammer may result. For this to occur on shore platforms the body of water needs to be confined so that the momentum of the water flow is not able to disperse laterally. It is thought that it is possible for water hammer to occur under certain wave breaking conditions (Trenhaile

1987). True water hammer is very rare and Bagnold (1939) argued that under natural conditions true water hammer could never occur due to the aeration of the wave.

It has been shown in section 5.3.3 that most waves are broken by the time they reach the platforms studied for this thesis and then flow across the platform as aerated bores. This specialised mode of wave erosion by water hammer is highly unlikely to occur on the platforms studied for this thesis.

It is possible however that small scale versions of wave shock and water hammer may occur as the wave flows across the platform. This will be discussed in section 6.1.3.4.

6.2.3 BROKEN WAVES.

6.2.3.1 HYDROSTATIC PRESSURE.

Hydrostatic force or the pressure applied by the water body itself has been cited as a mode of wave erosion (Sanders 1968a). This same concept has been referred to in a number of different ways. Tsujimoto (1987) called this force “wave pressure” and both the pressure of the water body itself (Trenhaile 1987) and the change in pressure resulting from the passage of waves across the rock surface (Zenkovich 1967, Tsujimoto 1987, Sunamura 1992) have been cited as modes of wave erosion. The hydrostatic pressure (p) applied by a column of water above a surface of rock can be calculated using equation 6.1. The force applied by a column of water is dependent on the gravitation force (g) applied by the water body itself (where ρ is the density of water) and the depth of the water (d).

$$p = \rho g d$$

Equation 6.1

As a wave moves over the platform water depth changes resulting in a change in the hydrostatic force applied. It is not made entirely clear how hydrostatic pressure erodes rock however the compression caused by the application of hydrostatic pressure may result in a weakening of the rock structure. This weakening could be enhanced by the successive compression and release caused by changing pressures. Changes in

hydrostatic pressure work at two distinct time scales. There are pressure changes resulting from tidally driven water level fluctuations that theoretically occur over a 12 hour period. However, the shore platform at KM3 is only covered by the tide for between 4–5 hours during the highest portion of the cycle. Pressure changes resulting from wave activity occur in relation to the wave period, which ranged from 6-8 seconds during the study period.

‘Whether these pressures are sufficient to cause deterioration of the rocks depends on whether the strain exceeds the tolerance of the material’ (Trenhaile 1987:1). If the hydrostatic pressure is greater than the compressive strength of the rock, erosion should occur. However Trenhaile (1987:1) also says that ‘we cannot be sure there is any relationship between wave pressure and erosional efficiency’ and erosional processes are ‘probably most efficient when pressures are high’.

It is possible to calculate hydrostatic pressure on KM3 at each of the sensor locations using recorded still water depths and equation 6.1 (table 6.1). Sensors were located near the seaward edge, in the middle and near the landward edge of the profile (figure 5.24). These hydrostatic pressures ranged from 0 N.m⁻² at low tide when there is no water covering the platform to a maximum of 12 400 N.m⁻² at high tide. When an average atmospheric air pressure of 1013 N.m⁻² is added it gives a total maximum pressure applied to the rock surface of up to 13 500 N.m⁻². Therefore, change from 1013 to 13 500 N.m⁻² occurred over approximately 2 hours.

Table 6.1: Hydrostatic pressures calculated at KM3.

| sensor | hydrostatic pressure (N.m ⁻²) | | | | | | |
|----------|---|--------------|--|-----------------------|------------------|------------------------|------------------|
| | from tidal influence | | | from wave influence | | | |
| | at low tide | at high tide | actual pressure high tide + atmospheric | eq. 5.1 (still water) | | eq. 5.2 (moving water) | |
| | | | | H _{ave} | H _{max} | H _{ave} | H _{max} |
| Sensor 1 | 0 | 12436 | 13449 | 4018 | 7032 | 3811 | 6557 |
| Sensor 2 | 0 | 10598 | 11611 | - | - | - | - |
| Sensor 3 | 0 | 10256 | 11269 | - | - | - | - |

Assessment of hydrostatic pressure applied by waves as they moved over the platform was possible at the seaward most sensor (sensor 1) where measures of wave height were recorded by the Vector (section 5.4.1.2.2). Hydrostatic pressures from waves are also shown in table 6.1. Wave height (H) was substituted for water depth (d) in order to obtain the maximum change in pressure as a wave crossed a point on the rock surface. Measures of both average significant wave height and maximum wave height were used. Maximum pressure fluctuations caused by the passage of waves were 7030 N.m^{-2} .

Calculation of pressure changes caused by waves using equation 6.1 assume a still body of water and neglect the effect of the velocity potential on hydrostatic pressure. Movement of water will change the amount of the pressure applied and can be accounted for by using equation 6.2 (Denny 1988) which utilises Bernoulli's' equation for unsteady flow.

$$p = (\rho g H) \left(\frac{\text{Cosh}(ks)}{\text{Cosh}(kd)} \right) \quad \text{Equation 6.2}$$

Where k is the wave number ($k = 2\pi/L$), s is the distance from the seabed and d is water depth. Wavelength (L) was calculated using linear wave theory (equation 6.3).

$$L = T \sqrt{gd} \quad \text{Equation 6.3}$$

Results in table 6.1 show that, in this case, accounting for the velocity potential of the flowing water reduces the amount of hydrostatic pressure applied.

Maximum water depths due to both the tidal oscillation and maximum wave heights on the shore platform at KM3 were measured at sensor 1 (figure 5.24). Therefore, addition of half the pressure from maximum wave height ($P_{H\text{max}}$) and the maximum pressure from the tide ($P_{\text{high tide}}$) at this point gives the maximum hydrostatic pressure that could have occurred on KM3 during the study period. This was $16\,965 \text{ N.m}^{-2}$. Even this maximum hydrostatic pressure was at least two orders of magnitude less than the compressive strength equivalents of the mudstone at this location. From point load

testing compressive strength of the mudstone at KM3 was shown to be $2.2 \times 10^7 \text{ N.m}^{-2}$ and from Schmidt hammer testing was shown to be $1.1 \times 10^7 \text{ N.m}^{-2}$ (table 4.4). Hence direct hydrostatic pressure alone would not be capable of causing erosion on the shore platform at KM3.

However, it may not be a simple case of direct hydrostatic pressure causing erosion. It may be that alternation of pressure, the application and the release, could contribute over time to weakening of the integrity of the rock structure just as the continued bending of a piece of wire may eventually cause it to snap. This has not been assessed here.

6.2.3.2 WATER MASS FRICTION / SHEAR STRESS.

Friction caused by the movement of the water mass itself over the rock has been described as a mode of wave erosion on shore platforms (Zenkovich 1967). This concept is given a number of different names by various authors. Sunamura (1992) refers to the 'to and fro' motion of water being effective for erosion and Sanders (1968a) talks about water abrasion. The similar concept of shear stress created by waves was proposed as a possible mode of erosion by Trenhaile (1987), Tsujimoto (1987), Denny (1988), Sunamura (1992) and Stephenson (1997a).

The modes of erosion named above may differ slightly in the execution of the process but all are based on the fundamental concept of water moving over a solid rock surface causing a frictional force. This frictional force is considered important in shallow water as the energy of a wave once broken is greater than that of an oscillatory wave of similar parameters due to the fact that the entire body of water is being translated forward (Zenkovich 1967). However turbulence and bottom friction act to reduce this energy at a significant rate directly after breaking.

This direct assault of the water across the rock surface will result in shear forces, which may lead to erosion. Quantifying these forces can be difficult. The notion of a 'to and fro' motion for example is difficult to parameterise. The frictional drag caused by flowing water over a stationary surface is also difficult to measure directly. However

equations are available which calculate a component of this in terms of the shear stress. Shear stress (τ) is the force per unit area resulting from the differing velocities of sequential layers of water. Force is exerted on a surface by water being dragged over it. The flow field of a layer of water closest to the surface is controlled by the frictional drag imposed on the flow by the underlying stationary surface. In successive layers of the water above this bottom layer velocities increase rapidly until flow is at the same velocity as the general flow (figure 6.3).

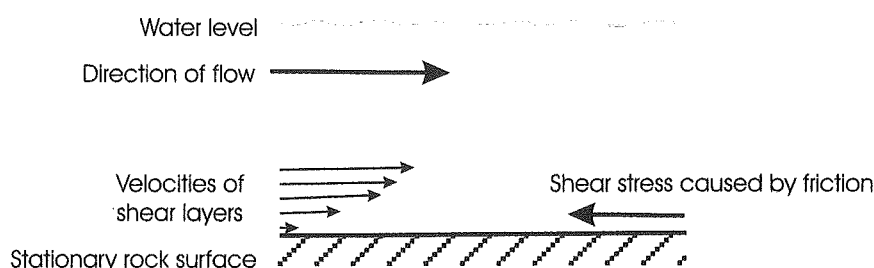


Figure 6.3: Shear stress caused by a body of water moving over a stationary rock surface.

As shear stress is a measure of the force per unit area applied by the moving water it can be calculated using equation 6.4 where the force, or shear, is proportional to the mass of the water (m) and its acceleration, $\left(\frac{du}{dt}\right)$.

$$\tau = m \frac{du}{dt} \quad \text{Equation 6.4}$$

From empirical evidence equation 6.5 has been established, relating τ to the velocity of the water itself (u).

$$\tau = C_f \rho u^2 \quad \text{Equation 6.5}$$

Where C_f is a dimensionless friction constant, ρ is the density of seawater and u is the velocity of the flow.

The friction coefficient (C_f) accounts for the effect of bottom friction and will vary depending on the surface roughness. Values used are usually ‘sound’ estimates based on empirical evidence. Procedures such as measuring wave height attenuation in a flume, direct measurement of wave energy loss, direct measurement of force and measurement of the velocity field have been used to gain values for C_f (Jonsson 1966). Tsujimoto (1987) states that a value of 0.01 is often used in shallow water regions. However in very shallow water the effect of friction is supposed to be more marked. Kamphuis (1975) presents an empirically derived wave friction factor design diagram where C_f depends on the type of flow and surface roughness, in the form of a Reynolds number. Values for C_f have an extreme range from 0.5 – 0.01 which can result in a difference of two orders of magnitude when using equation 6.5. It is therefore important to adopt the correct friction coefficient. Tsujimoto (1987) adopted $C_f = 0.15$ obtained from work by Kohno *et al* (1978 *in* Tsujimoto 1987) based on the reduction of wave height across a coral reef. This environment was considered to have similar morphology to a shore platform.

Assuming conservation of momentum of flow, it is possible to gain an indication of the energy loss to friction as waves flowed across the platform at KM3. From the average reduction in velocity measured between sensor 2 and sensor 3 and the known distance between the two an average reduction factor of 0.18 per metre was calculated. Therefore using a $C_f = 0.15$ as proposed by Tsujimoto (1987) is of similar magnitude to this result and suitable for the shore platform environment.

Tsujimoto (1987) calculated maximum shear stresses on shore platforms using equation 6.5. A lack of direct measurements of water velocity meant that he relied on solitary wave theory to calculate u (equation 6.6).

$$u = \sqrt{gH} \tag{Equation 6.6}$$

Combining equations 6.5 and 6.6 and using $C_f = 0.15$ as outlined above gives equation 6.7.

$$\tau = 0.15\rho gH_b$$

Equation 6.7

Tsujimoto (1987) used maximum wave breaking height (H_b) as his value of wave height as he considered this to be the point at which the most shear stress would be exerted on the shore platform (refer to section 5.3.1 for detail on how H_b was obtained). As noted previously the reliance of Tsujimoto (1987) on breaking wave height for calculation of shear stresses on shore platforms needs to be questioned in light of the fact that, at the shore platforms studied here, waves have broken by the time they reach the platform as shown in section 5.3.3. For the Japanese coast he found shear stress values of between 1 000 and 8 100 N.m^{-2} . Comparing these to the compressive strength of the rock he defined a demarcation between plunging cliff and shore platform initiation (Figure 6.4).

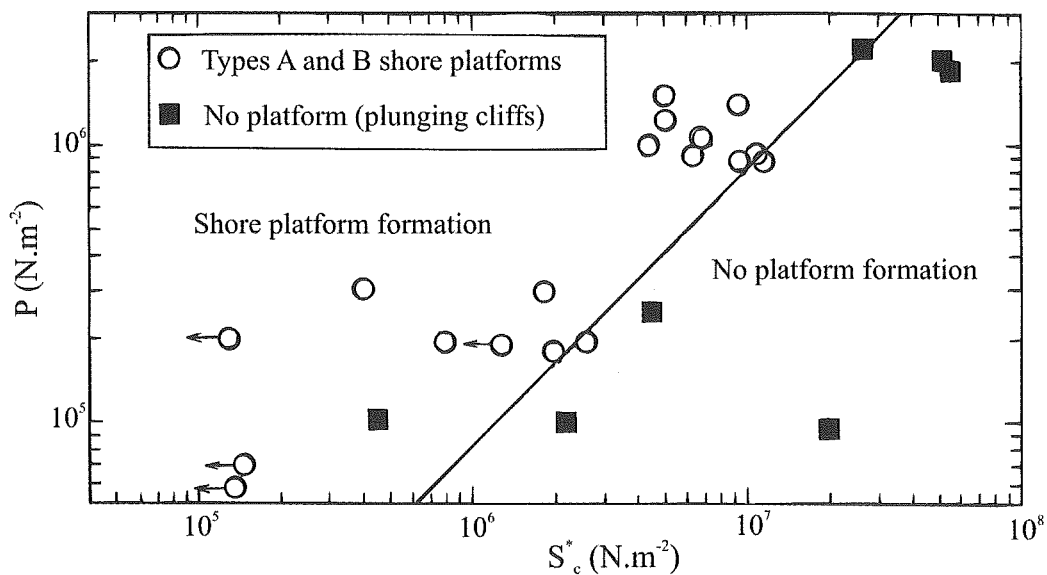


Figure 6.4: Demarcation for shore platform initiation (Tsujimoto 1987). Where P is pressure from calculated wave shear stresses and S^*_c is compressive strength of the rock gained from a combination of sonic and standard testing.

As the shear strengths shown in figure 6.4 are 0.081 of the compressive strengths of the rocks it is assumed that Tsujimoto (1978) considered shear stress alone was not the total assailing force of the waves although he does not outline any other facets of wave assailing force. He stated that maximum shear stresses were greater than the resistance forces offered by the rock and hence capable of erosion.

Stephenson (1997a) working on platforms on the Kaikoura peninsula used the same approach as Tsujimoto in calculating shear stress (equation 6.7). However instead of using H_b he used wave height (calculated from water pressure) measured directly on the platform by an S4 wave buoy. Calculated shear stresses were between 311 and 1 400 $N.m^{-2}$. He compared these directly with measured compressive rock strengths of the same platforms ($47 \times 10^6 N.m^{-2}$) and concluded that wave assailing force, in terms of shear strength was insufficient to cause erosion of the shore platform.

When assessing Stephenson's data of wave shear force and rock strength using Tsujimoto's demarcation diagram the shore platforms of his study fell within the "no platform formation" region.

Shear stresses were calculated using equation 6.7 for measurements made at sensor 1 on KM3 (section 5.4.1). Shear stress values calculated using equation 6.7 ranged from 302 – 1055 $N.m^{-2}$ (table 6.2). This range is similar to the range found by Stephenson (1997a).

Table 6.2: Shear stresses at KM3, calculated using equation 6.7 and wave height measured at sensor 1 as well as using equation 6.5 and direct measurement of flow velocity. Stresses are given in $N.m^{-2}$.

| date and start time of 18 minute recording | shear stresses ($N.m^{-2}$) | | | |
|--|-------------------------------|--------------|--------------------------------|--------------|
| | from eq. 5.7 and wave height | | from eq. 5.5 and flow velocity | |
| | τ_{max} | τ_{ave} | τ_{max} | τ_{ave} |
| 18/08/2001 13:00 | n/a | n/a | 218 | 20 |
| 18/08/2001 14:00 | 679 | 483 | 300 | 27 |
| 18/08/2001 15:00 | 754 | 543 | 317 | 40 |
| 18/08/2001 16:00 | 845 | 618 | 551 | 40 |
| 19/08/2001 14:00 | n/a | n/a | 320 | 22 |
| 19/08/2001 15:00 | 1041 | 664 | 394 | 32 |
| 19/08/2001 16:00 | 965 | 709 | 349 | 34 |
| 19/08/2001 17:00 | 950 | 603 | 425 | 35 |
| 19/08/2001 18:00 | 965 | 633 | 338 | 35 |
| 24/08/2001 07:00 | 513 | 347 | 348 | 30 |
| 24/08/2001 08:00 | 724 | 513 | 396 | 38 |
| 24/08/2001 09:00 | 799 | 528 | 472 | 35 |
| 24/08/2001 10:00 | 588 | 437 | 278 | 32 |
| 24/08/2001 11:00 | n/a | n/a | 243 | 20 |

Use of equation 6.7 to calculate shear stress has some drawbacks. The quantification of a suitable friction coefficient is problematic as outlined earlier. Another problem is that it relates wave height directly to shear stress occurring at the rock surface based on the relationship given in equation 6.6 rather than using water velocity directly. The current state of understanding of broken wave dynamics makes it difficult to rely on the proposition that the wave height is related directly to water velocity. In figure 5.64 it was shown that average water velocities did not strongly relate directly to water depth.

The relationship between flow velocities underneath a bore and the height of that bore has not been clearly established. To emphasise this fact a comparison of measured average flow velocities and flow velocities calculated from wave height and water depth recorded at the same time at sensor 1 is presented in figure 6.5. The equation used to calculate flow velocity from wave height (H) was $u = \sqrt{gH}$ and the equation used to calculate flow velocity from water depth (d) was $u = \sqrt{gd}$.

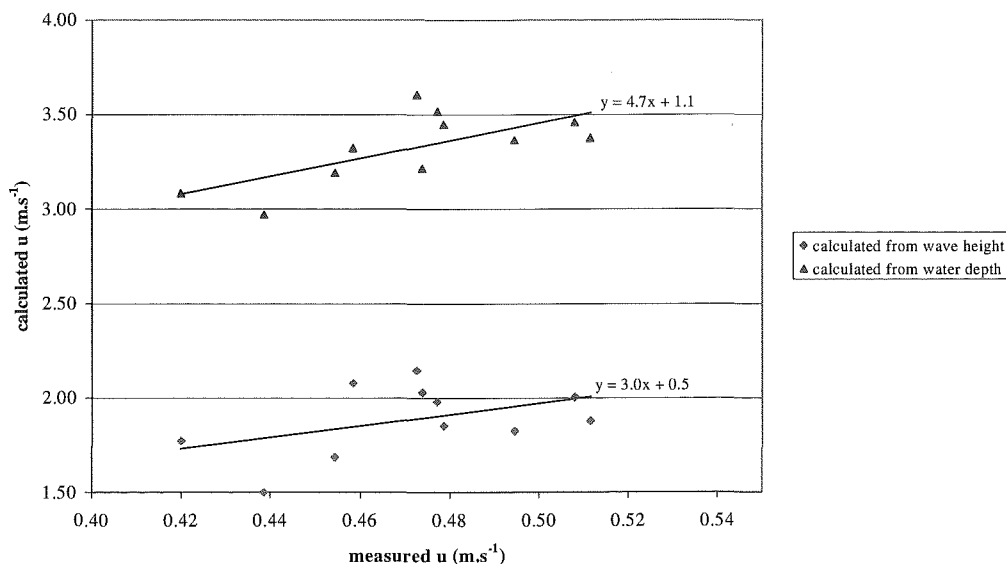


Figure 6.5: Comparison of average flow velocities measured directly at sensor 1 and flow velocities calculated using wave height and water depth measured at sensor 1 simultaneously.

Although figure 6.5 shows direct relationships between measured and calculated velocities it is evident that calculated velocities seriously overestimated the actual velocity. Neither method of calculation used accurately predicted actual flow velocity beneath the bores flowing across the platform at KM3.

Equation 6.6 from solitary wave theory applies to an unbroken wave. Therefore, as it is the velocity of the water that causes the shear stress and the relationship between this and wave height on a shore platform is not well understood, it would be best to use a measure of velocity directly. Ascertaining the actual shear stresses present under waves as they flow across shore platforms therefore requires further investigation. Table 6.2 includes shear stresses calculated using directly measured water velocities at sensor 1 and equation 6.5. These ranged from 25 –394 N.m⁻² and are considerably less than the shear stresses calculated using wave height for the same time periods. Using wave height in this instance overestimated shear stresses occurring. The lower values of τ obtained using water velocity directly also show the effect of friction slowing the flow velocities down as the broken wave flows across the surface.

Shear stresses given in table 6.2 are considerably less than those of values of rock strength measured for the mudstone at KM3. Bedrock strength was 2.2×10^7 N.m⁻² and surface strength was 1.1×10^7 N.m⁻² (table 4.4). Therefore, erosion of the rock by shear stresses caused by water flow alone is unlikely.

The efficacy of shear stress as a mode of wave erosion on a shore platform has been presented here at a very basic level. It suggests that shear forces are not great enough to cause erosion of the rock surface. It is possible however that other aspects of shear forces are important in the process of erosion. Turbulent forces may contribute to shear stress and it has been shown in section 5.4.3.3 that the flow environment on the shore platform is very turbulent. It is also not necessarily the shear stress itself that causes erosion but the change or sudden changes in shear stress.

6.2.3.3 CAVITATION.

Cavitation is the formation of the vapour phase in a liquid (Arndt 1981). It is proposed as a mode of erosion on shore platforms by Sanders (1968a) and Trenhaile (1987). The phenomenon of cavitation has been subjected to much research in the area of engineering where it has caused extensive damage to structures. However investigation into the geomorphic role of cavitation has been given little consideration and much of this has mainly been concentrated on the erosion of bedrock river channels (Whipple *et al* 2000). The term cavitation has been applied broadly and has been used to imply anything from the initial formation of bubbles to large-scale cavities (Arndt 1981). For the purposes of this study cavitation occurs where there is a reduction in local fluid pressure usually caused by high velocity flows below the vapour pressure of dissolved air causing the water to vaporise forming bubbles within the flow. This is a non-steady phenomenon, as the bubbles formed will implode when advected into regions of higher pressure (Arndt 1981, Whipple *et al* 2000). The stress and implosions created by the formation and collapse of the vapour pockets causes erosion of the rock surface. It is generally accepted that for cavitation to occur nuclei need to be present (Whipple *et al*. 2000). These are usually very small suspended sediment particles or air bubbles either embedded in the flow or in small cracks at the boundary surface (Arndt 1981).

A cavitation inception index (equation 6.8) is used to predict the onset of cavitation under given flow conditions. It is the ratio of the difference between hydrostatic pressure (p_o) and vapour pressure (p_v) to the free-stream dynamic pressure (Arndt 1981).

$$\sigma = \frac{P_o - P_v}{\frac{1}{2} \rho u^2} \quad \text{Equation 6.8}$$

Where ρ is the water density and u is the velocity of the flow. The critical value for σ , in principle, is unity however in practice it has been found to be commonly in the range of 2 – 3 (Arndt 1981). When σ is greater than the critical value there is no cavitation effect. Differences in σ reflect the importance of flow and environmental conditions in the initiation of cavitation e.g. flow depth and water temperature. Whipple *et al* (2000)

developed a graph giving conditions for cavitation inception based on flow depth and water velocity which is based on bedrock river channel evidence (figure 6.6)

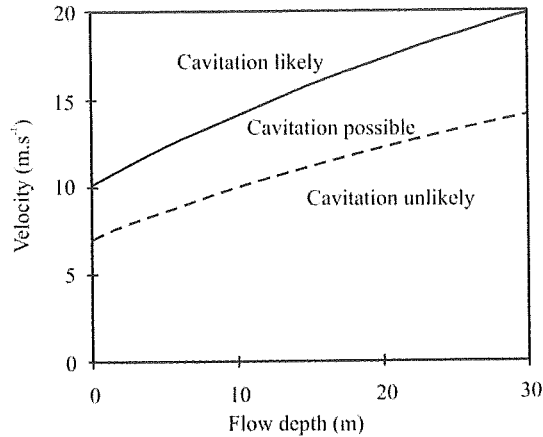


Figure 6.6: Critical velocities required for cavitation inception as a function of flow depth. Calculated for $\sigma = 4$ (possible cavitation – dashed line) and $\sigma = 2$ (probable cavitation – solid line) and a water temperature of 10°C (Whipple *et al* 2000).

They have assumed that when $\sigma \leq 4$ cavitation is possible and when $\sigma \leq 2$ cavitation is likely. They assert that cavitation is an important process in bedrock riverbed erosion but admit that it is difficult to find definitive evidence of cavitation as there is no known distinctive signature of cavitation damaged rock surfaces. Dahl (1965) also notes the difficulty of identifying cavitation signatures but suggests that cavitation erosion creates coarse surfaces. In Norway these surfaces have then been polished by abrasion beneath old ice flows to form the “plastically sculptured detail” that he was studying.

Although small air bubbles may be required within the flow to act as cavitation nuclei, aeration of the flow may also play a dual role in that too much aeration will vent pressures to the water surface and may cushion the collapse of cavitation pockets (Whipple *et al* 2000). The traditional view is that cavitation requires high velocities and non aerated water (Trenhaile 1987, Stephenson 1997a).

Using equation 6.8 it is possible to calculate σ for the conditions that were present on KM3 during the study period. The maximum velocity recorded was 2.54 m.s⁻¹ at sensor 2 on 19/08/01 and the average water temperature measured by the Vector during the

study period was 9.3°C. The vapour pressure of water is dependent on the temperature of that water. Water of 9.3°C has a vapour pressure of 1200 N.m⁻² (Stull 1995). This gives the smallest possible cavitation index for the measurement period of $\sigma = 3.3$ which is greater than the critical cavitation values presented by Arndt (1981). Therefore, according to Arndt's (1981) limits, cavitation would not occur in this environment. According to Whipple *et al.* (2000) who state that cavitation is possible between $\sigma = 2$ and $\sigma = 4$ in a fluvial environment cavitation may be possible under the conditions measured at KM3. However, using their guidelines for cavitation initiation given in figure 6.6 velocities would have needed to be in excess of 7.4m.s⁻¹ for it to be possible for cavitation to occur and in excess of 10.5m.s⁻¹ for it to be likely to occur given the maximum water depth of 1.2 m at KM3. These velocities were not reached on the shore platform at KM3 where maximum velocity recorded was 2.54m.s⁻¹. Cavitation is also likely to be severely inhibited by the large amount of aeration of the flow.

6.2.3.4 AIR COMPRESSION.

Air compression into rock cavities by waves is thought to be a mode of wave erosion on shore platforms (Sanders 1968a, Robinson 1977b, Trenhaile 1987). As waves flow across a shore platform air may be trapped between the wave and the rock, usually within joints, bedding planes, erosional clefts and other rock cavities. The forward impetuosity of the water causes compression of air into these cavities. This pressure will be released as the wave recedes (Trenhaile 1987). Such compression and release will cause stress on the surrounding rock thus leading to erosion. This mode of erosion requires the rock surface to be exposed to an alternation of air and water. It will therefore only occur along a small moving band as the tide rises and falls and the rocks are covered and uncovered by water. This definition of air compression within joints means this mode of wave erosion is limited both temporally and spatially assuming that once the platform surface is fully submerged the air will not be available for compression. Robinson (1977b) noted that this mode of erosion is more effective when it occurs in conjunction with sand wedging which acts to hold the joints open.

Trenhaile (1987) considered that there were some specific conditions under which air compression in joints may occur. High pressures could only be generated if the wave front or bore was parallel to the rock face and if the pressure could not be relieved laterally into areas of low pressure (Trenhaile 1987). So, for air compression to occur a cliffed section of rock is required onto which the wave can flow. As mentioned previously unbroken waves very rarely reach the landward cliff at KM3 (section 5.3.3) and when they do they lack the impetus required for compression to occur. It is unlikely that air compression is a mode of erosion on or near the landward cliff of this shore platform.

It is possible however that this mode of erosion occurs at a smaller scale as flows move across the platform. Shore platforms are not uniformly flat surfaces and often there are protuberances above the general surface of the rock. These protuberances may present the required conditions for air compression.

Quantification of this mode of erosion is difficult. Calculation of the force created is dependent on knowledge of the configuration of factors required for initiation of the process and an understanding of the scale, both temporal and spatial, at which the process operates.

Once a compression force has been quantified it is still difficult to assess the damage that it may be capable of. It needs to be compared to the strength of the rock at the point of compression. This will be a joint strength rather than a massive rock strength. The effect of, not only, the application of pressure but also the release of it should be considered. Air compression will be working at the mechanically weakest part of the rock which has the greatest surface area (figure 6.7). The assessment of changes in pressure on the rock structure at this point needs to take into account some measure of the elasticity of the rock. This is a very difficult thing to quantify (section 4.5).

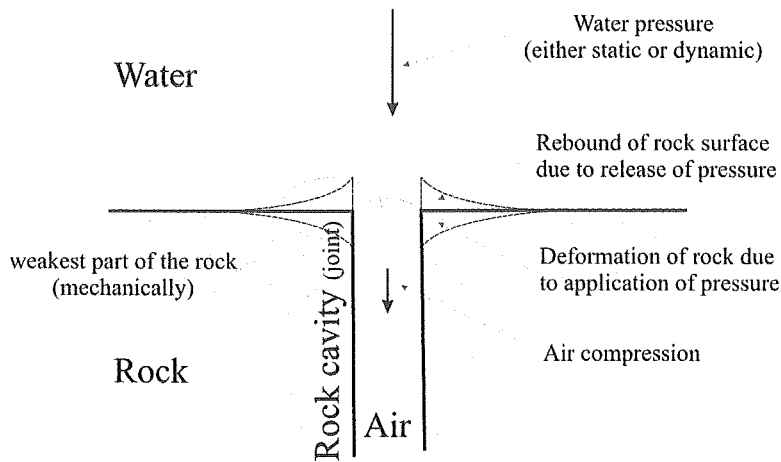


Figure 6.7: Deformation of rock surface at a joint due to application and release of water pressure (and consequent air compression and release). The extent of the deformation is unknown and probably exaggerated.

The only theory available to assess the pressure created by air compression in rock cavities was developed by Bagnold (1939) in relation to quantifying wave shock pressures. Creation of wave shock pressures and air compression within cavities are analogous situations meaning that this approach is also appropriate in the quantification of air compression pressures. Bagnold proposed a cylindrical piston-and-cup model where a pocket of air was compressed within a cavity by a 'piston' of water (Figure 6.8) and derived an equation (6.9) to describe the change in pressure ($P_{\max}-P_o$) due to air compression.

$$P_{\max} - P_o = \frac{2.7 \rho u^2 k}{D} \quad \text{Equation 6.9}$$

Where ρ is the water density, u the water velocity, k the length of the water column and D the width of the air pocket.

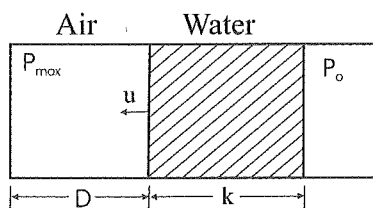


Figure 6.8: Bagnold's piston-and-cup model (Mitsuyasu 1966). Where D is the width of the air pocket, k is the length of the water column, P_o the initial (atmospheric) pressure, u the velocity of the water column and P_{\max} the pressure of the compressed air.

Mitsuyasu (1966) expanded this model by deriving an analytic solution for the equation of which he considered the first term on the right as a fairly good approximation (only the first term is presented in equation 6.10). He also presented a solution for an air cushion with leakage.

$$P_{\max} - P_o = \rho uk\sigma \sin \sigma \quad \text{Equation 6.10}$$

Where t is the time taken for compression and σ is given in equation 6.11.

$$\sigma = \left(\frac{P_o \gamma}{\rho k D} \right)^{1/2} \quad \text{Equation 6.11}$$

Where γ is a value for the adiabatic compression of the air.

Ramkema (1978) further developed Bagnold's model to account for adiabatic and isothermal air compression. Adiabatic air compression occurs when no heat exchange takes place and results in an increase of air temperature with increasing pressure. Isothermal air compression occurs when air remains at a constant temperature as pressure is applied.

Due to the impossibility of measuring the thickness of the air cushion in the field Trenhaile (1987) believed equations 6.9 and 6.10 to be of theoretical rather than practical interest. However in the case of air compression in a joint the thickness of the air pocket is constrained by the size of the joint itself. The geological survey conducted at KM3 (section 4.2) measured joint thicknesses across the profile. These varied between 0.5 mm to >6 mm. Although joints greater than 6 mm were evident Mitsuyasu (1966) considered air pockets of 6 mm to be the maximum size for shock pressures to occur.

In order to apply the equations of Bagnold (1939) or Mitsuyasu (1966) in the shore platform situation a number of assumptions have been made. Adiabatic compression of air was assumed to occur and the length of the water column was at least $k = 0.2H$ as

suggested by Bagnold (1939). Average wave height (H) measured on the platform was used for these calculations. Greater values of k lead to very slight but not significant increases in overall pressures.

Table 6.3 shows pressure changes calculated from applying the models of Bagnold and Mitsuyasu and using both average and maximum water velocities measured at sensor 2 on KM3 (section 5.4.3). Pressures were calculated for a range of joint thickness from 0.5 – 6 mm.

Table 6.3: Modelled air compression pressures in joints at KM3.

| Joint thickness - D (mm) | air compression pressures (kN.m ⁻²) | | | |
|-----------------------------|---|------------------|-------------------|------------------|
| | Bagnold's model | | Mitsuyasu's model | |
| | u _{max} | u _{ave} | u _{max} | u _{ave} |
| 0.5 | 2143 | 83 | 28 | 6 |
| 1.0 | 1071 | 42 | 24 | 5 |
| 1.5 | 714 | 28 | 18 | 4 |
| 2.0 | 536 | 21 | 15 | 3 |
| 2.5 | 429 | 17 | 12 | 2 |
| 3.0 | 357 | 14 | 11 | 2 |
| 3.5 | 306 | 12 | 9 | 2 |
| 4.0 | 268 | 10 | 8 | 2 |
| 4.5 | 238 | 9 | 7 | 1 |
| 5.0 | 214 | 8 | 7 | 1 |
| 5.5 | 195 | 8 | 6 | 1 |
| 6.0 | 179 | 7 | 6 | 1 |

Using Bagnold's model pressures from air compression in rock joints could be as great as $2.1 \times 10^6 \text{ N.m}^{-2}$ and as low as $6.9 \times 10^3 \text{ N.m}^{-2}$. As the models suggested generated pressures increased significantly with increased momentum of the impinging water mass and decreased with increased thickness of the air cushion.

Direct comparison of compressive strength of the rock measured by point load testing ($1.03 \times 10^6 \text{ N.m}^{-2}$) (section 4.5.3) to calculated air compression pressures shows that under Bagnold's regime rock erosion would occur at joints smaller than 1 mm when flow velocities are maximum and that erosion is likely to occur when joint thickness is less than 2 mm (pressures were within 68% of the rock strength). Using the Mitsuyasu

model regime, air compression pressures are an order of magnitude less than the compressive strength of the rock therefore should not be capable of erosion.

Added to this, shock pressures measured in either the laboratory or the field failed to achieve the maximum predicted theoretical levels (Bagnold 1939, Mitsuyasu 1966). However no measure of air compression of the nature described here has been made either in the laboratory or field so a comparison is impossible at this time.

This direct comparison of air compression pressures to rock compressive strength may be somewhat misleading as the rock strength measure used for comparison is that of the strongest most massive part of the rock, the bedrock, and air compression preferentially occurs in locations of lower and even the weakest rock strength, the joints and fractures. Unfortunately rock joint strength is very difficult to assess and no measure of it was possible for this thesis. The strength of the joint structure depends on factors such as the degree of weathering of the joint and the size of the fracture.

Accounting for the fact that air compression in joints takes place at the weakest part of the rock it is very likely that this mode of wave erosion is occurring at a scale of less than 2mm and is possibly also occurring at greater scales on the shore platform at KM3. Given that the specific requirements of no lateral leakage of confined air are met so that high pressures may result.

Air compression in joints is considered adequate in aiding erosion at the very least. A simplification of the process was necessary and it has given an indication of the magnitude of this mode of erosion and the scale at which it is likely to occur. Before conclusive comments can be made further investigation of this mode of wave erosion needs to be made accounting for short duration and high magnitude of shock pressures and the effect of application and release of pressure on the rock.

If air compression in joints is a feasible mode of wave erosion as is suggested here it would tend to form surfaces that are generally level while at the same time creating a

jagged surface as the air pressure would tend to blow the rock apart from within making use of the existing joint structure.

It is also possible that a similar process occurs at an even smaller scale and without the requirement of air being captured by the wave front. The nature of a bore is such that it is well aerated. This means that there are numerous small air pockets continuously available for use in the air compression process. It is conceivably possible for air compression at this scale to cause micro erosion.

6.2.3.5 QUARRYING / PLUCKING.

Quarrying is the plucking of chunks of rock (no specified size) from the rock surface. It is frequently cited as a mode of wave erosion on shore platforms (Sanders 1968a, Bradley and Griggs 1976, Robinson 1977b, Trenhaile 1987, Sunamura 1992). Quarrying seems to be a term used more to describe the end, observed morphologies rather than any specific process. A quarried or plucked surface is one from which largish (usually angular) chunks of rock have been picked directly from a surface leaving holes of a matching shape. There are a number of different hypotheses as to how this end result is achieved. Bradley and Griggs (1976) considered disintegration of bedrock particles was via fluid drag and changes in pressure. Removal of rock fragments by shock pressure, water hammer and air compression into joints was suggested by Sanders (1968a) and Trenhaile (1987). Pitty (1971) suggested that suction associated with turbulent eddies caused large blocks to be lifted and Robinson (1977b) proposed that pressure of water being forced into joints and cracks caused chunks of rock to be quarried.

There was visual evidence on the shore platforms studied that a limited amount of quarrying had taken place as seen by identification of locations from where blocks have been removed (figure 6.9). However direct assessment of the process was difficult.

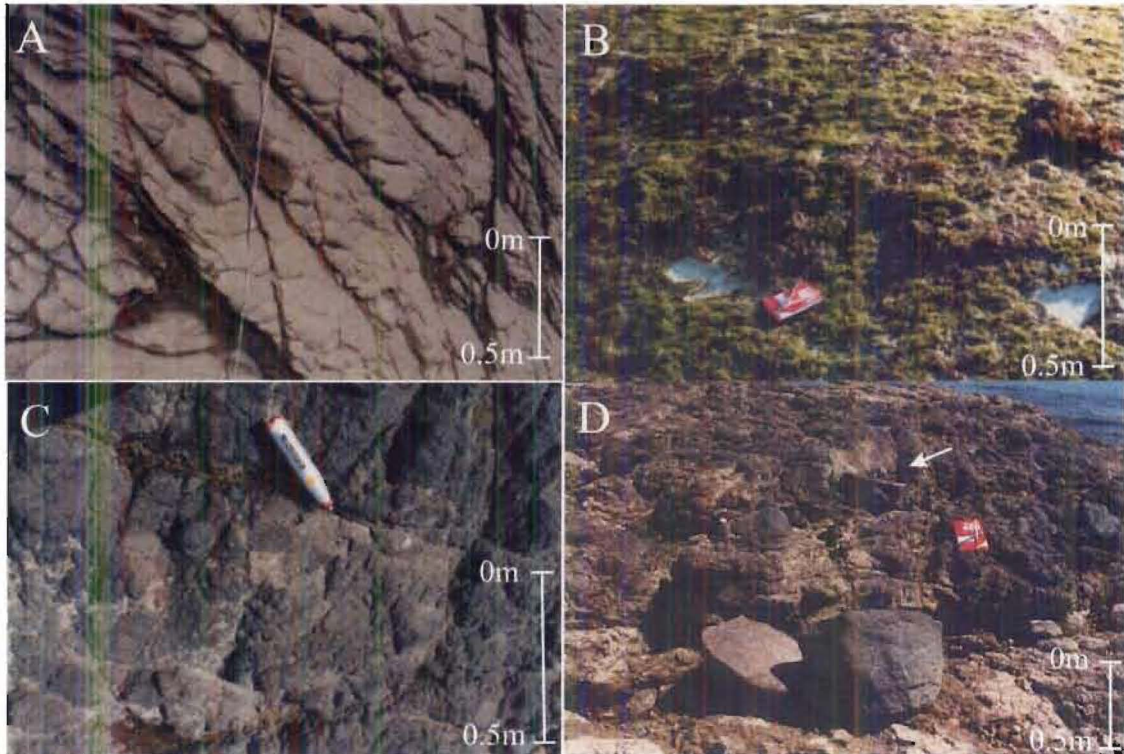


Figure 6.9: Evidence of wave quarrying on shore platforms. A. Mudstone platform at KM2 (27/11/2000). B. Limestone platform at KM7 (16/06/2001). C. Basalt platform at AK1 (25/10/1999). D. Basalt platform near AK2 (16/11/2000). The arrow indicates the location from where the boulder in the middle foreground of the picture was plucked. Scales shown in the photographs are approximate only.

Erosion by quarrying or plucking requires firstly the production of loose joint blocks and secondly the subsequent entrainment and transport of the loosened joint blocks. In the fluvial environment Whipple *et al* (2000) considered the production of loose joint blocks generally involved weathering, crack propagation and rock fracture. The same would hold for the marine environment. It is likely that the processes described in previous sections all contribute to the final effect of quarrying. Air compression within joints, for example, could be a primer for loosening and removal of chunks of rock defined by those joints. No direct quantification of quarrying as a mode of wave erosion was undertaken here.

The process of quarrying will be rate limited by one of two processes, either the production of joint blocks or the entrainment and transport of sediment. Production of

joint blocks is accomplished via processes described in previous sections with the addition of general weathering.

However in order to assess the feasibility and scale of quarrying on a shore platform some indication of the size of clasts (or chunks) that the waves are capable of moving is required. (This is undertaken in section 6.3). From this, quantification of how much force is actually required to move these rock chunks may be assessed. It may be possible to quantify the scale of quarrying that waves are capable of and define this limiting aspect of quarrying.

6.2.3.6 ABRASION.

Abrasion is a term that has been used to encompass a wide range of processes involving wear of rock surfaces via contact with sediment moved within a fluid flow. This may include the rubbing, splitting, chipping and cracking of the rock. It has been studied in fluvial, marine, aeolian and glacial environments (Marshall 1929, Kueuen 1964, Broadhead and Driese 1994, Ferguson *et al.* 1996). Robinson (1977b) defined abrasion on shore platforms as the wearing of the rock surface from erosion and smoothing by waves armed with detritus. Abrasion is also considered a mode of erosion on shore platforms by Norrman (1964), Zenkovich (1967), Bradley and Griggs (1976), Trenhaile (1987), Sunamura (1992).

Abrasion depends on the forces of water flow created by the passage of waves being enough to be able to entrain sediment. Assessment of the feasibility of abrasion as a mode of wave erosion must start with an assessment of the ability of the flow to entrain sediment. This is to be investigated in section 6.3. When the flow is strong enough to result in entrainment, loose stones, pebbles, sand and other debris will be rolled, swept and dragged across the surface of the shore platform, producing abrasion. Abraded areas of rock tend to be smoothed surfaces.

Abrasion requires not only the ability of the flow to move sediment but also a supply of sediment to be there for moving. Sediment may be present on shore platforms from

wave quarrying, rock fall from cliffs, beaches in close proximity and from sediment thrown on to the platform from the near shore environment (figure 6.10).

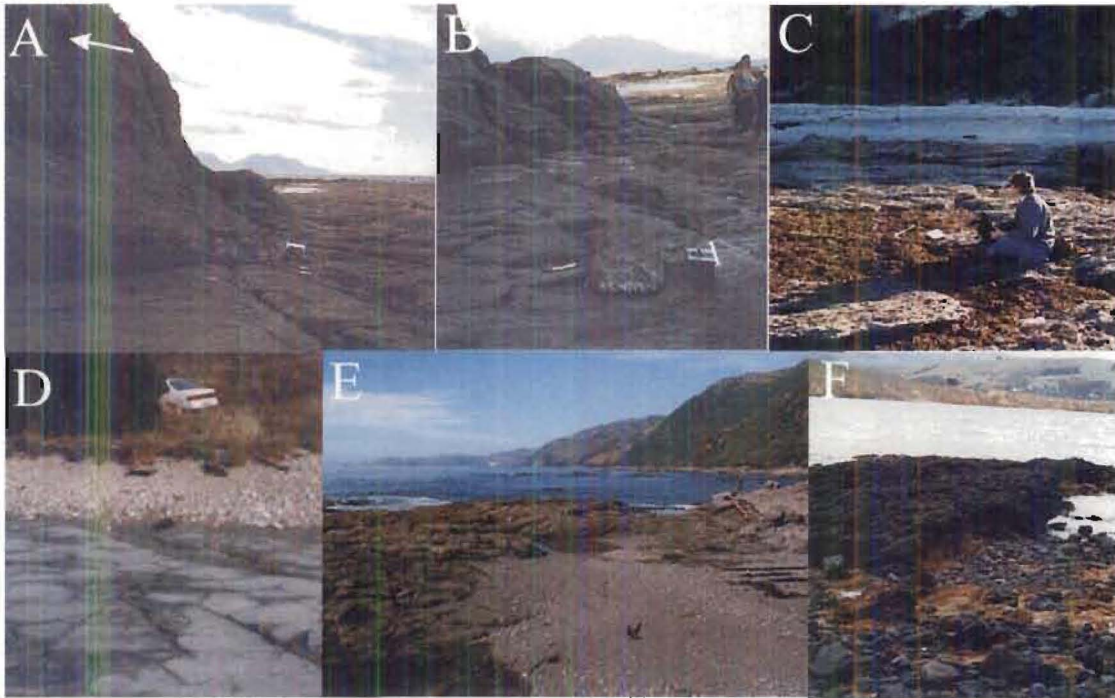


Figure 6.10: Sediment available for abrasion on shore platforms. A. Rock fall from the cliff near KM3 (5/06/2000). Arrow indicates location from where the rock fell. (Box indicated is 400mm in length). B. Rock thrown onto platform near KM3 (04/05/2002). Note seaweed and algae that has grown on it. (Box indicated is 400mm in length). C. Backshore limestone gravel beach at KM7 (24/05/1998). D. Backshore limestone gravel beach on mudstone platform at KM2 (05/05/2000). E. Greywacke gravel beach encroaching onto the shore platform at RM1 (12/02/1999). F. Loose sediment and blocks near AK1 (14/05/1998).

For the majority of the time surfaces of the shore platforms studied in this thesis were observed to be clear of loose sediment. Therefore the extent of abrasion as a mode of erosion could be questioned or quite site specific across the platform. When sediment was observed on the platform e.g. from cliff fall, it was usually removed by the next tide. Hence, some abrasion may have occurred in those instances but not on a continuous basis. Where a consistent supply of loose sediment was available e.g. gravel beaches on the backshore of the platforms, higher rates of down wear were measured and smoother surfaces were evident. MEM sites located within close proximity (<2m) of beaches (KM2A, KM7A and RM1A) showed rates of erosion significantly greater than those not within close proximity to sediment supplies (section 3.2).

Once sediment has been entrained there are a number of ways that it can be moved by the flow. Heavier particles may be rolled along the surface, slightly lighter ones could saltate or bounce and the lightest will be suspended within the flow. Type of movement will depend on the size, density and shape of the sediment and the velocity of the flow. This movement of sediment leads to the direct wearing down of the surface, breaking off chunks of rock and exerting stress on the rock through impact. The method of movement will determine the type and extent of abrasion that occurs.

No direct quantification of abrasion as a mode of wave erosion has been made here. However it has been shown to be a possible mode of wave erosion in at least some parts of the shore platforms studied for this thesis but not on a platform wide basis. The specifics of sediment entrainment will be discussed in section 6.3.

6.2.4 COMBINATIONS OF MODES.

Sections 6.2.1 to 6.2.3 presented modes of erosion separately and assessed the feasibility of each individual mode as an erosive process. On a discrete basis, the two modes of air compression in cavities and abrasion may be directly capable of causing erosion of the rock surface on the shore platform at KM3 under the flow regime described in Chapter 5. In reality however it is probable that modes of wave erosion do not work in isolation. A combination of different forces could contribute to the eventual disintegration of the rock. Figure 6.11 shows the distribution of modes of wave erosion resulting from the processes of mechanical wave action on hard rock shore platforms as hypothesised by Sanders (1968a). Most of the processes operate at the same levels on the same surfaces and therefore combined effects would be possible.

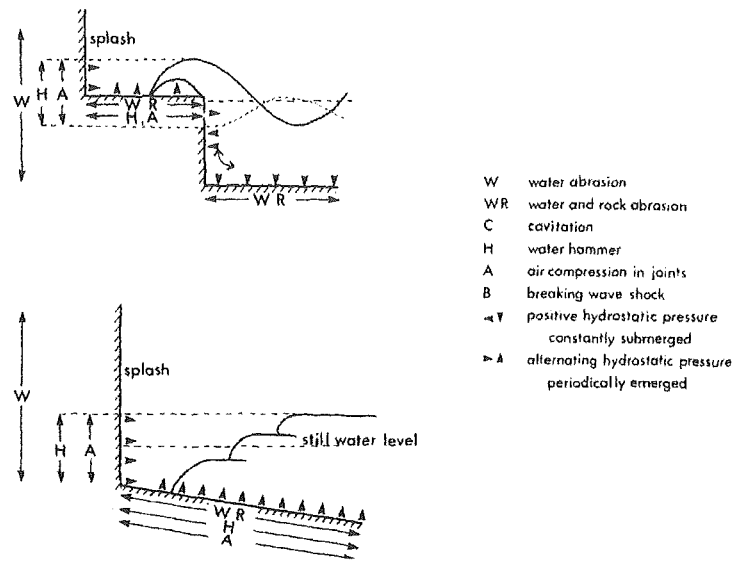


Figure 6.11: Modes of wave erosion and their distribution on shore platforms (Sanders 1968a).

In the fluvial situation Whipple *et al* (2000) presented a schematic illustration which showed a number of contributing modes of erosion as facilitation for the plucking of a bedrock block (figure 6.12). He noted that ‘Where the downstream neighbour of a block has previously been removed, both rotation and sliding become possible, and extraction is greatly facilitated.’ (Whipple *et al* 2000:496). All these processes shown in figure 6.12 operate in the marine environment with the only difference being that flow is not unidirectional but at the least bi-directional and rather more turbulent.

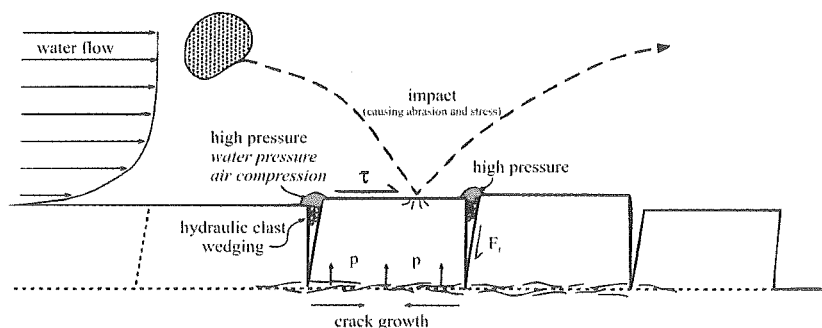


Figure 6.12: Schematic illustration of forces and processes contributing to erosion by plucking (after Whipple *et al* 2000). Processes not included by Whipple *et al* are indicated in italics.

Direct investigation and quantification of the capability of modes of wave erosion on shore platforms has not previously been undertaken in a comprehensive manner. As mentioned in section 6.2.2.1 shock pressure is the only proposed mode of wave erosion to have been measured directly in the laboratory and this was done with varying degrees of success. Direct measurement of modes of wave erosion in the field have been rare. Stephenson (1997a) measured water pressure changes resulting from the passage of waves. He did not directly assess their erosive capability, but rather converted the measure to shear stress and assessed the competence of this calculated value in producing erosion. He concluded from this that waves were not capable of erosion on the shore platforms at Kaikoura (Stephenson 2000). However by neglecting to measure aspects of the flow field other than pressure changes he did not account for other processes which have been shown to be capable of causing rock erosion, at least individually and almost certainly in combination.

More often, but still somewhat rarely, morphology has been used as an indicator of mode of wave erosion on shore platforms. Researchers have cited chunks missing from the surface of the rock face as evidence of wave quarrying (Mii 1962, Bradley and Griggs 1976, Robinson 1977b, Emery and Kuhn 1980, Trenhaile 1987, McKenna *et al.* 1992). Robinson (1977b) sited smooth surfaces as an indication of abrasion and rough surfaces as an indication of wave quarrying. He measured changes in these surfaces using MEM techniques and concluded that both processes were operating on shore platforms of Northeast Yorkshire, England. However these findings need to be approached with some caution, as morphology can be a somewhat ambiguous indicator of process. Trenhaile (1987:21) states, in reference to wave events, that 'the MEM technique is incapable of considering the quarrying of large rock fragments, and like other methods has difficulty in assessing the role of high magnitude low frequency, erosional events'. As outlined in section 3.1 an unsuccessful attempt was made in this thesis to measure larger erosion of this nature. The way in which the measurement of morphological changes are undertaken when looking for an indicator of process causing erosion will be dictated by the expected scale of the change caused by the mode of erosion. It has been shown in this chapter that wave processes may work at the smaller

scale as well as the larger expected quarrying scale and therefore might be detected via use of the MEM technique.

Two directions of research now need to be followed in order to elaborate on the erosive capabilities of waves. Firstly there is a need to assess the effect of the forces quantified in previous sections on the rock itself. The efficiency of the forces applied depends to a certain extent on the failure mode of the rock. Secondly the cumulative effects of combined modes of wave erosion need to be evaluated and quantified.

6.3 SEDIMENT ENTRAINMENT.

One of the features that makes a shore platform distinctive and unique from other marine environments is the general absence of loose sediment at the ocean – land interface. Shore platforms are surfaces of exposed bedrock that are usually bare of sediment, despite the fact that both continued down wearing of the horizontal surface and subaerial weathering of the landward cliff yield detritus. The size of this detritus ranges from granular to significantly sized blocks. If the sediment were not transported away formation of the shore platform would cease as rubble armoured the near horizontal surface.

Wave induced flows are fundamental in the process of sediment removal from shore platforms. Assertions have been made that sediment is easily transported off shore platforms (Bradley and Griggs 1976), but no quantification of the process has been undertaken. The competence of flows produced by waves and the processes by which sediment transport occur have not previously been studied in this environment. How large a piece of sediment are waves capable of transporting? The upper limit of entrainment must dictate the extent to which the bedrock needs to be broken down before removal is possible. This is an important consideration when debating the way shore platforms erode. Another is the question of what the sediment does to the rock surface as it is being moved. Entrainment and transportation of sediment is therefore a vital process in the formation of shore platforms and worthy of investigation. This

section looks at theories of sediment entrainment and transport, as they relate to the shore platform situation and quantifies the competence and capabilities of the process under the wave conditions described in Chapter 5.

6.3.1 SEDIMENT ENTRAINMENT THEORIES.

The majority of investigations into sediment entrainment and transport within fluid flows have been undertaken in the fluvial environment. Theories rely heavily on fluid mechanics with many different solutions based on assumptions of unidirectional, sometimes turbulent, fluid flow. There have been a number of comprehensive reviews outlining the physics of the processes and past research undertaken (for example Leopold *et al* 1964, Richards 1982, Goudie 1990, Carling and Dawson 1996). Therefore, a full review will not be presented in this thesis.

The basic physics behind theories of sediment movement by fluid flow is that the force applied to the sediment is great enough to overcome the specific gravity of the sediment particle. This force is either impact of water strike, drag force or turbulence generated lift (Inman 1949), and causes movement of the particle in the direction of flow. Generally, the size and amount of sediment moved increases with increasing flow velocity, however there are exceptions to this rule to be discussed later.

Sediment may be transported within the flow in three different ways (Norrman 1964, Richards 1982).

- 1). As bedload or contact load, which involves rolling, sliding and surface creep of the sediment. The rate of transport is usually between 2 – 15% of the flow velocity (Richards 1982).
- 2). By saltation or the bouncing along of sediment in episodes of temporary suspension and surface impact.
- 3). In suspension where the sediment is supported within the fluid by the vertical component of turbulent eddies and moves at the rate of the flow.

The three modes of transportation defined above follow a continuum of stages which are arbitrarily defined. Increasing flow intensity will cause a sediment particle of a given size to progress through each stage of transport as illustrated in figure 6.13. Sediment carried entirely within the flow is referred to as being in suspension and sediment moved along the bed surface is bedload (Komar 1998). The continuum of stages from one mode to the other makes definition of a boundary between the two difficult. Sundborg (1956) makes the distinction based on the concentration of suspended material within the flow with the transition between bedload and suspension being where concentration was between 20 – 30%.

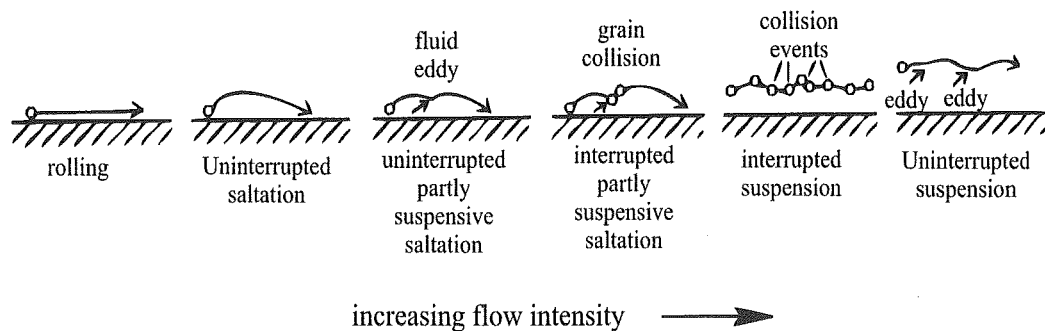


Figure 6.13: Sediment transport modes under conditions of increasing flow intensity. (Richards 1982:fig 4.2a)

Sediment may also be moved within the flow in solution. This method of sediment transportation requires processes aside from water flow and further discussion of it will not be undertaken here.

The most easily entrained particles are 0.18 mm in size (Inman 1949). Greater flow velocities are required to move particles both larger and smaller than this. Larger grains have a greater specific gravity to overcome and therefore require higher flows to initiate movement. Grains of 0.18 mm are thought to be just large enough to create or enhance turbulence within the flow, thus aiding entrainment (Inman 1949). Beds of particles smaller than 0.18 mm tend to present a smoother surface to the flow causing the drag forces to be more evenly distributed over the grains. Sediment of smaller size is also held together more strongly by cohesive forces (Zenkovich 1967). However, once

suspended within the flow the smallest particles will stay there for a significantly longer period of time than larger grained sediment.

Once a particle has been lifted above the bed even the slightest current will cause horizontal displacement during its gravitational fall (Norrman 1964). This horizontal displacement is aided by the fact that once set in motion, a lower velocity is required to keep sediment entrained (Hjulstrom 1939).

Entrainment of sediment depends on a number of important factors. The most influential factor is the velocity of the water (Hjulstrom 1939). This includes both the entrainment threshold velocity and the settling velocity of the sediment (Inman 1949). The threshold velocity (u_c) is the velocity required to initiate movement of a specific sediment particle. Other factors important in sediment entrainment include the character of the water (Hjulstrom 1939), the degree of bottom roughness (Inman 1949), the current characteristics, the range of sediment available (Kirk 1970) and aspects of the particle being entrained (Zenkovich 1967). The threshold velocity provides the initial force or impetus for movement. The character of the water dictates the viscosity of the flow. The degree of bottom roughness and current characteristics determine the turbulence of the flow. Turbulence enhances the ability of a laminar flow to entrain sediment by providing an additional lift force (Norrman 1964). These aspects of flow are combined to define the competence and capacity of that flow. Flow competence is the maximum particle size transportable by that flow and flow capacity is the maximum quantity of sediment transported (Richards 1982). The size range and amount of sediment available dictates what can be moved and the size, shape and specific gravity determine under what conditions it will be moved.

The importance of the combination of size, shape and specific gravity of a particle to sediment movement within a flow lead to the development of the concept of hydraulic size of a grain. Hydraulic size is the rate of fall of a particle in a motionless liquid (Zenkovich 1967). This is assessed easily for smaller sediments in a settling tube. However, larger, more expensive and, for this thesis, unavailable apparatus are required for sediment of the size being dealt with on shore platforms. Therefore, instead of

hydraulic size, a slightly less accurate but more readily available and comparable measure of sediment diameter (B-axis) has been used in the following section.

The calculation of threshold velocities is important when assessing the competence of a flow. Penck (1894 *in* Zenkovich 1967) developed a formula, based on empirical evidence, for initiation of sediment movement by a current over a horizontal surface (equation 6.12).

$$u_t = a\sqrt{r \tan \varphi} \tag{Equation 6.12}$$

Where u_t is the rate of flow, r the radius of the particle, a is a coefficient that depends on the shape of the particle and on friction and φ is the angle of rest of the given material. Zenkovich (1967) also gave a table of critical threshold velocities from various sources, some empirically derived and some theoretically derived. These are presented in figure 6.14 with the addition of critical entrainment velocities given by Sundborg (1956).

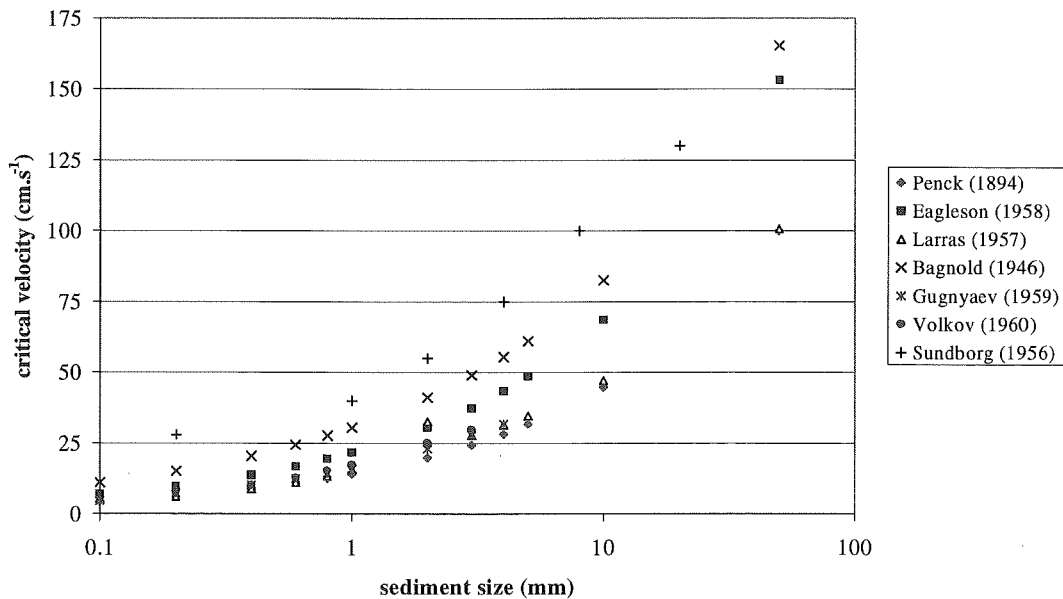


Figure 6.14: Critical entrainment threshold velocities for given sediment sizes. Data from Zenkovich (1967:table 7) and Sundborg (1956).

From figure 6.14 it can be seen that measurements, estimates and predictions of critical entrainment velocities vary for sediment larger than 0.1mm diameter. This makes quantification of the competence of a flow difficult.

Traditionally, critical conditions for entrainment have been determined by correlations between quantity of sediment movement and the difference between measured flows (Komar 1996). For direct evaluation of sediment entrainment thresholds empirical curves are available and widely used (Goudie 1990). One such curve was developed by Hjulsrom (1939), based on empirical evidence, and gives values for sediment erosion, transport and deposition in fluvial environments (figure 6.15).

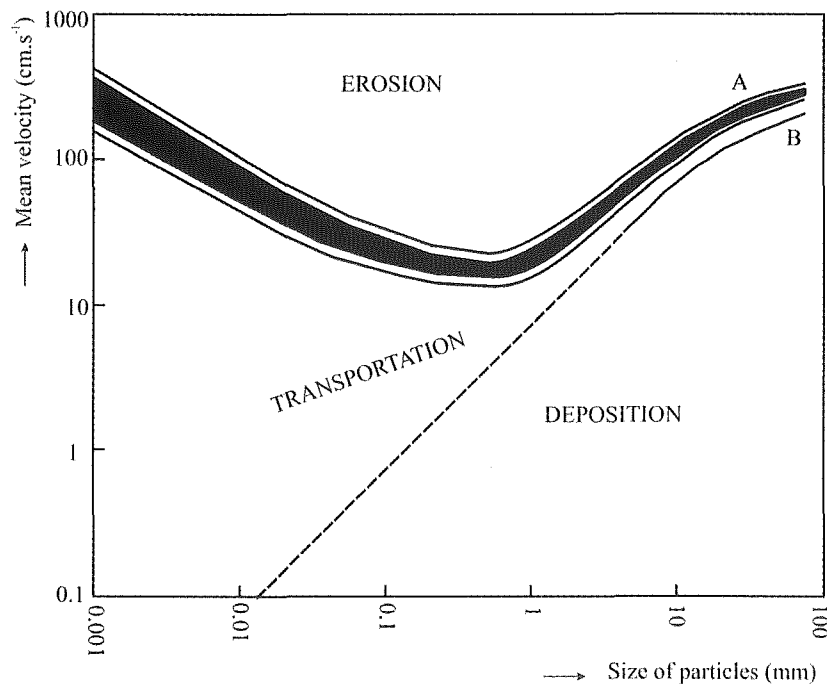


Figure 6.15: The Hjulsrom Curve showing entrainment and transport velocities for given sediment sizes. Logarithmic scale used. (Hjulsrom 1939).

This curve gives a simple graphical indication of the possible behaviour of a sediment particle as the flow regime changes. It applies for average velocity of flow at 1 m above a bed of uniform sized sediment. Hjulsrom (1939:10) regarded the use of average velocity as an independent variable 'as a temporary substitute until more data are (*were*) available'. This is because sediment entrainment is related directly to instantaneous flow rather than average flow and instantaneous velocities can vary significantly around

an average velocity (see section 5.4.3.3). Instantaneous velocities can be up to 3 times the average velocity in the fluvial environment (Richards 1982). Turbulence can be even greater in the coastal environment due to the bi-directional nature of flows. On KM3 a maximum instantaneous velocity difference of 3.8 times the average velocity was recorded and on average, maximum velocities were 3.3 times the average velocity during 18 minute periods (over all three sensors). The largest recorded change in velocity was from -2.5 m.s^{-1} to $+2.5 \text{ m.s}^{-1}$ (5.0 m.s^{-1} in total).

Variation in instantaneous velocity defines the turbulence of the flow and is fundamental to particle movement. Turbulence is by definition spatially and temporally random and can be described statistically (section 5.4.3.3). As turbulent fluctuations in flow are distributed around a mean velocity the initiation of particle motion will be a similarly distributed phenomena (Richards 1982). This, combined with the fact that there are many other factors which influence critical entrainment velocities, is the reason why Hjulstrom (1939) used a band (curve A) to define entrainment velocities rather than a single line.

Curve B on Hjulstrom's diagram gives the competency of flow in relation to sediment size and mean velocity. It shows the power of flow required to carry detritus and reflects the settling velocity of the particles (Hjulstrom 1939). It can be seen in figure 6.15 that the force required to put a particle in motion is greater than the force required to keep it in motion within the flow. Hjulstrom (1939) stated that for gravel sized sediment (1 – 10 mm) flow can decrease up to 30% before deposition begins. Zenkovich (1967) cited a range of 25 – 33% decrease in velocity. Greater divergence of the two curves occurs as sediment becomes progressively smaller. Changes in water viscosity will also effect the settling velocity of particles within the flow. Greater viscosity will result in a lessening of the settling velocity and an increase in the likelihood of the particle remaining in suspension. Increases in viscosity occur with decreases in water temperature or with increases in amounts of finer sediment in suspension. Therefore sediments are transported more easily in winter than in summer (Hjulstrom 1939).

Hjulstrom's curve has been shown to hold for sediment sizes in the middle ranges. However his extrapolation into both finer and coarser sediments was done with less success. Sundborg (1956) revised Hjulstrom's curve at the smaller sediment end accounting for cohesion of fine sediment. He found that consolidated sediment had a greater critical entrainment velocity than originally shown and that unconsolidated fine sediment had a lower one. His corrections are shown in figure 6.16 as dashed lines.

At the coarser end of the sediment spectrum it has been shown empirically that entrainment velocities are somewhat less than those originally anticipated or extrapolated in Hjulstrom's original curve (Novak 1973). Torpen (1956) offered a solution for sediment entrainment of coarser sediment sizes based on empirical evidence and theory developed specifically for coarser sediment. This gives two curves, the lower gives the bottom velocity for sliding and the upper the mean velocity for overturning of larger sediment. Figure 6.16 includes measured entrainment values for given sediment sizes collated in Novak (1973) and Torpen's (1956) solutions. A well defined velocity increase with increasing size is still evident but lower than predicted velocities were required to initiate entrainment of larger particles.

Possible reasons for this deviation at the coarse end of the sediment spectrum may result from:

- 1). Differences in shape, density and orientation of larger particles.
- 2). Bed roughness becomes more significant to coarse sediment transport.
- 3). The effective density of the water was increased due to sand and silt in suspension.
- 4). A velocity other than average 1m high free stream velocity was measured.

Differences in shape, density and orientation may result in the sediment proportionally presenting greater surface area to the force of the flow than smaller sediment does. This provides more leverage for the flow force and may aid in initiation of entrainment.

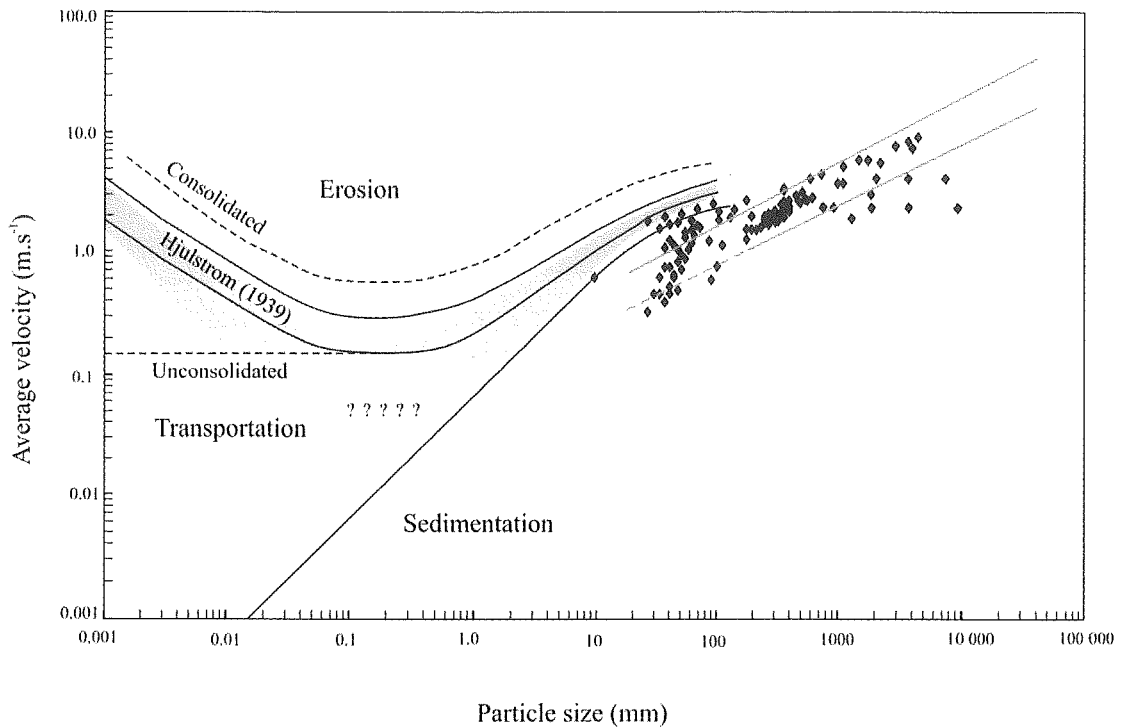


Figure 6.16: Hjulstrom's curve with corrections (*after* Novak 1973). Dashed lines show Sunborg's assessment of finer particle entrainment. Diamonds are empirical results from various sources (*in* Novak 1973). Grey lines are Torpen's (1956) solution for coarse sediment. Shaded area shows hypothesised bottom flow values for Hjulstrom's curve.

Bed roughness may be significant in a number of ways. Larger particles are usually sparsely distributed and do not reside within a bed of uniformly sized sediment. Therefore, there is greater surface area available to the force of the flow. Where large particles are grouped together within the flow, presenting a uniform sized sediment bed, the size of the sediment is such that each individual piece is capable of creating its own turbulent field, thus aiding entrainment.

Where a wide range of sediment is available for entrainment it is likely that smaller sediment, with lower critical entrainment velocities, will become entrained either before or at the same time as the larger sediment. Finer material usually travels in suspension making the entraining fluid more viscous and capable of picking up larger sediment at a lower velocity than anticipated by Hjulstrom's curve.

As it is the velocity of the flow, on the bed, that does the work of entrainment the use of mean 1m high free stream velocities in predicting sediment transport creates problems.

There is no accurate way to relate free stream mean velocity to instantaneous velocity at the bed in such diverse environments. However, Hjulstrom (1939:10) stated that “the velocities near the bottom of the stream would be approximately $10 - 20\text{cm.s}^{-1}$ less than those given on the chart.” The shaded curve on figure 6.16 gives average bed velocities obtained by applying this $10-20\text{cm.s}^{-1}$ reduction to Hjulstrom’s original curve. The lower limit of this bed velocity curve is difficult to define. From study of mixed bed sediment movement Sundborg (1956) observed that a minimum velocity of 0.15m.s^{-1} was required to initiate sediment movement. Any flow with velocity less than this was not capable of entraining sediment. This single straight-line threshold is in apparent conflict with Hjulstrom’s notion of a band of average velocities being responsible for the initiation of sediment movement. Therefore the lower portion of the shaded curve in figure 6.16 is an indication rather than an actual limit.

The empirical curves given in figure 6.16 are generally based on laboratory experiments where single clasts or sediment of a limited range of sizes have been subjected to measured flow conditions. This does not account for the differing nature of entrainment from mixed sediment beds. This and the problems outlined previously have guided recent sediment entrainment research. Komar (1996:136) stated that the critical problems of defining initial grain movement are determining “1) the distribution of flow shear stresses, and 2) the critical shear stress distribution of the bed material.” However, sediment movement across the shore platform environment involves individual sediment particles being entrained from a solid surface rather than the more complex mixed sediment beds on which of many recent sediment entrainment studies have focused. Therefore, indications of critical threshold velocities will be obtained from figure 6.16.

6.3.2 SEDIMENT MOVEMENT IN THE COASTAL ENVIRONMENT.

The theory presented in previous section was developed with fluvial applications in mind. In the study of sediment entrainment and transport in the coastal environment the principles of fluid flow are still fundamental and much of the fluvial work has been utilised. This has usually been in relation to longshore transport, sorting and deposition of sediments on beaches (for examples see Komar 1998). The major difference between

the two environments, the fact that flow is not unidirectional, has been addressed to some extent, usually in relation to the sorting and deposition of the sediment rather than entrainment.

Hjulstrom's curve was developed for rivers. However as stated in the abstract of his 1939 paper 'Transportation of detritus by moving water' many of the relations for river water apply to ocean water, with only a few differences. These differences were listed as 'the large masses of water involved, the slowness with which the water moves and the effect of tides'. It has been shown (section 5.4.3.1) that water flow on the shore platform at KM3 reaches significant velocities as it does in many other coastal surf zones (Kirk 1970). Therefore when applying this model to the shore platform environment the slowness with which the water moves is not an aspect that needs to be considered. The large masses of water involved in the coastal marine environment result in a less constrained flow when compared to the fluvial environment and the effect of the tides is to move the locus of flow across a range of elevations. Norrman (1964) listed the differences between fluvial conditions and the flow conditions near the bottom under waves as: oscillatory forward and backward motion, large and rapid variability and the great macro turbulence in relation to mean velocity. Basically, flow in the coastal environment is not unidirectional and is more turbulent.

Zenkovich (1967) stated that the displacement of material depends on wave parameters such as height, steepness and period. In saying this he was eluding to the relationship between these parameters and the flow field beneath the waves, as it is the velocity of the water that is fundamental to the process. Sediment transport theories that rely on wave parameters, such as height, do so under the assumption that the wave theory being applied holds at the location of study. Komar and Millar's (1975) relationship for prediction of initiation of sediment movement on beaches under wave action is probably the most widely used for the coastal environment (Goudie 1990). It is an empirical relationship that gives two equations relating critical threshold velocities to sediment entrainment for two ranges of sediment sizes. Their determination of the near bottom threshold velocity relied on linear wave theory.

Another theory of sediment movement within the coastal environment is based on the oscillatory nature of waves (Zenkovich 1967). As waves shoal their orbital motion becomes asymmetric. The crests increase in height and steepness and the troughs flatten. The resulting difference in magnitude and duration of velocities in the onshore and offshore directions causes coarser sediments to be transported onshore while finer sediments are transported offshore, with bands of sorted sediment being formed across the beach.

It has been shown previously (section 5.3), that neither linear wave theory nor solitary wave theory holds once the waves have reached the shore platform at KM3. Therefore these approaches will not be used here. Those related directly to flow will be used instead.

6.3.3 SEDIMENT MOVEMENT ON KM3.

Predicting exact amounts of sediment movement in a fluid flow is impossible due to the nature and complexity of the process. It is, however, possible to estimate, with some confidence, size ranges and potential distances of sediment movement. This section uses the most practical tools available to quantify what the potential for sediment movement was on the shore platform at KM3 under the conditions described in Chapter 5. These estimates will provide a good general picture of the process of sediment movement on the shore platform.

Figure 6.16 was used to obtain critical entrainment velocities for a range of sediment particle sizes. Values from the middle of the band representing flow at the bed on the revised Hjulstrom's curve were used rather than the usual free stream velocity at 1 metre above the bed (figure 6.16). Bed velocities were used as they relate directly to the point and process of entrainment. Also 1 metre high free stream velocities in a river would not correlate well to the marine shore platform environment where wave bores drive the pattern of flow. Unlike a river, a bore has a generally uniform average velocity through the entire water column. For sediment greater than 100mm in size a value from the

middle of Torpen's band was used (figure 6.16). It is, therefore, important to remember that the numbers for sediment entrainment and transport in this section represent a value from the middle of a band rather than a single value.

6.3.3.1 POTENTIAL SEDIMENT ENTRAINMENT ON KM3.

Table 6.4 gives critical entrainment velocities, at the bed, (u_t), for given groups of sediment sizes. The critical entrainment velocity shown is that of the largest grain in each class. The Udden-Wentworth grain size classification scale has been used (Lewis and McConchie 1994). For each sediment class the percentage of time conditions for entrainment were equalled or exceeded over each measured tidal cycle is given.

Table 6.4: Sediment entrainment. The competence of flow on KM3 averaged over each tidal cycle. Critical entrainment velocities (u_t) are maximas for each sediment size range and '% time' gives the percentage of time the flow was capable of carrying sediment in the given size range.

| sediment size (mm) | sediment category | u_t (m.s ⁻¹) | % time | | |
|--------------------|-------------------|----------------------------|----------|----------|----------|
| | | | 18/08/01 | 19/08/01 | 24/08/01 |
| < 0.05 | Silt and clay | <0.1 | 100.0 | 100.0 | 100.0 |
| 0.05 - 2.0 | Sand | <0.3 | 94.7 | 94.6 | 94.1 |
| 2.0 - 4.0 | Granules | <0.5 | 63.7 | 63.6 | 60.5 |
| 4.0 - 64 | Pebbles | <0.9 | 35.7 | 36.0 | 33.6 |
| 64 - 256 | Cobbles | <1.5 | 9.1 | 10.1 | 9.1 |
| 256 - 1000 | Boulders | <3.5 | 0.6 | 0.9 | 1.0 |
| 1000+ | Blocks | 3.5+ | 0.0 | 0.0 | 0.0 |

While the tide covered the platform flow was always capable of entraining silt, clay and fine sand. As critical entrainment velocities are higher than critical transport velocities, this means that these sizes of sediment, once entrained, were also likely to be transported in suspension during the entire time that the tide covered the platform. It was possible for sand to be entrained at least 94 % of the time and there was even potential for movement of boulders up to 1% of the time.

6.3.3.2 SEDIMENT ENTRAINMENT ON KM3.

As stated earlier, the fact that shore platforms are commonly bare of sediment, as is the case at KM3, means that sediment movement must occur. An indication of the representativeness of figures shown in table 6.4 can be gained from an analysis of sediment observed to have moved onto, over and/or off the shore platform near KM3. These ranged from the removal of silts, clays and sands, as observed by the MEM measurements, through to cobbles and boulders. The a, b and c axis of seven cobbles and boulders resting on the platform surface at low tide on 5/6/2000 and 4/5/2002 were measured (see figure 6.10 A and B). The B axis measurements ranged from 105 – 540 mm, classing some of these sediment as significantly sized boulders. All of these rocks were moved off the platform by water flow within four tidal cycles. Entrainment of the largest of these would have required a critical velocity of 2.3m.s^{-1} and once set in motion a critical transport velocity of 1.7m.s^{-1} . As is shown in table 6.4 these velocities did occur on KM3 during the measurement period.

The importance of sediment movement over shore platforms means that this process warrants closer investigation. Spatial differences in flow across the platform mean that the processes of sediment entrainment and transport will also be spatially diverse. Where does the sediment go and how quickly does it go there?

6.3.3.3 VECTOR SEDIMENT ENTRAINMENT SUMMATIONS.

Once sediment is entrained it is transported by the flow. In the fluvial environment flow is gravity driven and will generally result in sediment being transported down stream. Flow in coastal environments is driven primarily by waves, not gravity. In terms of sediment movement theory, this is the biggest difference between the fluvial and coastal environments. As with the fluvial environment the initial entrainment of sediment in the coastal environment is determined by the instantaneous velocity and turbulence. However, the transportation and place of eventual settlement of sediment are determined by the oscillatory motion and resulting asymmetric flow of the waves.

Generally in the coastal environment it has been reported that coarser sediment moves shoreward and finer sediment moves offshore due to the asymmetry of flow under waves (Zenkovich 1967, Komar 1998, Allan 1998). Norrman (1964:84) stated “it is typical of all exposed shores (around Lake Vattern) that there are no fine sediments... All material which does not settle in the intervals between the maxima of oscillatory motion will move out of the environment.” These studies have all been undertaken on beach environments where onshore impulses (swash) are usually greater than those offshore (backwash) due to the absorption of some wave energy within the mobile sediment bed. However, shore platforms are fundamentally different from beaches in that the ‘bed’ is solid rock and therefore does not absorb wave energy in the same way. Flows that come in across the top of the shore platform must also go back out across the top of the shore platform. They are only reduced in magnitude by the effect of friction, not the combined friction and percolation effects that occur with flow across mobile beds. The shore platform environment is therefore potentially more turbulent with a greater capacity for sediment transport in the offshore direction.

It is possible to evaluate the competence of the flow and net direction of transport of sediment using vector diagrams constructed in a similar manner to those in figure 5.48. Figures 6.17, 6.18 and 6.19 show the net trajectories of water flow for two different critical entrainment velocities over 18 minute periods recorded on the hour every hour while water covered the platform at KM3. A threshold velocity of 0.1 m.s^{-1} was used for figures 6.17A, 6.18A and 6.19A. This relates to the critical entrainment velocity of silts, clay and fine sands. A threshold velocity of 1.0 m.s^{-1} was used for figures 6.17B, 6.18B and 6.19B, relating to the critical entrainment velocity of 120 mm sized sediment. Each vector is the product of the magnitude of flow (m.s^{-1}) multiplied by the frequency of time flow was above the threshold velocity (%) in each of the eight directions. Resultant vectors, therefore, show both the direction and magnitude of the net impulse of water flow on sediment of the two sizes corresponding to the entrainment velocity thresholds used. Vectors were constructed in an excel spread sheet and redrawn to scale using CorelDraw. These vector flow summations represent impulses felt by sediment and therefore also represent the possible direction and magnitude of sediment movement. Sediment of the silt, clay and fine sand sizes are most likely to go directly into

suspension once entrained and will therefore follow the path of the water flow at the same velocity as the water itself. Larger sediment, once entrained by the flow, is more likely to remain as bed load. Although it will still follow the path of the water flow it will do so at a significantly slower velocity. The following description of vector flow summations refers to flow impulses felt by sediments of the given grain size.

Figures 6.17, 6.18 and 6.19 give an indication of what the general net impetus of water flow on sediment across KM3 was. It is important to note that the actual path followed by entrained sediment would have been far more complex. The dynamic nature of the successive impulses that a particle was subjected to can be seen in figure 5.44. This has implications for abrasive work done on the shore platform. The vector diagrams of figures 6.17, 6.18 and 6.19 show the cumulate results of these impulses.

Generally the flow became less competent closer to the landward cliff of KM3. This relates directly to the reduced magnitude of the flow recorded at sensor 3 when compared to flows at sensors 1 and 2. Flows at sensor 3 would have been able to entrain sand and smaller sediments but not sediments of 120 mm in size. However, this does not necessarily mean that sediment of 120 mm in size could not have been transported through this area once entrained within the flow elsewhere.

There were significantly different rates of flow for each sediment type with the smaller sediment being subjected to proportionally larger impulses.

Direction of sediment movement varied across the platform. For example on 18/08/01 offshore movement would have occurred over the seaward portion of the profile but onshore movement was shown over the mid and landward portions. For the majority of the time over which flow measurements were made, movement of both smaller and 120 mm sized particles over the seaward portion of the platform was generally in the seaward direction regardless of the movement of sediment across the remainder of the platform. Therefore if sediment were moved into this seaward zone it would be transported directly offshore. As the platform has a distinct seaward cliff, sediment would therefore be lost to the system.

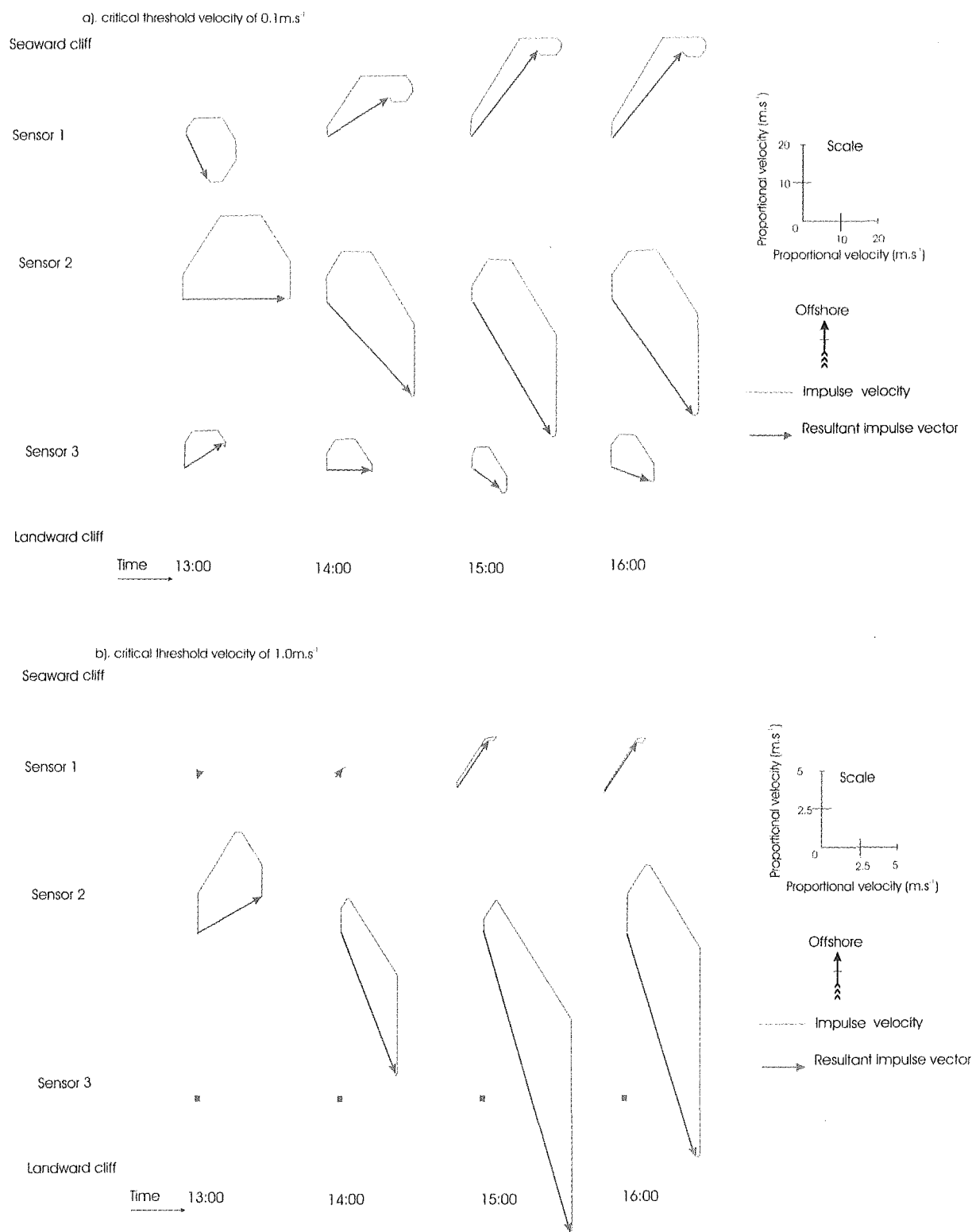


Figure 6.17: Vector summations of the impulse of water flow on sediment for critical threshold velocities of: a). 0.1 m.s^{-1} (silt, clay and fine sand), b). 1.0 m.s^{-1} (120 mm sediment). A vector summation of magnitude multiplied by frequency is given for each 18 minute reading at each sensor on 18/08/01. Note the different scales used for a and b.

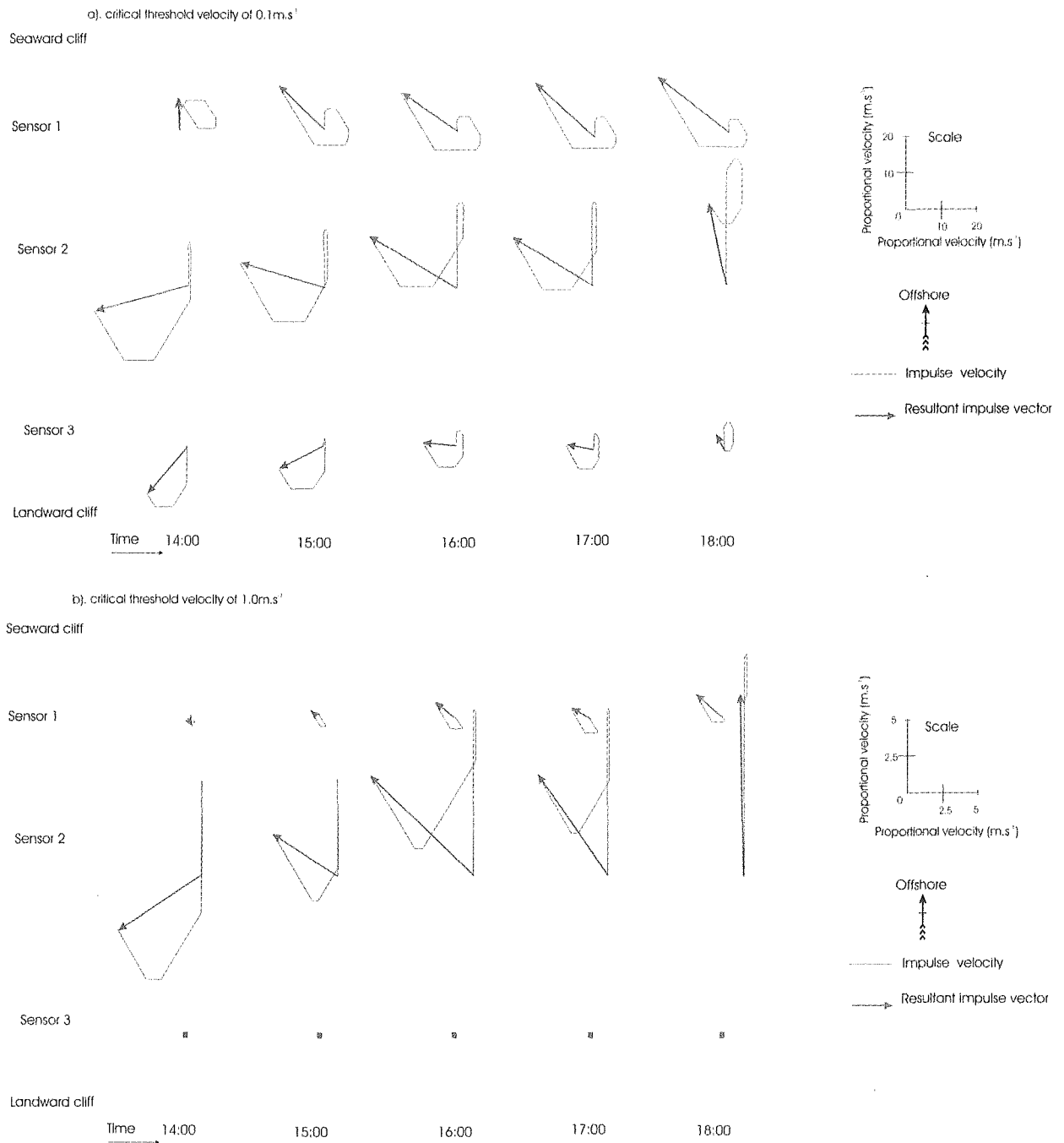


Figure 6.18: Vector summations of the impulse of water flow on sediment for critical threshold velocities of: a). 0.1 m.s^{-1} (silt, clay and fine sand), b). 1.0 m.s^{-1} (120 mm sediment). A vector summation of magnitude multiplied by frequency is given for each 18 minute reading at each sensor on 19/08/01. Note the different scales used for a and b.

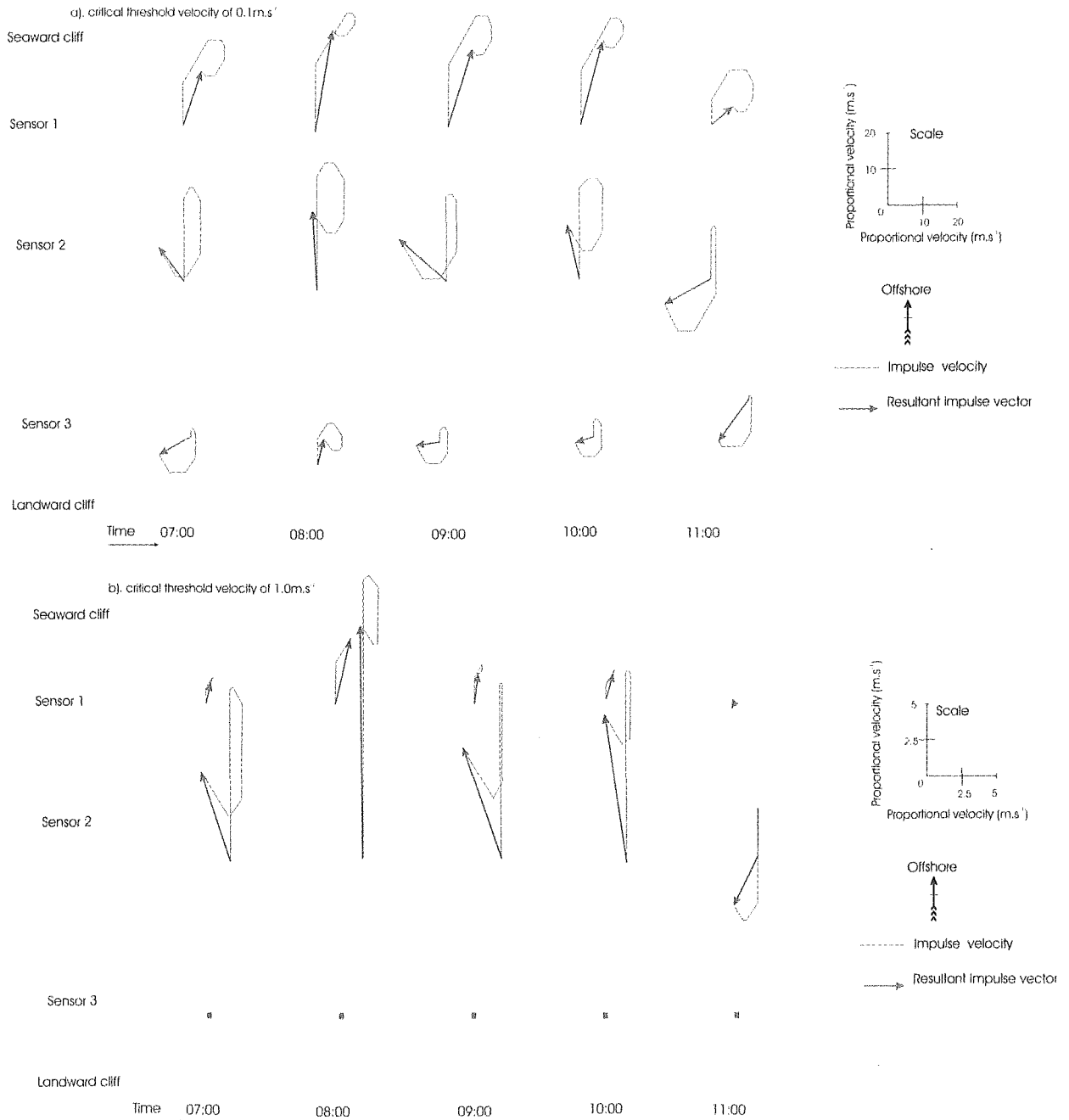


Figure 6.19: Vector summations of the impulse of water flow on sediment for critical threshold velocities of: a). 0.1 m.s^{-1} (silt, clay and fine sand), b). 1.0 m.s^{-1} (120 mm sediment). A vector summation of magnitude multiplied by frequency is given for each 18 minute reading at each sensor 24/08/01. Note the different scales used for a and b.

There were significant amounts of lateral movement of smaller sediment with slightly less lateral movement of larger particles.

Longshore direction of flow appears to be related directly to prevailing deepwater wave conditions. On 18/08/01 northerly swell was occurring and lateral movement of sediment was generally alongshore to the south. On 19/08/01 and 24/08/01 deepwater conditions had changed to a south to south-easterly swell and lateral movement of sediment tended alongshore to the north. As comprehensive deepwater directional wave data was not available, further analysis of this proposal is not possible.

There appeared to be changing potential sediment movement patterns with the rise and fall of the tide. For example on 19/08/01 there was a swing to seaward flow impulses with the fall of the tide. More data would be required to confirm any general patterns.

The vector flow summations of figures 6.17, 6.18 and 6.19 can be thought of as representative of sediment entrainment and transport through a compartment on the shore platform around the KM3 profile. Provided sediment particles are not constrained by morphology they will follow the trajectories shown by the resultant vectors. However, where particles go once they have moved out of this compartment will be dictated by the flow patterns and the morphology of the neighbouring compartment. As comprehensive grid sampling of platform flows was beyond the scope of this thesis it is assumed that flows recorded across the profile of KM3 are reasonably representative of general platform flows. Sampling sites were chosen to be as representative as possible. However, the dynamic nature of the system means that some variation will occur. There are a number of channels running across the platform, usually along joints, which may direct the lateral flow.

As smaller sediment travels in suspension it will go with the flow moving where the water takes it until the magnitude of the flow drops below the critical transport velocity for that size particle. The sediment will then be deposited. Larger sediment however tends to move as bed load and may be constrained by morphology. It is possible that it

may become trapped in crevices, joints or channels either by reduction in the flow below critical velocity levels due to morphological influences at these locations or by becoming wedged in place. Once wedged, sediment would require greater force to move it again. Sediment was observed collected in joints and channels on the platform near KM3. Channels may also encourage greater sediment movement by directing and intensifying flow. In some cases causing sediment to move off the platform. There are a number of large channels near KM3 (figure 6.20) which may modify the flow and hence the sediment trajectories.



Figure 6.20: Oblique photo of KM3 showing channels along jointing.

6.3.3.4 POTENTIAL SEDIMENT TRANSPORT DISTANCES.

It is possible to calculate the total net distance that sediment was potentially transported by multiplying the length of the resultant vectors in figures 6.17, 6.18 and 6.19 (as a percentage) by the amount of time over which the impulse flow force was applied to the sediment. Potential total net distances travelled by the finer sediment and 120 mm sized sediment are shown in table 6.5. A time period of 4 hours was used, as this was the length of time over which flow measurements were made. Water covered the platform for slightly longer than this. However, at early and late stages of coverage water depth was insufficient for flow measurement.

Table 6.5: Potential net distance, in metres, of sediment movement on KM3 over a tidal cycle (4 hour period).

| date and start time of 18 minute | potential sediment travel distance (m) | | | | | |
|--|--|-------------|----------|-------------|----------|-------------|
| | Sensor 1 | | Sensor 2 | | Sensor 3 | |
| | 1mm size | 120 mm size | 1mm size | 120 mm size | 1mm size | 120 mm size |
| 18/8/01 13:00 | 1945 | 3 | 3844 | 103 | 1809 | 0 |
| 18/8/01 14:00 | 2645 | 13 | 4867 | 213 | 1639 | 0 |
| 18/8/01 15:00 | 4161 | 78 | 5989 | 438 | 1304 | 0 |
| 18/8/01 16:00 | 4072 | ave | 5232 | ave | 1504 | ave |
| | 3206 | 81 | 4983 | 317 | 1564 | 0 |
| | | ave | | ave | | ave |
| | | 44 | | 268 | | 0 |
| 19/8/01 14:00 | 1369 | 11 | 3872 | 149 | 2296 | 0 |
| 19/8/01 15:00 | 2499 | 9 | 3517 | 116 | 1939 | 0 |
| 19/8/01 16:00 | 2759 | 35 | 3922 | 207 | 1313 | 0 |
| 19/8/01 17:00 | 3108 | 33 | 3583 | 179 | 1159 | 0 |
| 19/8/01 18:00 | 3517 | ave | 3233 | ave | 748 | ave |
| | 2650 | 51 | 3626 | 262 | 1491 | 0 |
| | | ave | | ave | | ave |
| | | 28 | | 183 | | 0 |
| 24/8/01 7:00 | 2321 | 31 | 1710 | 136 | 1495 | 0 |
| 24/8/01 8:00 | 4099 | 96 | 3142 | 339 | 1066 | 0 |
| 24/8/01 9:00 | 3131 | 45 | 2547 | 171 | 1008 | 0 |
| 24/8/01 10:00 | 3373 | 43 | 2225 | 215 | 797 | 0 |
| 24/8/01 11:00 | 1185 | ave | 2196 | ave | 2040 | ave |
| | 2822 | 3 | 2364 | 82 | 1281 | 0 |
| | | ave | | ave | | ave |
| | | 44 | | 189 | | 0 |

Total ave distance travelled by 1mm size sediment 2623

Total ave distance travelled by 120mm size sediment 82

Once entrained finer sediment (silt, clay and fine sand) with $u_t = 0.1\text{m.s}^{-1}$ moves as suspended load within the water column and will therefore follow the trajectory of the water itself. For finer sediment the maximum potential distance travelled was just less than 6000m and the minimum distance was 748m. On average over the entire profile finer sediment was transported 2.6 km over a tidal period (4 hours). This is a considerable distance and sufficient for sediment to be moved offshore regardless of direction of flow. The platform at KM3 is only 90 m wide and stretches laterally for approximately 500 m to the Northeast and approximately 1600 m to the Southwest, with a sharp 1.5 m drop to a lower limestone surface approximately 300 m to the south-west.

Figures 6.17B, 6.18B and 6.19B show net impulses of water flow above $u_t = 1.0\text{ m.s}^{-1}$. As sediment of 120 mm in size moves as bed load rather than in suspension it will not travel at the same velocity as the water flow. Richards (1982) reported that bed load sediment moved at 2 – 15 % of the impulse water velocity. Hjulstrom (1939) conducted an experiment investigating the velocity of different sized rolling particles in steady flow and found sediment movement rates of 30 – 60 % of impulse water velocity.

Ascertaining a velocity of bed load from water flow data is therefore problematic and confused by the behaviour of different particles within the same flow. For example larger particles tend to move faster and stop less frequently than smaller ones (Inman 1949). As no direct measurement of sediment entrainment velocities was possible, the value of 15% of water velocity has been used here. Using this best estimate of 120 mm sediment moving at 15 % of impulse water velocity potential distances travelled by these sized particles ranged from 438 to 0 m and average distance travelled for the whole platform was 82m. This is one to two orders of magnitude less than the distance travelled by the finer sediment but under favourable directional conditions still sufficient distance for sediment to be transported offshore.

6.3.3.5 LONGINOV'S METHOD.

The analysis in the previous section gives details on the distances and directions of sediment transport of two specific sediment sizes. It does not show the potential transport over all sediment size ranges. In order to assess sediment entrainment over the range of sediment sizes available a method developed by Longinov (*in* Zenkovich 1967:129 - 135) has been employed. This method calculates quantities which express both direction and intensity of sediment transport in the onshore and offshore directions for given sediment size categories. Longinov used pressure measurements from under waves which he correlated to fluid flow. He then related fluid flow to critical entrainment velocities of a range of sediment sizes and compared this to an estimate of the net direction of particle motion derived from the frequency of occurrence at given velocity intervals in both the onshore and offshore directions.

As flow velocities have been measured directly (Chapter 5) the correction for pressure is not required here. Critical velocities for a range of sediment sizes are given in table 6.4.

Longinov's method considered the distributions of net velocities (from pressure) in records lasting several minutes. The total range of velocities (u) in a record were divided into groups by absolute magnitude. The total time that each velocity group was directed onshore (positive impulse) or offshore (negative impulse) was calculated (i) and

expressed as a percentage of the total duration of the record ($i(\%)$). The onshore and offshore components were summed algebraically giving the net velocity deficit for each velocity range (Δi). The velocity deficit was multiplied by the mean velocity of the interval which gave net proportional velocity for each interval, expressed in relative magnitude independent of the length of the actual record ($u\Delta i$). The proportional velocities were summed from highest to lowest with allowance for sign, resulting in a proportional net velocity for each velocity group (Σ). This summation from highest to lowest was undertaken as each smaller group of sediment will be subjected to all impulses higher than their critical velocity.

A worked example of the calculations required to construct Longinov's impulse diagrams is presented in table 6.6. It uses data from sensor 1 on 18/08/01 13:00. The total amount of time for each group was expressed in seconds. Direction of flow was determined by placing each separate flow reading into an onshore (+) or offshore (-) bin. Onshore flows were defined as those that flowed through a 135° wedge centred on the onshore direction and likewise for offshore flows. For example a flow defined by the vector shown in figure 6.21 (dashed line) was classified as onshore and the absolute magnitude of this flow was then used in subsequent calculations. Actual directions of flow were used rather than component onshore (x) and alongshore (y) vectors as it is direct flow impulse which causes sediment movement rather than the constituents of that flow.

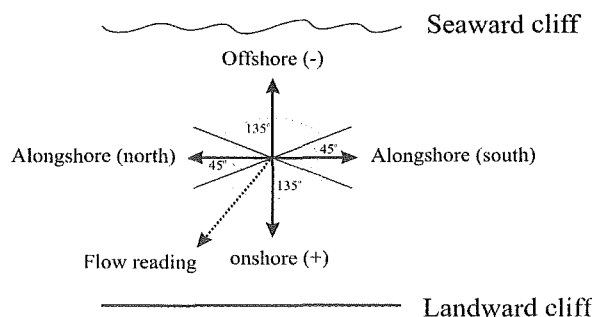


Figure 6.21: Definition sketch of flow direction as used when applying Longinov's method to the flow data recorded at KM3.

Table 6.6: Calculation table used for constructing a distribution graph of proportional net velocity for a range of sediments, using Longinov's method. For data from sensor 1 on 18/08/01 13:00.

| u (m.s ⁻¹) | i (seconds) | | i (%) | | Δi (%) | u Δi | Σ |
|------------------------|-------------|------|-------|-----|----------------|--------------|----------|
| | + | - | + | - | | | |
| 0.0-0.2 | 95.5 | 64.5 | 8.8 | 6.0 | 2.9 | 0.3 | 13.5 |
| 0.2-0.4 | 220.6 | 84.9 | 20.4 | 7.9 | 12.6 | 3.8 | 13.2 |
| 0.4-0.6 | 162.1 | 43.8 | 15.0 | 4.1 | 11.0 | 5.5 | 9.4 |
| 0.6-0.8 | 54.4 | 11.9 | 5.0 | 1.1 | 3.9 | 2.8 | 3.9 |
| 0.8-1.0 | 13.0 | 0.3 | 1.2 | 0.0 | 1.2 | 1.1 | 1.2 |
| 1.0-1.2 | 1.5 | 0.3 | 0.1 | 0.0 | 0.1 | 0.1 | 0.1 |
| 1.2-1.4 | 0 | 0 | 0 | 0 | 0 | 0 | 0 |
| 1.4-1.6 | 0 | 0 | 0 | 0 | 0 | 0 | 0 |
| 1.6-1.8 | 0 | 0 | 0 | 0 | 0 | 0 | 0 |
| 1.8-2.0 | 0 | 0 | 0 | 0 | 0 | 0 | 0 |
| 2.0-2.2 | 0 | 0 | 0 | 0 | 0 | 0 | 0 |
| 2.2-2.4 | 0 | 0 | 0 | 0 | 0 | 0 | 0 |
| 2.4+ | 0 | 0 | 0 | 0 | 0 | 0 | 0 |

total 547.1 205.5
 1080 = 100%

Net impulse diagrams have been constructed, following Longinov's method, for every 18 minute set of data recorded (figures 6.22, 6.23 and 6.24). Velocity groups are plotted on the x-axis in 0.2m.s⁻¹ intervals. Below this sediment sizes moved by these velocities are indicated. Impulses in the onshore/offshore direction are shown as bold lines. Due to the strength of the lateral component of the flow, alongshore impulses have also been calculated and graphed (fine lines). Alongshore flows were defined as those within a 45° wedge centred on either the northerly or southerly alongshore directions (figure 6.21). Curves are shown for each sensor.

Figures 6.22, 6.23 and 6.24 show that the proportional net velocities (or impulses) felt by sediment on the shore platform at KM3 were significant. The flow was always capable (competent) of moving sediment of sizes up to and including pebbles at all sites across the platform. Flow was most competent at sensor 2 in the middle of the platform where figures 6.22, 6.23 and 6.24 indicate that it was possible for boulders to be entrained.

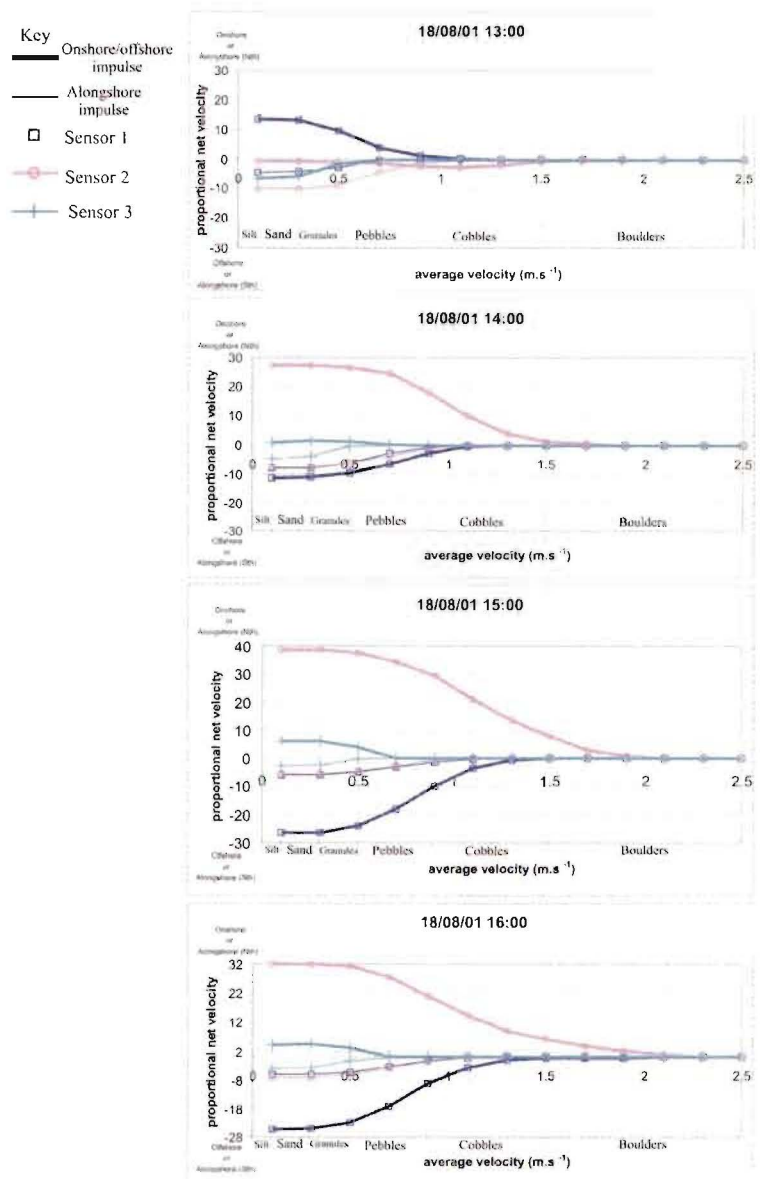


Figure 6.22: Proportional net velocity diagrams (constructed according to Longinov’s method) Calculated for each 18 minute period recorded while water covered the shore platform at KM3 on 18/08/01. Positive impulses were in the onshore or alongshore-north direction and negative in the offshore or alongshore-south direction. Curves are shown for each of the three sensors. A key is provided.

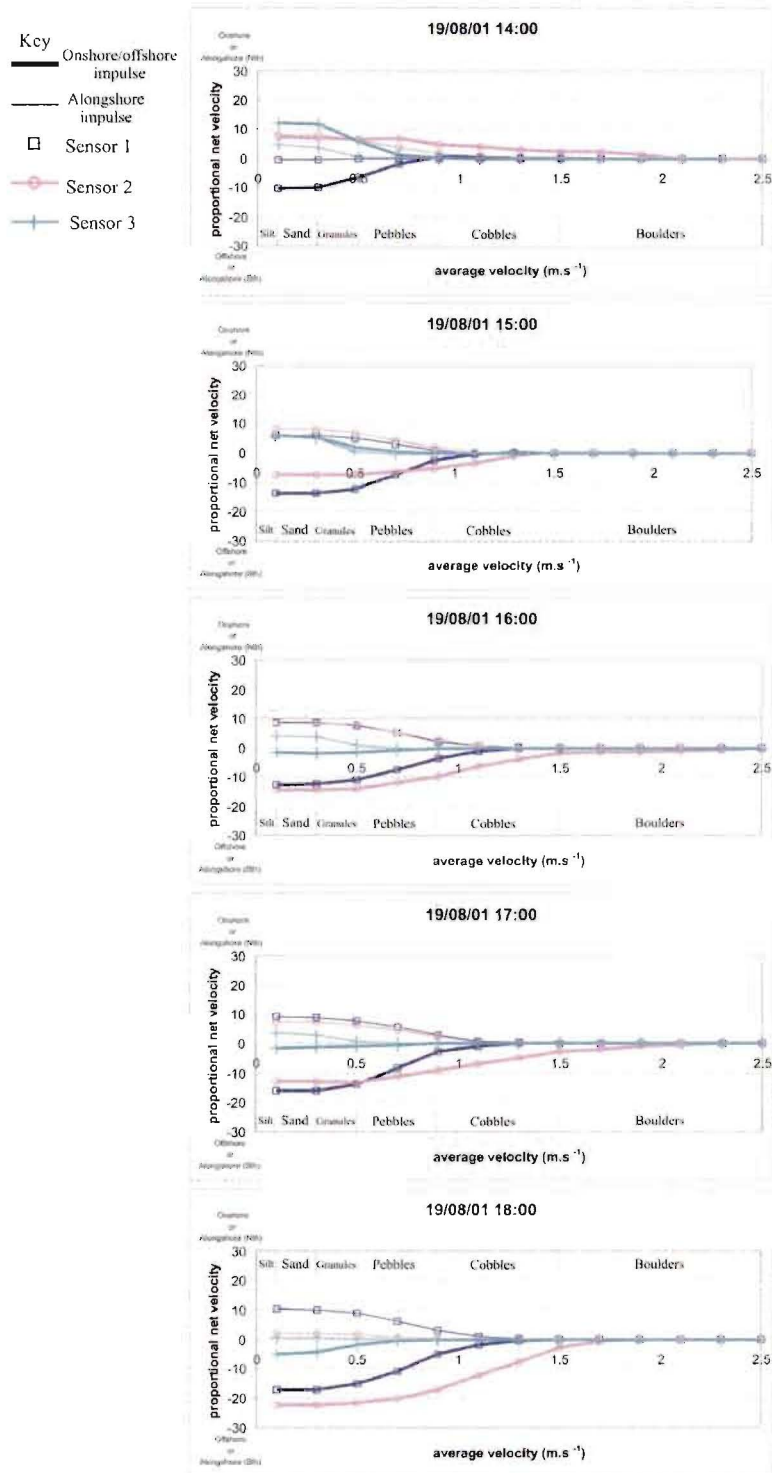


Figure 6.23: Proportional net velocity diagrams (constructed according to Longinov's method) Calculated for each 18 minute period recorded while water covered the shore platform at KM3 on 19/08/01. Positive impulses were in the onshore or alongshore-north direction and negative in the offshore or alongshore-south direction. Curves are shown for each of the three sensors. A key is provided.

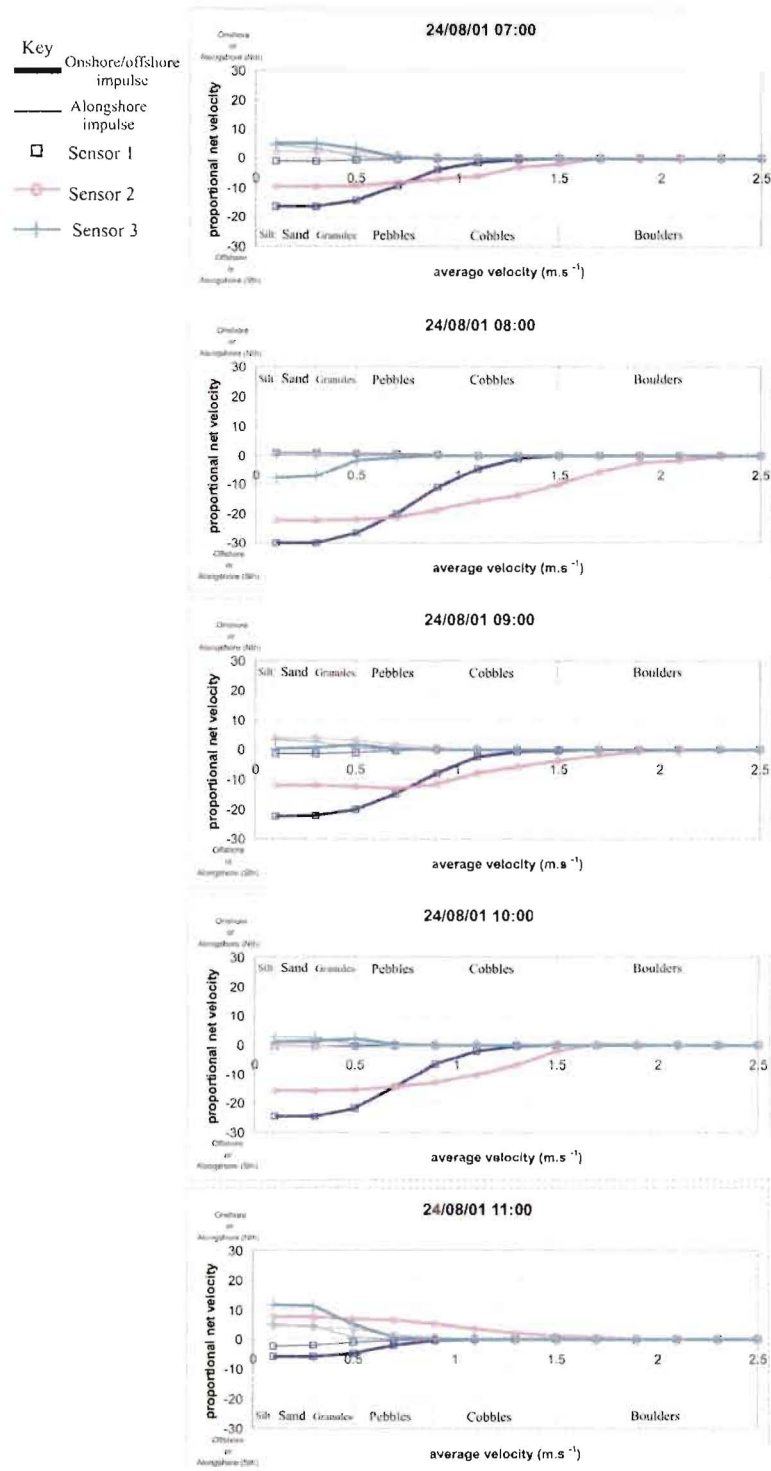


Figure 6.24: Proportional net velocity diagrams (constructed according to Longinov’s method) Calculated for each 18 minute period recorded while water covered the shore platform at KM3 on 24/08/01. Positive impulses were in the onshore or alongshore-north direction and negative in the offshore or alongshore-south direction. Curves are shown for each of the three sensors. A key is provided.

For the majority of the time sediment movement was directed offshore. This was especially the case at sensor 1 where only one 18 minute record (18/08/01 13:00) shows onshore impulse. Such a dominance of offshore sediment movement would explain the lack of sediment on shore platforms as once the sediment moves over the seaward cliff it is lost to the system. There were also net potential movements of sediment in the alongshore directions over a similar range of sediment sizes as the onshore / offshore ones. Although these are not of the same magnitude they would have still been competent at entraining sediment.

Where onshore movement of sediment was indicated there was also alongshore flow which would have prevented settling of sediment on the 'backshore' (near the seaward cliff) of the platform.

In general the greatest potential for movement of sediment was in the centre of the platform with the flow being competent over a wider range of sediments. However the magnitude of impulses at sensor 1 for silt – granule sized sediment was often higher than that at sensor 2. Finer sediment moved into and through the seaward portion of the platform would have been exposed to greater net impulse forces from the flow.

Figure 6.22 confirms the pattern evident in figure 6.17 of a dual pattern of sediment movement across the platform on the 18/08/01. There was a very strong offshore sediment movement over all size ranges over the seaward portion of the platform and even stronger onshore movement over the mid and landward portions of the platform. This pattern was not evident on either figure 6.23 or 6.24 where offshore movement was predominant over the entire platform.

On the 19/08/01 potential net movement at sensor 3 appeared to be related to the tide with onshore movement of sediment as the tide rose changing to an offshore movement as the tide fell (figure 6.23). This pattern, however, was not evident in either figure 6.22 or 6.24.

The diversity of these diagrams serves to emphasise the dynamic nature of sediment entrainment and transport over time on the shore platform at KM3. Significant differences in patterns of potential net sediment movement, not only between tides but also during tidal cycles themselves were evident. However, dominance of offshore movement is shown which explains the lack of sediment present on the shore platform at KM3 and on shore platforms in general.

This dominance of proportional offshore net velocity is not typical in coastal environments. Kirk (1970) showed a dominance of proportional net onshore pressure (related to velocity) over sediment sizes on mixed sand and gravel beaches at Kaikoura. There most potential net movement of sediment was onshore. However the potential net movement often showed asymmetry across the sediment size range. In some cases while smaller particles were subjected to net onshore impulses, coarser particles experienced net offshore impulses during the same time period. This is typical of many beach systems (Zenkovich 1967). Asymmetry such as this was not evident on the shore platform at KM3.

The analysis above has shown that there is potential for net movement of sediment over a large range of sizes up to and including small boulders under 'normal' flow conditions on KM3. This therefore defines the size that the rock of the platform needs to be broken down to before it can be transported offshore as sediment. This is not necessarily small with potential transport of boulders (B-axis of up to 1000mm) being shown.

However the fact that relatively little sediment was observed on the platform at KM3 would mean that little is available for transport, therefore the limiting factor in the process of sediment movement on, over and off shore platforms is the availability of sediment.

Vector summation analysis and Longinov's potential net velocity diagrams have provided a useful summary of the competence of the flow across the shore platform at KM3 in relation to average and instantaneous flows. There are however some drawbacks to these methods.

Critical velocities for sediment size ranges using Hjulstrom's curve have been obtained from the average velocity. Although the impulses felt by the sediment shown in the potential net velocity diagrams are related directly to the flow the actual size of particle shown to be moved by the impulses may vary slightly for reasons explained previously (section 6.2.1).

In using average values of flow velocity no account is made for the effect of turbulence as an aid to sediment entrainment. When greater levels of turbulence occur this provides additional lift forces and average horizontal flow forces required to entrain sediment are reduced. If turbulence contributes to the lift forces within the flow the amount of force required by the laminar component of flow to cause entrainment would be less. The issue of turbulence adding to the shear stress that a particle is subjected to within the flow is an area for further study.

Another problem with assessing the competence of flows over the shore platform at KM3 was that conditions recorded were fairly typical or 'normal'. The analysis does not include the effect of a 'big event'. In terms of sediment transport a 'big event' on the shore platform would be one with high velocity flows. Maximum velocities that flow on the shore platform at KM3 may reach are, as yet, undefined and as shown in section 5.4.2 it is difficult to predict which deepwater wave conditions will translate to 'big events' on the shore platform.

6.3.4 WAVE EFFECTIVENESS

The previous section quantified the magnitude of sediment movement over the shore platform at KM3 but it did not define which of flow actually did the greatest amount of work. By investigating the power of the flow it is possible to further elucidate the work done by waves as they cross the shore platform. McCave (1971) devised a parameter called wave effectiveness which is related to the power of the flow. The concept of wave effectiveness "rests on the notion that the geomorphic work that can be accomplished by

waves is the product of the mass rate of sediment transport and the frequency of occurrence of the transport.” (Kirk in prep.) Wave events with a maximum ‘magnitude and frequency’ product are the most efficient at causing change in an environment. This concept can be usefully applied to the shore platform situation even though it was originally developed for waves passing over a mobile bed of unconsolidated sediment.

McCave (1971) assumed that the instantaneous sediment transport rate was proportional to the available fluid power of the flow. He showed that power ($\omega = \tau u$) is proportional to the cube of the near bed velocity (u_p) (equation 6.13). See equation 6.5 for value of τ .

$$\omega \propto u_p^3$$

Equation 6.13

The amount of work done by the flow per unit area of bed is then a multiple of the power (u_p^3) and the percent of time for which a given velocity is exceeded (P). This is the wave effectiveness parameter and when plotted against a value proportional to the shear stress exerted by the flow on the bed (u^2) the resultant curves can be used to define conditions and locations of maximum wave effectiveness.

This suggests that there are some events of moderate to large magnitude and moderate frequency which account for the most change over a period of years. Those events with high magnitude and very low frequency and those with higher frequency but low magnitude will yield low wave effectiveness values.

Figures 6.25, 6.26 and 6.27 show wave effectiveness for each recorded 18 minute flow period. Although each cover only a small period of time it is possible to distinguish which parts of the flow were potentially most effective in terms of geomorphic work. The peak of each curve defines the conditions of maximum geomorphic work. From figures 6.25, 6.26 and 6.27 it is evident that the greatest potential geomorphic work was not accomplished by the maximum flow velocities and that total amounts of geomorphic work varied spatially across the platform and to a lesser extent temporally during the tide.

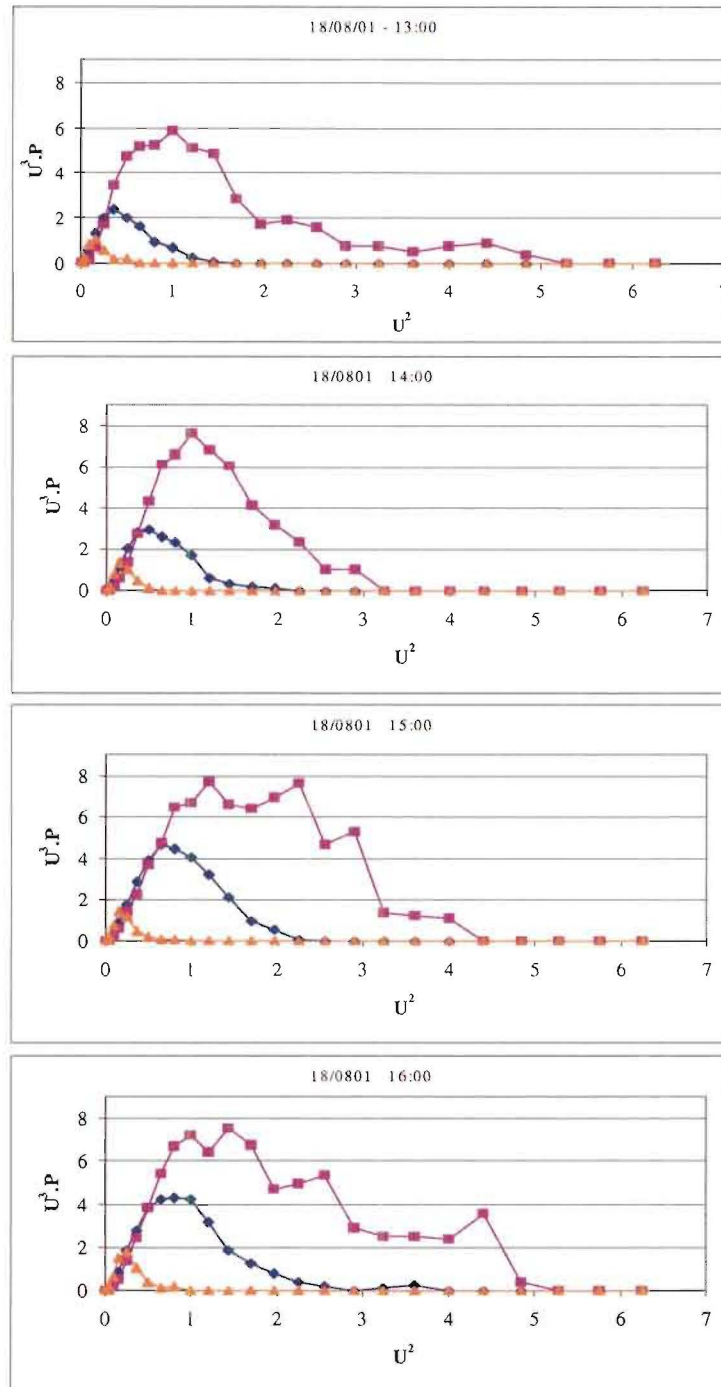


Figure 6.25: Wave effectiveness plots for 18 minute periods recorded at KM3 on the hour every hour while water covered the shore platform on 18/08/01. Wave effectiveness ($u^3.P$) is plotted against a proportional value for shear stress (u^2). Curves are shown for sensor 1 (\blacklozenge), sensor 2 (\blacksquare) and sensor 3 (\blacktriangle).

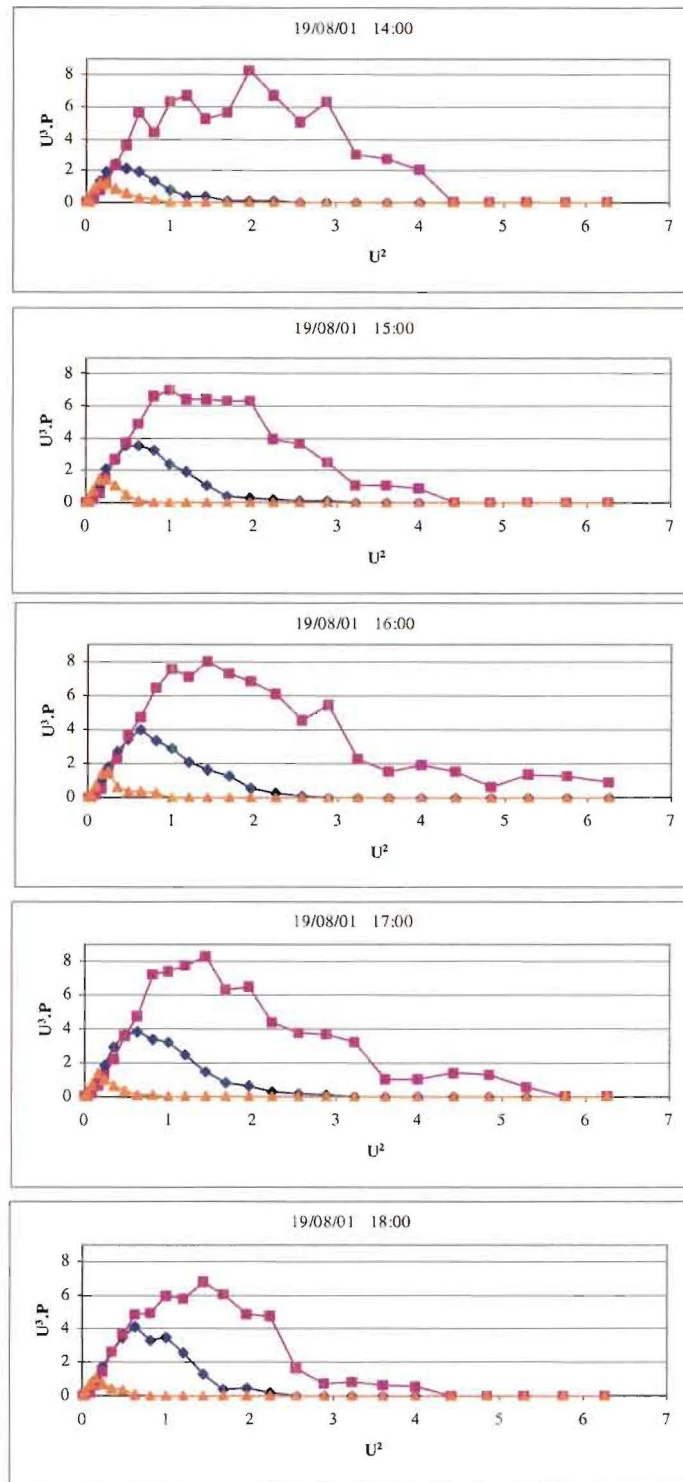


Figure 6.26: Wave effectiveness plots for 18 minute periods recorded at KM3 on the hour every hour while water covered the shore platform on 19/08/01. Wave effectiveness ($u^3.P$) is plotted against a proportional value for shear stress (u^2). Curves are shown for sensor 1 (\blacklozenge), sensor 2 (\blacksquare) and sensor 3 (\blacktriangle).

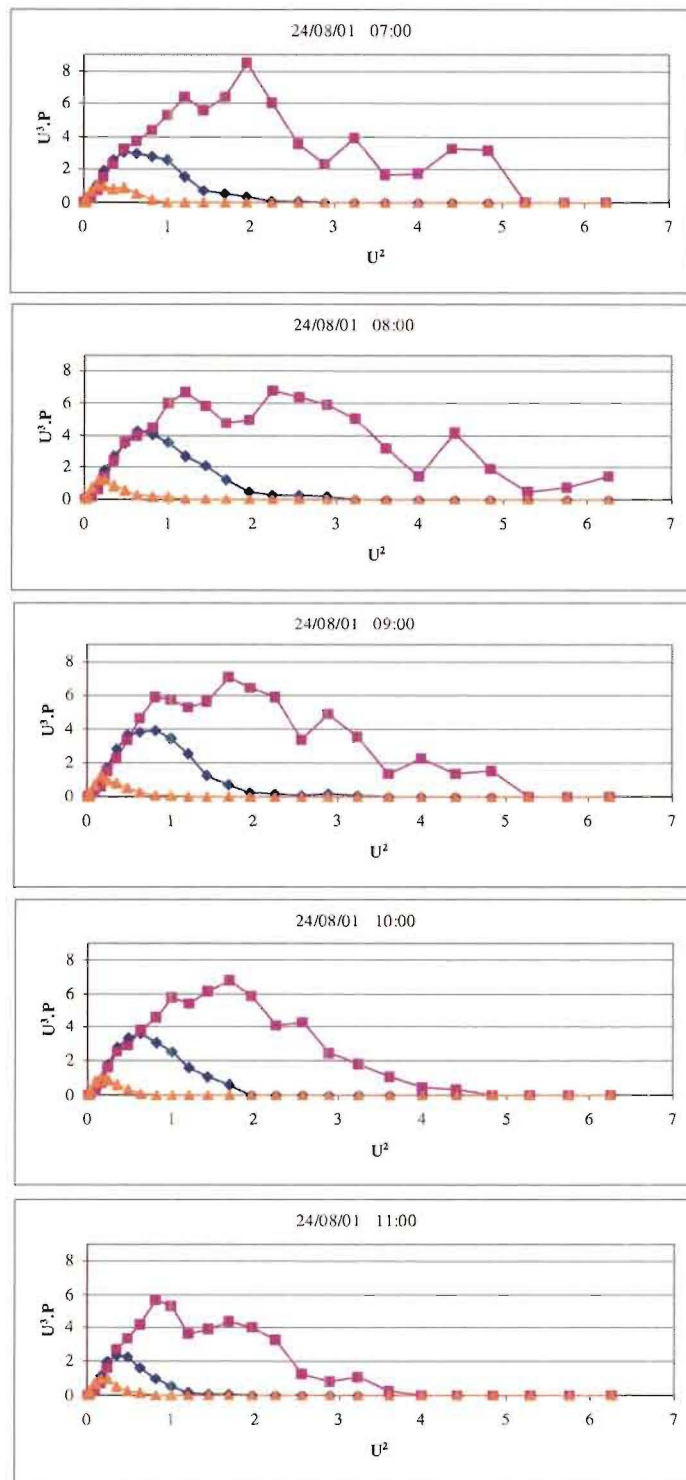


Figure 6.27: Wave effectiveness plots for 18 minute periods recorded at KM3 on the hour every hour while water covered the shore platform on 24/08/01. Wave effectiveness ($u^3.P$) is plotted against a proportional value for shear stress (u^2). Curves are shown for sensor 1 (\blacklozenge), sensor 2 (\blacksquare) and sensor 3 (\blacktriangle).

The greatest amount of work was potentially accomplished in the centre of the platform and the least on the landward portion at sensor 3. Sensors 1 and 3 showed consistent patterns with smooth peaked curves that modally had peaks of effectiveness at proportional shear stresses of 0.64 and 0.16 N.m^{-2} respectively. These values equate to velocities of 0.8 and 0.4 m.s^{-1} . The wave effectiveness curves at sensor 2 in the centre of the platform were somewhat less smooth with an average peak equivalent velocity value of 1.2 m.s^{-1} . The most effective flows at performing geomorphic work were in the centre of the platform. In some cases wave effectiveness peaks were reduced slightly as the tide receded from the platform. The peak $u^3.P$ values of sensors 1 and 2 were lowest during the 18 minutes from 11:00 on 18/08/01 as the tide receded.

Wave effectiveness curves presented in figures 6.25, 6.26 and 6.27 have provided insight into the general patterns of geomorphic work across the platform over the measurement period.

Both McCave (1971) and Kirk (in prep) related wave height to near bed orbital velocity via linear wave theory and constructed wave effectiveness curves using annual wave climate data. McCave (1971) did this for the North Sea and Kirk (in prep) for Lake Pukaki, New Zealand. From this they were able to define the types of waves that did the greatest geomorphic work annually. Kirk (in prep) found that annually waves of 2 m in height produced the greatest amounts of geomorphic work rather than those of the biggest events ($H=4\text{m}$). Although Kirk goes on to note that high magnitude events tend to produce large and durable changes in the shore profile even though the proportion of the total work accomplished on an annual basis may be low.

An analysis of annual flows on shore platforms would provide useful information on the type of waves which do the most geomorphic work in this environment. Once these annual work patterns are quantified the significance of storms in shore platform development can be assessed. However this type of analysis will not be possible until either long term recording of flows on shore platforms are made or a correlation between offshore wave conditions and onshore flows is established. Such a correlation would enable use of long term deepwater wave data described in section 5.2.2 to define annual

work patterns. As the effect of storms and work done during storms has been put forward as being important in the development of shore platforms (Trenhaile 1987) this would be an useful extension of this work. It may be that the effect of a big event is noticeable in terms of large blocks removed from the platform surface but the majority of the actual work of eroding the platform is done on a day to day basis by average sized flows.

Wave effectiveness curves provide measures of potential geomorphic work in terms of sediment movement. Geomorphic work in terms of direct erosion of the rock surface is not quantified. However an indication of the erosive power of the flow on the shore platform at KM3 was given by these curves through the use of shear stress. Quantification of the erosive work of flows using wave effectiveness would require greater knowledge and definition of the aspects of the flow that are fundamental to erosion of the rock surface on a shore platform.

Section 6.3 has discussed the potential for sediment entrainment on KM3 under the flow regime described in Chapter 5. However, there are a number of aspects of the flow regime that were not measured and therefore have not been included in this analysis. The effect of turbulence in providing lift forces has been mentioned but not quantified. Turbulence in the vertical was not measured at two and the sensors but the turbulence in the horizontal plane was shown in section 5.4.3.3 to be significant. Another aspect to flow that has not been investigated is that of acceleration. Variations in acceleration may provide further impetus to flow forces. The effects of these two aspects on sediment provide an avenue for future research.

The potential for sediment movement has been shown but the consequences of this movement have not been fully investigated. Consequences of sediment movement across shore platforms will be two fold. This movement will denude the shore platforms allowing erosion processes to continue unhindered by debris and the movement itself will cause stress to the rock surface. The quantification of this effect is unknown. When sediment is available for entrainment across the platform the path it takes and the type of entrainment that occurs will be important as to how it affects the platform surface and

whether it aids in the erosion of that rock. It has been shown that the sediment is taken offshore and warrants further research.

6.4 SUMMARY.

It has frequently been asserted in the literature that waves do the work of erosion on shore platforms (Mii 1962, Suzuki *et al.* 1970, Bradley and Griggs 1976, Takahashi 1977, Sunamura 1978, Tsujimoto 1987, Trenhaile 1999). However, it is less frequently outlined as to exactly how this erosive work is accomplished. A number of authors have given lists of different possible mechanisms of wave induced erosion (Sanders 1969a, Trenhaile 1987, Sunamura 1992) but the lack of knowledge as to the flow regime across shore platforms has hindered both confirmation and elucidation of these processes. No quantification of their effects has been undertaken until now.

Characterisation of the flow regime across the shore platform at KM3 (Chapter 5) provided data with which to investigate the feasibility of suggested mechanisms of wave induced erosion. This has been carried out in this chapter. Where possible quantification of these processes has been undertaken. The second half of the chapter discussed the potential for sediment movement across the shore platform under the measured flow conditions.

The forces caused by each mode of erosion were quantified where possible and compared to the rock strength as given in Chapter 4, to assess the ability of each mode to erode the rock surface. Of the potential modes of erosion investigated in this chapter air compression and abrasion were shown to be most capable of causing erosion. Other modes were not individually capable of erosion as assessed but in combination may be.

Clapotis will not occur on the shore platforms studied for this thesis as the specific configurations required, of water, waves and rock face do not occur. It was shown that true shock or impact pressures and water hammer are unlikely to occur on shore platforms but that small scale versions of these modes may result in localised erosion where conditions are compatible.

The maximum hydrostatic pressure on KM3 was 12400 N.m^{-2} which was significantly less than the resistance force offered by the rock of the platform. This mode of erosion was not considered capable of eroding the rock in isolation. However, the alternation of pressure that occurs in this environment as successive waves pass over a surface may contribute to weakening of the integrity of the rock over time and hence erosion. No quantification of this aspect was possible.

Measures of shear stress were between $302 - 1055 \text{ N.m}^{-2}$. This was considerably less than the resistance force offered by the rock surface. Therefore, shear stress as measured here is not a successful mode of erosion. However, measurement of flow was in the horizontal plane only. This means that turbulence has not been fully accounted for in this calculation of shear stress. Further investigation is warranted before shear forces of waves as a mode of erosion of rock surface is rejected completely.

A cavitation index was calculated and comparisons to cavitation thresholds given in the literature were made, showing that cavitation is unlikely on shore platforms. Cavitation is also considered unlikely due to the high level of aeration of the flow, however, localised regions of high velocity may create the conditions required for initiation of cavitation.

The theoretical pressures attained by air compression within rock cavities could be as high as $2.1 \times 10^6 \text{ N.m}^{-2}$ which is great enough to counter the resistance force of the rock in specific conditions. These require small fractures or cavities in the rock surface and a supply of air. Air compression in fractures and joints of less than 6mm is considered adequate in aiding erosion of the rock surface, at the very least.

Abrasion was shown to be possible in some locations on the shore platform due to the competence of the flow to entrain sediment but is limited in extent to locations where sediment is readily available.

The movement of sediment across and off the shore platform is an important and unique aspect of the shore platform environment. The lack of sediment on shore platforms is evidence that transportation across platforms occurs. Measurements of flow across KM3 provided data for assessment of the competence and capacity of the flow. This is the first time an assessment of sediment transport in the shore platform environment has been undertaken.

The flow was competent to transport sediment up to the size of large boulders (B-axis of up to 1000mm) and silt, sand and pebbles (B-axis of up to 64mm) could be entrained from locations across the entire platform. This possible range of sizes that may be transported defines the size that the rock needs to be broken down to by processes of erosion on shore platforms before it is removed. The direction of movement of sediment 120mm in size was shown to be generally offshore and over one tidal cycle it was shown that for sediment of this size movement could potentially be moved 82m on average. This is enough distance for sediment to be transported offshore. Smaller sized sediment would be carried much greater distances in the same amount of time.

Sediment transport over KM3 by wave induced flows is likely to be restricted only by supply of sediment. Flow has been shown to be competent of moving sediment of significant size.

An analysis of the effectiveness of measured flows showed that it may not be the biggest events that do the most work on shore platforms. This is an important consideration when discussing modes of erosion and events that are likely to contribute to shore platform development.

CHAPTER SEVEN

WEATHERING

7.1 INTRODUCTION

Structures formed by weathering have been widely identified on shore platforms and have often been presented as evidence for the occurrence of weathering processes (Bartrum 1916, 1935, Bartrum and Turner 1928, Wentworth 1938, Hills 1949, Mii 1962, Bird and Dent 1966, Healy 1968, Sanders 1968a). However the importance of weathering as a set of processes of shore platform formation is debated (Trenhaile 1987, Stephenson and Kirk 2000b). The role of weathering in shore platform development has been identified by different researchers in at least three broadly different ways.

- 1). As fundamental to the formation of shore platforms (Bartrum 1916, 1935, Nott 1994, Stephenson and Kirk 2000b).
- 2). As a method of weakening the rock to the point where it becomes susceptible to wave erosion. (Tsujimoto 1987, Sunamura 1992, 1994, Trenhaile 2001)
- 3). As a modifier of the surface after initial formation has been accomplished. (Wentworth 1938, 1939, Bartrum 1935, Hills 1949, 1972, Sanders 1968a).

Weathering is a complex set of assailing forces operating to erode shore platforms. The importance of weathering in reducing the inherent strength of the rock was mentioned in section 4.7 but not discussed fully. In this chapter the assailing forces of weathering processes with respect to shore platform surface change will be discussed.

Before discussion of the processes of weathering on shore platforms is conducted a general understanding of weathering processes is required. A brief overview of mechanisms of weathering will be given in order to allow identification of weathering processes on the shore platforms studied for this thesis. An exhaustive list of weathering processes is not provided but those thought to be relevant to the shore platform environments studied for this thesis are included.

There are a number of comprehensive reviews of weathering, e.g. Ollier (1969) and Yatsu (1988) which give detailed discussions on many aspects of processes.

7.2 WEATHERING MECHANISMS.

Yatsu (1988:2) defines weathering as “the alteration of rocks or minerals *in situ*, at or near the surface of the earth and under the conditions which prevail there”. This embodies the essential concept of what weathering is. However, some authors have outlined more comprehensive criteria. Ollier (1969:1) states that weathering is “the breakdown and alteration of materials near the Earth’s surface to products that are more in equilibrium with the newly imposed physico-chemical conditions.”

Processes of weathering can be divided broadly into categories of mechanical weathering and chemical weathering. Mechanical weathering involves the physical disintegration of rock and chemical weathering involves the decomposition of minerals and chemicals within the rock (Yatsu 1988). Weathering is often separated into a third category of biological effects but most of these are expressed through either mechanical or chemical processes (Ollier 1969). However, for convenience biological weathering will be addressed separately as many biological effects combine both mechanical and chemical processes.

7.2.1 MECHANICAL WEATHERING.

Mechanical processes of rock weathering include frost action, salt weathering, mineral expansion through hydration and thermal stresses, alternation of wetting and drying and biological effects.

7.2.1.1 FROST ACTION.

Frost action is the result of volume expansion of water on freezing. Water expands about 9% on freezing at 0°C (Ollier 1969) and when this expansion occurs in the pore spaces between minerals or in fractures it causes physical stress within the rock. This eventually leads to fatigue of the rock structure or mechanical wedging off of fragments.

Frost weathering will only be effective on shore platforms in cold environments where alternating freeze thaw temperatures occur (Sunamura 1992).

The ready source of saturation and alternating freeze-thaw cycles within the intertidal zone mean that the coastal environment may be particularly suited for frost action in cold climates (Trenhaile 1987). Processes and effects of frost action on shore platforms have been investigated. However an understanding of precise mechanisms is still poor (Trenhaile and Rudakas 1981, Hansom 1983, Trenhaile and Mercan 1984, Robinson and Jerwood 1986, Dionne and Brodeur 1988). Trenhaile and Rudakas (1981) noted that considerable differences in the susceptibility of various lithologies to frost action makes for a difficulty in the understanding of planation of an intertidal zone consisting of alternating series of rock types.

Frosts occur on average between 38 – 69 days per year in the environments where field sites for this study are located (section 2.4). However, as noted in section 2.4, weather stations are located at altitudes higher than sea level and fewer frosts will occur where the shore platforms are located at sea level. Therefore frost action can not play a significant role in the continuous erosion of the marine shore platforms studied for this thesis. At Lake Waikaremoana frosts may occur at lake level so it is possible that frost action may play some role in the weathering of rock at these sites.

7.2.1.2 SALT WEATHERING.

Salt weathering is the fragmentation of rocks by the crystallisation of salts (Wellman and Wilson 1965). Crystal growth within the rock interstices produces stresses, leading to their widening and resulting in granular disintegration or fragmentation of the rock in much the same manner as ice growth. Possible mechanisms of crystal growth are described in Wellman and Wilson (1965).

The necessary conditions for salt crystal growth include a supply of salts, sites where salt can accumulate and cyclic changes in humidity or temperature (Wellman and Wilson 1965, Sanders 1968a). In the shore platform environment inundation by

seawater and subsequent evaporation may lead to concentration of saline solution within pore spaces or fractures in the rock. Adequate concentrations of salts need to be built up before flushing by subsequent water flows in order for salt crystal growth to be possible. Initiation of salt crystal growth also requires heat or rapid evaporation and crystallisation may be enhanced by biological activity (Sanders 1968a, Ollier 1969). Salt weathering is therefore restricted to a specific zone where both seawater flooding and evaporation occur and on rocks that allow entry of seawater. The first requirement is met in the inter-tidal location of shore platforms. The ability of the rocks of shore platforms studied in this thesis to allow entry of seawater will be investigated in section 7.3.4.3.

The conditions required for salt weathering mean that this process should be most efficient in hot arid areas. However salt weathering has been reported in Antarctica (Ollier 1969) and therefore it is not strictly spatially restricted.

Wellman and Wilson (1965) credited salt weathering with being responsible for many unusual topographic forms including coastal platforms. However most studies of shore platform processes treat it as a secondary influence within a wider weathering process of water layer weathering. It is seen as modifying surfaces created by other means, rather than a primary agent. No direct quantification of the effects of salt weathering on shore platforms has been published.

7.2.1.3 MINERAL EXPANSION.

Some minerals expand when hydrated. When these minerals are incorporated within the rock structure such expansion can lead to fatigue and disintegration of the rock (Ollier 1969, Sunamura 1992). Minerals most susceptible to hydration are clays. Hydrated clay particles may be drawn from the rock lattice into suspension in the surrounding water and subsequently flushed from the rock with the introduction of new fluid, without going into solution.

Expansion of some minerals can also result from heating of the rock. This may also lead to fatigue and disintegration (Sunamura 1992).

7.2.1.4 WETTING AND DRYING.

Alternation of wetting and drying causes some minerals, mostly clays, to swell on wetting and shrink on drying. These internal changes within rocks can lead to initiation of micro crack formation, widening of existing cracks or disintegration of the rock (Yatsu 1988).

The ready mechanism of wetting and drying on shore platforms in the form of tidal oscillations has meant that this process has been cited as a primary cause of erosion on shore platforms (Bartrum 1916, Wentworth 1938, 1939, Stephenson and Kirk 2000b). Stephenson and Kirk (2000b) showed that the shore platform environment at Kaikoura was an ideal location for weathering by this mechanism by quantification of wetting and drying cycles induced from tidal inundation on these platforms. For wetting and drying to be an effective weathering agent on shore platforms clay minerals must be present in the rock. Investigation of the effect of wetting and drying on the shore platform rocks studied in this thesis is detailed in section 7.3.4.2.

Water layer weathering has been used to collectively refer to processes which cause lowering, smoothing and levelling of intertidal rocks associated with pools of standing water (Bartrum and Turner 1928, Bartrum 1935, Wentworth 1938, Hills 1949, Bird and Dent 1966, Healy 1968, Sanders 1968a Takahashi 1977, Stephenson and Kirk 2000b). This process was originally named water-level weathering (Wentworth 1938) but was subsequently renamed water-layer weathering to avoid connotations of a processes that worked at sea level (Hills 1949).

Mechanisms causing water layer weathering have not been fully defined but “most workers agree that the processes include alternate wetting and drying, salt crystallisation, chemical weathering and the movement of solutions through rock capillaries” (Trenhaile 1987:52).

7.2.2 CHEMICAL WEATHERING.

Chemical weathering processes include solution of chemicals and minerals within the rock, changes in chemical structure and biological effects.

7.2.2.1 SOLUTION.

Solution is the dissolving of elements or minerals from the rock into liquid form. Dissolvable minerals are usually calcium carbonate based and are drawn into solution through chemical reaction with carbon dioxide (CO₂) present in the water. The fact that seawater is saturated or supersaturated with calcium carbonate has lead researchers to question the effectiveness of solution in marine environments (Ollier 1969). However, solution of shore platform limestone by sea water has been observed and attributed to algal influence and nocturnal activity of some inter-tidal organisms that produce CO₂ (Emery 1946, Trudgill 1976a). Trudgill (1976b) attributed 10% of the total erosion he measured on shore platforms at Aldabra Atoll, Indian Ocean to solution of this type.

Solution of shore platform surfaces is only possible where the content of rocks have dissolvable elements or minerals such as calcium carbonate. The limestone at Kaikoura is calcium carbonate rich but the four other rock types studied for this thesis are not. Therefore only the limestone is likely to be susceptible to weathering of this nature.

Dissolving of rocks can occur also via various other chemical processes including hydrolysis and oxidation-reduction (Yatsu 1988). The result of these processes would be difficult to distinguish from that of solution.

7.2.3 BIOLOGICAL WEATHERING.

Biological weathering is the breaking down of rock caused by flora and fauna and utilises both mechanical and chemical processes. Ollier (1969:51-52) summarises the

most important effects of biological weathering into eight categories. Those effects that are relevant to weathering of shore platform rock are:

- “1). Simple breaking of particles, as by eating or burrowing of animals, or pressure exerted by growing roots.
- 2). Simple chemical effects, as when solution is enhanced by the CO₂ produced by respiration.
- 4). Complex chemical effects such as chelation, and the formation of complexes of organic-mineral substances.
- 5). Effects on surface moisture...
- 6). Effects on ground temperature...
- 7). Effects on pH of surfaces...
- 8). Protection from erosion by reducing exposure of the surface.”

In existing discontinuities of the rock the biological action of root growth will increase pressure on these fractures and may lead to widening and eventual failure of the rock (Yatsu 1988). Also possible detachment of plants from the rock structure may result in removal of rock fragments. For one year at Macquarie Island, Southern Ocean, Smith and Bayliss-Smith (1998) documented losses of at least 1.56 tonnes of rock per km of coast from a shore platform using measurements of freshly quarried bedrock attached to bull-kelp (*Durvillaea antarctica*) uprooted during storms. Boring and grazing of marine organisms may also reduce the mechanical strength of the rocks on shore platforms and result in erosion (McLean 1967, Trudgill 1976a).

Chemical mechanisms of biological weathering include the use of chelation agents by plants. These agents enable the extraction of ions from normally insoluble solids (Ollier 1969). Other biological organisms such as algae and grazing beasts enable chemical alteration of rock-forming minerals, causing weakening of the rock structure (Yatsu 1988). Detailed descriptions of biological effects of marine organisms on rocks can be found in Trenhaile (1987) or Denny (1988).

Biological effects of weathering may also be protective. The moisture holding abilities of algae have been credited with causing a reduction in the number of wetting and

drying cycles a rock surface would undergo and hence reducing weathering potential (Stephenson and Kirk 2000b). Marine vegetation and organisms such as barnacles and mussels are also capable of providing protection for the rock surface by reducing exposure to other elements that may induce weathering. (Except when forcibly removed to provide sustenance for field assistants!). Hills (1949) suggested that growth of algae and vegetation over shore platform surfaces prevented wave quarrying.

Biology is often afforded a secondary role in the erosion of shore platforms but the degree of biological weathering that occurs on shore platforms will depend on the morphogenetic environment. Some authors credit significant amounts of weathering on shore platforms to contributions from biological activity (Trudgill 1976a, 1976b, Healy 1968) and in reference to shore platform weathering Hills (1968) stated that “indeed the only agents (of weathering) known to be so narrowly limited are organisms that grow on the platform.”

A separate description of each weathering mechanism has been given here as a matter of convenience. However, these mechanisms do not often work in isolation. “Mechanical and chemical processes proceed almost spontaneously and interrelatedly” (Sunamura 1992:70).

The type and extent of weathering on shore platforms will be dependent on the morphogenetic environment (Ollier 1969). In tropical environments processes of chemical weathering may dominate and in cold climates mechanical processes of ice action may have major influence on platform formation. In temperate environments a combination of such processes would be possible.

Nott (1994) attributed chemical and biological weathering the dominant role in formation of shore platforms on the tropical Darwin Coast, Australia and a number of studies have emphasised the importance of ice action in shore platforms developed in cold climates (Trenhaile and Rudakas 1981, Hansom 1983, Trenhaile and Mercan 1984, Robinson and Jerwood 1987, Dionne and Brodeur 1988).

The climatic requirements of some processes of weathering therefore restrict the locations where they will operate. Many processes of chemical weathering require the higher temperatures which occur in the tropics, and ice action requires the colder temperatures of higher latitudes. Dionne and Brodeur (1988) stress that “the importance of shore ice and frost weathering in shore platform development varies with latitude, lithology, geographic setting and hydraulic factors.”

7.3 MEASUREMENT OF WEATHERING ON SHORE PLATFORMS.

Quantification and assessment of weathering on shore platforms has rarely been undertaken in a rigorous manner with very few direct measurements being conducted (Trenhaile 1987). Assessment of the influence of weathering on shore platform development has generally been interpreted from observation of morphology (Bartrum 1916, 1935, Wentworth 1938, 1939, Mii 1962, Hodgkin 1964, Sanders 1968a, Robinson 1977c, Spencer 1981, Hansom 1983, Robinson and Jerwood 1987, Dionne and Brodeur 1988, Nott 1994). Wentworth (1938, 1939) carefully described the weathered features of shore platforms on Oahu, Hawaii and from this hypothesised processes of shore platform development. Other investigations of weathering on shore platforms have generally followed Wentworth’s methodology. Unfortunately, morphology is at best, an ambiguous indicator of process.

A few researchers have supported observational evidence with more rigorous investigations of weathering on shore platforms (Sanders 1986a, Trudgill 1976a, 1976b, Spencer 1981, Trenhaile and Rudakas 1981, Trenhaile and Mercan 1984, Stephenson and Kirk 2000b). Laboratory tests have been conducted to ascertain susceptibility of shore platform rocks to certain aspects of weathering processes such as saturation levels of rocks (Sanders 1986a, Trenhaile and Rudakas 1981, Trenhaile and Mercan 1984). Stephenson and Kirk (2000b) calculated frequency of occurrence of wetting and drying cycles on shore platforms at Kaikoura, and used this as an indication of the capacity of weathering processes in erosion of those platforms. In doing this they made an assumption that, the mechanism of wetting and drying, induced weathering on these shore platforms and used this as an indicator of weathering rather than direct

measurement. MEM techniques have been used to directly measure the effects of biological weathering but not the actual processes themselves (Trudgill 1976a, 1976b, Spencer 1981).

Sunamura (1992, 1994) and Trenhaile (2001) have incorporated weathering as a factor in shore platform development through rock strength calculations. However, no direct measurement of weathering processes was reported and a method for calculation of a representative percentage reduction in rock strength from weathering on shore platforms is unclear.

Tsujimoto (1987) incorporated aspects of weathering through direct *in situ* measurement of rock strength using sonic testing (section 4.5). Sonic testing indicates both the presence of fractures and changes in bedrock strength.

A measure of weathering has also been incorporated, implicitly, in shore platform research through the use of rock strength defined by Schmidt hammer rebound tests (Suzuki *et al.* 1970, Takahashi 1977, Sunamura 1978, Tsujimoto 1987, Trenhaile *et al.* 1998, Stephenson and Kirk 1998, 2000b, 2001). The Schmidt hammer measures the surface strength of rock, which reflects both the intact strength and degree of weathering of the rock (section 4.5.2.2).

7.3.1 ASSESSMENT OF WEATHERING MADE FOR THIS STUDY.

The difficulty inherent in direct quantification of weathering processes on shore platforms meant that no such measurements were made for this study. However, an indication of the degree of weathering of each rock surface was gained from the reduction of rock strength at the surface (section 4.5.6). Morphological evidence of weathering was observed and laboratory tests of the susceptibility of each rock type to aspects of weathering mechanisms were conducted.

7.3.2 REDUCTION OF ROCK STRENGTH.

An indication of the reduction of rock strength at the surface of each shore platform was calculated from a ratio of the compressive strength of the bedrock and the compressive strength of the surface rock, with the ratio expressed as a percentage. From this the degree of reduction in strength of surface rock compared to bedrock strength was obtained. This is an indication of the degree of weathering of the rock surface. All platform surfaces showed reduction in rock strength at the surface. The greywacke surface was weaker than the bedrock by 34%, the mudstone at Kaikoura was 48% weaker, the limestone surface strength was reduced by 77%, the basalt by 88% and the mudstone at Lake Waikaremoana by 91%. This indicates weathering of all shore platform surfaces studied. However, this may not be a true indication of the total amount of weathering the shore platform rock has undergone as surface layers may have been weakened to the extent that this top layer of weathered material may have been removed.

This has shown that the surfaces of all shore platforms studied have been subjected to weathering but the degree of weathering each has undergone and the mechanisms through which weathering has occurred are still in question.

7.3.3 MORPHOLOGICAL EVIDENCE.

Another indication that weathering of shore platform surfaces has occurred can be obtained from morphological evidence. This is a good starting point in identification of weathering processes on shore platforms but it must be remembered that it does not define the processes.

Features formed by weathering observed on the shore platforms during the study period varied from profile to profile and not all were observed on all platforms. Water-layer weathering in the form of flat shallow pools was observed on the mudstone at Kaikoura (figure 7.1a). Honeycomb weathering, thought to be associated with salt crystallisation (Yatsu 1988) was observed on the mudstone near KM3 and at various other locations around the Peninsula (figure 7.1b). Salt crystallisation was observed intermittently on

all the marine shore platform surfaces studied. Figure 7.1a shows the clearest example of this near KM3. Disintegration of mudstone at Lake Waikaremoana from wetting and drying was evident on much of the mudstone shoreline. Figure 7.1c shows disintegration of mudstone blocks at Lake Waikaremoana, on a moss surface approximately 2m above the mean water level as an illustration of the effect. Hydration causing swelling of the clay minerals within the rock was observed at isolated locations on the Kaikoura mudstone (figure 3.3). Solution patterns were observed on isolated areas of the surface on the limestone (figure 7.1d).

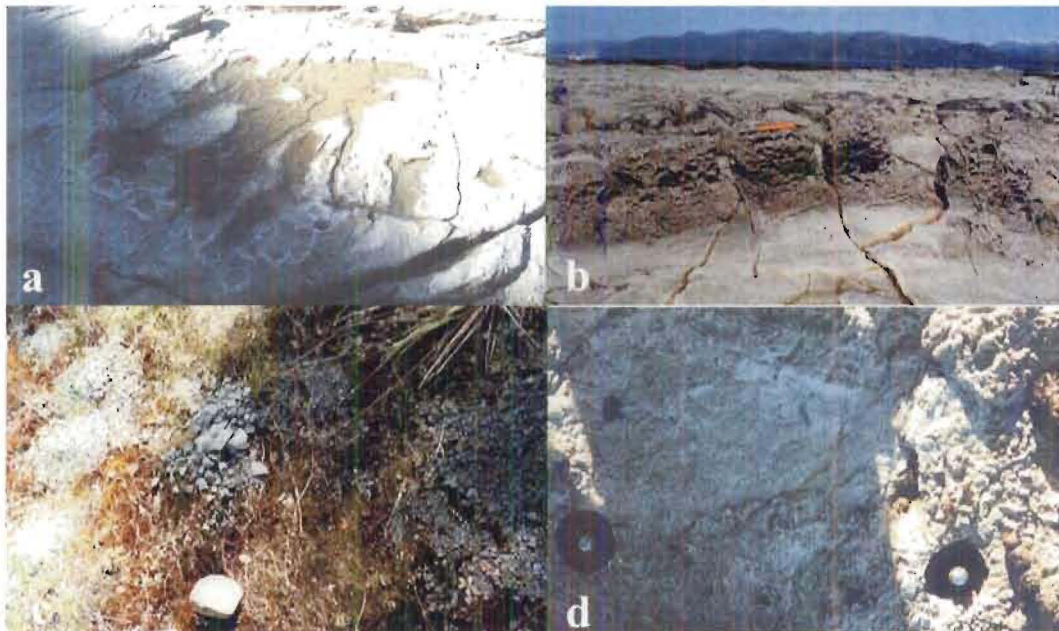


Figure 7.1: Weathered features observed on shore platforms studied for this thesis. a). Salt crystallisation and water-layer weathering on Kaikoura mudstone near KM3 (pen in the centre of the picture is 135 mm in length) b). Honeycomb weathering on Kaikoura mudstone (pen is 135mm in length) c). Disintegration of Lake Waikaremoana mudstone from wetting and drying (block in foreground is approximately 140mm in width) d). Solution on limestone at KM7 (bolts are 150mm apart).

Evidence of biological weathering was also observed on all shore platforms studied. Mechanical erosion by plant roots was observed on some parts of the platforms at Lake Waikaremoana and a variety of marine vegetation and organisms were variously established on each marine shore platform. Lower elevations of KM7 were usually covered in marine vegetation (figure 7.2a). Seaweeds established at KM7 and variously on other profiles studied included, Neptune's necklace (*Hormosira banksii*), Sea lettuce

(*Ulva lactuca*) and Zig zag weed (*Cystophora torulosa*). Species of algae present included *Corallina officinalis* and *Lithothamnion* species. Bull kelp (*Durvillaea antarctica*) is extensively established on the seaward cliffs of KM3, RM1, AK1 and AK2. Barnacles (*Chaemosipho* species) were observed on the seaward portions of the platforms formed in greywacke (RM1) and basalt (AK1 and AK2). Holes created by boring molluscs (*pholids*) were observed in basalt near AK1 (figure 7.2b). Feeding patterns in algae were observed on the limestone at KM7 (figure 7.2d) and home-scars left by limpets (*Cellana* species) were observed on both the Kaikoura mudstone (figure 7.2c) and the limestone (figure 7.2e). This is by no means an exhaustive list of all the biological weathering activity on the shore platforms studied. Rather it highlights biological weathering observed on shore platforms during the study period. Further discussion of biological weathering effects on shore platform morphology is not presented here and is an area for further research, possibly calling on the substantial body of literature that exists on the biology of the intertidal zone (see Denny 1988).

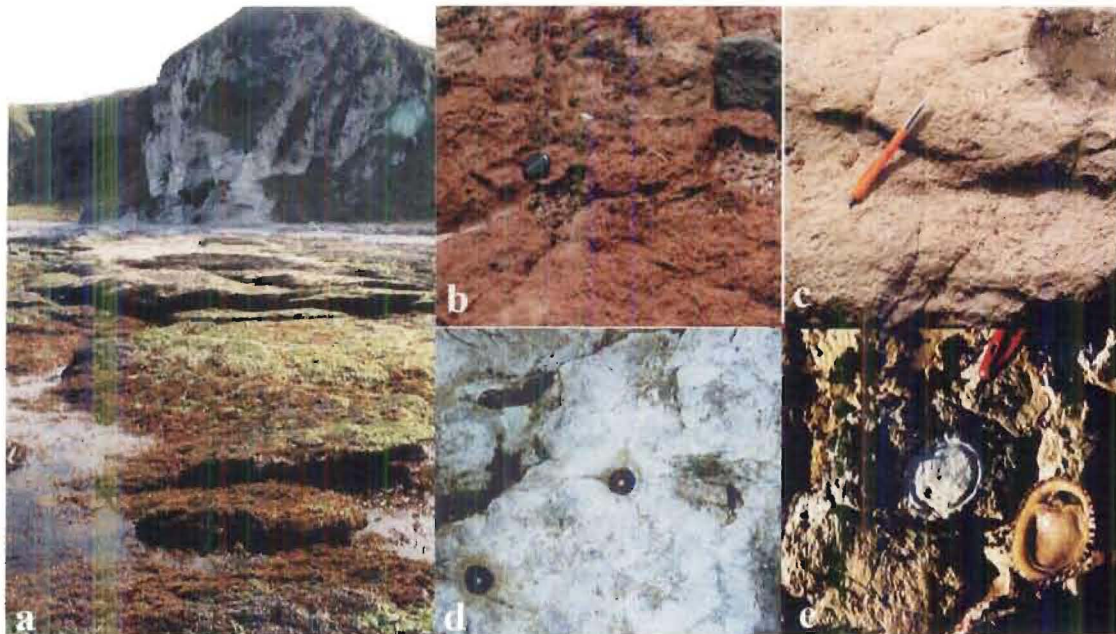


Figure 7.2: Evidence of biological weathering observed on shore platforms. a). Establishment of marine vegetation on limestone at KM7 (distance from foreground to cliff is approximately 60m) b). Boring mollusc burrows on basalt near AK3 (lens cap is 50mm in width) c). Limpet home-scar on mudstone near KM3 (pen is 135mm in length) d). Feeding patterns in algae on limestone at KM7 (bolts are 150mm apart) e). Limpet home-scar on limestone near KM7 (limpet is approximately 40mm long). See text for full scientific names of biology.

7.3.4 SUSCEPTIBILITY TESTS.

Although the observation of weathered features reported in the previous section suggests that weathering processes were operating on the shore platforms studied fuller analysis is required. As direct measurements of weathering processes on the shore platforms were not possible in this study it was considered important to gain an indication of the susceptibility of the rocks to various weathering mechanisms.

The susceptibility of a rock to weathering varies according to the rock texture, strength of bonding, degree of fracturing, permeability, porosity, saturation-coefficient and water absorption (Trenhaile 1987).

A direct investigation of the chemical and mineral composition of the rocks could provide indication of their susceptibility to chemical weathering. However, Ollier (1969:53) stated that “chemical composition alone is not a sure indication of weatherability”. Without knowing the precise mechanisms of weathering it is possible to test for susceptibility by replication of certain aspects of process and exclusion of others (Sanders 1968a). Therefore rather than following a strictly chemical approach, testing of shore platform rock susceptibility to weathering was undertaken using methods that replicated aspects of natural processes as closely as possible.

Three different tests of rock susceptibility to weathering were conducted in the laboratory on rock samples from each of the five lithologies studied for this thesis. A standard geomechanical test called a slake-durability test, a wetting and drying test and a saturation test. Blocks of rocks ($\sim 0.4\text{m}^2$) were collected from locations close to study profiles and smaller samples were cut from each of these for each susceptibility test.

7.3.4.1 SLAKE-DURABILITY.

The slake-durability test is a standard engineering test “intended to assess the resistance offered by a rock sample to weakening and disintegration when subjected to two standard cycles of drying and wetting” (Brown 1981:92). It is designed to give a factor

accounting for possible rock strength reduction due to weathering for work in engineering geology.

7.3.4.1.1 METHOD.

The procedure utilised for this test followed the method set out in Brown (1981). For each shore platform rock type a representative sample consisting of 10 rock lumps each between 40-60g was prepared. Lumps were roughly spherical and corners rounded prior to testing. The sample of each rock type was placed in a separate drum comprised of a mesh cylinder of diameter 140mm and a length of 100mm with solid ends. Each sample was dried at 30°C to a constant mass. Temperatures used for drying were lower than those recommended in order to replicate the natural environment more closely. Each drum was placed in a trough filled with tap water to a level 20mm below the axis of the drum. The rock lumps within the drums were unobstructed. The drums were rotated at a constant speed of 20rpm for 10 minutes. The sample and drum were dried to a constant mass and weighed. The process was repeated once more using a new lot of tap water. A slake-durability index (I_{d2}) giving percentage mass of sample remaining after two slaking cycles was calculated using equation 7.1.

$$I_{d2} = \frac{B}{A} \times 100\% \quad \text{Equation 7.1}$$

Where B is the dry mass of the sample after two cycles and A is the initial dry mass of the sample. The apparatus used is shown in figure 7.3.



Figure 7.3: Slake-durability testing apparatus.

7.3.4.1.2 RESULTS.

The slake durability for each rock type is given in table 7.1.

Table 7.1: Slake durability index ($I_{(d2)}$) for each rock type.

| Rock type | slake-durability |
|---------------------------------|------------------|
| basalt | 96.6 |
| mudstone (Kaikoura) | 94.2 |
| limestone | 98.3 |
| greywacke | 99.8 |
| mudstone (Lake Waikaremoana) | 95.7 |

The Kaikoura mudstone had the lowest slake-durability index losing 5.8% of its mass under this type of testing. The rock type most resistant to slake-durability testing was the greywacke, which lost only 0.2% of mass after testing.

Although the slake-durability test is a standard weathering test it does not reflect weathering processes only. The rolling of the drum induces impact or mechanical action between the 10 lumps of rock in the sample. The result of this mechanical action on the 10 lumps of the sample gives an indication of the rocks susceptibility to abrasion. At the end of two cycles, edges on the lumps of the samples of Kaikoura mudstone, limestone and Lake Waikaremoana mudstone had all been well rounded. Edges on the basalt lumps were less rounded and some small chips had broken from the surfaces. Edges on the greywacke were not visibly rounded but some small chips had broken from the surfaces. This indicates that the mudstones and limestone are more susceptible to wear by abrasion than the greywacke and basalt. These latter two rock types appear to be more brittle in nature.

Under conditions where abrasion is able to occur the shore platforms formed in the mudstones and limestone should result in smoother surfaces with higher erosion rates. These three rock types all had roughness coefficients showing smoother surfaces than

either basalt or greywacke (table 2.2) and were visually smoother on the micro scale (figure 2.23).

However, the lack of loose sediment generally observed on the shore platforms studied (section 2.6) means that abrasion of rock surfaces is not likely on a platform wide scale. It may account for greater rates of erosion in isolated areas where beach sediment is within close proximity such as at KM2A, KM3A and KM7A. These three MEM sites had higher rates of erosion than the average rates for the profile on which each was located (see section 8.4).

7.3.4.2 WETTING AND DRYING.

In the marine shore platform environment tides form a ready mechanism that provides regular cycles of wetting and drying. Wetting and drying has been cited as a dominant mechanism of erosion on shore platforms (Wentworth 1938, Stephenson and Kirk 1998, 2000b) but mechanisms and effects of this type of weathering are still poorly understood. Therefore, it is important to test this assertion.

7.3.4.2.1 METHOD.

A simple wetting and drying test was conducted to test the susceptibility of each rock type to wetting and drying as a mechanism of weathering. Samples of each rock type were cut into roughly similar sized and shaped blocks and were air dried for longer than 2 weeks. Preparation methods meant that it was not possible to retain the original moisture content of the rock, so sample blocks were allowed to come to equilibrium with the ambient conditions as shore platform surfaces would in the natural environment. Two samples of each rock type were tested. The initial mass of each sample was measured. Samples were alternately immersed in water and then dried for between 6-8 hours for each event. The length of soaking and drying episodes was chosen to replicate the tidal cycle as closely as possible. Fresh water was used for the Lake Waikaremoana samples and seawater for the other 4 rock types in order to reflect natural conditions. Samples were oven dried at a constant temperature of 35°C. However it was found that rock samples did not dry completely in a 6 hour period. Consequently 12 hour periods

of drying were interspersed through the testing period to ensure complete drying of each sample in order to make all samples comparable. Even though drying intervals were varied each sample was subjected to an identical regime. The process was repeated for 10 cycles of wetting and drying. Samples were weighed after each period of drying and mass loss as a percentage of the original mass was calculated. Fragments of rock smaller than approximately 1cm³ and broken completely from the main body of the sample were removed prior to weighing.

7.3.4.2 RESULTS.

Figure 7.4 shows percentage loss of mass from initial mass of each rock sample after drying. Both Kaikoura mudstone and Lake Waikaremoana mudstone were most susceptible to weathering by wetting and drying with the Kaikoura mudstone losing up to 20% by mass from one sample after 10 cycles. The Lake Waikaremoana mudstone disintegrated into pieces smaller than 1cm³ during the first cycle (figure 7.4 and 7.5). Extrapolation of mass loss at the same rate recorded for the first cycle gives losses of 50% and 33% for each of the samples after 10 cycles. One sample of the basalt (sample A) lost 0.9% of mass after 10 cycles. The remaining basalt sample (sample B), the limestone and the greywacke samples showed changes of less than 0.25% by mass.

The Kaikoura mudstone lost mass through breaking into small pieces (figure 7.5) and also from dissociation of clay particles from the rock as observed by the muddiness of the water after soaking. The Lake Waikaremoana mudstone also lost mass from breaking and dissociation of clay particles. No visible changes occurred on the greywacke samples during progressive cycles. The only observed change on the limestone was the removal of a small flake from the surface of one sample. Both the basalt samples changed colour very slightly, becoming redder in appearance. This could be an indication that oxidation of ferric minerals occurred. One basalt sample (sample A) (figure 7.5) showed some granular disintegration. The other basalt sample (sample B) (figure 7.5) showed no change in the physical appearance of the rock, however some salt crystallisation was observed close to a fracture on the surface of this sample.

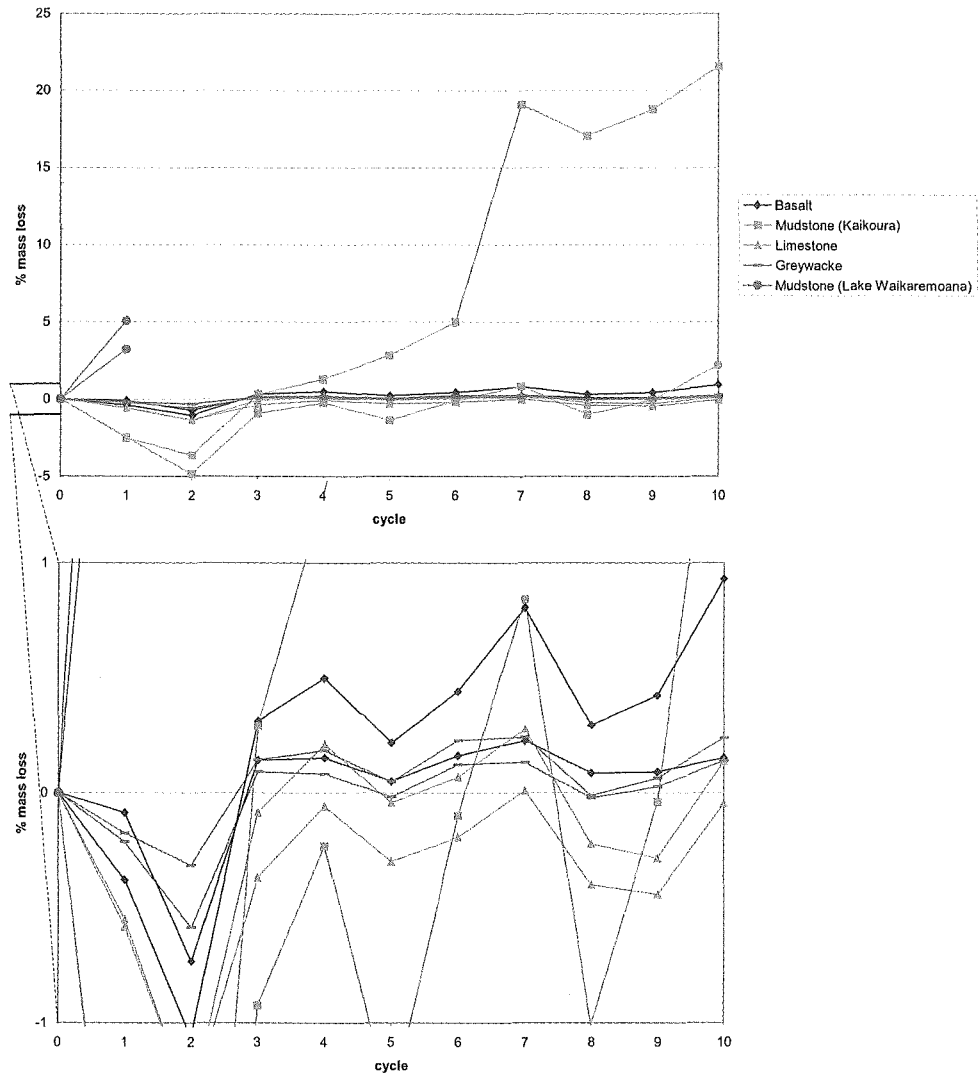


Figure 7.4: Reduction in mass of samples from initial mass after wetting and drying cycles. The lower graph shows greater detail of the vertical scale between 1 and -1 % mass loss.

Figure 7.4 shows that during the testing some samples increased in mass when compared to initial mass. Such an increase in mass reflects incomplete drying of a sample at the end of a cycle. To eliminate discrepancies that may have arisen from different absorption rates of each rock type (section 7.3.4.3) cycles 4, 7 and 10 included 12 hour drying periods. Figure 7.6 shows the average percentage mass loss for each rock type after cycles that included 12 hours of drying.

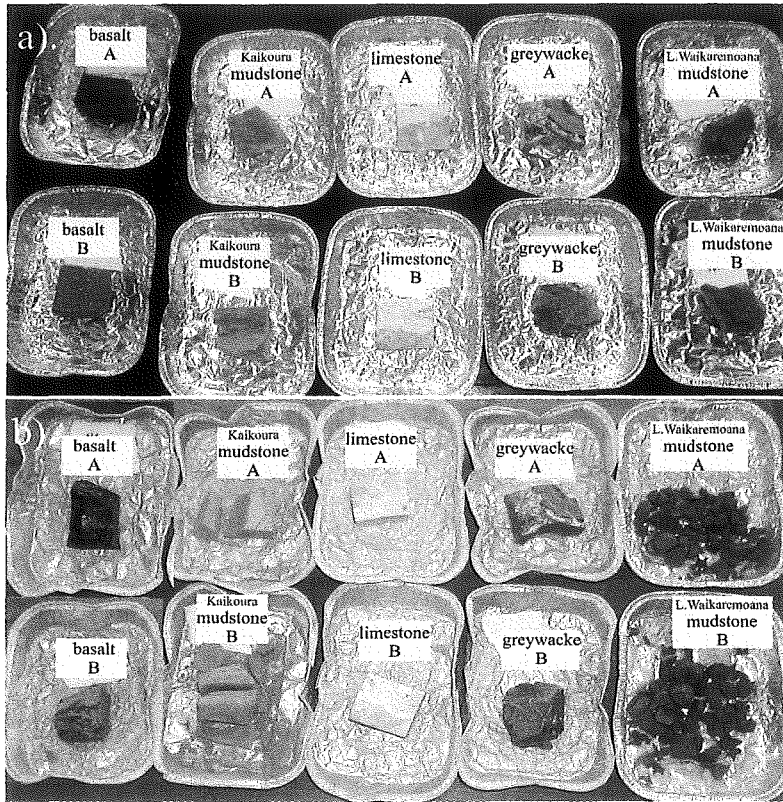


Figure 7.5: Samples subjected to wetting and drying susceptibility testing. a). prior to testing b). after 10 wetting and drying cycles. Trays are approximately 140mm in width.

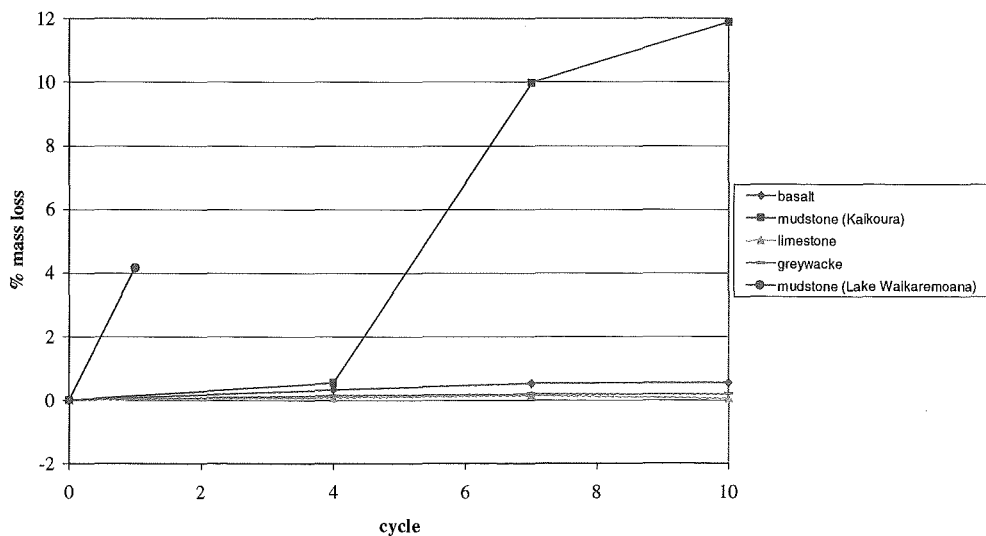


Figure 7.6: Susceptibility of each rock type to 10 cycles of wetting and drying. Average reduction in mass as a percentage is shown for each rock type. Only percent mass loss after 12 hour drying cycles have been included.

The fact that none of the samples dried completely in 6-8 hours at a constant temperature of 35°C is important when considering wetting and drying cycles of shore platform rocks in the natural environment. It means that weathering mechanisms utilising wetting and drying cycles will be focused only in the very top surface layers of the rock. This includes not only expansion and contraction of clay particles from wetting and drying as was evident on the mudstone but also salt crystallisation. The observation of salt crystal formation on some samples during this test shows that this weathering mechanism may occur under conditions of wetting and drying alone. However conditions required for salt crystal growth are difficult to recreate in the laboratory and therefore susceptibility of each rock type to salt weathering is unknown.

The two basalt samples were chosen to represent different portions of the rock. It was shown in section 4.5.4 that the strength of the basalt was extremely variable. This test has shown that this variation was also evident in the susceptibility of the basalt to weathering processes in the form of wetting and drying. As not all of the basalt in which the shore platforms at AK1 and AK2 are formed is susceptible to wetting and drying this would lead to differential weathering and possible armouring of the platform surface by less susceptible parts of the rock. This is reflected in the relative roughness of the surface (table 2.2).

Although Lake Waikaremoana does not have tides causing regular wetting and drying cycles the level of the lake does fluctuate, facilitating this mechanism of weathering. Also high rainfall (section 2.4.5) contributes to cycles of wetting and drying. The high susceptibility of the Lake Waikaremoana mudstone to this mechanism of weathering, an estimated 42% mass loss in 10 cycles, helps to explain the high rate of erosion of shore platforms formed on the mudstone at Lake Waikaremoana. Once weathered, surface debris are easily removed by wave action and surface flooding. Given the high susceptibility of the Lake Waikaremoana mudstone to this form of weathering and the conducive environmental conditions it is likely to be the dominant component in the development of these shore platforms.

The Lake Waikaremoana mudstone, Kaikoura mudstone and parts of the basalt are susceptible to weathering by wetting and drying. The limestone, greywacke and parts of the basalt are not.

7.3.4.3 SATURATION.

For salt weathering to occur, conditions conducive to salt crystallisation must be met. Rocks must, in the first instance, allow entry of salt water. An indication of the capacity of a particular rock type to meet this condition can be obtained from a saturation test. In this test the amount of water a rock absorbed on immersion was monitored until saturation occurred.

The ability of rock to absorb water will enhance the likelihood of salt crystallisation and hydration within the lattice structure of the rock leading to internal pressures both in pore spaces and in micro fractures resulting in disintegration of the rock.

7.3.4.3.1 METHOD.

Samples of rock from each shore platform were cut into blocks of approximately 45cm³. All were of a similar shape and size so that each had the same exposed surface area. One sample from each rock type was prepared with the exception of basalt. Two basalt samples were tested to represent differences in the nature of this rock. These have been outlined previously (sections 4.5.4 and 7.3.4.2). Samples were air dried for at least 2 weeks. As noted in section 7.3.4 this allowed samples to become adapted to ambient atmospheric conditions. Initial sample mass was measured before immersion in water for 70 hours. Fresh water was used for the Lake Waikaremoana mudstone sample and seawater for the other rock types. Water temperature was approximately 16°C. At specified intervals samples were removed from the water, towel dried to remove excess surface water, weighed and returned to the water as quickly as possible. After 70 hours of immersion, samples were oven dried at 60°C until a constant dry mass was obtained.

7.3.4.3.2 RESULTS.

The initial water content of each sample was obtained from a comparison of dry mass with initial mass of the samples. Sample B of the basalt had the highest initial water content by mass of 2.9%. Other samples had water contents of between 2.0% (Kaikoura mudstone) and 0.4% (greywacke) (table 7.2). After 30 minutes of immersion the Kaikoura mudstone attained a higher percentage water content by mass than the basalt (sample B) but other than this, water content rankings were maintained during the experiment (table 7.2).

Table 7.2: Water content in sample as a percent of dry mass before and after 70 hours of immersion in water (i.e. at saturation).

| Rock sample | Water contained in sample as a % of dry mass | |
|---------------------------------|--|---|
| | initial water content | water content at saturation (after 70 hours immersion) |
| basalt (A) | 0.9 | 1.5 |
| basalt (B) | 2.9 | 6.0 |
| mudstone (Kaikoura) | 2.0 | 9.1 |
| limestone | 1.6 | 3.9 |
| greywacke | 0.4 | 0.9 |
| mudstone (Lake Waikaremoana) | 1.7 | 3.2 |

Figure 7.7 shows the intake of water by each sample as a percentage of the initial mass. Samples showed inverse exponential patterns of water intake and had reached saturation, or were very close to saturation after 70 hours of immersion in water. The Lake Waikaremoana mudstone sample broke into pieces after 2 hours of immersion and had reached a water content of 3.2% at this time. The intake of water by the Lake Waikaremoana mudstone sample during the first 30 minutes of immersion shows a slightly differing pattern of water uptake from the patterns of water intake of other samples. This was probably the result of mass loss from the sample due to disintegration.

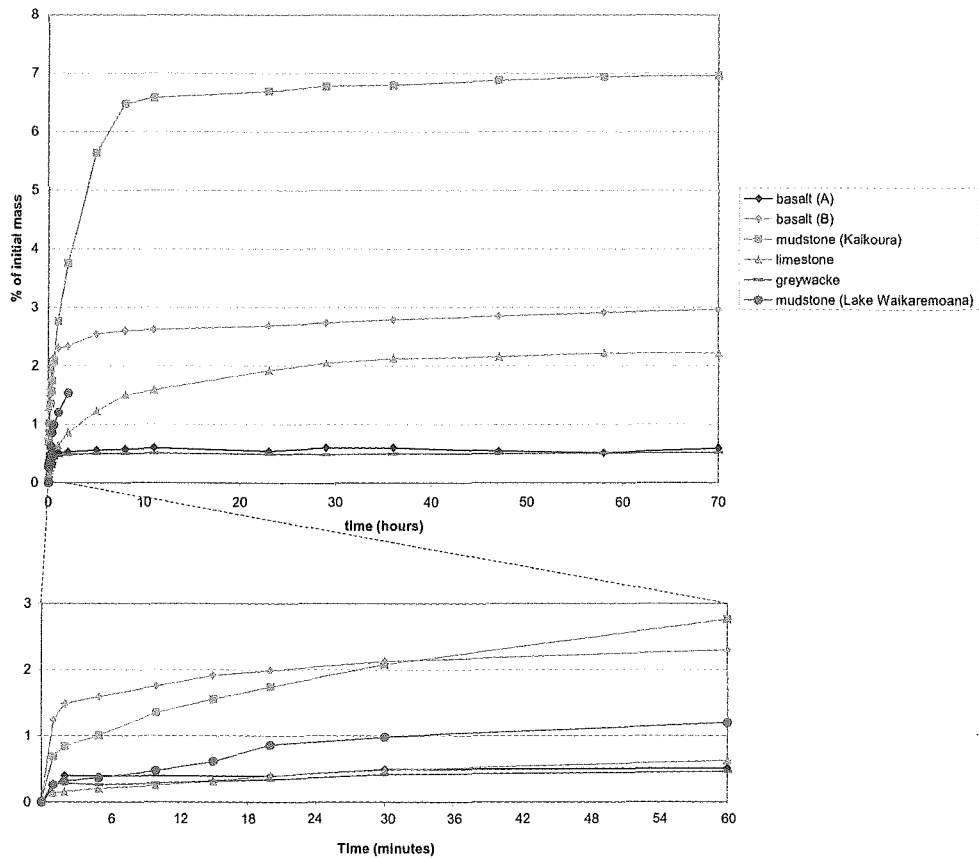


Figure 7.7: Water intake of rock samples over 70 hours of immersion expressed as a percentage of initial sample mass. The lower graph shows greater detail of the horizontal scale for the first 60 minutes of immersion.

Basalt (sample A) and the greywacke absorbed the least water before reaching saturation each increasing to just 0.5% of initial mass. Much of this water intake would have been through penetration of the micro fractures of the rocks. Absorption of water by limestone increased gradually until it reached saturation of 3.8% of initial mass after 36 hours. All other rock types became saturated within 7 hours with greywacke and basalt (sample B) reaching saturation levels within 30 minutes.

Figure 7.7 shows that significant amounts of water were absorbed by all rock types, when compared to mass at saturation, within the first half hour of immersion and even the first 10 minutes. The rapidity of entry of water into the rock will determine the type of water fluctuations that may induce salt weathering on each platform. The slower rate

of absorption to saturation shown on the limestone means that tidal oscillations will be important for providing saline solution to the rock. The rapid rate of absorption to saturation on the greywacke and basalt will allow entry of saline solution and encourage salt growth from wave activity and short term fluctuations such as seiches within enclosed water bodies. A seiche with an average period 245s and average amplitude of 0.48m was recorded by pressure sensor measurement within the Akaroa Harbour on 06/02/02 (see section 5.2.3.2 for detail on pressure sensor).

All rock types tested absorbed water (figure 7.7). Therefore the first condition for salt crystal growth may be met on all shore platforms studied for this thesis. This is confirmed by the intermittent observation of salt crystals on all the marine platforms. However, at Lake Waikaremoana the second condition for salt crystal growth, a supply of saline fluid, is not met. Therefore, the Lake Waikaremoana mudstone is unlikely to be subjected to salt weathering, at least on a Lake wide scale. The degree of susceptibility of each rock type to salt weathering will be controlled by the total amount of water absorbed before saturation is reached. The Kaikoura mudstone, limestone and parts of the basalt absorbed greater amounts of water and are therefore more susceptible to salt weathering than the greywacke and parts of the basalt.

Destruction by salt crystallisation is most effective on porous, fractured or cleavable rocks (Sanders 1968a) and this test has shown that all rock types studied are capable of absorbing water and may therefore be susceptible to those mechanisms of weathering to a degree depending on their relative intake. The mudstone at Kaikoura was most susceptible and the greywacke and parts of the basalt were least susceptible.

7.4 WEATHERING AS A CONTROL IN SHORE PLATFORM MORPHOLOGICAL CHANGE.

The control exerted by weathering in shore platform development can be investigated through a comparison of the susceptibility of rock to weathering and the rate of surface change on platforms. If weathering is a dominant process in shore platform development as suggested by Stephenson and Kirk (2000b) shore platforms formed in

rocks with greater susceptibility to weathering should have greater rates of surface erosion. Also, as weathering weakens the rock structure thereby reducing the rock strength, as suggested by Trenhaile (2001), it would be expected that those rocks more susceptible to weathering would erode at a greater rate.

Figure 7.8 plots the three measures of rock susceptibility to weathering made in this thesis against rate of surface change for each study site. This shows that there were no clearly definable direct relationships between rock susceptibility to each type of weathering, as assessed by the three tests conducted and the rate of surface change. For slaking the correlation was $r = 0.33$, for wetting and drying the correlation was $r = 0.60$ and for saturation the correlation was $r = 0.17$. However, generally figure 7.8 shows there is a trend of higher rates of erosion (negative surface change) on rock types more susceptible to weathering when comparing all three types of weathering. Two points deviate markedly from the trend being grouped in the lower left portion of the plot. Both are results from testing of Lake Waikaremoana rock samples. One of these points is that of Lake Waikaremoana mudstone percentage of water intake. As the sample tested disintegrated before saturation was reached this result may not be a true indication of the total percentage of water intake possible by this rock type.

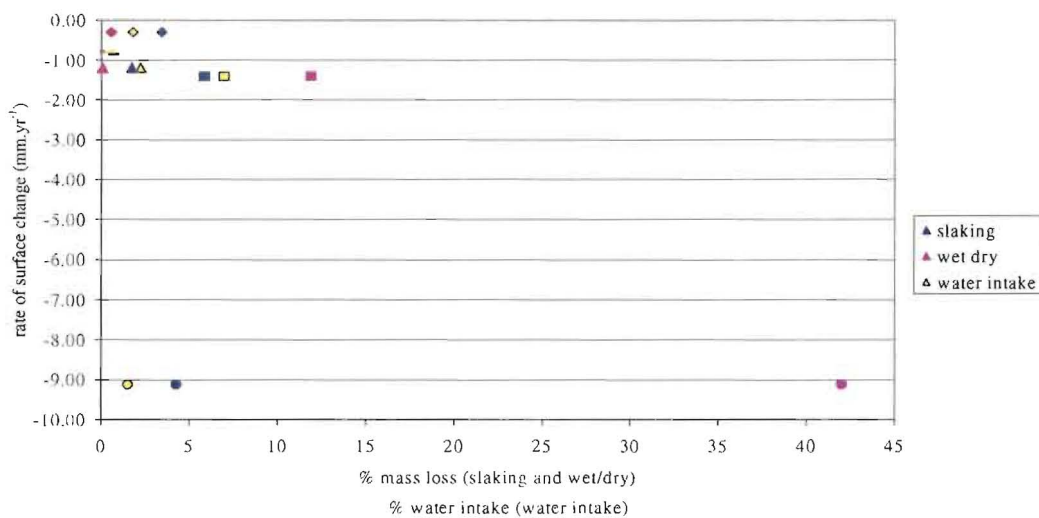


Figure 7.8: Correlation of susceptibility of shore platform rocks to weathering and rate of surface change. Each rock type is plotted using a different symbol; greywacke (—), limestone (▲), basalt (◆), Kaikoura mudstone (■) and Lake Waikaremoana mudstone (●).

This general trend shown in figure 7.8 is not strong enough ($r = 0.49$) to state that there is a direct relationship shown between susceptibility to weathering and rate of surface change of the shore platform rocks. This suggests that weathering is not a dominant control in development of the shore platforms studied for this thesis.

One reason for this lack of correlation between weathering and shore platform development may be that only three specific tests for assessing susceptibility of rocks to weathering were conducted. It is likely that all mechanisms of rock weathering that occur on shore platforms have not been assessed or that mechanisms work in combination. The wide ranging possibilities of processes and combinations of processes capable of weathering rocks have meant that exhaustive tests of susceptibility to weathering were not possible. However, the three aspects of weathering assessed were chosen on the basis that the type and amount of weathering is primarily determined by climatic conditions (see section 7.2). In a temperate climate moderate amounts of both chemical and mechanical action are expected. Therefore weathering processes of salt crystallisation, wetting and drying and processes associated with saturation of the rock are considered to be dominant modes of weathering of the shore platforms studied given the temperate climate. The three tests used were also chosen to replicate processes most commonly observed and documented on shore platforms (Bartrum and Turner 1928, Wentworth 1938, 1939, Hills 1949, Mii 1962, Bird and Dent 1966, Sanders 1968a, Stephenson and Kirk 1998, 2000b). Testing was conducted in a manner that also replicated natural conditions on shore platforms as closely as was possible in a laboratory situation.

As with indices of rock strength the methods used to test for susceptibility of rocks to weathering, determines, to a certain extent, the results obtained. It has been shown that cycles of wetting and drying are not necessarily a useful measure of weathering processes on all shore platforms and should be used in conjunction with other tests to enable fuller description of weathering processes on shore platforms.

In considering the contribution of weathering to shore platform development it is important to understand that no one single mechanism or process is responsible for

weathering on all shore platforms. Platforms formed in different lithologies are susceptible to different types of weathering.

7.5 SUMMARY.

This chapter has further characterised the nature of the shore platform rocks by detailing their susceptibilities to some weathering processes. It has also discussed the mechanisms by which processes of weathering erode shore platform rocks and investigated the control that some of these processes have on development of the shore platforms studied for this thesis.

Weathering has occurred on surfaces of all shore platforms studied for this thesis. All surfaces showed a surface strength greatly reduced from that of the bedrock. The surface strength of the greywacke had reduced the least from bedrock strength (34%) and the Lake Waikaremoana mudstone showed the greatest reduction in strength at the surface (91%).

However, it was not possible to quantify actual weathering rates *in situ* on the platforms. Therefore an indication of the susceptibility of each rock type to different aspects of weathering was gained from three laboratory tests designed to replicate particular natural processes that have been identified as mechanisms of weathering. The tests were a slake-durability test, a wetting and drying test and a saturation test. The nature of analysis undertaken here means that presentation of absolute values of weathering was not possible. Rather susceptibility is given in relative terms between different rock types.

Testing showed that the Kaikoura mudstone, the Lake Waikaremoana mudstone and parts of the basalt were susceptible to weathering from wetting and drying. Ten cycles of wetting and drying caused percent mass losses of samples of each of these rocks of between 0.9% and an estimated 41%. Limestone was susceptible to solution weathering, although this was not tested directly but inferred from observation of morphology. Salt

weathering was possible on all rock types studied, with the exception of the Lake Waikaremoana mudstone. However, salt weathering was more likely on the Kaikoura mudstone, the limestone and parts of the basalt. This was inferred from water content at saturation, which was highest on the Kaikoura mudstone at 9.1% of dry mass and from rate of water intake. The greywacke and parts of the basalt were least susceptible to processes of weathering tested in this thesis.

The degree of susceptibility of rocks to processes of weathering in laboratory tests showed only a weak negative relationship to the rate of surface change of the shore platforms studied in this thesis. It has therefore been shown that weathering processes may have some effect on shore platform development but not necessarily a controlling one.

CHAPTER EIGHT

SPATIAL VARIATION AND SHORE PLATFORM DEVELOPMENT

8.1 INTRODUCTION.

This chapter examines causes of spatial variations in shore platform location and morphology. It discusses the role of rock type and other process factors in the spatial location of shore platforms and in their profile form, to further elucidate processes controlling shore platform formation.

It is established that shore platforms form only within the coastal zone, at or near mean water level (Dana 1849, Johnson 1919, Bartrum 1935, Wentworth 1938, 1939, Challinor 1949, Jutson 1954, Mii 1962, Sanders 1968a, Trenhaile 1972, 1974b, 1987, 1999, Sunamura 1978, 1992, Trenhaile and Layzell 1981, Tsujimoto 1987, Stephenson and Kirk 2000a, 2000b). However the precise spatial location of shore platforms in the vertical dimension has not been defined with respect to water level (Trenhaile 1987, Stephenson 2000). Shore platforms have some, as yet, unclear relationship to the water level or range of water levels at the coast. Once removed from this active coastal environment either by tectonic activity or changes in relative sea level, shore platforms cease evolving. Examples of this include the relict shore platforms of the Kaikoura Peninsula (figure 2.3) that have been lifted above the coastal zone by tectonic activity and the relict shore platforms on the southwest flanks of Banks Peninsula (section 2.4.3) isolated from the coast by lower sea levels and an accreting beach system.

There have been various notions proposed within the literature about shore platform change over time. However, the question of exact equilibrium form and location with respect to water level remains unanswered. Do shore platforms achieve an equilibrium form and if so what kind of form is this? Or, given that they are erosive, do they continue widening and lowering indefinitely? If there is an equilibrium form what factors or combinations of factors control this?

Some authors assert that wave action is the dominant erosive force in shore platform development (Dana 1849, Jutson 1939, 1949, Edwards 1941, Challinor 1949, So 1965, Trenhaile 1974a, 1978, 1999, Bradley and Griggs 1976, Sunamura 1978, 1992, Tsujimoto 1987, McKenna *et al.* 1992) so that after an unspecified amount of time the elevation of platforms must bear some relation to the base level to which wave action occurs and width must be determined by dissipation of wave energy across the horizontal surface of the evolved platform. Eventually the platform will tend towards a static form that fully dissipates the erosive or assailing force of the waves. Models of shore platform evolution presented by Sunamura (1992) and Trenhaile (2000) both suggest that shore platforms will attain final static equilibrium forms given sufficient time with a constant sea level. The unspecified amount of time taken to achieve this form will depend on the wave assailing force and the resistance offered to this by the rock strength.

Other authors suggest that weathering is a more effective erosive force than marine action in shore platform development (Bartrum 1916, Nott 1994, Stephenson and Kirk 2000b) and therefore shore platforms will erode down to some elevation related to water level but will continue widening indefinitely. Bartrum (1916) specified this elevation as that of permanent saturation of the rock.

Each of these proposals defines a very different equilibrium of shore platforms and different criteria for controls on shore platform development and form. They also imply different spatial distributions of shore platforms with respect to morphogenetic conditions.

Previous chapters have outlined measured change on selected shore platforms and described mechanisms of processes causing change. Where possible the potential and actual change caused by processes of wave action and weathering have been outlined and quantified. The relative roles of each of the erosive processes thought to control shore platform morphology and surface change have also been investigated. This chapter examines the spatial distribution of shore platforms with respect to morphogenetic conditions and erosive processes and discusses the relationships between erosive processes and the morphology of shore platforms within a spatial context. Factors controlling shore platform development and

morphology are investigated, as is the equilibrium form of shore platforms. To do this, some information previously presented will be re-examined in greater detail to emphasise and elucidate spatial variations in shore platform morphology and development.

Sections 8.2, 8.3 and 8.4 of this chapter each examine different scales of variation in shore platform distribution, morphology and rate of development from wider to site-specific scales. These scales are New Zealand wide, individual profile scale and micro scale. Each scale is discussed individually but they are not necessarily discrete. For example, the way the rock breaks down at the micro scale may dictate the type of surface that occurs at the profile scale and the way the rock breaks down may be dictated by larger scale distributions of climate. Section 8.5 of the chapter presents a way of looking at shore platform development taking account of the mechanisms of processes and the role these processes play in the form and development of shore platforms as discussed in earlier chapters.

8.2 SHORE PLATFORM DEVELOPMENT IN THE NEW ZEALAND TEMPERATE CLIMATE.

Shore platforms, as distinguished by similarities in morphology, occur in many varied coastal environments. The shore platforms studied for this thesis were located at various positions around New Zealand (figure 2.1). New Zealand has a temperate climate and although shore platforms studied were spatially dispersed the climatic conditions at each are broadly similar. There is a moderate temperature range of mean maximum monthly temperatures between 22.5°C at Akaroa in January and 7.7°C at Kaikoura in July. Temperatures fall below 0°C on occasion enabling frost conditions, which are more frequent at Lake Waikaremoana profile sites than other sites. Rainfall is moderate, ranging from 2148 mm.yr⁻¹ at Lake Waikaremoana, to 638 mm.yr⁻¹ at Akaroa (section 2.4). A temperate climate encourages moderate amounts of biological activity, moderate amounts of chemical activity (Ollier 1969) and opportunity for semi-regular wetting and drying cycles. There are some differences between the mountain lake environment at Lake Waikaremoana and the marine environments of the east coast of the South Island but in general climates are similar.

All the marine shore platforms studied for this thesis are exposed to micro tidal conditions and the hydroelectric power operating restrictions of Lake Waikaremoana constrain water levels to within a 3m range. This is slightly greater than the micro tidal conditions of the east coast of the South Island.

Other aspects of the morphogenetic environments of the study sites differ. Shore platforms studied were formed in five different rock types (section 4.2) while wave environments offshore from the exposed Kaikoura peninsula and Raramai Point profiles (KM2, KM3, KM7 and RM1) were found to be significantly different from the enclosed Robinson's Bay Point (AK1 and AK2) and Lake Waikaremoana (WK1 and WK2) profiles (section 5.2.3).

Therefore, shore platforms studied for this thesis were all located within a temperate climate and had similar tidal ranges, but were formed in different rock types and exposed to different wave environments. Despite the differing morphogenetic and lithological conditions these shore platforms appear to have similar form and dimensions.

To test this assumption a non-parametric statistical test (Wilcoxon rank sum test) was performed on measured shore platform morphological parameters of width and gradient. This was done to ascertain if shore platforms from these different environments were essentially of the same population in terms of the shape parameters of width and gradient. The Wilcoxon rank sum test (McClave and Sincich 2000) is designed for comparison of independent samples based on a ranking of those samples. It must be noted that the small number of data of 8 profiles in all hinders statistical comparison of measured shore platform parameters.

Populations were chosen based on rock type. This gave test statistics of $T=16$ for width and $T=18$ for gradient. For two-tailed tests at .05 significance level the null hypotheses that the widths and gradients of shore platforms studied for this thesis are from the same populations, could not be rejected. This statistical test showed that the shore platforms studied are essentially similar in width and gradient despite being from differing environments.

Rate of surface change on marine profiles studied have been shown to be similar in magnitude ranging from erosion of 1.41mm.yr^{-1} on the Kaikoura mudstone to erosion of 0.29mm.yr^{-1} on the basalt. The rate of surface change on the profiles at Lake Waikaremoana was almost an order of magnitude greater than this eroding at an average rate of 9.13mm.yr^{-1} . It was stated in section 8.1 that within the shore platform literature it has been suggested that shore platform form and formation is controlled by over-riding sets of processes, either wave assailing forces or weathering processes. The range of environments in which shore platforms studied for this thesis occur makes closer investigation of this notion possible. This section revisits the question of control of processes, described previously in this thesis, in platform width, gradient and rate of surface change as an indication of development.

The role of weathering on control of shore platform morphology was discussed in Chapter 7. An indication of the susceptibility of each lithology in which shore platforms were formed to different types of weathering was obtained through three different laboratory tests. From these tests it was possible to assess relative amounts of weathering caused by each different mechanism at each location. The three tests assessed rock susceptibility to weathering by wetting and drying, saturation and salt crystallisation. These are three of the more common forms of weathering in the temperate environment (Ollier 1969). Susceptibility to each differed on each of the five rock types. Figures 7.6 and 7.7 and table 7.1 showed that susceptibility to weathering varied considerably on each lithology. Rock types most susceptible to weathering were the Lake Waikaremoana mudstone and the Kaikoura mudstone, while rocks least susceptible to weathering were the greywacke and parts of the basalt.

There was no correlation between measures of susceptibility of each rock type to weathering and morphometric parameters of shore platforms or rate of surface change (figure 7.8). This suggests that the processes of weathering, as tested for in this thesis are not a dominant control on shore platform development for the shore platforms studied.

Chapter 5 discussed the role of waves in control of shore platform development and figure 5.9 showed that the parameter of significant wave height used to describe the wave environments offshore from each profile was not correlated to morphology or surface change. Much of this lack of correlation has been attributed to changes in the wave characteristics as the waves moved onshore, caused by offshore profiles and the shore platform morphology itself.

The control of rock characteristics on morphology and surface change were discussed in Chapter 4. Figures 4.7 and 4.9 show no correlation between aspects of lithology and platform width or gradient. Rock strength was assessed in three different ways (section 4.5). These related to bedrock strength, surface strength and rock mass strength. It was shown in figure 4.13 that bedrock strength did not correlate with platform width, gradient or rate of surface change. Correlations of varying degrees were shown between parameters of width, gradient and surface change and rock strength and mass strength. These ranged from a strong correlation of $r=0.82$ between mass strength and surface level change to the weaker correlation of $r=0.59$ between surface strength and surface level change. The correlations shown between aspects of rock strength and shore platform morphometric parameters show that rock strength does in part control shore platform morphology. However correlations were not strong enough to say that rock strength is the dominant control.

This lack of correlation between erosive processes occurring on shore platforms and morphometric parameters over all the shore platforms studied for this thesis suggests that although there may be a fundamental form to shore platforms there is no one dominant process controlling this form or surface change of the shore platforms studied.

It may be possible that a dominant process causing erosion of shore platforms has not yet been identified, but it is more likely that combinations of processes already identified result in the shore platform structure. The variety of morphogenetic conditions in which shore platforms develop suggests that there is a component of equifinality to shore platform formation based on the mix of erosive processes that work at each site.

This notion of different combinations of processes causing shore platform development is further developed by an examination of which processes are capable of eroding specific rock types.

There are a large number of different processes operating within the coastal environment that can erode rock into the near horizontal flat surface of a shore platform. Some of these processes work on some rock types but not all processes work on all rock types that shore platforms are formed in.

The character of the rock itself partly dictates the type of process that can erode it. The chemical and mineral composition of the rock controls the rate and location of penetration of water and hence the type of weathering and the rate and amount of weathering. Some of the erosive assailing force comes from the properties of the rock as well as the fluid action itself. Therefore the resisting force of rock is not only a force that opposes erosion but also a factor that may or may not facilitate erosion.

The rock types shown to be most susceptible to weathering in this thesis were the mudstones both at Kaikoura and Lake Waikaremoana. The greywacke at Raramai Point was shown, of those mechanisms of weathering tested, to be susceptible to only salt weathering and only to a limited extent. Therefore erosion of shore platforms by weathering is more likely to occur on the mudstone of the Kaikoura Peninsula (KM2 and KM3) and the mudstone at Lake Waikaremoana (WK1 and WK2) than on the greywacke at Raramai Point (RM1).

The effectiveness of erosive processes of waves also depends in part on the character of the rock in terms of constriction of flow and presence of conditions conducive to rock fragment removal. For example processes of rock plucking by waves on each rock type are constricted in extent by the availability of suitable rocks to pluck. This is dictated by the nature of fractures within the rock. Where rock is highly fractured, such as the greywacke at RM1, blocks will be more readily plucked from the platform surface as opposed to the smoother less fractured surfaces on the Kaikoura mudstone at KM2 and KM3.

Flows constricted by topographic constraints on shore platforms are likely to increase in velocity and therefore in ability to erode via processes related to shear stresses. Rougher rock surfaces, such as those of the basalt and greywacke (section 2.6.10) are likely to encourage or create more turbulence of the wave induced flow as it crosses over them. This would probably have a dual effect of greater lift in the flow encouraging greater displacement of blocks, but also greater dissipation of wave energy. Rougher surfaces, on the micro scale also provide greater opportunity for trapping of air bubbles and consequent micro scale pressures as described in section 6.1.3.4.

Different rock types offer different resistances to erosion and also different controls on the types of processes that occur and the extent of change caused by those processes. As shore platforms are formed in a wide variety of rock types offering different types of resistance to erosive processes, different combinations of erosion processes must operate from rock type to rock type in order to achieve the same result of erosion of a near horizontal surface. It has been shown for the platforms studied in this thesis that there is no one dominating process of those processes studied, which controls the form and development of shore platforms.

8.3 PROFILE SCALE.

The distinctive profile form of shore platforms provides definable elements of morphology such as width, gradient and elevation (section 2.5) which are similar for all shore platforms studied for this thesis. Some local variations in shore platform profile such as ramparts do occur in different locations but the profile shapes are all essentially similar. This section discusses the spatial variations of development and controls on development across the profile and in relation to surface elevation.

The form of the profile is controlled directly by changes that occur at the water-land interface. These changes are in turn controlled by a variety of erosional processes. To understand the processes controlling development of the profile, knowledge of changes that create it are necessary.

The amount of change that is required to form a shore platform in the coastal zone will depend on the initial shoreline before formation begins and the final equilibrium form of the platform profile. Although exact detail of shore platform equilibrium form is yet to be determined it has been assumed here on the basis of observational evidence that platforms tend towards a near horizontal surface within the intertidal zone. Further discussion of equilibrium form of shore platforms will be conducted in section 8.5. The antecedent shoreline conditions will not influence the type of changes required to form a shore platform, but will control the amount and spatial distribution of change across the platform.

Shore platforms appear to have eroded into a wide variety of initial shore profiles. However, identification of initial profile shape is difficult due to the dynamic changes that have occurred during platform formation. In some situations it is possible to propose an initial shape of the shoreline before shore platform development began from the form of the profile either side of the platform. For example, gradients of slopes either side of the platforms at WK1 and WK2 are similar (figures 2.18 and 2.19) and a continuation of a line connecting these slopes across the eroded shore platform region is possible. This gives an hypothesised antecedent profile of a steep valley slope.

The topography either side of the marine shore platforms studied for this thesis is cliffed in most cases, making estimation of antecedent shore profiles difficult. Initial shape may be dictated by spatially variable factors such as rock structure, or temporally changeable factors such as tectonic movement.

The rate of surface change documented in this thesis (section 3.4) is great enough that, if it is representative of past rates of change then only relatively brief, ~1000 year, stands of sea level are required for the formation of shore platforms to occur. It is therefore, entirely possible that in some instances current shore platforms are reworking shore platforms that were formed under previous conditions and have remained dormant within the landscape. At Kaikoura ongoing tectonic uplift (Ota *et al.* 1996) gives the possibility that platforms cut at lower stands of sea level could have been raised through the plane of present sea level thereby initiating polycyclic development of platforms. Ota *et al.* (1996) gave an average rate of uplift of the

Kaikoura Peninsula of 1.1 mm.yr^{-1} . The average rate of down wear of the Kaikoura Peninsula platforms measured for this study was 1.30 mm.yr^{-1} . At this high rate of down wear only a few thousand years would be required for shore platforms to establish. When this rate is compared to the amount of uplift that has occurred the concept of polycyclic development of shore platforms in this region is feasible. This presents the possibility that antecedent shoreline profiles of current shore platforms may have been relict shore platforms.

The antecedent conditions may dictate the rate of development of shore platforms, in that different amounts of rock at each elevation need to be eroded to form a near horizontal surface. However it seems unlikely that these conditions dictate final morphology. The processes of erosion working on shore platforms tend towards near horizontal flat surfaces (section 8.4). The lack of knowledge of antecedent slope or shape of study profiles means no conclusions on control of antecedent profiles on current shore platform morphology can be drawn from this study. This question provides an opportunity for further research using laboratory studies simulating shore platform development on models with different antecedent profile shapes. Laboratory studies described to date have used cliffs as initial profiles (Sanders 1968b, Sunamura 1991).

Notwithstanding antecedent conditions it is possible to derive patterns of surface change required to form a near horizontal wholly eroded surface. Logically, areas of higher elevation need to erode at a greater rate to form a horizontally flat surface. The extreme case of this is an antecedent profile consisting of a cliff face.

The assumption that the equilibrium form of shore platforms is that of a near horizontal flat surface has been made on the basis of observation and the noted tendency of erosion processes to work towards flat surfaces. This assumption is made pending further elaboration. All shore platforms studied for this thesis have surfaces with gradients of 3° or less.

Measures of surface change made at MEM sites spaced at regular intervals along shore platform profiles (section 2.6) provide a means to investigate patterns of surface change on shore platforms. Figure 8.1 plots elevation of each MEM site with

respect to mean sea level against average rates of surface change. This shows a trend for greater rates of erosion at higher elevations but the scatter of points around the line of best fit means that it is a weak trend only. The correlation between the two factors is not strong ($r=0.38$).

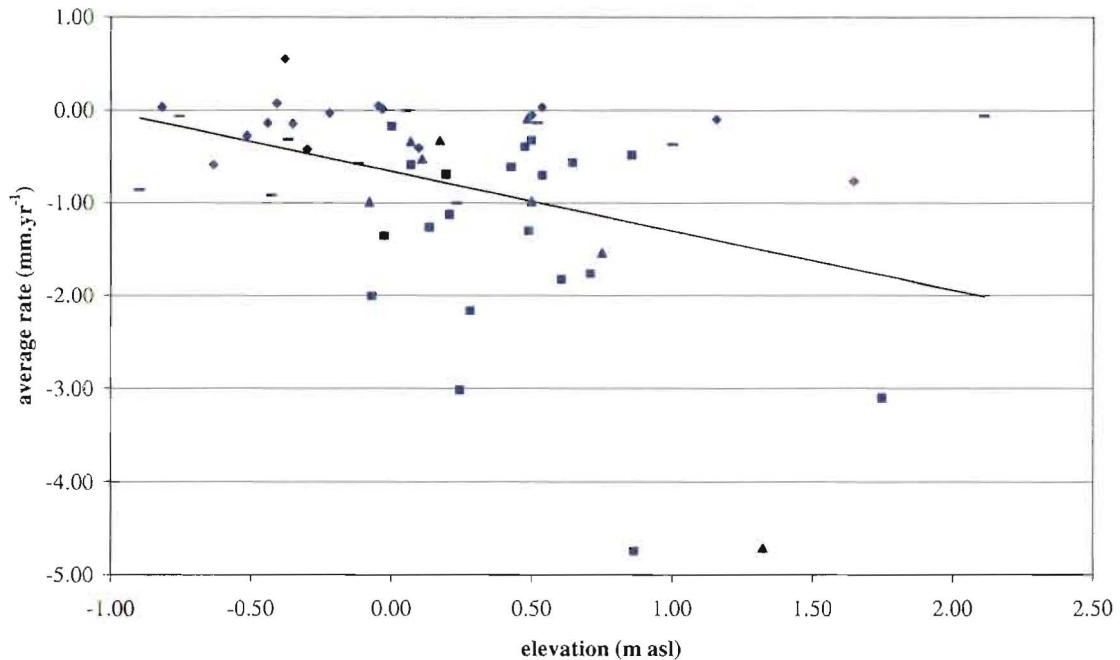


Figure 8.1: Elevation of MEM sites above mean sea level vs. average rate of surface change recorded at MEM sites. Results from each rock type are shown with a different symbol; greywacke (—), limestone (▲), basalt (◆) and Kaikoura mudstone (■). Lake Waikaremoana results have not been shown on the graph to allow greater detail to be seen.

When the trends of surface change related to elevation of each individual profile are given separately (see different symbols in figure 8.1 and figure 8.2) different patterns are discernable (figure 8.2). The limestone at KM7 shows a very strong negative trend of higher rates of erosion at higher elevations with good correlation of the relationship ($r=0.84$). The trends shown for the Kaikoura Peninsula mudstone profiles, KM2 and KM3 are also strongly negative with higher rates of erosion at higher elevations on the profile, although correlations are not as strong as that of KM7. Correlation for KM2 was $r=0.69$ and for KM3 was $r=0.44$. Neither the basalt profiles (AK1 and AK2) nor the greywacke profile (RM1) show a relationship between rate of surface change and elevation. Surface change was relatively constant at all elevations across these three profiles.

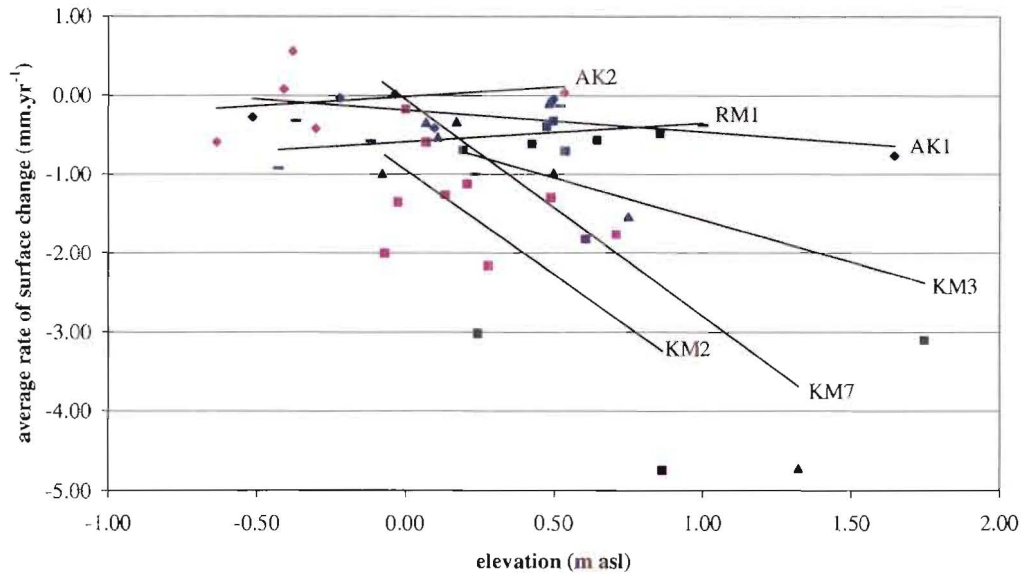


Figure 8.2: Elevation of MEM sites above mean sea level vs. average rate of surface change recorded at MEM sites. Trend lines for each profile are labelled. Results from each rock type are shown with a different symbol: greywacke (—), limestone (▲), basalt (◆) and Kaikoura mudstone (■).

Figure 8.1 shows that generally, over all profiles studied higher elevations are eroding at a faster rate as suggested earlier but at a profile scale different patterns occurred with higher elevations not eroding at a faster rate on all profiles (figure 8.2).

If shore platform development is evolutionary in nature, it may be postulated that optimum gradients based on the combination of processes operating will be reached after certain periods of time have passed. If higher elevations erode at greater rates the surface will eventually attain a uniform level and no differential rates based on elevation will be possible. Interaction of shore morphology and processes causing erosion on shore platforms will allow the platform to establish an equilibrium form. Once reached this form may continue eroding but will remain constant in shape unless the interaction of morphology and processes changes. On this basis figure 8.2 suggests that the morphologies of AK1, AK2 and RM1 have reached an equilibrium gradient.

It could be that these platforms have reached their optimum gradients in relation to the balance of processes operating and that the surfaces are eroding at uniform rates or that other factors control rates locally e.g. rock hardness or topographic features.

It is interesting to note that gradients of these three profiles are steeper than those that showed clear negative relationships of erosion rates at higher elevations (KM2, KM3 and KM7). RM1, AK1, and AK2 all have gradients of between 1° and 1.5° and KM2, KM3 and KM7 have gradients less than 1° (table 2.2).

For profiles on different rock types there may be specific angles of slope of shore platforms. The angle would depend on such factors as the rock strength, wave flow patterns, weathering, the combination of erosive processes occurring and the ability of each of these processes to cause erosion on that particular rock type.

Models of shore platform development implicitly or explicitly describe patterns of surface level change across a profile. These are based on assumptions that processes have the ability to produce differential cross shore patterns of erosion.

Parallel retreat models suggest a retreat of the platform by uniform down wear across the entire near horizontal surface and related back cutting of the landward cliff. Taken to its conclusion this implies a two faceted surface, as shown in Challinor's (1949) diagram (figure 1.3) with uniform down wear on the landward portion of the surface and no down wear on the seaward.

Sunamura's (1992) model of shore platform development (figures 1.5 and 1.6) is based on the assumption that wave assailing force is the primary mode of erosion of shore platforms and therefore has a related distribution pattern of erosion in the vertical dimension which corresponds to wave force (figure 1.6). This distribution of force is based on the oscillatory motion of deepwater waves and reduces exponentially with depth below still water level. The model shows erosion above the point where wave force and rock resisting force are equal. It is implied that the erosion of a horizontal surface is based on the vertical distribution of wave strength with greater rates of erosion closer to still water level due to the greater assailing force at this point (Sunamura 1992). In his classification of shore platforms

Sunamura (1992) describes a flat horizontal surface (figure 2.8). Antecedent conditions given in Sunamura's (1992) model are of a cliff although patterns of erosion outlined would hold for any initial shore profile. Eventually dissipation of the wave energy would be such across the platform that wave assailing force at each point on the platform would be equal and zero, therefore development would stop.

However, if wave assailing force is the dominant cause of erosion it could be expected that the profile surface would mirror, in form, the vertical distribution of the wave assailing force. This implies a convex surface not the flat one described in figure 2.8. Laboratory modelling of shore platform development by Sunamura (1991) showed the development of convex profiles. However, very few field observations of shore platforms describe convex surfaces. Shore platform profiles studied for this thesis were essentially flat with the exception of the Lake Waikaremoana (WK1 and WK2) profiles which were concave. It might be that the convex effect is too subtle to detect in field studies or that other factors disturb its formation e.g. the adaptation of wave flows by the shore platform morphology (section 5.3).

The location of MEM sites at reasonably regular intervals across shore platform profiles studied for this thesis (section 2.6) allows cross profile patterns of surface change to be examined and compared to the outcomes of the models described above.

In order to enable comparison between profiles of different widths the location of each MEM site on its profile was calculated as a ratio of the total length of the profile, where 0 represents sites at the foot of the landward cliff and 1 represents sites on the top of the seaward cliff or at the seaward edge of the platform. Some sites occurred outside of these two boundaries due to installation requirements.

Figure 8.3 shows a scatter plot of the position of each MEM site on its profile plotted against average rate of surface change measured at that site. Points are mostly scattered within a broad band across the plot. There was a slight trend towards greater rates of erosion nearer the landward cliff, however, no strong correlation exists.

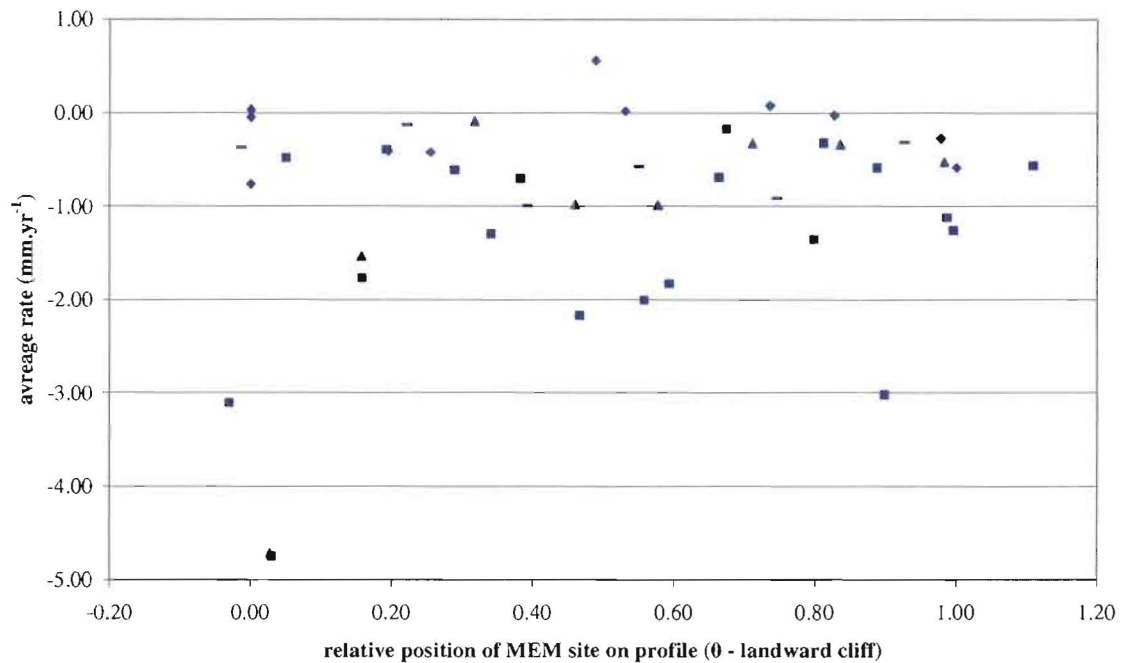


Figure 8.3: Position of MEM site on the profile vs. average rate of erosion at that site. Position on the profile is given as a proportion of the width of each profile. 0 is the location of the landward cliff and 1 is the location of the seaward cliff. Results from each rock type are shown with a different symbol; greywacke (—), limestone (▲), basalt (◆) and Kaikoura mudstone (■). Lake Waikaremoana results have not been shown on the graph to allow greater detail to be seen.

The figure shows that there were no discernable cross-shore patterns of erosion rates on the shore platforms studied. This could be viewed as essentially uniform surface change or down-wear across the entire platform profile in all cases.

Possible patterns of erosion across shore platforms were further investigated by construction of bar graphs of measured rates of surface change at each MEM site normalised across each profile. Average rates of surface change were calculated for each profile. The rate of surface change for each individual MEM site along that profile is then given in relation to this. Normalised rates of surface change are presented for each profile in figure 8.4 a – h.

There is no clear consistent pattern evident in the distribution of rates of erosion across the platforms studied. One reason for this may be that wave assailing force at the shore platforms has a different vertical distribution than that shown in Sunamura's (1992) model (figure 1.6).

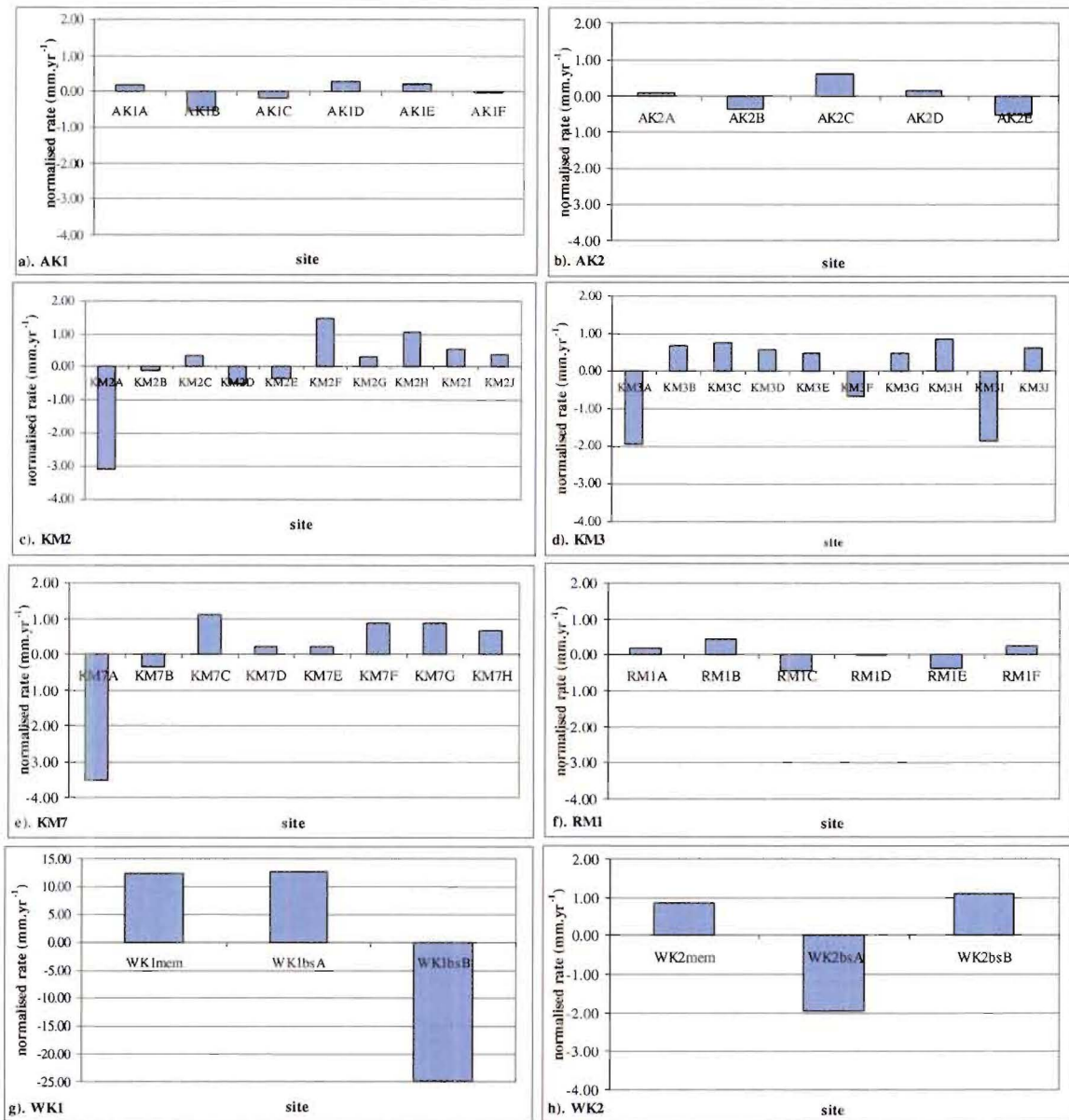


Figure 8.4: Normalised rates of erosion for each profile a). AK1 b). AK2 c). KM2 d). KM3 e). KM7 f). RM1 g). WK1 and h). WK2.

The distribution shown in figure 1.6 is related to the deepwater motion of waves. In section 5.3.3 it was shown that by the time waves have progressed from deepwater onto the shore platforms all but the smallest have broken and they propagate as bores and no longer in the oscillatory manner of deepwater waves. Therefore, distribution of wave energy in the vertical plane is different to that shown in figure 1.6. Theoretically, average velocity is uniform through the entire depth of the bore therefore distribution of wave assailing force essentially becomes uniform in the

vertical dimension. In this way the morphology of the offshore slope and the platform itself controls the wave processes on the shore platform.

8.4 MICRO SCALE.

Processes causing erosion on shore platforms tend towards change at the micro scale and this change is reflected at the local scale in the form of the profile. This section discusses the scale of mechanisms causing erosion on shore platforms and the form created by these mechanisms.

Water layer weathering, described in detail by Wentworth (1938), includes a combination of processes of wetting and drying and salt crystallisation and erodes rock towards a flat horizontal surface via the use of shallow pools of water. The edges of these shallow pools are progressively eroded so that adjacent pools merge. For this type of weathering to be effective the rock surface needs to be conducive to forming shallow pools. Figures 4.1 – 4.5 show the nature of rock surfaces studied for this thesis. The smooth surfaces of the Kaikoura mudstone and sections of the limestone provide favourable pool forming surfaces. The greywacke, basalt and the Lake Waikaremoana mudstone do not.

Salt crystallisation on its own works within the rock structure or joints to fracture off small sections of rock. It will only work where saline water is able to penetrate the rock and therefore only on the top layer of the rock. Although the actual individual nature of the processes would be to cause a jagged fractured surface at the micro scale over a larger area of rock the tendency would be to erode where water is able to penetrate. This would be at the surface or top layer of the rock. Salt weathering works in conjunction with waves, which wash the debris away so weathering can continue on newly exposed rock surfaces.

Wave action may work in a number of ways to cause erosion of the shore platform surface (Chapter 6). The action of water flow across a surface will be to smooth it at the large scale. At the micro scale some roughness may occur from plucking of loose blocks surrounded by joints but essentially the flow is working to make the smoothest surface to flow over. Structures protruding into the flow will be exposed

to the greatest stresses and are therefore more likely to break off than the lower parts of the surface. Turbulence may alter this trend at the micro scale enhancing plucking or setting up eddies. The possible air compression action described in section 6.1.3.4 requires rough surfaces on the micro scale for capture of air bubbles. It was suggested that fracture size of less than 6mm was suitable for this process.

Both these groups of processes, weathering and waves are controlled by rock character. Mudstone at Kaikoura is more susceptible to weathering processes and flakes easily but has a smoother less fractured surface which makes it less susceptible to wave processes of plucking. The greywacke is highly fractured and potentially more easily eroded by wave action than weathering processes.

The high spatial variability of rock strength and surface structure at the micro scale across the shore platforms studied (figures 4.12 and 2.22) would mean that the processes described here would also be spatially varied in distribution across platforms. The exception to this spatial variation is the action of water flow, which is not constrained by differences in rock surface strengths at the micro scale. However, it is constrained by larger scale fractures and fissures in the rock surface.

Most of the erosive processes working on shore platforms tend towards near horizontal flat surfaces or are constrained by other factors in such a way that this occurs. This dictates the distinctive near horizontal flat surface form of shore platforms.

8.5 SHORE PLATFORM DEVELOPMENT.

Processes causing change on shore platforms described in this thesis have all been shown to have the capacity to cause erosion of shore platforms. However, it has been shown that over all the shore platforms studied, no one process controls morphology and that the morphology both responds to processes and controls processes. For this reason a geomechanical model of shore platform development does not provide an adequate framework within which to view shore platform development. This section presents a different way in which shore platform development can be conceptualised.

There is a vertical zone at the coast in which shore platform forming processes occur. The extent of the zone is determined by the mechanisms of the erosive processes and the vertical fluctuations of water level controlled by tidal and other influences. Within that zone, the occurrence of shore platforms, the form shore platforms take and their rate of development is dependent on the interaction between the processes of erosion and the responses of the morphology. This interaction can be conceptualised generally through a process – response model (figure 8.5).

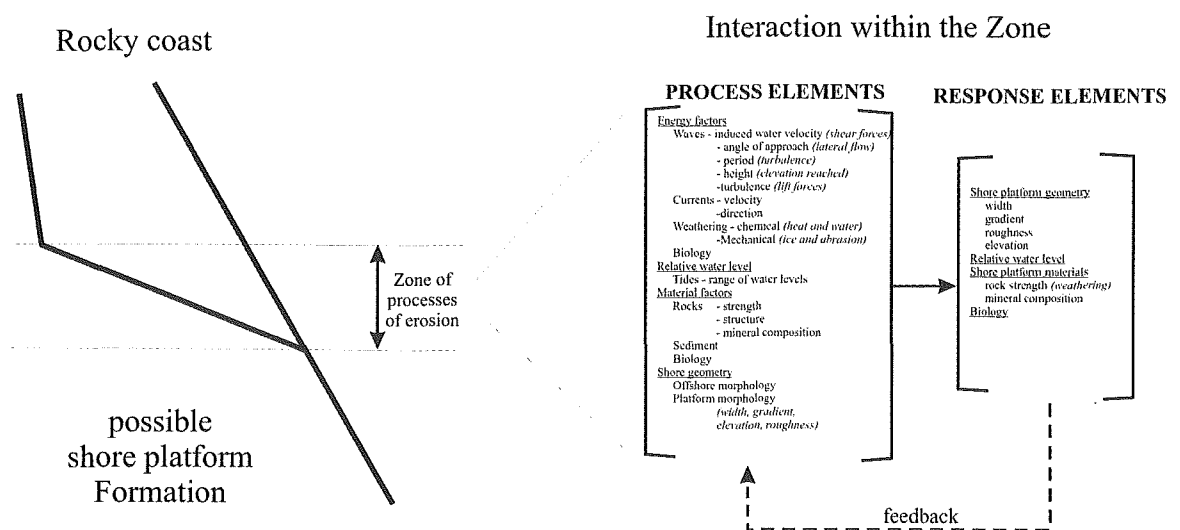


Figure 8.5: A model of shore platform development. Defining the zone of formation and the interaction of processes within that zone which, over time defines the form of the profile.

8.5.1 THE FORMATION (EROSION) ZONE.

As stated in section 8.1 shore platforms only develop at the coast at or near mean water level. This is within a zone where air, water and rocks interact. Once removed from the unique combination of processes that occur there, these features no longer evolve in the form of a shore platform. Removal from the zone may be the result of tectonic movement, changes in sea or water level either up or down, or erosion of the rock surface below the zone. For this reason it may be useful to think of the development of shore platforms in terms of a vertical zone of processes. As formation of shore platforms only occurs within this zone it must be one or more of the processes or, the unique combination of processes that occur within this coastal

zone that are fundamental in shore platform development. This section discusses the processes of erosion that work within the zone and the boundaries of the zone.

This shore platform formation zone may be defined in two ways.

- 1) By identification of erosive processes on shore platforms and the requirements and spatial restrictions of the mechanisms by which they operate.
- 2). Through identification of morphology and the limits of this morphology in comparison to other factors.

8.5.1.1 SPATIAL RESTRICTIONS ON EROSION PROCESSES.

Many processes capable of causing erosion on shore platforms and the mechanisms by which they work have been discussed in this thesis. This section recalls some of those processes and places them in a spatial context. Not all erosive processes that work on shore platforms have been discussed and it is acknowledged that other processes may also lead to erosion on shore platforms. However, they are considered to contribute relatively little to overall erosion.

The collective erosive processes of wave action (Chapter 6) are restricted in the elevation to which they work by water level variations and the intensity of the general wave environment on the platform. Water level variations in the marine environment are driven primarily by the tide and have well defined upper and lower limits. In the Lake Waikaremoana environment water levels are driven by input volumes of water in relation to outflow rates. Wave action is then superimposed onto these limits to give absolute levels to which waves may work. The maximum wave height and runup on the shore platform added to the upper tidal or lake level limit and the influence of storm surge will give the upper boundary of the vertical extent of possible erosive work done by waves. The activity of the general wave environment must dictate to some extent the size of bores crossing the shore platform and therefore the elevation to which they reach. However, the relationship between deepwater and onshore wave energy and height is a complex one. As shown in figure 5.35 it is not necessarily the highest energy deepwater waves that deliver the

highest energy to the shore platform. Wave heights at the platform edge are controlled by the nearshore and the morphology of the platform itself.

Water flow is also controlled by the morphology of the platform itself. It was shown in section 5.4.3 that average velocity and intensity of turbulence vary consistently with location on the shore platform. Flow may also be constricted and changed by aspects of relief on the shore platform. Further research is required to establish full understanding of these morphology – wave induced flow interactions.

Water flow across the rock is required for many of the mechanisms of wave erosion outlined in Chapter 6 to operate. Therefore a depth of water above the rock surface is required. This requirement is again dictated by tidal levels in relation to the shore platform.

The effectiveness of wave erosion will also be restricted to zones where rock structure is such that it is susceptible to erosion by the wave forces exerted. For example, fractured rock may make blocks available for plucking or provide small cavities in which air compression can occur.

The collective erosive processes of weathering require interaction of air, water and rock. This gives a definite lower boundary to operation of weathering on shore platforms at the level of permanent inundation or saturation (the lowest tidal level). This requirement of interaction of air, water and rock also means that there is no upper level restriction to weathering processes as rain may provide the water element at any vertical level above the level of permanent saturation. However, weathering is intensified by regular wetting and drying and intrusion of salt water, which occurs within the tidal zone.

As shown in section 7.3.4 saturation of some rocks requires as little time as 10 minutes to occur. Therefore the upper limit of intensified weathering could be areas reached by wave inundation at the highest tidal level. It was shown in section 7.3 that the intensity and type of weathering is controlled by rock type. Therefore the spatial distribution of rock type will dictate the spatial distribution of erosive processes of weathering. Rocks without clay content such as the greywacke at RM1

will not support weathering by wetting and drying alone. Distribution of weathering is restricted by rock characteristics both in terms of vertical distribution and depth of penetration into the rock. In laboratory testing, saturated rocks did not dry fully in 6 hours (section 7.3.4.2). This suggests that weathering action is confined to the surface layer only.

For continued weathering to occur on shore platforms, removal of debris by wave action is required in order to expose fresh un-weathered surfaces. Most weathering processes will only be effective until armouring occurs, so to be effective they must work in conjunction with the process or processes that remove the sediment from the platform. Therefore the zone of continuous intensified weathering is restricted by the vertical extent of wave action to elevations where flows occur of sufficient velocity to be able to transport debris away.

The processes of erosion on shore platforms described in this thesis are either restricted between, or are most effective between, the lowest tidal level and the highest level of wave activity. The vertical zone in which waves are able to erode shore platform rock surfaces is restricted for the most part to between tidal limits. The lower limit to which weathering works is the level of permanent inundation and the upper limit of intensified weathering is the highest reached by wave action.

These vertical boundaries of shore platform development have previously been described in the literature either explicitly or implicitly through identification of process – morphology relationships (Bartrum 1916, Trenhaile 1978, 1987, 1999, Trenhaile and Layzell 1981, Tsujimoto 1987, Sunamura 1992). For example, Bartrum (1916) suggested that shore platforms erode to a level of permanent saturation of the rock. The vertical distribution of wave action is controlled by tide range (Bartrum 1935, Bradley and Griggs 1976, Trenhaile 1987, Tsujimoto 1987, Sunamura 1992, McKenna *et al.* 1992) and Trenhaile (1972, 1974a, 1997, 1999) has shown a positive relationship between platform gradient and tidal range. Steeper platform gradients occur in regions with greater tidal ranges.

8.5.1.2 MORPHOLOGICAL LIMITS.

Another indication of the boundaries of the shore platform formation zone can be obtained from shore platform morphology.

If the view that shore platform formation is constrained within a zone of processes is accepted then morphology will also be constrained within the boundaries of this zone. If development of shore platform morphology is constrained within this zone, classification of the zone may be possible from direct investigation of the vertical distributions of platform boundaries.

Using morphology to define the boundaries of the zone of formation, and assuming that the shore platform boundaries defined in section 2.5.2 are the limits of the shore platforms studied for this thesis, it is possible to compare the vertical distribution of each study profile with respect to mean sea level using hypsographic curves (figure 2.22). The lower limits of all study profiles were at elevations higher than 1.13m below mean sea level and the upper limits of morphology ranged between 0.65 m amsl to 2.13 m amsl. The majority of the surface of each shore platform was between 0.5m either side of mean sea level. Lake Waikaremoana shore platforms covered a greater range of elevations being more steeply sloping. Surfaces of KM2, KM3 and KM7 were predominantly at higher elevations than those of AK1, AK2 and RM1.

Hypsographic curves shown in figure 2.21 may define the zones absolutely in the vertical dimension but not in relation to process. Therefore, hypsographic curves for each profile have been redrawn scaled to tidal variations (figure 8.6 and 8.7). Vertical elevations have been given as a proportion of tidal level at that profile, where 0 is the lowest level of the tide and 100 is the highest level of the tide.

Cumulative frequencies of shore platform surface elevations between average tidal levels were constructed for figure 8.6. Lake Waikaremoana profiles have not been included in this figure as the lake is non-tidal. Figure 8.6 shows that not all levels of the shore platform profiles studied are within the mean tidal levels. Therefore, the entire morphology of shore platforms studied does not occur between mean tidal

ranges. Mean tidal range does not fully define the boundaries of shore platforms or the zone of formation.

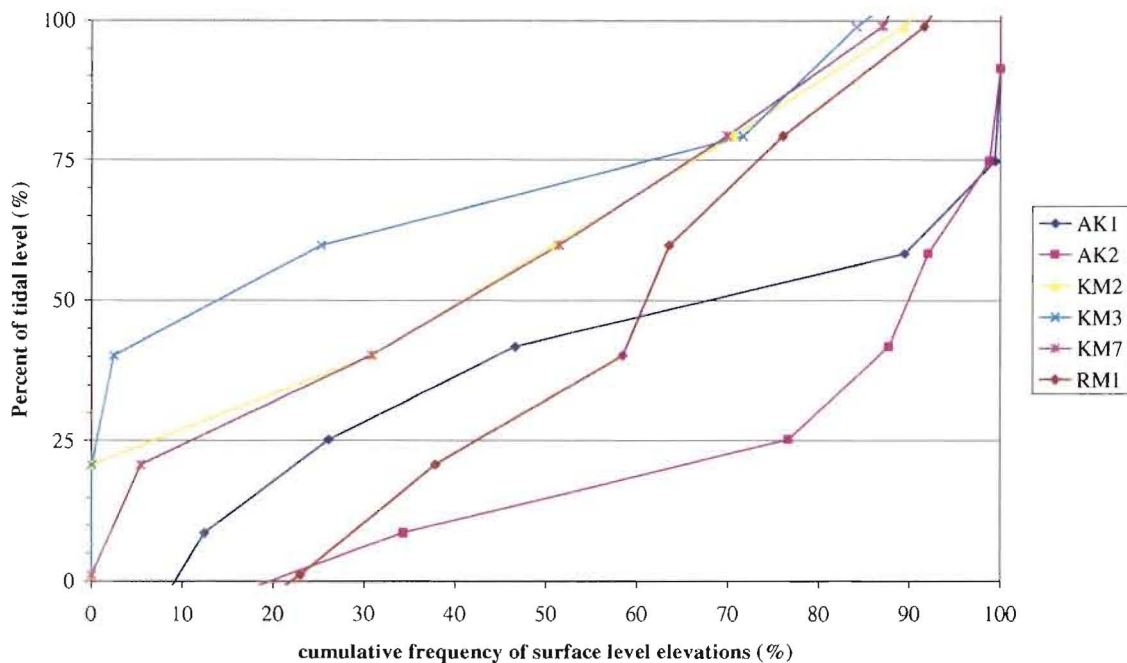


Figure 8.6: Hypsographic curves showing frequency of elevation with respect to mean tidal levels at 0.25m intervals for marine study profiles.

Figure 8.7 shows a similar comparison of cumulative frequencies of surface elevation but this time scaled to maximum tidal ranges recorded at each location. The maximum operating range of Lake Waikaremoana has been used in this figure to give what is essentially a maximum ‘tidal’ range. The majority of elevations on all shore platforms were within the limits of maximum tidal range. The elevations of all profiles were constrained by the lowest tidal level. However upper limits of KM7, WK1 and WK2 were outside the highest tidal level. This shows that definition of the upper vertical limit of the zone of formation requires consideration of the role of storm surge and wave splash in raising the water level above that of the highest tide on occasion.

From investigation of both the restrictions on erosion processes and the bounds of morphology the vertical extent of the zone of shore platform formation has been defined as between the lowest tidal level and the upper limit of wave action which is influenced by the highest tidal or water level and wave conditions. This zone defines an area where shore platform formation may be possible. Whether shore platforms

occur and the form that they take depends on the complex interactions of processes within the zone.

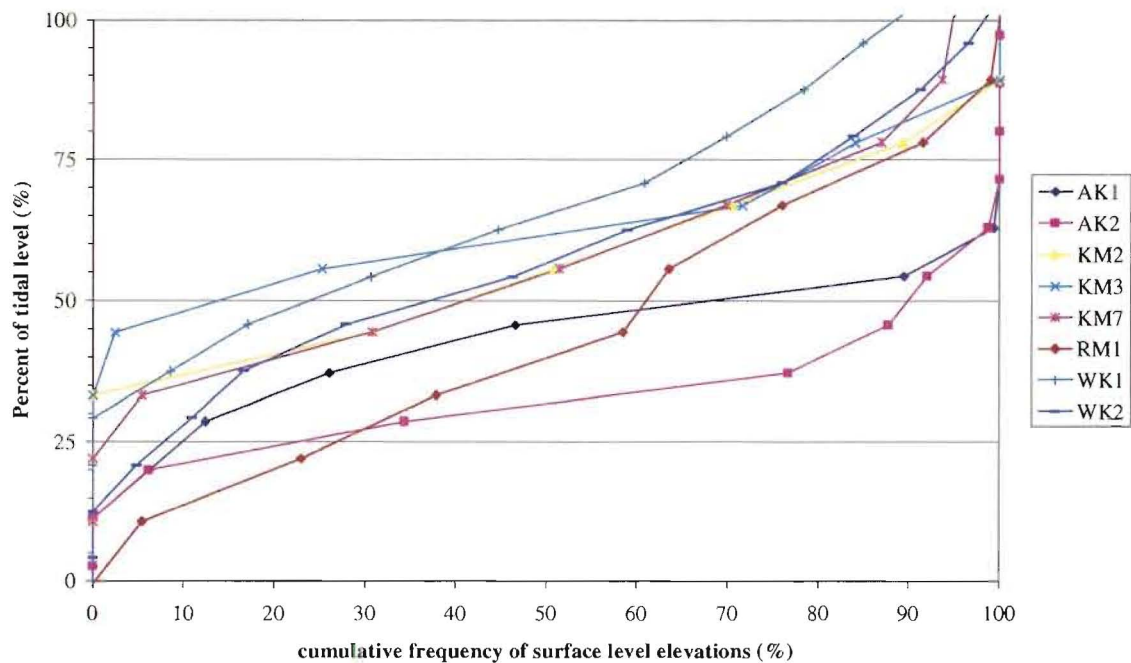


Figure 8.7: Hypsographic curves showing frequency of elevation with respect to maximum and minimum tidal levels at 0.25m intervals for all study profiles.

8.5.2 PROCESS – RESPONSE MODEL (WITHIN THE ZONE OF FORMATION).

It has been shown that no one process necessarily dominates erosion of shore platforms studied for this thesis (section 8.2). Different processes or combinations of processes occur in different locations dependent on both the erosional process factors and morphological responses to these factors. Process factors include the wave environment, weathering and rock characteristics. It is important to note that responses and controls on shore platform morphology are more complex than a straight geomechanical model of balance between opposing forces would tend to suggest. Sunamura’s (1992) model of shore platform development states that where wave assailing forces are greater than the resisting forces of the rock, shore platforms will develop. However, investigation of relationships between processes and shore platform morphology as well as processes and rate of shore platform development in the form of surface change for this thesis have shown that great variation and complexity in these relationships occurs. This complexity is exemplified in the location of shore platforms around Akaroa Harbour where rock type is similar and

wave energy varies due to shoaling and protection of the harbour topography. Shore platforms occur where the assailing force of the waves has been shown to be lowest, at the head of the harbour (figures 5.6 and 5.7), and not on the exposed cliffs of the harbour entrance.

Therefore the morphology of shore platforms, in terms of width, gradient and elevation is, in general not the result of control by one over riding influence or set of processes producing assailing forces but a complex combination of erosive processes and morphological control over these processes which may differ from location to location. The complex interactions of processes and responses within the zone of erosion can be interpreted using an adaptation of Krumbein's (1964) process – response model for beaches. This adaptation is shown in figure 8.8.

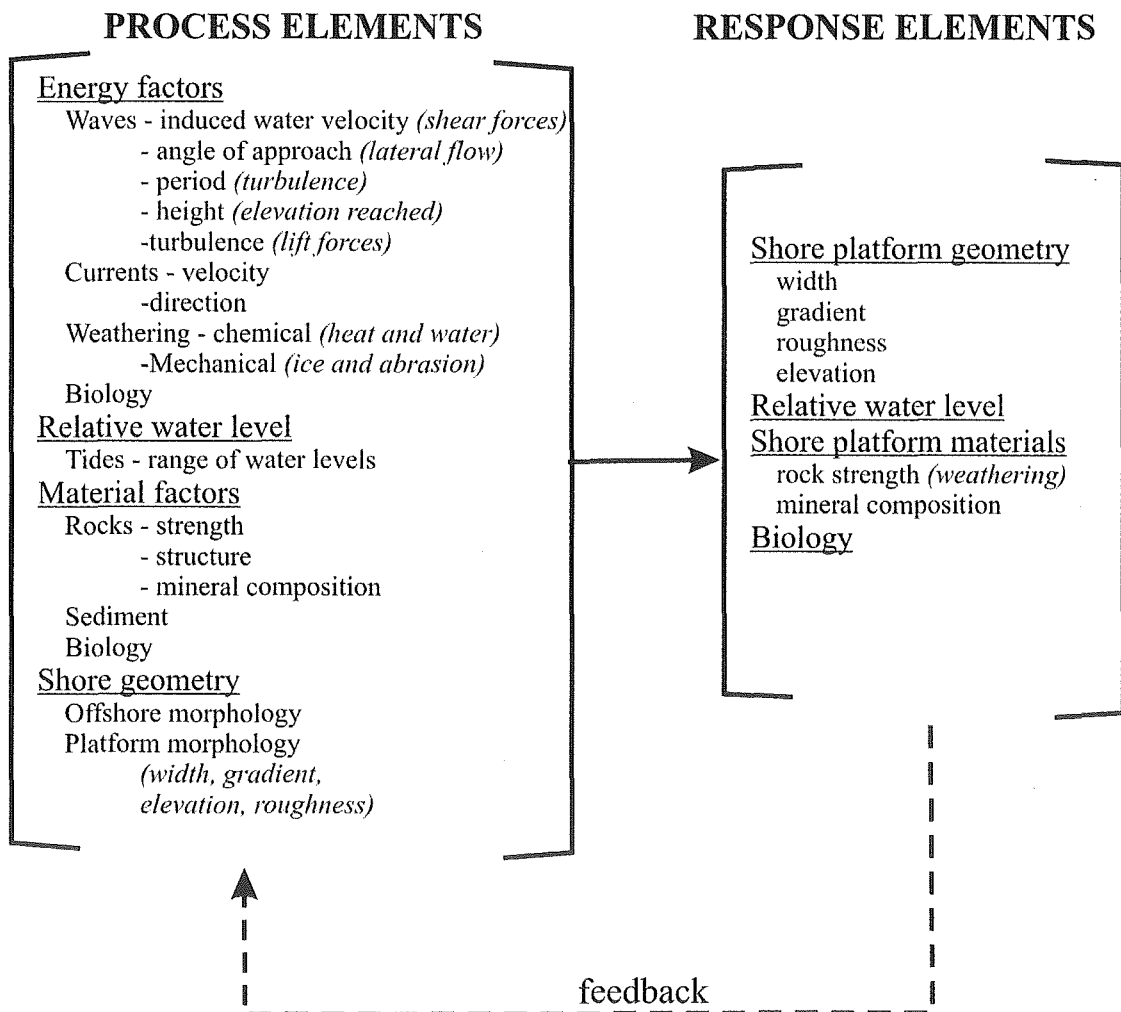


Figure 8.8: Conceptual process – response model for shore platforms (after Krumbein 1964).

This process response model (figure 8.8) details process elements and response elements on shore platforms and shows linkages between the two. Processes elements are given in terms of energy factors, relative water level, material factors and shore geometry. These elements dictate, to a greater or lesser extent erosive processes that occur on shore platforms. Response elements include shore platform geometry, relative water level, shore platform materials and biology. These are all elements of shore platforms that respond or change with actions of processes. A feedback loop is included in the model as the response of some elements may have consequences for how process elements operate. For example, the shore platform geometry has been shown in Chapter 5 to effect transformations in wave action. Some elements such as platform morphology and biology are included on both sides of the model as these factors may act as both a process element and a response element in shore platform development.

After a sufficient amount of time process and response elements will attain an equilibrium profile form. This form will be retained even though erosion may continue, until a change in either process or response elements occurs.

The equilibrium profile form may vary in absolute dimensions from location to location where process and response elements vary. It was suggested in section 8.3 that the lack of erosional pattern related to elevation across the profiles at AK1, AK2 and RM1 meant that these profiles may have reached an optimum gradient, one where processes and responses have reached a point where they are adapted. On the Kaikoura Peninsula profiles (KM2, KM3 and KM7) higher elevations are still eroding at a greater rate. Therefore, process and response elements have not reached an optimum gradient with respect to the gradient of the surface.

Recognition of optimum width attained by different shore platforms is more difficult to detect in terms of a measurable pattern. This would require knowledge of the relative positions of the landward and seaward edges of shore platforms. As noted by Stephenson (2001) this is difficult to measure. From analysis of aerial photographs taken 52 years apart he concluded that there was no detectable retreat of the seaward edge of the shore platforms on the Kaikoura Peninsula. Edwards (1941) suggested that the width of shore platforms was determined by the relative rate of

retreat of the landward and seaward cliffs but offered no field evidence of seaward cliff retreat. Sunamura (1992) stated that no seaward cliff retreat was possible based on distribution of wave assailing force in relation to the seaward edge of the platform.

The lack of information on relative cliff retreat for shore platforms studied in this thesis means that no conclusions can be made as to the possible width attained when process and response elements are adapted. However, the width of relict platforms on the Kaikoura Peninsula are over 1km in some locations (figure 2.2). Assuming that environments when these shore platforms were formed were similar to those forming the current platforms it is unlikely that the profiles at KM2, KM3 and KM7 have attained an equilibrium width and will continue to widen for a considerable time.

The complex interactions described by the process-response model of figure 8.8 suggest that development of shore platforms may be the result of equifinality. In different locations, different processes of erosion may dominate but result in similar morphology.

8.6 SUMMARY.

At the beginning of this chapter a number of questions were posed concerning the equilibrium of shore platforms. Past propositions in the literature concerning the evolution of shore platforms implicitly or explicitly assume an equilibrium form. If weathering is considered the dominant process causing erosion on shore platforms there should be down-wear of platforms to a base level and continued widening of the shore platforms indefinitely. If waves are considered to be the dominant form of erosion, down-wear should occur to a level related to the base level of wave activity and shore platform form and width should be static when the platform has reached a form that fully dissipates the wave energy. What then is the equilibrium form of a shore platform and how does this form develop?

On the shore platforms studied for this thesis it was shown that no single process of erosion or set of processes measured dominated despite similarity of shore platform

form in terms of width and gradient. Processes measured included aspects of weathering, wave action and rock characteristics and shore platforms were from differing process environments.

This lack of dominance of one process suggests that shore platforms are formed through a complex interaction of processes that are not necessarily the same at each location.

It has been proposed here that shore platforms will only form within a vertical zone defined at the lower boundary by the lowest tidal level and at the upper boundary by the highest level of wave action. This upper boundary is dependent on tides and wave conditions. Within this zone erosion will continue as long as there is contact between the air, water and rock.

The rate of erosion and response of the rock in profile form depends on the complex interaction of erosive process elements and response elements and can be conceptualised through a processes-response model (figure 8.8).

It is an important conclusion that erosive processes do not only dictate form but that form may also influence processes. The equilibrium form for one set of environmental conditions may be slightly different to another, although the processes of erosion all tend towards a near horizontal flat surface.

Once the morphology has adapted to erosive processes and erosion processes have adapted to the morphology the shore platform will have attained an equilibrium form. However, as long as the zone of formation still exists with the interaction of the air, water and rock, erosion of the shore platform will continue to occur. The nature of the processes of erosion on shore platforms are such that erosion will occur indefinitely within this zone.

The shore platform may reach a constancy of form but continuing erosion may still occur causing the position of the form to retreat over time. Shore platforms are wholly erosional therefore no accretional additions can be made. The equilibrium form of shore platforms for the sites studied in this thesis is expressed as a near

horizontal flat surface with shallow gradient and an, as yet, unspecified width. The exact form is defined by the combination of processes within the zone of erosion and the responses of both, morphology to processes and processes to morphology. Processes include rock characteristics, wave induced processes, weathering, biological action and shore geometry.

The shore platforms studied in this thesis are formed in rock types with differing characteristics and control the response of the rock to processes of erosion. Therefore, shore platforms formed in different rock types must have been developed by a range of different processes or combinations of processes. This highlights the possibility of equifinality in shore platform development.

CHAPTER NINE

CONCLUSIONS.

This thesis has quantified surface level change on shore platforms formed in five different lithologies at various locations around New Zealand and has investigated several processes of erosion on those shore platforms. It will be recalled that this work was undertaken with the following objectives as stated in Chapter 1.

- 1). Investigation of the control of rock type on shore platform morphology and shore platform development.
- 2). Investigation of the nature and activity of some processes of wave action and weathering as causes of change on shore platforms.
- 3). Quantification of change and of patterns of change for elucidation of both control and processes occurring on shore platforms.
- 4). To develop measures of processes that are more appropriate for use in shore platform studies.
- 5). Investigation of the concept of equilibrium as it applies to shore platform development.

Conclusions have been reached in relation to these five objectives. However, because of the integrated nature of the conclusions they will be stated as a whole rather than on the basis of each individual objective. The examination of processes and their relationships to morphology and morphological change on shore platforms has highlighted the narrowness of the commonly used geomechanical approach in providing a universal description of shore platform development. The integrated approach of this thesis suggests shore platform development is not the result of the balance between resisting forces of the rock and the assailing forces of waves, but rather a complex combination of factors. Therefore, an alternative model for looking at the development of shore platforms has been presented in this thesis. This will also be summarised.

Shore platforms formed in five different rock types on coastlines around New Zealand were selected for study in this thesis. They are all located within temperate climates and are on the shores of both fresh and salt-water bodies with micro and effectively meso tidal ranges. The platforms studied all had near horizontal flat surfaces located within the intertidal zone.

To enable investigation of morphology, eight profiles in all were established across the study platforms. Micro-erosion meter (MEM) sites were installed at reasonably regular intervals across the profiles for monitoring and quantifying surface level change. This permitted comparisons of measurements made on all rock types. Sites were surveyed approximately every two to three months for three years, except for the Lake Waikaremoana sites that were surveyed once a year for three years.

The profiles crossed shore platforms eroded into basalt, greywacke, limestone and two types of mudstone and were all of similar morphology despite differing morphogenetic environments. The components of morphology were defined according to criteria rigorously established in this thesis. Platform width ranged from 40.4m to 89.1m and gradients were between $2^{\circ}41'$ and $0^{\circ}26'$. Mean elevations of profiles varied between 0.81m above mean water level and 0.37 m below mean water level. All profiles showed broadly similar distributions of elevation with at least 60% of the surface constrained within a narrow range of elevations between 1m above mean water level to 0.7m below mean water level.

Measurement of surface level change showed vertical changes in both the negative (downward) and positive (upward) directions on all the marine shore platform surfaces. On the mudstone at Lake Waikaremoana only surface change in the negative direction was measured. Positive changes in surface level were interpreted as surface swelling and negative as surface contraction or erosion. The largest amount of surface change recorded over the study period was 50+ mm of surface lowering on WK1bsA. The greatest amount of surface change recorded on the marine shore platforms was 11.85mm of surface lowering at KM2A. Maximum erosion rates of 12.82 mm.yr^{-1} were measured at WK1mem. Maximum erosion rate on marine platforms studied were 4.75 mm.yr^{-1} at KM2A. Average rate of erosion measured in

the basalt was 0.29mm.yr^{-1} , on the greywacke was 0.78mm.yr^{-1} , on the limestone was 1.19mm.yr^{-1} , on the Kaikoura mudstone was 1.41mm.yr^{-1} and on the Lake Waikaremoana mudstone was 9.13mm.yr^{-1} .

None of the changes measured appeared to display cyclic patterns but there were patterns of change that showed sequential expansion and contraction of all rock surfaces except the Lake Waikaremoana mudstone. The temporal scale of these surface change patterns was not defined but it was shown that considerable changes were evident over periods of weeks and even over the period of a single day. This is a significant finding as previous identification of the swelling phenomena has reported temporal patterns of change in the order of months (Stephenson and Kirk 2001).

Surface change at the micro scale (less than 12.5cm^2) differed in spatial dispersion from rock type to rock type. Greywacke and basalt both displayed highly active surfaces with 20-30 nodes of movement over the study period. Change occurred in a more uniform way on the Kaikoura mudstone and limestone with only 3-4 nodes of movement evident on the surface plots of measurement over the study period. The high level of change evident on the greywacke and basalt occurred without corresponding erosion and shows the remarkable robustness of these two rock types. They are able to absorb large amounts of surface change without disintegrating. On the Kaikoura mudstone and limestone, surfaces appeared to be less active in nature but greater rates of erosion occurred suggesting that these rock types are less robust. The changes on the Lake Waikaremoana mudstone were both dynamic in nature and highly erosive. This rock type is unable to withstand net erosion when subjected to changes of surface level.

Given the dynamic nature of surface change a method for calculating average rates of change was developed that did not rely solely on two surveys of the surface level. This has been called a multiple duration method and it utilised the regular surveys of MEM sites to give surface level change over a range of durations. From this a best fit line was plotted that gave average rate of surface change. Surface change was further characterised by calculation of a residual from each plot, which gave an indication of the amplitude of rock surface expansion and contraction at that site. The average annual rates presented earlier were calculated using this method.

Construction of multiple duration graphs showed that at each site average surface change calculated from surveys separated by shorter intervals had a wider degree of variability than those separated by longer intervals. It was an unexpected finding that measured surface change rates are a function of duration of the record, especially, as it was also found that short term rates measured over three years represent longer term rates measured over 24+ years. From the patterns shown in these data it was concluded that durations of greater than 600 days between surveys avoided the shorter term influence of surface expansion and contraction.

There was very little variation in average rates of surface change evident across the study profiles. This led to the conclusion that erosion rates are consistent across shore platforms in this study. There was a slight trend of higher erosion rates at higher elevations across profiles. This pattern was most noticeable on the Kaikoura mudstone and limestone but did not occur on the profiles formed in the greywacke and basalt.

The MEM technique has been utilised in this thesis to measure surface level change on shore platforms. The accuracy of this technique over the short term has been questioned (Trenhaile 1987). However, it has been shown that short term, three year measurements of surface change are representative of longer term, 24+ year measurements. It has also been shown that rates of surface level change measured using the MEM have sufficiently high magnitudes that they can have formed the current shore platforms in the times that water levels have been in their present relative levels at each study site. This suggests that the MEM technique provides an adequate measure of surface level change on shore platforms provided surveys are made over durations of greater than approximately 600 days.

Although the MEM technique has been shown to be suitable for measuring surface level change on shore platforms, future research augmenting micro scale observations with larger scale surface measurements may prove worthwhile. These could be undertaken through development of photogrammetry techniques.

9.1 CONTROL OF ROCK TYPE.

Prior to investigation of the control of rock type on shore platform development, characterisation of each rock type was made to facilitate comparison between them in this thesis. Characterisation of rock types was made through description of lithology of each profile and three different indices of rock strength.

Orientation of the dip and strike of rock in which each profile was formed varied considerably. There was no pattern evident between platform orientation and bedrock dip and/or strike. This showed that shore platforms are wholly erosional in origin and have formed, for the most part, regardless of the lines of weakness within the rock.

Three indices of rock strength were obtained from three different tests of rock strength: point load, Schmidt hammer and rock mass assessment. Each of these indices represented a slightly different aspect of rock strength. Point load testing gave a measure of bedrock strength, Schmidt hammer testing gave a measure of rock surface strength and rock mass strength assessment gave an index for the strength of the whole body of rock in which the platform was formed.

Average bedrock strengths ranged from a maximum of 2.14MPa on the greywacke to a minimum of 1.03MPa on the Kaikoura mudstone. Surface strength measures in the form of Schmidt hammer rebound numbers gave a ranking of the five rock types in the order of greywacke (44), Kaikoura mudstone (32), limestone (31), basalt (22) and Lake Waikaremoana mudstone (19). The rock mass index also ranked greywacke strongest (72) but showed a different order of the other four rock types with basalt (63), Kaikoura mudstone (61), limestone (60) and Lake Waikaremoana mudstone (50). The strength of the five different rock types ranged from the greywacke, which was moderately strong to the Lake Waikaremoana mudstone which was very weak.

For both the point load testing and the Schmidt hammer testing there was a range of results, which gave standard deviations around the mean strength. Standard deviation was especially high for point load testing with basalt showing the maximum variation

of $\pm 110\%$. This evident diversity of strength within single rock types could be expected to result in differential weathering and erosion rates on the platforms.

The degree of rock strength control of shore platform morphology varied according to the measure of strength used. Generally bedrock strength was not correlated to morphology or morphological surface change. Surface strength correlated positively to platform width showing wider platforms in stronger rock. This observation contradicts concepts of rock strength control of shore platform morphology given in the literature (Trenhaile 1987). Both mass strength and surface strength showed a negative trend when compared to platform gradient. As rock strength increased platform gradient decreased. No robust explanation for this relationship has been offered. There were negative trends between all three indices of rock strength and platform elevation with respect to mean water level. It was a surprising finding that shore platforms formed in stronger rock types occurred at lower elevations. No strong trends were shown between indices of rock strength and rate of surface level change, where surface level change has been used as an indicator of shore platform development.

Overall relationships between rock strength and shore platform morphology were complex. This work has highlighted a complexity in the control of rock strength on shore platform morphology.

The different indices of rock strength showed differing relative strengths for each rock type. This has emphasised the fact that an appropriate means of characterising the rock strength needs to be used. This needs to be one which reflects the nature of the forces that are causing erosion. It was concluded that measures of surface strength using the Schmidt hammer and the rock mass strength index are the most appropriate indices of rock strength to use in shore platform studies. These were the measures of rock strength that showed the strongest correlations to aspects of morphology and surface change. As it has been shown that erosive processes operate at the rock surface it is logical that measures of strength at this point are the most appropriate to characterise the resistance presented to erosion.

9.2 WEATHERING PROCESSES.

An investigation of the degree of weathering of each shore platform was obtained from a comparison of compressive strength equivalents of bedrock and surface rock strength of each rock type. Reductions of rock strength measured were 34% on the greywacke, 48% on the Kaikoura mudstone, 77% on the limestone, 88% on the basalt and 91% on the Lake Waikaremoana mudstone. It was concluded that this indicates a weakening of the rock at the surface on all shore platforms studied. However, this may not be a true indication of the total amount of weathering the shore platform has undergone.

Investigation of the activity of weathering processes was not possible directly, but an assessment of the susceptibility of the five different rock types to weathering was possible. This revealed much about the nature of weathering and its possible activity on the shore platforms studied. Three tests for susceptibility to weathering were conducted. One was a standard slake durability test, which gives a mass loss after two rotation cycles in a drum immersed in water. Mudstone at Kaikoura lost the greatest mass in this testing, losing 5.8% of the sample mass. The greywacke was least susceptible losing just 0.2% of the sample mass. A wetting and drying test showed Lake Waikaremoana mudstone, Kaikoura mudstone and parts of the basalt were susceptible to weathering by wetting and drying with percent mass loss of between 41% to 0.9% over 10 cycles. Limestone, greywacke and parts of the basalt were not susceptible to weathering by wetting and drying. A saturation test showed that salt weathering was possible on all five rock types. However, salt weathering is unlikely at Lake Waikaremoana due to a lack of supply of saline solution. It had greater potential on those rocks that absorbed the highest amount of water as a percent of dry mass on saturation. Saturation amounts as a percent of dry mass were 9.1% on the Kaikoura mudstone, 3.2% on the Lake Waikaremoana mudstone, 3.9% on the limestone, between 1.5% and 6.0% on the basalt and 0.2% on the greywacke.

It has been shown that not all of the rock types in which the shore platforms are formed are susceptible to certain mechanisms of weathering. The three tests that were conducted showed that greywacke was not very susceptible to these processes of

weathering. This means that the contribution of weathering to shore platform development at RM1 on the greywacke would be significantly less than those profiles on the other rock types more susceptible to processes of weathering.

A weak negative correlation was shown when the degree of susceptibility of rocks to processes of weathering was compared to rate of surface change. It was concluded from this that weathering processes may have some effect on shore platform development but not a controlling one.

Weathering processes were not assessed directly but rather by tests of rock susceptibility to specific processes of weathering. This gives a measure of possible relative effects of weathering. No more appropriate measure of weathering processes has been suggested. However, the complex nature and variety of possible weathering processes on shore platforms means that a wide range of tests should be considered. It was shown that not all rock types in which the shore platforms are formed are susceptible to weathering by wetting and drying. Therefore, indicators of wetting and drying alone are not sufficient to assess processes of weathering on shore platforms.

9.3 WAVE PROCESSES.

Offshore wave environments at each study site have been described to levels of detail supportable by the few data available. At KM2, KM3, KM7 and RM1 maximum significant wave height is 6.7m and average significant wave height is 1.8m. At AK1 and AK2 maximum significant wave height is 1.3m and average significant wave height is 0.6m. At WK1 and WK2 maximum significant wave height is 0.8m and average significant wave height is 0.2m. Comparison of these wave heights and parameters of shore platform morphology found a weak trend of wider platforms in areas of more active wave environments but no relationship between significant wave height and gradient or rate of surface change was evident. From this it was concluded that the offshore wave environment does not directly control shore platform development.

Further analysis of offshore waves at each study site showed that the offshore topographies are such that all but the smallest waves break before reaching the seaward edge of any of the profiles studied in this thesis. This finding questions the use of deepwater wave parameters or calculated wave breaking height as indicators of onshore platform wave assailing forces and shows that waves move onto and across shore platforms as bores or smaller reformed waves.

Simultaneous measurement of deepwater and onshore wave parameters showed that significant changes occurred as waves propagated onto shore platforms. Wave period was slightly longer onshore, with average significant period of 6.7s, than in deepwater with average significant wave period of 6.4s. Wave height reductions of over 67% between deepwater and on the shore platform were recorded. Water particle velocity changes of between +46% and -72% were measured. Wave energy and energy flux reduced dramatically as waves propagated onshore with 90% or more being lost. The relationship between deepwater and onshore wave energy was not a direct one and it was shown that it was not necessarily the highest energy waves that delivered the highest energy to the shore platform.

From these differences in deepwater and onshore platform wave parameters it can be concluded that the nature and activity of wave action on shore platforms is not readily related to that in deepwater.

The nature and activity of wave action on shore platforms was investigated through measurement of wave induced flows on the shore platform at KM3. Three sensors located at KM3 near the seaward edge, in the centre and near the landward edge of the platform recorded flows. These are the first measurement of velocity fields on shore platforms reported in the geomorphic literature.

Near the landward edge of the platform average velocities were $0.45\text{m}\cdot\text{s}^{-1}$ with a maximum velocity of $1.89\text{m}\cdot\text{s}^{-1}$ recorded. In the centre of the platform average velocities were higher at $0.66\text{m}\cdot\text{s}^{-1}$ and a maximum velocity of $2.54\text{m}\cdot\text{s}^{-1}$ was recorded. Velocities at the landward sensor were on average $0.26\text{m}\cdot\text{s}^{-1}$ and a maximum of $0.99\text{m}\cdot\text{s}^{-1}$. This showed that consistent dissipation of energy as waves flowed across the platform did not occur. These flow velocities were not related to

tidal level or offshore wave conditions and it has been concluded that flow velocity on the shore platform at KM3 is primarily controlled by another parameter such as the morphology of the platform itself. Strong lateral components to flows were measured at all three locations across the shore platform under varied deepwater wave conditions. Flow was shown to be very turbulent both in terms of uniformity and steadiness. Variations of up to 112% of the average flow velocity were measured.

These findings have consequences for understanding where erosion by wave action may occur on shore platforms. Rock surfaces will be subjected to forces from multiple directions rather than just onshore or offshore directions.

Direct measurement of wave action on the shore platform at KM3 enabled assessment of different modes of erosion proposed in the literature. Where possible, quantification of the forces of each mode of erosion was undertaken and from this the capacity of each mode to cause erosion of the rock surface was assessed. It was concluded that individually air compression and abrasion were the only two modes that created forces great enough to directly erode the rock surface. The maximum calculated force created by air compression within cavities of the rock was $2.1 \times 10^6 \text{ N.m}^{-2}$. This is greater than the measured surface strength of the rock. The flow was shown to be competent to move sediment. Therefore in locations where sediment is available on the platform erosion by abrasion is possible. Modes of Clapotis, shock pressures, water hammer, hydrostatic pressure, shear stress and cavitation were all shown to be incapable of erosion on an individual basis. However it was noted that modes of wave erosion do not work in isolation and combined action may be capable of erosion at least on the micro scale.

The process of wave action transporting sediment from shore platforms is an integral component of shore platform development, yet has not previously been investigated in the geomorphic literature. From direct measures of flow on the shore platform at KM3 it was possible to assess the competence and capacity of wave induced activity. Flows across the platform were competent of entraining silts, clays and sands (up to 2mm in diameter) at all locations across the platform while the tide covered the surface. There was potential for movement of large boulders (B-axis of up to 1000mm) up to 1% of the time. The capacity of the flow was limited by sediment

supply. From this it can be concluded that sediment of a large range of sizes could be transported across shore platforms.

There was a dominance of offshore net velocity and hence sediment transport was almost all offshore. This is not typical in coastal environments but explains why little unconsolidated sediment is evident on shore platforms.

Analysis of the effectiveness of flows lead to the conclusion that it is not the more extreme events that do the most geomorphic work on shore platforms. This is an important consideration when discussing events that are most likely to contribute to shore platform development. As yet, magnitudes of events have not been defined, but of the flows measured those that were most effective near the landward margin of the platform were 0.4m.s^{-1} , in the centre of the platform were 1.2m.s^{-1} and at the seaward margin were 0.8m.s^{-1} . These are considerably less than the fastest flows of up to 2.54m.s^{-1} .

The most appropriate measures to characterise wave processes on shore platforms are those of flow measured directly on the shore platforms. It was shown that deepwater wave parameters did not relate directly to wave parameters measured on the shore platform. It was also shown that all but the smallest waves have broken before reaching the edge of the shore platforms studied for this thesis. This means that calculated measures of breaking wave height are not readily useful to characterise the wave environment at these shore platforms. Therefore, until clear relationships between deepwater and onshore platform wave parameters are established, onshore platform measures of wave action should be utilised.

It has been shown that, there is still little understanding of the controls of flow onto and across shore platforms. As it was not necessarily the highest energy waves that delivered the highest energy to the shore platform, use of deepwater wave parameters to indicate onshore platform wave induced forces should be made with caution. Wave theory developed for sand beaches should not be applied to shore platform environments until greater understanding is attained. Use of Linear wave theory has been shown to overestimate flow velocities and distribution of flow on the shore platform at KM3. Therefore, given the current state of understanding of controls on

flow dynamics onto and across shore platforms it is recommended that the best assessment of wave action on shore platforms is that of flow measured directly on the platform.

The large amounts of turbulence measured at KM3 mean that average flow velocities alone may not be adequate for quantification of the erosive power of flow on shore platforms. The contribution of turbulence when assessing wave induced forces needs to be considered. This has only been undertaken to a limited extent in this thesis and is an area that warrants further research.

9.4 THE NATURE OF THE EQUILIBRIUM OF SHORE PLATFORMS.

This investigation of the nature and activity of processes of wave action and weathering occurring on shore platforms has led to the conclusion that no single process controls shore platform development over all the shore platforms studied for this thesis. Shore platform development is complex.

It is concluded from observation of morphology and a greater understanding of some processes of erosion that shore platforms tend towards near horizontal flat surfaces within the intertidal zone. Shore platforms reach an equilibrium form but continue to erode holding this form. It has been proposed that shore platform development occurs within a vertical zone bounded by the lowest level of low tide and the highest level of wave activity. Within this zone processes will continue as long as there is interaction between air, water and rock. The development and form of shore platforms within this zone will depend on the interaction of process and response elements. The form attained by platforms may vary slightly depending on the interaction between processes and responses. However, after this form has been achieved erosion will continue until the rock surface moves out of the zone. The form will only change if the process or response elements change. Shore platform equilibrium is, therefore, dynamic.

In order to conceptualise shore platform development a model has been proposed based on the process – response model of Krumbein (1964) adapted for the shore

platform environment. Process elements and response elements are given and the interaction between the two sets of elements involves a feedback link. Some elements are in both categories as they function as both a process and a response on shore platforms. The equilibrium form of a shore platform depends on the unique combination and interaction of process and response elements at each location.

9.5 FURTHER RESEARCH.

This thesis has quantified and elucidated many of the processes of erosion occurring on shore platforms developed in different rock types. In doing so it has provided greater insight into shore platform development. The expected outcome of better understanding of some important mechanisms causing erosion on shore platforms was achieved and in some cases this leads to a better understanding of processes and their relationships to morphology and morphological change. Greater elucidation of this on a range of rock types has led to the conclusion that a simple geomechanical model of resistance balanced against force does not provide an adequate conceptual frame work in which to investigate shore platform development. There is no single set of processes that dominates shore platform development. For this reason a conceptual model for shore platform development has been presented, where form is defined by the interaction of process and response elements. This appears to give a more universally applicable way of viewing shore platform development.

This proposed model of shore platform development should now be tested against data from other shore platforms environments and further modified with greater understanding of both response and process elements of shore platforms. Although this thesis has quantified and elucidated some process and response elements, further research is required to more fully understand others and the interactions that occur.

In terms of processes of wave action this thesis has shown that there are no direct relationships between deepwater and on shore platform wave parameters. Definition of the relationship between wave action in deepwater and on the shore platform requires further investigation. Flow measurements were conducted only at one location and these observations now need to be extended onto differing shore platform environments to ascertain whether the same relationships are evident. Also,

assessment of both turbulence and acceleration on wave induced forces needs to be incorporated into analysis, to further clarify the role these may play in rock surface erosion.

More detailed study and testing of shore platform rock susceptibility to weathering is required to understand the full influence of processes of weathering. Greater understanding of patterns of surface change would also enable further elucidation of processes. This could include larger scale monitoring of surface change and definition of the temporal and spatial patterns of surface change.

REFERENCES

- Allan, J. C., 1998. Shoreline development at Lake Dunstan, South Island, New Zealand. *Unpub. Doctor of Philosophy Thesis, University of Canterbury, Christchurch.*
- Allan, J. C., Stephenson, W. J., Kirk, R. M. & Taylor, A. J., 2002: Lacustrine shore platforms at Lake Waikaremoana, North Island, New Zealand. *Earth Surface Processes and Landforms*, 27, 207-220.
- Allan, J. C., Stephenson, W. J., Taylor, A. J. & Kirk, R. M., 1999: *Monitoring shoreline change and development at Lake Waikaremoana for shoreline management.* Christchurch: Electricity Corporation of New Zealand
- Arndt, R. E. A., 1981: Cavitation in fluid machinery and hydraulic structures. *Annual review of fluid mechanics*, 13, 273-328.
- Bagnold, R. A., 1939: Interim report on wave pressure research. *Journal of the institution of civil engineers (London)*, 12, 202-226.
- Bal, A. A., 1997: Sea caves, relict shore and rock platforms; evidence for the tectonic stability of Banks Peninsula, New Zealand. *New Zealand Journal of Geology and Geophysics*, 40 (3), 299-305.
- Bartrum, J. A., 1916: High water rock platforms: a phase of shoreline erosion. *transactions of the New Zealand Institute*, 48, 132-134.
- Bartrum, J. A., 1924: The shore platform of the west coast near Auckland: its storm wave origin. *Report to the Australian Association of Science*, 16, 493-495.
- Bartrum, J. A., 1926: Abnormal shore platforms. *Journal of Geology*, 34, 793-806.
- Bartrum, J. A., 1935: Shore Platforms. *Report of the 22nd meeting of the Australian and New Zealand Association for the advancement of Science*, 22 (Jan 1935), 135-143.
- Bartrum, J. A. & Turner, F. J., 1928: Pillow lavas, peridotites and associated rocks from northernmost New Zealand. *transactions of the New Zealand Institute*, 59, 98-138.
- Bascom, W., 1980: *Waves and Beaches.* Anchor Press/Doubleday: Garden City.
- Bird, E. C. F. & Dent, O. F., 1966: Shore platforms on the south shore of New South Wales. *Australian Geographer*, 10, 71-80.
- Bradley, W. C. & Griggs, G. B., 1976: Form, genesis and deformation of central California wave-cut platforms. *Geological Society of America Bulletin*, 87, 433-449.
- Broadhead, T. W. & Driese, S. G., 1994: Experimental and natural abrasion of conodonts in marine and eolian environments. *Palaios*, 9 (6), 546-560.
- Brown, E. T. (ed), 1981: *Rock Characterization Testings and Monitoring.* Pergamon Press:
- C.E.R.C. & Center, C. E. R. (ed), 1984: *Shore Protection Manual.* US Corp of Army Engineers:
- Carling, P.A. & Dawson, M. R. (ed), 1996: *Advances in Fluvial Dynamics and Stratigraphy.* John Wiley & Sons: Chichester.
- Castilla, J. C., Steinmiller, D. K. & Pacheco, C. J., 1998: Quantifying wave exposure daily and hourly on the intertidal rocky shore of central Chile. *Revista Chilena de Historia Natural*, 71, 19-25.
- Challinor, J., 1949: A principle in coastal geomorphology. *Geography*, 34 (166), 212-215.
- Charmichael, R. S. (ed), 1989: *Physical Properties of Rocks and Minerals.* CRC Press: Florida

- Cotton, C. A., 1951: Seacliffs of Banks Peninsula and Wellington: Some criteria for coastal classification. *New Zealand Geographer*, 7 (2), 103-120.
- Cotton, C. A., 1963: Levels of planation of marine benches. *Zeitschrift für Geomorphologie*, 7, 97-110.
- Dahl, R., 1965: Plastically Sculptured detail forms on rock surfaces in Northern Nordland, Norway. *Geografiska Annaler*, 47 (A), 83-140.
- Dana, J. D., 1849: *Geology - United States Exploring Expedition 1838 - 1842*.
- Day, M. J. & Goudie, A. S., 1977: Field assessment of rock hardness using the Schmidt hammer. *British Geomorphological Research Group Technical Bulletin*, 18, 19-22.
- Denny, M. W., 1985: Wave forces on intertidal organisms: A case study. *Limnology and Oceanography*, 30 (6), 1171-1187.
- Denny, M. W., 1988: *Biology and the mechanics of the wave-swept environment*. Princeton University Press.
- Dietz, R. S., 1963: Wave-base marine profile of equilibrium, and wave-built terraces: a critical appraisal. *Geological Society of America Bulletin*, 74, 971-990.
- Dingwall, P. R., 1966. Bay-Head sand beaches of Banks Peninsula. *Unpub. Master of Arts Thesis, University of Canterbury, Christchurch*.
- Dionne, J. C. & Brodeur, D., 1988: Frost weathering and ice action in shore platform development with particular reference to Quebec, Canada. *Zeitschrift für Geomorphologie*, Supplement Band 71, 117-130.
- Duckmanton, N. M., 1974. The Shore platforms of the Kaikoura Peninsula. *Unpub. Master of Arts Thesis, University of Canterbury, Christchurch*.
- Edwards, A. B., 1941: Storm wave platforms. *Journal of Geomorphology*, 4, 223-236.
- Edwards, A. B., 1951: Wave action in shore platform development. *Geological Magazine*, 88, 41-49.
- Elgar, S. & Raubenheimer, B., 2001: Current meter performance in the surf zone. *Journal of Atmospheric and Oceanic Technology*, 18 (10), 1735-1746.
- Emery, K. O., 1941: Rate of surface retreat of sea cliffs based on dated inscriptions. *Science*, 93, 617-618.
- Emery, K. O., 1946: Marine solution basins. *Journal of Geology*, 54, 209-228.
- Emery, K. O. & Kuhn, G. G., 1980: Erosion of rock shores at LaJolla, California. *Marine Geology*, 37, 197-208.
- Emery, K. O. & Kuhn, G. G., 1982: Sea cliffs: Their processes, profiles and classification. *Geological Society of America Bulletin*, 93, 644-654.
- Everard, C. E., Lawrence, R. H., Witherick, M. E. & Wright, L. W., 1964: *Raised beaches and marine geomorphology. Present views on some aspects of the geology of Cornwall and Devon*. Royal Geological Society of Cornwall.
- Ewans, K. C. & Kibblewhite, A. C., 1992: Spectral features of the New Zealand deep-water ocean wave climate. *New Zealand Journal of Marine and Freshwater Research*, 26, 323 -338.
- Ferguson, R., Hoey, T., Wathen, S. & Werritty, A., 1996: Field evidence for rapid downstream fining of river gravels through selective transport. *Geology*, 24 (2), 179-182.
- Flemming, N. C., 1965: Form and relation to present sea level of Pleistocene marine erosion features. *Journal of Geology*, 73, 799-811.
- Gaylord, B., 1999: Detailing agents of physical disturbance: wave-induced velocities and accelerations on a rocky shore. *Journal of Experimental Marine Biology and Ecology*, 239, 85-124.
- Gaylord, B., 2000: Biological implications of surf-zone flow complexity. *Limnology and Oceanography*, 45 (1), 174-188.

- Gill, E. D., 1972: The relationship of present shore platforms to past sea levels. *Boreas*, 1, 1-25.
- Gill, E. D. & Lang, J. G., 1983: Micro-erosion meter measurements of rock wear on the Otway coast of southeast Australia. *Marine Geology*, 52, 141-156.
- Goda, Y., 1990: Random wave interaction with structures. In: Herbich, J.(ed) *Handbook of Coastal and Ocean Engineering*.
- Gorman, R. & Laing, A., 2001: Bringing wave hindcasting to the New Zealand coast. *ICS 2000 Proc.*, 30-37.
- Goudie, A. (ed), 1990: *Geomorphological Techniques*. Routledge: London
- Guza, R. T. & Thornton, E. B., 1982: Swash oscillations on a natural beach. *Journal of Geophysical Research-Oceans*, 87 (C1), 483-491.
- Hansom, J. D., 1983: Shore platform development in the south Shetland Islands, Antarctica. *Marine Geology*, 53, 211-229.
- Healy, T. R., 1968: Bioerosion on shore platforms developed in the Waitemata Formation, Auckland. *Earth Science Journal*, 2, 26-37.
- Herbich, J. B. (ed), 1990: *Handbook of Coastal and Ocean Engineering: Wave phenomena and coastal structures*. Gulf Publishing Company: Huston
- High, C. J. & Hanna, F. K., 1970: A method for the direct measurement of erosion on rock surfaces. *Geomorphological Research Group Technical Bulletin*, 5, 1-25.
- Hills, E. S., 1949: Shore Platforms. *Geological Magazine*, 86, 137-152.
- Hills, E. S., 1972: Shore platforms and wave ramps. *Geological Magazine*, 109, 81-88.
- Hjulstrom, F., 1939: Transportation of Detritus by moving water. In: Trask, P. D.(ed) *Recent Marine Sediments*, U.S. Geological Survey.
- Hodgkin, E. P., 1964: Rate of erosion of intertidal limestone. *Zeitschrift fur Geomorphologie*, 8 (4), 385-392.
- Hucka, V., 1965: A rapid method of determining the strength of rock in situ. *International Journal of Mechanical Mining Science*, 2, 127-134.
- I.A.H.R., 1989: List of sea-state parameters. *Journal of Waterway, Port, Coastal and Ocean Engineering*, 115 (6), 793-808.
- I.S.R.M., 1985: Suggested method for determining point load strength. *International Journal of Rock Mechanical Mining Science and Geomechanics*, 22 (2), 51-60.
- Inman, D. L., 1949: Sorting of sediments in the light of fluid mechanics. *Journal of Sedimentary Petrology*, 19 (2), 51-70.
- Johnson, D. W., 1919: *Shore Processes and Shoreline Development*. Wiley and sons: New York.
- Johnson, J. W., O'Brien, M. P. & Isaacs, J. D., 1948: *Graphical construction of wave refraction diagrams*. U.S. Hydrographic Office
- Johnson, M. E. & Libbey, L. K., 1997: Global review of Upper Pleistocene (substrate 5e) rockyshores: Tectonic segregation, substrate variation and biological diversity. *Journal of Coastal Research*, 13 (2), 297-307.
- Jonsson, I. G., 1966: Wave boundary layers and friction factors. *Proceedings of the 10th conference on coastal engineering. Tokyo, Japan*, 127-148.
- Jutson, J. T., 1939: Shore platforms near Sydney, New South Wales. *Journal of Geomorphology*, 2, 237-250.
- Jutson, J. T., 1949: The shore platforms of Lorne, Victoria. *Proceedings of the Royal Society of Victoria*, 61, 43-59.
- Jutson, J. T., 1954: The shore platforms of Lorne, Victoria, and the processes operating thereon. *Proceedings of the Royal Society of Victoria*, 65, 125-134.

- Kamphuis, J. W., 1975: Friction factor under oscillatory waves. *Journal of the waterways harbours and coastal engineering division*, 101 (2), 135-144.
- Kelsey, H. M. & Bocheim, J. G., 1994: Coastal landscape evolution as a function of eustasy and surface uplift rate, Cascadia margin, Southern Oregon. *Geological Society of America Bulletin*, 106 (6), 840-853.
- Kirk, R. M., 1970. Swash zone processes: An examination of relations between water motion and foreshore response on some mixed sand and shingle beaches, Kaikoura, New Zealand. *Unpub. Doctor of Philosophy Thesis, University of Canterbury, Christchurch.*
- Kirk, R. M., 1972: *Statistical summary of sea state observations in New Zealand 1971*. Christchurch: Geography Department, University of Canterbury
- Kirk, R. M., 1973: *Statistical summary of sea state observations in New Zealand 1972*. Christchurch: Geography Department, University of Canterbury
- Kirk, R. M., 1974: *Statistical summary of sea state observations in New Zealand 1973*. Christchurch: Geography Department, University of Canterbury
- Kirk, R. M., 1975a: Aspects of surf runup processes on mixed sand and gravel beaches. *Geografiska Annaler*, 57 (ser A), 117-133.
- Kirk, R. M., 1975b: *Statistical summary of sea state observations in New Zealand 1974*. Christchurch: Geography Department, University of Canterbury
- Kirk, R. M., 1977: Rates and forms of erosion on intertidal platforms at Kaikoura Peninsula, South Island, New Zealand. *New Zealand Journal of Geology and Geophysics*, 20 (3), 571-613.
- Kirk, R. M., 2001: Marine processes and coastal landforms. In: eds Sturman, A. P. & Spronken-Smith, R.(ed) *The Physical Environment: A New Zealand Perspective*, Oxford University Press: Oxford.
- Kirk, R. M., In preparation: Wind wave modelling of shoreline erosion processes for Lake Pukaki, South Island, New Zealand.
- Komar, P.D., 1996: Entrainment of sediments from Deposits of Mixed Grain Sizes and Densities. In: eds Carling, P.A. & Dawson, M. R. (ed), *Advances in Fluvial Dynamics and Stratigraphy*. John Wiley & Sons: Chichester.
- Komar, P. D., 1998: *Beach Processes and Sedimentation*. Prentice Hall: New Jersey.
- Komar, P. D. & Gaughan, M. K., 1972: Airy wave theory and breaker height prediction. In: *13th Coastal Engineering Conference*, pp. 405-418, American Society of Civil Engineers.
- Komar, P. D. & Miller, M. C., 1975: On the comparison between the threshold of sediment motion under waves and unidirectional currents with a discussion of the practical evaluation of the threshold. *Journal of Sedimentary Petrology*, 45 (1), 362-367.
- Kraus, N. C., Lohrmann, A. & Cabrera, R., 1994: New acoustic meter for measuring 3D laboratory flows. *Journal of Hydraulic Engineering*, 120 (3), 406-412.
- Krumbein, W. C., 1964: A geological process-response model for analysis of beach phenomena. *U.S. Army Corp. of Engineers Beach Erosion Board Annual Bulletin*, 17, 1-19.
- Kuenen, P. H., 1964: Experimental abrasion: 6. surf action. *Sedimentology*, 3, 29-43.
- Lane, S. N., Chandler, J. H. & Butler, J. B., 1996: Roughness parameterisation for hydraulic models. In: *Paper presented to the Annual Conference of the RGS-IBG*: Strathclyde.
- Lane, S. N., Chandler, J. H. & Richards, K., 1998: Landform monitoring, modelling and analysis: Land form in geomorphological research. In: eds Lane, S. N., Richards, K. & Chandler, J. H.(ed) *Landform Monitoring, Modelling and Analysis.*, John Wiley and sons: Chichester.

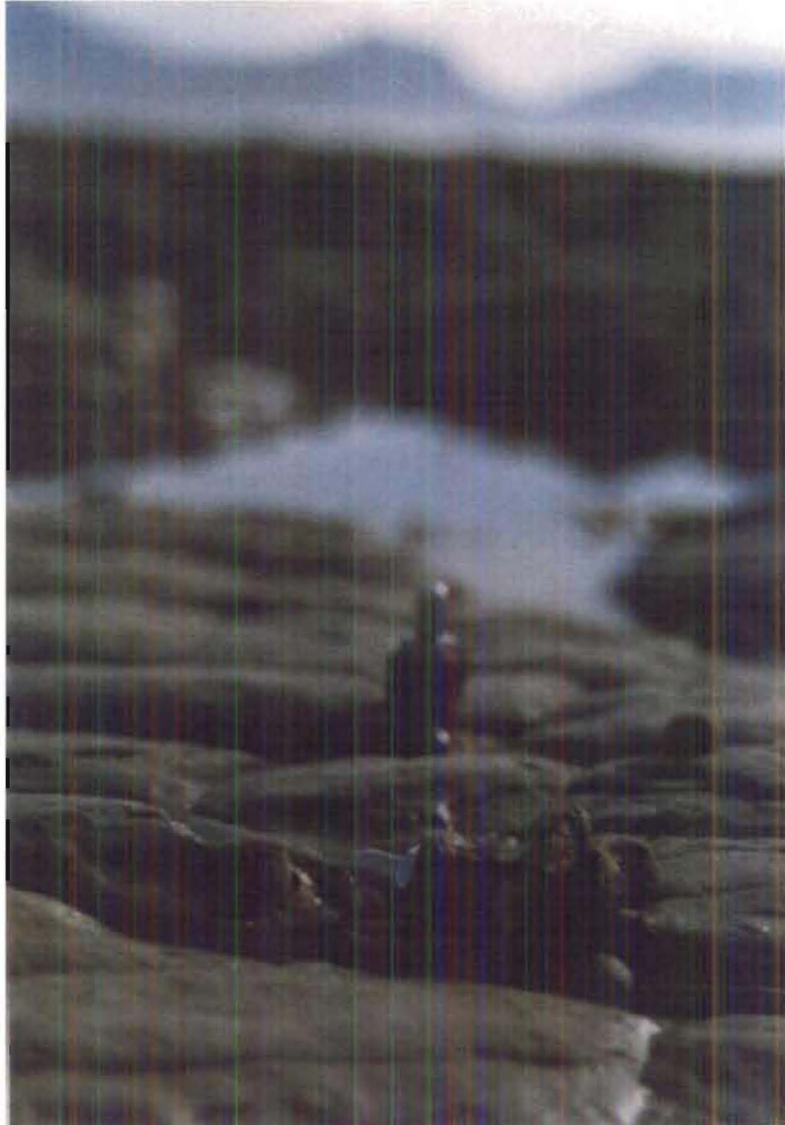
- Lawrie, A., 1993: Shore platforms at +6-8 m above mean sea level on Banks Peninsula and implications for tectonic stability. *New Zealand Journal of Geology and Geophysics*, 36 (4), 409-415.
- Lensen, G. J., 1975: Geological map of New Zealand, Sheet 16 - Kaikoura, Department of Scientific and Industrial Research.: Wellington.
- Leopold, L. B., Wolman, M. G. & Miller, J. P., 1964: *Fluvial Processes in Geomorphology*. W.H. Freeman and Co.
- Lewis, D. W. & McConchie, D., 1994: *Practical Sedimentology*. Chapman and Hall: New York.
- Longuet-Higgins, M. S., 1952: On the statistical distribution of the heights of sea waves. *Journal of Marine Research*, 11 (3), 245-266.
- MacKenzie, B. R. & Kiorboe, T., 1995: Encounter rates and swimming behaviour of pause-travel and cruise larval fish predators in calm and turbulent laboratory environments. *Limnology and Oceanography*, 40 (7), 1278-1289.
- Macky, G. H., Latimer, G. J. & Smith, R. K., 1995: Wave climate of the Western Bay of Plenty, New Zealand 1991-1993. *New Zealand Journal of Marine and Freshwater Research*, 29, 311-327.
- Marshal, P., 1927: The origin of Lake Waikaremoana. *Transactions and Proceedings of the New Zealand Institute*, 57, 237-244.
- Marshal, P., 1929: Beaches gravels and sands. *transactions of the New Zealand Institute*, 60, 342-365.
- Matthews, 1992. Shoreline erosion and sedimentology of Lake Waikaremoana. *Unpub. Master of science Thesis, University of Waikato, Hamilton*.
- McCave, I. N., 1971: Wave effectiveness at the sea bed and its relationship to bed-forms and deposition of mud. *Journal of Sedimentary Petrology*, 41 (1), 89-96.
- McClave, J. T. & Sincich, T., 2000: *Statistics*. Prentice Hall: Upper Saddle River.
- McKenna, J., Carter, R. W. G. & Bartlett, D., 1992: Coast erosion in northeast Ireland. - Part II. Cliffs and shore platforms. *Irish Geography*, 25 (2), 111-128.
- McLean, J. F., 1967. Objective description of shore platforms on the northeast coast of the South Island. *Unpub. Master of Arts Thesis, University of Canterbury, Christchurch*.
- McLean, R. F., 1967: Erosional burrows in beachrock by the tropical sea urchin, *Echinometra lucunter*. *Canadian Journal of Zoology*, 45 (1), 586-588.
- McLean, R. F., 1968: *Statistical summary of sea state observations in New Zealand 1967*. Christchurch: Geography Department, University of Canterbury
- McLean, R. F., 1972: *Sea conditions off the Northeast Coast, South Island, New Zealand: Ship Reports Jan - June 1967*. Christchurch: Geography department, University of Canterbury
- McLean, R. F. & Davidson, C. F., 1968: The role of mass-movement in shore platform development along the Gisbourne coastline, New Zealand. *Earth Science Journal*, 2 (1), 15-25.
- Merel, A. P. & Farres, P. J., 1998: The monitoring of soil surface development using analytical photogrammetry. *Photogrammetric Record*, 16 (92), 331-345.
- Mii, H., 1962: Coastal geology of Tanabe Bay. *The Science Reports of the Tohoku University, Sendai, Japan (2nd series - Geology)*, 31 (1), 1-93.
- Miller, L. R., Leverette, S., O'Sullivan, J., Tochko, J. & Theriault, K., 1974: Field measurements of impact pressures in surf. In: *14th Conference of Coastal Engineering*, pp. 1761-1777.
- Mitsuyasu, H., 1966: Shock pressure of breaking wave. In: *10th conference on coastal engineering*, pp. 268-283.

- Mottershead, D. N., 1989: Rates and patterns of bedrock denudation by coastal salt spray weathering : a seven-year record. *Earth Surface Processes and Landforms*, 14, 383-398.
- Munk, W., 1944: *Proposed uniform processes for observing waves and interpreting instrument records*. 26, S.I.O.
- Nadaoka, K. & Yagi, H., 1998: Shallow-water turbulence modelling and horizontal large-eddy computation of river flow. *Journal of Hydraulic Engineering-ASCE*, 124 (5), 493-500.
- Norrman, J. O., 1964: Lake Vättern: Investigations on shore and bottom morphology. *Geografiska Annaler*, 46 (1-2), 7-238.
- Nott, J., 1994: The influence of deep weathering on coastal landscape and landform development in the monsoonal tropics of northern Australia. *Journal of Geology*, 102 (5), 509-522.
- Novak, I. D., 1973: Predicting course sediment transport: The Hjulstrom curve revisited. In: Morisawa, M.(ed) *Fluvial Geomorphology*.
- Nowell, A. R. M. & Church, M., 1979: Turbulent flow in a depth-limited boundary layer. *Journal of Geophysical Research-Oceans*, 84 (C8), 4816-4824.
- Ollier, C., 1969: *Weathering*. Oliver and Boyd: Edinburgh.
- Ota, Y., Pillans, P., Berryman, K., Beu, A. & Fujimori, T., 1996: Pleistocene coastal terraces of Kaikoura Peninsula and the Marlborough coast, South Island, New Zealand. *New Zealand Journal of Geology and Geophysics*, 39, 51-73.
- Pickrill, R. A. & Mitchell, J. S., 1979: Ocean wave characteristics around New Zealand. *New Zealand Journal of Marine and Freshwater Research*, 13 (4), 501-520.
- Pitty, A. F., 1971: *Introduction to Geomorphology*. Methuen and co: London.
- Ramkema, C., 1978: A model law for wave impacts on coastal structures. In: *16th Coastal Engineering Conference*, pp. 2308-2327.
- Richards, K., 1982: *Rivers - Form and Processes in Alluvial Channels*. Methuen: London.
- Robinson, D. A. & Jerwood, L. C., 1986: Frost and salt weathering of chalk shore platforms near Brighton, Sussex, U.K. *Transactions of the Institute of British Geographers*, 12, 217-226.
- Robinson, L. A., 1977a: The morphology and development of the Northeast Yorkshire shore platform. *Marine Geology*, 23 (237-255).
- Robinson, L. A., 1977b: Marine erosive processes at the cliff foot. *Marine Geology*, 23 (257-271).
- Robinson, L. A., 1977c: Erosive processes on the shore platform of Northeast Yorkshire, England. *Marine Geology*, 23, 339-361.
- Sanders, N. K., 1968a. The development of Tasmanian Shore Platforms, *University of Tasmania*.
- Sanders, N. K., 1968b: Wave tank experiments on the erosion of rocky coasts. *Papers and proceedings of the Royal Society of Tasmania*, 102, 11-16.
- Selby, M. J., 1980: A rock mass strength classification for geomorphic purposes: with tests from Antarctica and New Zealand. *Zeitschrift fur Geomorphologie*, 24 (1), 31-51.
- Sewell, R. J., Weaver, S. D. & Reay, M. B., 1992: *Geology of Banks Peninsula*, Institute of Geological and Nuclear Sciences.
- Shulmeister, J. & Kirk, R. M., 1993: Evolution of a mixed sand and gravel barrier system in North Canterbury, New Zealand, during Holocene sea-level rise and still-stand. *Sedimentary Geology*, 87, 215-235.
- Shulmeister, J., Soons, J. M., Berger, G. W., Harper, M., Holt, S., Moar, N. & Carter, J. A., 1999: Environmental and sea level changes on Banks Peninsula

- (Canterbury, New Zealand) through three glaciation-interglaciation cycles. *Palaeogeography, Palaeoclimatology, Palaeoecology*, 152, 101-127.
- Smith, J. M., 1991: *Wind-wave generation on restricted fetches*. US Army Engineer Waterways Experiment Station, Coastal Engineering Research Centre
- Smith, J. M. B. & Bayliss-Smith, T. P., 1998: Kelp-plucking: Coastal erosion facilitated by bull-kelp *Durvillaea antarctica* at subantarctic Macquarie Island. *Antarctic-Science.*, 10 (4), 431-438.
- So, C. L., 1965: Coastal platforms of the Isle of Thanet, Kent. *Transactions of the Institute of British Geographers*, 37, 147-156.
- Spencer, T., 1981: Micro-topographic change on calcarenites, Grand Cayman Island, West Indies. *Earth Surface Processes and Landforms*, 6, 85-94.
- Steers, J. A. (ed), 1971: *Applied Coastal Geomorphology*. MacMillan: London
- Stephenson, W. J., 1997a. Development of shore platforms on Kaikoura Peninsula, South Island, New Zealand. *Unpub. Doctor of Philosophy Thesis, University of Canterbury, Christchurch.*
- Stephenson, W. J., 1997b: Improving the traversing micro-erosion meter. *Journal of Coastal Research*, 13 (1), 236-241.
- Stephenson, W. J., 2000: Shore platforms: A neglected coastal feature? *Progress in Physical Geography*, 24 (3), 311-327.
- Stephenson, W. J., 2001: Shore platform width - A fundamental problem. *Zeitschrift fur Geomorphologie*, 45 (4), 511-527.
- Stephenson, W. J. & Kirk, R. M., 1996: Measuring erosion rates using the micro-erosion meter: 20 years of data from shore platforms, Kaikoura Peninsula, South Island, New Zealand. *Marine Geology*, 131 (3-4), 209-218.
- Stephenson, W. J. & Kirk, R. M., 1998: Rates and patterns of erosion on inter-tidal shore platforms, Kaikoura Peninsula, South Island, New Zealand. *Earth Surface Processes and Landforms*, 23 (12), 1071-1085.
- Stephenson, W. J. & Kirk, R. M., 2000a: Development of shore platforms on Kaikoura Peninsula, South Island, New Zealand II: The role of subaerial weathering. *Geomorphology*, 32 (1-2), 43-56.
- Stephenson, W. J. & Kirk, R. M., 2000b: Development of shore platforms on Kaikoura Peninsula, South Island, New Zealand Part one: The role of waves. *Geomorphology*, 32 (1-2), 21-41.
- Stephenson, W. J. & Kirk, R. M., 2001: Surface swelling of coastal bedrock on inter-tidal shore platforms. *Geomorphology*, 41 (1), 5-21.
- Stull, R. B., 1995: *Meteorology Today for Scientists and Engineers*. West Publishing Company.
- Sturman, A. P. & Tapper, N. J., 1996: *The Weather and Climate of Australia and New Zealand*. Oxford University Press: Oxford.
- Suggate, R. P., 1965: Late Pleistocene geology of the northern part of the South Island, New Zealand. *New Zealand Geological Survey Bulletin*, 77, 91.
- Sunamura, T., 1973: Coastal cliff erosion due to waves-field investigations and laboratory experiments. *Journal of the Faculty of Engineering, University of Tokyo.*, 32, 1-86.
- Sunamura, T., 1975: A laboratory study of wave-cut platform formation. *Journal of Geology*, 83, 389-397.
- Sunamura, T., 1978: Mechanisms of shore platform formation on the southern coast of the Izu Peninsula, Japan. *Journal of Geology*, 86, 211-222.
- Sunamura, T., 1983: Processes of sea cliff and platform erosion. In: Komar, P. D.(ed) *CRC Handbook of Coastal Processes and Erosion*.
- Sunamura, T., 1991: The elevation of shore platforms: A laboratory approach to the unsolved problem. *Journal of Geology*, 99, 761-766.

- Sunamura, T., 1992: *Geomorphology of Rocky Coasts*. John Wiley and Sons.
- Sunamura, T., 1994: Rock control in coastal geomorphic processes. *Transactions, Japanese Geomorphological Processes*, 15 (3), 253-272.
- Sundborg, A., 1956: The river Klarälven: a study of fluvial processes. *Geografiska Annaler*, 38 (2), 125-316.
- Suzuki, T., Takahashi, K., Sunamura, Y. & Terada, M., 1970: Rock mechanisms on the formation of washboard-like relief on wave-cut benches at Arasaki, Miura Peninsula, Japan. *Geographical Review of Japan*, 43, 211-222.
- Sverdrup & Munk, W., 1947: *Wind sea and swell*. U.S. Hydrological Office
- Takahashi, K., 1977: *Shore platforms in Southwestern Japan-Geomorphological study*. Coastal Landform Study Society Southwestern Japan.: Osaka.
- Taylor, D. I., 2003a. Habitat-forming intertidal algae across wave-exposures: An experimental evaluation of plant and herbivore interactions. *Unpub. Doctor of Philosophy Thesis, University of Canterbury, Christchurch*.
- Taylor, D. I., 2003b: Ph.D. Scuba diver, Kaikoura. *Personal Communication*. January 2003
- Thais, L. & Magnaudet, J., 1996: Turbulent structure beneath surface gravity waves sheared by the wind. *Journal of Fluid Mechanics*, 328, 313-344.
- Thomas, M. L. H., 1986: A physically derived exposure index for marine shorelines. *Ophelia*, 25 (1), 1-13.
- Thompson, E. F. & Vincent, C. L., 1984: Shallow water wave height parameters. *Journal of Waterway Port Coastal and Ocean Engineering*, 110 (2).
- Thompson, E. F. & Vincent, C. L., 1985: Significant wave height for shallow water design. *Journal of Waterway Port Coastal and Ocean Engineering*, 111 (5), 828-842.
- Thornbury, W. D., 1954: *Principles of Geomorphology*. Wiley: New York.
- Thornton, E. B. & Guza, R. T., 1983: Transformation of wave height distribution. *Journal of Geophysical Research-Oceans*, 88 (C10), 5925-5938.
- Torpen, B. E., 1956: Large rocks in river control works. *Civil Engineering*, 26, 586-591.
- Trenhaile, A. S., 1972: The shore platforms of the Vale of Glamorgan, Wales. *Transactions of the Institute of British Geographers*, 56, 127-144.
- Trenhaile, A. S., 1974a: The geometry of shore platforms in England and Wales. *Transactions of the Institute of British Geographers*, 62, 129-142.
- Trenhaile, A. S., 1974b: The morphology and classification of shore platforms in England and Wales. *Geografiska Annaler*, 56A (1-2), 103-110.
- Trenhaile, A. S., 1978: The shore platforms of Gaspé, Quebec. *Annals of the Association of American Geographers*, 68, 95-114.
- Trenhaile, A. S., 1980: Shore platforms: a neglected coastal feature. *Progress in Physical Geography*, 4 (1), 1-23.
- Trenhaile, A. S., 1987: *The Geomorphology of Rock Coasts*. Clarendon Press: Oxford.
- Trenhaile, A. S., 1999: The width of shore platforms in Britain, Canada and Japan. *Journal of Coastal Research*, 15 (2), 353-364.
- Trenhaile, A. S., 2000: Modelling the development of wave-cut shore platforms. *Marine Geology*, 166, 163-178.
- Trenhaile, A. S., 2001: Modelling the effect of weathering on the evolution and morphology of shore platforms. *Journal of Coastal Research*, 17 (2), 398-406.
- Trenhaile, A. S. & Layzell, M. G. J., 1981: Shore platform morphology and the tidal duration factor. *Transactions of the Institute of British Geographers*, 6, 82-102.

- Trenhaile, A. S. & Mercan, D. W., 1984: Frost weathering and the saturation of coastal rocks. *Earth Surface Processes and Landforms*, 9, 321-331.
- Trenhaile, A. S., Pepper, D. A., Trenhaile, R. W. & Dalimonte, M., 1998: Stacks and notches at Hopewell Rocks, New Brunswick, Canada. *Earth Surface Processes and Landforms*, 23 (11), 975-988.
- Trenhaile, A. S. & Rudakas, P. A., 1981: Freeze-thaw and shore platform development in Gaspé, Quebec. *Geographic Phys. Quat.*, 35, 171-181.
- Trudgill, S. T., 1976a: The marine erosion of limestones on Aldabra Atoll, Indian Ocean. *Zeitschrift für Geomorphologie*, Supplementband 26, 164-200.
- Trudgill, S. T., 1976b: The subaerial and subsoil erosion of limestone on Aldabra Atoll, Indian Ocean. *Zeitschrift für Geomorphologie*, Supplementband 26, 201-210.
- Trudgill, S. T., 1987: Bioerosion on intertidal limestone, Co. Clare, Eire. *Marine Geology*, 74, 111-121.
- Tsujimoto, H., 1987: Dynamic conditions for shore platform initiation. *Science Reports of the Institute of Geoscience, University of Tsukuba*, 8 (Section A), 45-93.
- Tucker, M. J., 1963: Analysis of records of sea waves. *Proceedings of the Institution of Civil Engineers*, 26, 305-316.
- Viles, H. A. & Trudgill, S. T., 1984: Long term re-measurements of micro-erosion meter rates, Aldabra Atoll, Indian Ocean. *Earth Surface Processes and Landforms*, 9, 89-94.
- Walsh, J., 2002: *Canterbury directional wave buoy quarterly report: Nov 2000 - Jan 2001*. Christchurch: National Institute of Water and Atmosphere for ECan and CCC
- Wellman, H. W. & Wilson, A. T., 1965: Salt weathering, a neglected geological erosive agent in coastal and arid environments. *Nature*, 205, 1097-1098.
- Wentworth, C. K., 1938: Marine bench-forming processes: water-level weathering. *Journal of Geomorphology*, 1 (1), 6-32.
- Wentworth, C. K., 1939: Marine bench-forming processes: Solution benching. *Journal of Geomorphology*, 2 (1), 3-25.
- Whipple, K. X., Hancock, G. & Anderson, R. S., 2000: River incision into bedrock mechanics and relative efficacy of plucking, abrasion and cavitation. *Geological Society of America Bulletin*, 112 (3), 490-503.
- Williams, A. T. & Roberts, G. T., 1995: The measurement of pebble impacts and wave action on shore platforms and beaches: the swash force transducer (swashometer). *Marine Geology*, 129 (1-2), 137-143.
- Williams, R. B. G. & Robinson, D. A., 1983: The effect of surface texture on the determination of the surface hardness of rock using the Schmidt hammer. *Earth Surface Processes and Landforms*, 8, 289-292.
- Williams, R. B. G., Swantesson, J. O. H. & Robinson, D. A., 2000: Measuring rates of surface downwearing and mapping microtopography: the use of micro-erosion meters and laser scanners in rock weathering studies. *Zeitschrift für Geomorphologie*, Supplementband 120, 51-66.
- Yatsu, E., 1988: *The Nature of Weathering, An Introduction*. Sozsha: Tokyo.
- Zenkovich, V. P., 1967: *Processes of Coastal Development*. Oliver and Boyd: London.



The end of a data set.